

8 June 2007 | S10

Science

 AAAS

**"I feed my cells Lifeline™ Media.
I wouldn't consider anything else."**



"I care about my cells and need them to thrive. The people at Lifeline Cell Technology understand and care about my cells too. Their cell culture experience dates back to the 1980's, to the introduction of Normal Human Cell Systems. Their philosophy is to provide quality-tested products that are guaranteed to perform. Best of all, their technical staff is accessible and knowledgeable."

At Lifeline Cell Technology we produce Stem Cell and Primary Cell products for your research. Stem Cell products include Mitomycin C Treated Fibroblasts with Serum Free Medium and ags-Neural Stem Cells, *a unique cellular model of stroke*. Try our primary human cell products, including Endothelial Cells, Dermal Fibroblasts, Serum Free or Low Serum Media, Growth Factors and Reagents. Lifeline products are consistently manufactured and rigorously tested.

Call us at 301.845.7787. We'll be pleased to help you with your research needs and give you the specialized attention you and your cells deserve.



Call Lifeline Technical Service and Sales at 301.845.7787
Science readers - please visit lifelinecelltech.com/science for a SPECIAL OFFER.
Lifeline Cell Technology - 10 East Frederick Street - Walkersville, MD 21793

Lifeline Cell Technology is an International Stem Cell company.
©2007 Lifeline Cell Technology. All Rights Reserved.



**Nothing in life is to be feared.
It is only to be understood.**

Marie Curie

Scientist (1867-1934)

We work to encourage vision and creativity that extends well beyond the short-term. Shimadzu believes in the value of science to transform society for the better. For more than a century, we have led the way in the development of cutting-edge technology to help measure, analyze, diagnose and solve problems. The solutions we develop find applications in areas ranging from life sciences and medicine to flat-panel displays. We have learned much in the past hundred years. Expect a lot more.

www.shimadzu.com

 **SHIMADZU**



Get attached to illustra for faster nucleic acid sample prep.

New illustra™ nucleic acid sample prep kits from GE Healthcare give you optimal yield and purity. What's more, they do this in as little as half the time it takes the best competing products. Whether you're purifying nucleic acids in plasmid, blood, tissue, cells or bacteria, you'll find that superior results and outstanding reproducibility come easily with illustra mini and midi kits.

With more than 20 years' experience in nucleic acid research, we're bringing science to life and helping transform healthcare. We call it Life Science Re-imagined.

www.gelifesciences.com/illustra

Speed is crucial to the sundew plant's success.
It reacts rapidly, bending its tentacles to bind its prey.
Some species can do this in just tenths of a second.



imagination at work



COVER

Flowers of monkshood, *Aconitum napellus*, extend laterally from a main stem and open successively toward the apex. This arrangement is one of only three basic flowering structures observed in nature, reflecting the way developmental mechanisms and natural selection interact to constrain biological form, as described on [page 1452](#).

Photo: Karen Lee

DEPARTMENTS

- 1387 [Science Online](#)
- 1389 [This Week in Science](#)
- 1395 [Editors' Choice](#)
- 1398 [Contact Science](#)
- 1401 [Random Samples](#)
- 1403 [Newsmakers](#)
- 1503 [New Products](#)
- 1504 [Science Careers](#)

EDITORIAL

- 1393 [New Cooperation in East Asia](#)
by Hiroshi Nagano and
Christopher T. Hill

NEWS OF THE WEEK

- Teams Reprogram Differentiated Cells—Without Eggs
Reprogramming, Take Two 1404
- MIT Colleague Quits to Protest Sherley Dismissal 1405
- Gravity Distorts Big Bang Afterglow, Opening
New Window on Cosmos 1407
- SCIENCESCOPE** 1407
- Mongkol Na Songkhla: Thai Health Minister Defends
Controversial Drug-Patent Policy 1408
- Saudi Arabia: Graduate University Launched With
\$10 Billion Endowment 1409
- Whales (Mostly) Win at Whaling Commission Meeting 1411

NEWS FOCUS

- Pushing the Scary Side of Global Warming 1412
- A New Take on Tau 1416
- A Tame Virus Runs Amok 1418
- 210th American Astronomical Society Meeting 1420
- Black Holes: Galactic Homebodies?
- Exoplanet Jackpot Shows Astronomers Are Looking for
Worlds in All the Right Places
- 'Pristine' Galaxy Gives a Glimpse of Purity



LETTERS

- Adult Versus Embryonic Stem Cells: Treatments 1422
S. Smith, W. Neaves, S. Teitelbaum
Response D. A. Prentice and G. Tarne
- Making Singapore a Research Hub C. Cao
- Making Data on Iraqi Mortality Rates Available
G. Burnham, S. Doocy, L. Roberts

CORRECTIONS AND CLARIFICATIONS 1425

BOOKS ET AL.

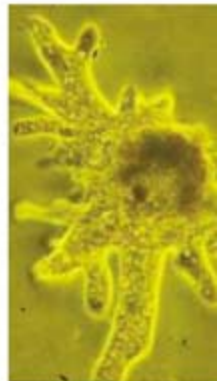
- The Edge of Evolution** The Search for the Limits of
Darwinism M. J. Behe, reviewed by S. B. Carroll 1427
- Evolution and the Levels of Selection** 1428
S. Okasha, reviewed by D. Jablonski

POLICY FORUM

- Practical Experiences in Dual-Use Review 1432
E. M. Davidson, R. Frothingham, R. Cook-Deegan

PERSPECTIVES

- Cracking the Supersolid 1435
P. Phillips and A. V. Balatsky
- Sister Act 1436
D. D. Moore
- Long Live Electronic Coherence! 1438
W. W. Parson
>> [Report p. 1462](#)
- [Listening to the Crackle of Subducting Oceanic Plates](#) 1439
A. Rietbrock
>> [Report p. 1472](#)
- [Deglaciation Mysteries](#) 1440
R. F. Keeling
>> [Research Article p. 1456](#)
- [Site-Seeing by Sequencing](#) 1441
S. Fields
>> [Report p. 1497](#)



1428

RNAi solutions by QIAGEN

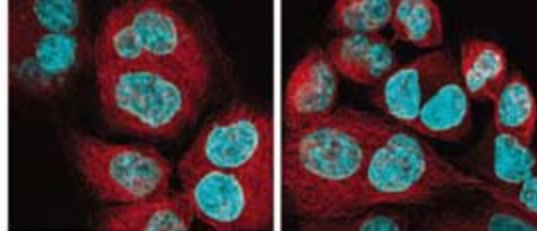
Knock down reliably

- Predesigned and validated siRNA
- Flexible, user-defined siRNA plates and sets
- Custom siRNA design and synthesis
- Matching siRNA and RT-PCR assays
- miRNA purification kits and assays

Contact QIAGEN today or visit www.qiagen.com/goto/RNAi.



Sample & Assay Technologies



SCIENCE EXPRESS

www.scienceexpress.org

APPLIED PHYSICS

Wireless Power Transfer via Strongly Coupled Magnetic Resonances
A. Kurs et al.

The magnetic resonance between two induction coils can be used to power a remote device through space over a distance of 2 meters.

[10.1126/science.1143254](https://doi.org/10.1126/science.1143254)

CELL BIOLOGY

**Parallels Between Cytokinesis and Retroviral Budding—
A Role for the ESCRT Machinery**

J. G. Carlton and J. Martin-Serrano

Cytokinesis, the process by which daughter cells are physically separated during cell division, uses the same machinery as viruses like HIV use to bud from infected cells.

[10.1126/science.1143422](https://doi.org/10.1126/science.1143422)

NEUROSCIENCE

Dentate Gyrus NMDA Receptors Mediate Rapid Pattern Separation in the Hippocampal Network

T. J. McHugh et al.

Rats are able to distinguish a new environment from a similar one because of distinct patterns of synaptic strengthening in the dentate gyrus.

[10.1126/science.1140263](https://doi.org/10.1126/science.1140263)

ASTROPHYSICS

Rapid Formation of Supermassive Black Hole Binaries in Galaxy Mergers with Gas

L. Mayer et al.

Simulations demonstrate that drag by the surrounding gas, rather than by nearby stars, slows galactic black hole pairs enough for them to coalesce within 1 million years.

[10.1126/science.1141858](https://doi.org/10.1126/science.1141858)

TECHNICAL COMMENT ABSTRACTS

ECOLOGY

Comment on "From Plant Traits to Plant Communities: A Statistical Mechanistic Approach to Biodiversity" 1425

S. H. Roxburgh and K. Mokany

[full text at www.sciencemag.org/cgi/content/full/316/5830/1425b](http://www.sciencemag.org/cgi/content/full/316/5830/1425b)

Comment on "From Plant Traits to Plant Communities: A Statistical Mechanistic Approach to Biodiversity"

C. O. Marks and H. C. Muller-Landau

[full text at www.sciencemag.org/cgi/content/full/316/5830/1425c](http://www.sciencemag.org/cgi/content/full/316/5830/1425c)

Response to Comments on "From Plant Traits to Plant Communities: A Statistical Mechanistic Approach to Biodiversity"

B. Shipley, D. Vile, É. Garnier

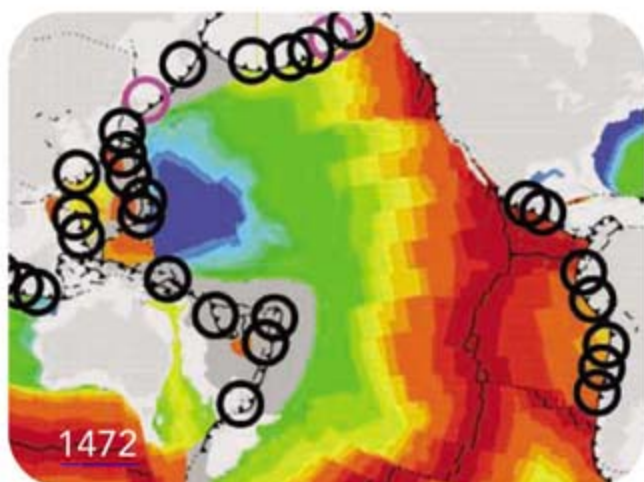
[full text at www.sciencemag.org/cgi/content/full/316/5830/1425d](http://www.sciencemag.org/cgi/content/full/316/5830/1425d)

REVIEW

PHYSICS

Imaging Atomic Structure and Dynamics with Ultrafast X-ray Scattering 1444

K. J. Gaffney and H. N. Chapman



BREVIA

ECOLOGY

Expansion of Industrial Logging in Central Africa 1451

N. T. Laporte et al.

Satellite images from 1973 to 2003 document the expansion of logging in tropical African forests and show that logging road construction is accelerating.

RESEARCH ARTICLES

EVOLUTION

Evolution and Development of Inflorescence Architectures 1452

P. Prusinkiewicz et al.

A combination of modeling and experiments explains why certain types of flower clusters are likely to be found in nature while others are absent.

CLIMATE CHANGE

Marine Radiocarbon Evidence for the Mechanism of Deglacial Atmospheric CO₂ Rise 1456

T. M. Marchitto et al.

Carbon-14 dates from a sediment core imply that Pacific deep waters stored CO₂ during glacial times and then vented it as deglaciation started, accelerating the temperature rise.

>> *Perspective p. 1440*

REPORTS

APPLIED PHYSICS

Monochromatic Electron Photoemission from Diamondoid Monolayers 1460

W. L. Yang et al.

Self-assembled layers of diamondoids, clusters of nanodiamonds with exposed hydrogens, efficiently emit electrons at one particular energy.

[CONTENTS continued >>](#)

Biomarker Discovery WEBINAR



Join our panel of experts in a **LIVE**
online seminar on **June 20, 2007**

Brought to you by the *Science* Business Office

Discovery of Autoantibody Biomarkers for Cancer and Autoimmune Disease

Autoantibodies have been documented to be valuable biomarkers in a range of cancers, in addition to autoimmune diseases. A number of discovery platforms are available for the identification of disease-specific autoantibodies. Protein microarrays provide a rapid and sensitive platform for the screening of autoantibodies in easily accessible biological fluids including sera, plasma, and urine.

Participating Experts:

Eng M. Tan, M.D.

Department of Molecular
and Experimental Medicine
Scripps Research Institute
La Jolla, CA

Michael Snyder, Ph.D.

Department of Molecular, Cellular,
and Developmental Biology
Yale University
New Haven, CT

Paul Predki, Ph.D.

Vice President for Research
and Development, Proteomics
Invitrogen Corporation
Carlsbad, CA

You will meet with a panel of experts to:

- ▶ Learn about the promise of autoantibodies as biomarkers for cancer and autoimmune disease.
- ▶ Obtain insight into how to advance your biomarker discovery research using proteomics approaches.
- ▶ Hear about the successful application of protein arrays to biomarker discovery in ovarian cancer.
- ▶ Have your questions answered by the experts live and in real time.

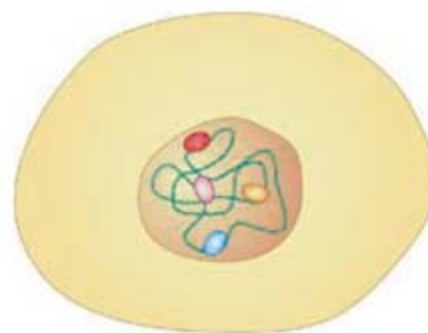
Register now!

**For more information and
complimentary registration online visit**

www.sciencemag.org/webinar



Webinar sponsored by Invitrogen



**1441 &
1497**

REPORTS CONTINUED...

CHEMISTRY

Coherence Dynamics in Photosynthesis: Protein Protection of Excitonic Coherence 1462

H. Lee, Y.-C. Cheng, G. R. Fleming

Spectroscopy reveals that two electronically excited domains in a bacterial photosynthetic reaction center are kept in phase by the protein to promote efficient energy transfer.

>> *Perspective p. 1438*

CHEMISTRY

Stepwise Quenching of Exciton Fluorescence in Carbon Nanotubes by Single-Molecule Reactions 1465

L. Cognet et al.

Electron-hole pairs diffuse across semiconducting carbon nanotubes, visiting thousands of sites before they are quenched in a light-producing reaction.

GEOPHYSICS

Seismic Evidence for Deep-Water Transportation in the Mantle 1468

H. Kawakatsu and S. Watada

Seismic images show how water flows on the surface of a subducting slab into the deep mantle beneath northeastern Japan.

GEOPHYSICS

Global Prevalence of Double Benioff Zones 1472

M. R. Brudzinski et al.

In all 15 of Earth's subduction zones—not just a few, as previously thought—earthquakes occur in two parallel regions, on top of the descending plate and within it.

>> *Perspective p. 1439*

PLANT SCIENCE

A Meta-Analysis of Effects of Bt Cotton and Maize on Nontarget Invertebrates 1475

M. Marvier, C. McCreedy, J. Regetz, P. Kareiva

A meta-analysis of 41 studies shows that fields of cotton or corn containing a transgenic insecticide harbor lower populations of certain invertebrates compared to untreated fields.

EVOLUTION

An Ancient Mechanism Controls the Development of Cells with a Rooting Function in Land Plants 1477

B. Menand et al.

A transcription factor that controls formation of hair-like organs in haploid mosses was co-opted to form a nonhomologous but functionally similar organ in diploid land plants.

MEDICINE

Polony Multiplex Analysis of Gene Expression (PMAGE) in Mouse Hypertrophic Cardiomyopathy 1481

J. B. Kim et al.

Covering beads with multiple copies of a sequence tag allows precise measurement of RNA expression and can detect as little as one molecule of messenger RNAs in three cells.

GENETICS

RNA Maps Reveal New RNA Classes and a Possible Function for Pervasive Transcription 1484

P. Kapranov et al.

Analysis of all the RNA transcribed from the human genome reveals three new classes of RNA that may be functionally important.

GENETICS

A Common Allele on Chromosome 9 Associated with Coronary Heart Disease 1488

R. McPherson et al.

A Common Variant on Chromosome 9p21 Affects the Risk of Myocardial Infarction 1491

A. Helgadottir et al.

About one of every four Caucasians carry a sequence variation at a regulatory region of chromosome 9 that confers an elevated risk of heart disease.

IMMUNOLOGY

Attenuation of Allergic Contact Dermatitis Through the Endocannabinoid System 1494

M. Karsak et al.

Endogenous cannabinoids released from neurons usually inhibit allergic skin responses; in mice in which they are absent, allergic reactions are exacerbated.

MOLECULAR BIOLOGY

Genome-Wide Mapping of in Vivo Protein-DNA System Interactions 1497

D. S. Johnson, A. Mortazavi, R. M. Myers, B. Wold

Chromatin immunoprecipitation and high-throughput sequencing identify the nearly 2000 specific DNA binding sites for a neuronal transcription factor.

>> *Perspective p. 1441*

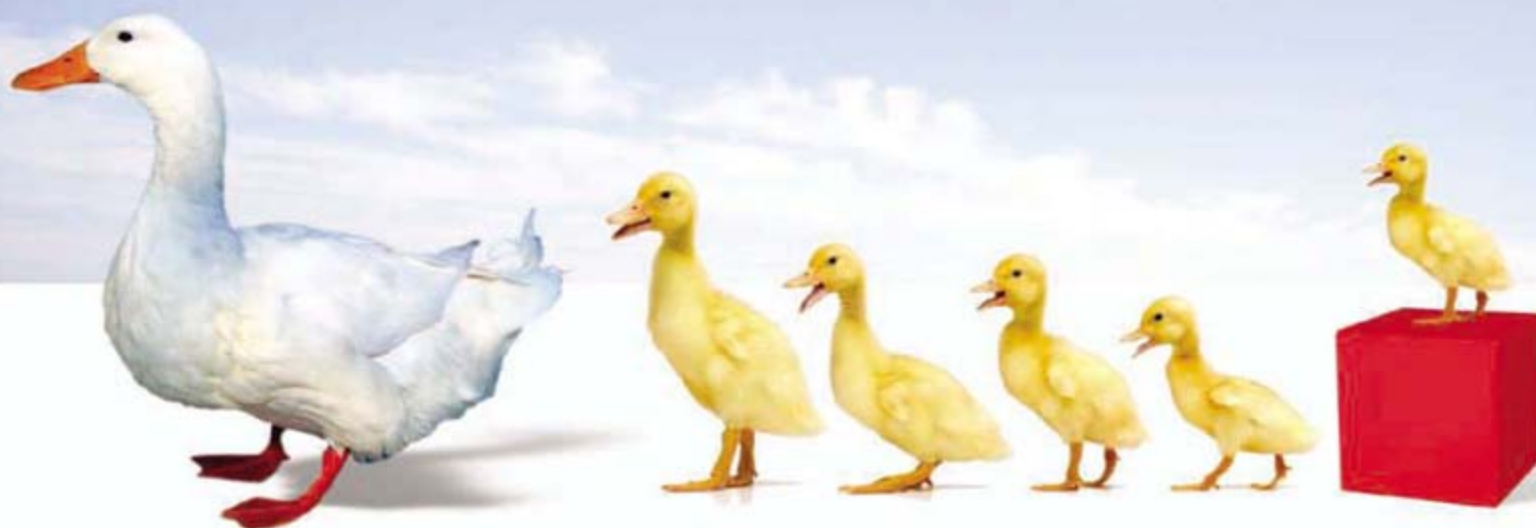


ADVANCING SCIENCE. SERVING SOCIETY

SCIENCE (ISSN 0036-8075) is published weekly on Friday, except the last week in December, by the American Association for the Advancement of Science, 1200 New York Avenue, NW, Washington, DC 20005. Periodicals Mail postage (publication No. 484460) paid at Washington, DC, and additional mailing offices. Copyright © 2007 by the American Association for the Advancement of Science. The title SCIENCE is a registered trademark of the AAAS. Domestic individual membership and subscription (51 issues): \$142 (\$74 allocated to subscription). Domestic institutional subscription (51 issues): \$710; Foreign postage extra: Mexico, Caribbean (surface mail) \$55; other countries (air assist delivery) \$85. First class, airmail, student, and emeritus rates on request. Canadian rates with GST available upon request, GST #1254 88122. Publications Mail Agreement Number 1069624. Printed in the U.S.A.

Change of address: Allow 4 weeks, giving old and new addresses and 8-digit account number. Postmaster: Send change of address to AAAS, P.O. Box 96178, Washington, DC 20090-6178. Single-copy sales: \$10.00 current issue, \$15.00 back issue prepaid includes surface postage; bulk rates on request. Authorization to photocopy material for internal or personal use under circumstances not falling within the fair use provisions of the Copyright Act is granted by AAAS to libraries and other users registered with the Copyright Clearance Center (CCC) Transactional Reporting Service, provided that \$18.00 per article is paid directly to CCC, 222 Rosewood Drive, Danvers, MA 01923. The identification code for Science is 0036-8075. Science is indexed in the Reader's Guide to Periodical Literature and in several specialized indexes.

CONTENTS continued >>



Elevate!

INNOVATION @ WORK

Elevate your understanding of the Epigenome with Sigma's Imprint™ DNA Modification Kit.

Sigma offers a complete solution for DNA methylation analysis with the Imprint DNA Modification Kit. This product contains all of the reagents necessary for complete bisulfite conversion and subsequent purification of DNA samples.

- **Fastest Kit Available** - procedure takes less than 2 hours to complete as compared to overnight methods
- **Unparalleled Sensitivity** - only 50 pg or 20 cells required for modification
- **Complete Conversion** - greater than 99% conversion of unmethylated cytosines
- **Robust** - more than 50% DNA recovery through treatment and purification

For more information, please visit sigma.com/mod50



Communication by vibration.

SCIENCE NOW

www.sciencenow.org DAILY NEWS COVERAGE

Flu-Fighting Fetuses

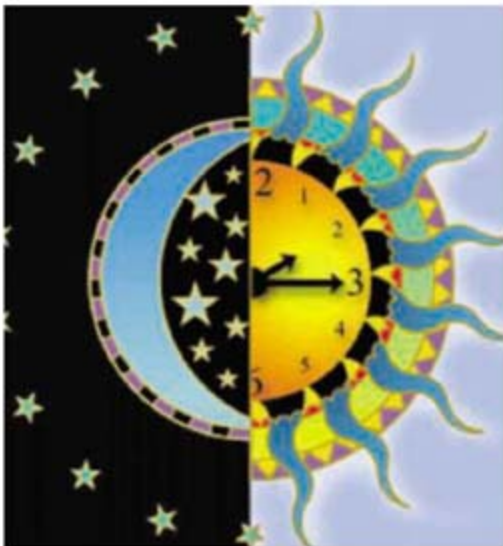
Babies have complex immune systems, even before they are born.

Rumble, Rumble. Who's There?

Elephants can distinguish friend from stranger by paying attention to ground vibrations.

Through a Lens, Darkly

Astronomers weigh some dark matter in the fringe of the Milky Way.



Circadian biology.

SCIENCE'S STKE

www.stke.org SIGNAL TRANSDUCTION KNOWLEDGE ENVIRONMENT

PERSPECTIVE: In SYNC—The Ins and Outs of Circadian Oscillations in Calcium

T. Imaizumi, J. I. Schroeder, S. A. Kay

A slow oscillation in cytoplasmic calcium may function in circadian signaling.

PERSPECTIVE: IL-33—A Sheep in Wolf's Clothing?

M. Gadina and C. A. Jefferies

IL-33 joins the exclusive group of cytokines with nuclear as well as receptor-mediated functions.

FORUM: Zinc Signals 2007

E. M. Adler

Read the reports of this meeting devoted to zinc signaling.



Business requires a variety of skills.

SCIENCE CAREERS

www.sciencerecareers.org CAREER RESOURCES FOR SCIENTISTS

UK: Hidden Talents, Hungry Markets— Ph.D.s Have Many Skills to Offer Industry

K. Zala

You will need a number of business-related skills to land a job outside academia.

US: Opportunities—Postdoc to IPO, One Young Scientist's Entrepreneurial Journey

P. Fiske

As a postdoc, Avi Speer had a great idea that he took all the way to an initial public offering.

US: Living the Issue

B. Benderly

A family health crisis led lab scientist Adil Shamoo to a new passion and a new career in bioethics.

NETHERLANDS: From the Archives— So It's a Small World, So What?

D. van Vlooten

How can the six degrees of separation help you find a job or funding?

Separate individual or institutional subscriptions to these products may be required for full-text access.



in a word, trust.

T4 DNA Ligase from New England Biolabs

WHEN YOU NEED LIGASE, TURN TO THE INDUSTRY STANDARD

New England Biolabs is dedicated to providing our customers with guaranteed enzyme performance. Our recombinant T4 DNA Ligase is the most extensively used ligase for cloning experiments. It is available at exceptional value, and an even greater value when purchased in large quantities for high throughput technologies. For cohesive, blunt, simple or complex reactions, make T4 DNA Ligase from NEB your first choice.

■ T4 DNA Ligase*

Regular Concentration

For standard cloning reactions

M0202S/L

High Concentration

For large or difficult constructs

M0202T/M

■ Quick Ligation™ Kit*

For ligation of cohesive or blunt-end DNA fragments in 5 minutes at room temperature. See our website for more details.

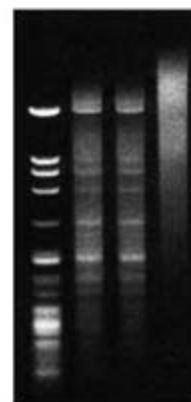
M2200S/L

Advantages:

- Quality – Highly pure enzyme with no lot-to-lot variation
- Convenience – Choose original T4 DNA Ligase or the Quick Ligation Kit to meet the demands of a variety of reaction conditions
- Flexibility – Active at room temperature or 16°C; reaction times run from 5 minutes to overnight
- Robustness – Active in a variety of reaction buffers

 = Recombinant

*NEB ligase products are BSA-free



0 0.1 0.2 1.0
T4 DNA Ligase (µl)
Ligation of blunt-ended HaeIII fragments of Lambda DNA using various amounts of T4 DNA Ligase (400,000 cohesive end units/ml) in a 20 µl reaction volume. Reactions were incubated for 30 minutes at 16°C.



0 10 20 30 60
Time (min)
Ligation of HindIII fragments (4-base overhang) of Lambda DNA using 1 cohesive end unit (1 µl of 1:400 dilution) of T4 DNA Ligase. Reactions were incubated at 25°C.

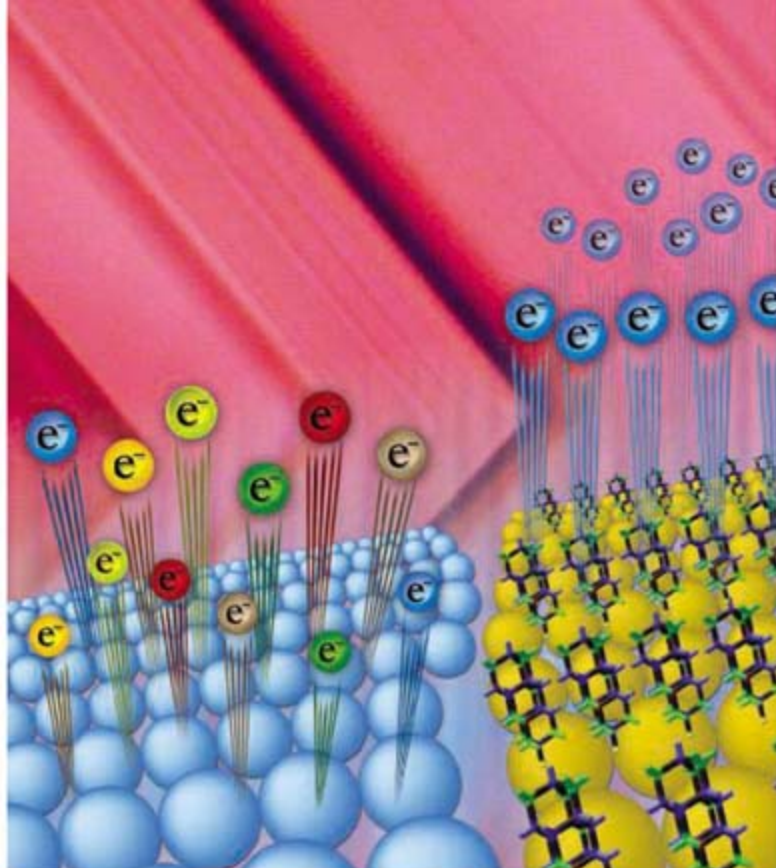
For more information and our international distribution network, please visit www.neb.com

New England Biolabs, Inc. is an ISO 9001 certified company

New England Biolabs Inc. 240 County Road, Ipswich, MA 01938 USA 1-800-NEB-LABS Tel. (978) 927-5054 Fax (978) 921-1350 info@neb.com

Canada Tel. (800) 387-1095 info@ca.neb.com • **China** Tel. 010-82378266 beijing@neb-china.com • **Germany** Tel. 0800/246 5227 info@de.neb.com

Japan Tel. +81 (0)3 5669 6191 info@neb-japan.com • **UK** Tel. (0800) 318486 info@uk.neb.com



<< Electron Emits with Ease

Negative electron affinity materials readily emit electrons, which make them potentially useful in field-emission displays and electron microscopes. Bulk diamond is known to be one such material, but issues with emission uniformity and electronic transport have led to a search for other candidates. Diamondoids (C_{22} and higher polymantanes) are molecules that have been extracted from petroleum, which contain 4 to 11 diamond-crystal cages terminated by hydrogen atoms. A photoemission study by **Yang *et al.*** (p. 1460) of functionalized self-assembled monolayers of diamondoids shows that they are also negative electron affinity materials and can provide a nearly monochromatic source of photoemitted electrons.

X-ray Visions

The success of x-ray diffraction for determining atomic structures has inspired further efforts to extend its use to materials that are less crystalline in nature and to determine structural changes on the time scales characteristic of changes in electronic structure and bonding.

Gaffney and Chapman (p. 1444) discuss a new generation of x-ray facilities whose incident beams start out as electron bunches from a linear accelerator and are then converted to coherent pulses of x-rays. The pulsed nature of the x-ray beam allows characterization of ultrafast dynamics, and the beam's coherence will allow imaging of noncrystalline materials with atomic resolution.

Harvesting Light Coherently

Photosynthesis relies on the remarkable efficiency of energy transfer among the complex protein domains that absorb sunlight and channel energy into chemical reactions. **Lee *et al.*** (p. 1462; see the Perspective by **Parson**) used a two-color photon-echo spectroscopic technique to explore the early dynamics of energy transfer between two components of the photosynthetic reaction center from purple bacteria. Upon photoexcitation, a bacteriopheophytin and accessory bacteriochlorophyll stay coherently in phase within each protein for significantly longer times than do the individual components across the ensemble. Modeling of the data implicates vibrational coupling through

the protein structure in maintaining this coherent state and thereby facilitating efficient energy migration.

Stepwise Quenching

When excited by visible light, semiconducting single-walled carbon nanotubes (SWNTs) generate highly mobile excitons, and processes that annihilate these excitons lead to characteristic fluorescence in the near infrared. Chemical reactions at the sidewalls of the nanotube, such as protonation, can quench this photoluminescence. **Cognet *et al.*** (p. 1465) have used the quenching process to follow side-wall reactions by placing SWNTs in agarose gels and diffusing in reversible reactants (acids or bases) or irreversible reagents (diazonium salts). Stepwise changes in luminescence correspond to quenching of excitons at localized sidewall sites. An analysis of these stepwise changes reveals that the excitons move in a diffusional manner and explore ~10,000 sites during their lifetimes.



Earthquakes Zones in Parallel

Benioff zones are strips of descending plates in subduction zones that host earthquakes. Some areas are known to host double Benioff zones (parallel strips where earthquakes occur), but it

has been thought that most of these zones occur as single swaths. **Brudzinski *et al.*** (p. 1472; see the Perspective by **Rietbrock**) analyzed databases of earthquakes and located earthquakes within the descending slabs of lithosphere. Two parallel seismic stripes, rather than a single broad zone, were found in most cases. The widespread occurrence of double Benioff zones sets limits on the formation mechanisms of earthquakes.

From Variety to Variation

Flowers and groupings of flowers (inflorescences) come in an astonishing variety of shapes and sizes; however, theoretically many more possibilities could have evolved. To explain why the biological forms we see in nature represent such a small part of theoretical possibilities, **Prusinkiewicz *et al.*** (p. 1452, published online 24 May; see the cover) combine genetic and theoretical studies on inflorescence architecture. By showing how interactions between development and selection operate within higher-dimensional fitness spaces, the authors reveal likely routes and constraints on the evolution of biological forms. Furthermore, the study tests this model by examining the expression of two genes that influence architecture in the model plant, *Arabidopsis*.

Transcriptional Profiling of Tissue

The progression of a tissue from a healthy to a diseased state is typically accompanied by

Continued on page 1391

Dharmacon
now sold as
Thermo Scientific

© 2007 Thermo Fisher Scientific Inc. All rights reserved.

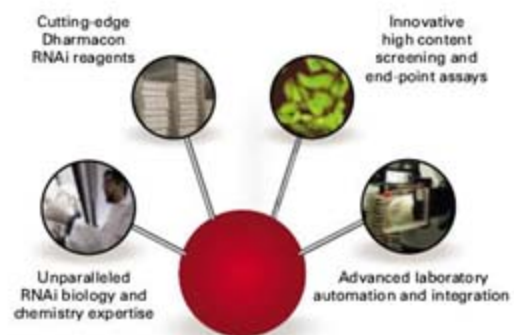


Progressive RNAi-based screening & profiling solutions with RNAi Discovery and Therapeutics Services.

The Thermo Scientific brand of products now includes complete RNAi-based screening solutions to accelerate drug discovery and therapeutic development by combining advanced Thermo Scientific Dharmacon RNAi reagents, assay technology and lab automation. Services can range from a single screen to multi-component program projects that support critical drug discovery activities.

- Target identification
- Target validation
- Drug rescue, repositioning, and patent extension
- Biomarker discovery
- RNAi therapeutic technology development
- RNAi screening consultation and training

visit www.thermo.com/dharmacon or call 800-235-9880

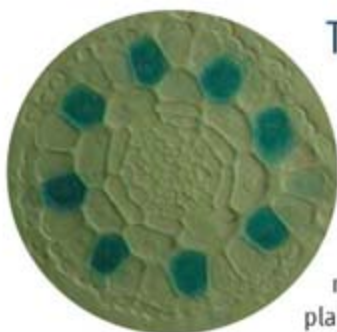


Fully Integrated RNAi Services

Access to unmatched RNAi expertise, advanced reagents and bioinformatics tools enables the rapid evolution of hits to drug target leads.

Continued from page 1389

changes in the expression of hundreds to thousands of genes. A number of existing methods allow these transcriptional changes to be monitored, each method with its own strengths and weaknesses. **Kim *et al.*** (p. 1481) describe polony multiplex analysis of gene expression, or PMAGE, that allows for more precise quantification of transcripts and detection of low-abundance transcripts. Application of PMAGE to a mouse model of hypertrophic cardiomyopathy revealed changes in the expression of many low-abundance transcripts even before the appearance of pathological changes in the heart.



The Root of the Problem

Mosses exhibit a relatively primitive life-style with only a haploid gametophyte phase, compared with flowering plants, which have two distinct phases in their life cycle—a brief haploid gametophyte phase employed during reproduction, and the diploid sporophyte phase, which makes up the physical bulk of the plant.

Menand *et al.* (p. 1477) analyzed angiosperm root hairs and their moss counterparts, rhizoids. Root hairs in the diploid angiosperm plants bury themselves in the soil and absorb nutrients. In the haploid mosses, rhizoids or caulonema perform a similar nutrient absorption and anchoring function, but are not related to root hairs at the cellular level. However, it now seems that related transcription factors direct the development of both cell types, indicating a closer relationship than previously assumed.

related transcription factors direct the development of both cell types, indicating a closer relationship than previously assumed.

Importance of Non-Gene Transcription

Much larger proportions of many eukaryotic genomes are transcribed into RNA than can be accounted for by their protein coding potential. The function of this “non-gene” transcription is unclear.

Kapranov *et al.* (p. 1484, published online 17 May) analyzed both long and short unannotated RNAs in human cells and found that a significant fraction of the longer transcripts may serve as precursors for the shorter RNAs. The short RNAs tend to cluster at the 5' and 3' ends of genes, and their numbers are often correlated with the expression of the underlying gene. Many of the 5' RNAs are found in conserved regions, suggesting that they may play important roles in gene or genome-related functions.

Probing the Genetics of Heart Disease

Certain life-style factors, such as smoking, greatly increase the risk of developing heart disease, but genetic factors also contribute. In independent studies, **McPherson *et al.*** (p. 1488, published online 3 May) and **Helgadottir *et al.*** (p. 1491, published online 3 May) used genome-wide association scanning to identify DNA sequence variants at chromosome 9p21 that increase the risk of heart disease in Caucasian populations. The 20 to 25% of Caucasians with two copies of the so-called “risk allele” had a 30 to 40% higher risk of heart disease compared with individuals with no copies of this allele. The genomic region of interest falls outside the boundaries of annotated protein-coding genes, so the mechanism by which it influences heart disease remains mysterious. Intriguingly, DNA sequence variants within the same general region of chromosome 9p21 have recently been shown to increase the risk of type 2 diabetes.

Allergy-Blocking Transmitters

The endocannabinoid system performs various regulatory functions and has been implicated in a growing number of physiological roles, both in the central and peripheral nervous systems and in peripheral organs. **Karsak *et al.*** (p. 1494) now find that this influence extends to regulation of allergic response. Mice lacking the two known cannabinoid receptors showed a strong tendency toward developing cutaneous contact sensitivity in response to distinct allergens. Blocking the receptors with antagonists had a similar effect, while absence of the gene encoding an enzyme responsible for breaking down cannabinoids increased resistance of mice to contact sensitivity. The regulation of the endocannabinoids or their receptors might be useful in treating allergies, although their role in the wider context of human allergy needs to be explored.

CREDIT: MENAND ET AL.

The Art of Global Discovery Chemistry



CHEMBRIDGE CORPORATION IS THE WORLD'S LARGEST GLOBAL DISCOVERY CHEMISTRY CRO AND PREMIER PROVIDER OF ADVANCED SCREENING LIBRARIES FOR SMALL MOLECULE DRUG DISCOVERY. PLEASE VISIT WWW.CHEMBRIDGE.COM



HEALTH NEWS

Breast cancer cure rate reaches 100%

Scientists disclose
treat

Someday, a researcher will make the breakthrough discovery that leads to the final victory in the fight against breast cancer. When that great day comes, we hope to have played a supporting role. To learn about scientists making significant discoveries today, visit www.promega.com/today.

©2007 Promega Corporation

TODAY COULD
BE THE DAY


Promega



Hiroshi Nagano is executive director at the Japan Science and Technology Agency, Tokyo, Japan. E-mail: hnagano@va.rosenet.ne.jp



Christopher T. Hill is professor of Public Policy and Technology in the School of Public Policy at George Mason University in Arlington, VA. E-mail: chill2@gmu.edu

New Cooperation in East Asia

THIS YEAR MARKS A NEW ERA FOR SHARED SCIENTIFIC PURSUITS AMONG CHINA, JAPAN, and Korea. The three nations have embarked on a new cooperative venture to support and manage science and technology. Preliminary meetings of agency officials and nongovernmental associations over the past several years culminated in a ministerial meeting earlier this year that resulted in a joint statement.* The consensus is an epoch-making event for these countries, given that although each continues to reach out to assume a larger role in world affairs, the three have tended to bump up against one another over such matters as ownership and control of natural resources, immigration, and commerce.

Nations have long used collaboration in science to advance knowledge and enhance diplomatic relationships. As neighbors in East Asia, these three ancient nations share many aspects of history and culture. In recent decades, China, Japan, and Korea have enjoyed remarkable economic and social progress, although they were in profoundly different economic, political, and diplomatic circumstances when they began their rise to new prominence. Today, the three countries face a host of common challenges in health, ecological, and energy-related matters. The trilateral statement was forged to specify cooperative efforts across a broad range of disciplines, in approaches that anticipate both fundamental and problem-driven research. The work will affect the interface of modern and traditional medicine, energy technology (including the peaceful use of nuclear energy), and disaster prevention and mitigation (to limit environmental deterioration). Of particular interest is the planned Trilateral Bioinformatics Network, which will facilitate communication among scientists working in life sciences. Moreover, the tripartite statement is not limited to cooperation in R&D programs. The three countries have agreed to cooperate in following international standards for protecting intellectual property and to explore ways of enhancing scientific integrity.

This is all good news, particularly considering that each country is also currently undergoing dramatic change, expansion, and reform in its scientific and technological institutions. China and Korea are building new universities. Japan has extensively introduced competitive processes for research evaluation. Corporate investments are expanding in all three countries. Thus, although each nation is developing an independent strategy of its own to bolster science and technology, there is clear intent to build and support collaboration among their remarkably strong scientific and technological activities. That is a welcome development that deserves international recognition.

A key element of the trilateral statement is a series of planned meetings of leaders of the agencies that oversee science and technology policy, planning, and evaluation. The meetings are intended to assess progress made at each evaluation point, including the exchange of young scientists among the three countries. The joint statement envisions meetings at levels ranging from joint workshops for researchers to ministerial meetings in 2009 and 2011, and expects to hold meetings of agency officials in 2008 and 2010. And although it is far too early to expect accomplishments, there are already strong indications of progress. At the annual meeting of the American Association for the Advancement of Science in February, agency leaders and researchers from China, Japan, and Korea discussed their latest work on policy issues of common interest, such as the mobility of human resources and evaluation of research programs. The work of these agencies should be of interest in North America, Europe, and elsewhere, because each is engaged in imaginative analyses of national trends in scientific and technological performance and outcomes.

The challenge for China, Japan, and Korea will be to sustain the spirit of the joint statement through inevitable changes in national leadership and priorities, as well as developments in the world political situation. The hope is to transform that new collaborative spirit into meaningful advances in science and technology, leading to real solutions for important shared problems. With a new determination to cooperate, the East Asian region is strengthening its status as a region committed to making science a driver of global societal and economic development in the 21st century.

— Hiroshi Nagano and Christopher T. Hill

*Joint Statement of the First Trilateral Korea-Japan-China Ministerial Meeting on Science and Technology Cooperation, Seoul, 12 January 2007 (www.mext.go.jp/english/kagaku/07012314.htm).





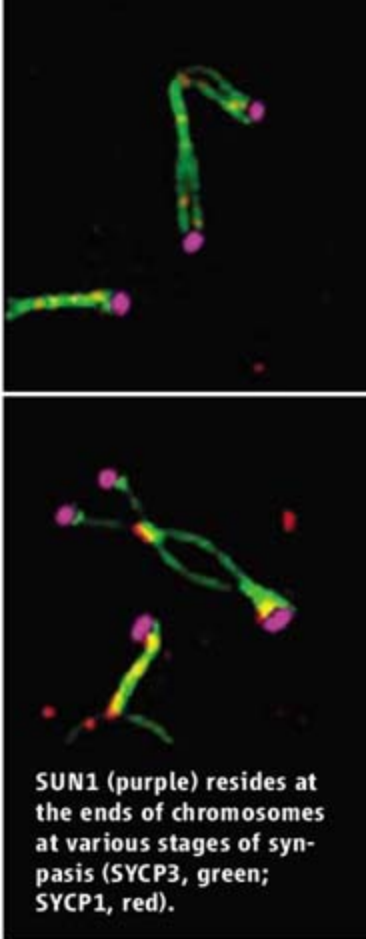
“The unknown has always fascinated me, and research is the best way to satisfy my curiosity.”

How do cells react to changed conditions? Which molecular processes control the regulation mechanisms? What genetic changes take place? Conversely: what is the effect on organisms when their genomes are transformed? Answering questions like these creates the foundation for breakthroughs in medicine, industry, and agriculture. Finding these answers requires sharp cell images and accurate micromanipulation, now unified in a single system. With the **Leica AM6000**, it is possible to view and manipulate cells simultaneously – with absolute reproducibility and minimum effort.

Prof. Stéphane Viville, Institute of Genetics and Molecular and Cellular Biology, Illkirch, France and Reproductive Biology Service SIHCUS-CMCO, Functional Unit Preimplantation Diagnostics, Schiltigheim, France

www.leica-microsystems.com

Leica
MICROSYSTEMS



SUN1 (purple) resides at the ends of chromosomes at various stages of synapsis (SYCP3, green; SYCP1, red).

DEVELOPMENT

Starting at the End

As sex cells divide during meiosis, homologous chromosomes pair up, form a synaptonemal complex with the aid of the lateral element SYCP3 and the transverse element SYCP1, and exchange genetic material. This recombination takes place before chromosome segregation and results in increased genetic diversity. Before pairing, however, the telomeric regions (the ends) of chromosomes can be observed to localize and cluster at the nuclear envelope. By generating knockout mice, Ding *et al.* show that the protein SUN1 participates in attaching telomeres to the nuclear membrane. When SUN1 is eliminated, telomeres no longer adhere to the nuclear envelope, and chromosomes are defective in synapsis and recombination. This results in mice that are infertile because of a failure to produce male and female gametes. Hence, telomeric clustering is necessary for successful meiosis in mice and is required for proper spermatogenesis and oogenesis. — BAP

Dev. Cell **12**, 10.1016/j.devcel.2007.03.018 (2007).

APPLIED PHYSICS

Quantum Dots Heated into Harmony

The cavity quantum electrodynamics framework, in which an atom in a cavity is coupled to the cavity's optical modes, is being explored as a potential building block for quantum information-processing architectures. However, atom mobility within the cavity can hinder control of the process. The use of artificial atoms, or quantum dots, confined to a high-quality optical cavity is one possible solid-state solution to the dynamics issue. Despite being designed to be identical, though, the dots can differ slightly from one another in size and atomic composition, thereby giving rise to distinct excitation spectra for each dot. This spectral variability is expected to cause a problem for communication between dots in an ensemble. By heating individual quantum dots through the laser excitation of a nearby connected heat pad, Faraon *et al.* show that the spectra of individual dots can be tweaked by up to 1.8 nm, thus providing the possibility of tuning the excitation spectra of an ensemble of quantum dots. — ISO

Appl. Phys. Lett. **90**, 213110 (2007).

SURFACE SCIENCE

Long Intervals in the Islands

Interactions between adsorbates on metal surfaces are often direct and short-range in nature; repulsions, for example, can lead to lower cover-

ages than steric packing would predict. Longer-range interactions can arise indirectly, such as through interactions with the surface states of the metal. Nanayakkara *et al.* explored these longer-range effects for adsorbed Br atoms on the close-packed Cu(111) surface. They deposited phenyl bromide on the surface and heated it to 600 K in vacuum. Biphenyl molecules desorbed and the Br atoms had sufficient mobility to form islands on the surface (shown at right).

Scanning tunneling microscopy at 4 K revealed that the nearest-neighbor island separations were half-multiples of the Fermi wavelength of this surface. The strong interaction of the Br atoms with the surface potential affected the island spacing even at distances of more than 50 Å. — PDS

Phys. Rev. Lett. **98**, 206108 (2007).

GEOCHEMISTRY

Mantle Melting Mechanisms

During Earth's history, heavy metals gradually decoupled from silicate rocks and sank toward the core, which became differentiated from the overlying mantle. Signatures of this process can be traced in the distribution of highly siderophile elements (Re and the platinum group elements Os, Ir, Ru, Pt, and Pd) that are chemically associ-

ated with iron. These elements tend to concentrate in base metal sulfides rather than in silicate-based minerals. Over time, they then fractionate and particular elements become sequestered in different types of sulfides, depending on the ways in which they melt. In low-sulfur rocks, their distributions are less well understood.

Luguet *et al.* have analyzed the distribution of highly siderophile elements in four rock samples from the low-sulfur harzburgite lenses in the Lherz massif in the French Pyrenees.

The platinum group elements were found to concentrate in rare, micrometer-sized minerals (sulfides and alloys) in the intergranular spaces. These are thought to be the residues of base metal sulfides that were lost from these rocks after a high degree (up to 25%) of partial melting. Because of their high melting temperatures and high Os content, these minerals may preserve Os isotope compositions after several rounds of mantle melting, possibly explaining the patchy Os distribution of the connecting upper mantle. — JB

Geochim. Cosmochim. Acta
10.1016/j.gca.2007.04.011 (2007).

MICROBIOLOGY

Form Follows Function

Strains of *Prochlorococcus* cyanobacteria contribute nearly half of the photosynthesis in the open ocean. Different ecotypes have distinct

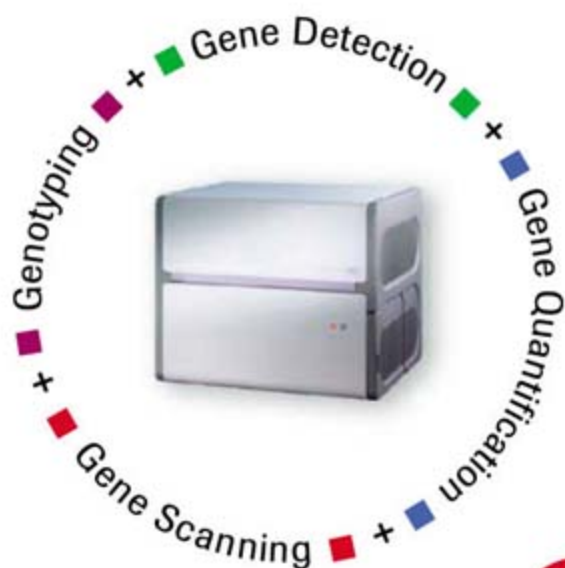
Continued on page 1397



www.roche-applied-science.com

LightCycler® 480 Real-Time PCR System

Looking for more versatility in real-time PCR?



We have what you need to accomplish more... now and in the future.

Choose the LightCycler® 480 System (96- and 384-well format) – and get the power and flexibility to meet changing research needs.

- **Gene Detection:** Benefit from an advanced optical system and enhanced multiplexing capabilities to perform multitarget analysis.
- **Gene Quantification:** Utilize sophisticated software and unique algorithms to generate highly accurate gene quantification data.
- **Genotyping:** Achieve reliable genotyping results based on superior post-PCR melting curve analysis.
- **Gene Scanning:** Employ the innovative high-resolution melting (HRM) method to scan genes for unknown variations.

Be prepared for the evolving demands of real-time PCR.

Learn more about our cutting-edge technologies that provide versatility without compromise – visit www.lightcycler480.com today!

For general laboratory use. Not for use in diagnostic procedures.

This LightCycler® 480 Real-Time PCR System is licensed under U.S. Patent 6,814,934 and corresponding claims in its non-U.S. counterparts and under one or more of U.S. Patents Nos. 5,038,852, 5,656,493, 5,333,675, or corresponding claims in their non-U.S. counterparts, for use in life science, by implication or by estoppel under any patent claims or for any other implication.

The product is covered in-part by US 5,871,908, co-exclusively licensed from Evotec OAI AG. Parts of the Software used for the LightCycler® 480 System are licensed from Idaho Technology Inc., Salt Lake City, UT, USA.

LIGHTCYCLER is a trademark of Roche. Other brands or product names are trademarks of their respective holders. © 2007 Roche Diagnostics GmbH. All rights reserved.



Diagnostics

Roche Diagnostics GmbH
Roche Applied Science
68298 Mannheim
Germany

Continued from page 1395

morphologies. The tiny and spherical MED4 strain holds a 1.66-Mb genome and appears to prefer surface waters. In contrast, the larger (2.41-Mb genome) and ovoid MIT9313 ecotype is abundant in deeper (>50 m) subtropical and tropical waters.

By rapid freezing of hydrated cultured cells and cryoelectron microscopy, Ting *et al.* were able to document a substantially divergent cellular organization and structure in these bacterial strains. The MED4 strain possesses a thinner cell wall and a less extensive intracytoplasmic (photosynthetic) membrane system in comparison to MIT9313. The authors also find differences in key genes required for the biosynthesis of the cell wall peptidoglycan, where the greater similarity of these genes in MIT9313 and *Synechococcus* WH8102 correlates with their much thicker peptidoglycan layers. Overall, it seems that MIT9313 cells are better adapted for photosynthetic growth at low irradiance levels in deeper waters, although nutrient transport could also influence cell size and shape. — CA

J. Bacteriol. **189**, 10.1128/JB.01948-06 (2007).

BIOCHEMISTRY

Tinkering with Protein Structure

A few years ago, a new protein (Top7) was made from scratch. A computational algorithm provided a sequence of amino acids that had been designed to fold into a stable structure unlike any previously deposited in the public data-

bases; lo and behold, it did. Top7 consists of three substructures: a pair of two β -strand-one α -helix modules (A and C) separated in the sequence by a single β strand (module B), with the five β strands forming a hydrogen-bonded β sheet.

Using atomic force microscopy and steered molecular dynamics, Sharma *et al.* have assessed the mechanical resistance of Top7 to being pulled apart and compared these parameters to those of the canonical elastomeric module I27 of titin. They find that theory and experiment fit well, providing an average unfolding force of 155 pN that acts to strip off module A from B-C by breaking the hydrogen (and other) bonds between these substructures. Welding



Top7 (green) construct used in measuring unfolding forces.

β -strands 1 and 3 with a disulfide revealed that 170 pN was needed to lever module C away from the A-B assembly, whereas interrupting one of the hydrogen bonds linking β -strands 3 and 5 was sufficient to lower the unfolding force to 125 pN. These results together illustrate the power of combining computational and biochemical approaches to the design and refinement of protein structure. — GJC

Proc. Natl. Acad. Sci. U.S.A. **104**, 9278 (2007).



www.stke.org

<< NEMO: An Adaptive Regulator

Nuclear factor κ B (NF- κ B), a transcription factor critical in the immune response to pathogens, is maintained in the inactive state by an inhibitory protein (I κ B). The I κ B kinase (IKK) complex activates NF- κ B by dissociating I κ B, and NEMO, also known as IKK γ , is a regulatory subunit of this complex. Zhao *et al.* show that in addition to this role in NF- κ B activation, NEMO helps to activate the interferon regulatory factors IRF3 and IRF7, which, in combination with NF- κ B and activator protein 1, stimulate the transcription of type I interferons (IFN- α and - β) in virally infected cells. Experiments with mouse embryo fibroblasts deficient in the gene encoding NEMO showed that the efficient production of IFN- α and the subsequent expression of signal transducer and activator of transcription 1 (STAT1) required NEMO, but not IKK β (a subunit required for NF- κ B activation), suggesting that NEMO was not acting through the NF- κ B pathway. Reporter gene assays also demonstrated the dependence of IRF3- and IRF7-mediated gene expression on NEMO. In the NEMO knockout cells, overexpression of TBK1 (an IKK-related kinase that is upstream of IRF3 and IRF7 activation) restored reporter gene activation, and NEMO was also required for activation of the kinase activity of TBK1, placing NEMO upstream of TBK1 in the path to IRF3 and IRF7 activation. However, NEMO did not interact directly with TBK1 (or the related kinase IKK ϵ); instead, immunoprecipitation studies with transfected cells showed that TANK (TRAF family member-associated NF- κ B activator) was required for the formation of a trimeric complex of TANK, NEMO, and either IKK ϵ or TBK1. Mutational and deletion analyses suggest that different regions of NEMO participate in NF- κ B versus IRF activation. — NRG

Nat. Immunol. **8**, 592 (2007).

We've got your KO mice
and ES Clones
CLICK ON IT



www.stke.org

713-677-7429 | 888-377-TIGM

TEXAS INSTITUTE FOR GENOMIC MEDICINE



Amazing!

INNOVATION @ WORK

Over 4,000 high quality antibodies from a single source

Sigma's AMAZING collection of high quality antibodies:

- Includes monoclonals, polyclonals, secondaries, conjugates and custom services
- Validated using a variety of methods – WB, IHC, IF, IP, ELISA
- Easily explored through Sigma's award-winning online tools
- Supported by Sigma's world-renowned technical service to assist you with your specific antibody requirements

Sigma is your source.

Go to sigma.com/antibody and be Amazed!

Search for your antibody of interest using these convenient online tools at sigma.com/antibody

- Antibody Explorer
- PathFinder

Your Favorite Gene Search matches your gene of interest to thousands of Sigma antibodies



sigma.com/yfg

sigma.com

Accelerating Customers' Success through Leadership in Life Science, High Technology and Service
SIGMA-ALDRICH CORPORATION • BOX 14508 • ST. LOUIS • MISSOURI 63178 • USA

SIGMA

Deadline extended
to August 1.

Get published in *Science*, win a trip to Stockholm, \$25,000 – and earn the respect of Nobel laureates

Established in 1995, the GE & *Science* Prize for Young Life Scientists seeks to bring science to life by recognizing outstanding Ph.D.s from around the world and rewarding their research in the field of molecular biology.

This is your chance to gain international acclaim and recognition for yourself and your faculty, and to turn your scientific ideas into reality. If you were awarded your Ph.D. in molecular biology* during 2006, describe your work in a 1000-word essay. Then submit it for the 2007 GE & *Science* Prize for Young Life Scientists. A panel of distinguished scientists selects one Grand Prize winner and four regional winners. **Deadline extended to August 1.**

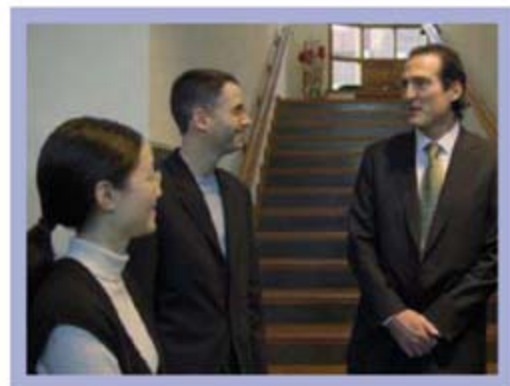
There are few awards more rewarding in science than the *Science*/AAAS and GE Healthcare-sponsored prize – just ask the Grand Prize winner for 2006. In addition to having her essay published in *Science*, Irene Chen received \$25,000, was flown to the awards ceremony in Stockholm, Sweden, and got to pick the brains of Nobel laureates Andrew Fire and Craig Mello.**

GE & *Science* Prize for Young Life Scientists:
Life Science Re-imagined.

For more information, go to
www.gehealthcare.com/science



Grand Prize winner Irene Chen presents her research to a captivated audience



Chen and fellow Prizewinner Ron Milo find common ground with Nobel laureate Craig Mello

Established and presented by:



* For the purpose of this prize, molecular biology is defined as "that part of biology which attempts to interpret biological events in terms of the physico-chemical properties of molecules in a cell" (*McGraw-Hill Dictionary of Scientific and Technical Terms*, 4th Edition).

**Nobel Prize 2006 winners in Physiology or Medicine for their discovery of RNA interference – gene silencing by double-stranded RNA.



Chadwick letter to the Royal Society.



Wartime Memories

RECENTLY UNSEALED DOCUMENTS FROM WORLD WAR II ILLUSTRATE that French physicists had an early lead in the race to produce a nuclear reactor. The papers were given to Britain's Royal Society for safekeeping in 1940 and 1941 by James Chadwick, discoverer of the neutron and leader of Britain's wartime nuclear research. The society opened them to honor the 75th anniversary of Chadwick's Nobel Prize-winning discovery.

In the papers, French citizens Hans von Halban and Lew Kowarski discuss how to make a nuclear reactor and generate plutonium. Before fleeing to Britain, the pair worked in Paris with Frédéric Joliot-Curie. After German scientists discovered nuclear fission in 1939, the three realized it should be possible to make a reactor to generate power and patented the idea.

Halban and Kowarski likely gave the papers to Chadwick to establish the priority of their findings, says Chadwick biographer Andrew Brown, a research fellow at Harvard's John F. Kennedy School of Government. During the war, researchers couldn't publish results for fear of revealing secrets, and many looked to Chadwick, known for his integrity, to keep tabs on their work. Ironically, Brown says, Chadwick took a dim view of priority squabbles: "He thought that people shouldn't be concerned with their reputations when the survival of the country was at stake."

Sino-Scientific Literacy

The first-ever survey of the scientific knowledge of county-level bureaucrats in China indicates that if the Asian giant is going to take over the world, a little more homework is called for.

Last year, 945 civil servants in 17 provinces and municipalities took the test. Only 12.2% passed. Respondents were required to choose the right definitions for seven scientific terms, correctly judge the truth of at least 10 of 22 scientific statements, and not hold any superstitions.

Almost two-thirds were able to choose correct definitions for terms such as "molecule," "DNA," and "Internet" and to correctly rate 10 of 22 statements (such as "the father determines a child's sex") as true or false. But only 36% picked correct definitions for "probability," "controlled experiment," and "scientific research." The survey also showed that more than half believed in

superstitions, such as fortune-telling by reading the face (held by 28%).

"Civil servants should take the lead in promoting national scientific literacy," says Cheng Ping of the China National School of Administration, which announced the results of the survey last month. Civil servants, along with young people, farmers, and urban laborers, are targets of China's new National Scheme for Scientific Literacy. In a similar survey of the general population in 2003, only 2% passed.

Saving the Coelacanth

The coelacanth, a rare fish that hasn't changed significantly in 300 million years, seems to be popping up all over. So much, in fact, that it's in danger of being overfished. On 11 June in Dar es Salaam, scientists and officials will meet to discuss creating a Coelacanth Marine

Protected Area near Tanga in northern Tanzania.

Equipped with an oil-filled spine and limb-like fins, the coelacanth can weigh more than 100 kilograms. It was thought to be extinct until a live one was discovered off South Africa in 1938. Although specimens have been found up and down the East African coast and even in Indonesia, the main population was thought to be in the Comoros Islands. But in the past 3 years, many more—32 so far—have been caught off Tanzania, most of them in Tanga, 800 km north of the Comoros. "It looks like more coelacanths have

survived than people initially thought," says marine biologist Eric Verheij, acting director of the Nature Conservancy's Palau office, who was the first to identify a Tanga coelacanth.

The ancient fish started showing up in wide-mesh gill nets that were laid to catch sharks at depths of 40 to 200 meters when shrimp trawlers were operating nearby.

Anthony Ribbink, head of the African Coelacanth Ecosystem Programme in Grahamstown, South Africa, says they are now being killed at a "quite frightening" rate. At the meeting in Dar es Salaam, the discussions will center on how to get the fishermen to lay their shark nets elsewhere.

Coelacanth caught in April.



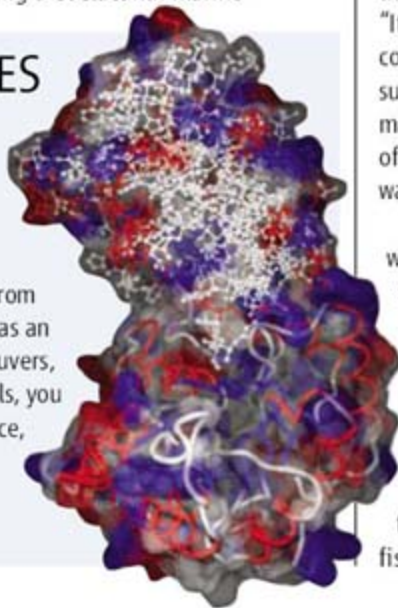
CREDITS (TOP TO BOTTOM): CORBIS; ROYAL SOCIETY; E. M. MACHUMU; PROTEIN MOVIE GENERATOR

NET WATCH

MOLECULAR HOME MOVIES

The new Protein Movie Generator (PMG) provides an online studio for budding scientific Walt Disneys. Produced by two researchers at the University of Paris, the site makes it easy to create animations that put molecules in motion.

PMG starts with files from the Protein Data Bank or trajectories from molecular simulations. Users can then script simple scenarios, such as an enzyme pirouetting to display its active site, or more complex maneuvers, such as a ligand gliding in to dock with its receptor. If you prefer stills, you can use PMG to craft molecular graphics. This illustration, for instance, bares some of the internal structure of triosephosphate isomerase, one of the sugar-slicing enzymes of glycolysis. >> bioserv.rpbs.jussieu.fr/~autin/help/PMGtuto.html



THE
DR. PAUL JANSSEN AWARD
FOR BIOMEDICAL RESEARCH

THE SELECTION COMMITTEE

OF

THE DR. PAUL JANSSEN AWARD
FOR BIOMEDICAL RESEARCH

INVITES NOMINATIONS FOR
THE 2008 AWARD



2006 WINNER:

DR. CRAIG MELLO

FOR HIS ROLE IN THE DISCOVERY OF RNA INTERFERENCE (RNAi)
AND THE ELUCIDATION OF ITS BIOLOGICAL FUNCTIONS

Please go to www.pauljanssenaward.com for more information
Deadline for nominations is December 1, 2007

2008 Selection Committee

Dr. Solomon Snyder
Chairman

Dr. Linda Buck

Dr. Jean-Marie Lehn

Dr. Craig Mello

Dr. Hartmut Michel

Dr. Edward Scolnick

Sir Richard Sykes

Johnson & Johnson

©Johnson & Johnson Pharmaceutical Services, LLC 2007



BEATING A KILLER. Developing an affordable malaria vaccine for Africa, where a million children die from the disease every year, is the tall challenge awaiting French physician Christian Loucq, who last week was named director of the PATH Malaria Vaccine Initiative (MVI) in Bethesda, Maryland. Loucq had been interim director of MVI, which has received \$265 million from the Bill and Melinda Gates Foundation, since February.

Movers

Loucq has worked primarily in marketing and sales positions for half a dozen vaccine companies—including Pasteur Merieux Connaught and SmithKline Beecham—in India, Thailand, China, Belgium, the United Kingdom, and elsewhere. His ability to lead, listen, and network will make up for his inexperience in vaccine development and malaria science, predicts Thomas Monath, a former chief scientific officer at vaccine producer Acambis, where Loucq was vice president from 2002 until 2006. “He’s a great choice,” Monath adds.

POLITICS

POLITICAL PRO. The man chosen by President George W. Bush to be the next U.S. surgeon general knows his way around Washington, D.C. Cardiologist James W. Holsinger Jr. served for 26 years in senior posts throughout the Department of Veterans Affairs before becoming its chief medical director and then undersecretary of health during the early 1990s. An M.D.-Ph.D.



graduate of Duke University, Holsinger is a professor of preventive medicine at the University of Kentucky in Lexington and a former chancellor of the medical center. Holsinger has declined comment while his nomination is pending before the

Senate, but the White House said he will focus on combating childhood obesity.

ON CAMPUS

WAR OF WORDS. Evolutionary biologist Robert Trivers was 6 hours away from delivering a talk at Harvard University on self-deception and the role it played in Israel’s 2006 invasion of Lebanon when organizers cancelled the 27 May event. Trivers claims that the cancellation was payback for his recent letter in *The Wall Street Journal* attacking an op-ed piece by Harvard law professor Alan Dershowitz, a well-known defender of many of Israel’s policies. “It was a very humiliating and

degrading experience,” says Trivers, who had to call several friends and relatives to ask them not to come.

Trivers (right), a professor at Rutgers University in New Brunswick, New Jersey, had sent a letter on departmental stationery to Dershowitz a few weeks earlier saying that “if there is a repeat of Israeli butchery toward Lebanon, and if you decide once again to rationalize it publicly, look forward to a visit from me. Nazis—and Nazi-like apologists such as yourself—need to be confronted directly.”



Dershowitz says he had nothing to do with the disinvitation from Martin Nowak, who heads Harvard’s Program for Evolutionary Dynamics. But Dershowitz admits he was planning to hand out copies of Trivers’s letter at the event “in an exercise of my right to free speech.” Dershowitz has also filed a complaint with Rutgers administrators. Nowak couldn’t be reached for comment, and a Harvard spokesperson was unable to confirm or deny Trivers’s version of the story.

Three Q’s >>

By day, **Clark Olson** is a professor of database systems and computer vision at the University of Washington, Bothell. By night, he’s a king of fantasy sports, a hobby in which individuals create and manage imaginary teams of real players that compete with one another based on their season’s statistics. Olson’s computational and algorithmic skills have earned him five straight top-three finishes in an international rating system of online fantasy players, plus about \$5000 in winnings every year.



Q: How well do you know the games themselves?

Sports knowledge isn’t crucial to doing well at fantasy sports. More important are knowing where to get good information, being able to analyze stats, and developing successful strategies for building a strong team.

Q: How much of your decision-making is art and how much is science?

I’m not sure there is any art at all. I try to make every decision based upon principled analysis. For some moves, new information makes analysis trivial.

Q: Who will be more successful this season: your fantasy picks or your favorite baseball team, the Seattle Mariners?

It is extremely unlikely that the Mariners will finish as well in their league as I do in the ESPN Uber contest, where I am in fourth place overall. However, if success is measured in revenue, then I can’t compete with the Mariners.

Got a tip for this page? E-mail people@aaas.org

A Thai view of
drug patents

1408

The big
deal on
whaling

1411

STEM CELLS

Teams Reprogram Differentiated Cells—Without Eggs

Scientists this week reported major advances toward a central goal of stem cell research: directly reprogramming fetal mouse cells so that they are indistinguishable from embryonic stem (ES) cells. The technique, which they say should also work on adult cells, could one day enable researchers to generate cell lines tailored to individual patients without the use of eggs or embryos.

“The papers are stunning,” says Harvard stem cell researcher Chad Cowan. “Amazing, ... very exciting,” adds Stephen Duncan of the Medical College of Wisconsin in Milwaukee. The advances, which are sure to have political implications as well, are reported in two papers in *Nature*—written by groups headed by Shinya Yamanaka of Kyoto University in Japan and by Rudolf Jaenisch at the Massachusetts Institute of Technology—and in another paper by Konrad Hochedlinger at Harvard, which was published in the inaugural issue of *Cell Stem Cell*.

The three reports extend a finding made last year by Yamanaka’s team. By inserting various combinations of genes related to pluripotency active in mouse ES cells, the researchers discovered a combination of four genes that, when introduced into skin cells from mice’s tails, conferred ES-like properties upon them (*Science*, 7 July 2006, p. 27).

But the tail cells did not completely mimic ES cells, and many scientists were skeptical.



Neat trick. A normal embryo developed by Jaenisch’s group entirely from reprogrammed fetal mouse cells.

“When Shinya first claimed this, I would say that 90% of the field said ‘No way.’ It seemed so stunning that it could happen like that,” says Cowan. Now it’s clear not only that it happened but also that with an alteration in the original formula, scientists have generated what they believe are fully pluripotent cell populations from both fetal and adult mouse fibroblasts.

The three teams all began by following Yamanaka’s procedure, using a viral vector to introduce copies of genes for four transcription factors active in ES cells: Oct4, Sox2, c-Myc, and Klf4. Because the reprogramming works for only one in every 1000 cells, the researchers needed to weed out the non-starters. Yamanaka did this by looking for the activity of a gene that, as it turned out, selected for cells that were incompletely reprogrammed. In the new studies, the scientists used the expression of Oct4 and Nanog—well-known pluripotency markers.

The cells selected using these markers appear to have all the same traits as ES cells. To test this hypothesis, the researchers tagged the reprogrammed cells, called induced pluripotent stem (iPS) cells, with a fluorescent dye and injected them into early-stage mouse embryos. Some of the resulting chimeric animals had descendants of the iPS cells throughout their bodies. The researchers confirmed this by successfully breeding the chimeras to normal mice. This showed that iPS cells had made it to the germ line in the chimeras.

Together, the three papers give a convincing picture of the reprogramming phenomenon, says Cowan. Jaenisch says his iPS cells passed the “most stringent” test of pluripotency, which involves being injected into tetraploid embryos. Created by fusing two normal embryos, tetraploid embryos are incapable of development beyond forming a placenta. But when they are injected with normal pluripotent cells, the embryos develop into mice that are entirely the products of the introduced cells. In Jaenisch’s experiment, the iPS cells came from reprogrammed fetal cells, but the researchers are confident that the strategy will work with cells generated from adult fibroblasts, says Hochedlinger, a co-author.

In the study led by Hochedlinger, the team thoroughly explored the epigenetics—changes that modify chromosomes and control gene expression—of iPS cells, demonstrating that the epigenetic signatures of their genes are the same as those in ES cells.

But the Yamanaka study showed a big downside to the strategy. The only author to study the offspring of the chimeras after birth, he observed that 20% of the 121 mice developed tumors. That finding, Yamanaka notes, shows the danger of using retroviral vectors, which can turn on cancer-causing genes.

This highlights what Jaenisch calls ▶

Reprogramming, Take Two

In the same issue of *Nature*, Harvard’s Kevin Eggan reported another reprogramming advance: nuclear transfer (also called research cloning) using a fertilized mouse egg, or zygote. Early attempts in the 1980s to clone animals by transferring the nucleus of a somatic cell into a zygote failed, leading to a focus on doing the procedure with unfertilized oocytes. Human eggs, however, are difficult to obtain.

Now Eggan and colleagues have shown that if nuclear DNA is removed from the dividing mouse zygote at just the right moment, it will successfully reprogram an introduced nucleus from a somatic cell. In this experiment, the researchers succeeded in creating both new lines of ES cells and apparently healthy cloned mice.

This work, says Cowan, suggests that to create patient-specific human ES cell lines, researchers could make use of fertilized eggs that would otherwise be discarded at fertility clinics, sidestepping the problematic issue of egg donation. “It’s an exciting paper,” says cloning researcher Robert Lanza of Advanced Cell Technology Inc. in Worcester, Massachusetts.

—C.H.



“major, major problems which need to be resolved” if this work is to be applied to humans. Once the appropriate human transcription factors are identified, scientists will have to find ways to introduce the factors without retroviruses or to safely activate the relevant genes within the cell.

A likely alternative would be the use of small molecules to penetrate cell walls and turn on production of the necessary transcription factors. “Now that we know there’s a mechanism by which this [reprogramming] can happen, there will be an aggressive search to find small molecules that can activate these pathways,” predicts Duncan. “It will take a lot of

work, but the fact that the pathways exist gives you a [place] to start. ... This is huge.”

It’s still a long road to potential therapies with reprogrammed adult cells. But Cowan is optimistic: “The most amazing thing about these papers is you now take this whole idea of reprogramming out of the hands of cloning specialists and put it into the hands of anyone who can do molecular and cell biology.” In some ways, he says, “it’s a much simpler system than we thought.” As a result, he predicts, “we’re really going to see this process accelerate.”

Coincidentally, the advances were announced the day before the House was

scheduled to vote on a Senate-passed bill loosening restrictions on ES cell lines available to federally funded researchers. The measure was expected to pass but to be vetoed by President George W. Bush in a replay of the events of last summer (*Science*, 28 July 2006, p. 420).

In this environment, the reprogramming studies are likely to be seized on by critics of ES cell research as further evidence that there is no need for the contentious practice of destroying early embryos to obtain stem cells. Hochedlinger and others hasten to point out that research needs to progress on all fronts because all systems “have their limitations.”

—CONSTANCE HOLDEN

ACADEMIC TENURE

MIT Colleague Quits to Protest Sherley Dismissal

The head of a biomedical innovation center at the Massachusetts Institute of Technology (MIT) in Cambridge has resigned to protest the school’s treatment of an African-American colleague in the biological engineering department. Frank Douglas, who is also black, says he will leave MIT on 30 June—the termination date for his colleague, James Sherley. An MIT spokesperson says that Douglas’s decision would have no impact on the institution’s stance regarding Sherley, who went on a 12-day hunger strike in February after being denied tenure (*Science*, 16 February, p. 920).

A stem cell researcher and the winner of a 2006 Director’s Pioneer Award from the National Institutes of Health (NIH), Sherley began a fast on 5 February to fight what he claims was a racist decision by MIT to reject his bid for tenure. MIT says that race played no role in the decision. When Sherley ended his strike, MIT put out a statement expressing a commitment to address his concerns about fairness and to “continue to work toward resolution of our differences with Professor Sherley.” In the weeks that followed, however, MIT administrators made it clear that they would neither reopen Sherley’s tenure case nor review how his grievances had been handled.

Douglas is a chemist and pharmaceutical industry veteran who was hired in 2005 to establish MIT’s Center for Biomedical Innovation. He holds faculty appointments in the science, engineering, and management

schools. In a 1 June letter to MIT Associate Provost Claude Canizares, Douglas expressed dismay that MIT, “after having agreed to arbitration, which led to Prof. Sherley ending his hunger strike, now, has negated that



On principle. Frank Douglas says MIT’s handling of James Sherley’s protest reflects an environment that is hostile to African Americans.

agreement and insists on his departure on June 30th, 2007. ... I leave because I would neither be able to advise young Blacks about their prospects of flourishing in the current environment, nor about avenues available to effect change when agreements or promises are transgressed.”

Douglas says he has no opinion on whether Sherley deserved tenure but is frustrated by MIT’s “lack of desire” to resolve the issue. “Does the institution really believe that Prof. Sherley would have ended his hunger strike if he really understood that ‘continue(ing) to work towards resolution of differences’ meant no arbitration process and a pre-agreement that he should leave regardless of the outcome of the resolution of those differences?,” he asks, saying that as a minority, he felt obligated to speak out.

In a 3 June reply to Douglas, Canizares wrote, “I can state categorically that MIT did not agree, implicitly or explicitly, to arbitration or to extend Professor Sherley’s faculty appointment beyond June 30.” The next day, MIT issued a statement saying that Douglas’s decision was based on inaccurate information, and that it hoped he would reconsider his resignation.

Outsiders familiar with MIT’s environment do not think Douglas’s departure will have much impact. “The administration is inclined to take the same approach that governments take while dealing with terrorists: They won’t negotiate,” says Philip Phillips, an African-American solid state physicist at the University of Illinois, Urbana-Champaign, who was denied tenure at MIT 16 years ago. Instead, he predicts, MIT will treat Douglas as it did Sherley—“as just another irrational person.”

—YUDHIJIT BHATTACHARJEE



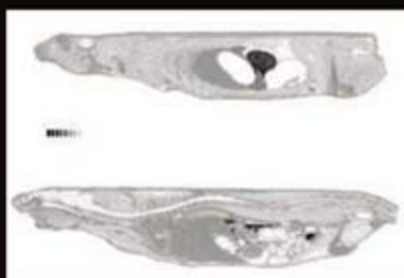
HIGHLY VERSATILE BIO-IMAGING SYSTEM

FLA-7000

473nm 532nm 635nm 650nm 670nm

A multi-functional, high-performance, compact system with enhanced modularity to meet your life science needs

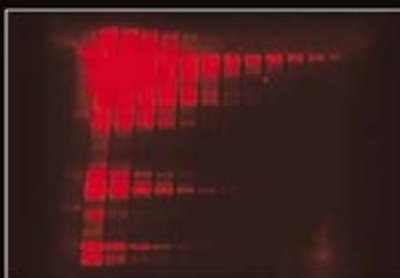
RADIOISOTOPE



WBA, ¹⁴C, Excitation 650nm, Filter B390, 50μm
Data courtesy of Institute of Whole Body Metabolism

A radioisotope-labeled sample image can be acquired with high throughput and high sensitivity using Fujifilm's unique proprietary technology: Integrated Imaging Plate technology and high-speed detection technology (Light Collecting Guide).

FLUORESCENCE



Western Blotting with Alexa Fluor® 680, MouselgG, Excitation 670nm, Filter R710, 50μm

A maximum of four lasers are optionally available for use with the following: LD473nm, SHG532nm, LD635nm, LD650nm and LD670nm. This enables the system to be upgraded to cover a broader range of fluorescent dyes including near-IR.

DIGITIZING



Silver-stained BSA, SDS-PAGE, Excitation 473nm, Filter Y520, 50μm

Able to take digitized (Gel Documentation) images of silver-stained gel or CBB-stained gel.

<http://lifescience.fujifilm.com>

FUJIFILM Corporation 7-3, Akasaka 9-Chome Minato-ku, Tokyo 107-0052, Japan, Tel: +81-3-6271-2158, Fax: +81-3-6271-3136 · E-mail: sginfo@fujifilm.co.jp

FUJIFILM Medical Systems U.S.A., Inc. 419 West Avenue, Stamford, CT 06902, U.S.A, Tel: +1-866-902-3854, Fax: +1-203-327-6485 · E-mail: don.wilke@fujimed.com

FUJIFILM Europe GmbH Heesenstr. 31, 40549 Dusseldorf, Germany, Tel: +49-211-5089-174, Fax: +49-211-5089-9144 · E-mail: lifescience@fujifilmeurope.de

FUJIFILM (U.K.) Ltd., Unit 12 St Martins way, St Martins Business Centre, Bedford, MK42 0LF, U.K, Tel: +44-1234-245291, Fax: +44-1234-245293 · E-mail: lifesciences@fuji.co.uk

富士胶片(中国)投资有限公司 31st floor, Hong Kong New World Tower, No. 300 Hual Hai Zhong Road, Shanghai, P.R China, Tel: +86-21-3302-4655 ext.363, Fax: +86-21-6384-3322 · E-mail: wgxiang@fujifilm.com.cn

COSMOLOGY

Gravity Distorts Big Bang Afterglow, Opening New Window on Cosmos

The best picture of the infant universe is distorted as if in a fun-house mirror, cosmologists report. Ironically, the aberration may lead to a clearer view of how the young universe evolved.

The observation marries two of cosmologists' more fruitful pursuits. Researchers have analyzed the afterglow of the big bang, known as the cosmic microwave background (CMB), to nail down the precise age and composition of the universe. Meanwhile, others have studied how light from distant galaxies is deflected by the gravity from vast filaments of "dark matter" stretching through space, a phenomenon known as "weak lensing." Now, a team of young upstarts has detected weak lensing of the CMB itself.

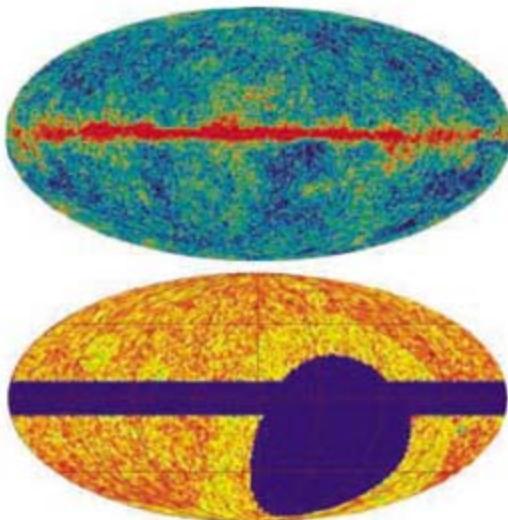
Researchers were certain that the CMB would show the lensing distortion, but they were eager to find the effect because it could be used to probe the evolution of the structure of the universe, says David Spergel, a cosmologist at Princeton University. "What they saw is what they expected," he says, "but this is groundbreaking because this is a new tool that could be very powerful."

To spot the effect, Kendrick Smith of the University of Chicago in Illinois and colleagues started with the portrait of the CMB produced by NASA's orbiting Wilkinson Microwave Anisotropy Probe (WMAP). The temperature of the microwaves varies slightly from point to point across the sky. By analyzing the hot and cold blotches, WMAP researchers have deduced that the universe is 13.7 billion years old and consists of 4% ordinary matter, 22% dark matter, and 74% weird space-stretching "dark energy" (*Science*, 19 December 2003, p. 2038).

With images of galaxies, lensing makes the elliptical shapes tend to align with their neighbors in the sky, like fish in a swirling school (*Science*, 17 March 2000, p. 1899). In the case of the CMB, a clump of dark matter in the foreground should magnify the splotchy pattern behind it. In principle, researchers could spot the effect by scrutinizing the CMB alone. In practice, that "auto-correlation" technique isn't yet feasible because WMAP can't quite bring the microwave pattern into sharp enough focus.

So the team compared the CMB map to one pinpointing 1.8 million galaxies that was produced by the Very Large Array (VLA) of radio telescopes in New Mexico. The galaxies

trace the dark matter filaments, so the spots in the sky where galaxies are most numerous should also line up with the patches in the CMB that appear to be magnified. The comparison makes the effects of lensing clear, much as superimposing two patterns of seemingly random dots might reveal a picture partially encoded in each, the researchers reported in a paper posted last week to the arXiv preprint server (www.arxiv.org).



Double vision. Cosmologists detected the gravity-induced distortion of the cosmic microwave background (top) by comparing it with a galaxy map.

Lensing of the CMB could enable researchers to probe how the dark-matter web evolved even before galaxies formed. But that will require autocorrelation analysis of higher precision data from future projects such as the South Pole Telescope; the Atacama Cosmology Telescope at Cerro Toco, Chile; and the European Planck satellite, says Christopher Hirata, a cosmologist at the Institute for Advanced Study in Princeton, New Jersey. Hirata and his colleagues will soon publish an independent observation of the CMB lensing.

The advance was made by three of the field's younger members. Smith and Oliver Zahn of the Harvard-Smithsonian Center for Astrophysics in Cambridge, Massachusetts, are graduate students, and Olivier Doré of the University of Toronto is a postdoc. They were able to make their mark because the WMAP and VLA data are open to the public. If that had not been the case, Smith says, "two graduate students and a postdoc probably wouldn't have been the drivers" for the project.

—ADRIAN CHO

Measuring Health Work

Using a \$105 million gift from the Bill and Melinda Gates Foundation, the University of Washington, Seattle, has created the Institute for Health Metrics and Evaluation (IHME).

"How do we know the investments in global health we're making are having the impact we want?" asks health economist Christopher Murray, who will head a staff of 130.

Murray is moving to Seattle from Harvard because billionaire Larry Ellison rescinded his pledge of \$115 million to create a similar institute when university president Lawrence Summers resigned. "I'm deeply unhappy that we lost Chris," says Barry Bloom, dean of Harvard's School of Public Health. "One needs health metrics to hold countries accountable for the health of their people. That's what he does, and he does it better than anyone else."

Murray contends that policymakers—especially in developing countries—need better data on mortality, immunization rates, and disease burdens. IHME will train graduate students and issue reports that evaluate specific programs funded by the Gates Foundation and other new players in the global health arena as well as the flow of aid.

—JON COHEN

Russian Double Trouble

MOSCOW—A governmental office auditing the Russian Foundation for Basic Research (RFBR) has claimed that the funding agency misspent about \$8 million in fiscal year 2006. RFBR manages about \$150 million, or about 6% of the Russian government's basic research budget. But the audit released last month by the Russian Accounts Chamber called RFBR's activities "unsatisfactory." The \$8 million in question was awarded to two projects already funded in other ways, it said, and last year 96 other research projects receiving about \$800,000 were halted due to "unsatisfactory quality" or because the projects closed down.

RFBR Director Vladimir Lapshin defended his agency, calling the audit "some kind of a mishmash." Grants that were occasionally given to already-funded projects make up a "negligible" sum, Lapshin says, adding that terminating unsatisfactory projects was a result of solid peer-review. Several senior Russian scientists, who asked not to be named, expressed fear that the audit could be a prelude to shutting down RFBR or allowing state officials to take control of its budget.

—ANDREY ALLAKHVERDOV AND
VLADIMIR POKROVSKY



Hard-nosed negotiator. Critics of Thailand's compulsory licenses have double standards, insists health minister Mongkol Na Songkhla, pictured in his office.

MONGKOL NA SONGKHLA INTERVIEW

Thai Health Minister Defends Controversial Drug-Patent Policy

BANGKOK—Thailand's audacious moves to break drug patents have earned it raves from many governments and patient advocates—and the ire of big pharma. Thailand has asserted its right, under a World Trade Organization provision for coping with public health needs, to make or import generic versions of two AIDS drugs—efavirenz and lopinavir/ritonavir—and clopidogrel, a heart medication (*Science*, 11 May, p. 816). Several countries say they will follow in Thailand's footsteps. Brazil has already invoked a compulsory license for Merck's efavirenz.

Thailand has paid for its activism. In March, Abbott Laboratories, which makes lopinavir/ritonavir, withdrew applications to sell seven new medications in Thailand. And the Office of the U.S. Trade Representative has put Thailand on its Priority Watch List and will reportedly decide next month whether to slap tariffs on certain Thai exports.

At the center of this firestorm is Mongkol Na Songkhla. A 65-year-old medical doctor, Mongkol was appointed minister of public health by Thailand's military-installed government last October. Described by colleagues as a down-to-earth workaholic with a sharp sense of humor, Mongkol, in an interview with *Science* last week, insisted that the com-

pulsory licenses are aimed solely at helping poor people and that Thailand has borne "unfair" criticism. He also revealed that his ministry has offered an olive branch to drug companies.

—RICHARD STONE

There are reports that Thailand may issue compulsory licenses on two more drugs, and that you have set a limit of five drugs.

Compulsory licensing [CL] is not a routine action. It is a very special, exceptional one. If we want to do CL for our poor people, we cannot do more than five drugs.

Why five? How did you arrive at that limit?

Cost. We don't want to interfere with R&D, with innovation, with the investment of the companies. Twenty percent of Thai people can pay from their own pocket and never want to use generic drugs. Government employees prefer to use the originals. And foreigners who come to get health services in Thailand, they never get the generic drugs. But the majority—about 80% of our people—never has a chance to use the original product.

It's been reported that the next two drugs that might be issued compulsory licenses are cancer drugs.

People guess this from my criteria, from the cost of drugs to people. ... I cannot confirm. We have a committee to consider this. I never make [these] decisions by myself. I'm only the gateway.

Some critics claim the licensing is more of a negotiating strategy to force drug companies to come down in price. Is that a fair observation?

Maybe, maybe. You see, more than 2 years ago we invited the drug companies to come and negotiate. They never wanted to sit and talk with our committee. And right now it is easier for us to invite them.

You certainly got their attention.

Yes.

On balance, do you think the focus on compulsory licensing has been positive for Thailand?

I don't think it's positive, because some people have a double standard. Why don't they criticize other countries, especially developed countries that do CL?

What would you have done differently?

We did it too transparently. I don't think the other countries announced their intention to do compulsory licensing. Everyone knows the details of our negotiations. This is maybe too transparent.

As a medical doctor, you must be particularly distressed with Abbott's action to withdraw drugs it had intended to sell here. Have you conveyed that to them?

They want me to stop doing CL before negotiations. That is very tough.

You will not agree to that?

Yes, I will not.

Do you think the rift with the drug companies can be healed?

It will take time. I have proposed that they sell another version of their original products of the same quality but different packaging for the poor, at a lower price.

Is it possible in Thailand to tightly control the distribution of a second version for poor people?

Sure, because this would only be for non-commercial use. It cannot be used in private clinics or [private] hospitals.

How have drug companies reacted to this idea?

I am still waiting [for their reaction].

SAUDI ARABIA

Graduate University Launched With \$10 Billion Endowment

Saudi Arabia is using some of its vast oil wealth to create what it hopes will be a world-class graduate research institution.

The King Abdullah University of Science and Technology (KAUST), which is scheduled to open in the fall of 2009, will have a \$10 billion endowment—the sixth largest in the world. Although the university won't open for more than 2 years, officials said this week that they will prime the pump by awarding some 500 undergraduate scholarships this year and next to students around the world, with the understanding that the recipients will form KAUST's inaugural classes. They are also launching a \$100-million-a-year global research partnership program to fund work by scientists who agree to become affiliated with the new university.

"We realized that we cannot wait until when we open, in September 2009, to begin our research program," says Nadhmi Al-Nasr, KAUST's interim president. "We also wanted to find researchers working on things that have the potential to benefit Saudi Arabia."

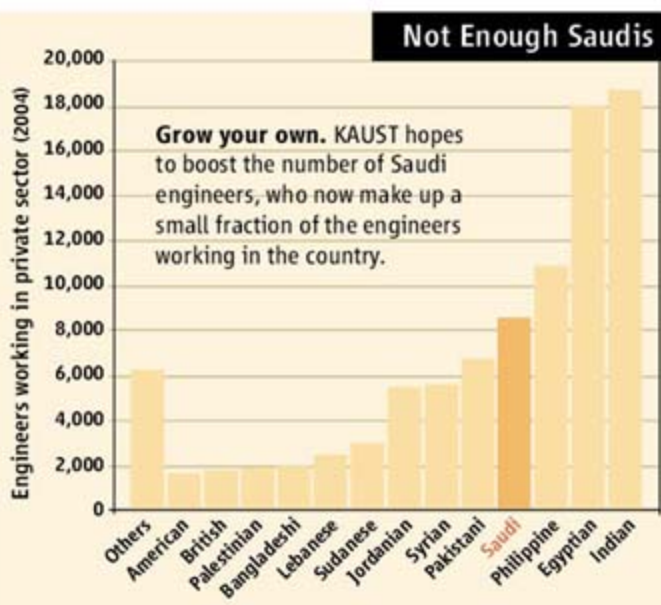
The university is the brainchild of the country's current ruler. It's being built from scratch on a tract along the Red Sea, some 80 km north of Jeddah. The project, which includes constructing a surrounding city of 15,000, was given to Saudi Aramco, the government-owned oil giant, and is being overseen by the Minister of Petroleum and Mineral Resources. But once completed, the university will be financially and administratively independent of the Saudi government, says Al-Nasr, who's on leave from his post as vice president for engineering at Saudi Aramco.

"KAUST will have its own governing board of trustees as well as its own endowment," he explains. Government officials also decided to place it outside the purview of the ministry of higher education. "The kingdom is in the midst of reassessing its entire system of higher education," Al-Nasr explains. "So it would not make sense to try to build KAUST within the existing bureaucracy."

The university will be organized around

multidisciplinary research institutes. The initial ones will encompass energy and the environment, biosciences and engineering, materials science and engineering, and applied mathematics and computational science. Accordingly, the first round of global partnerships will lure faculty members by tackling challenges such as desalination, carbon capture and hydrogen-rich fuels, and computational linguistics.

KAUST has hired some academic heavyweights to help it jump-start the school. Al-Nasr says the Institute of International Education, which runs the U.S.-based Fulbright Program, will manage the student scholarship program, while the Washington Advisory Group (WAG) will handle the competitive grants program using a National Science Foundation-style merit-review system. The university will



eventually have a capacity for 2000 graduate students and 600 faculty members and researchers, and Al-Nasr hopes as many as one-fifth of the students will be Saudis.

"I think it's a potential game changer for the region," says WAG's Frank Rhodes, president emeritus of Cornell University and an adviser to the university. Adds Richard Sykes, rector of Imperial College London and another adviser: "I don't think that it'll be too difficult to get good people to come for a short time. The issue will be, 'Can you sustain the quality over time?'" KAUST hopes to have a founding president on board by January 2008.

—JEFFREY MERVIS

Stem Cell Patents Defended

The Wisconsin Alumni Research Foundation (WARF) says that its three patents covering the derivation of human embryonic stem (ES) cells and the cells themselves comprise work that represents "true innovation." The foundation responded last week to a March ruling by the U.S. Patent and Trademark Office that earlier work with mouse cells "anticipated" the first-ever derivation of human cells in 1981 by James Thomson of the University of Wisconsin, Madison. WARF disputed that contention, citing certain unique chemical requirements for human cells. In a declaration, Colin Stewart of the Institute of Medical Biology in Singapore said that Thomson's achievement "managed to accomplish what others had for years tried and failed to do."

Not so, says Jeanne Loring, a molecular biologist at the Burnham Institute in San Diego, California, who believes Thomson simply applied known mouse methods to primate cells to which he had access few others had. The patent office has 2 months to decide whether WARF's patents are invalid.

—ELI KINTISCH

Glacial Progress

With a baseline inventory of its glaciers set in 2002, Chinese scientists now hope to obtain a comprehensive picture of how glaciers in western China have responded to climate change in recent years. The new glacier inventory project will use remote sensing and field surveys to compile data for comparison with the baseline established by China's first survey, which began in 1978 and took more than 20 years to complete. A team of researchers this month will head out to the Qilian Mountains in Qinghai Province to begin fieldwork. Liu Shiyin, a project leader at the Chinese Academy of Sciences' Cold and Arid Regions Environmental and Engineering Research Institute in Lanzhou, hopes the \$2.6 million project will help quantify glacier retreat and warming impacts, such as drought or sea-level rise. Western China's glaciers feed 10 major rivers.

—HAO XIN

Ecology Lab Gets Execution Stay

After funding was cut by the Department of Energy, officials last month planned to close the Savannah River Ecology Lab on 31 May (*Science*, 18 May, p. 969). Now, the University of Georgia has given the lab a 1-month reprieve, although it hasn't told Director Paul Bertsch whether its financial support will do more than pay for salaries and benefits. Lawmakers are investigating the situation.

—ELI KINTISCH

The power of small **x8**

1 μ l analysis — increased throughput

The NanoDrop® ND-8000
8-Sample Spectrophotometer

1 μ l samples. No cuvettes. No dilutions.



Revolutionary technology. **8 readings in under 30 seconds.** The NEW NanoDrop® ND-8000 8-Sample Spectrophotometer is powerful — eight 1 μ l samples at once.

Full spectrum UV/Vis analysis of 1 μ l samples for quantitation, purity assessments and more: nucleic acids, microarrays, proteins and general spectrophotometry.

Measurement is quick and easy — pipette up to eight samples and measure. Each sample is read using two path lengths to achieve an extensive

dynamic range (e.g., 2-3700 ng/ μ l dsDNA), virtually eliminating the need for dilutions. Then just a quick wipe clean and you're ready for your next samples. What could be easier — or more powerful?

And for the power of small in single-sample absorbance or fluorescent measurements, check out the NanoDrop® ND-1000 Spectrophotometer or the NanoDrop® ND-3300 Fluorometer (ultra low fluorescent detection limit of sample mass — e.g., 2 pg dsDNA).

Ready to experience the power of small x8? **Test a NanoDrop® ND-8000 8-Sample Spectrophotometer in your own lab.**

FREE one-week evaluation www.nanodrop.com
302.479.7707



 **NanoDrop**



Big supporters. Greenpeace and other volunteers form a human whale to express their views at the Anchorage meetings.

CONSERVATION BIOLOGY

Whales (Mostly) Win at Whaling Commission Meeting

ANCHORAGE, ALASKA—Whales and environmentalists were the big winners at this year's 4-day meeting of the International Whaling Commission (IWC) here, with a majority of member nations reaffirming the organization's 21-year moratorium on commercial whaling. The meeting also passed a resolution calling for Japan to "suspend indefinitely" its scientific whaling in the Southern Ocean Whale Sanctuary and to change its plans for lethal research on endangered humpbacks and fin whales (*Science*, 27 April, p. 532).

But the meeting of 400-plus delegates from 71 countries from 28 to 31 May was hardly a joyful reunion. Rather, like any unhappy family, IWC members exchanged insults and accused each other of bad faith and broken promises—sentiments that added to the ever-growing divide between those who fancy a whale steak and those who prefer their cetaceans whole, alive, and swimming in the ocean's waters.

And in the final hour, Japan, which strongly favors a resumption of commercial whaling, announced that it was considering a divorce. The IWC has spurned its "original role as a natural resource management organization," Akira Nakamae, one of Japan's deputy commissioners, said at the meeting. "Japan upholds the principle of using all living marine resources," he said, and may form "a new organization with other countries" that follow that principle.

Last year's IWC gathering had a very different outcome: Japan and its pro-whaling allies narrowly passed a symbolic resolu-

tion calling for an end to the moratorium on commercial whaling. Given the rise in abundance of some whale species, Japan has also asked the Convention on International Trade in Endangered Species to review the status of great whales; CITES currently prohibits trade in these cetaceans or their products. But the IWC voted 37–4 for a resolution saying that the whaling moratorium was still needed and asking CITES, which meets this week, to defer to IWC on the question of whales.

Japan chose "not to participate" in that vote and others, underscoring the widening gulf between pro- and antiwhaling nations. However, the IWC did throw a lifeline to the Gulf of California's highly endangered vaquita dolphin (*Phocoena sinus*), pledging support for Mexico's plans to save it from extinction.

Some IWC members also strongly criticized Japan's scientific whaling. Japan kills more than 1000 whales each year (primarily minke) in the Southern Ocean and North Pacific and sells the meat. That is the largest number of whales harpooned by any IWC nation. A majority of the commission—with Japan and its allies not participating—approved a resolution that expresses "deep concern at [Japan's] continuing lethal research" and states that the program does "not address critically important research needs." Delegates from several nations delivered far harsher words: "The practice of scientific whaling by Japan flies in the face of the whole purpose of this convention and demeans the IWC," charged Malcolm Turnbull, Australia's

deputy commissioner and a member of parliament. "Show goodwill toward the people of Australia, and drop the humpbacks if not the program itself," he asked in an appeal echoed by others.

Australia's request was based "on emotion, not science," responded Joji Morishita, a deputy commissioner from Japan. "We are proud of our scientific program and its achievements," he said, noting that the hunts will go ahead as planned for the winter of 2007–08. The IWC has no authority to force Japan to curb research whale hunts, which require only a "special permit" issued by the Japanese government itself.

The IWC prides itself on using science to guide its decisions, although science was invoked in so many ways that the New Zealand delegation finally noted that the term had a "very elastic meaning." Prior to the full meeting that ended last week, the IWC's Scientific Committee gathered for 2 weeks in Anchorage to discuss everything from the status of the world's whale species, to whale deaths as a result of entanglement in fishing nets, to whale-watching tours and pollution. The resulting 100-plus-page *Report of the Scientific Committee* then served as the basis for the full meeting's discussions.

Indeed, it was because the U.S. delegation made the case with strong scientific data that the meeting attendees voted unanimously to support subsistence hunts of Western Arctic bowhead whales by certain Alaskan Eskimo aboriginal whaling communities—a request expected to be controversial. "The data were compelling and show that the Western Arctic bowhead population is healthy and recovering," said Douglas DeMaster, a deputy commissioner on the U.S. delegation. "This hunt is also sustainable."

Japan had hoped to persuade the IWC commissioners to allow four coastal communities to resume hunting North Pacific minke whales, a request they have made at the last 20 IWC meetings. Such a limited hunt would not "negatively impact the abundant minke" and would alleviate "suffering in the villages," said Nakamae. But in contrast to the Western Arctic bowhead whales, there are few data about these minke whale populations, which are already killed as bycatch, says DeMaster. And few countries agreed that Japan's village whalers, who would sell the whale meat, are equivalent to native subsistence hunters. Japan has threatened to leave the IWC before but has not. Still, it is not clear whether it will participate in the 2008 IWC meeting, planned in Santiago, Chile.

—VIRGINIA MORELL

Virginia Morell is a writer in Ashland, Oregon.



Pushing the Scary Side Of Global Warming

Greenhouse warming might be more disastrous than the recent international assessment managed to convey, scientists are realizing. But how can they get the word out without seeming alarmist?

CLIMATE MODELER JAMES HANSEN knows all about sounding the alarm. In the summer of 1988, drought wracked the country, fire was consuming Yellowstone National Park, and the nation's capital sweltered. Even the Senate hearing room where Hansen was testifying was warm and stuffy—the Democrats had opened the windows the night before. Then Hansen, dubbed NASA's top climate scientist by the media, shouted "Fire!" in the crowded theater: "With a high degree of confidence," he declared, greenhouse warming had arrived. Although many of his colleagues agreed, none chimed in with support; they could not share his high degree of confidence. Still, Hansen's lone authoritative voice was enough to send the media into a years-long brouhaha over global warming.

That uproar quieted within a few years, but Hansen, still the director of NASA's Goddard Institute for Space Studies (GISS) in New York City, finds himself at the head of an informal movement to again rouse the public

and policymakers. This time he worries that sea level could rise several disastrous meters by the end of the century, as the warming he heralded sends the great ice sheets rumbling toward the sea. If nothing is done to rein in greenhouse gas emissions, he says, "I just can't imagine that you could keep sea-level rise under a meter." Then the sea would flood many kilometers inland along the world's low-lying coasts, from Florida to Bangladesh.

That was Hansen's warning to Congress in late April, but it's not the message that came out of the U.N.'s Intergovernmental Panel on Climate Change (IPCC) in early February. Many news reports gave the impression that the prestigious international assessment actually downgraded the risk of imminent sea-level rise to a small fraction of a meter.

So Hansen seems to be out on a limb, again. This time, however, he's got company. No longer reticent, other scientists are going public about how bad things might get by the

end of the century. "The IPCC has been overly cautious in not wanting to give any large number to [future] sea-level rise," says climate researcher Stefan Rahmstorf of the Potsdam Institute for Climate Impact Research in Germany.

Scientists are still trying to strike a balance between their habitual caution and growing concern over uncertain but disastrous greenhouse outcomes. "Most scientists don't want to, but I think we need a way to explore" the extreme end of the range of possibilities, says glaciologist Robert Thomas of NASA contractor EG&G at Wallops Flight Facility in Virginia. Thomas says scientists need "a better way" than IPCC's consensus approach, "so we can communicate with the public without becoming scaremongers."

Naturally cautious

Seldom have mainstream climate scientists spoken out about the scary possibilities of



◀ **A goner?** Greenland's ice has been accelerating toward the sea lately, and no one is sure why.

30,000 comments from reviewers. The report was in turn boiled down to a 21-page "Summary for Policymakers" (SPM). Its central projection of sea-level rise by the century's end—0.34 meter—came within 10% of the 2001 number. And by getting a better handle on some uncertainties, it even brought down the upper limit of its projected range, from 0.89 to 0.59 meter.

The SPM did add that "larger values [of sea-level rise] cannot be excluded." Whatever has accelerated ice-sheet flow to the sea, the report said, might really take off with further warming—or not. "Understanding of these effects is too limited" to put a number on what might happen at the high end of sea-level rise, it concluded. Lacking such a number, the media tended to go with the comforting 0.34-meter projection or ignore sea level altogether.

Some scientists believe IPCC did as well as it could in assessing the sea-level threat. "Since 2001, nature has revealed some pretty remarkable behavior in the ice sheets," says glaciologist Waleed Abdalati of NASA's Goddard Space Flight Center (GSFC) in Greenbelt, Maryland, who manages NASA's ice-observation program. That behavior has included the catastrophic collapse of the Larsen B ice shelf—which triggered glacier accelerations—and the galloping glaciers draining the Greenland ice sheet, which have doubled their pace. But "we just don't have the capacity to quantify" that sort of ice-sheet behavior, he notes, so "the best you can do is point to some red flags. The language of the SPM does that, if you're looking for it."

Quantifying ice-sheet behavior does indeed have its limitations, says climate and sea-level modeler Jonathan Gregory of the University of Reading, U.K., who coordinated the production of the sea-level section in the IPCC projections chapter. A predictive model cited by IPCC would melt more Greenland ice as the air warms, he says, because that is a well-understood and quantifiable process. However, the model would not include the effect of that glacial meltwater lubricating the base of the Greenland ice sheet. Although researchers have seen signs that such lubrication speeds the ice sliding into the sea, they aren't yet able to model it. "If

No longer alone. James Hansen was a lone voice in 1988 but has company now in the greenhouse spotlight.

there are no models to give us some numbers," says Gregory, "all you can do is make numbers up. It wouldn't be appropriate to make up numbers."

Going beyond such physically based models—for example, by extrapolating from past trends—wouldn't be such a good idea either, Gregory says. Lessons taken from how sea level rose as the 20th century warmed, he says, would be useless in predicting sea-level rise in this century if the underlying causes change. "If you don't know what is causing the relationship" between warming and sea-level rise, he says, "is that really a good basis for making projections?"

A bolder assessment

Scientists are well aware of the hazards of straying far from the hard science of climate change, but some are eager to change the IPCC process and even move beyond it. They would begin with wording. "IPCC gets an A+ for scientific assessment," says climate modeler Richard Somerville of the Scripps Institution of Oceanography in San Diego, California, "but a gentleman's C for communication." The communication problem is largely a matter of structure, says geoscientist Michael Oppenheimer of Princeton University. "All the facts are there in the [main-report] chapter," he says, "but the SPM didn't tie those facts together in a coherent statement of risk that would allow a policymaker to make an informed decision."

Beyond the IPCC's language, a number of climate scientists think the report missed an opportunity to broaden public appreciation of the risk of the most dangerous climate change. "If you don't understand the physics, your uncertainty is larger," says Thomas. That greater uncertainty extends the range of possible ice losses to higher, more dangerous levels. But IPCC didn't capture that increased risk, says climate modeler Michael MacCracken of the Climate Institute in Washington, D.C.



global warming. "Most people [in the field] realize this really is an extremely serious problem we're facing" in sea-level rise, says Thomas. But no one understands just why the great ice sheets of Greenland and West Antarctica have accelerated their slide to the sea in recent years (*Science*, 24 March 2006, p. 1698). Will the acceleration continue? Speed up? Slow down? Stop? In the face of such uncertainty, most climate scientists have traditionally let IPCC speak for them. When they've gone public, it was usually to counter greenhouse contrarians arguing for an inconsequential warming with trivial impacts.

In the latest report, its fourth since 1990, the IPCC spoke for scientists in a calm, predictably conservative tone (*Science*, 9 February, p. 754). It is, after all, an exhaustive, many-tiered assessment of the state of climate science based exclusively on the published literature. In IPCC's Working Group I report on the physical science of climate, 600 authors contributed to an 11-chapter report that drew

If you want to
extract gDNA
from 10ml of
whole blood...

Talk to Tecan



Freedom EVO® gDNA XL for large scale purification of genomic DNA

Products like the new Freedom EVO gDNA XL have made Tecan market leaders in automated molecular biology. It offers reproducible results, a fully automated hands-free process from crude blood samples to highly purified genomic DNA. It's designed for a variety of downstream applications such as single and multiplex PCR, restriction digestion, real-time PCR – and all this at any throughput up to 96 samples a day.

We recognise how hard it is to get enough gDNA for your needs from low volumes of blood. So Tecan has teamed up with the leading companies in DNA purification technologies to develop Freedom EVO systems which are able to handle up to 10ml blood samples. This is just one example of how Tecan is in touch with what our customers want most.

To find out more about the Freedom EVO gDNA XL or any of our products, please talk to Tecan on any of the numbers below.

www.tecan.com

 **TECAN.**

Liquid Handling & Robotics | Detection | Sample Management | Components | Services & Consumables

Austria +43 62 46 89 33 Belgium +32 15 42 13 19 China +86 10 586 95 936 Denmark +45 70 23 44 50 France +33 4 72 76 04 80 Germany +49 79 51 94 170
Italy +39 02 215 21 28 Japan +81 44 556 7311 Netherlands +31 18 34 48 17 4 Portugal +351 21 000 82 16 Singapore +65 644 41 886 Spain +34 93 490 01 74
Sweden +46 31 75 44 000 Switzerland +41 44 922 89 22 UK +44 118 9300 300 USA +1 919 361 5200 Other +43 62 46 89 33

A big part of IPCC's problem, say MacCracken and others, was its strict adherence to the use of models. By IPCC standards, "if it's not in a model, it's speculation," says Rahmstorf. By ignoring factors that can't yet be modeled, he says, IPCC came up with deceptively reassuring numbers.

More numbers

Although forewarned, some researchers are generating numbers for public consumption by going beyond physics-based models. In a paper published in *Science* in January, too late for the IPCC to consider it, Rahmstorf took "a semiempirical approach to projecting future sea-level rise." He determined how much sea level rose in the 20th century per year per degree and projected that rate through the 21st century, with its expected warming. That projection produced a sea-level rise in 2100 of 0.5 to 1.4 meters above the 1990 level, well above the IPCC's projection of 0.18 to 0.59 meter.

Then, Rahmstorf and six co-authors, including Hansen, published a paper in *Science* on the day the IPCC report was released. They pointed out that warming had been running toward the high side of IPCC projections during the past few decades, while sea levels rose at the upper limit of projections. "These observational data underscore the concerns about global climate change," the authors wrote. IPCC had clearly not exaggerated sea-level rise, they said, and may even have underestimated it. Reinforcing their message, news stories published a few days before the IPCC report's release quoted Rahmstorf and other scientists lamenting the expected shortcomings on sea-level projections.

That was more media attention than suited some climate researchers. "When we speak to the public, we should not rely on the new result," argues Hans von Storch of the GKSS Institute for Coastal Research in Geesthacht, Germany. "The newest results are not necessarily the best ones. The IPCC should represent a certain filter. That every taxicab driver knows about [the latest result] is a bit premature."

Some scientists would have IPCC reach even farther back to try to deal with "factors that you don't understand," as MacCracken puts it. He notes that paleoclimatologists and geologists have extracted records of ancient

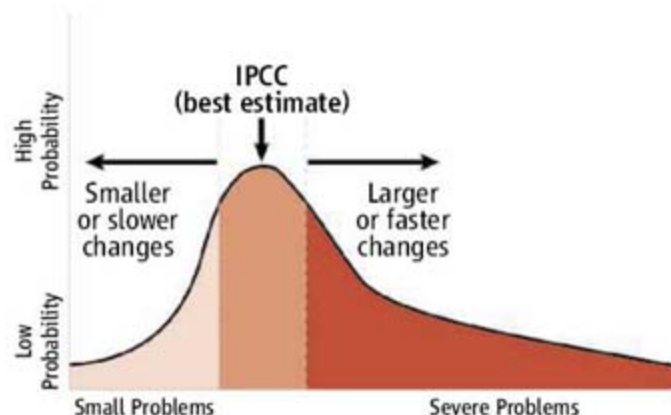
sea level for times when Earth was warmer or colder than today. In the case of the penultimate warm interglacial 120,000 years ago, the globe was only about 1°C warmer—a temperature we could reach by 2100—but sea level was 4 to 6 meters higher. Even though that warmth had millennia to shrink the great ice sheets back then, MacCracken says, history still suggests that the world's ice is more vulnerable than IPCC's modeling implies.

Another way

Gregory calls projections drawing on such studies "a scientific hunch." Hansen prefers "insight," but whatever it is called, Hansen says, you won't find much of it in an IPCC report. IPCC "overall does a good job," he says, but "there are limitations on that process. Everybody in [sea-level] research is much more concerned than 6 or 7 years ago" when the previous report came out, he says; yet the latest message from IPCC was seemingly unchanged. "There is a role for something in addition."

As an example of an alternative to the IPCC report, Hansen cites the U.S. National Academy of Sciences' climate change report of 1979. Chaired by the late meteorologist Jule Charney, then at the Massachusetts Institute of Technology, the small committee delivered, among other things, a best estimate and range for the sensitivity of climate to greenhouse gases, a central figure in climate science. IPCC never ranged far from those numbers, and this year it confirmed them. "There were huge uncertainties back then," says Hansen, "yet the Charney report came up with an estimate by coming at it from different angles. That's what you need to do with sea level."

Hansen practices a multipronged approach himself. With colleagues at GISS, he draws on several lines of evidence—climate modeling, recent observations, paleoclimate records, and the basic physics of the greenhouse—to "gain insight into how the world works." That approach helped him to see greenhouse warming under way in 1988, he says. Now it is revealing positive feedbacks in the ice-climate



Asymmetry. The climate debate has focused on problems judged most likely (center) or least damaging (left), but the greatest risk may be at the extreme (right).

system that can allow modest warming to accelerate losses from the ice sheets. The world is on a "slippery slope," Hansen has written, that could lead to meters of sea-level rise in the next century or two unless people take immediate actions to cut greenhouse gas emissions.

As in 1988, Hansen's pursuit of such insights has put him at odds with many in the climate community. "Maybe he's still within the error bars," says glaciologist Robert Bindshadler of GSFC, but "I'm not prepared to put centuries on [the timing] rather than millennia." No matter. Hansen has again taken to the bully pulpit as NASA's top climate scientist, publishing in peer-reviewed journals, testifying to Congress, writing op-ed articles, and appearing in documentaries. Only last week in a GISS press release announcing a new publication, Hansen warned of disastrous effects—including increasingly rapid sea-level rise—if greenhouse gas emissions continue apace for even a couple more decades. And a few days later, he took his boss, NASA Administrator Michael Griffin, to task for publicly questioning the need to tackle global warming. Hansen's take: "remarkably uninformed."

Besides a streamlined IPCC process and individual scientist activism, Oppenheimer sees another approach: using expert elicitation to broaden the assessment of uncertainty. This survey technique grills selected experts in private on the state of the science. Without the drive to reach a consensus, the experts "give a different view of the probability of various outcomes," says Princeton's Oppenheimer. Ultimately, these and other methods will be needed, he says. "You really need a broad, thorough, and comprehensive assessment of uncertainty and risk," he says. "There is no one answer to the assessing of uncertainty."

—RICHARD A. KERR

"IPCC gets an A+ for scientific assessment, but a gentleman's C for communication."

—Richard Somerville,
Scripps Institution of
Oceanography

ALZHEIMER'S DISEASE

A New Take on Tau

The search for drugs to combat neuron-destroying diseases is prompting researchers to take a fresh look at a familiar suspect

When it comes to combating Alzheimer's disease, neurobiologists need all the help they can get. So far, efforts to develop drugs that halt or reverse the relentless brain degeneration caused by the disorder have met with only modest success. The few approved therapies slow cognitive decline, but only temporarily, possibly because they don't target the root cause of the disease.

Drugs that may do that are in the pipeline, however. They're aimed at reducing production of amyloid beta ($A\beta$), a protein fragment thought to be the instigator of the nerve cell death driving Alzheimer's disease (*Science*, 3 November 2006, p. 781). And now researchers are taking a closer look at another possible target, a protein called tau that is involved in the pathology of a number of neurodegenerative diseases, including Alzheimer's.

Tau has taken a back seat to $A\beta$ for the past several years, but recent work with animal models and with cells in lab culture suggests that focusing on tau could pay off. Treatments that reduce the formation within the brain of certain mutant taus, or even of the normal protein itself, can alleviate memory loss and other neurological deficits in

mice that have been genetically engineered to develop brain pathology similar to that in human Alzheimer's brains.

Although a lot more work will be needed before any of these early experiments pay off in the clinic, tau researchers are more optimistic than before. The findings "open up a new potential [Alzheimer's] treatment; reducing tau might complement the anti-amyloid strategy," says Lennart Mucke of the University of California, San Francisco, School of Medicine, whose lab is among those doing the work.

And big pharma is taking note as well. For example, Merck & Co. Inc. has just hired Michael Hutton, a tau researcher at the Mayo Clinic in Jacksonville, Florida, to head up a new effort to develop tau-based drugs for Alzheimer's disease. "I'm putting my money where my mouth is," Hutton says. "I do think tau is a great therapeutic target."

Tau resurgent

For more than 20 years, neurobiologists have known that both $A\beta$ and tau are prominent in the abnormal structures that stud the brains of Alzheimer's patients: $A\beta$ is located in the so-called plaques that form outside

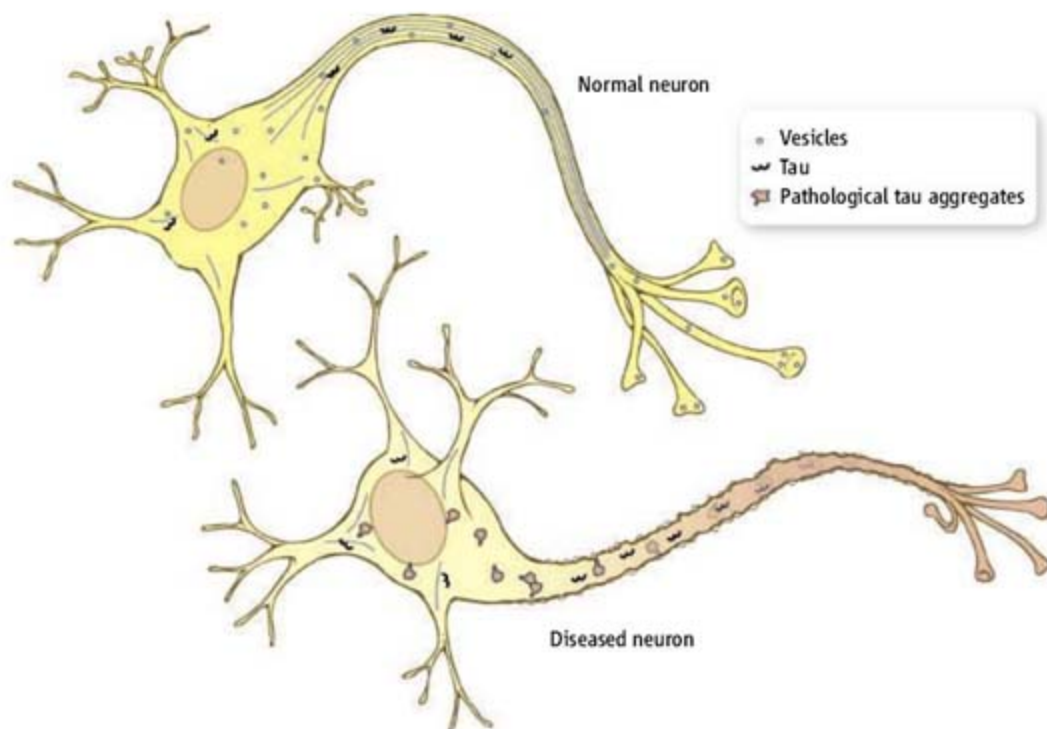
dead and dying nerve cells, whereas tau appears inside neurons in a mesh of proteins called neurofibrillary tangles (NFTs). For a time, a controversy raged about which protein causes the brain neurons to degenerate. The tide began to swing in $A\beta$'s favor after the discovery about 16 years ago that mutations in the *APP* gene, which makes the larger protein from which $A\beta$ is clipped, cause some hereditary Alzheimer's cases.

Indeed, no mutations in the tau gene have ever been linked to the disease, and today even many tau experts concede that $A\beta$ -linked abnormalities initiate brain neuron loss. "There's no doubt that $A\beta$ [toxicity] is a fairly early event in Alzheimer's disease pathology and that tau is likely downstream," says Christopher Eckman, also at the Mayo Clinic in Jacksonville.

But tau researchers got a boost about 10 years ago, when several teams found that mutations in the gene for the tau protein cause some cases of a less common but devastating dementia known as FTL (for frontotemporal lobar degeneration). This discovery showed that abnormal forms of the protein can cause nerve degeneration and as a result, memory loss and other neurological deficits. The work also buttressed the case that counteracting tau's effects might help Alzheimer's patients. "Focusing on tau [for Alzheimer's therapy] makes perfectly good sense," says Zaven Khachaturian, senior science adviser to the Alzheimer's Association in Chicago, Illinois.

In the past few years, researchers have begun to test the idea of targeting tau, using various mouse models of Alzheimer's disease. The most recent example, described in the 4 May issue of *Science* (p. 750), comes from Mucke's group. These researchers used a genetically altered mouse strain that carried a mutant human *APP* gene and varying numbers of the mouse tau gene—either zero, one, or the normal complement of two copies. Because these mice carry the mutant *APP* gene, all their brains developed structures resembling the amyloid plaques of Alzheimer's brains. But as is commonly seen in such modified mice, none had tangles or neuron loss.

Mucke and his colleagues found that, as the animals aged, those with two tau gene copies became impaired in their ability to learn the Morris water maze, which requires that the animals find an underwater platform. Animals with one copy were less impaired, whereas those with no tau gene learned as readily as normal controls did—results indicating that the absence of tau somehow prevents the behavioral deficits that would otherwise occur in animals with mutant *APP*.



When tau goes bad. In a normal neuron (top), tau stabilizes the microtubules (blue lines) that transport materials to the nerve terminals. But in Alzheimer's disease, tau loses its ability to bind to the microtubules and forms abnormal aggregates. The microtubules degenerate, impairing neuronal function.

Yet the tau reduction had no effect on A β deposition. The animals lacking tau “had brains full of amyloid plaques but could solve the water maze in a snap,” Mucke says. Further work indicated that tau might contribute to neuronal malfunction by making brain neurons hyperexcitable, which can ultimately lead to their death.

Other researchers have also found that reducing tau can alleviate memory loss in mouse models. For their experiments, a team led by Karen Hsiao Ashe of the University of Minnesota Medical School in Minneapolis and the Mayo’s Hutton created a strain of mice bearing a mutant human tau gene combined with regulatory sequences that allowed it to be turned off by the antibiotic doxycycline. As the researchers reported about 2 years ago, as these mice age, they accumulate NFTs in brain neurons where the tau gene is active.

What’s more, the animals’ brains shrink as a result of nerve cell death, and the mice show a marked deterioration in their ability to learn the water maze. But suppressing expression of the mutant tau gene with doxycycline improved the animals’ memories and halted the neuronal losses without affecting NFT accumulation (*Science*, 15 July 2005, p. 476).

Last year, Frank LaFerla and his team at the University of California, Irvine, reported on a mouse model that they engineered to develop both plaques and tangles. Treatment with two antibodies, one directed at A β and the other at tau, preserved the animals’ ability to learn. Both antibodies were needed. “If we reduce A β without reducing tau, we don’t improve [the animals’] learning and memory behavior,” LaFerla says.

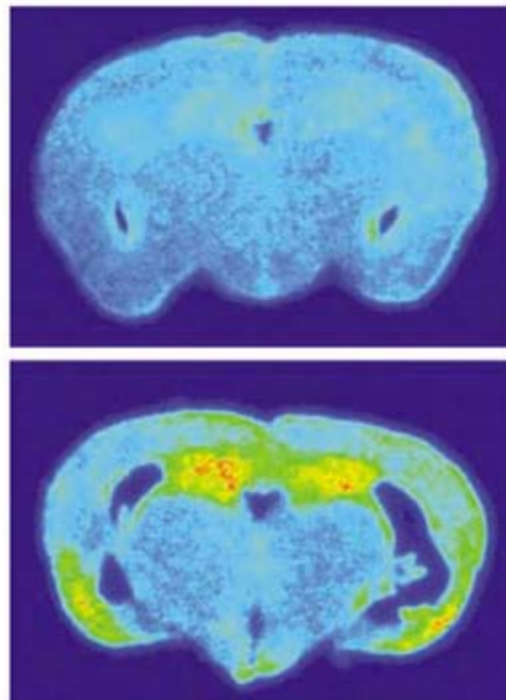
But which tau?

In addition to showing that tau can play a role in cognitive decline, these studies also shed light on what Hutton calls a “massive uncertainty”: What form of tau damages neurons? Identifying the culprit could be important for guiding efforts to develop therapies; those trying to stop A β buildup, for example, continue to wrestle with whether to target soluble or insoluble forms.

For most of the 100 years since Alois Alzheimer described the plaques and tangles in his patients’ brains, researchers focused on the tangles with their insoluble tau as the species at fault. But Ashe and her colleagues found that when they turned off tau formation in their animals, NFTs continued to accumulate despite the other improvements. Similarly, the LaFerla team’s antibodies were directed at soluble tau as well as soluble A β and did not reduce

plaques or tangles. Some form of tau “before the tangles [develop] is causing the memory problems,” Ashe concludes.

Further evidence that a nontangle form of tau causes neuronal damage comes from Virginia Lee, John Trojanowski, and their colleagues at the University of Pennsylvania School of Medicine in Philadelphia. When these researchers tracked the changes in brain neurons in mice bearing a mutant



Inflammatory link. A mouse brain (bottom) bearing a mutant human tau gene shows extensive microglial cell activation at 9 months (yellow to red colors). The brain at top is from a 9-month-old control.

tau gene, they found that the synapses, which are the connections between neurons, deteriorated at 3 months of age—long before NFTs appeared.

By this same early age, microglial cells, the brain’s immune cells, became activated, presumably due to the presence of the mutant tau, the researchers reported in the February issue of *Neuron*. This suggests that the microglia might be contributing to the neuronal damage by causing inflammation—an idea that got a boost when Lee, Trojanowski, and their colleagues treated the animals with an immunosuppressant. “We delayed everything,” Lee says. “The tangles decreased, the neuronal loss decreased, and the animals lived longer.” These results tie in with other evidence suggesting that inflammation plays a role in Alzheimer’s etiology and that anti-inflammatory drugs might help.

Still, tau abnormalities could contribute in other ways to neuronal degeneration and these, too, suggest therapeutic strategies. Normal tau binds to, and stabilizes, the micro-

tubules, which run through the neuronal axon and help transport nutrients, proteins, and other materials back and forth between the cell body and the synapse. For reasons not yet understood, tau becomes excessively phosphorylated in Alzheimer’s brains and as a result no longer binds properly to the microtubules. The microtubules in turn deteriorate, ultimately leading to nerve cell death.

Some drugs, including the taxols used to treat breast cancer, stabilize microtubules. About 2 years ago, Lee, Trojanowski, and their colleagues showed that one of these drugs, paclitaxel, improved axonal function and ameliorated the neurological problems of mice carrying a human tau gene. Lee notes, however, that the taxols and other microtubule-stabilizing drugs kill dividing cells and are thus too toxic, especially for long-term use. Her group is currently working to develop less toxic taxol derivatives.

Other researchers are taking a different tack, aiming to inhibit the kinases that add phosphates to tau. Some of these have shown promise in animal models. For example, Hutton’s team, working with that of Hanno Roder at Sirenade Pharmaceuticals in Martinsried, Germany, found that an inhibitor of a kinase called ERK2 reduced the excessive tau phosphorylation occurring in mice carrying a human tau gene and also reduced the animals’ difficulties in moving.

Similarly, LaFerla and his colleagues have evidence from their mouse model that interventions thought to be protective against Alzheimer’s disease, including learning interventions and dietary intake of omega-3 fatty acids, might work partly by decreasing levels of enzymes that phosphorylate tau. But at least in their model, A β reductions also appear to be necessary for neurological protection.

All of this work in mice raises the obvious question of whether the results are relevant to Alzheimer’s disease and other so-called tauopathies such as FTL. But there is at least one hint that inhibiting tau phosphorylation could help people afflicted by the conditions. The drug memantine is one of the few approved for treating Alzheimer’s disease. And although it wasn’t designed to inhibit phosphorylation, Khalid Iqbal and his colleagues at the New York State Institute for Basic Research in Developmental Disabilities on New York’s Staten Island have evidence from cell studies that the drug decreases tau phosphorylation and inhibits neurofibrillary degeneration. “I don’t understand,” Iqbal says, “how anyone can think about Alzheimer’s and not think about tau.”

—JEAN MARX



SMALLPOX VACCINE

A Tame Virus Runs Amok

The massive response that saved a child from a rare infection demonstrated the strength of U.S. medicine—and the vulnerability of U.S. biodefenses

On 3 March, doctors treating a 2-year-old boy in a Chicago hospital were alarmed by the angry rash that covered his body. They checked out the usual suspects—chickenpox and herpes simplex, which can have serious consequences for children, like this one, with eczema. But lab tests ruled out both. As the rash worsened days later, forming ring-like, indented pustules on half of the boy's body, the hospital's staff learned that the father, a soldier in Iraq, had been vaccinated for smallpox several weeks before. The vaccine—or contact with recent vaccinees—can trigger a life-threatening rash in people with eczema, one that looks much like smallpox itself.

What happened next was a race straight out of a TV medical drama. Doctors and at least two dozen outside experts, including a veteran of the smallpox eradication campaign, worked around the clock for days to diagnose and treat the boy's disease, known as eczema vaccinatum. Ultimately, they made a bold decision to try an experimental drug; it may have helped save the child's life. Today,

despite severe skin loss, the boy is back at home in Indiana, healthy except for possible scarring where the pustules formed.

The incident, described in the 18 May issue of *Morbidity and Mortality Weekly Report (MMWR)*, offers a mixed view of U.S. efforts to defend against a bioweapons attack, had this been the first in a wave of smallpox cases. On the one hand, a half-dozen federal and local agencies deserve good marks for working together to diagnose and treat a mysterious infectious disease. The experimental drug was developed with funds from the U.S. biodefense research program. But as a test of how quickly the system might contain a disease, the results seem not so good: If the boy's illness had been caused by a real smallpox release, notes poxvirus program chief Inger Damon of the Centers for Disease Control and Prevention (CDC) in Atlanta, Georgia, there likely would have been casualties.

The *MMWR* report also highlights the risks of the Department of Defense's (DOD's) smallpox vaccination program,

Mass campaign. DOD has given the smallpox vaccine to 1.2 million U.S. soldiers.

which uses a vaccine formulation that many consider outmoded (*Science*, 20 December 2002, p. 2312). Moreover, the soldier should not have been vaccinated, the *MMWR* report says. "It does not mean the program is broken," because the rate of side effects has been very low overall, says infectious-disease physician Luciana Borio of the Center for Biosecurity at the University of Pittsburgh in Pennsylvania, but the incident underscores the need for safer vaccines, which are now in the works.

Live virus

The current smallpox vaccine is an old formulation made with live vaccinia virus, a relatively benign cousin of the variola virus that causes smallpox. Serious side effects in immunocompromised patients and children are rare but well-known; former chancellor of the University of Colorado Health Sciences Center Vincent Fulginiti, 75, an expert on these adverse events, saw eczema vaccinatum cases often in the 1960s through 1972, when children were routinely immunized for smallpox.

After wild smallpox was declared eradicated in 1979, vaccinations continued only for members of the U.S. military. They had to be protected, the government decided, because they might be the first to encounter the lethal virus if secret stocks were deployed by an enemy. That program ended in 1990. In 2002, however, in the wake of the post-9/11 anthrax attacks, the Bush Administration resumed vaccinations for soldiers, but included screening so that people at risk for side effects would be excluded.

Why the father of the Indiana boy was not screened out is not known. Before he was vaccinated in January in anticipation of deployment to Iraq, he had received an educational pamphlet and briefing warning about possible side effects. He was also given a form asking whether he had a history of eczema, which he did. People with this skin condition or those who have household contacts with it are not supposed to receive the smallpox vaccination. For privacy reasons, DOD declined to disclose the soldier's answers on the screening form.

Then, in February, when his deployment was delayed, the soldier made a visit home. Although a scab from the vaccination had fallen off, he later told DOD, he kept the site covered as instructed. In late February, his 28-month-old son, who also had eczema, developed a fever and rash. On

3 March, after his family visited an Indiana emergency room, the child was transferred to Comer Children's Hospital, part of the University of Chicago in Illinois.

Doctors there took skin samples from the child and tested them for herpes and varicella; the tests were negative. Meanwhile, the lesions had spread over about 80% of the child's body and had worsened: Each pustule was circular, with a dimple in the middle, says University of Chicago pediatric infectious-disease physician John Marcinak, who coordinated the boy's care. Another viral culture tested positive for an unidentified virus. On 7 March, Marcinak says, he and pediatric dermatologist Sarah Stein, who by this time had been told of the father's vaccination, began to suspect vaccinia: "From a clinical standpoint, it all fit."

Marcinak and colleague Surabhi Vora contacted CDC, which set up conference calls with various CDC and Army experts to analyze digital photos. The Illinois Department of Public Health also supplied polymerase chain reaction tests of skin scrapings from the child and his mother, who had developed a milder rash. Those tests showed the presence of a poxvirus. At that point, says Fulginiti, who was on the daily calls, he knew "it was eczema vaccinatum."

The Chicago doctors began the standard treatment, injecting vaccinia immune globulin, or antibodies from people given the vaccine, which a U.S. marshal had hand-carried on a flight from CDC's biodefense stockpile. The boy was given narcotics for pain, sedated, and put on a ventilator. Two days later, his condition worsened. "We weren't sure he was going to survive," Marcinak says. Next, his team tried a second-line drug, cidofovir, normally stocked by hospitals for AIDS patients with cytomegalovirus eye infections but approved by the U.S. Food and Drug Administration (FDA) off-label for complications from smallpox vaccination. Cidofovir seemed to be of limited help; the boy's abdomen had filled with fluid and his kidneys were failing, a condition that could have been exacerbated by the second drug.

On the next conference call on Saturday, 10 March, CDC's Damon suggested one more thing: an experimental smallpox antiviral drug, ST-246. "The condition of the child on the weekend was just so grim," Damon says, that they wanted to try any-

thing that might give him a chance.

The drug had first been discovered through a routine small-molecule screen for compounds that inhibit poxviruses. It had later been improved, reducing toxicity. With funding from the National Institutes of Health's biodefense program, SIGA Technologies Inc. in Corvallis, Oregon, reported last year in experiments at CDC that ST-246 protects monkeys against variola infections; it has also conducted a phase I clinical safety trial. Hours after Damon suggested using ST-246 that Saturday, FDA approved emergency use of the drug to treat the sick boy.

That night, SIGA Chief Scientific Officer Dennis Hruby tucked a vial in his pocket and flew to Chicago from Corvallis in a private jet paid for by billionaire Ronald Perelman, an investor in SIGA. The boy got an initial dose through a stomach tube Sunday morning. "The next day, he started to slowly get better," Marcinak says. He also received skin grafts.

On 7 April, the boy moved out of the intensive care unit into a regular bed; 12 days later, he went home. "He looks very good right now," says Marcinak. The grafts are healing well, he says, but it is too soon to tell whether he will have scarring.

Researchers say they may never know exactly what saved the boy's life because he was receiving three drugs (cidofovir lingers

SIGA received \$16.5 million from the National Institute of Allergy and Infectious Diseases last fall to conduct further clinical trials and scale up production of ST-246. But whether the federal government will eventually purchase ST-246 for the biodefense stockpile is not known, Borio says.

Adequate screening?

Some public health experts are now raising questions about DOD's procedures for identifying soldiers for whom the smallpox vaccine is too risky. But others say DOD, which has excluded 116,000 of 1.3 million potential vaccinees, has done a good job. Overall, side effects have occurred at "a much, much lower rate than would have been expected," says vaccine expert John Modlin of Dartmouth Medical School, including the one eczema vaccinatum case and 61 cases of mild vaccinia rash in contacts. But the Indiana case is "a very important reminder that we can't become lax about screening," he says.

Dryvax, the old vaccine, apparently has other side effects as well, including myopericarditis, inflammation of the heart, which has occurred in 140 soldiers so far. Most people recover, says Modlin, but in a few, heart muscles may be permanently weakened.

A new vaccine produced by cell cultures was supposed to be slightly safer. But data presented last month to the FDA vaccine

advisory panel by the manufacturer, Acambis in Cambridge, U.K., suggest a comparable rate of myopericarditis cases, says Modlin, a panel member. Although the panel found the vaccine safe and effective for the U.S. stockpile, "in my view, [the myopericarditis risk] should" prompt DOD to conduct a new risk-benefit analysis.

It is sobering to consider what might have happened if the Indiana boy's rash had been the first case in a wave of smallpox cases from a bioterror attack. The intense response—more than 20 experts on daily conference calls for a month—could not have been sustained for dozens of patients or more,

Damon notes. The current system would have been overwhelmed "if 10,000 people had had an [smallpox] infection," says Hruby. That's why it is so important, he says, to develop standard therapies that can be tested in advance and kept on the shelf.

—JOCELYN KAISER

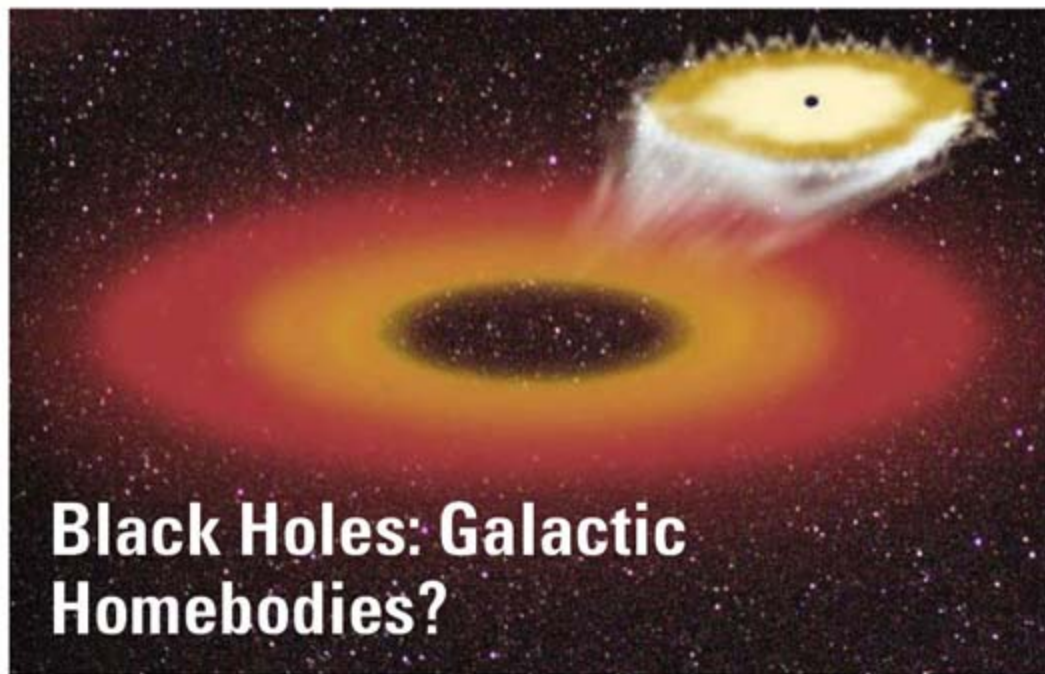


Poxvirus's mark. These lesions broke out on a 2-year-old boy after he contracted vaccinia from his father and developed eczema vaccinatum, a rare side effect.

in the body for a week) as well as extraordinary medical care. Moreover, analyses of daily blood samples that could reveal when virus levels dropped have been inconclusive so far, Damon says. Still, he adds, "I think it [ST-246] was certainly a component" in the boy's recovery.

MEETING BRIEFS >>

210TH MEETING OF THE AMERICAN ASTRONOMICAL SOCIETY | 27–31 MAY | HONOLULU, HAWAII



Black Holes: Galactic Homebodies?

Rogue black holes hurtling through space may be nothing to worry about, a new analysis concludes.

When galaxies collide, the black holes at their cores should eventually merge in a violent collision, imparting a high-velocity kick that might shoot the newly merged black hole out of the joined galaxies. In fact, recent simulations have suggested that the recoil velocity could occasionally reach 3000 kilometers per second, more than enough for the black

hole to escape its galaxy's gravity. Yet searches do not find galaxies without central black holes. "When we actually look around at galaxies, all galaxies appear to have black holes," says Christopher Reynolds of the University of Maryland, College Park. "So why aren't there these empty-nest galaxies?"

In a new search for black holes traveling away from their host galaxies, Erin Bonning of the Observatoire de Paris, Meudon, and collaborators at the University of Texas,

Austin, examined 2600 quasars cataloged by the Sloan Digital Sky Survey. Quasars are fountains of energy powered by supermassive black holes at the centers of distant galaxies. A black hole being ejected from its host galaxy would drag some of the surrounding matter with it and would retain its quasarlike appearance. But the quasar's extra motion would make its redshift differ from that of the galaxy. The survey saw no convincing evidence for such shifts, the astronomers said at the meeting.

"For some reason, we do not get large kicks in quasars," said Bonning. "This is an interesting nondiscovery."

Astrophysicists at the University of Maryland, College Park, presented a possible explanation for the lack of large kicks. The simulations forecasting high-velocity ejections assume that the merging black holes are spinning rapidly, with their spin axes in the same plane as their galactic orbits. According to these models, configurations capable of kicking the final black hole out of the merged galaxies should occur in about 10% of galactic collisions.

But such a spin orientation is unlikely to persist throughout the merger process, Tamara Bogdanovic and her Maryland colleagues reported at the meeting. In gas-rich merging galaxies, their analysis showed, the two black holes will become embedded

Exoplanet Jackpot Shows Astronomers Are Looking for Worlds in All the Right Places

As news stories go, finding a new extrasolar planet is now about as surprising as another athlete arrest or celebrity trip to rehab. But recent, rapid increases in the number of known exoplanets have begun to reveal some noteworthy patterns, with implications for understanding the formation of planets and the prospect for life on some of them.

Planets around distant stars typically betray their presence when astronomers observe wobbles in stellar motion induced by the subtle tugs of the planet's gravity. Until recently, the search for such wobbles focused mostly on stars similar to the sun. Now surveys of other star types, from dim red dwarfs to massive subgiants, are showing that all varieties of stellar parents produce planetary offspring.

"Every sort of star we've looked at has a planet of some sort," says Alan Boss of the Carnegie Institution of Washington.

At the meeting, planet hunter Jason Wright of the University of California (UC), Berkeley, noted that 28 newcomers have been added to the planetary roster in the past year, bringing the total to 236. Of the recent additions, four orbit "A stars," said UC Berkeley's John A. Johnson.

In general, A stars, which are more than 1.3 times the mass of the sun, are poor candidates for planet searches, as their high temperatures and rapid spins make it hard to get precise velocity measurements by measuring shifts in the color of the light they emit. But as A stars age, they evolve

into "retired A stars," expanded subgiants with cooler temperatures and slower spins, making planet detection more feasible.

Using the Keck Observatory in Hawaii and the Lick Observatory in California, Johnson and collaborators scanned 150 subgiants, adding the four planets orbiting retired A stars to the six that had been discovered previously. The 10 A-star planets orbit at greater distances than planets of sunlike stars do, Johnson notes. All but one are farther from their parent stars than Earth is from the sun, and none is closer than 80% of the Earth-sun distance.

"This is very intriguing," Johnson said. "It's probably telling us something about how planets migrate from where they were born in closer to the star and how stellar mass affects that migration process."

A stars also appear more likely than other stars to possess Jupiter-sized planets. Jupiters are found in orbit around 4% to 5% of sunlike stars; 8% to 9% of retired A stars have them, Johnson said.

Such findings hint that increased attention to A stars could further inflate the planetary lineup. "They're twice as likely to have a planet as a sunlike star," says Johnson. "This means that there's probably a treasure trove of planets waiting for us around these retired A stars."

On the lightweight side of the solar-mass divide, smaller, dimmer stars known as red dwarfs, or M stars, have also begun to attract more attention

in a spinning disk of gas that will twist their axes until the black holes are spinning upright. As a result, the kick velocity after their merger will be less than 200 km per second, far short of the speed required to escape the merged galaxies' gravity.

"Ejection should not be common in such cases," Bogdanovic says.

Collisions of gas-poor galaxies might still eject black holes with high velocities, she says. But without surrounding gas to give off radiation, such wandering black holes would be extremely difficult to detect.

Another possible explanation for the missing rogue black holes is that they are not initially spinning rapidly enough to be ejected, but that seems unlikely, said Reynolds. A survey of black hole spins, reported by Maryland graduate student Laura Brenneman, found a range of spin rates, some approaching the maximum possible spin velocity.

"So the logical possibility," Reynolds said, "is that something upsets the orientation of the black holes as they are merging."

'Pristine' Galaxy Gives A Glimpse of Purity

A small but speedy dwarf galaxy hurtling toward the Andromeda galaxy has provided astronomers some reassurance about their favorite model of galaxy formation, along with hope for improved understanding of

star formation.

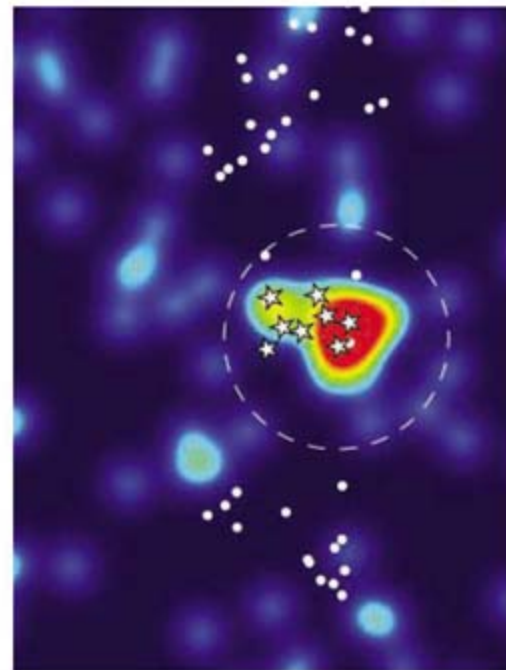
Andromeda XII, discovered in 2006, is dim even by dwarf galaxy standards, with a brightness of only about 100,000 suns. But new results, reported at the meeting, show that it is exceptionally fast, falling toward the Andromeda galaxy at 281 kilometers per second. At that speed, it may be moving too rapidly to be trapped by the gravity of the Local Group of galaxies, which includes Andromeda and our own Milky Way.

Jorge Peñarrubia of the University of Victoria in British Columbia and his colleagues established the speed of Andromeda XII using the DEIMOS spectrograph at the Keck II telescope on Mauna Kea, Hawaii. (A paper on the new findings is to be published in the *Astrophysical Journal*.) The quickness of Andromeda XII suggests that it formed far from the Local Group and is making its first visit, says Peñarrubia. The dwarf's arrival, he adds, fulfills predictions by the standard model of galaxy formation from cold dark matter, exotic nonluminous material that dominates the mass of both dwarfs and larger galaxies.

Dwarf galaxies contain from 50 to 500 times as much dark matter as ordinary matter, Peñarrubia said: "According to cold dark matter theory, the dwarfs are building blocks of galaxies. If you understand dwarfs, you learn about how galaxies form."

If it is entering the Local Group for the first time, Andromeda XII should be free from gravitational disturbances induced by the gravity of the group's larger galaxies.

"Andromeda XII is pristine; its properties are those it had when it was formed," said Peñarrubia. Consequently, it offers astronomers an unusual opportunity to study star formation and dark matter distribution. In dwarf galaxies that have already



Passing through. Stars mark confirmed members of the Andromeda XII dwarf galaxy, making its first visit to the Local Group of galaxies.

entered the Local Group, gravitational interactions may have altered the location of dark matter and obscured the history of star formation.

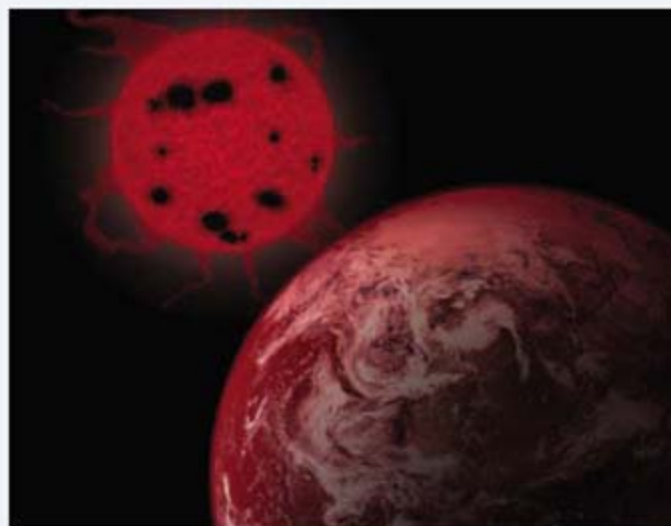
—TOM SIEGFRIED

Tom Siegfried is a writer in Los Angeles, California.

from planet hunters. A recent media frenzy accompanied news of a planet orbiting the red dwarf Gliese 581 because of its potential habitability (*Science*, 27 April, p. 528). The planet's orbit may be locked around its star in a way that keeps one side in the sun and one side in the shade, and the shady side's temperature may resemble Hawaii's, said Edward Guinan of Villanova University in Pennsylvania.

Guinan and collaborators have been studying the long-term habitability of M-star planets, particularly with regard to x-ray or ultraviolet radiation emissions that would endanger life. The danger would be especially high during the early days of the star's life, they reported, because young red dwarfs emit frequent stellar flares that would bathe nearby planets with deadly radiation. But nascent life on planets with atmospheres and magnetic fields would be protected from such emissions, Guinan noted.

After about 2 billion years, red



Prime location? Slow-burning red-dwarf stars might outperform our sun as hosts for life-bearing planets.

dwarfs settle down into an exceptionally long period of stability, as they burn their nuclear fuel slowly and maintain a fairly constant temperature for billions of years. That makes long-term prospects brighter for life on M-star planets than on Earth, where the sun will become intolerably hot in just a few billion years.

"M stars ... are suitable hosts for harboring life," said Guinan. "Your habitable zone will last for 20, 30, 40 billion years as the star's magnetic activity dies down."

M stars are the most numerous stars in the galaxy, and many are close enough to Earth to be available for detailed follow-up study, including attempts to directly image planets themselves.

"All these results make the case strongly that we're on the right track" for success in such imaging missions, said Boss.

"These studies are showing us that the frequency of planetary systems is really larger than what one might have guessed as recently as 10 years or so ago," he said. "Planetary systems are not rare oddballs. They really are quite common." —T.S.



LETTERS

edited by Etta Kavanagh

Adult Versus Embryonic Stem Cells: Treatments

D. A. PRENTICE AND G. TARNE USED THEIR LETTER "TREATING DISEASES WITH ADULT STEM CELLS" (19 Jan., p. 328) to try to defend Prentice's previous claim that "over 65 human diseases" have been "effectively treated through adult stem cells" (1). Now Prentice and Tarne say that what he really meant was that adult stem cell treatments for 65 diseases are being tested for possible efficacy.

Clearly, enrollment of an experimental therapy in a clinical trial does not mean that it is an effective therapy. The purpose of clinical trials is, first, to establish safety and, second, to document efficacy. Many promising experimental therapies fail when they reach larger Phase II or III trials. Such is the case with adult stem cell therapy for heart attacks and breast cancer—two conditions for which Prentice and Tarne improperly claimed that adult stem cells provide effective therapy [see the Supporting Online Material of our Letter "Adult stem cell treatments for diseases?," 28 July 2006, p. 439 (2)].

Prentice and Tarne's Letter perpetuates some of the same false representations of research with which we took issue in our original Letter. The GDNF infusion trials they referenced do not document any contribution of stem cells to the apparent improvements in Parkinson's patients. A careful reading of the cited papers shows that stem cells were not even studied (3, 4). Further, they cite a case report of a single patient as evidence that bone marrow transplantation can be used to correct hair loss—a condition that remains on their posted list of adult stem cell treatments (5).

In an interview published in the *Chicago Tribune* shortly after our Letter was published online, Prentice admitted that some of his citations were unwarranted. "We've cleaned up that list now," he said. Asked how the errors occurred, Prentice said, "I think things just got stuck in" (6).

In their Letter, Prentice and Tarne further disregard scientific accuracy by stating,

"We stand by our statement that Prentice and those who repeat his claims mislead laypeople and cruelly deceive patients."

—Smith *et al.*

that database (7). A repeat of Prentice's search found "system," "systemic," "brain stem," and the verb "stem" (as in "which stem from") in the last 10 listings of trials recruiting patients (647–656), but no mention of stem cells. The first 10 all relate to the use of stem cell transplants to replace blood-forming cells destroyed when chemotherapy or radiation is used as the primary treatment of the patient's disease (8). There are three trials for stem cell therapy in multiple sclerosis, but none for Parkinson's disease or spinal cord injury.

Prentice's erroneous claims are widely used and further embellished by opponents of embryonic stem cell research. For example, Focus on the Family set up a Web site last year opposing what they called "unproven, unsafe, and unethical experiments" with embryonic stem cells. The Web site referenced Prentice's claims and falsely asserted that patients "have access to adult stem cell therapy which currently provides safe and successful treatments for more than

70 diseases and injuries.... These are tangible therapies that are available today" (9).

We stand by our statement that Prentice and those who repeat his claims mislead laypeople and cruelly deceive patients.

SHANE SMITH,¹ WILLIAM NEAVES,^{2*}
STEVEN TEITELBAUM³

¹Children's Neurobiological Solutions Foundation, 1826 State Street, Santa Barbara, CA 93101, USA. ²Stowers Institute for Medical Research, 1000 East 50th Street, Kansas City, MO 64110, USA. ³Department of Pathology and Immunology, Washington University, 660 South Euclid Avenue, St. Louis, MO 63110, USA.

*To whom correspondence should be addressed. E-mail: William_Neaves@stowers-institute.org

References and Notes

1. J. Shea, "Doctors: Adult stem cells, cord blood hold most promise," posted on Catholicspirit.com on 27 October 2005 (accessed 7 Feb. 2007 at www.catholicspirit.com/stories/2005/oct/1027doctors.html).
2. See Supporting Online Material on *Science Online* at www.sciencemag.org/cgi/content/full/1129987/DC1.
3. S. Gill *et al.*, *Nat. Med.* **9**, 589 (2003).
4. S. Love *et al.*, *Nat. Med.* **11**, 703 (2005).
5. B. Seifert *et al.*, *Blood* **105**, 426 (2005).
6. J. Manier, J. Graham, "Experts rip Rove stem cell remark; researchers doubt value of adult cells," *Chicago Trib.*, 19 July 2006, p. 1.
7. See www.clinicaltrials.gov/ct/search?term=stem+cell (accessed 7 Feb. 2007).
8. See annotated list of examples of currently recruiting clinical trials retrieved on 7 Feb. 2007 at www.clinicaltrials.gov/ct/search?term=stem+cell; available as Supporting Online Material on *Science Online* at www.sciencemag.org/cgi/content/full/316/5830/1422b/DC1.
9. The Web site "Women's Voices Against Cloning," which is paid for by Focus on the Family (accessed 7 Feb. 2007 at www.citizenlink.org/images/votenocloning/learn-missourians.html).

Response

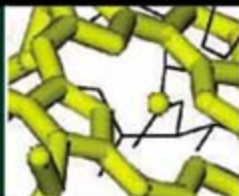
SMITH *ET AL.* CRITICIZED AN EARLIER COMPILATION of peer-reviewed studies with results showing benefits for patients with 65 conditions from nonembryonic stem cells. In our Letter "Treating diseases with adult stem cells" (19 Jan., p. 328), we thanked them for detecting a few technical errors in this list, but added that these do not affect our central claim—in fact, such health improvements have now been documented in patients with over 70 conditions [see the Supporting Online Material that accompanied our Letter (1)].

In none of these studies do the authors state merely that they are about to "test" whether adult stem cells may benefit patients or that they have begun "enrollment" in clinical trials. Rather, all these studies (including



Supersolid mystery

1435



How energy flows

1438

“On one point we agree with Smith *et al.*—It is gravely wrong to mislead laypeople and cruelly deceive patients.”

—Prentice and Tarne

those on breast cancer and heart damage) are reports of completed trials in which patients with these conditions benefited.

They question our reference to the use of GDNF for Parkinson’s patients. The focus of this therapeutic approach was improvement in patient health, which was achieved in these studies (2–4), rather than basic investigation of GDNF’s mode of action. However, the finding that trophic factors such as GDNF act by stimulating endogenous stem cells has existed for years, has been demonstrated in animal models, and has been proposed by several authors for treating neurodegenerative diseases in humans [e.g., (5–9)]. Regarding the patient case report they criticize, this was hardly mere “hair loss,” but rather complete remission of alopecia universalis (10).

We thank them for pointing out the vagaries of the NIH search engine, although we note that they only looked at trials currently recruiting patients, and not the complete list of trials. We had chosen a search term similar to that used by Dr. Battey, Chief of the NIH Stem Cell Task Force, who reported 563 adult stem cell clinical trials in 2004 (11). Closer analysis shows that currently there are only 1229 trials listed at clinicaltrials.gov that are related to the use of adult stem cells (12). Will all these trials automatically translate into safe, reliable, and widely available treatments? We do not know. That does not mean we should deny or belittle the tangible benefits that published approaches have already provided to some patients—benefits that remain lacking from any approach using embryonic stem cells. To suppress the evidence would be a disservice to patients.

In this context, we note that Neves and Teitelbaum were very prominent in the well-funded political coalition designed to amend the Missouri constitution in 2006 to authorize human embryo cloning and embryonic stem cell research. The Web site of this coalition, Missouri Coalition for Life-Saving Cures (13), continues to list “more than 70 diseases and

injuries that could benefit from stem cell research,” despite the lack of evidence regarding embryonic stem cells for such a claim and the widespread consensus that some of these conditions, such as Alzheimer’s disease, are extremely unlikely candidates for a stem cell treatment in the future. On one point we agree with Smith *et al.*—It is gravely wrong to mislead laypeople and cruelly deceive patients.

DAVID A. PRENTICE^{1,2*} AND GENE TARNE²

¹Family Research Council, 801 G Street, NW, Washington, DC 20001, USA. ²Do No Harm: The Coalition of Americans for Research Ethics, 1100 H Street, NW, Suite 700, Washington, DC 20005, USA.

*To whom correspondence should be addressed. E-mail: dap@frc.org

References and Notes

1. See Supporting Online Material at www.sciencemag.org/cgi/content/full/1129987/DC1; list also posted at the Web site of Do No Harm: The Coalition of Americans for Research Ethics, www.stemcellresearch.org.
2. S. Love *et al.*, *Nat. Med.* **11**, 703 (2005).
3. J. T. Slevin *et al.*, *J. Neurosurg.* **102**, 216 (2005).
4. S. S. Gill *et al.*, *Nat. Med.* **9**, 589 (2003).
5. A. Hermann *et al.*, *Expert Opin. Biol. Ther.* **4**, 131 (2004).
6. T. L. Limke, M. S. Rao, *J. Cell Mol. Med.* **6**, 475 (2002).
7. J. Fallon *et al.*, *Proc. Natl. Acad. Sci. U.S.A.* **97**, 14686 (2000).
8. S. S. Magavi *et al.*, *Nature* **405**, 951 (2000).
9. C. G. Craig *et al.*, *J. Neurosci.* **15**, 2649 (1996).
10. B. Seifert *et al.*, *Blood* **105**, 426 (2005).
11. *Congressional Rec.*, 9 Sept. 2004, pp. H6955–H6958.
12. Using the search term: stem cell; initial search shows clinical trials recruiting patients; click box in upper left to show all trials, including those no longer recruiting patients, analyzing each trial listed for relatedness to use of adult stem cells. Accessed 7 May 2007. For an analysis of differing results using similar search terms, see table S1 in the Supporting Online Material on *Science Online* at www.sciencemag.org/cgi/content/full/316/5830/1422b/DC1.
13. See www.missouricures.com/diseases.php (accessed 15 Mar. 2007).

Making Singapore a Research Hub

AS A SCIENCE POLICY ANALYST WHO WORKED in Singapore for several years, I witnessed the Singaporean government’s ambitions to turn the city-state into a world-class hub of biomedical research, ranging from basic research to manufacturing (“An Asian tiger’s bold experiment,” D. Normile, *News Focus*, 6 Apr.,



Lab partner.

Pipetman®

Just what you’re looking for in your lab:

- A detail-oriented, high-quality performer
- 30+ years experience
- Reliable and quickly adaptable
- Proudly upholds stringent industry-wide ISO standards
- Can handle small-to-large volumes of work
- Low maintenance, affordable and easy to work with

 Only (and always) from Gilson.

Put it to work for you.
1-800-GILSON1
www.pipetman.com



p. 38). In addition to the skepticism expressed in the article by Lee Wei Ling, one of Singapore's top biomedical scientists, about the dependence of the nation on the international talent pool for leaders of its biotech effort, Singapore faces other challenges.

First, biotech research is uncertain and it can take many years to achieve a breakthrough. Furthermore, advances in understanding pathways operating in human beings are not automatically translatable into commercialized, profitable products. It is not unusual for a pharmaceutical company to spend 10 years and billions of dollars developing a new drug. Although improvements in drug-screening technologies, automation of the screening process, and advances in genomics may change the "hit-or-miss" drug discovery process and shorten the development cycle, pharmaceutical companies will continue to see high rates of failure and enormous development costs. It remains to be seen whether Singaporeans are ready to embrace uncertainties and tolerate failures.

Second, the talent challenge may not be easily resolved. Singapore has started using a government fellowship program to send students

abroad. But it will take at least 10 years—the normal time for a doctoral degree plus postdoctoral research experience—for them to become independent researchers and longer to become internationally renowned. Also, in contrast to the United States, where the biotech industry has benefited from strong entrepreneurial efforts by academic scientists, their counterparts in Singapore, as civil servants, operate in a highly rigid, hierarchical system where moves between academia and industry are rare. Also, Singaporean youngsters may not be willing to stick to tedious benchwork that may or may not lead to financial rewards.

Finally, research in Singapore profited from the ethical debates that mired stem cell and cloning research in the United States. Less restrictive rules may have been an inducement to some foreign biotech companies to set up operations in Singapore. Of course, that does not mean Singapore has no regulatory framework to review research and enforce any recommended ethical code. But Singapore's advantage may not last if the research environment becomes more open in other countries. More importantly, there should be better opportunities for civil society

in Singapore to debate the issues related to biotech research. Citizens have the right to know much more about the risks and benefits associated with the biomedical sciences conducted in Singapore than they do now. Public understanding is at least as important as deep pockets and a deep talent pool.

CONG CAO

Neil D. Levin Graduate Institute of International Relations and Commerce, State University of New York, 33 West 42nd Street, New York, NY 10036, USA.

Making Data on Iraqi Mortality Rates Available

FOLLOWING OUR 2004 IRAQ MORTALITY SURVEY (1, 2), we made the data available to interested parties, and it has been our intent from the beginning to make the data from our 2006 study available so that our mortality estimations could be assessed by other scientists ("Iraq mortality study authors release data, but only to some," J. Kaiser, News of the Week, 20 Apr., p. 355). At the time the study was published, Iraqi colleagues requested that we delay release, as they were very fearful that some-

Don't Let Spreadsheet Programs Limit Your Choices

The Simplest and Most Effective Way to Analyze and Graph Data!

SigmaPLOT

Exact Graphs for Exact Science

SigmaPlot allows you to:

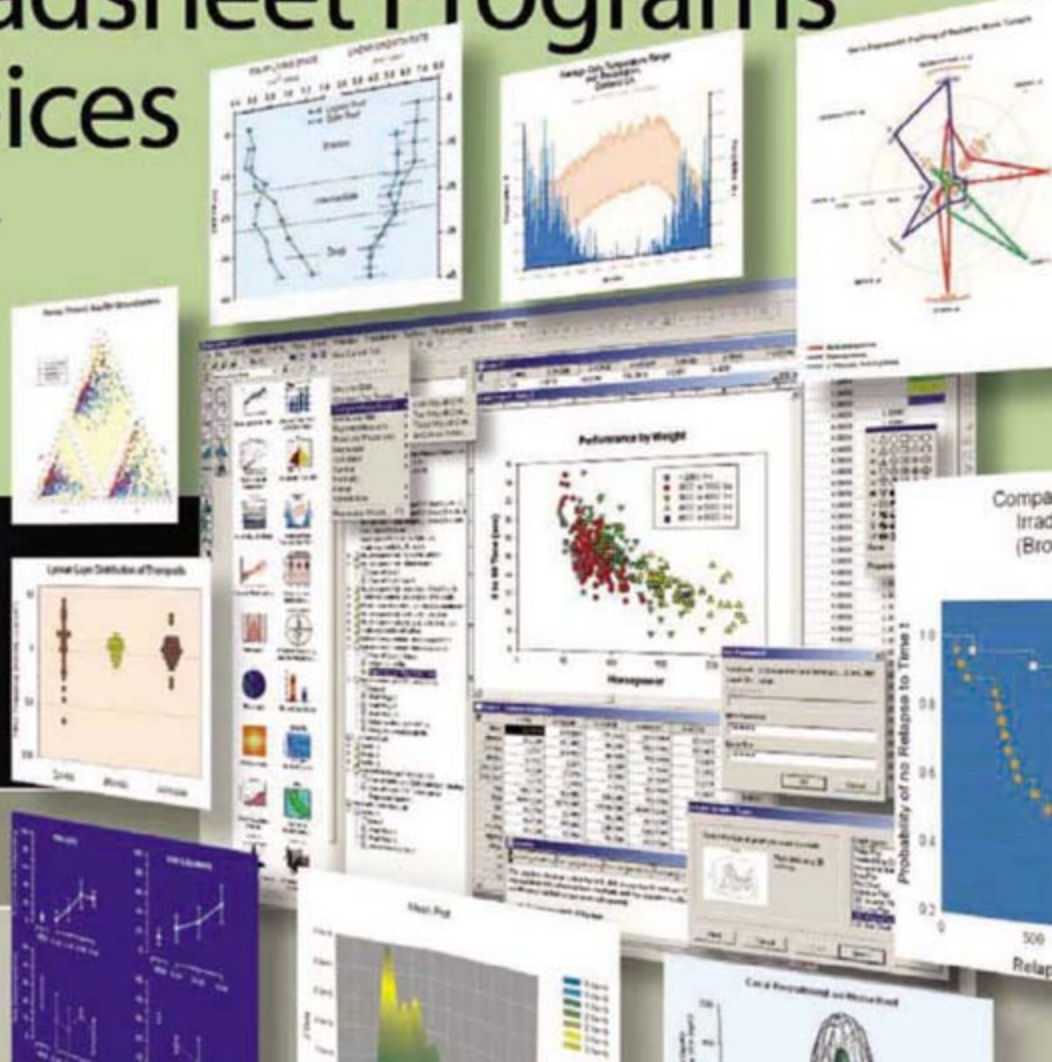
- > Choose from over 80 different 2-D and 3-D graph types
- > Customize every element of your graphs
- > Import, analyze & manage data quickly and easily
- > Fit your data easily and accurately with the Regression Wizard and the Dynamic Fit Wizard
- > Instantly access SigmaPlot from Microsoft® Excel
- > Publish your work anywhere easily
- > Streamline your work by automating repetitive tasks

FREE interactive demos & 30-day trial software available at www.systat.com
Call 1-800-797-7401 or email info@systat.com

Preferred by over 150,000 researchers worldwide

"I've tested other programs, but have never been able to make the same quality of technical graphs and figures I can make with SigmaPlot."

- Fred N. Scatena, Research Hydrologist



how streets, houses, and neighborhoods might be identified through the data with severe consequences. We agreed to wait for 6 months and have now made the data available.

From the beginning, we have taken the position that protecting participants is paramount, and thus we will not be releasing any identifiers below the level of governorate. The demand by some for street names seems to arise from the erroneous belief that only main streets were sampled, when in fact, where there were residential streets that did not intersect with the selected commercial street, these too were included in the sampling frame for identification of the start house. In any event, our interviewers reported that most, although not all, violent deaths occurred away from the location of residence.

The Iraq war continues to be a highly polarizing event. Following the release of the 2004 data set, we saw the distortion and manipulation of data by some to support pre-established positions. For the 2006 data, we decided on a more cautious approach, not releasing data to persons or groups with connections to pro-war or anti-war organizations. We continue to encourage others to pursue the collection of population-based data on mortality to further strengthen the measurement methods for the consequences of conflict on the host populations. It is our hope that accurate data will lead to a stronger international commitment to the protection of those unwillingly caught up in conflict.

GILBERT BURNHAM,¹ SHANNON DOOCY,¹
LES ROBERTS²

¹Department of International Health, Johns Hopkins Bloomberg School of Public Health, 615 North Wolfe Street, Baltimore, MD 21205, USA. ²Mailman School of Public Health, Columbia University, 3209 Country Route 2, Cincinnati, NY 13040, USA.

References

1. L. Roberts, R. Lafta, R. Garfield, J. Khudhari, G. Burnham, *Lancet* **364**, 1857 (2004).
2. G. Burnham, R. Lafta, S. Doocy, L. Roberts, *Lancet*, published online 12 Oct 2006, DOI: 10.1016/S0146-6736(06)69491-9.

CORRECTIONS AND CLARIFICATIONS

Policy Forum: "Environmental monitoring network for India" by P. V. Sundareshwar *et al.* (13 Apr., p. 204). On page 204, in the first column, first paragraph, the next-to-last sentence, the reference citation (3) should be (2) and "not" should read "no." The corrected sentence is, "Although FLUXNET and other observation networks cover diverse vegetation types within a 70°S to 30°N latitude band (2) and different oceans (5, 6), there are no comprehensive and reliable data from African and Asian regions." The authors were members of an Indo-U.S. bilateral workshop on INDOFLUX. In the legend to the first figure, reference citations (24–26) should be (22–24). In the credit line, the word "(SOURCE)" should be removed.

Perspectives: "High bond orders in metal-metal bonding" by F. Weinhold and C. R. Landis (6 Apr., p. 61). In the second

sentence of the second paragraph, the phrase "As was the case following Cotton's report in 1973" is incorrect. The report appeared in 1964.

TECHNICAL COMMENT ABSTRACTS

COMMENT ON "From Plant Traits to Plant Communities: A Statistical Mechanistic Approach to Biodiversity"

Stephen H. Roxburgh and Karel Mokany

Shiple *et al.* (Reports, 3 November 2006, p. 812) developed a quantitative method for predicting the relative abundance of species from measured traits. We show that the method can have high explanatory power even when all trait and abundance data are randomly and independently generated, because of a mathematical dependence between the observations and predictions. We also suggest a potential solution to this problem.

Full text at www.sciencemag.org/cgi/content/full/316/5830/1425b

COMMENT ON "From Plant Traits to Plant Communities: A Statistical Mechanistic Approach to Biodiversity"

Christian O. Marks and Helene C. Muller-Landau

Shiple *et al.* (Reports, 3 November 2006, p. 812) predicted plant community composition and relative abundances with a high level of accuracy by maximizing Shannon's index of information entropy (species diversity), subject to constraints on plant trait averages. We show that the entropy maximization assumption is relatively unimportant and that the high accuracy is due largely to a statistical effect.

Full text at www.sciencemag.org/cgi/content/full/316/5830/1425c

RESPONSE TO COMMENTS ON "From Plant Traits to Plant Communities: A Statistical Mechanistic Approach to Biodiversity"

Bill Shipley, Denis Vile, Éric Garnier

We maintain that there is no circularity or structural bias in our model that inflates its predictive ability beyond the sampling bias inherent in the r^2 statistic. When replacing observed average traits by environmental variables, the generality and predictive ability depends on one's empirical ability to predict these average values. Finally, maximizing rather than minimizing entropy given constraints is justified by axioms of information theory and is not an ecological assumption.

Full text at www.sciencemag.org/cgi/content/full/316/5830/1425d

Letters to the Editor

Letters (~300 words) discuss material published in *Science* in the previous 3 months or issues of general interest. They can be submitted through the Web (www.submit2science.org) or by regular mail (1200 New York Ave., NW, Washington, DC 20005, USA). Letters are not acknowledged upon receipt, nor are authors generally consulted before publication. Whether published in full or in part, letters are subject to editing for clarity and space.




Lab director.

Pipetman
Concept®

Just what you're
looking for in your lab:

- A true pioneer in the field, one of a kind in the industry
- A high-tech wiz, exceptionally computer savvy
- Adapts quickly to a multitude of job functions and lab protocols
- Easy to train and extremely intuitive
- Ability to track and report on every detail of a project
- Easy to read and guarantees high productivity
- Communicates well in both single-channels and multichannels
- Can manage small-to-large volumes of work

 Only (and always)
from Gilson.

Put it to work for you.
1-800-GILSON1
www.pipetman.com



FREE
with registration

Science Alerts in Your Inbox

Get daily and weekly E-alerts on the latest breaking news and research!



Get the latest news and research from *Science* as soon as it is published. Sign up for our e-alert services and you can know when the latest issue of *Science* or *Science Express* has been posted, peruse the latest table of contents for *Science* or *Science's* Signal Transduction Knowledge Environment, and read summaries of the journal's research, news content, or Editors' Choice column, all from your e-mail inbox. To start receiving e-mail updates, go to:

<http://www.sciencemag.org/ema>



EVOLUTION

God as Genetic Engineer

Sean B. Carroll

"The Lord hath delivered him into mine hands."

Those are the words that Thomas Huxley, Darwin's confidant and staunchest ally, purportedly murmured to a colleague as he rose to turn Bishop Samuel Wilberforce's own words to his advantage and rebut the bishop's critique of Darwin's theory at their legendary 1860 Oxford debate. They are also the first words that popped into my head as I read Michael J. Behe's *The Edge of Evolution: The Search for the Limits of Darwinism*. In it, Behe makes a new set of explicit claims about the limits of Darwinian evolution, claims that are so poorly conceived and readily dispatched that he has unwittingly done his critics a great favor in stating them.

In *Darwin's Black Box: The Biochemical Challenge to Evolution (1)*, Behe had forwarded the notion that certain biochemical systems were "irreducibly complex," could not have evolved stepwise by Darwinian mechanisms, and thus were intelligently designed. Since that earlier book, Behe has played a key role in the intelligent design (ID) movement, including a star turn as a defense witness in the 2005 Dover school board case. Despite his testimony—or, I should say, partly because of what he said (2)—ID was ruled to be a religious concept and its teaching in public schools unconstitutional.

Behe, a professor of biochemistry at Lehigh University, has found an audience among various flavors of creationists who find Darwinian evolution incompatible with their religious views and see scientific validation in Behe's claims. Clearly, this book's main audience would be that constituency, although they will find some parts very discomfiting. For instance, Behe explicitly accepts the ability of random mutation and selection to account for the variation within and differences between closely related species (but not higher taxa

such as vertebrate classes). He also accepts (as he has before) the 4.5-billion-year age of Earth and that we share a common ancestor with chimpanzees. That certainly won't go over well in some camps.

Behe also explores some examples of Darwinian evolution at the molecular level, including an extensive treatment of the evolutionary "trench warfare" fought between humans and malarial parasites over the millennia—all in the context of what Darwinian evolution "can do." So what's the problem?

The problem is what Behe asserts Darwinian evolution can't do: produce more "complex" changes than those that have enabled humans to battle malaria or allowed malarial parasites to evade the drugs we throw at them. Behe's main argument rests on the



assertion that two or more simultaneous mutations are required for increases in biochemical complexity and that such changes are, except in rare circumstances, beyond the limit of evolution. He concludes that "most mutations that built the great structures of life must have been nonrandom." In short, God is a genetic engineer, somehow designing changes in DNA to make biochemical machines and higher taxa.

But to arrive at this conclusion, Behe relies on invalid assertions about how genes and

proteins evolve and how proteins interact, and he completely ignores a huge amount of experimental data that directly contradicts his faulty premises. Unfortunately, these errors are of a technical nature and will be difficult for lay readers, and even some scientists (those unfamiliar with molecular biology and evolutionary genetics), to detect. Some people will be hoodwinked. My goal here is to point out the critical flaws in Behe's key arguments

and to guide readers toward some references that illustrate why what he alleges to be beyond the limits of Darwinian evolution falls well within its demonstrated powers.

Behe's chief error is minimizing the power of natural selection to act cumulatively as traits or molecules evolve

stepwise from one state to another via intermediates. Behe states correctly that in most species two adaptive mutations occurring instantaneously at two specific sites in one gene are very unlikely and that functional changes in proteins often involve two or more

sites. But it is a non sequitur to leap to the conclusion, as Behe does, that such multiple-amino acid replacements therefore can't happen. Multiple replacements can accumulate when each single amino acid replacement affects performance, however slightly, because selection can act on each replacement individually and the changes can be made sequentially.

Behe begrudgingly allows that only "rarely, several mutations can sequentially add to each other to improve an organism's chances of survival." Rarely? This, of course, is the everyday stuff of evolution. Examples of cumulative selection changing multiple sites in evolving proteins include tetrodotoxin resistance in snakes (3), the tuning of color vision in animals (4),

cefotaxime antibiotic resistance in bacteria (5), and pyrimethamine resistance in malarial parasites (6)—a notable omission given Behe's extensive discussion of malarial drug-resistance.

Behe seems to lack any appreciation of the quantitative dimensions of molecular and trait evolution. He appears to think of the functional features of proteins in qualitative terms, as if binding or catalysis were all or nothing rather than a broad spectrum of affinities or rates. Therefore, he does not grasp the funda-

The Edge of Evolution

The Search for the Limits of Darwinism

by Michael J. Behe

Free Press, New York, 2007.

331 pp. \$28, C\$33.99.

ISBN 9780743296205.

The reviewer, the author of *The Making of the Fittest*, is at the Laboratory of Molecular Biology, Howard Hughes Medical Institute, University of Wisconsin, Madison, WI 53706, USA. E-mail: sbcarroll@wisc.edu

mental reality of a mutational path that proteins follow in evolving new properties.

This lack of quantitative thinking underlies a second, fatal blunder resulting from the mistaken assumptions Behe makes about protein interactions. The author has long been concerned about protein complexes and how they could or, rather, could not evolve. He argues that the generation of a single new protein-protein binding site is extremely improbable and that complexes of just three different proteins "are beyond the edge of evolution." But Behe bases his arguments on unfounded requirements for protein interactions. He insists, based on consideration of just one type of protein structure (the combining sites of antibodies), that five or six positions must change at once in order to make a good fit between proteins—and, therefore, good fits are impossible to evolve. An immense body of experimental data directly refutes this claim. There are dozens of well-studied families of cellular proteins (kinases, phosphatases, proteases, adaptor proteins, sumoylation enzymes, etc.) that recognize short linear peptide motifs in which only two or three amino acid residues are critical for functional activity [reviewed in (7–9)]. Thousands of such reversible interactions establish the protein networks that govern cellular physiology.

Very simple calculations indicate how easily such motifs evolve at random. If one assumes an average length of 400 amino acids for proteins and equal abundance of all amino acids, any given two-amino acid motif is likely to occur at random in every protein in a cell. (There are 399 dipeptide motifs in a 400-amino acid protein and $20 \times 20 = 400$ possible dipeptide motifs.) Any specific three-amino acid motif will occur once at random in every 20 proteins and any four-amino acid motif will occur once in every 400 proteins. That means that, without any new mutations or natural selection, many sequences that are identical or close matches to many interaction motifs already exist. New motifs can arise readily at random, and any weak interaction can easily evolve, via random mutation and natural selection, to become a strong interaction (9). Furthermore, any pair of interacting proteins can readily recruit a third protein, and so forth, to form larger complexes. Indeed, it has been demonstrated that new protein interactions (10) and protein networks (11) can evolve fairly rapidly and are thus well within the limits of evolution.

Is it possible that Behe does not know this body of data? Or does he just choose to ignore it? Behe has quite a record of declaring what is impossible and of disregarding the scientific literature, and he has clearly not learned any

lessons from some earlier gaffes. He has again gone "public" with assertions without the benefit (or wisdom) of first testing their strength before qualified experts.

For instance, Behe once wrote, "if random evolution is true, there must have been a large number of transitional forms between the *Mesonychia* [a whale ancestor] and the ancient whale. Where are they?" (12). He assumed such forms would not or could not be found, but three transitional species were identified by paleontologists within a year of that statement. In *Darwin's Black Box*, he posited that genes for modern complex biochemical systems, such as blood clotting, might have been "designed billions of years ago and have been passed down to the present ... but not 'turned on'." This is known to be genetically impossible because genes that aren't used will degenerate, but there it was in print. And Behe's argument against the evolution of flagella and the immune system have been dismantled in detail (13, 14) and new evidence continues to emerge (15), yet the same old assertions for design reappear here as if they were uncontested.

The continuing futile attacks by evolution's opponents reminds me of another legendary confrontation, that between Arthur and the Black Knight in the movie *Monty Python and the Holy Grail*. The Black Knight, like evolution's challengers, continues to fight even as each of his limbs is hacked off, one by one. The "no transitional fossils" argument and the "designed genes" model have been cut clean off, the courts have debunked the "ID is science" claim, and the nonsense here about the edge of evolution is quickly sliced to pieces by well-established biochemistry. The knights of ID may profess these blows are "but a scratch" or "just a flesh wound," but the argument for design has no scientific leg to stand on.

References

1. M. J. Behe, *Darwin's Black Box: The Biochemical Challenge to Evolution* (Free Press, New York, 1996).
2. Kitzmiller et al. v. Dover Area School District et al., Memorandum Opinion, 20 December 2005; www.pamd.uscourts.gov/kitzmiller/decision.htm.
3. S. L. Geffeney et al., *Nature* **434**, 759 (2005).
4. S. B. Carroll, *The Making of the Fittest: DNA and the Ultimate Forensic Record of Evolution* (Norton, New York, 2006).
5. D. M. Weinreich, N. F. Delaney, M. A. DePristo, D. L. Hartl, *Science* **312**, 111 (2006).
6. W. Sirawaraporn et al., *Proc. Natl. Acad. Sci. U.S.A.* **94**, 1124 (1997).
7. V. Neduva et al., *PLoS Biol.* **3**, e405 (2005).
8. R. P. Bhattacharyya, A. Reményi, B. J. Yeh, W. A. Lim, *Annu. Rev. Biochem.* **75**, 655 (2006).
9. V. Neduva, R. B. Russell, *FEBS Lett.* **579**, 3342 (2005).
10. Y. V. Budovskaya, J. S. Stephan, S. J. Deminoff, P. K. Herman, *Proc. Natl. Acad. Sci. U.S.A.* **102**, 13933 (2005).
11. P. Beltrao, L. Serrano, *PLoS Comput. Biol.* **3**, e25 (2007).
12. M. J. Behe, in *Darwinism, Science or Philosophy?*, J. Buell, V. Hearn, Eds. (Foundation for Thought and Ethics, Richardson, TX, 1994), pp. 60–71.
13. A. Bottaro, M. A. Inlay, N. J. Matzke, *Nat. Immunol.* **7**, 433 (2006).
14. M. J. Pallen, N. J. Matzke, *Nat. Rev. Microbiol.* **4**, 784 (2006).
15. R. Liu, H. Ochman, *Proc. Natl. Acad. Sci. U.S.A.* **104**, 7126 (2007).

10.1126/science.1145104

EVOLUTION

A Multilevel Exploration

David Jablonski

In the natural world, as in human societies, complexity is almost always organized hierarchically. From the nested structures of armies and corporations to the classical biological progression from molecule to cell to tissue to body to species, the "particles" at each level tend to be grouped into ever more inclusive units. However, despite the ubiquity of natural hierarchies, their evolutionary implications have been anything but clear.

Evolution and the Levels of Selection is a major contribution toward putting this controversial area on a coherent conceptual and philosophical footing. Samir Okasha's argument hinges on two components,

neither of them new but here powerfully and creatively integrated and extended. First is the fundamental distinction between two disparate kinds of multilevel selection (MLS), often conflated despite their formal introduction 20 years ago (1), with even earlier precedents. The failure to appreciate this distinction has generated an enormous amount of confusion, at times bordering on fury, and Okasha's use of this conceptual framework brings exceptional clarity and precision to a wide range of issues. In essence, for MLS1 the sole focal level is the individual (at any level), but its fitness depends partly on the group to which it belongs. The classic example is the seeming paradox of altruism: how can selection drive behavior that aids others at the

Evolution and the Levels of Selection

by Samir Okasha

Clarendon Press, Oxford,
2006. 275 pp. \$55, £30.
ISBN 9780199267972.

The reviewer is in the Department of Geophysical Sciences and Committee on Evolutionary Biology, University of Chicago, 5734 South Ellis Avenue, Chicago, IL 60637, USA. E-mail: djablons@uchicago.edu

Receive a free TaqMan® Low Density Array Upgrade and 20 Free TaqMan® Array cards*
Visit 7900HT.com to learn more.

Proven Performance in Labs Everywhere. Customized for Yours.



Applied Biosystems 7900HT Fast Real-Time PCR System Meets Your Changing Needs.



The gold standard in real-time PCR

Used by researchers all over the world and referenced in hundreds of journals, the Applied Biosystems 7900HT Fast Real-Time PCR System is the recognized gold standard in real-time PCR.



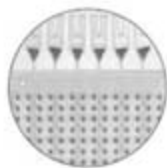
Interchangeable blocks

Configurable and highly flexible, the 7900HT Fast System offers user-interchangeable thermal cycling blocks, cycling times as low as 35 minutes and automated plate loading/unloading for higher throughput.



The world's largest collection of assays

Choose from over 2 million TaqMan® Gene Expression, Genotyping and miRNA Assays.



Easy, pre-loaded assays in a micro fluidic card format

For the ultimate in ease-of-use, order your assays pre-loaded in the 384-well TaqMan® Low Density Array.

To see how the 7900HT Fast System meets your changing research needs, visit www.7900HT.com

AB Applied Biosystems

* Receive a Low Density Array Upgrade and 20 Free TaqMan® Low Density Array cards with the purchase of an Applied Biosystems 7900HT Fast Real-Time PCR System. This offer cannot be combined with other promotions or discounts. Offer valid until March 31, 2006. Void where prohibited. This offer is for US customers only — International customers please inquire with your local sales office. Other restrictions may apply. All prices exclude any applicable delivery and/or local tax. Please contact your local Sales Representative for other details of this offer. <http://www.7900HT.com>

For Research Use Only. Not for use in diagnostic procedures. The Applied Biosystems 7900HT Fast Real-Time PCR System is covered by U.S. Patents Nos. 6,563,581 and 6,719,949. The Applied Biosystems 7900HT Fast Real-Time PCR System base unit equipped with its sample block module is an Authorized Thermal Cycler for PCR and may be used with PCR licenses available from Applied Biosystems. Its use with Authorized Reagents also provides a limited PCR license in accordance with the label rights accompanying such reagents. This instrument is licensed under U.S. Patent No. 6,814,934 and corresponding claims in its non-U.S. counterparts and under one or more of U.S. Patents Nos. 5,038,852, 5,656,493, 5,333,675, 5,475,610 or 6,703,236, or corresponding claims in their non-U.S. counterparts, for use in research. Purchase of this instrument does not convey any right to practice the 5' nuclease assay or any of the other real-time methods or rights under any other patent claims or for any other application expressly, by implication, or by estoppel. Applied Biosystems and AB (Design) are registered trademarks and Applied is a trademark of Applied Biosystems Corporation or its subsidiaries in the US and/or certain other countries. TaqMan is a registered trademark of Roche Molecular Systems, Inc. ©2007 Applied Biosystems. All rights reserved.

actor's expense? Under MLS1, altruists have lower fitnesses within their groups than selfish individuals, but groups containing a higher proportion of more altruists contribute more individuals to the global population. Okasha (a philosopher of science at the University of Bristol) greatly clarifies this process and shows how its logic can apply to many evolutionary problems, from the operation of selfish intracellular elements to the origin of complex cells.

In contrast, MLS2 involves multiple focal levels, with selection operating on units at each of those levels simultaneously and with effects cascading both upward and downward. The classic example is species selection, where

ness that can provide a formal separation of levels of selection. One of the real pleasures of this book is watching Okasha view a succession of problems in multilevel selection through the lens of the Price equation in its different forms. It proves a powerful conceptual tool, although it does not always perform ideally. For example, Okasha finds the Price equation to be theoretically inferior to an alternative called contextual analysis as an approach to detecting MLS1.

Okasha is not quite as precise on the notion of emergent properties, another highly contentious area in the multilevel selection debates. Okasha recognizes the existence of such properties, irreducible to characters at

of opposing concepts of emergence, see (3).]

The final chapter derives fresh insights from Okasha's integrative framework for some of the most profound evolutionary events in the history of life. The evolutionary transitions to new kinds of individuals—from prokaryote to eukaryote, unicell to multicellular organism—must have entailed the subordination of lower-level units into a larger whole. Okasha makes a strong argument that such transitions involve both types of multilevel selection, operating in succession. His deep understanding of the evolutionary models and his integration of the philosophical issues really pay off here. This chapter alone is worth the price of the book.

Elsewhere in the book, however, MLS2 seems to get short shrift. This is a shame,

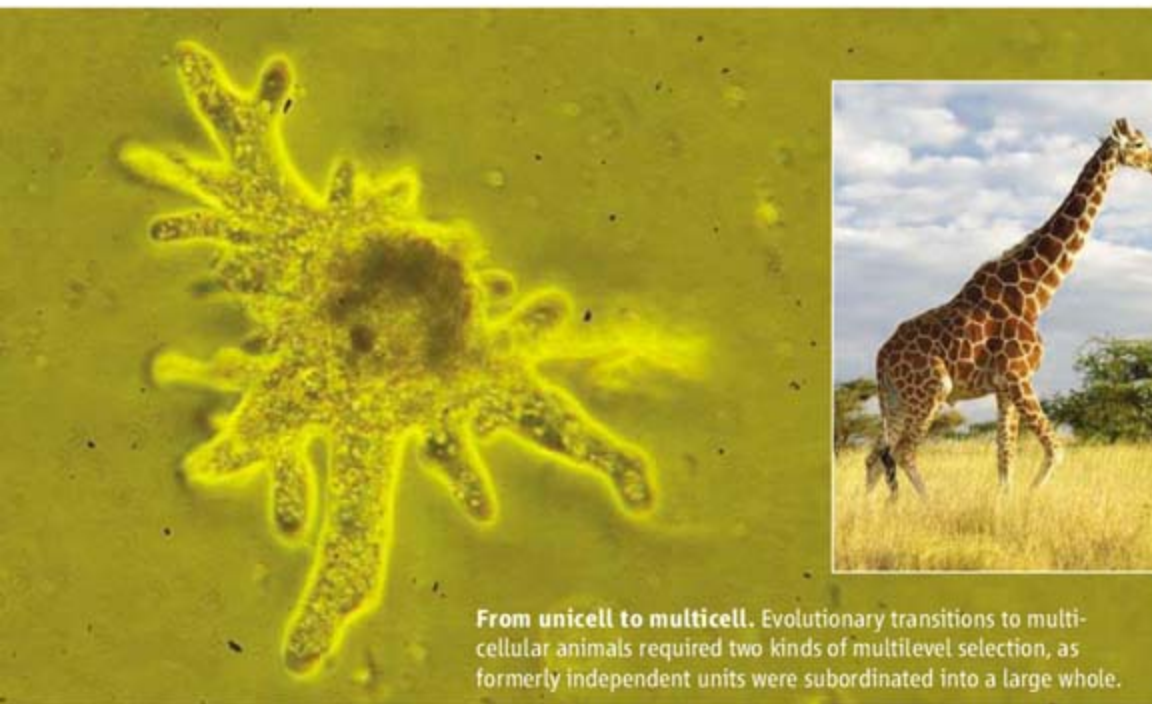
because that is another growth area that could benefit from closer philosophical attention. As Okasha notes, most workers concede the plausibility of MLS2; the uncertainty lies in the efficacy of processes above and below the traditional dynamics of bodies within populations. But species selection receives the shortest chapter in the book, and the burgeoning macroecological literature on the size, position, phylogenetic distribution, and organismic correlates of geographic range (accepted by Okasha as a potential factor in strict-sense species selection) is not mentioned. Nor is the even larger paleontological and neontological literature on comparative analyses of

clades, where organismic and species properties are tested for their statistical associations with differential diversification rates. I was eager to see Okasha bring his conceptual arsenal more fully to bear on these and other nearly unexplored potential sources of data and theory. [(4) offers an entry into these aspects of the debate.]

A hierarchical view of the evolutionary process, with potentially opposing, reinforcing, or orthogonal forces in play at multiple levels, may be harder to grapple with than the more traditional view, but Okasha has greatly clarified many of the central issues. I can't imagine anyone working on multilevel selection—or attempting to dismiss it—without reading this book.

References

1. I. L. Heister, J. Damuth, *Am. Nat.* **130**, 582 (1987).
2. S. J. Gould, *The Structure of Evolutionary Theory* (Harvard Univ. Press, Cambridge, MA, 2002); reviewed by D. J. Futuyma, *Science* **296**, 661 (2002).
3. T. A. Grantham, *Palaeontology* **50**, 75 (2007).
4. D. Jablonski, *Palaeontology* **50**, 87 (2007).



From unicell to multicell. Evolutionary transitions to multicellular animals required two kinds of multilevel selection, as formerly independent units were subordinated into a large whole.

both organisms within populations and species within lineages are subject to differential survival and reproduction according to heritable variation. Variations in speciation rates, extinction rates, or both can thus drive large-scale evolutionary changes independent of the fitnesses of the organisms within those species and can indirectly shift the mean phenotypes of lineages. Okasha notes that such indirect effects, often termed “upward and downward causation,” are the essence of multilevel selection. When is the differential proliferation of a given biological property on some level the result of direct selection at that level, and when is it a by-product of processes at a lower or higher level? (As Okasha makes clear for the first time, these cross-level processes are fundamentally different under MLS1 and MLS2.)

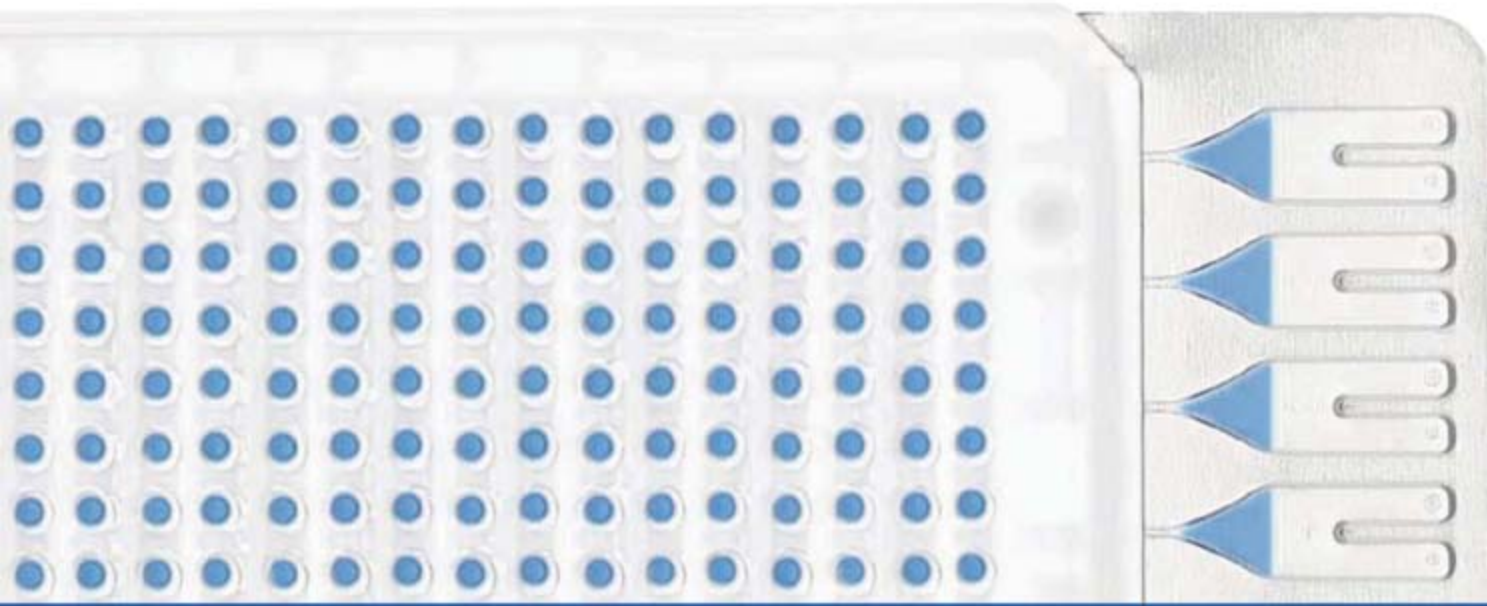
To address this problem, Okasha applies the second major element of his argument: the Price equation, a general statistical statement of the covariance between a character and fit-

ness at lower hierarchical levels, but does not see them as required for the operation of multilevel selection. For him, the essence of the problem is the emergent relation between a character and fitness at a given level. This is a reasonable stance, although not the only one possible. In fact, in several places Okasha skates very close to treating emergent species properties as integral to the operation of species selection, as did Stephen Jay Gould in his magnum opus (2). For example, Okasha accepts that the increased frequency over time of gastropod species having larvae that do not feed in the plankton should be classified as species selection because “[d]ifferences in species’ fitness were not caused by differences in the fitnesses of their constituent organisms, but by differences in the extent of within-species gene flow.” [Such gene flow, with the associated genetic population structure, is arguably a species-level property; for a lucid analysis

Now Available!

Custom panels in smaller, 10-card order sizes.

384 Wells. Preloaded for TaqMan® Performance.



Readily available TaqMan® Arrays deliver speed, accuracy and sensitivity to your real-time PCR gene expression analysis.

TaqMan® Low Density Array Gene Signature Panels are readily available, expertly-designed, focused gene sets that don't require liquid handling robots or complex pipetting to use. Simply add your cDNA and TaqMan® Universal PCR Master Mix into the eight sample ports of this micro fluidic card and instantly run 384 real-time PCR reactions on the 7900HT Fast Real-Time PCR System. The Gene Signature Panels come pre-loaded with TaqMan® Gene Expression Assays, so you get the accuracy, reproducibility, and specificity that only TaqMan® Assays can provide. It's the fast and affordable way to validate microarray hits and screen pathways and biomarkers without the worry and difficulty associated with 96-well plates or individual tubes.

Order from the growing portfolio of TaqMan® Low Density Array Gene Signature Panels:

- Human or Mouse GPCR Panel
- Human or Mouse Immune Panel
- Human, Mouse, or Rat Endogenous Control Panel
- Human Protein Kinase Panel
- Human Apoptosis Panel
- Human ABC Transporter Panel

More panels will be available soon! Register to receive new Gene Signature Panel product announcements or suggest a panel of your own at tlda.appliedbiosystems.com



The perfect combination: the TaqMan Low Density Array and Applied Biosystems 7900HT Fast Real-Time PCR System.

AB Applied Biosystems

Applied Biosystems is committed to providing the world's leading technology and information for life scientists. Applied Biosystems consists of the Applied Biosystems and Celeris Genomics businesses. For Research Use Only. Not for use in diagnostic procedures. Practice of the patented 5' Nuclease Process requires a license from Applied Biosystems. The purchase of TaqMan® Low Density Array Gene Signature Panels includes an immunity from suit under patents specified in the product insert to use only the amount purchased for the purchaser's own internal research when used with the separate purchase of an Authorized 5' Nuclease Core Kit. No other patent rights are conveyed expressly, by implication, or by estoppel. For further information on purchasing licenses contact the Director of Licensing, Applied Biosystems, 850 Lincoln Centre Drive, Foster City, California 94404, USA. The TaqMan® Low Density Array is covered by U.S. Patents Nos. 6,514,750 and 6,942,837. Micro Fluidic Card developed in collaboration with 3M Company. Applied Biosystems and AB (Design) are registered trademarks and Applied is a trademark of Applied Biosystems or its subsidiaries in the US and/or certain other countries. TaqMan is a registered trademark of Roche Molecular Systems, Inc. ©2007 Applied Biosystems.

SCIENCE AND SECURITY

Practical Experiences in Dual-Use Review

E. Megan Davidson,¹ Richard Frothingham,² Robert Cook-Deegan^{3*}

Bioscience is under increased scrutiny for “dual-use” concerns. Dual-use in this sense refers to research with the potential both to generate valuable scientific knowledge and to be used for nefarious purposes, with serious consequences for public health or the environment (1). In April 2007, the U.S. National Science Advisory Board for Biosecurity (NSABB) released draft guidance for local and federal oversight of such research (2). NSABB proposed that individual researchers identify substantive dual-use concerns in their work and confer with local institutional bodies in managing risks. Since 2004, the Southeast Regional Center of Excellence for Emerging Infections and Biodefense (SERCEB) has reviewed research project applications for dual-use potential. Of 27 proposals for internal SERCEB funding, 10 contained “dual-use research of concern” as defined by the NSABB, some prompting further action (3). This high “hit rate” is mainly attributable to SERCEB’s research focus on pathogens and host defenses. The rate would not be nearly as high for biomedical and bioengineering research more broadly.

SERCEB’s experience is relevant to current debates on identification and management of dual-use research risks. Formal dual-use review with analysis of risk management options might enable some valuable research to move forward, which would otherwise be forgone because of biosecurity concerns.

SERCEB Dual-Use Review (2004–07)

SERCEB has been funded since 2003 by the National Institute of Allergy and Infectious Diseases to develop drugs, vaccines, and diagnostics for biodefense and emerging infections. In addition to research programs, SERCEB has a Policy, Ethics, and Law (PEL) Core (4).

SERCEB first encountered dual-use concerns in 2004 when its Steering Committee reviewed project proposals for internal funding. One application proposed creating a



reverse genetic system to study a viral hemorrhagic fever (VHF)—a high scientific priority but also a serious dual-use concern. Having read the Fink Report (5), the Steering Committee asked the PEL Core to review this and other proposals for dual-use concerns. Little guidance for dual-use review existed then. The sparse literature available addressed review of publications on completed research, rather than prospective review for funding and oversight (6). The NSABB had yet to be formed, and two reports from the U.S. National Academies addressing dual-use concerns had not yet been released (7, 8). SERCEB’s review of the VHF proposal is summarized as example 1 in the supporting online material (SOM) (9).

This case illustrates a common theme in the dual-use cases reviewed by SERCEB. Any genetic manipulation of a pathogen has some potential to enhance virulence, although attenuation is the more likely result. This principal investigator (PI) considered discovery of a hypervirulent mutant to be unlikely, but not impossible, and noted the difficulty of identi-

The U.S. government is debating how to handle national security risks posed by bioscience research. A research consortium shares lessons learned from their research oversight scheme.

fying hypervirulence in a pathogen that is nearly 100% fatal in the animal model. The PI proposed methods to manage the risk by attenuating the virus. Although the PI proposed to deal with publication issues raised by a dual-use discovery by suppression and reporting to “an appropriate governmental institution,” the PEL Core recommended that plans for publication be deferred until and unless a dual-use concern actually resulted, at which time the PI would discuss publication strategies and content with the SERCEB Steering Committee. Generally, we would favor modification of publications when feasible rather than the suppression of scientific results.

In a second case from 2004 (9), the objective was to enhance efficacy of vaccines by blocking activation of T cells responsible for limiting immune response. The dual-use concern was that experi-

mental interventions might result in discovery of methods for suppressing immunity and overwhelming the host response to a pathogen. The SERCEB queries and investigator responses suggested destruction of research materials and suppression of research results, both drastic responses to dual-use concerns. Today, SERCEB would be more likely to recommend other management approaches, such as placing stocks in physically secure spaces, training all personnel involved in dual-use issues before beginning research, and modifying publications to report results but limiting details about methods that could enable misuse, rather than suppressing publication completely.

Two issues became apparent during SERCEB dual-use review: few investigators were aware of the dual-use dilemma, and technical expertise was critical in assessing dual-use risk. SERCEB addressed the first problem through education and awareness training, as recommended by the Fink Report and underscored by the NSABB. In September 2005, the PEL Core released an online education

¹Duke University Medical Center, Durham, NC 27710, USA. ²Duke Human Vaccine Institute, Duke University Medical Center, Durham, NC 27710, USA. ³Institute for Genome Sciences and Policy, Duke University, Durham, NC 27708, USA. *Author for correspondence. E-mail: bob.cd@duke.edu

module to introduce researchers to dual-use issues, to present prominent cases, to describe relevant laws and regulations, and to highlight scientists' responsibilities to promote biosecurity (10). By May 2007, more than 450 individuals had completed this module (11).

The need for technical expertise was addressed by engaging investigators in the dual-use review. They were asked to consider the likelihood that their work would increase the dangerousness of an agent through increased pathogenicity or broadened host range or would enhance its dispersal and, thus, its potential as a biological weapon and to consider the magnitude of possible harm. This model of posing questions directly to potential PIs resembles the "points-to-consider" process used by NIH for some clinical research (12). Examples of questions posed in a recent proposal evaluation are shown in the figure on page 1432 (9).

Reviewers and investigators have jointly developed plans to minimize and manage dual-use risks. Strategies have included training, laboratory security, experimental design, sponsor notification, and prepublication review. Training has included requiring lab members to take the online module and facilitating lab group discussions. Experimental design changes to mitigate dual-use risk include substituting a marker protein for a toxin in a proof-of-principle experiment and replacing a virulent microbe with an attenuated strain to obtain information of equal scientific value through safer means. During publication, authors could often reduce dual-use potential by limiting details on production methods while conveying key scientific results. For projects with significant dual-use concern, investigators were also asked to develop response plans for dual-use discoveries by determining to whom such discoveries would be reported, and how to communicate results. These risk-management strategies enhance foresight and allow investigators to share responsibility with relevant stakeholders. SERCEB review has resulted in modifications to proposed research, but no projects have been halted or publications stopped because of dual-use concerns.

Discussion

The NSABB draft guidance of April 2007 recommends making education on dual-use issues a required component of research ethics training. The SERCEB experience supports this recommendation, as many investigators were unaware of dual-use issues in their own research. NSABB draft guidance also calls for individual investigators to determine

whether their research poses dual-use risks of concern. If so, it recommends they be considered by an institutional committee. As suggested by the Fink Report, Institutional Biosafety Committees (IBCs) are one possibility. Dual-use research poses potential biosafety hazards about which IBCs are legitimately concerned. For example, enhanced biosafety procedures would be required for a pathogen with enhanced virulence, increased infectivity, or a broadened host range. One problem with delegating risk identification entirely to investigators is that, in our experience, sensitivity to dual-use concerns is highly subjective. Indeed, those most sensitive to risk are also more likely to have thought through risk reduction and avoidance. The least-sensitive investigators may be the greatest risk.

Although formal regulations have yet to be devised, three of six SERCEB IBCs have assumed responsibility for dual-use review. In 2006, Duke University and the University of Florida revised their recombinant DNA registration forms to include questions identifying dual-use potential (13, 14). Emory University's Institutional Health and Biosafety Committee established a Biosecurity Subcommittee to consider dual-use concerns. The three other SERCEB universities are considering their options and awaiting more specific guidance from NSABB and NIH. As noted by the NSABB, some dual-use research (such as research to enhance pathogen dispersal or delivery) would not normally come to IBCs, because their primary responsibility is the review of recombinant DNA research. It may prove worthwhile to create regional or national review bodies to which novel or complex dual-use cases can be referred.

Responsibility to recognize and address dual-use discoveries begins with investigators, but it cannot end there. Policy-makers and administrators should provide researchers with information that will enable them to identify dual-use concerns, as well as institutional resources to assist in their management. Institutions and funding organizations need to develop mechanisms to assist investigators in conducting dual-use review and in devising plans of action when dual-use materials and information are discovered. Some scientists have expressed legitimate concern that attention to dual-use issues will stymie their research. At institutions with significant commitments to research on pathogens and toxins, benefits of raising awareness and devising contingency plans are likely to outweigh costs. Scientists and research oversight bodies will need to make modest investments in dual-use education, review, and reporting. Our hope is that our experience and the experience of other

institutions will contribute to development of effective and balanced local review approaches and will avoid extreme policies that could impede research.

SERCEB's dual-use review policies have changed with growing experience from 2004 to 2007. This has been a learning process that we expect will become more clearly defined over time.

References and Notes

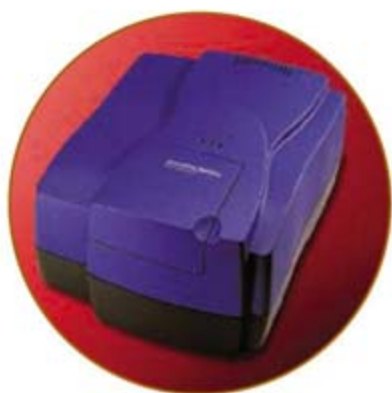
1. R. M. Atlas, M. Dando, *Biosecur. Bioterror.* **4**, 276 (2006).
2. Working Group on Oversight Framework Development, draft report presented at meeting of the National Science Advisory Board for Biosecurity, National Institutes of Health, Bethesda MD, 19 April 2007.
3. Working Group on Oversight Framework Development, Dual Use Criteria Working Group status report presented at meeting of the National Science Advisory Board for Biosecurity Meeting, National Institutes of Health, Bethesda MD, 30 March 2006.
4. Southeast Regional Center of Excellence for Emerging Infections and Biodefense (SERCEB), Policy, Ethics and Law Core; www.serceb.org/pel.
5. Committee on Research Standards and Practices to Prevent the Destructive Application of Biotechnology, *Biotechnology Research in an Age of Terrorism* (National Academies Press, Washington, DC, 2004). Referred to throughout as "the Fink Report;" authoring committee chaired by molecular geneticist Gerald R. Fink.
6. Journal Editors and Authors Group, *Science* **299**, 1149 (2003).
7. Committee on Genomics Databases for Bioterrorism Threat Agents, *Seeking Security: Pathogens, Open Access, and Genomic Databases* (National Academies Press, Washington, DC, 2004).
8. Committee on Advances in Technology and the Prevention of Their Application to Next Generation Biowarfare Threats, *Globalization, Biosecurity, and the Future of the Life Sciences* (National Academies Press, Washington, DC, 2006).
9. Further information (questions, PI responses, and PEL Core recommendations) is presented in the Supporting Online Material.
10. SERCEB: Policy, Ethics and Law Core, "The Dual-Use Dilemma in Bioscience Research" (SERCEB, Durham, NC, 2005); www.serceb.org/pel/module.
11. As of 9 May 2007, 333 individuals from SERCEB institutions had completed the module. Other users are from various organizations, including NIH, Centers for Disease Control and Prevention, and the World Health Organization.
12. Such a process was adopted by the Human Gene Therapy Subcommittee of the Recombinant DNA Advisory Committee (Office of the Director, NIH, Bethesda, MD, April 2002); www4.od.nih.gov/oba/rac/guidelines/guidelines.html.
13. Duke University Occupational and Environmental Safety Office, "Recombinant DNA Registration Form" (Duke University, Durham, NC, March 2006); www.safety.duke.edu/LabSafety/Docs/ibcform_2006update.doc.
14. University of Florida Department of Environmental Health and Safety, "Recombinant DNA Research Registration" (University of Florida, Gainesville, FL, 2006); www.ehs.ufl.edu/Bio/Files/rdna.doc.
15. Support was provided by the Southeast Regional Center of Excellence for Emerging Infections and Biodefense (NIH/NIAID grant U54 AI 057157), and Duke University School of Medicine.

Supporting Online Material

www.sciencemag.org/cgi/content/full/316/5830/1432/DC1

10.1126/science.1142873

More Microarray Applications



Molecular Devices offers the most broadly applicable microarray scanning and analysis package on the market. With the industry-leading Axon GenePix® system, you can perform virtually any fluorescent microarray application in a standard microscope slide format.

- ⊕ Gene Expression: Easily scan and analyze 1-color to 4-color arrays from any source, whether home-brewed or commercially manufactured
- ⊕ Comparative Genomic Hybridization (CGH): Unique AutoPMT function in Axon GenePix Pro ensures optimal scans using all array features
- ⊕ Protein array: Non-confocal 64 μm focal depth ensures optimal imaging of membrane-slide protein arrays, and surface scanning allows the use of non-transparent substrates
- ⊕ ChIP-Chip and Methylation: Visualize results in genomic context with Axon Acuity® software's Chromosome Viewer
- ⊕ And many others: If it's fluorescent and fits within a standard slide format, we can accommodate it.

Arcturus® Microgenomics and Axon Microarray Tools

- ⊕ **NEW!** Arcturus Turbo Labeling™: RNA/DNA labeling for microarrays
- ⊕ Axon GenePix 4100A, 4000B, 4200A, and 4200AL microarray scanners for the full spectrum of applications and throughput
- ⊕ Axon GenePix Pro 6 image analysis and Axon Acuity 4 microarray informatics software

Expect more. We'll do our very best to exceed your expectations.

Molecular Devices

now part of MDS Analytical Technologies

tel. +1-800-635-5577 | www.moleculardevices.com

SmartShutter™ Stepper-Motor Driven Shutter

- As fast as 8msec from trigger to open or close
- Choose between fast or "soft" speeds
- Programmable control of exposure time delay
- Free running or timed interval operation
- Variable aperture settings for neutral density
- Life tested to over 100 million cycles
- 25mm, 35mm or 50mm shutters available
- Modular repairable design
- USB or TTL control



SUTTER INSTRUMENT

ONE DIGITAL DRIVE, NOVATO, CA 94949
PHONE: 415.883.0128 | FAX: 415.883.0572
EMAIL: INFO@SUTTER.COM | WWW.SUTTER.COM

Science Classic

The complete
Science archive
1880–1996

Fully integrated with
Science Online
(1997–today)

Available to institutional
customers through a site license.
Contact ScienceClassic@aaas.org
for a quote.

Information: www.sciencemag.org/classic



PHYSICS

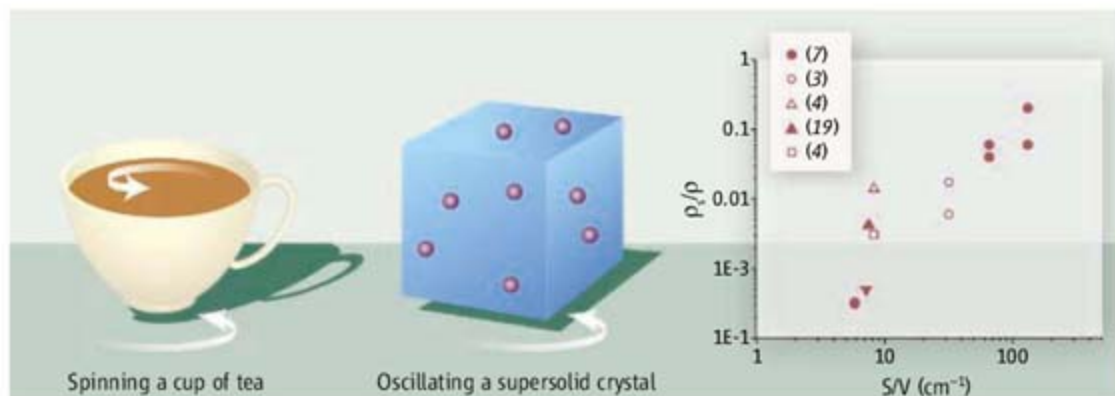
Cracking the Supersolid

Philip Phillips and Alexander V. Balatsky

We routinely teach physics students that the rotational motion of a rigid body is strongly determined by its moment of inertia. However, calculating this basic property in the usual way would be futile in the case of a supersolid (1). A supersolid is one of the truly enigmatic quantum states of matter, whereby atoms that remain locked in crystalline order can also resist rotation if the crystal is rotated (see the figure). Indeed, it is the richness of quantum mechanics that permits this seemingly paradoxical behavior. Experiments on solid helium-4 show that anywhere from 0.14 to 20% (2–6) of the atoms remain still while the rest rotate with the container. In this situation, the nonrotating atoms are detected as a “missing moment of inertia” (MMI). The current debate regarding the observation of MMI in solid helium-4 centers on whether superflow (and hence supersolidity) is the root cause or whether some other, perhaps nonequilibrium, phase is responsible. Several groups have recently reported results that may help narrow down the underlying mechanisms.

The phenomenon of MMI is well known in superfluids. At sufficiently low temperature, the angular momentum of a rotating container of liquid helium-4 disappears if the rotation is so slow that vortices are not excited. This effect is a benchmark test of equilibrium superfluidity. MMI in a superfluid requires that (i) the single-atom wave functions extend over the entire sample, and (ii) some fraction of atoms Bose-condense. For a perfect crystalline solid—that is, one in which the number of atoms equals the number of lattice sites—neither of these conditions can be satisfied.

To obtain both crystallinity and MMI, Andreev and Lifshitz (7) and others (1, 8) focused on the quantum mechanical motion associated with vacancy (missing atom) or interstitial (atom between lattice sites) defects. Such defects occur, in principle, in any solid, and they can Bose-condense at sufficiently low temperature. In such a scenario, the



Super strangeness. (Left) A normal liquid rotates with its container. (Center) Superfluids and supersolids, on the other hand, include atoms that remain stationary while the rest of the material oscillates. (Right) Rittner and Reppy (6) noticed that all of the experimental values for the MMI (the ratio of supersolid density ρ_s to total density ρ) fall onto a universal curve as a function of the surface-to-volume ratio. [Graph adapted from (6)]

defects are the superfluid while the helium-4 atoms maintain long-range crystal order.

Although the vacancy scenario has been adopted (9) to explain the MMI in the 2004 experiments of Kim and Chan (2) on solid helium-4, such explanations leave a residue. First, accurate calculations indicate that vacancy-type defects separate into distinct phases in pure solid helium-4 rather than form a supersolid (10).

Second, the experimental bounds on the number of defects determined by Simmons and colleagues (11) is far lower (0.3%) than the modest superfluid fraction of 2% seen in the early experiments of Kim and Chan. In fact, on the basis of the expression for the Bose condensation temperature in the dilute regime, it is straightforward to show that vacancy defects with a density of 0.3% already condense at 200 mK, the onset temperature for the MMI in the Kim and Chan experiments—a further indication that the defect scenario cannot quantitatively explain the data.

Third, Blackburn *et al.* (12) have observed no low-temperature anomaly in the Debye-Waller factor (the reduction of x-ray or neutron scattering intensity because of thermal atomic motion) below the onset temperature of the MMI in the Kim and Chan experiment. Absence of such an anomaly casts doubt on the MMI being associated with a true phase transition driven by defects.

Fourth, Rittner and Reppy (6) have shown that the MMI signal is acutely sensitive to the quench time for solidifying the liquid. In one extreme, they found the MMI to be absent in fully annealed samples. This experiment is

Recent experimental and theoretical work shows that frozen helium must have atomic disorder rather than perfect crystallinity for it to become a supersolid.

still in dispute, as not all groups (13–15) have been able to eliminate the MMI by sample annealing. In the other extreme, the MMI increased to an astounding 20% (see the figure) in samples in which the solidification from the liquid occurred in less than 2 min (6). A narrow annular region that maximized the surface-to-volume ratio enabled such rapid cooling of the sample and ensured a high degree of frozen-in disorder. This striking feature suggests that supersolidity is not intrinsic to pure solid helium-4. Rather, some kind of disorder, dislocation-induced plasticity, or glassy ordering (16–18) is the efficient cause.

Ultimately, the sharp test of supersolidity is persistent mass flow, much the way a persistent electrical current flows in a superconductor. The key success thus far is that of Sasaki *et al.* (19), who observed mass flow only in samples containing grain boundaries. However, the precise relationship between this experiment and the torsional oscillator measurements is unclear because mass flow was observed at temperatures (1.1 K, not far from the bulk superfluid transition temperature) vastly exceeding the onset temperature for MMI in the torsional oscillator experiments (5), namely $T_c = 0.2$ K.

The team led by Beamish (20) has looked specifically for pressure-induced mass flow through two parts of the sample separated by a set of micrometer-sized capillaries, and they have seen no telltale signature. Relying on the fact that true superflow should exhibit a thermodynamic signature, Todoshchenko *et al.* (21) measured the melting curve of helium-4 between 10 and 320 mK. They observed no

deviation from the expected behavior in ultra-pure samples with a helium-3 concentration of 0.3 parts per billion. Such an experiment is not sufficient to rule out superflow in the highly polycrystalline samples, but it is a clear indication that superflow is not intrinsic to the pure helium-4 but rather is an extrinsic disorder-driven effect. In fact, the dramatic effect that helium-3 impurities have on enhancing T_c (4) is a further indicator that disorder is pivotal.

Hence, the question remains: Is the observation of MMI in the torsional oscillator experiments now seen by numerous groups around the world an example of true superflow? Short of a direct observation of persistent mass flow, it is essential that thermodynamic measurements (21) be carried out on the polycrystalline samples of Rittner and Reppy (6). In addition, neutron scattering and x-ray tomography measurements below 200 mK on the polycrystalline samples could offer unprecedented insight into the defect structure that enables the observed MMI.

Ultimately, if disorder is key, then several questions arise. Why is the signal (2) for helium in vycor (silica glass) so anomalously low? Vycor has a surface-to-volume ratio that exceeds any of the samples shown in the figure by four orders of magnitude, whereas its MMI is only 0.4%. Can grain boundaries account for a 20% MMI? Can a system in which 20% of the atoms flow along grain boundaries be properly thought of as a crystal? What is the quantitative theory behind the helium-3 enhancement of T_c seen by Clark and Chan (4)?

In light of the disorder data, there are two classes of theoretical proposals left standing. First, there are the theories (16, 17) that rely on some sort of disordered supercomponent present in solid helium-4. In fact, one of us (P.P.) has collaborated on calculations (17) that provide a quantitative explanation of the enhancement of T_c caused by helium-3 impurities on the basis of this model. Within such a model, one can argue that the absence of MMI in the pure system arises because helium-4 atoms in a hexagonal close-packed lattice form a Mott insulator (which prevents flow). Disorder is expected to destroy a bosonic Mott state and give rise to a superfluid.

Then there are proposals from a collaboration involving one of us (A.V.B.) for bosonic glassy states in which MMI is obtained without ever invoking superflow (18). Torsional oscillator experiments ultimately measure the changes in mechanical properties, so the connection to MMI is indirect and requires interpretation. The idea here is that the mechanical response of the solid, and hence the torsional oscillator properties, are changing at the onset of the glass state. The challenge for theory and

experiment is to characterize bulk helium-4 samples with enough precision to decide on such nonsuperflow scenarios.

All of these recent experiments plainly show that the standard textbook supersolid falls short as an adequate explanation of the experiments. What is clear is that the true answer is hidden in the disorder.

References and Notes

1. A. J. Leggett, *Phys. Rev. Lett.* **25**, 2543 (1970).
2. E. Kim, M. H. W. Chan, *Nature* **427**, 225 (2004).
3. E. Kim, M. H. W. Chan, *Science* **305**, 1941 (2004); published online 2 September 2004 (10.1126/science.1101501).
4. A. C. Clark, M. H. W. Chan, *J. Low Temp. Phys.* **138**, 853 (2005).
5. E. Kim, M. H. W. Chan, *Phys. Rev. Lett.* **97**, 115302 (2006).
6. A. S. C. Rittner, J. D. Reppy, *Phys. Rev. Lett.* **98**, 175302 (2007).
7. A. F. Andreev, I. M. Lifshitz, *Sov. Phys. JETP* **29**, 1107 (1969).
8. G. V. Chester, L. Reatto, *Phys. Rev.* **155**, 88 (1967).
9. P. W. Anderson, W. F. Brinkman, D. A. Huse, *Science* **310**, 1164 (2005); published online 3 November 2005 (10.1126/science.1118625).
10. M. Boninsegni *et al.*, *Phys. Rev. Lett.* **97**, 80401 (2006).
11. S. M. Heald, D. R. Baer, R. O. Simmons, *Phys. Rev. B* **30**, 2531 (1984).
12. E. Blackburn *et al.*, <http://arxiv.org/abs/cond-mat/0702537> (2007).
13. E. Kim, M. H. W. Chan, *Phys. Rev. Lett.* **97**, 115302 (2006).
14. A. Penzev *et al.*, <http://arxiv.org/abs/cond-mat/0702632> (2007).
15. K. Shirahama *et al.*, *Bull. Am. Phys. Soc.* **51**, 450 (2006).
16. M. Boninsegni, N. Prokof'ev, B. Svistunov, *Phys. Rev. Lett.* **96**, 105301 (2006).
17. J. Wu, P. Phillips, <http://arxiv.org/abs/cond-mat/0612505> (2006).
18. A. V. Balatsky, Z. Nussinov, M. Graf, S. Trugman, *Phys. Rev. B* **75**, 094201 (2007).
19. S. Sasaki, R. Ishiguro, F. Caupin, H. J. Maris, S. Balibar, *Science* **313**, 1098 (2006); published online 27 July 2006 (10.1126/science.1130879).
20. J. Day, J. Beamish, *Phys. Rev. Lett.* **96**, 105304 (2006).
21. I. A. Todoshchenko, H. Alles, H. J. Junes, A. Ya. Parshin, V. Tsepelin, <http://arxiv.org/abs/cond-mat/0703743> (2007).
22. P.P. is supported in part by NSF grant DMR0605769. A.V.B. is supported by the U.S. Department of Energy (US BES E 304) and Los Alamos National Laboratory (LDRD 2005 1164 DR).

10.1126/science.1143866

PHYSIOLOGY

Sister Act

David D. Moore

Particular fibroblast growth factors function as metabolic hormones and act through a certain signaling cascade design to control specific states of homeostasis.

All biologists know that the myriad enzymatic pathways that extract energy from metabolites and convert them to essential products are literally the biochemical basis for life. Many also view these reactions as an indigestible list of obtuse facts, which makes it all the more impressive that the late Dr. Robert Atkins, creator of the popular high-protein, high-fat, low-carbohydrate diet, was able to pass on a relatively obscure aspect of this process to a substantial fraction of the public—namely, that ketone bodies, produced from metabolizing fat, accumulate when you fast, allowing the body to use fat instead of carbohydrates for energy. Like all metabolic processes, the production of ketone bodies from fat (a process called ketogenesis) is regulated. As Atkins stressed, “burning” of fat is blocked by insulin in response to eating carbohydrates but is activated by starvation and also by a low-carbohydrate “ketogenic” diet. Two recent papers in *Cell Metabolism* (1, 2) have identified a remarkable and unexpected role for an obscure growth factor in

this process. A third paper in the *Proceedings of the National Academy of Sciences* (3) reveals how another protein facilitates this growth factor's effect on metabolism.

The human genome encodes 22 members of the fibroblast growth factor (FGF) family (4). Most function in diverse processes such as development and wound healing. But three members—FGF19 (FGF15 in the mouse), FGF21, and FGF23—have recently emerged as metabolic hormones. FGF19 modulates bile acid biosynthesis, and itself is regulated by farnesoid X receptor (FXR), a nuclear receptor that is activated by bile acids (5). FGF23 regulates phosphate and calcium homeostasis, and its expression is controlled by the vitamin D receptor (6, 7). FGF21 has a variety of beneficial effects on undesirable metabolic parameters. For example, treating obese mice (genetically engineered to lack leptin, a hormone that controls appetite) with FGF21 decreases the concentrations of serum glucose and triglycerides and increases insulin sensitivity (8). Similar results were observed in obese rhesus monkeys (9). Inagaki *et al.* (1) and Badman *et al.* (2) now show that FGF21 expression in the liver of fasted mice is activated by the nuclear hormone receptor

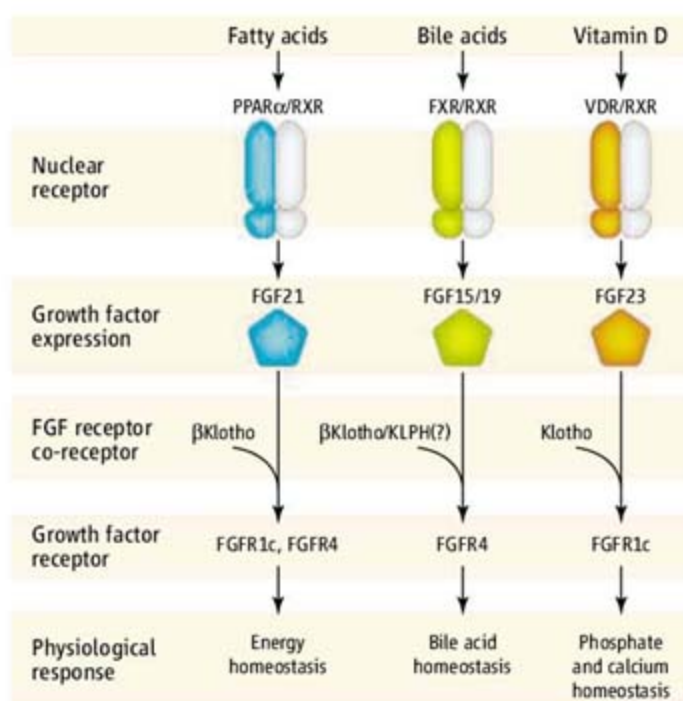
The author is in the Department of Molecular and Cellular Biology, Baylor College of Medicine, Houston, TX 77030, USA. E-mail: moore@bcm.edu

peroxisome proliferator-activated receptor α (PPAR α , also known as NR1C1).

Like other nuclear hormone receptors, PPAR α directly regulates gene expression in response to low molecular weight signaling molecules. But unlike the well-known nuclear receptors that respond to endocrine hormones, PPAR α belongs to a new group of metabolic receptors that respond to common metabolites (10, 11). In the case of PPAR α , fatty acids can function as endogenous signaling ligands, and it is well documented that PPAR α functions in the liver to induce the expression of enzymes that promote fatty acid oxidation. This represents an elegantly simple regulatory circuit in which the presence of the energy source activates an enzymatic pathway that causes its own combustion.

In fatty acid oxidation, the straight carbon chains are chopped into two-carbon bits in the form of acetyl-coenzyme A (CoA). Among the many potential fates of acetyl-CoA is conversion into four-carbon ketone bodies that are released by the liver and used by other tissues, particularly the brain, as an energy source. As Inagaki *et al.* and Badman *et al.* show, FGF21 promotes fatty acid oxidation and diverts its output to ketone body production.

Both groups show that the dramatic induction of FGF21 expression in the livers of fasted mice is absent in transgenic mice lacking PPAR α . Badman *et al.* used RNA interference to decrease endogenous FGF21 expression, which resulted in markedly increased triglyceride levels in both the liver and serum of mice fed a ketogenic (low carbohydrate, high fat) diet. This was associated with decreased expression of fatty acid-oxidizing enzymes and also 3-hydroxy-3-methylglutaryl (HMG)-CoA synthase 2 (HMGCS2) and carnitine palmitoyltransferase 1a (CPT1a), key enzymes in ketone body production that are both gene targets of PPAR α . Inagaki *et al.* extended previous reports on the effects of both FGF21 treatment and transgenic overexpression of FGF21 in the mouse liver to demonstrate increased ketogenesis. Thus, in transgenic mice genetically engineered to overexpress FGF21, the normally low ketone body concentration in serum was increased severalfold, though the transgene did not further augment the elevated levels in fasted mice. Acute FGF21 treatment partially rescued the defective ketone body production



Patterns in metabolic pathways. Three different signaling pathways that regulate homeostasis may share a common design, involving a nuclear receptor, a fibroblast growth factor (FGF), an FGF receptor, and a member of the Klotho family of proteins. Each nuclear receptor forms a dimer with the retinoid X receptor (RXR); the Klotho proteins interact with distinct FGF receptor isoforms. Each pathway contributes to the broader mechanisms by which each nuclear receptor influences homeostasis.

observed in fasted mice lacking PPAR α . Surprisingly, increased ketogenesis in the fed FGF21-overexpressing transgenic mice was not associated with elevated messenger RNA expression of HMGCS2 or CPT1a in the liver, although an increase in protein expression suggests possible posttranscriptional alteration in enzyme activity.

A bigger surprise seen with the FGF21-overexpressing transgenic mice was a dramatic increase in hepatic expression of several lipases usually found only in the pancreas. This was coupled with increased expression of more conventional lipases (and thus, lipolysis) in white adipose tissue. Inagaki *et al.* suggest that these increases in lipase activity may promote ketogenesis by augmenting the supply of fatty acids in the liver.

Here the story takes a bizarre turn. Mice maintained in constant darkness also express the same pancreatic enzymes in the liver and other peripheral tissues (12). Li and colleagues ascribe this phenomenon to increased concentration of 5'-adenosine monophosphate (5'-AMP) and showed that treatment with 5'-AMP induces torpor in mice (12). Torpor is an extreme example of decreased energy output that is associated with drastically reduced body temperature. Inagaki *et al.* show that when FGF21-overexpressing transgenic mice were fasted for 24 hours, their body temperature declined dramatically and

locomotor activity ceased. Decreased body temperature was also observed in fasting wild-type mice when they were infected with an FGF21-expressing adenovirus or treated with a synthetic PPAR α agonist. These observations clearly link the FGF21-PPAR α pathway to torpor, but the specific relationship with 5'-AMP signaling remains to be explored. More broadly, in combining the current results on fasting and ketogenic response with previous results on glucose metabolism, it is evident that FGF21 is emerging as a regulator of overall energy balance.

It is intriguing that the link between FGF21 and PPAR α completes a tidy pattern. Each of the three metabolic FGFs is now closely tied to a functionally complementary nuclear receptor signaling pathway. Determining whether this pattern extends to downstream signaling molecules is complicated by the responses of the relatively limited number of FGF receptors to multiple FGFs (4). A major advance in this area was recently provided by yet another unexpected connection. *Klotho* was initially identified as a mouse locus

that, when mutated, causes progeria, or premature aging (13). Remarkably, interaction with Klotho protein converts two specific isoforms of FGF receptor 1 from general FGF receptors to specific FGF23 receptors (14), a role that is nicely supported by striking similarities in the phenotypes of mice lacking either *Klotho* or FGF23. In Greek mythology, *Klotho*, along with *Lakhesis* and *Atropos*, was one of three sisters responsible for spinning, measuring, and cutting the thread representing the fate of each individual. And just as might be predicted, *Klotho*'s awkwardly named sister β Klotho was very recently found to combine with either of two FGF receptor isoforms to confer a specific response to FGF21 (3). The possibility of a simple three-way nuclear receptor-FGF-Klotho sister pattern (see the figure) is supported by the existence of another close relative, *Klotho*-LPH related protein (KLPH) (15). But as Macbeth learned, the pronouncements of the three weird sisters must be interpreted with caution. Thus, mice lacking β Klotho (16) show bile acid defects similar to those in mice lacking either FGFR4 or FGF15, rather than the triglyceride or glucose metabolic defects that would be anticipated from disrupting FGF21 signaling. Perhaps such phenotypes will emerge. At this early stage, however, the basis for downstream signaling is one of a number of tangles in the

FGF21 and FGF15/19 threads that remain to be teased apart.

References

1. T. Inagaki *et al.*, *Cell Metab.* **5**, 415 (2007).
2. M. K. Badman *et al.*, *Cell Metab.* **5**, 426 (2007).
3. Y. Ogawa *et al.*, *Proc. Natl. Acad. Sci. U.S.A.* **104**, 7432 (2007).
4. V. P. Eswarakumar, I. Lax, J. Schlessinger, *Cytokine Growth*

- Factor Rev.* **16**, 139 (2005).
5. T. Inagaki *et al.*, *Cell Metab.* **2**, 217 (2005).
 6. T. Shimada *et al.*, *J. Bone Miner. Res.* **19**, 429 (2004).
 7. O. I. Kolek *et al.*, *Am. J. Physiol. Gastrointest. Liver Physiol.* **289**, G1036 (2005).
 8. A. Kharitonov *et al.*, *J. Clin. Invest.* **115**, 1627 (2005).
 9. A. Kharitonov *et al.*, *Endocrinology* **148**, 774 (2007).
 10. L. Michalik *et al.*, *Pharmacol. Rev.* **58**, 726 (2006).
 11. A. I. Shulman, D. J. Mangelsdorf *N. Engl. J. Med.* **353**, 604 (2005).

12. J. Zhang, K. Kaasik, M. R. Blackburn, C. C. Lee, *Nature* **439**, 340 (2006).
13. M. Kuro-o *et al.*, *Nature* **390**, 45 (1997).
14. I. Urakawa *et al.*, *Nature* **444**, 770 (2006).
15. S. Ito, T. Fujimori, Y. Hayashizaki, Y. Nabeshima, *Biochim. Biophys. Acta* **1576**, 341 (2002).
16. S. Ito *et al.*, *J. Clin. Invest.* **115**, 2202 (2005).

10.1126/science.1144837

BIOPHYSICS

Long Live Electronic Coherence!

William W. Parson

Plants and photosynthetic bacteria use pigment-protein “antennas” to absorb light and transfer the energy to reaction centers, which trap the energy in electron-transfer reactions. On page 1462 of this issue, Fleming and co-workers (1) provide new insights into how energy flows from the antenna pigments to the sites of photochemical activity.

The authors study the reaction center of purple photosynthetic bacteria (see the figure). If the bacteriopheophytins in this reaction center are excited with light at 750 nm, the excitation moves to the accessory bacteriochlorophylls and then to the bacteriochlorophyll dimer within 100 to 200 fs (2–4). The dimer then transfers an electron to one of the bacteriopheophytins via the intervening bacteriochlorophyll.

In thinking about how energy flows through these systems, a recurring issue is whether excitations jump stochastically from molecule to molecule or whether groups of pigments act together as “supermolecules.” The answer hinges largely on how rapidly interactions with the surroundings destroy electronic coherence created by excitation.

Excitation of a complex containing two pigments leads to a combination of the ground state and states in which one or the other molecule is excited. The dynamical properties of an ensemble of such complexes can be expressed as a matrix, in which the diagonal elements are the probabilities of finding a complex in a given state and the off-diagonal elements represent the electronic coherence between pairs of states.

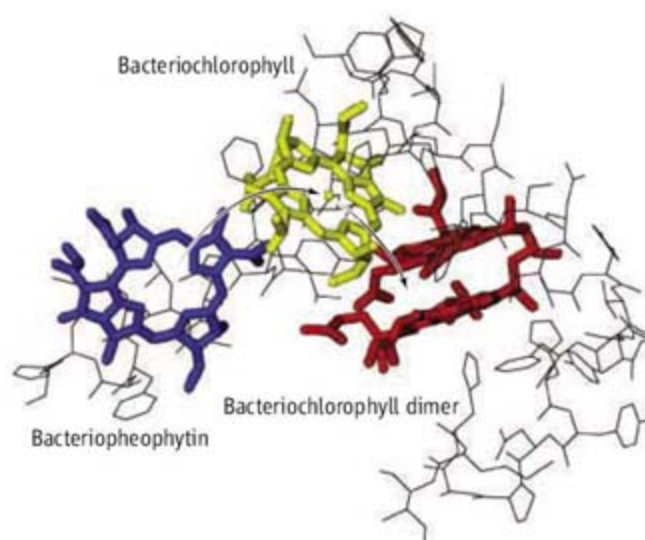
If the ensemble is excited with a short pulse of light, one or more off-diagonal elements will initially be nonzero. These elements oscillate at

frequencies proportional to the energy differences between states—much like the beats in the sound of two bells ringing at slightly different frequencies. The amplitudes of these coherences will eventually decay to zero as the contributions from different members of the ensemble get out of phase. But as long as electronic coherence remains, the ensemble will exhibit oscillatory spectroscopic features, and a second or third pulse of light can reverse dephasing caused by static variations of the energies, resulting in emission of a photon echo analogous to a spin echo in nuclear magnetic resonance (5, 6).

Oscillatory fluorescence indicative of vibrational coherence is well known in reaction centers and antenna complexes and typically lasts for several picoseconds (7, 8). Most investigators have assumed that electronic coherence decays much more quickly, because electronic excitation is associated with a larger redistribution of charge and is therefore more sensitive to fluctuating fields from the surroundings. Two recent studies by Fleming and co-workers (1, 9) call this assumption into question.

In both experiments, two laser pulses were focused on the sample in a spatially and temporally controlled manner, and a photon echo after a third pulse was measured. Engel *et al.* (9) studied an antenna complex from green sulfur bacteria that has seven bacteriochlorophylls per protein subunit. They found that a pulse resonant with one of the absorption bands of the complex could bring oscillations initiated earlier by light resonant with a different band back into phase. The resulting echo was seen even when the delay between the

Synchronized excitations may be key to energy transfer in photosynthetic bacteria.



Correlated effects. In the reaction center of purple photosynthetic bacteria, energy is transferred from a bacteriopheophytin (blue) via an accessory bacteriochlorophyll (yellow) to the adjacent bacteriochlorophyll dimer (red); part of the surrounding protein is shown in black (11). Fleming and co-workers (1, 9) suggest that some of the protein’s vibrational modes could have correlated effects on the excitation energies of multiple pigments.

second and third pulses was 660 fs, indicating that the complex retained electronic coherence for at least this long.

Lee *et al.* (1) have now used separate pulses of 750- and 800-nm light to generate coherence between excited states of the bacteriopheophytins and bacteriochlorophylls in bacterial reaction centers. Photon echoes after a third pulse showed that electronic coherence between the two excited states persisted for hundreds of femtoseconds.

The authors suggest that electronic coherence is preserved in pigment-protein complexes because some of the protein’s vibrational modes have correlated effects on the transition energies of multiple pigments. These vibrational modes thus affect the energy differences between pigments less than their absolute energies—allowing electronic coherence to be preserved. For exam-

The author is at the Department of Biochemistry, University of Washington, Seattle, WA 98195, USA. E-mail: parsonb@u.washington.edu

ple, motions of an α -helix might cause similar changes in the electrical fields acting on several pigments bound to that helix.

Electronic coherence could facilitate energy migration by allowing excitations to be sensed simultaneously at multiple sites within the protein. These ideas remain to be explored by detailed molecular-dynamics simulations and quantum calculations. It seems clear, however, that a complete description of energy migration in photosynthetic complexes will have to include electronic coherence.

Recent work by Woodbury and co-workers (10) addresses how motions of the reaction

center protein affect the rate of electron transfer from the bacteriochlorophyll dimer to the initial electron acceptors. Their results suggest that the energies of the electron-transfer states may be more strongly coupled to protein motions than are the shorter-lived excited states probed in the photon-echo experiments by Fleming and co-workers (1, 9).

References

1. H. Lee, Y.-C. Cheng, G. R. Fleming, *Science* **316**, 1462 (2007).
2. R. J. Stanley, B. King, S. G. Boxer, *J. Phys. Chem.* **100**, 12052 (1996).
3. M. H. Vos, J. Breton, J. L. Martin, *J. Phys. Chem. B* **101**, 9820 (1997).

4. B. A. King, T. B. McAnaney, A. deWinter, S. G. Boxer, *J. Phys. Chem. B* **104**, 8895 (2000).
5. S. Mukamel, *Principles of Nonlinear Optical Spectroscopy* (Oxford Univ. Press, Oxford, 1995).
6. W. W. Parson, *Modern Optical Spectroscopy with Examples from Biophysics and Biochemistry* (Springer, Berlin, 2006).
7. M. H. Vos, M. R. Jones, C. N. Hunter, J. Breton, J.-L. Martin, *Proc. Natl. Acad. Sci. U.S.A.* **91**, 12701 (1994).
8. M. H. Vos, F. Rappaport, J.-H. Lambry, J. Breton, J.-L. Martin, *Nature* **363**, 320 (1993).
9. G. S. Engel *et al.*, *Nature* **446**, 782 (2007).
10. H. Wang *et al.*, *Science* **316**, 747 (2007).
11. U. Ermler, G. Fritsch, S. K. Buchanan, H. Michel, *Structure* **2**, 925 (1994).

10.1126/science.1143907

GEOPHYSICS

Listening to the Crackle of Subducting Oceanic Plates

Andreas Rietbrock

Areas called subduction zones occur under the ocean where one section of Earth's crust (the lithosphere) collides with another and descends into the mantle (see the figure). Although these zones are of substantial scientific interest, they also have great social and economic importance. Most of the world's disastrous earthquakes and volcanoes take place at subduction zones, as well as geological processes that generate many of the ore deposits on Earth.

We can map the path of the descending lithospheres by measuring the abundant seismic activity in the subduction zone. Since it was first observed in the early 1930s, however, the precise nature and cause of this seismicity has been debated. On page 1472, Brudzinski *et al.* report a major step forward in our understanding of the geophysical and geochemical processes at work in these seismic regions (1).

The deep layers of seismic activity in subducting regions are called Wadati-Benioff zones (WBZs) and can be found as deep as 700 km. Originally, WBZs were believed to be single layers of seismic activity, but they have turned out to be more complex. The first convincing observation of a double WBZ beneath northern Honshu, Japan, was made by Hasegawa *et al.* (2), and they reported a separation distance between the two layers of about 30 to 40 km. Since then, the geoscience community has been

puzzled by the relative rarity of double WBZs.

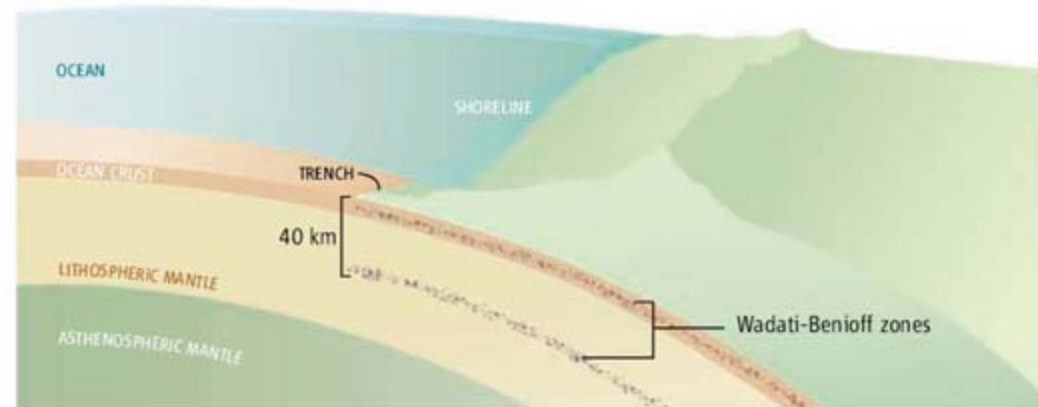
Recently, as a result of a huge increase in seismological data collected and the availability of new data-processing tools, hints of double WBZs with much smaller separation distances (<10 km) have been found in many different subduction zones (3). Brudzinski *et al.* have taken these observations further and propose that double layering of seismicity is an inherent feature of WBZs in the depth range between 50 and 300 km (which they refer to as double Benioff zones, or DBZs).

The origin of WBZ seismicity has been controversial for several reasons. Brittle failure or, more precisely, sudden slip along a pre-existing fault or plate interface is the cause for most of the earthquakes in Earth's crust (<50 km depth). However, due to the high temperature and pressure at the depth level of WBZ

Double zones of seismic activity now appear to be a general feature of tectonic plates pushed deep into Earth, providing new clues to the sources of deep earthquakes.

seismicity the material will instead undergo ductile deformation, which inhibits earthquake faulting. Therefore, different processes are necessary for the generation of WBZ seismicity.

A commonly accepted model for this deeper activity is dehydration embrittlement, in which fluids released by hydrous minerals of the crust and mantle of the slab can lead to high pore pressures, reduce the effective stress on preexisting faults, and hence promote the occurrence of earthquakes (4). In the upper layer of seismicity, researchers believe that a mineral transformation from basalt to eclogite in the oceanic crust is the main reaction promoting earthquakes and causing an increase of seismicity in this depth range. As yet, there is no such consensus about which of the numerous possible hydrous minerals might explain the lower band of seismicity in double WBZs.



Double seismicity. At subduction zones, one tectonic plate descends under another. Earthquakes occur along surfaces called Wadati-Benioff zones (WBZs) to depths of more than 700 km. Brudzinski *et al.* have now found that double WBZs may be a general feature of subduction zones. From these observations, detailed geophysical and geochemical processes inside them can be deduced.

The author is in the Department of Earth and Ocean Sciences, Liverpool University, Liverpool L69 3GP, UK. E-mail: A.Rietbrock@liverpool.ac.uk

Brudzinski *et al.* have now found a direct correlation whereby older oceanic plates show a greater distance between regions of seismicity. They conclude, based on thermal-petrological models developed by Hacker *et al.* (5), that dehydration of the mineral antigorite is responsible for the seismicity in the lower layer of double WBZs.

Although the detailed geophysical explanation presented by Brudzinski *et al.* for the double seismic zone might be debatable, they observe that double WBZs are the rule and not the exception during subduction of oceanic lithosphere. This provides an important new constraint for all models developed to explain the occurrence of WBZ seismicity. However,

further work on the stress accumulation and dissipation in the lithosphere during subduction is necessary to understand the faulting mechanism causing seismicity in double WBZ or even triple WBZ, as proposed for some regions beneath Japan (6).

Brudzinski *et al.* show that, as the number of seismological stations and the availability of digital seismic traces increases, the global earthquake catalog will become accurate enough to delineate the fine structure of seismicity (on the order of a few kilometers) on a global scale. This accuracy will increase in the near future as a result of large seismological observation initiatives like EarthScope in the United States or the NERIES program

(Network of Research Infrastructures for European Seismology) in Europe, which will make more high-quality digital data readily available for seismologists worldwide.

References

1. M. R. Brudzinski, C. H. Thurber, B. R. Hacker, E. R. Engdahl, *Science* **316**, 1472 (2007).
2. A. Hasegawa, N. Umino, A. Takagi, *Tectonophysics* **47**, 43 (1978).
3. A. Rietbrock, F. Waldhauser, *Geophys. Res. Lett.* **31**, 10.1029/2004GL019610 (2004).
4. S. Kirby, *Rev. Geophys.* **33**, 287 (1995).
5. B. R. Hacker, G. A. Abers, S. M. Peacock, *J. Geophys. Res.* **108**, 2029 (2003).
6. T. Igarashi, T. Matsuzawa, N. Umino, A. Hasegawa, *J. Geophys. Res.* **106**, 2177 (2001).

10.1126/science.1141921

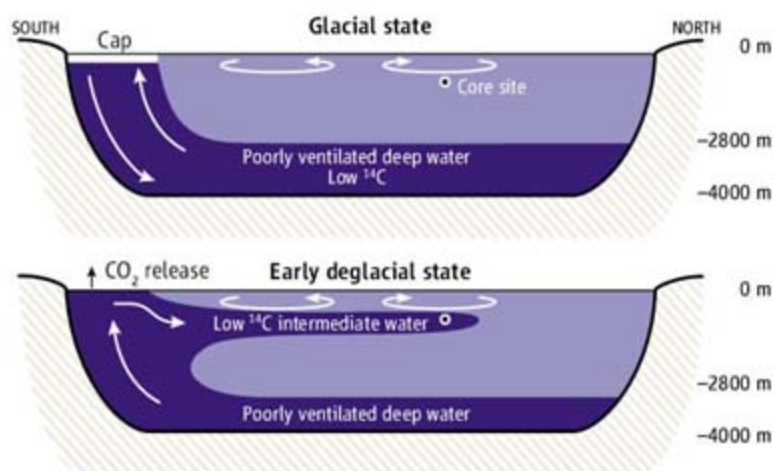
ATMOSPHERE

Deglaciation Mysteries

Ralph F. Keeling

Between 19,000 and 11,000 years ago, the Earth emerged from the last glacial period. During this deglaciation, the carbon dioxide (CO_2) concentration in the atmosphere rose from 180 to 265 parts per million (ppm). Over the same period, the radiocarbon content of the CO_2 fell by ~35%. A simple but unproven explanation for both changes is an increase in the rate at which the ocean's subsurface waters were renewed by exchange with aerated surface waters—a process known as ventilation. A ventilation increase could increase atmospheric CO_2 concentration by releasing excess CO_2 that had accumulated in subsurface waters by the decomposition of sinking detritus. On page 1456 in this issue, Marchitto *et al.* (1) bolster the case for such a ventilation increase and offer insight into how the increase may have occurred.

To track changes in past ventilation, most researchers have turned to measurements of the radiocarbon (^{14}C) content of shells of foraminifera, a ubiquitous marine microorganism. Radiocarbon is produced naturally in the upper atmosphere by cosmic rays and spreads through the ocean as part of the pool



Deep-water ventilation. This cross section of the Pacific Ocean shows how poorly ventilated water may have been delivered to intermediate depths during deglaciation, as suggested by Marchitto *et al.* (Top) Ventilation of the deep ocean by sinking around Antarctica was partially suppressed by a cap formed by sea ice or a layer of low-salinity water. (Bottom) This cap was removed during early deglacial warming, exposing upwelled deep waters to the atmosphere, releasing radiocarbon-depleted CO_2 . The density of the poorly ventilated waters was reduced by freshening and warming. With reduced density, the water could spread widely at intermediate depths, displacing waters of similar density.

of dissolved carbon. Because of radioactive decay, waters that are more isolated from the atmosphere (that is, more poorly ventilated) have lower $^{14}\text{C}/^{12}\text{C}$ ratios, as do the shells that grow in these waters. The radiocarbon age of a fossil shell therefore reflects the age of the shell plus the age of the water in which it lived. By subtracting the radiocarbon ages of surface-dwelling (planktonic) and bottom-dwelling (benthic) foraminifera, picked from the same layer of a sediment core, it is possible to estimate age difference of surface and deep

Results from a sediment core provide insights into ocean circulation changes during the last deglaciation.

waters, which is a measure of the deep-water ventilation rate.

This technique, applied to numerous sediment cores, has thus far mainly yielded the unremarkable result that the ventilation rate of the glacial ocean was very similar to that of today's ocean, at least down to a depth of ~2800 m (2). Thus, if there was a major change in ocean ventilation during deglaciation, this change must have occurred in ocean waters below that depth. However, despite some tantalizing results (3), no general picture has emerged for waters below 2800 m, because of methodological difficulties related to the low sedimentation rates that typically characterize cores from these depths.

Marchitto *et al.* focus on a sediment core recently hauled up off Baja California from a depth of 700 m, seemingly too shallow for studying deep ventilation. The core contains bands corresponding to a set of millennial climate oscillations first discovered in ice cores from Greenland, allowing absolute dates to be fixed within the core. Using these dates, the authors correct the $^{14}\text{C}/^{12}\text{C}$ ratios of benthic foraminifera for radioactive decay, thus establishing the original $^{14}\text{C}/^{12}\text{C}$ ratio of the water in which the foraminifera lived. The technique does not require $^{14}\text{C}/^{12}\text{C}$ measurements on planktonic

The author is at the Scripps Institution of Oceanography, University of California, San Diego, CA 92093, USA. E-mail: rkeeling@ucsd.edu

foraminifera, which are subject to potentially large systematic errors.

The results show two periods during deglaciation when the bottom water at their site had unexpectedly low $^{14}\text{C}/^{12}\text{C}$ ratios. The water was so old that it must have been delivered to the site by upwelling from greater depth, presumably from below 2800 m. The oldest waters found by Marchitto *et al.* have an age of ~4000 years. For comparison, the oldest waters in the modern ocean have an age of ~2300 years.

The study provides the strongest evidence to date that the glacial ocean contained some very poorly ventilated water somewhere in its depths. The low- ^{14}C periods coincide with the periods when atmospheric radiocarbon decreased and atmospheric CO_2 increased most rapidly during deglaciation. The results are thus a convincing fingerprint of a process that flushed excess carbon from an isolated deep reservoir toward the surface, thereby driving the atmospheric changes.

Today, waters below 2800 m are ventilated by two routes. One involves the sinking of aerated surface waters in the North Atlantic, the other sinking of such waters near Antarctica. During the last glacial period, both routes probably weakened, with the southern route possibly influenced by sea ice or surface freshening (see the figure, top panel). During glacial times, the deep ocean would thus have been less ventilated than it is today.

But how could low- ^{14}C waters get to Marchitto *et al.*'s core site during deglaciation? Much of the upwelling of deep water occurs

today around Antarctica, resulting in the formation of Antarctic Intermediate Water, a low-salinity water mass that spreads northward at intermediate depths. Marchitto *et al.* hypothesize that a similar process occurred during deglaciation, allowing upwelled water to spread northward to their site (see the figure, bottom panel). However, the evidence for this southern pathway is circumstantial.

The results help to reconcile the reconstructed trends in atmospheric radiocarbon with the estimated trends in the production of radiocarbon by cosmic rays—a comparison that seems to demand an increase in ocean ventilation during deglaciation (4). They support theories that attribute the bulk of the glacial-interglacial CO_2 change to changes in ocean ventilation (5, 6).

The study also provides support for a theory for how the glacial ocean differed from today's ocean as a result of the cooling of deep waters to nearly the freezing point. Cooling to this extent is expected to allow the salty brine that is released during sea ice formation to accumulate more easily in the deep ocean (7). This idea is supported by sediment pore-water studies (8). By blocking the input of fresh water from precipitation, sea ice could also reduce the conversion of upwelled deep water into low-salinity Antarctic Intermediate Water (7). A strengthening of intermediate-water formation during deglaciation is consistent with a breakdown of this state caused by warming.

The study nevertheless leaves the skeptics

with arrows in their quiver. Marchitto *et al.*'s low- ^{14}C waters are so old that they start to stretch credibility, especially considering that the deep reservoir from which the water was drawn must have been even older. (This follows because some mixing with younger water would unavoidably have occurred during upwelling and transit to the site.) How could prior studies have overlooked deep waters this old?

If Marchitto *et al.*'s interpretation is correct, evidence for old water at intermediate depths should be present throughout the South Pacific in sediments of the appropriate age and depth. If subsequent work supports the findings, we may look back at this study as a key turning point in the quest to understand glacial and interglacial CO_2 changes.

References

1. T. M. Marchitto, S. J. Lehman, J. D. Ortiz, J. Flückiger, A. van Geen, *Science* **316**, 1456 (2007); published online 10 May 2007 (10.1126/science.1138679).
2. W. Broecker *et al.*, *Paleoceanography* **22**, PA2206 (2007).
3. L. D. Keigwin, S. J. Lehman, M. S. Cook, *Eos* **87**, PP44A07 (2006).
4. K. Hughen *et al.*, *Science* **303**, 202 (2004).
5. J. R. Toggweiler, J. L. Russell, S. R. Carson, *Paleoceanography* **21**, PA2005 (2006).
6. B. B. Stephens, R. F. Keeling, *Nature* **404**, 171 (2000).
7. R. F. Keeling, B. B. Stephens, *Paleoceanography* **16**, 112330 (2001).
8. J. F. Adkins, K. McIntyre, D. P. Schrag, *Science* **298**, 1769 (2002).

Published online 10 May 2007;
10.1126/science.1142326.
Include this information when citing this paper.

MOLECULAR BIOLOGY

Site-Seeing by Sequencing

Stanley Fields

Every few years, a new technology comes along that dramatically changes how fundamental questions in biology are addressed. The impact of the technology is not always appreciated at first—when it is used only by those involved in its development—but becomes clear once the technology begins to spread to the broader scientific community. A well-known example is the DNA microarray, which became widely available to biologists about a decade ago and has since been applied to an ever-expanding set of questions such as

determining the profile of genes expressed in a specific cell type. Now it is ultrahigh-throughput DNA sequencing that is making the transition from development to widespread use. Johnson and colleagues are in the vanguard of this movement. On page 1497 of this issue (1), they report that an advanced DNA sequencing technology (from Solexa/Illumina) can be used to identify all the locations in the human genome where a specific protein binds. They do this with a speed and precision that goes beyond what has been achieved with previous technologies.

DNA-binding proteins control transcription, replication, DNA repair, and chromosome segregation. Given the importance of these proteins, identifying their binding sites

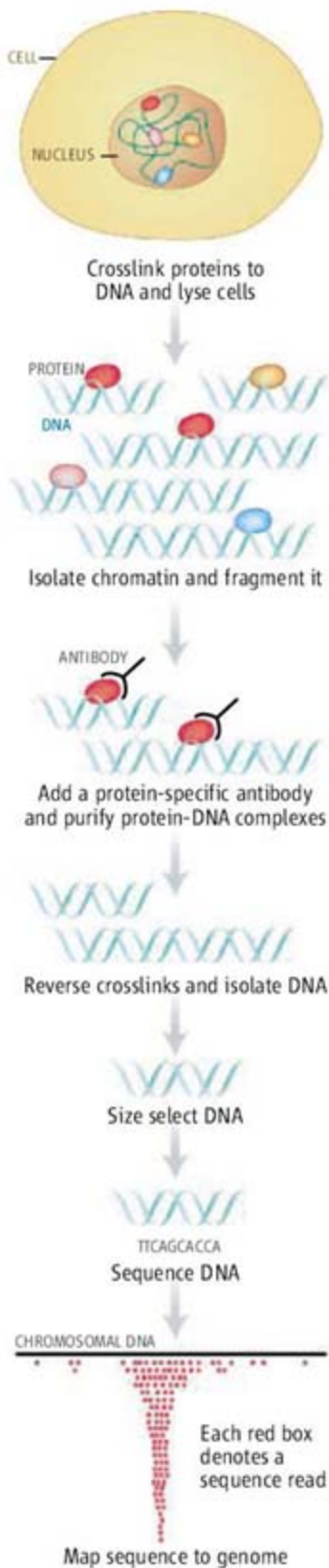
An advance in DNA sequencing is a crucial component of a rapid, precise, and relatively inexpensive way to identify transcription factor binding sites at a whole-genome level.

throughout the genome has occupied much attention in recent years. The most common method of locating these sites within a living cell is known as chromatin immunoprecipitation (ChIP). In this approach, cells are treated with a reagent, typically formaldehyde, that crosslinks protein and DNA, and then the cells are lysed. Chromatin (the complex of proteins and DNA in chromosomes) is isolated, the DNA is sheared into small fragments, and an antibody is added to precipitate the protein and its associated DNA. The DNA that is liberated after reversal of the protein-DNA crosslinks is then analyzed. In the initial uses of this method, researchers analyzed the DNA to determine whether single genes were enriched by the immunoprecipitation.

The author is in the Departments of Genome Sciences and Medicine, Howard Hughes Medical Institute, University of Washington, Seattle, WA 98195-5065, USA. E-mail: fields@u.washington.edu

The classic genomic application of this approach—which began about 5 years ago—analyzes not single genes but all precipitated DNA fragments by using them as probes on a DNA microarray, giving rise to the pithy (albeit repetitive) moniker: ChIP-chip. A microarray is an ordered arrangement of defined DNA fragments immobilized on a surface. It is used to identify DNA sequences present in a sample through the hybridization of complementary strands. Pioneered in the yeast *Saccharomyces cerevisiae* (2, 3), ChIP-chip was quickly applied to mammalian cells to identify binding sites for transcription factors (4, 5). More recently, it has found new applications in the analysis of the distribution across the genome of modified histones and histone binding proteins (6, 7). To improve this technique, Johnson *et al.* dispense with the “chip” of ChIP-chip and identify protein-bound DNA fragments by direct DNA sequencing (see the figure), a method they call ChIPSeq.

The focus of their study is a protein called neuron-restrictive silencer factor or repressor element-1 silencing transcription factor (indicated here as NRSF), a mammalian transcriptional repressor that silences the expression of neuronal genes in nonneuronal cell types and in neuronal progenitor cells (8, 9). Many NRSF binding sites have been well characterized and comprise a 21-base pair DNA sequence motif containing two nonidentical half-sites of 10 base pairs each. Johnson *et al.* recovered DNA samples from chromatin treated with a monoclonal antibody against NRSF and mapped the DNAs to the human genome by determining their nucleotide sequences (see the figure). Control DNA samples were derived from chromatin not treated with the antibody. For this approach to work, they needed to sequence many fragments, and they did: Two to 5 million sequences were



Protein binding, across the genome. The ChIPSeq method described by Johnson *et al.* identifies binding sites across the whole human genome for a specific protein. The control for this procedure omits the antibody step. The final panel shows a cluster of individual sequence reads (red boxes) that map back to the same region of the genome and locate a protein binding site.

“read” at 25 nucleotides per read. They then used an algorithm they developed to map these reads to the genome and identify regions where reads cluster together. They found all locations in the genome that met two criteria: at least 13 independent sequence reads and an enrichment of at least fivefold relative to the control. The largest cluster contained 6718 reads; in other words, a single NRSF binding site was found 6718 times in the sequence data.

What does this study reveal about NRSF binding sites? NRSF binding was detected at nearly all of its canonical motifs in the genome, indicating that all sites are accessible to the protein in the cell type analyzed (a human T cell line). Most sites bound by the factor were also identified, indicating that the sequencing approach is comprehensive. As befits a repressor, binding of NRSF near promoters (DNA regions where transcription factors bind to control their target genes) correlated with low levels of transcription of the associated genes. New binding motifs were also discovered, including those having two half-sites with noncanonical spacing between them, and those composed of only individual half-sites. Finally, genes bound to NRSF are high-

ly enriched for functions involved in synaptic transmission and nervous system development.

What are the advantages of ChIPSeq over ChIP-chip? For one, the whole genome can be assayed by a sequencing approach, rather than only those DNA regions captured on a microarray. However, this advantage diminishes as genome tiling arrays, which present the whole genome in an arrangement of overlapping DNA fragments, approach the resolution of just a few nucleotide bases. ChIPSeq also avoids the complications of array hybrid-

ization, such as probes with different optimal temperatures for binding to their complementary strands, probes that hybridize to more than one DNA sequence, and interference of hybridization by DNA secondary structure. Furthermore, ChIPSeq, as currently performed, is only half the cost of human whole-genome tiling arrays. Perhaps most usefully—given the increasing number of genome sequences now available—ChIPSeq can immediately be applied to any of those genomes, rather than only those for which microarrays are available.

With the success of this study, the localization of binding sites for many other proteins—including transcription factors, structural components of chromatin, modified histone proteins, and the enzymes that modify them—will likely be mapped by ultrahigh-throughput DNA sequencing. However, current high-throughput sequencing approaches (Solexa/Illumina and the 454 Life Sciences platforms) are not limited to identifying the sites in the genome visited by DNA binding proteins. They will find considerable use in resequencing genomes; a recent well-publicized example is the genome of James D. Watson. They will be used to discover new genes, such as those encoding small RNAs and microRNAs. And as Johnson *et al.* point out, the large number of individual sequence reads provides a direct count of the sequences present in any sample. Thus, gene expression profiles of cells and tissues, comparative genome hybridization between, for example, DNA from normal versus tumor cells, the messenger RNAs that are present on polysomes and being translated to proteins, and numerous other nucleic acid measurements can be accomplished easily, cheaply, and accurately by a sequencing approach. The technology that is most threatened by the widespread adoption of ultrahigh-throughput sequencing? The DNA microarray.

References

1. D. S. Johnson, A. Mortazavi, R. M. Myers, B. Wold, *Science* **316**, 1497 (2007).
2. B. Ren *et al.*, *Science* **290**, 2306 (2000).
3. V. R. Iyer *et al.*, *Nature* **409**, 533 (2001).
4. C. E. Horak *et al.*, *Proc. Natl. Acad. Sci. U.S.A.* **99**, 2924 (2002).
5. A. S. Weinman *et al.*, *Genes Dev.* **16**, 235 (2002).
6. C. L. Liu *et al.*, *PLoS Biol.* **3**, e328 (2005).
7. D. K. Pokholok *et al.*, *Cell* **122**, 517 (2005).
8. J. A. Chong *et al.*, *Cell* **80**, 949 (1995).
9. C. J. Schoenher, D. J. Anderson, *Science* **267**, 1360 (1995).

Career advice, insight and tools.

Turn to the experts for the big picture.
Visit www.ScienceCareers.org



Your career is too important to leave to chance. So to find the right job or get career advice, turn to the experts. At ScienceCareers.org we know science. And we are committed to helping take your career forward. Our knowledge is firmly founded on the expertise of *Science*, the premier scientific journal, and the long experience of AAAS in advancing science around the world. Put yourself in the picture with the experts in science. Visit www.ScienceCareers.org.

ALBERT EINSTEIN and related rights TM/© of The Hebrew University of Jerusalem, used under license. Represented by The Roger Richman Agency, Inc., www.albert-einstein.net.

ScienceCareers.org

We know science



Discover the
leading resource in
the life sciences ...

Encyclopedia of

 Life
ELS Sciences

www.els.net

Spanning the entire spectrum of life science research, the *Encyclopedia of Life Sciences* features thousands of specially commissioned and peer-reviewed articles, most of which are accompanied by colour images and tables.



- Available in print and online
- Over 3,500 original articles
- Contributions from 5,000 of the world's leading scientists
- Introductory, advanced and keynote articles
- More than 9,000 illustrations and figures

Original 20 Volume
print set

Hardcover
978-0-470-01617-6
£3150 / \$5670 / €4899

NEW 6
Supplementary
print volumes

Hardcover
978-0-470-06141-1
£795 / \$1435 / €1249, valid until 30 June
2007 - thereafter £995 / \$1795 / €1549

26 Volume print set (20 Volumes + 6
Supplementary volumes)

Hardcover
978-0-470-06651-5
£3550 / \$6390 / €5499, valid until
30 June 2007 - thereafter
£4145 / \$7465 / €6449



HOW TO ORDER

EUROPE, MIDDLE EAST,
ASIA & AFRICA

John Wiley & Sons Ltd
Tel: +44 (0)1243 843294
Fax: +44 (0)1243 843296

E-mail:
cs-books@wiley.co.uk
www.wiley.com

NORTH, CENTRAL &
SOUTH AMERICA

John Wiley & Sons Inc
Tel: 877 762 2974
Fax: 800 597 3299
E-mail: custserv@wiley.com
www.wiley.com

GERMANY, SWITZERLAND
& AUSTRIA

Wiley-VCH Verlag GmbH
Tel: +49 6201 606 400
Fax: +49 6201 606 184
E-mail: service@wiley-vch.de
www.wiley-vch.de



Imaging Atomic Structure and Dynamics with Ultrafast X-ray Scattering

K. J. Gaffney¹ and H. N. Chapman²

Measuring atomic-resolution images of materials with x-ray photons during chemical reactions or physical transformations resides at the technological forefront of x-ray science. New x-ray-based experimental capabilities have been closely linked with advances in x-ray sources, a trend that will continue with the impending arrival of x-ray-free electron lasers driven by electron accelerators. We discuss recent advances in ultrafast x-ray science and coherent imaging made possible by linear-accelerator-based light sources. These studies highlight the promise of ultrafast x-ray lasers, as well as the technical challenges and potential range of applications that will accompany these transformative x-ray light sources.

Many seminal advances in the natural sciences can be linked to the measurement of critical structures with atomic resolution. X-ray diffraction has proven to be among the most powerful tools for determining the atomic structures that catalyze fundamental advances in scientific disciplines ranging from biology to solid state physics. Although all objects scatter x-rays, crystal formation has been an essential step in the measurement of atomic-resolution structures for the majority of materials. Because of the regular arrangement of atoms in a crystal as opposed to an amorphous material, the x-ray scattering from the repeating structural unit adds coherently at periodically arranged Bragg peaks. This amplification greatly reduces the x-ray fluence required to measure a high-resolution diffraction pattern, but away from the Bragg peaks the scattered intensity remains too weak to measure, losing much of the information contained in the continuous molecular transform of the underlying structural unit. Even so, crystallography has remained the only method to measure diffraction at the large scattering angles required for the determination of high-resolution structures. The inability to crystallize important samples, however, has impeded progress in materials science and structural biology (1).

Measuring the continuous x-ray scattering pattern directly from a nonperiodic object, a lensless imaging technique inspired by crystallography, provides an alternative method for structure determination (2). This imaging technique requires the illuminating x-ray beam to maintain phase coherence across the entire width of the object, or across many repeating structural units in crystallography, in order to retrieve structural information. To coherently

illuminate an object with the full fluence of an x-ray beam requires the source to possess laser-like properties.

For coherent imaging, as with crystallography, x-ray exposure determines the achievable resolution, and radiation damage sets the maximum dose. The necessity of limiting the dose without the benefit of Bragg amplification inhibits coherent imaging from achieving atomistic resolution at synchrotrons designed to produce high average, but low peak, flux and has limited the technique to relatively large objects (3, 4), such as cells (5). Delivering the radiation dose to the sample in an extremely intense single x-ray pulse before the onset of radiation degradation provides a strategy for high-resolution x-ray imaging without crystallization (6, 7). Spontaneous synchrotron radiation cannot generate the peak coherent intensities necessary for imaging with a single pulse of light, but free electron lasers operating in the extreme ultraviolet have demonstrated that "instantaneous imaging" can be achieved (8) and x-ray-free electron lasers (XFEL) (9) have the promise of making atomic-resolution imaging possible (7).

More than sample preparation and radiation damage limit the utility of x-ray crystallography. An additional limitation has been the inability to observe atomic-level structure on the time scale of atomic motion. Direct visualization of these dynamics with x-ray scattering would greatly enhance our ability to study the nonequilibrium properties of materials and the pathways followed during infrequent equilibrium events, such as chemical reactions. Although time-resolved measurements have been made with use of the nominally 100-ps synchrotron pulses (10, 11), these sources are insufficient for single-shot diffractive imaging and for most measurements of structural dynamics. Single-shot x-ray imaging requires an extremely high per-pulse coherent flux, which can only be achieved with an x-ray laser, and both methodologies require fs

duration x-ray pulses to image materials before the onset of x-ray damage and to temporally resolve atomic and molecular motions. Synchrotron pulses would need to be roughly a thousand times shorter than their typical duration to achieve this temporal resolution, which cannot be accomplished at standard beam currents.

Linear electron accelerators provide an alternative approach to generating x-rays that bypass the dominant limitations of synchrotrons. In a linear accelerator, the electrons do not recirculate, making it possible to generate a much brighter electron beam. Brightness represents the product of transverse spot size, divergence, energy spread, and pulse duration of a particle beam. The short electron pulse durations make it possible to generate fs x-ray pulses with per-pulse x-ray fluences comparable to those of synchrotrons. The Stanford Linear Accelerator Center (SLAC) built just such a facility, the Sub-Picosecond Pulse Source (SPPS), demonstrating the unique opportunity linear accelerators provide as ultrafast x-ray sources.

Whereas the SPPS generated spontaneous x-rays like a synchrotron, the tremendous brightness of linear accelerator electron beams makes lasing at x-ray wavelengths possible (12). The FLASH facility (13) at the Deutsches Elektronen Synchrotron currently generates extreme ultraviolet (UV) laser light with photon energies ranging from 20 to 200 eV. The Linac Coherent Light Source (LCLS) (14) at SLAC will be the world's first XFEL starting in 2009, with other XFEL facilities scheduled to follow (15, 16). These facilities will generate x-ray photons with energies ranging from 800 eV to 12 keV.

The wavelength of the radiation at FLASH limits the spatial resolution to tens of nanometers. With the arrival of the LCLS and future facilities, x-ray beams with peak brightness 10^9 times brighter than that of current synchrotrons will be produced (17). This combination of high peak brightness, Å wavelengths, and fs pulse durations provide the necessary ingredients for pursuing atomic-resolution imaging and ultrafast science.

Femtosecond X-ray Scattering Studies of Structural Dynamics

Ultrafast laser spectroscopy has transformed our understanding of dynamics in the natural sciences. A few canonical measurements, coupled with theory and simulation, have provided robust atomic-scale descriptions of important structural transformations. However, for many important processes our interpretations remain largely speculative. This has driven the development of short-pulse x-ray (18–20) and electron (21) sources for probing dynamics.

For the majority of experimental studies of dynamics, a laser pulse initiates the transient phenomena by promoting electrons into nonequilibrium excited states. For ultrashort laser pulses, this electronic excitation impulsively modifies the potential energy surface of the atomic

¹PULSE Center, Stanford Linear Accelerator Center, Stanford University, Stanford, CA 94305, USA. E-mail: kgaffney@slac.stanford.edu ²Lawrence Livermore National Laboratory, Livermore, CA 94550, USA. E-mail: henry.chapman@llnl.gov

nuclei. This excited-state potential-energy surface determines the structural pathway followed after laser excitation. Determining the shape of the potential energy surface represents the critical, but generally difficult, objective of experimental studies of nonequilibrium structural dynamics.

The laser disordering and melting of semiconductors represent a classic demonstration of the limitations of optical studies and the potential of ultrafast x-ray sources for studying structural dynamics. Early experimental work demonstrated that intense fs pulse excitation of a silicon crystal led to a sub-ps increase in the reflectivity (22). Although absorption of the laser generates an increased reflectivity because of the direct excitation of carriers, the magnitude of the observed change could not be explained by this effect alone and led to the conclusion that intense laser excitation causes a semiconductor to metal transition. Because Si forms a metallic liquid, metal formation was attributed to crystal melting.

The rate of this purported phase transition exceeds the rate of energy transfer from the excited electrons to the crystal vibrations, leading to the supposition that the melting occurs nonthermally. Theoretical studies have supported this supposition by predicting that excitation of roughly half an electron per atom generates a crystal instability that spontaneously leads to crystal melting (23). Although ultrafast changes in the visible reflectivity led to this hypothetical nonthermal melting mechanism, these optical studies cannot unambiguously confirm the conjecture.

This puzzling situation made nonthermal melting a natural phenomenon for illustrating the viability of fs x-ray scattering (24). Studies of laser-excited InSb crystals with laser plasma-generated fs x-ray pulses observed a large amplitude decay of the (111) Bragg peak intensity in less than a ps (24). These measurements provided the first direct experimental evidence that large-scale atomic disordering proceeded concurrently with the large increase in optical reflectivity, but they could not identify the melting

mechanism because of the limited source intensity.

The higher x-ray fluence and shorter pulse duration of the SPPS x-ray source provided a new opportunity to determine the mechanism for nonthermal melting of InSb (25–27). Initial measurements demonstrated that, for the first half ps after laser excitation, the atoms disorder inertially. The constant velocity dynamics of the ionic cores observed in the experiment occur with a thermal velocity distribution unchanged by laser excitation and generate large-scale increases in crystal disorder. Only at substantially higher carrier densities was accelerated disordering observed as predicted by theory (23, 27). Inertial dynamics do not, however, eliminate the ionic memory of the crystallographic lattice. The average atomic positions in the crystal have not changed, only the width of the distribution for the nuclei (Fig. 1, A and B). This demonstrates that the formation of a liquid requires collisions that randomize ionic momenta. The observation of diffusive atomic motion on the ps time scale suggests the emergence of liquid dynamics (26), but observing the formation and structure of the nascent liquid phase cannot be achieved with crystallography. Observing the short-range order of the liquid phase requires the measurement of diffuse scattering, as has been achieved with ultrafast electron diffraction measurements of laser melting of aluminum (28) and which could be carried out with an XFEL source.

Although linear accelerator-based ultrafast x-ray sources have higher per-pulse flux than alternative ultrafast x-ray sources (18–20), they lack the inherent time synchronization between the x-ray probe and the laser excitation pulse of these alternative sources. In a laser pump linear accelerator-derived x-ray probe measurement, the laser pulses must be synchronized to the x-ray pulses. Synchronizing the laser to the radio frequency field that accelerates the electrons nominally achieves this goal but does not ensure high-quality synchronization. The residual timing jitter between the x-ray and laser pulses results in shot-to-shot variations in their relative times of arrival that, when averaged over multiple pulse pairs, has a standard deviation of roughly 1 ps for the SLAC linear accelerator (29). Any experiment that averaged the signal from multiple pulses without accounting for this jitter would have ps time resolution, even with 100-fs pulses.

Seeing time synchronization as the primary technical challenge to studying ultrafast dynamics with x-ray laser sources, the SPPS collaboration developed an electro-optic sampling (EOS) technique for measuring timing jitter on a shot-to-shot basis by cross-correlating the laser pulses used for sample excitation with the electric field from the electron bunch used to produce the x-ray pulses (29). Ideally, the cross correlation would be between laser and x-ray pulses, but the weak x-ray-matter interaction makes this much more challenging. A laser pump x-ray probe investigation of coherent vibrational motion in a

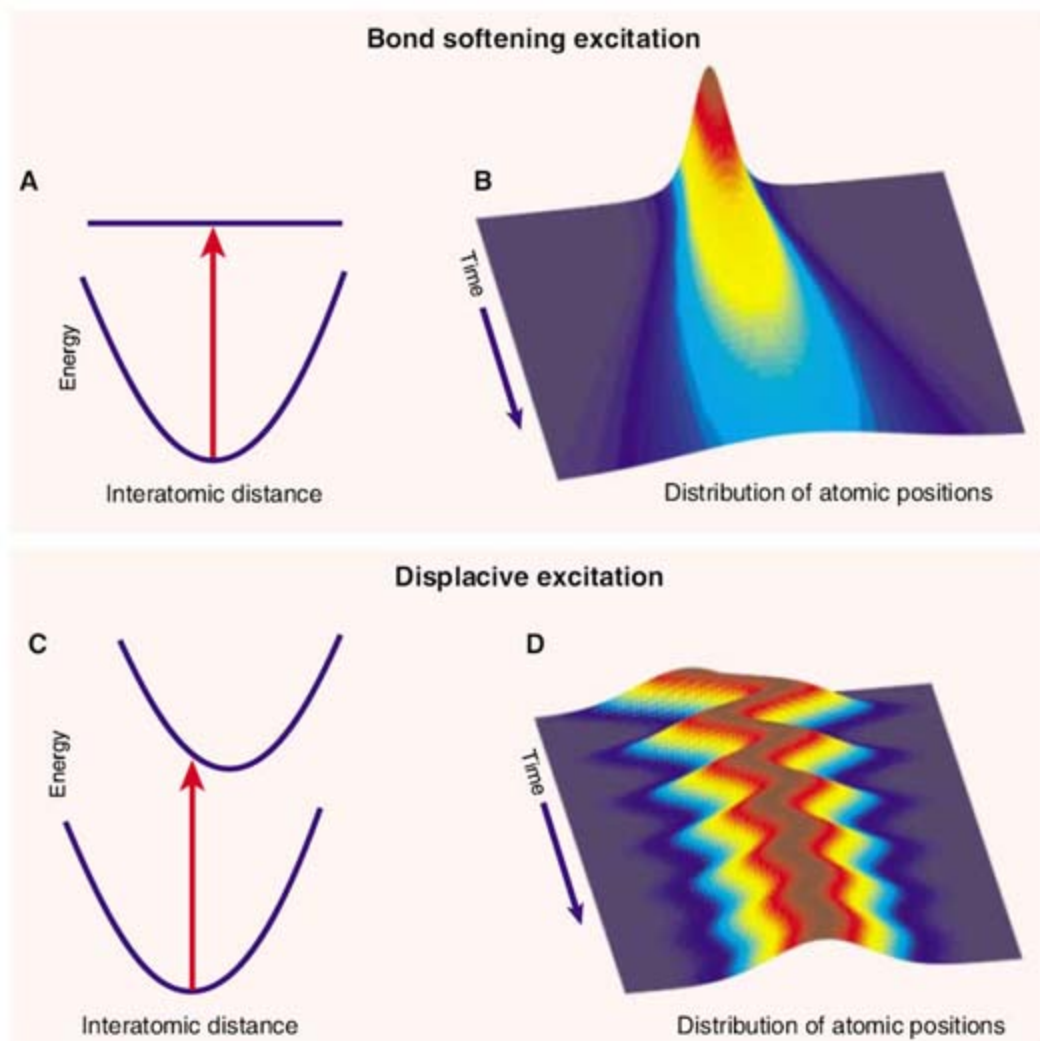


Fig. 1. (A) Schematic representation of photogenerated softening of the interatomic potential in InSb (25). (B) Time-dependent distribution of atomic positions following bond softening. The initial Gaussian distribution broadens linearly with time and with a velocity determined by the root mean square atomic velocities before laser excitation. (C) Schematic representation of a photogenerated shift in the equilibrium bond length in a bismuth crystal (30, 34). (D) Time-dependent distribution of atomic positions after displacive vibrational excitation. The frequency of the coherently excited vibration determines the period of the oscillation in average atomic position, whereas the magnitude of the shift in equilibrium position determines the amplitude of the oscillation.

bismuth crystal confirmed the ability of the EOS measurement to accurately determine the shot-to-shot time delay (30).

In this study, fs laser pulse excitation of bismuth changes the equilibrium structure of the unit cell and leads to coherent vibrational motion (31–33) (Fig. 1, C and D). This coherent motion generates large-amplitude oscillations, in particular Bragg peaks such as the (111) reflection (34). This experimental observation of strong ~300-fs period oscillations in the (111) Bragg diffraction intensity rigorously demonstrated the utility of EOS as a timing diagnostic (29, 30). These measurements also provided a detailed characterization of the excited state potential, further demonstrating the utility of ultrafast x-ray scattering for the

study of structural dynamics. Coherent vibrational motion in a ferroelectric crystal has also been observed with ultrafast x-ray diffraction by using laser-sliced x-ray pulses from a synchrotron (35). X-ray slicing sources represent an important development in ultrafast x-ray science with performance attributes distinct from XFEL sources. A complementary discussion of nonthermal melting and displacive excitations, as well as a discussion of data analysis, can be found in the Supporting Online Material (SOM) text.

Coherent X-ray Imaging with Atomic Resolution

Electromagnetic radiation can be used to image objects with a spatial resolution ultimately

limited by the wavelength, λ , of the radiation. Image formation can be simply described as interferometry; the light scattered by an object must be recombined so that it interferes at the image plane. Performing this reinterference directly with an aberration-free lens makes diffraction-limited imaging possible with visible radiation. In the simple case of illumination with a coherent plane wave, the achievable resolution equals $d = \lambda / \sin \theta$, where θ represents the highest scattering angle collected by a lens or detector. At x-ray wavelengths, however, manufacturing lenses that accept and redirect light scattered at high angles becomes increasingly difficult. Focal sizes of tens of nanometers can be achieved (36), but atomic-resolution lenses do not appear feasible.

Imaging at near-atomic resolution can be achieved without lenses by conducting the reinterference of the scattered light computationally. The numerical determination of the image from the measured x-ray scattering pattern requires that the phase of the diffracted light be determined in order to apply the correct phase shift to each reinterfering spatial frequency. Because the detection of the scattering pattern only measures the intensity of the scattering radiation rather than the amplitude, no phase information can be directly measured. A variety of methods have been developed for alleviating the information deficit in crystallography, such as examining the wavelength dependence of the diffraction pattern near an atomic absorption edge or by knowing part of the structure or a similar structure. With coherent diffractive imaging, an alternative route to reconstructing the scattered x-rays into an image can be used.

Sayre has noted that the continuous diffraction pattern of a coherently illuminated unit cell contains twice the information obtained from the diffraction pattern of a crystalline arrangement of identical copies of that unit cell (2, 37). If adequately sampled, this pattern provides the exact amount of information needed to solve the phase problem and deterministically invert the x-ray scatter pattern into an image of the scattering object. The past several decades have seen substantial advances in the experimental and numerical techniques re-

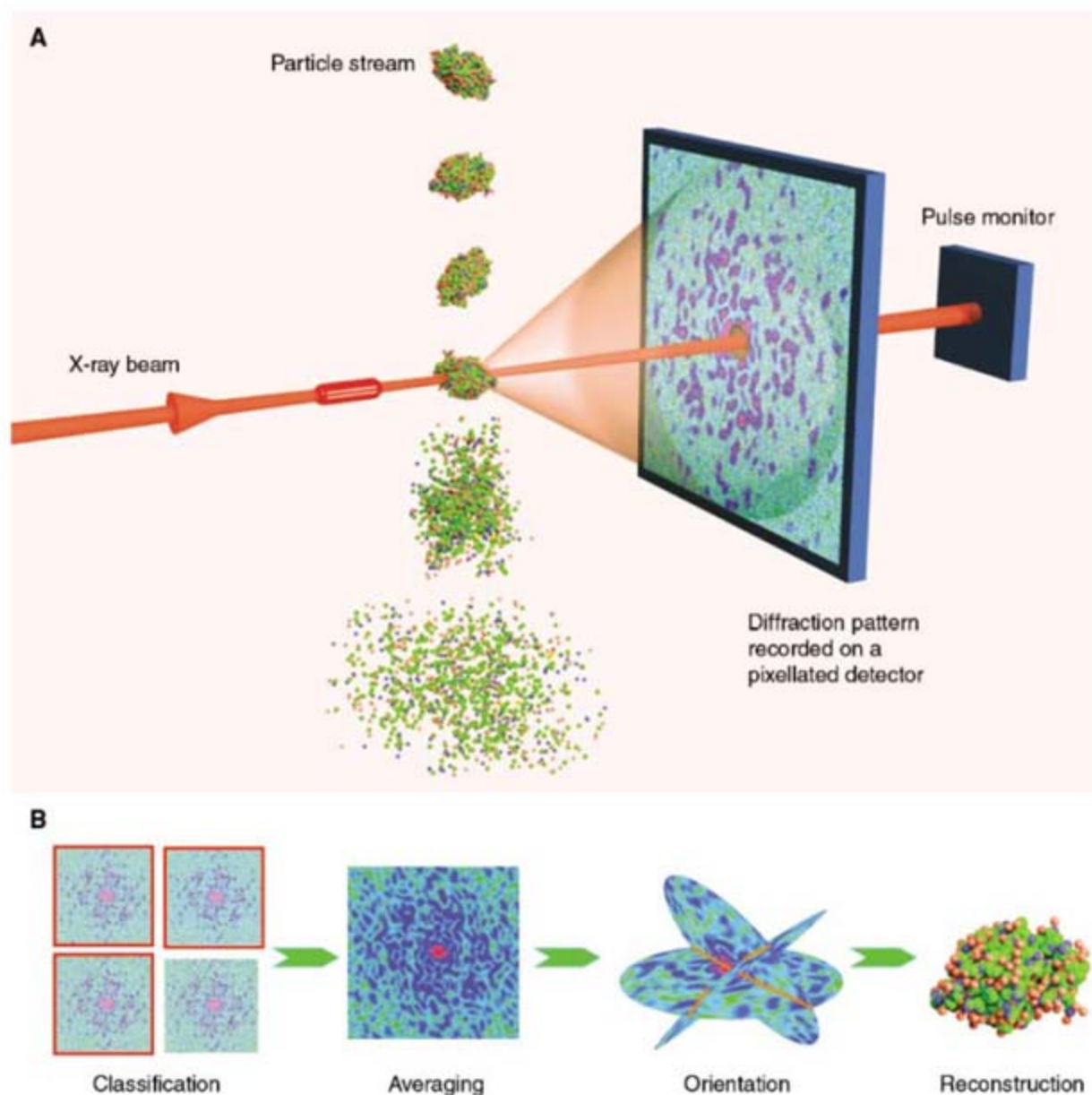


Fig. 2. Schematic depiction of single-particle coherent diffractive imaging with an XFEL pulse. **(A)** The intensity pattern formed from the intense x-ray pulse (incident from left) scattering off the object is recorded on a pixelated detector. The pulse also photo-ionizes the sample. This leads to plasma formation and Coulomb explosion of the highly ionized particle, so only one diffraction pattern [a single two-dimensional (2D) view] can be recorded from the particle. Many individual diffraction patterns are recorded from single particles in a jet (traveling from top to bottom). The particles travel fast enough to clear the beam by the time the next pulse (and particle) arrives. The data must be read out from the detector just as quickly. **(B)** The full 3D diffraction data set is assembled from noisy diffraction patterns of identical particles in random and unknown orientations. Patterns are classified to group patterns of like orientation, averaged within the groups to increase signal to noise, oriented with respect to one another, and combined into a 3D reciprocal space. The image is then obtained by phase retrieval.

quired for coherent diffractive imaging (3). Coherent diffractive x-ray imaging experiments have primarily used iterative algorithms for image reconstruction, with resolutions approaching 10 nm having been achieved (4, 5).

Radiation damage limits the highest resolution achievable with coherent diffractive imaging. When using 8-keV x-ray photons to image low atomic number materials such as a biomolecule, for every scattered photon that contributes to the diffraction pattern there are about 10 x-ray photons absorbed. This absorption deposits energy into the sample and leads to sample degradation. When exposed to high average brightness synchrotrons, biological materials can withstand doses of roughly 200 photons/Å² with cryogenic cooling. For a noncrystalline protein surrounded by vitreous ice, the number of scattered photons varies as 1/θ⁴. An exposure of 200 photons/Å² gives statistically significant signal only for feature sizes larger than $d = 10$ nm, much too coarse for imaging molecular or atomic structures, which have angstrom scale features.

Delivering the radiation dose to the sample before radiation-induced structural degradation provides a strategy to exceed the exposure limit set by the radiation damage threshold at synchrotron facilities. Solem and Baldwin (6) first proposed x-ray laser flash imaging microscopy. Neutze *et al.* extended this concept to the use of XFEL pulses to image single nanoscopic particles at near-atomic resolution (7). They used a molecular dynamics simulation to model the interaction of a focused XFEL pulse on a single biomolecule. They simulated the influence of x-ray photo-ionization, electronic relaxation, illuminated particle charging, and the resultant Coulomb explosion while simultaneously calculating the x-ray scattering pattern (Fig. 2). They predict that x-ray lasers will allow fluences 10⁵ times larger for biological imaging than presently achievable with synchrotron radiation if the x-rays are delivered to the sample before the Coulomb explosion. This simulation indicates that the pulse will need to be tens of fs in duration or shorter for the explosion to have a minimal influence on the x-ray scattering pattern. For biological objects, the increased x-ray dose should allow single-pulse images to be acquired with about 1-nm resolution. Higher-resolution images will be achievable with more strongly scattering high-atomic-number materials. In addition to these molecular dynamics simulations, hydrodynamic calculations have modeled the influence of an intense ultrafast x-ray pulse on the atomic structure of a macromolecule or cluster (38, 39).

Despite the enormous increase in allowed fluence, atomic-resolution imaging of single particles will require averaging of multiple images (7, 40). This will need to be done serially, with a new, identical particle being delivered on every x-ray shot. Ideally, the particle should be the only scattering object in the beam path, requiring them to be introduced into vacuum and efficiently

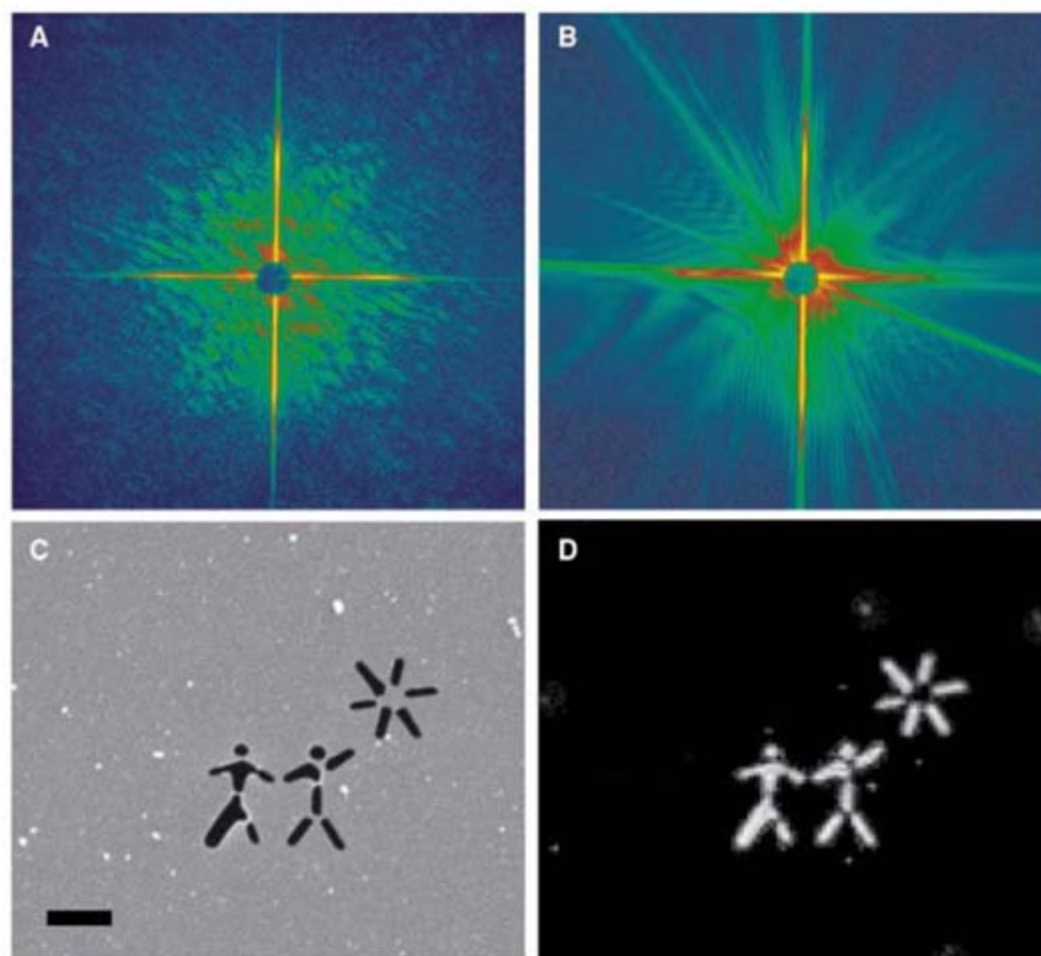


Fig. 3. (A) Diffraction pattern recorded with a single FEL pulse from a test object placed in the 20- μm focus of the beam (8). (B) The diffraction pattern recorded with a second FEL pulse selected with a fast shutter, showing diffraction from the hole in the sample created by the first pulse. (C) Scanning electron microscope image of the test object, which was fabricated by ion-beam milling a 20-nm-thick silicon nitride membrane. The scale bar denotes 1 μm . (D) The image reconstructed from the single-shot diffraction pattern shown in (A).

transported to the interaction volume. For randomly oriented particles, the requirement of orienting each single-pulse single-particle diffraction pattern sets the minimum scattering intensity. By following strategies similar to those used in single-particle cryoelectron microscopy (41), it will be possible to classify data into groups of similar orientation and vastly increase the signal-to-noise ratio by averaging. These classes must then be assembled into a three-dimensional coherent diffraction pattern (40), which will be phased (Fig. 2). Alternatively, the gas-phase particles could be aligned by a nonresonant laser pulse (42), greatly easing the single-pulse signal to noise required for computational alignment and averaging.

The single-pulse diffractive image of a micrometer-sized test object recorded at FLASH provides a dramatic illustration of the “flash” imaging technique (8) (Fig. 3). This demonstrates that an interpretable coherent diffraction pattern with excellent signal to noise can be collected from a small isolated object in a single FEL pulse. The focused pulse can destroy all material in its path, including the detector, and it was not previously obvious whether a diffraction pattern could be recorded without a large background

resulting from scattering from a beam stop, from the focusing optics, or from plasma radiation from the sample. These effects were prevented by using a novel graded multilayer mirror that only reflects the elastically scattered light from the sample onto a charge-coupled device (CCD) detector located in the optical far field and harmlessly passes the strong undiffracted beam through a hole in the mirror. The pulse that recorded the diffraction pattern heated the sample up to about 60,000 K, which ablated and melted. Nevertheless, the image is recorded to the 62-nm diffraction limit of the detector aperture, showing no effects of damage. Compared with diffractive imaging at synchrotrons, which is difficult because of the low coherent flux available and the need to filter a single coherent mode from an incoherent source, imaging with the FEL is straightforward and requires no spatial or spectral filtering of the illuminating pulse.

Future Prospects

The importance of ultrafast x-ray scattering and imaging measurements extends beyond the particular phenomena and materials studied to date. Excited state potential energy surfaces govern the evolution of nonequilibrium systems and also the

dynamics and kinetics of rare events in equilibrium systems, such as thermal phase transitions and chemical reactions. The SPPS collaboration has demonstrated that fs x-ray scattering can determine the topography of the excited state potential energy surface with unprecedented detail. Despite the success of the SPPS collaboration, the low flux of the source determined the scope of the scientific program. At the LCLS, the integrated x-ray production in 10 s of lasing will exceed the total x-ray photon production at the SPPS during its 3-year lifetime.

The increased flux will make possible diffuse scattering measurements for a wide variety of materials. For the vast majority of ultrafast phenomena, the transformations in structure will be localized in space and occur on the angstrom length scale. These changes in short range order will be manifest in the diffuse scattering. Femtosecond-resolution diffuse scattering measurements will be particularly important for studies of solution phase chemical dynamics (11) and order-disorder phase transition studies (28). Learning how to exploit the coherence of the x-ray pulses for studies of dynamics will also be an important aspect of the initial science programs at XFEL facilities. With coherent imaging techniques, the absolute structure, not just the average structure, can be measured. This should prove to be an important attribute for the investigation of first-order phase transitions, where deviations from the average structure, such as defects and imperfections, nucleate phase transformations. Time-resolved FEL imaging with an ultrafast optical pump will follow from practices developed at synchrotron slicing sources and the SPPS. Techniques for pumping samples with FEL pulses and probing the resultant dynamics with time-delayed FEL pulses will require further experimental development. One promising approach involves splitting the FEL pulse at or near the sample with use of a section of an optical element destroyed by the FEL pulse, along with the sample (43). Despite the many experimental and technical challenges that will exist at x-ray-free electron laser sources, the unprecedented peak brightness of XFEL radiation should open the field of ultrafast x-ray science

to a range of applications and phenomena approaching those studied with ultrafast lasers and x-ray synchrotrons.

The field of coherent x-ray diffractive imaging will benefit tremendously from the construction of x-ray laser sources. The FLASH free electron laser has demonstrated the feasibility of "instantaneous" imaging and provided a unique opportunity to prepare for the enormous peak brightness and power needed for atomic-resolution imaging. Major technical and experimental advances have been achieved in the past 2 years, although many challenges remain. These advances, in conjunction with the expected flux and time resolution of x-ray laser sources, will enable x-ray imaging with unprecedented spatial resolution. With XFEL sources, the dream of atomic-resolution imaging may become reality.

References and Notes

- Z. Dauter, *Acta Crystallogr.* **D62**, 1 (2006).
- D. Sayre, *Struct. Chem.* **13**, 81 (2002).
- J. W. Miao, H. N. Chapman, J. Kirz, D. Sayre, K. O. Hodgson, *Annu. Rev. Biophys. Biomol. Struct.* **33**, 157 (2004).
- H. N. Chapman *et al.*, *J. Opt. Soc. Am. A* **23**, 1179 (2006).
- D. Shapiro *et al.*, *Proc. Natl. Acad. Sci. U.S.A.* **102**, 15343 (2005).
- J. C. Solem, G. C. Baldwin, *Science* **218**, 229 (1982).
- R. Neutze, R. Wouts, D. van der Spoel, E. Weckert, J. Hajdu, *Nature* **406**, 752 (2000).
- H. N. Chapman *et al.*, *Nat. Phys.* **2**, 839 (2006).
- An x-ray-free electron laser uses a fs-duration bunch of high-energy electrons as the gain medium in a single pass laser. Acceleration of these high-energy electrons in an oscillatory magnetic field causes the electrons to spontaneously emit x-ray photons. This radiation emitted in the first few periods of the magnetic field interacts with the electron bunch, causing it to form many microbunches. Each microbunch within the fs-duration macropunch emits coherently, creating many sub-fs pulses of x-ray light contained within a roughly 100-fs-duration macropulse.
- F. Schotte *et al.*, *Science* **300**, 1944 (2003).
- H. Ihee *et al.*, *Science* **309**, 1223 (2005); published online 14 July 2005 (10.1126/science.1114782).
- R. Tatchyn *et al.*, *Nucl. Instrum. Methods* **A375**, 274 (1996).
- V. Ayvazyan *et al.*, *Eur. Phys. J. D* **37**, 297 (2006).
- www-ssl.slac.stanford.edu/lcls/.
- <http://xfel.desy.de/>.
- www-xfel.spring8.or.jp/.
- Brightness provides a particularly important metric for single-shot imaging, because brightness determines the deliverable x-ray flux on an extremely small sample.
- R. W. Schoenlein *et al.*, *Science* **287**, 2237 (2000).
- C. Spielmann *et al.*, *Science* **278**, 661 (1997).
- M. M. Murnane, H. C. Kapteyn, M. D. Rosen, R. W. Falcone, *Science* **251**, 531 (1991).
- J. C. Williamson, J. M. Cao, H. Ihee, H. Frey, A. H. Zewail, *Nature* **386**, 159 (1997).
- C. V. Shank, R. Yen, C. Hirlimann, *Phys. Rev. Lett.* **50**, 454 (1983).
- P. Stampfli, K. H. Bennemann, *Phys. Rev. B* **46**, 10686 (1992).
- A. Rousse *et al.*, *Nature* **410**, 65 (2001).
- A. M. Lindenberg *et al.*, *Science* **308**, 392 (2005).
- K. J. Gaffney *et al.*, *Phys. Rev. Lett.* **95**, 125701 (2005).
- P. B. Hillyard *et al.*, *Phys. Rev. Lett.* **98**, 125501 (2007).
- B. J. Siwick, J. R. Dwyer, R. E. Jordan, R. J. D. Miller, *Science* **302**, 1382 (2003).
- A. L. Cavalieri *et al.*, *Phys. Rev. Lett.* **94**, 114801 (2005).
- D. M. Fritz *et al.*, *Science* **315**, 633 (2007).
- T. K. Cheng *et al.*, *Appl. Phys. Lett.* **57**, 1004 (1990).
- S. Hunsche, K. Wienecke, T. Dekorsy, H. Kurz, *Phys. Rev. Lett.* **75**, 1815 (1995).
- T. E. Stevens, J. Kuhl, R. Merlin, *Phys. Rev. B* **65**, 144304 (2002).
- K. Sokolowski-Tinten *et al.*, *Nature* **422**, 287 (2003).
- A. Cavalleri *et al.*, *Nature* **442**, 664 (2006).
- C. Liu *et al.*, *J. Appl. Phys.* **98**, 113519 (2005).
- D. Sayre, *Acta Crystallogr.* **5**, 843 (1952).
- S. P. Hau-Riege, R. A. London, A. Szoke, *Phys. Rev. E* **69**, 051916 (2004).
- Z. Jurek, G. Faigel, M. Tegze, *Eur. Phys. J. D* **29**, 217 (2004).
- G. Huldt, A. Szoke, J. Hajdu, *J. Struct. Biol.* **144**, 219 (2003).
- U. Adiga *et al.*, *J. Struct. Biol.* **152**, 211 (2005).
- H. Stapelfeldt, T. Seideman, *Rev. Mod. Phys.* **75**, 543 (2003).
- S. P. Hau-Riege *et al.*, *Phys. Rev. Lett.* **98**, 145502 (2007).
- K.J.G. thanks the SPPS collaboration, in particular J. B. Hastings, A. M. Lindenberg, and D. A. Reis, as well as the U.S. Department of Energy (DOE) and the W. M. Keck Foundation for financial support. H.N.C. thanks J. Hajdu and Lab-Directed Research and Development support at Lawrence Livermore National Laboratory. This work was performed in part under the auspices of the DOE by University of California, Lawrence Livermore National Laboratory, under contract W-7405-Eng-48.

Supporting Online Material

www.sciencemag.org/cgi/content/full/316/5830/1444/DC1
SOM Text
Fig. S1
References

Q

Who inspires
brainwaves while
I study water waves?



AAAS

“ I study the mathematical equations that describe the motion of water waves. Different equations represent different waves – waves coming onto a beach, waves in a puddle, or waves in your bathtub. Then when I’ve surfed the math, I like nothing better than to spend the rest of the day surfing the waves.

This field is very important. The better we can model water waves, the better we can predict the patterns of beach erosion and natural disasters such as the tsunami in South East Asia. And this research can be applied to all sorts of regions around the world.

Being a member of AAAS means I get to learn about areas of interest I might not otherwise encounter. It gives me valuable opportunities to exchange ideas with colleagues in other fields. And this helps me find new approaches to ” my own work.

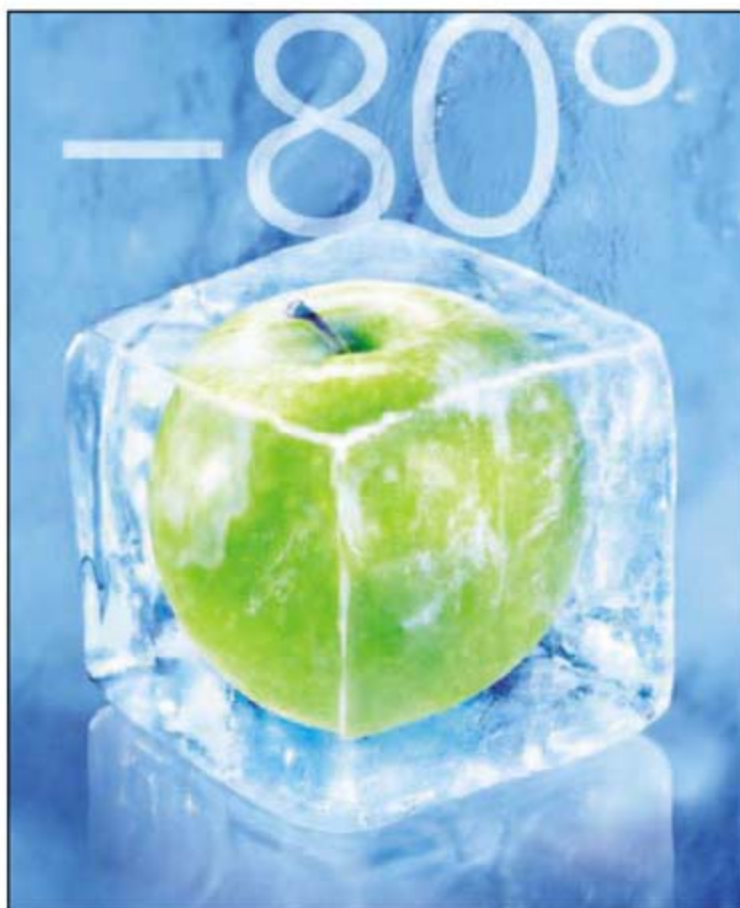
Dr. Katherine Socha is an assistant professor of mathematics at St. Mary’s College, Maryland. She’s also a member of AAAS.

See video clips of this story and others at www.aaas.org/stories

Katherine Socha, Ph.D.
Assistant Professor of Mathematics
and AAAS member



ADVANCING SCIENCE. SERVING SOCIETY



REMP offers small, medium and large scale automated systems and stores to suit your needs without having to compromise on the quality of sample processing and storage.

Sample Safe



The REMP Sample Safe™ is a compact, scalable, fully automated and easy to use storage solution that operates at temperatures down to -80°C . It is supporting all SBS standard produced MTPs and DWPs. Combined with the unique, patented REMP Tube Technology™, it minimizes the degradation of valuable samples caused by freeze/thaw cycles significantly and helps to obtain highly reproducible data sets for your research. The REMP Sample Safe™ is designed to fit any lab and is able to grow with your storage needs.

www.remp.com

REMP
sample management

 **TECAN** • REMP is a Tecan Group company

1,000's OF GRANTS MILLIONS IN FUNDING



GrantsNet. The first comprehensive science grants database.

GrantsNet is expanding its listings of some 900 funding programs from private foundations and not-for-profit organizations to include 400 to 500 new entries from the grants.gov site. **This provides the first comprehensive database of funding opportunities** to research scientists and administrators, career counselors, financial aid specialists, and undergraduate and graduate students. For listings, go to www.grantsnet.org

ScienceCareers.org

We know science

 AAAS

Expansion of Industrial Logging in Central Africa

Nadine T. Laporte,* Jared A. Stabach, Robert Grosch, Tiffany S. Lin, Scott J. Goetz

Central Africa's dense humid forests have long been regarded as among the most pristine on Earth, but in recent decades industrial logging has become the most extensive form of land use in the region. Currently more than 600,000 km² (30%) of forest are under logging concessions, whereas just 12% is protected. Logging-related disturbance in the region alters ecosystem composition and biodiversity (1), opens remote areas to poaching (2), and modifies numerous functional attributes of the ecosystem (3). Laws and regulations are in place to improve forest management at national and regional scales, but limited resources are available to enforce regulations or to provide technical support (4). Here, we report on the use of over 300 Landsat satellite images, covering 4 million km², to track the progression of logging roads for three decades preceding 2003 (5). We document accelerating rates of logging road construction in much of the region and show that monitoring with satellite remote sensing provides a practical approach to map changes associated with logging activities.

We mapped 51,916 km of logging roads within the forested region (Fig. 1). This is a conservative estimate, because not all areas had recent cloud-free satellite images (5) and logging roads are converted to public roads where population density is high. Logging roads accounted for 38% of the length of all roads, ranging from 13% in the Democratic Republic of Congo (DRC) to >60% in Gabon and the Republic of Congo (ROC). The combined road density (public and logging) was 0.07 km km⁻² and, considering logging roads only, 0.03 km km⁻². The highest logging road densities (0.09 km km⁻²) were in Cameroon and Equatorial Guinea (EG), where most of the forest was cut at least once. Logging in these two countries and in Gabon has extended inland in recent decades after the earlier harvesting of coastal forest.

The most rapidly changing area was in northern ROC, where the rate of road construction increased from 156 km year⁻¹ for the period 1976–1990 to over 660 km year⁻¹ after 2000. Evidence for a new frontier of logging expansion was documented within the DRC, which currently contains 63% of

the total remaining forest of the region and has the lowest measured logging road density (0.01 km km⁻²) of all Central African nations. Rates of logging road construction increased within DRC, particularly in a 50,000-km² region of north-central DRC, where the rate of road development progressed from 336 km year⁻¹ (1986–1990) to 456 km year⁻¹ (2000–2002). We expect industrial logging concessions to expand, with commensurate increases in the rates of logging and road building associated with foreign investment (6).

With the exception of the Okoumé forests of Gabon (7), most of the industrial logging is selective and focused on high-value tree species for export (for example, African mahoganies). We estimated 5% (89,715 km²) of the total forested area as disturbed and 29% (567,782 km²) as more likely to have increased wildlife hunting pressure because of easier access and local market opportunities offered by new logging towns (5). The greatest amount of forest disturbance (15%) occurred in Cameroon and EG, compared with just 1% within the DRC. In addition, we used finer resolution (4-m) satellite imagery to document disturbance created by logging skid trails and tree felling. These locally disturbed areas had canopy gaps that were five to six times larger than those in adjacent unlogged forests. Gaps created by tree fall ranged from 200 to 600 m² in size and, together with skid trails, accounted for 9% of the area in which logging occurred.

To date, few reliable data sets have been available to monitor the changes taking place in remote areas of the Congo Basin, but regular monitoring with satellite remote sensing provides a consistent approach to monitor both legal and illegal logging activities. In the context of the rapid frontier expansion, the conservation of forested landscapes and sustainable timber production is crucial for Central African nations and their inhabitants.

References and Notes

1. J. R. Malcolm, J. C. Ray, *Conserv. Biol.* **14**, 1623 (2000).
2. J. G. Robinson, K. H. Redford, E. L. Bennett, *Science* **284**, 595 (1999).
3. J. S. Hall, D. J. Harris, V. Medjibe, P. M. S. Ashton, *For. Ecol. Manage.* **183**, 249 (2003).
4. The Central Africa Forests Commission, www.comifac.org.
5. Materials and methods are available on *Science Online*.
6. P. Buys, U. Deichmann, D. Wheeler, "Road network upgrading and overland trade expansion in sub-Saharan Africa" (Policy Research Working Paper WPS 4097, World Bank, Washington, DC, 2006); available online at www.worldbank.org/reference.
7. L. J. T. White, *J. Trop. Ecol.* **10**, 309 (1994).
8. Supported by NASA grants NNG05GD14G and NNS06AA06A. We thank E. Davidson, R. A. Houghton, and D. Nepstad for comments on the manuscript.

Supporting Online Material

www.sciencemag.org/cgi/content/full/316/5830/1451/DC1

Materials and Methods

Fig. S1

Table S1

References and Notes

8 February 2007; accepted 26 April 2007

10.1126/science.1141057

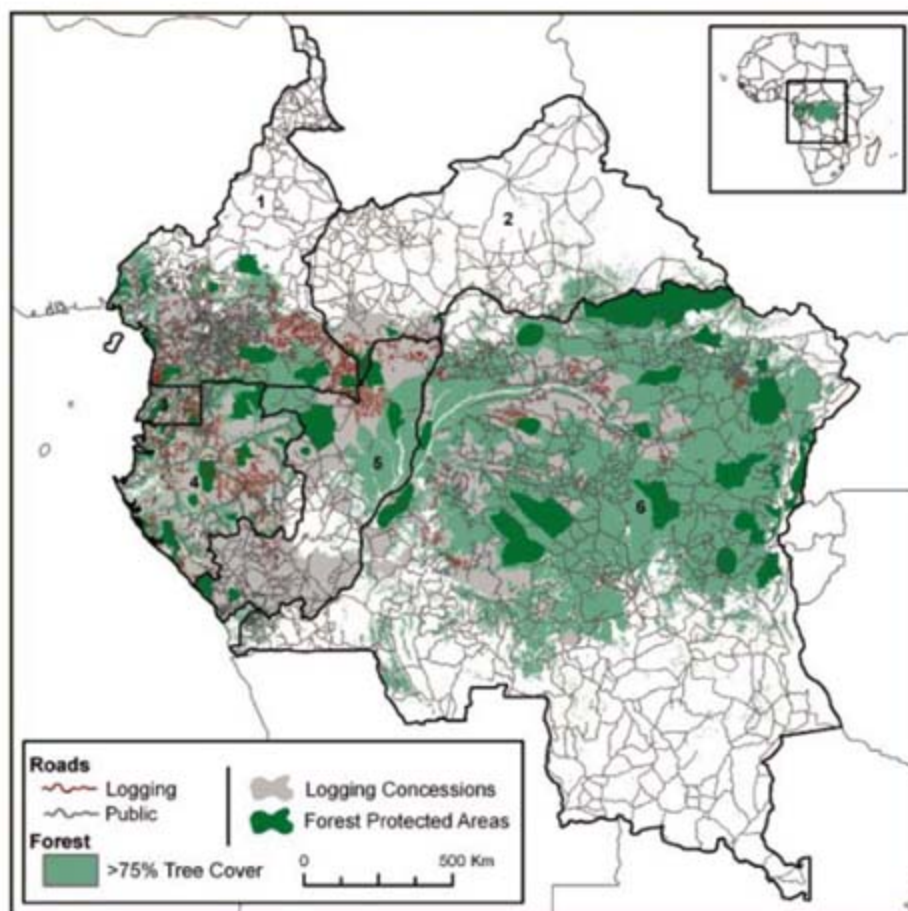


Fig. 1. Logging concessions and road distribution in Central Africa: Cameroon (labeled on the map as 1), Central African Republic (2), Equatorial Guinea (3), Gabon (4), Republic of Congo (5), and Democratic Republic of Congo (6). A more detailed graphic of logging roads for a portion of the region is provided in fig. S1.

Woods Hole Research Center, Falmouth, MA 02540, USA.

*To whom correspondence should be addressed. E-mail: nlaporte@whrc.org

Evolution and Development of Inflorescence Architectures

Przemyslaw Prusinkiewicz,¹ Yvette Erasmus,^{2*} Brendan Lane,¹ Lawrence D. Harder,³ Enrico Coen^{2†}

To understand the constraints on biological diversity, we analyzed how selection and development interact to control the evolution of inflorescences, the branching structures that bear flowers. We show that a single developmental model accounts for the restricted range of inflorescence types observed in nature and that this model is supported by molecular genetic studies. The model predicts associations between inflorescence architecture, climate, and life history, which we validated empirically. Paths, or evolutionary wormholes, link different architectures in a multidimensional fitness space, but the rate of evolution along these paths is constrained by genetic and environmental factors, which explains why some evolutionary transitions are rare between closely related plant taxa.

Organisms display great diversity in shape and architecture, but the range of observed forms represents only a small fraction of what is theoretically possible (1, 2). For example, when patterns of shell coiling are considered within a mathematically defined space of possible forms (morphospace), the observed forms are restricted to only a subregion of this space (3). One explanation for such restrictions is selection (4). However, it is likely that developmental and genetic mechanisms also play a role. For example, the absence of vertebrates with more than four limbs is thought to reflect an interplay between both developmental and selective constraints (5, 6). Developmental mechanisms restrict the range of genetic and phenotypic variation available for selection, whereas selection influences the evolution of developmental processes. Such two-way interactions can be unravelled using morphospaces based on developmental genetic mechanisms. We take this approach for the evolution of inflorescences, which has a history of both theoretical and molecular genetic analysis.

The arrangement of flowers on a plant reflects an iterative pattern of developmental decisions at the growing tips, or meristems. Each iteration occurs over a time interval known as a plastochron (7), during which a meristem may either switch to floral identity or continue to produce further meristems and, hence, branches. As the number of iterations rises, the number of the-

oretically possible structures increases rapidly (8). However, only a small subset of these structures corresponds to inflorescences observed in nature (Fig. 1). They are grouped into three broad architectural types: (i) panicles, which comprise a branching series of axes that terminate in flowers; (ii) racemes, which comprise axes bearing flowers in lateral positions or lateral axes that reiterate this pattern; and (iii) cymes, which comprise axes that terminate in flowers and lateral axes that reiterate this pattern (9–11) (Fig. 1, D to I). The appearance of each inflorescence type varies according to the arrangement of lateral meristems around the stem (phyllotaxy), the pattern of internode lengths, and additional variations on the three architectural themes. Although panicles, racemes, and cymes are all found among flowering plants, a restricted range of types is evident at local taxonomic levels: Genera seldom include species with both racemes and cymes.

These observations raise two related questions. First, what determines the extent of morphospace occupied by inflorescences in nature: Why do we find these three main architectural types and not more or fewer? Second, what constrains evolution within the occupied morphospace, imposing a local barrier between racemes and cymes?

A unifying inflorescence model. Previously, distinct developmental models have been postulated for different inflorescence types (12, 13), leading to a fractured view of phenotypic space. From an evolutionary perspective, however, inflorescence types should be related to each other through genetic changes. A developmental model that encompasses different architectural types within a single parameter space is thus needed. To construct it, we considered meristems giving rise to shoots or flowers as two extremes of a continuum. The variable that characterizes this continuum is called vegetativeness (*veg*), with high levels of *veg* corresponding to shoot meristem identity and low levels to flower meristem identity. The *veg* level may be related to many factors such as plant age, meristem position, internal state of a meristem, and the environment (14–17). For simplicity, we identify the factors influencing *veg* as plant age *t*, measured from the beginning of inflorescence development, and/or the internal state of the meristem.

If *veg* is high and does not change with time, an indeterminate vegetative branching structure is generated (Fig. 2A). For the plant to produce flowers, *veg* must decline in some or all meristems during growth. The simplest assumption is that *veg* decreases in all meristems equally. The resulting architecture is a panicle of flowers, which form at time *T* when low levels of *veg* are reached (Fig. 2B).

To generate further architectural types, we assume that meristems can be in one of two internal states, A and B, such that meristems in these states attain low levels of *veg* at different

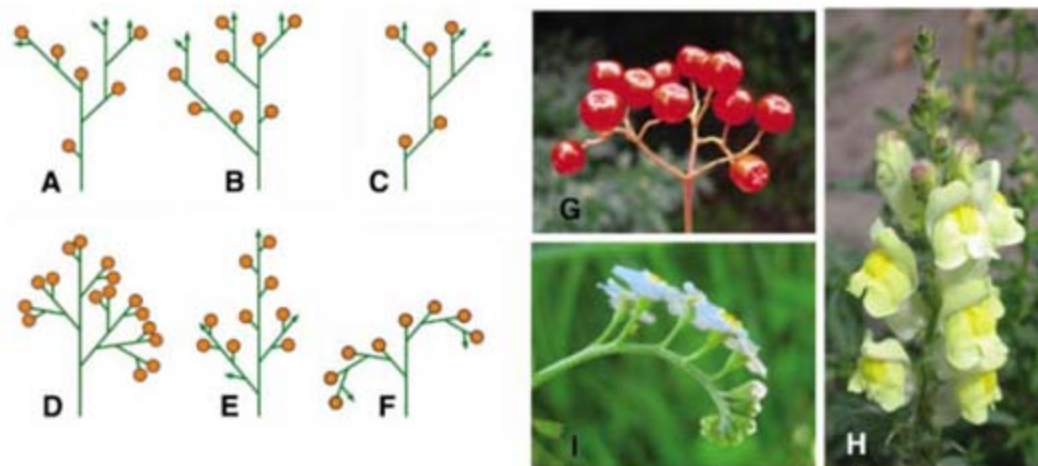


Fig. 1. Hypothetical and observed inflorescence structures. Arrows, meristems; circles, flowers. (A to C) Inflorescence structures not observed in nature. (D to F) Three main classes of inflorescence architectures: panicle (D), raceme (E), and cyme (F). (G to I) Species illustrating inflorescence types: (G) fruiting panicle of *Sorbus aucuparia*, (H) flowering raceme of *Antirrhinum majus*, (I) flowering cyme of *Myosotis arvensis*.

¹Department of Computer Science, University of Calgary, 2500 University Drive N.W. Calgary, Alberta T2N 1N4, Canada. ²Department of Cell and Developmental Biology, John Innes Centre, Colney Lane, Norwich NR4 7UH, UK. ³Department of Biological Sciences, University of Calgary, 2500 University Drive N.W. Calgary, Alberta T2N 1N4, Canada.

*Present address: Institute of Molecular Plant Science, Daniel Rutherford Building, Kings Buildings, Mayfield Road, Edinburgh, EH9 3JR, UK.

†To whom correspondence should be addressed. Email: enrico.coen@bbsrc.ac.uk

times, T_A and T_B . Suppose that the apical meristem of the main axis is in state A, whereas all lateral meristems are in state B. If $T_B < T_A$, lateral meristems will attain floral identity more quickly than does the apical meristem, yielding a raceme in the upper part of the plant (red path in Fig. 2C). However, lateral apices in the lower part of the inflorescence will also rapidly progress toward floral identity, producing a graded series of panicles (orange path in Fig. 2C). This

result is inconsistent with the structure of lateral branches of compound racemes, which typically do not terminate in flowers (Fig. 1E).

To resolve this discrepancy, we postulate that state B is transient. All lateral meristems are formed in state B, but they have two possible fates afterwards. If *veg* is sufficiently low, the meristem becomes a flower (red path, Fig. 2D). Otherwise, the meristem reverts to state A and produces a branch (orange path, Fig. 2D). The

rationale for this reversion is that a newly created meristem (state B) changes its identity once it becomes the terminal meristem of the next-order branch (state A). Biologically, state B represents the stage when a meristem is newly formed (immature), whereas state A represents a more advanced stage of meristem development (mature). We call the resulting model the transient model.

A key feature of the transient model is that it can generate cymes as well as racemes and panicles, thus accounting for these inflorescence types within a single framework. In cymes, lateral meristems repetitively create meristems in two different states: a terminal meristem giving rise to a flower, and a lateral meristem giving rise to a branch (Fig. 1F). This can be captured with the transient model by setting $T_A < T_B$. Immature lateral meristems then take longer to attain floral identity than do mature meristems, creating the reverse of the situation for racemes (Fig. 2E).

The region of morphospace generated by the transient model is illustrated in Fig. 3. The main diagonal ($T_A = T_B$) corresponds to panicles, flanked by racemes on one side ($T_A > T_B$) and cymes on the other ($T_A < T_B$). This planar region represents only a slice of the entire morphospace. For example, the hypothetical forms shown in Fig. 1, A to C, do not lie in this region and could only be generated with more complex mechanisms. The transient mechanism may therefore account for the restriction of observed inflorescence types to a small region of morphospace. Potentially adaptive architectures may not be attained in nature because they cannot be produced by developmental processes captured by the transient mechanism.

Integration of models with developmental and molecular genetics. To assess the plausibility of the transient model, we related it to underlying genetic mechanisms. We focused on two architectural genes from *Arabidopsis*, *TERMINAL FLOWER 1 (TFL1)* and *LEAFY (LFY)* (18–23), as they produce phenotypes that displace the wild-type plant in orthogonal directions in morphospace (Fig. 3). Compared to wild-type *Arabidopsis*, which produces branched racemes, mutants lacking *TFL1* activity produce inflorescences with short axes that terminate in flowers, whereas mutants lacking *LFY* produce highly branched inflorescences bearing shootlike flowers.

We incorporated genes into the transient model by postulating that *TFL1* increases *veg* and *LFY* reduces *veg* in meristems (Fig. 4A). The wild-type *Arabidopsis* architecture results from high *TFL1* and low *LFY* activity in state A meristems (yielding high *veg*) and high *LFY* and low *TFL1* activity in state B meristems (yielding low *veg*). This pattern of gene expression is produced by assuming that: (i) *LFY* and *TFL1* inhibit each other (18, 20, 22), (ii) *TFL1* expression is inhibited in state B, (iii) *LFY* is less sensitive to *TFL1* inhibition in state B [this enhances *LFY* in B meristems and allows *LFY* to attain high activity even in plants overexpressing

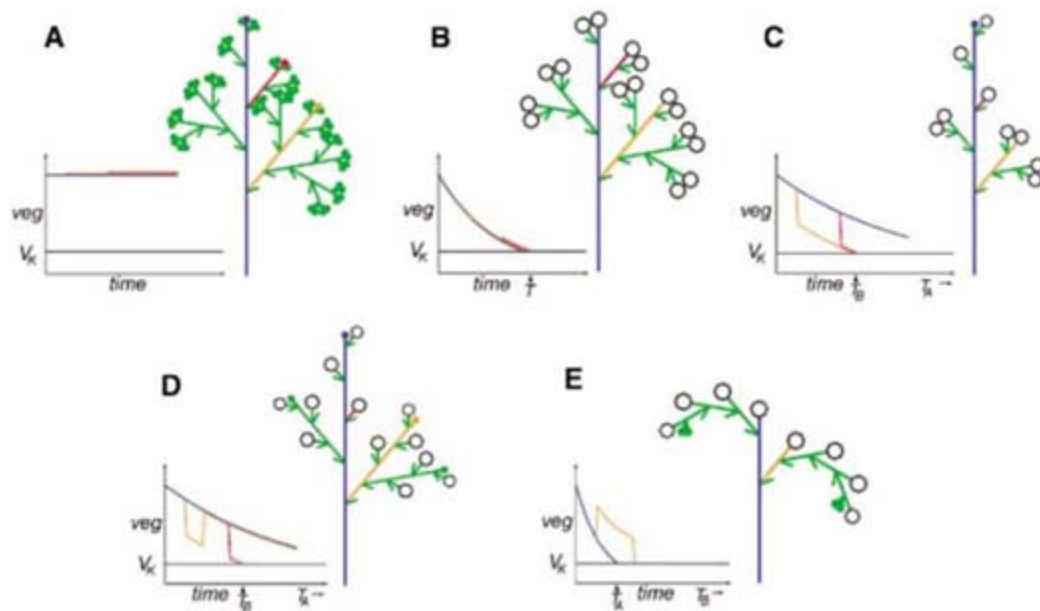


Fig. 2. Architectures and time course of *veg* decline for various inflorescence models. Small filled circles, meristems; white circles, flowers. Colors highlight paths of representative meristems: main meristem, blue; lowest lateral meristem, orange; third lateral meristem from bottom, red. Plots show the time course of *veg* decline in selected meristems after their initiation. (A) Level of *veg* does not change with time; an indeterminate vegetative branching structure results. (B) *veg* declines at a similar rate in all meristems and yields flowers upon reaching threshold V_K at time T ; a panicle results. (C) *veg* in apical meristems (state A) reaches threshold V_K at time $T_A > T_B$ for lateral meristems (state B). The resulting structure is a compound raceme, with lower branches terminating in flowers. (D) Transient model in which lateral meristems are initially in state B but revert to state A if *veg* does not reach the threshold V_K ; a raceme with indeterminate branches is produced for $T_B < T_A$. (E) Transient model in which $T_B > T_A$ yields a cyme.

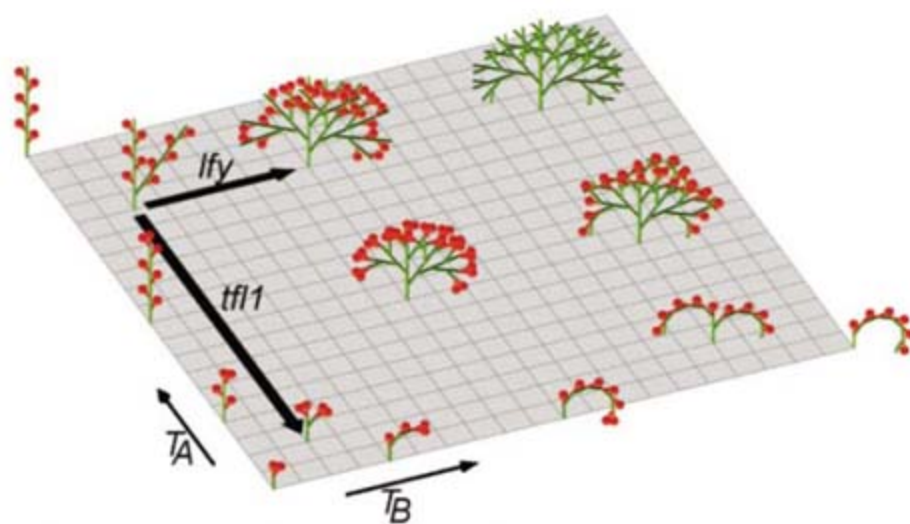


Fig. 3. Morphospace for the transient model. Different phenotypes are generated by varying the times T_A and T_B at which flowers begin to form. Values along each axis range from 0 to 10 plastochrons. Black arrows, pointing away from the wild-type architecture of *Arabidopsis*, indicate the effect of *tfl1* and *lfy* mutations [under inductive conditions (20)]. Inflorescences are shown at six plastochrons.

TFL1 (24)], and (iv) the levels of *TFL1* and *LFY* increase with plant age (21, 25). The shootlike flowers observed in *lfy* mutants (20) and plants overexpressing *TFL1* (22, 24) are captured by assuming that they correspond to intermediate *veg* levels, lying between the levels for normal shoots and flowers.

With these assumptions, the transient model largely accounts for mutant and overexpression phenotypes of *Arabidopsis* (Fig. 4, B to H, and

SOM text) and for observed patterns of gene expression. According to the model, a lateral meristem that gives rise to a branch is initially in state B, which corresponds to relatively low *TFL1* and high *LFY*. This pattern reverses when the meristem switches back to state A. These features agree with experimental data: *TFL1* expression is low in newly formed lateral primordia and only increases later (22). Furthermore, *LFY* is expressed early in primordia that will give rise

to lateral branches but is absent from mature lateral shoot meristems (25, 26). The transient model thus provides a functional explanation for observed expression patterns.

Evolutionary origins and implications of the transient mechanism. Both the range of architectural types observed in flowering plants and molecular genetic data lend support to the transient mechanism, but the evolutionary origin of this mechanism is unclear. To elucidate it, we

Fig. 4. Incorporating *LFY* and *TFL1* genes into the transient model for *Arabidopsis*. (A) Interactions between genes, time, *veg*, and growth underlying the model. Growth increases the number of modules and hence influences the spatial pattern of gene expression. Gene activity affects *veg* and hence influences whether a meristem will continue to generate more modules or whether it will cease growing. Arrowheads indicate up-regulation; bars, down-regulation. Growth promotes production of meristems in state A or B, with state B reverting to A unless the floral threshold is reached. (B to H) Wild-type, mutant, and transgenic phenotypes generated by the model with the

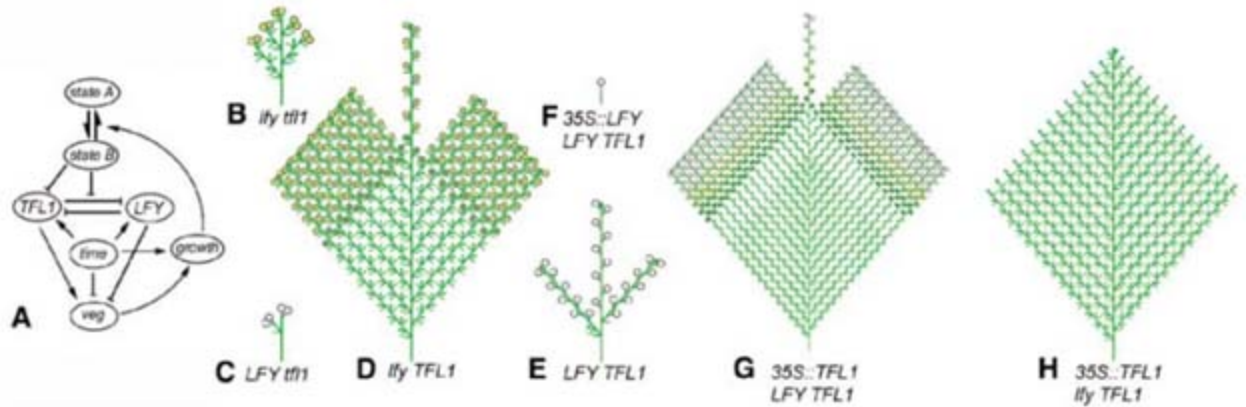
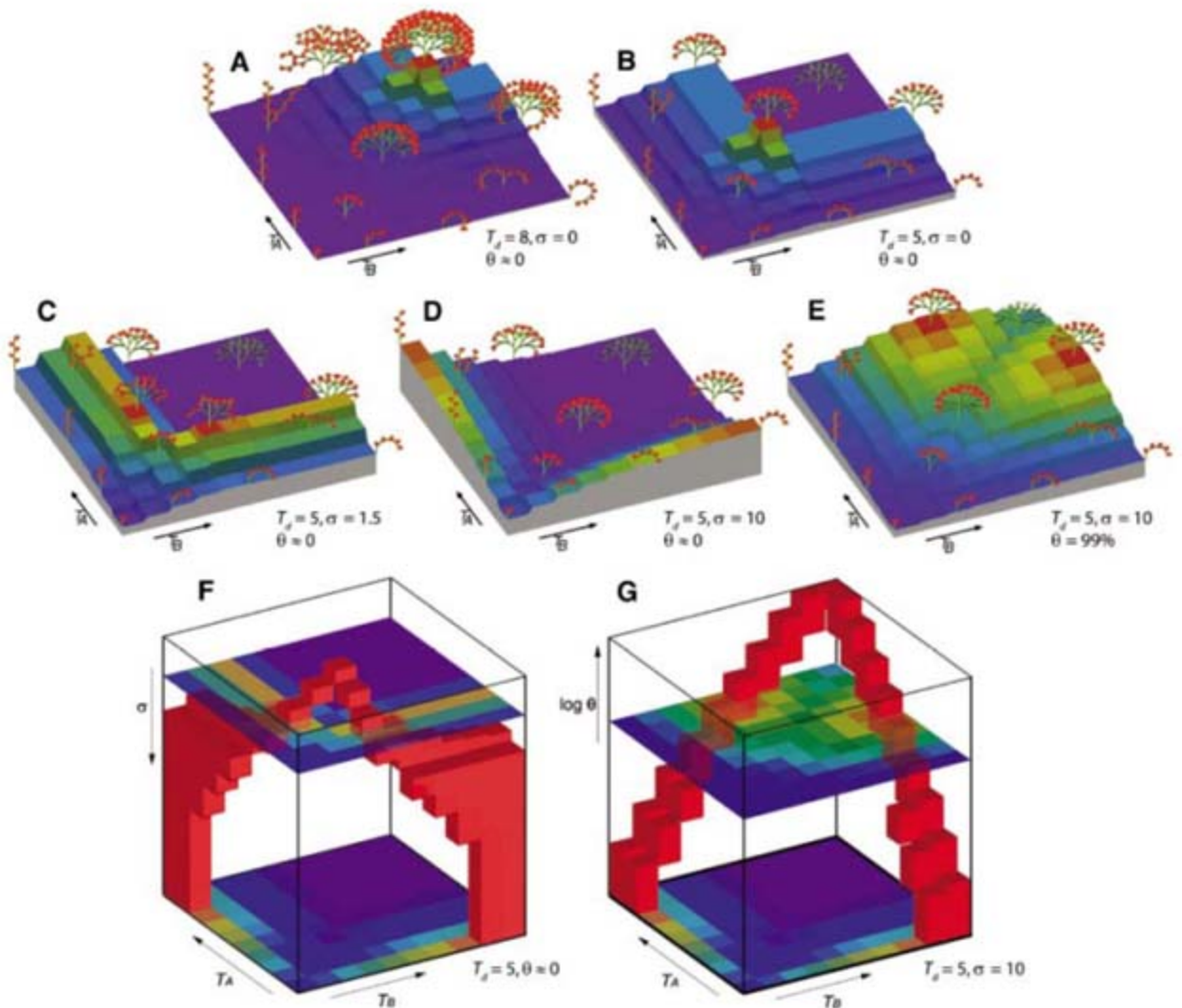


Fig. 5. (A to E) Two-dimensional fitness landscapes. Fitness levels are indicated by height and color. For each genotype, fitness is calculated over seasons with an average duration T_d and standard deviation σ , assuming that fraction θ of mature plants survives from one season to the next. Plants illustrate the architecture generated at time T_d . (A) For annuals with fixed growth duration, the optimal inflorescence is a panicle, represented by a single adaptive peak. (B) If T_d is reduced, the optimal architecture is a less highly branched panicle. (C) When σ is increased, two peaks arise corresponding to compound racemes and cymes. (D) With a further increase in σ , the peaks diverge. Optimal architectures are simple racemes and cymes. (E) Increased longevity θ shifts the peaks toward panicles. (F and G) Regions of high fitness in 3D fitness spaces. Horizontal sections correspond to the high-fitness regions in 2D fitness landscapes. (F) Path capturing the relation between architecture and σ . Colored sections correspond to figures (C) (top) and (D) (bottom). (G) Wormhole capturing the relation between architectures and longevity θ . Colored sections correspond to figures (D) (bottom) and (E) (top).

interactions shown in (A), assuming inductive conditions (20). Circles indicate flowers, color-coded according to *veg* levels. White, normal flower; yellow/green, shootlike flower). Arrows indicate branches. (For detailed explanation, see SOM.)



considered the fitness of different architectures in the region of morphospace generated by the transient model (SOM text).

With unlimited pollination and a growing season of fixed length, the optimal inflorescence architecture is a panicle. This is because the plant can delay flowering by keeping its meristems in a vegetative state until the latest time needed for fruit production, thus maximizing branching and the number of fruits (Fig. 5, A and B). However, if the length of the growth seasons varies from year to year, a plant that delays flowering too long may fail to produce any fruits by the end of a short season. This would reduce fitness, particularly if annual seed production is essential for genotype survival. The best strategy may thus be for a plant to “hedge its bets” (27–32) and generate flowers sequentially during a season, so that some flowers are produced early if the season is short but more flowers can still be produced later if the season is long. Racemes and cymes, in which only a fraction of meristems switch to floral identity at any time, may then have higher fitness values than panicles. This is illustrated in Fig. 5, C and D, in which racemes and cymes form separate adaptive peaks in the fitness landscape for annual plants, with the positions of the peaks depending on the standard deviation of growth duration.

To the extent that the impact of variable season length increases from tropical to more temperate conditions, our model predicts higher frequencies of racemes and cymes in temperate compared with tropical climates, and the opposite trend for panicles. To test these predictions, we extracted the incidence of each architectural type in different climatic zones from the Watson and Dallwitz database of angiosperm families (33) (fig. S1A). Although this database is not ideal for our purposes, as it aggregates characters for all species in the same family, it reveals significant trends. Consistent with our predictions, cymes are relatively more frequent in more temperate conditions ($P < 0.01$), whereas panicles show the opposite trend ($P < 0.001$). Racemes are also more frequent in temperate than tropical conditions, but not significantly ($P > 0.2$).

In addition to the environmental influences, positions of peaks in the theoretical fitness landscapes depend on factors under genetic control, such as plant longevity. If a plant is perennial (i.e., lives more than 1 year), the negative impact of short seasons in an uncertain environment is reduced by spreading the risk over multiple years (Fig. 5E). We found no significant associations of raceme or panicle architectures with longevity, but cymes are significantly less common in families with only woody perennials and more common in families with annuals, as predicted (fig. S1B) ($P < 0.05$). Furthermore, this trend is observed in temperate but not tropical families. Although we have focused on the effects of environmental uncertainty, similar theoretical fitness landscapes involving interactions between internal and external factors

could also be generated by considering the effects of limitations on pollination rate.

Although these results provide a rationale for sequential patterns of flower production, they do not explain why the transient mechanism evolved rather than other developmental mechanisms. One possibility is that the transient mechanism arose more readily because it built on the pre-existing developmental process of meristem establishment. Establishing a new lateral meristem requires a period of time during which genes needed for meristem maintenance become activated (34). The transient mechanism could have arisen by coupling *veg* levels to this basic transition of meristems from a newly initiated (immature) to an established (mature) state. Thus, the evolution of the transient mechanism may reflect an earlier developmental genetic constraint that biased the variants available for selection toward this mechanism (6).

Evolution between racemes and cymes. In uncertain or pollinator-limited environments, racemes and cymes can represent equivalent adaptive solutions separated by a valley in the fitness landscape (Fig. 5, C to E). Such low-fitness valleys may have been circumvented in various ways during evolution. One is through changes in the environment. Figure 5F shows fitness landscapes that have been calculated for different degrees of environmental uncertainty and combined to form a three-dimensional (3D) fitness space, with the vertical axis representing the standard deviation in growth duration. An inverted U-shaped high-fitness region connects racemes, panicles, and cymes. Connecting paths may also occur through variation in genetically controlled factors. For example, a path emerges when plant longevity is varied along the vertical axis (Fig. 5G). Connecting paths of this type are common features of higher dimensional genotypic spaces (35, 36). We propose the general term “evolutionary wormhole” for such high-dimensional connections.

Movement along evolutionary wormholes that connect racemes and cymes appears limited, as individual genera seldom include both architectures. This constraint may arise because moving along wormholes requires coordinated changes of several parameters, involving multiple genetic steps. Large jumps between regions of high fitness are thus unlikely; moreover, gene segregation would generate low-fitness phenotypes. In addition, mutations required to move along some stretches of a wormhole, such as crossing between racemes and cymes, involve changes in regulatory interactions rather than simple loss or reduction of function. For example, creating a cyme in *Arabidopsis* would require changing the *LFY* and *TFL1* promoters or other genes that interact with *LFY*, *TFL1* or *veg*, such that *veg* becomes high in state *B* and low in state *A* (the reverse of wild type). Such mutations are likely to be rare. Thus, evolution of inflorescences is constrained by the nature of the developmental genetic mechanism, as well

as by the interaction between organism and environment.

Conclusion. The diversity of inflorescence architectures reflects an interplay between development and selection at several levels. We propose that a relatively simple developmental mechanism—the transient model—underlies the restriction of inflorescence types to a small region of morphospace. This mechanism offers a selective advantage in dealing with environmental limitations and uncertainty over a simpler mechanism that can generate only panicles. Although similar advantages might also be achieved through other developmental mechanisms, the transient mechanism may have evolved because it co-opted a previously available developmental transition from the immature to mature state of apices. Within the confines of the morphospace spanned by the transient model, inflorescence architectures cannot evolve freely but are restricted to following paths of high fitness or evolutionary wormholes. The combination of theoretical and experimental approaches described here shows how development and selection can interact during evolution to carve out biological forms from the vast space of theoretical possibilities.

References and Notes

- G. R. McGhee, *Theoretical Morphology* (Columbia Univ. Press, New York, 1999).
- K. J. Niklas, *The Evolutionary Biology of Plants* (Univ. of Chicago Press, Chicago, 1997).
- D. M. Raup, A. Michelson, *Science* **147**, 1294 (1965).
- D. M. Raup, *J. Paleontol.* **41**, 43 (1967).
- R. Raff, *The Shape of Life* (Univ. of Chicago Press, Chicago, 1966).
- J. Maynard Smith et al., *Q. Rev. Biol.* **60**, 265 (1985).
- R. O. Erickson, F. J. Michelini, *Am. J. Bot.* **44**, 297 (1957).
- I. M. H. Etherington, *Proc. R. Soc. Edinb.* **59**, 153 (1939).
- W. Troll, *Die Infloreszenzen I* (Gustav Fischer Verlag, Stuttgart, Germany, 1964).
- W. Troll, *Die Infloreszenzen II* (Gustav Fischer Verlag, Jena, Germany, 1969).
- F. Weberling, *Morphology of Flowers and Inflorescences* (Cambridge Univ. Press, Cambridge, 1992).
- P. Prusinkiewicz, A. Lindenmayer, *The Algorithmic Beauty of Plants* (Springer-Verlag, New York, 1990).
- E. A. Kellogg, in *Monocots: Systematics and Evolution*, K. L. Wilson, D. A. Morrison, Eds. (CSIRO, Collingwood, Australia, 2000), pp. 84–88.
- G. G. Simpson, C. Dean, *Science* **296**, 285 (2002).
- T. Sachs, *Plant Cell Environ.* **22**, 757 (1999).
- D. Barthelemy, *Acta Biotheor.* **39**, 309 (1991).
- L. E. Gatsuk, O. V. Smirnova, L. I. Vorontsova, L. B. Zaugol'nova, L. A. Zhukova, *J. Ecol.* **68**, 675 (1980).
- F. Parcy, K. Bomblies, D. Weigel, *Development* **129**, 2519 (2002).
- D. Weigel, J. Alvarez, D. R. Smyth, M. F. Yanofsky, E. M. Meyerowitz, *Cell* **69**, 843 (1992).
- E. A. Schultz, G. W. Haughn, *Development* **119**, 745 (1993).
- D. Bradley, O. Ratcliffe, C. Vincent, R. Carpenter, E. Coen, *Science* **275**, 80 (1997).
- O. J. Ratcliffe, D. J. Bradley, E. S. Coen, *Development* **126**, 1109 (1999).
- S. Shannon, D. R. Meeks-Wagner, *Plant Cell* **3**, 877 (1991).
- O. J. Ratcliffe et al., *Development* **125**, 1609 (1998).
- M. A. Blazquez, L. N. Soowal, I. Lee, D. Weigel, *Development* **124**, 3835 (1997).
- J. Long, M. K. Barton, *Dev. Biol.* **218**, 341 (2000).
- K. R. Hopper, T. Rosenheim, T. Prout, J. Oppenheim, *Oikos* **101**, 219 (2003).

28. D. King, J. Roughgarden, *Theor. Popul. Biol.* **21**, 194 (1982).
 29. D. Cohen, *J. Theor. Biol.* **12**, 119 (1966).
 30. D. King, J. Roughgarden, *Theor. Popul. Biol.* **22**, 1 (1982).
 31. P. Haccou, Y. Iwasa, *Theor. Popul. Biol.* **47**, 212 (1995).
 32. E. Kussell, S. Leibler, *Science* **309**, 2075 (2005).
 33. L. Watson, M. J. Dallwitz, *The Families of Flowering Plants: Descriptions, Illustrations, Identification, and Information Retrieval*. Version: 29 July 2006 <http://delta-intkey.com> (1992 onward).
 34. T. Keller, J. Abbott, T. Moritz, P. Doerner, *Plant Cell* **18**, 598 (2006).
 35. A. C. Whibley *et al.*, *Science* **313**, 963 (2006).
36. S. Gavrillets, *Fitness Landscapes and the Origin of Species*, S. Levin, H. Horn, Eds., Monographs in Population Biology (Princeton Univ. Press, Princeton and Oxford, 2004).
37. We thank J. Avondo for help with visualizing 3D fitness landscapes, M. Claus for helpful discussions on bet-hedging, and C. Thébaud for advice on inflorescence databases. This research was funded by grants from Human Frontier Science Program (E.C. and P.P.), Natural Sciences and Engineering Research Council of Canada (P.P. and L.H.), and the Biotechnology and Biological Sciences Research Council, UK (E.C.).

Supporting Online Material

www.sciencemag.org/cgi/content/full/1140429/DC1

Materials and Methods

SOM Text

Fig. S1

References

SOM Programs

25 January 2007; accepted 30 April 2007

Published online 24 May 2007;

10.1126/science.1140429

Include this information when citing this paper.

Marine Radiocarbon Evidence for the Mechanism of Deglacial Atmospheric CO₂ Rise

Thomas M. Marchitto,^{1,2*}† Scott J. Lehman,^{1,2*} Joseph D. Ortiz,³ Jacqueline Flückiger,²‡ Alexander van Geen⁴

We reconstructed the radiocarbon activity of intermediate waters in the eastern North Pacific over the past 38,000 years. Radiocarbon activity paralleled that of the atmosphere, except during deglaciation, when intermediate-water values fell by more than 300 per mil. Such a large decrease requires a deglacial injection of very old waters from a deep-ocean carbon reservoir that was previously well isolated from the atmosphere. The timing of intermediate-water radiocarbon depletion closely matches that of atmospheric carbon dioxide rise and effectively traces the redistribution of carbon from the deep ocean to the atmosphere during deglaciation.

Radiocarbon measurements of calendrically dated hematyctic corals (1) and planktonic foraminifera (2, 3) indicate that the radiocarbon activity ($\Delta^{14}\text{C}$) of the atmosphere during the latter part of the last glacial period [~20,000 to 40,000 years before the present (yr B.P.)] ranged from ~300 to 800 per mil (‰) higher than it was during the pre-nuclear modern era (Fig. 1C). Although reconstructions of Earth's geomagnetic-field intensity predict higher cosmogenic ^{14}C production rates during the glacial period, production was apparently not high enough to explain the observed atmospheric enrichment (2–5). Rather, a substantial fraction of the atmosphere's $\Delta^{14}\text{C}$ buildup must have been due to decreased uptake of ^{14}C by the deep ocean. This requires a concomitant ^{14}C depletion in a deep-ocean dissolved inorganic C reservoir that was relatively well isolated from the atmosphere. Renewed ventilation of this reservoir could theoretically explain the drop in atmospheric $\Delta^{14}\text{C}$ (Fig. 1C) and the rise in atmospheric CO₂ (6) across the last deglaciation. Most workers point to the Southern Ocean as a

locus of deglacial CO₂ release, based on the similarity between atmospheric CO₂ and Antarctic temperature records (6) and on numerous conceptual and numerical models (7–9). If correct, we would expect some signature of the low- ^{14}C deep-ocean C reservoir to be spread to other basins via Antarctic Intermediate Water (AAIW). Here, we report a strong radiocarbon signal of the deglacial release of old C, recorded in an intermediate-depth sediment core from the northern edge of the eastern tropical North Pacific.

Intermediate water $\Delta^{14}\text{C}$ reconstruction.

Marine sediment multi-core/gravity-core/piston-core triplet from sediment layer MV99-MC19/GC31/PC08 was raised from a water depth of 705 m on the open margin off the western coast of southern Baja California (23.5°N, 111.6°W) (10). The site is today situated within the regional O₂ minimum zone that exists because of a combination of high export production and poor intermediate-water ventilation. Various sediment properties in MC19/GC31/PC08 vary in concert with the so-called Dansgaard-Oeschger (D-O) cycles that characterized the Northern Hemisphere climate during the last glacial period (11). Originally discovered in Greenland ice cores, D-O cycles also exist in a number of lower-latitude locations that were probably teleconnected to the North Atlantic region through the atmosphere (2, 12, 13). Off the coast of Baja California, the sedimentary concentrations of organic C, Cd, Mo, and benthic foraminifera all decreased sharply during D-O stadials (cold periods in Greenland) (11, 14). Together, these proxies are consistent with reduced productivity during stadials, caused

by either decreased coastal upwelling or a deepening of the regional nutricline related to the mean state of the tropical Pacific (11).

Diffuse spectral reflectance (DSR) provides a 1-cm resolution stratigraphy for GC31/PC08. After R-mode factor analysis, the third factor of DSR (Fig. 1A) exhibits the strongest correlation to the productivity proxies and to Greenland climate (11). We used this DSR record to apply a calendar-age model to MC19/GC31/PC08, based on correlation to $\delta^{18}\text{O}$ (an air-temperature proxy) in Greenland ice core GISP2 (Greenland Ice Sheet Project 2) (15). Resulting calendar ages were then combined with 50 benthic foraminiferal radiocarbon ages [19 of which were published previously (10)] to calculate age-corrected intermediate-water $\Delta^{14}\text{C}$ (16). To evaluate the partitioning of ^{14}C between the atmosphere and the ocean, we compared intermediate-water $\Delta^{14}\text{C}$ to that of the atmosphere (Fig. 1C), as reconstructed from tree rings (17), U-Th-dated corals (1, 17), and planktonic foraminifera from Cariaco Basin off Venezuela (3). Calendar ages for Cariaco Basin were originally based on the correlation of lithologic climate proxies to the GISP2 $\delta^{18}\text{O}$ record (2), which has been layer-counted with visual and chemical techniques (15). However, Hughen *et al.* (3) recently demonstrated that the Cariaco Basin ^{14}C calibration yields much better agreement with coral results older than ~22,000 yr B.P. when an alternate age model is used, based on correlation to the U-Th-dated Hulu Cave speleothem $\delta^{18}\text{O}$ record from eastern China (13). Because DSR in GC31/PC08 is more similar to the Greenland isotope record than to the lower-resolution Hulu Cave record, we continued to use the GISP2 correlation but applied simple provisional age adjustments to GISP2 older than 23,400 yr B.P., using four tie points to Hulu Cave (Fig. 1B and fig. S1). We do not suggest that this age model is necessarily superior to the original one (15), but this exercise is necessary for comparing our data to the most recent (and most consistent) atmospheric $\Delta^{14}\text{C}$ reconstructions (1, 3, 17). The resulting age model for MC19/GC31/PC08, based on 21 tie points, yields a very constant sedimentation rate (fig. S2) and gives us confidence that our calendar-age assignments for ^{14}C samples between tie points are reliable to within a few hundred years (table S1).

Baja California intermediate-water radiocarbon activities are plotted in red in Fig. 1C. The

¹Department of Geological Sciences, University of Colorado, Boulder, CO 80309, USA. ²Institute of Arctic and Alpine Research, University of Colorado, Boulder, CO 80309, USA.

³Department of Geology, Kent State University, Kent, OH 44242, USA. ⁴Lamont-Doherty Earth Observatory, Columbia University, Palisades, NY 10964, USA.

*These authors contributed equally to this work.

†To whom correspondence should be addressed. E-mail: tom.marchitto@colorado.edu

‡Present address: Environmental Physics, Institute of Biochemistry and Pollutant Dynamics, Eidgenössische Technische Hochschule Zürich, 8092 Zürich, Switzerland.

modern activity, based on a local seawater measurement of -131% at 445 m and the nearest Geochemical Ocean Section Study profile (18), is estimated to be -170% , in good agreement with the core top value. Comparable offsets from the contemporaneous atmosphere were maintained throughout the Holocene (typically $\sim 100\%$ between 0 and 10,000 yr B.P.) and during the latter part of the glacial period (roughly 200% between 20,000 and 30,000 yr B.P.) (19). Radiocarbon activities before 30,000 yr B.P. show increased scatter that may be related to the greater influence of slight contaminations on older samples.

Overall, it is clear that intermediate waters mainly followed atmospheric $\Delta^{14}\text{C}$ over the past 40,000 yr, except during the last deglaciation. Activities dropped sharply just after 18,000 yr B.P., reaching minimum values of $\sim -180\%$ between 15,700 and 14,600 yr B.P., roughly 450% lower than that of the contemporaneous atmosphere. For comparison, the lowest $\Delta^{14}\text{C}$ values found in the modern ocean (in the North Pacific near 2-km water depth) are depleted by $\sim 240\%$, relative to the preindustrial atmosphere (18). A second comparably large depletion event began sometime between 13,500 and 12,900 yr B.P. and ended between 12,100 and 11,600 yr B.P. The magnitude of ^{14}C depletion

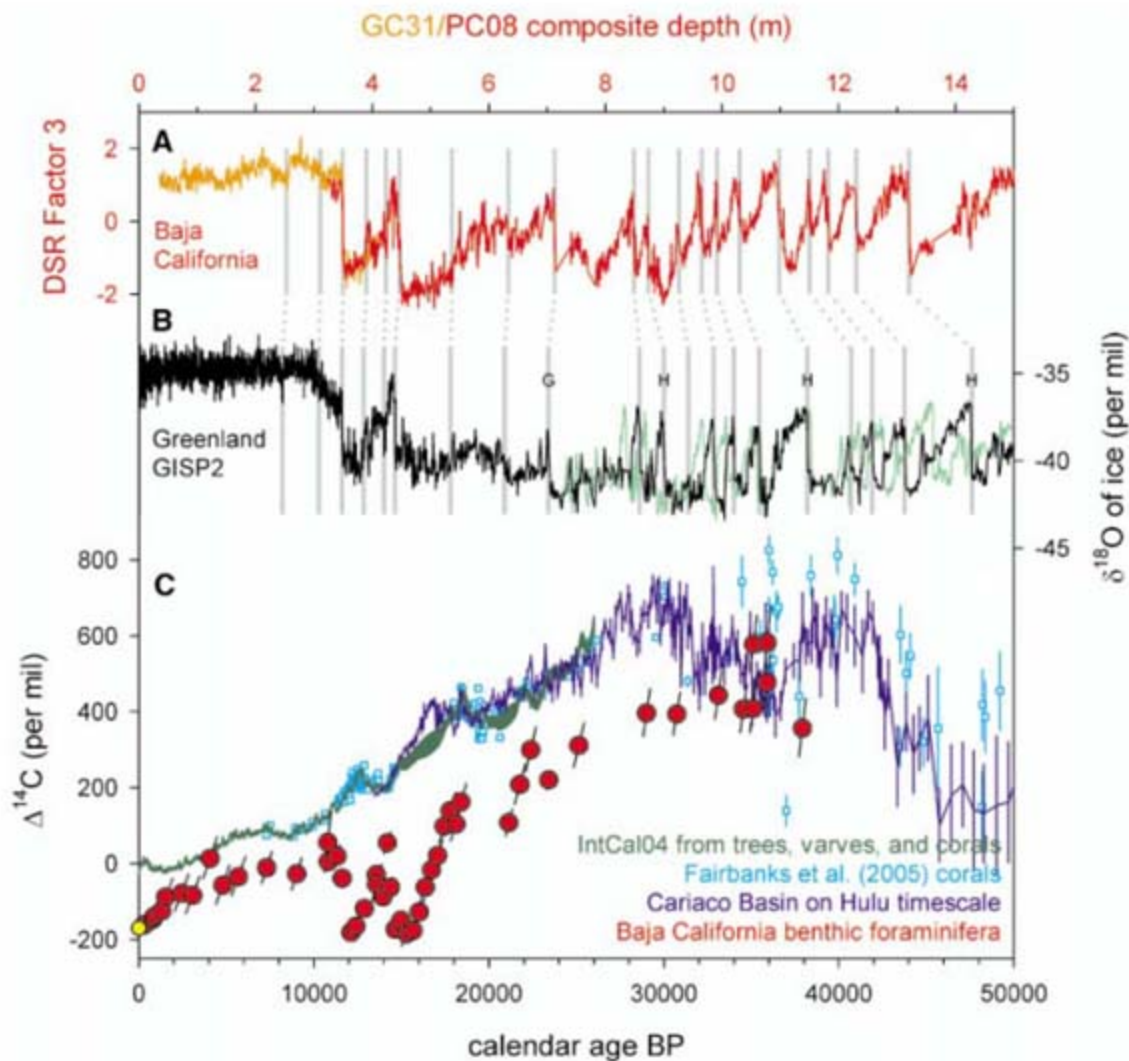
we reconstructed during these two deglacial events is much too great to attribute to changes in dynamics of the North Pacific thermocline (20) and must instead record a large change in the initial ^{14}C activity of waters advected to the site. Such depleted waters could have been sourced only from the deepest, most isolated regions of the glacial ocean (21).

Link to atmospheric history. In Fig. 2, we compare the timing of reconstructed intermediate-water and atmospheric $\Delta^{14}\text{C}$ changes with the deglacial record of atmospheric CO_2 from the East Antarctic Dome C ice core (6). The latter is shown on a GISP2 layer-counted time scale based on a simple synchronization of CH_4 variations between the Dome C and GISP2 ice cores (supporting online material text and table S2). It is immediately apparent that the atmospheric $\Delta^{14}\text{C}$ decline and CO_2 rise occurred in parallel, with a synchronous, intervening plateau appearing in both records. There is a slight (and still unreconciled) difference in the timing of the start of the deglacial atmospheric $\Delta^{14}\text{C}$ decline between the Cariaco Basin (3) and IntCal04 (17) reconstructions, but we take the deglacial onset of the atmospheric CO_2 rise and the atmospheric ^{14}C decline to be essentially synchronous. We now also find that these changes were associated with a prominent decline in $\Delta^{14}\text{C}$ of intermediate

water in the eastern North Pacific that must record the redistribution of aged C from the deep ocean to the surface. After 14,600 yr B.P., intermediate-water activities rebounded to higher values, coincident with the plateau in both the atmospheric CO_2 rise and the atmospheric $\Delta^{14}\text{C}$ drop. The leveling of the atmospheric records and the increase in ^{14}C activity of intermediate waters are all indicative of a reduction in the flux of aged C to the upper ocean and atmosphere from below. After $\sim 12,800$ yr B.P., the atmospheric CO_2 rise and $\Delta^{14}\text{C}$ drop resumed, and intermediate-water activities again reached minimum values of $\sim -180\%$, indicating a resumption of C redistribution from the deep ocean to the surface. By 11,500 yr B.P., the large deglacial atmospheric shifts were mostly completed, and intermediate-water activities finally reached modern values.

As pointed out by Monnin *et al.* (6), the deglacial rise of atmospheric CO_2 closely followed the rise in East Antarctic temperatures (Fig. 3A), implying that the ocean's release of C to the atmosphere was associated with changes in the Southern Ocean. Deep convection of the Southern Ocean both ventilates much of the ocean interior and returns to the atmosphere much of the C extracted by photosynthesis in the sunlit surface of the global ocean. During the last

Fig. 1. Intermediate-water and atmospheric $\Delta^{14}\text{C}$ records. (A) Diffuse spectral reflectance factor 3 from Baja California composite sediment core MV99-GC31/PC08, plotted versus depth (top axis) (11). Gray lines show tie points to the Greenland record that were used to derive the calendar-age model. (B) $\delta^{18}\text{O}$ of Greenland ice core GISP2 (15) on a provisional revised time scale (black, bottom axis). The new time scale deviates from the original time scale (green) for calendar ages older than 23,400 yr B.P. (vertical line labeled G). The new time scale is based on linear interpolation between point G and three tie points whose ages are derived from U-Th-dated Hulu Cave (vertical lines labeled H) (13). (C) Atmospheric radiocarbon activities based on tree rings, planktonic foraminifera from Cariaco Basin varve-counted sediments, and U-Th-dated corals (dark green) (17); additional recent coral measurements (light blue) (1); and planktonic foraminifera from Cariaco Basin, based on an age model derived from the correlation of sediment reflectance to Hulu Cave (dark blue) (3). Red circles show intermediate-water activities from benthic foraminifera in MC19/GC31/PC08. The yellow circle is an estimate for modern bottom waters at this site. Error bars are based on compounded uncertainties in radiocarbon ages and calendar ages.



glacial period, density stratification of the Southern Ocean surface and/or extensive sea-ice coverage are suggested to have isolated deep waters from the atmosphere (7–9), permitting the buildup of a larger deep-ocean C reservoir and a consequent drawdown of atmospheric CO₂. Sediment pore water chlorinity and δ¹⁸O measurements, combined with benthic foraminiferal δ¹⁸O, indicate that deep Southern Ocean waters were the saltiest and densest waters in the glacial ocean (22). Such high salinities point to brine formation beneath sea ice as an important mode of formation. At deglaciation, a progressive renewal of deep convection or upwelling in association with documented sea-ice retreat (23) [and possibly with poleward-shifting westerlies (8)] would have provided for the simultaneous delivery of ocean heat and sequestered C to the atmosphere. This transition occurred in two major steps, beginning with relatively early (~18,000 years ago) and gradual increases in temperature and CO₂ that were temporarily interrupted by the Antarctic Cold Reversal (ACR). Major transients in our record of Δ¹⁴C in intermediate-depth waters of the eastern North Pacific conform to this Antarctic schedule, consistent with the redistribution of C from the abyss to the upper ocean and atmosphere in connection with changes in deep convection of the Southern Ocean.

δ¹³C provides a tracer that is complementary to Δ¹⁴C, though with a far smaller dynamic range in seawater. During the last glacial period, the deep Southern Ocean contained the ocean's lowest δ¹³C values, suggesting a local accumulation of remineralized C and/or poor ventilation (24). Spero and Lea (25) argued that during the early part of the last deglaciation, Southern Ocean sea-ice retreat (23), combined with increased deep convection and northward Ekman transport, imparted transient low δ¹³C values to AAIW and Subantarctic Mode Waters and that this signal was recorded by deep-dwelling planktonic foraminifera in various ocean basins, including the eastern tropical North Pacific. These waters should also have carried a low Δ¹⁴C signature, and we suggest that this is the signal we observe off the coast of Baja California. Today, AAIW is barely traceable as a distinct water mass north of the equator in the eastern tropical Pacific (26). We argue that the northward penetration of AAIW during deglaciation was greater than it is today (27) and was at times fed by extremely ¹⁴C-depleted waters sourced from the abyss by deep overturning in the Southern Ocean. Sea-ice retreat could have allowed the upwelled deep waters to gain buoyancy from precipitation, converting some fraction of these waters into AAIW without substantial mixing with warmer thermocline waters (28), which would otherwise dampen the Δ¹⁴C signal. There is evidence that vertical stratification of the North Pacific also varied on an Antarctic climate schedule (29), so northern deep waters may have supplemented the supply of aged C to the Baja California site. However,

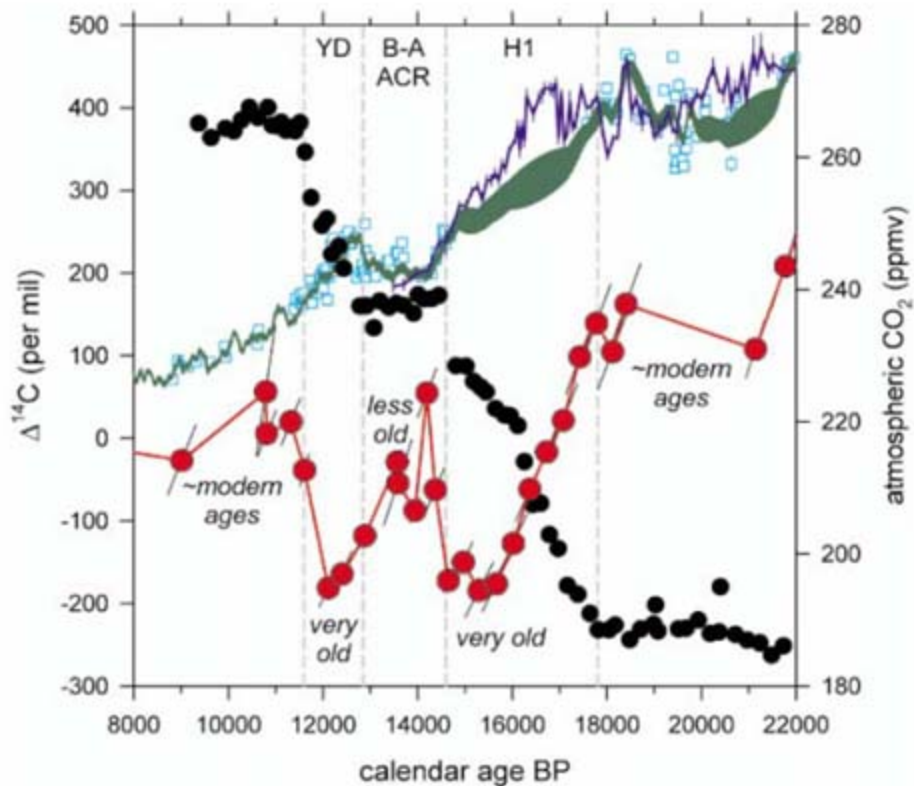


Fig. 2. Baja California intermediate-water Δ¹⁴C during the last deglaciation (red), compared with atmospheric Δ¹⁴C (dark green, light blue, and dark blue) (1, 3, 17), and atmospheric CO₂ from Antarctica Dome C (6) placed on the GISP2 time scale (black), as discussed in the text. Vertical dashed gray lines show the ages of Bolling-Allerød (B-A) and Younger Dryas (YD) boundaries, based on the GISP2 δ¹⁸O record, and the start of Heinrich event 1 (H1), based on the ²³¹Pa/²³⁰Th record from Bermuda Rise (34). The ACR is contemporaneous with the Bolling-Allerød. ppmv, parts per million by volume.

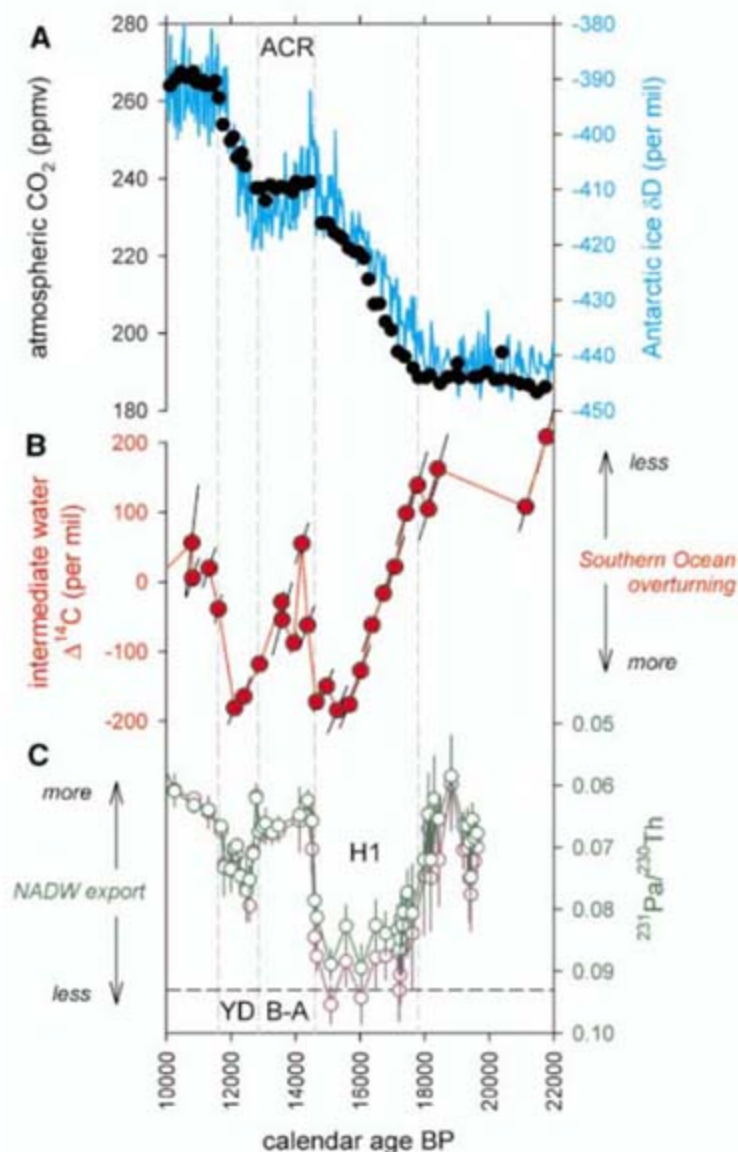
the interaction of strong circumpolar winds with bathymetry in the Southern Ocean provides for much more effective vertical pumping (30) than do conditions in the North Pacific, and therefore southern sources probably dominated the Δ¹⁴C changes in our record.

North-south teleconnections. Numerous observational and modeling studies indicate an inverse relationship between Antarctic and North Atlantic temperature variations that may be due to altered interhemispheric ocean-heat transport and/or opposing local deep-water formation histories (28, 31–33). Insofar as Δ¹⁴C of the intermediate-depth Pacific provides an inverse proxy for the strength of deep convection in the Southern Ocean, our results provide strong evidence for tight, inverse coupling of deep-water formation between hemispheres. This is clearly demonstrated by the covariation of intermediate-depth Pacific Δ¹⁴C and the formation history of North Atlantic Deep Water (NADW) [or its glacial analog, Glacial North Atlantic Intermediate Water (GNAIW)], based on measurements of ²³¹Pa/²³⁰Th from sediments in the western North Atlantic (34) (Fig. 3C). The near-cessation of ²³¹Pa export beginning just after 18,000 yr B.P. records a collapse of GNAIW that has been linked to a massive discharge of glacial ice and fresh water to the North Atlantic, known as Heinrich event 1. After a recovery during the Bolling-Allerød warm phase, another marked weakening of NADW/GNAIW is documented during the Younger

Dryas cold period, probably also triggered by a discharge of glacial meltwater (34). Both periods of NADW/GNAIW reduction were times of intermediate-depth Pacific Δ¹⁴C decline and atmospheric CO₂ rise.

It is often difficult to identify triggers in a tightly coupled system, but the relationships described above suggest that the Antarctic climate schedule may have been paced by ice sheet and meltwater forcing around the North Atlantic. Support for this conclusion comes from our observation that although major inflections in the Δ¹⁴C and ²³¹Pa/²³⁰Th records in Fig. 3 were almost exactly synchronous, the large Δ¹⁴C decrease (i.e., Southern Ocean ventilation increase) during Heinrich event 1 occurred more gradually than did the associated decrease in GNAIW export. This relationship is consistent with relatively slow circum-Antarctic warming due to anomalous ocean-heat transport (33), leading to sea-ice retreat (23) [and possibly poleward-shifting westerlies (8)] and, consequently, a progressive increase in deep overturning of the Southern Ocean. Alternatively, Southern Ocean overturning may have been instigated by NADW/GNAIW reductions through the requirement (35) that global rates of deep-water formation balance global deep upwelling, which is forced mainly by winds and tides. The abrupt rise in atmospheric Δ¹⁴C at the start of the Younger Dryas [+80% in just 180 years (36)] (Fig. 2) may record the time elapsed before the Southern Ocean could begin respond-

Fig. 3. Southern and northern ocean-atmosphere changes during the last deglaciation, compared with intermediate-water $\Delta^{14}\text{C}$. **(A)** Atmospheric CO_2 (black) and ice core deuterium (δD) temperature proxy (light blue) from Antarctica Dome C (6), placed on the GISP2 time scale. **(B)** Baja California intermediate-water $\Delta^{14}\text{C}$. **(C)** Inverted decay-corrected excess $^{231}\text{Pa}/^{230}\text{Th}$ in Bermuda Rise sediments, based on two methods to calculate excess (green and purple) (34). The horizontal dashed line shows the water-column production ratio for these isotopes (0.093); lower values are primarily due to Pa export by vigorous NADW. Vertical dashed lines show the ages of climatic boundaries, as in Fig. 2. Error bars are based on compound uncertainties in radiocarbon ages and calendar ages.



ing to reduced NADW formation, leading to the brief absence of deep-ocean sinks for ^{14}C (32).

Recent work shows that deep North Atlantic radiocarbon activities also increased abruptly during the Bolling-Allerod because of renewed formation of NADW and that they temporarily decreased during the Younger Dryas, when NADW formation was again briefly restricted (37, 38). In light of our new record, this pattern of deep-ocean change was probably limited to the North Atlantic (arising from deep circulation changes within the basin), whereas the intermediate-depth North Pacific record tracks the overall redistribution of C from the deep ocean to the atmosphere.

Implications for the deep C reservoir. Finally, our results bear on recent questions concerning reconstructed rates of atmospheric $\Delta^{14}\text{C}$ decline during deglaciation and implied ^{14}C aging of glacial deep waters. Although subject to uncertainties (19), decay projection of our first deglacial $\Delta^{14}\text{C}$ minimum back to the surface ocean (39) gives an apparent ventilation age of ~4000 years, implying that the inferred deep Southern Ocean source waters were at least that old. This is broadly consistent with the minimum deep-ocean age estimated from the

atmospheric record, assuming that the old reservoir filled half of the ocean's volume (40). Ages of up to 5000 years have been reported for glacial deep waters near New Zealand (41), but more northerly sites in the Pacific show little difference from today, at least at depths shallower than ~2 km (40). We infer that the greatest ^{14}C depletion of the glacial deep ocean was probably concentrated in the Southern Ocean region (and deepest Pacific), coincident with the highest densities (22) and lowest $\delta^{13}\text{C}$ values (24).

References and Notes

- R. G. Fairbanks *et al.*, *Quat. Sci. Rev.* **24**, 1781 (2005).
- K. Hughen *et al.*, *Science* **303**, 202 (2004).
- K. Hughen, J. Southon, S. J. Lehman, C. Bertrand, J. Turnbull, *Quat. Sci. Rev.* **25**, 3216 (2006).
- C. Laj *et al.*, *Earth Planet. Sci. Lett.* **200**, 177 (2002).
- R. Muscheler *et al.*, *Earth Planet. Sci. Lett.* **219**, 325 (2004).
- E. Mannin *et al.*, *Science* **291**, 112 (2001).
- D. M. Sigman, E. A. Boyle, *Nature* **407**, 859 (2000).
- J. R. Toggweiler, J. L. Russell, S. R. Carson, *Paleoceanography* **21**, PA2005 (2006).
- B. B. Stephens, R. F. Keeling, *Nature* **404**, 171 (2000).
- A. van Geen *et al.*, *Paleoceanography* **18**, 1098 (2003).
- J. D. Ortiz *et al.*, *Geology* **32**, 521 (2004).
- R. J. Behl, J. P. Kennett, *Nature* **379**, 243 (1996).
- Y. J. Wang *et al.*, *Science* **294**, 2345 (2001).
- W. E. Dean, Y. Zheng, J. D. Ortiz, A. van Geen, *Paleoceanography* **21**, PA4209 (2006).

- P. M. Grootes, M. Stuiver, *J. Geophys. Res.* **102**, 26455 (1997).
- Materials and methods are available as supporting material on Science Online. In the supporting material, we also present our $\Delta^{14}\text{C}$ values calculated with the original GISP2 chronology (15) and compare them to the original Cariaco record (2), based on correlation to GISP2 (fig. S3).
- P. J. Reimer *et al.*, *Radiocarbon* **46**, 1029 (2004).
- G. Ostlund, H. Craig, W. S. Broecker, D. Spencer, *GEOSecs Atlantic, Pacific and Indian Ocean Expeditions*, vol. 7, *Shorebased Data and Graphics* (U.S. Government Printing Office, Washington, DC, 1987).
- Throughout most of this paper, we discuss our $\Delta^{14}\text{C}$ values with respect to the contemporaneous atmosphere, rather than calculating ventilation ages by decay projection (39) because of large uncertainties in initial surface-ocean reservoir ages and the possibility of multiple intermediate- and deep-water sources with different ventilation histories.
- U. Mikolajewicz, T. J. Crowley, A. Schiller, R. Voss, *Nature* **387**, 384 (1997).
- The deglacial injection of low- ^{14}C intermediate waters along the Baja California margin did not noticeably overprint the DSR or other O_2 -sensitive productivity proxies recorded in GC31/PC08. Although $\Delta^{14}\text{C}$ and O_2 are broadly correlated in the modern ocean, they can also be decoupled (18) through air-sea exchange. Hence, deglacial intermediate waters were very depleted in $\Delta^{14}\text{C}$ but apparently not drastically depleted in O_2 .
- J. F. Adkins, K. McIntyre, D. P. Schrag, *Science* **298**, 1769 (2002).
- R. Gersonde, X. Crosta, A. Abelmann, L. Armand, *Quat. Sci. Rev.* **24**, 869 (2005).
- U. S. Minnemann, C. D. Charles, *Earth Planet. Sci. Lett.* **201**, 383 (2002).
- H. J. Spero, D. W. Lea, *Science* **296**, 522 (2002).
- P. C. Fiedler, L. D. Talley, *Prog. Oceanogr.* **69**, 143 (2006).
- S. Schulte, F. Rostek, E. Bard, J. Rullkötter, O. Marchal, *Earth Planet. Sci. Lett.* **173**, 205 (1999).
- R. F. Keeling, B. B. Stephens, *Paleoceanography* **16**, 112 (2001).
- S. L. Jaccard *et al.*, *Science* **308**, 1003 (2005).
- J. R. Toggweiler, B. Samuels, *Deep-Sea Res.* **42**, 477 (1995).
- T. J. Crowley, *Paleoceanography* **7**, 489 (1992).
- W. S. Broecker, *Paleoceanography* **13**, 119 (1998).
- R. Knutti, J. Flückiger, T. F. Stocker, A. Timmermann, *Nature* **430**, 851 (2004).
- J. F. McManus, R. Francois, J.-M. Gherardi, L. D. Keigwin, S. Brown-Leger, *Nature* **428**, 834 (2004).
- W. Munk, C. Wunsch, *Deep-Sea Res.* **45**, 1977 (1998).
- K. A. Hughen, J. R. Southon, S. J. Lehman, J. T. Overpeck, *Science* **290**, 1951 (2000).
- L. C. Skinner, N. J. Shackleton, *Paleoceanography* **19**, PA2005 (2004).
- L. F. Robinson *et al.*, *Science* **310**, 1469 (2005).
- J. F. Adkins, E. A. Boyle, *Paleoceanography* **12**, 337 (1997).
- W. Broecker *et al.*, *Science* **306**, 1169 (2004).
- E. L. Sikes, C. R. Samson, T. P. Guilderson, W. R. Howard, *Nature* **405**, 555 (2000).
- We thank D. Lopez, J. Turnbull, and C. Wolak for laboratory assistance; J. Southon for accelerator mass spectrometry analyses; A. Pearson for providing an unpublished seawater $\Delta^{14}\text{C}$ measurement; and T. Blunier for providing Dome C EDC 3 time scale and for valuable discussions on synchronization of the different ice cores. This manuscript was improved by comments from R. Keeling and two anonymous reviewers. Support was provided by NSF grants OCE-9809026 and OCE-0214221.

Supporting Online Material

www.sciencemag.org/cgi/content/full/1138679/DC1

Materials and Methods

SOM Text

Figs. S1 to S3

Tables S1 and S2

References

11 December 2006; accepted 27 April 2007

Published online 10 May 2007;

10.1126/science.1138679

Include this information when citing this paper.

Monochromatic Electron Photoemission from Diamondoid Monolayers

W. L. Yang,^{1,2} J. D. Fabbri,¹ T. M. Willey,³ J. R. I. Lee,³ J. E. Dahl,⁴ R. M. K. Carlson,⁴ P. R. Schreiner,⁵ A. A. Fokin,^{5,6} B. A. Tkachenko,⁵ N. A. Fokina,⁵ W. Meevasana,¹ N. Mannella,^{1,2} K. Tanaka,^{1,2} X. J. Zhou,^{1,2} T. van Buuren,³ M. A. Kelly,¹ Z. Hussain,² N. A. Melosh,¹ Z.-X. Shen¹

We found monochromatic electron photoemission from large-area self-assembled monolayers of a functionalized diamondoid, [121]tetramantane-6-thiol. Photoelectron spectra of the diamondoid monolayers exhibited a peak at the low-kinetic energy threshold; up to 68% of all emitted electrons were emitted within this single energy peak. The intensity of the emission peak is indicative of diamondoids being negative electron affinity materials. With an energy distribution width of less than 0.5 electron volts, this source of monochromatic electrons may find application in technologies such as electron microscopy, electron beam lithography, and field-emission flat-panel displays.

Diamondoids are molecules with cage structures that can be superimposed upon bulk diamond. These diamond-crystal cages are fused together and terminated by hydrogen. Adamantane is the smallest member, consisting of a single diamond cage; tetramantane, a higher diamondoid, is constructed by four cages. Since the discovery of higher diamondoids in petroleum, together with selective functionalization techniques (1–3), these materials have attracted interest because of their potential to combine the properties of diamond and nanomaterials. In addition to the optical, mechanical, and thermal properties of bulk diamond, hydrogen-terminated diamond surfaces have negative electron affinity (NEA), an important consideration in the development of electron emitters [reviewed in (4)]. However, difficulties in emission uniformity, electron injection, and electron transport have hindered the use of bulk diamond for this purpose (4). The primary challenge for electron emitters therefore remains to find a material that would realize uniformly large, highly efficient, and highly monochromatic electron emission. Diamondoids are an interesting candidate for electron emission, because they are essentially fully hydrogen-terminated diamond clusters. Indeed, recent quantum Monte Carlo calculations predict NEA for diamondoids up to 1 nm in size (5).

Large-area self-assembled monolayers (SAMs) of a functionalized diamondoid, [121]tetramantane-

6-thiol (2, 3), were assembled on Ag or Au substrates (6, 7). Thin films of unsubstituted [121]tetramantane were also fabricated by evaporating tetramantane powder at 50° to 80°C onto cleaned Au substrates in situ. Photoemission spectroscopy (PES) and near-edge x-ray absorption line structure (NEXAFS) measurements were performed (6) to analyze electron-emission properties and the molecular orientation of the SAMs. Several different samples with different bias voltages (0 to 9 V) were measured to check reproducibility. We observed obvious changes in the spectra after certain periods of beam exposure. All PES data shown here were collected at 30 K with less than 30 min of x-ray exposure.

The molecular orientation of the [121]tetramantane-6-thiol SAMs was characterized by polarization-dependent NEXAFS, a technique used extensively to study alkanethiolate SAMs (8–10). Figure 1A shows the total electron yield NEXAFS spectra of [121]tetramantane-6-thiolate on Au. The NEXAFS spectra resemble those from bulk and gas-phase [121]tetramantane (11, 12), indicating a high-purity film of tetramantane-thiol adsorbed on the surface. The angular dependence seen in the NEXAFS spectra implies that the tetramantane-thiol forms well-ordered monolayers with a preferential orientation. Absorption intensity of a NEXAFS resonance from a C 1s orbital depends directly on alignment between the linearly polarized incident x-rays and the transition dipole moment into a particular unoccupied orbital (8, 9). The angular dependence is simulated by summing over each atomic center with transition dipole moments oriented along the bonds (8, 9). These simulations agree with the experimental data (Fig. 1B) when the tetramantane-thiol, with the z axis of the molecule defined by the S-C bond, is tilted by $30 \pm 10^\circ$ from the surface normal (Fig. 1C) (6). Additionally, the affinity of the thiol for the metal leads to thiolate-bound monolayers (7, 13–15), as confirmed by S 2p core-level x-ray photoelectron spectroscopy (16) (fig. S2).

The key results of this work are seen in the PES spectra of [121]tetramantane-6-thiol SAMs grown on Ag (Fig. 2A) and Au (Fig. 3A) substrates. An emission peak appears for both surfaces at about 1-eV kinetic energy, the onset of the spectra at low kinetic energy. The intensity of the peak exceeds all the valence band features. For SAMs grown on Ag and Au, the sharp peak comprises about 68% and 17% of the total electron yield, respectively. This peak intensity

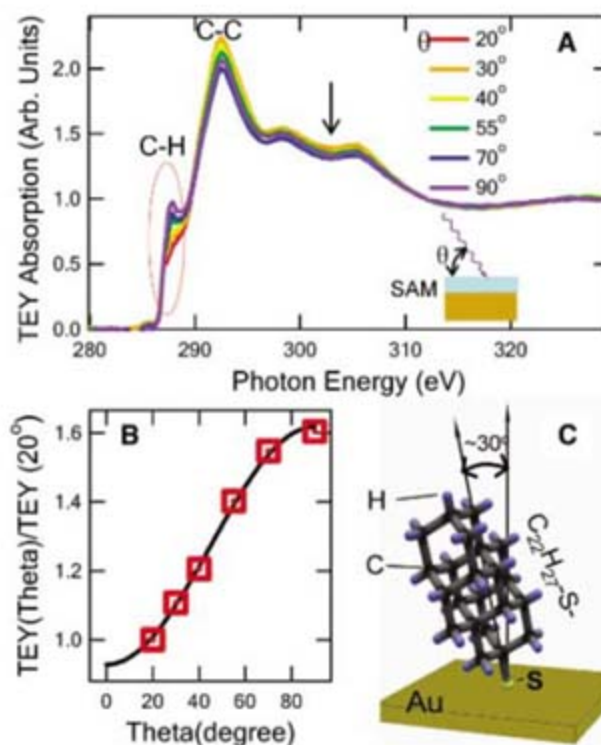


Fig. 1. (A) Polarization-dependent total electron yield NEXAFS spectra collected on [121]tetramantane-6-thiol SAMs prepared on Au. Total electron yield (TEY) is plotted against photon energy at different beam incident angles. The leading-edge peak at 287.6 eV (red oval) is assigned to transitions from the C 1s core level to the unoccupied (C-H) σ^* orbitals, and the peak at about 292.5 eV is assigned to (C-C) σ^* orbitals (8, 10, 11). The second gap indicated by the arrow is the characteristic signature of diamondoids (11, 12). (B) Comparison between experiments and theoretical simulations. Red squares represent the experimental ratio of (C-H) σ^* spectral weight between data at different angles and that at 20°. The black line is the calculated ratio based on the molecular geometry as shown in (C), with a polar angle of 36.5° (6).

¹Geballe Laboratory for Advanced Materials, Stanford University, Stanford, CA 94305, USA. ²Advanced Light Source, Lawrence Berkeley National Laboratory, Berkeley CA 94720, USA. ³Lawrence Livermore National Laboratory, Livermore, CA 94550, USA. ⁴MolecularDiamond Technologies, Chevron Technology Ventures, 100 Chevron Way, Richmond, CA 94802, USA. ⁵Institut für Organische Chemie, Justus-Liebig University Giessen, Heinrich-Buff-Ring 58, 35392 Giessen, Germany. ⁶Kiev Polytechnic Institute, pr. Pobedy 37, 03056 Kiev, Ukraine.

Fig. 2. (A) Photoelectron spectra of [121]tetramantane-6-thiol SAMs grown on Ag substrates, collected with 55-eV photon energy. The strong peak at 1-eV kinetic energy contains 68% of the total photoelectrons. The dotted line is a 50-times enlargement of valence band features. The inset shows the same spectra in a double logarithm plot. (B) Photoelectron spectrum collected on [121]tetramantane-6-thiol SAM covered by C_{60} sublimed in situ. The strong electron-emission peak disappears after C_{60} coverage. (C) Photoelectron spectrum collected on an annealed [121]tetramantane-6-thiol SAM. As in (B), the peak observed for the pristine SAM vanishes after the in situ annealing to 550°C. The difference between the spectrum in (C) and a pure Ag PES spectrum could be partially due to residual S atoms still bound to the surface after annealing.

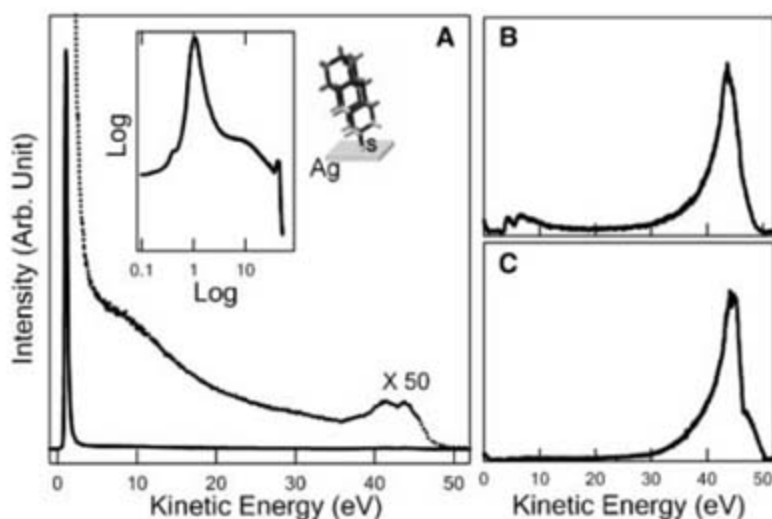


Fig. 3. (A) Photoelectron spectra of [121]tetramantane-6-thiol SAMs grown on Au substrates. The sharp peak at 1 eV contains about 17% of the total photoelectrons. The inset shows a double logarithm plot. (B) Photoelectron spectra of unsubstituted [121]tetramantane films prepared in situ on Au substrates. The inset is an enlargement of the low-kinetic energy part of the spectrum showing only a small peak.

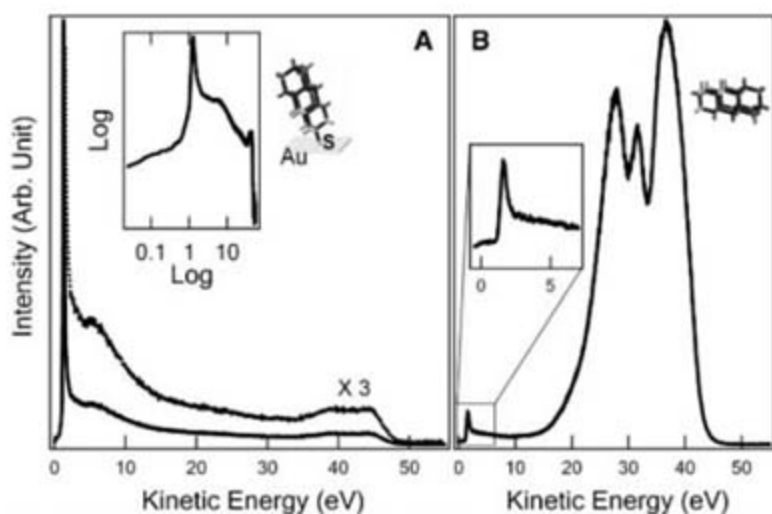
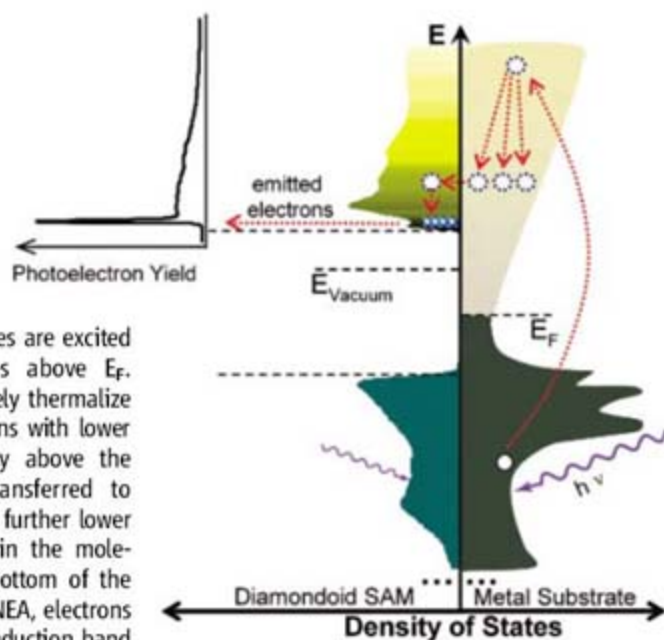


Fig. 4. Schematic of the electron-emission process on diamondoid SAM surfaces. E_F is the Fermi level of the metal substrate, sitting in the energy gap of diamondoid. The vacuum level (E_{vacuum}) is below the conduction-band minimum of the diamondoid, a characteristic of NEA. The dotted red line depicts the high-probability electron emission.

First, electrons in metal substrates are excited by photons into unoccupied states above E_F . Second, the excited electrons effectively thermalize in the metal, producing more electrons with lower energy. Third, electrons with energy above the conduction band minimum are transferred to diamondoid moieties. These electrons further lower their energies by exciting phonons in the molecules, and they accumulate at the bottom of the conduction band. Finally, because of NEA, electrons accumulated at the bottom of the conduction band emit into vacuum spontaneously and generate a peak at the low-kinetic energy threshold. Electron emission takes place also at high-kinetic energy levels, but with much lower photoelectron yield. Although this scenario roughly explains the existence of the electron-emission peak, more theoretical understanding is needed to fully explain the results.



is several times as strong as that found for hydrogen-terminated diamond surfaces [e.g., (4, 17–19)]. Even with a logarithm plot (insets), one can still see a sharp feature instead of the typical exponential decay of secondary electrons in this energy range.

To ensure that this unusual electron emission originates from the diamondoid monolayers, we applied two different techniques to cover or remove the monolayer in situ. Coating the diamondoid SAM with one monolayer of C_{60} , which was evaporated onto the SAM surface, caused the sharp emission feature to vanish (Fig. 2B). The valence band of the C_{60} covered surface is neither from tetramantane-thiol nor from C_{60} (20), but the origin of these features is not clear at present. The diamondoid SAM was also removed by annealing a SAM sample to 550°C in situ. Given that the thermal stability of conventional alkane thiol SAMs is ~70°C (21), this treatment should remove the diamondoid, and as shown in Fig. 2C, the low-kinetic energy peak completely disappears after annealing (22).

To investigate the importance of a monolayer of functionalized diamondoid versus a thin film of diamondoid, we compared [121]tetramantane-6-thiol SAMs with [121]tetramantane films. Figure 3B shows the PES spectrum of the [121]tetramantane film. The spectrum shows a small peak at low kinetic energy, in sharp contrast with the data for [121]tetramantane-6-thiol SAMs (Figs. 2A and 3A). Two factors may contribute to this difference. One is the poor electron conductivity within the thicker films versus that through the monolayers, and the other is the role that the thiol groups play in the SAM samples. Notably, this result indicates that the strong electron emission does not occur solely from the diamondoid surface, but that the metal substrate is also intimately involved in the process.

We further confirmed that the sharp peak remains at the same energy position with varying photon excitation energy (fig. S3). This rules out the possibility of core-level excitations and suggests that this sharp feature is not from electrons directly excited by photons, but from electrons accumulated at an intrinsic energy level of the molecules.

PES has been used widely for studying NEA materials, and a sharp feature at a low-kinetic energy threshold is often evident in the spectra of NEA (4, 17–19, 23, 24). Thus, the emission peak presented in this work provides direct evidence that certain functionalized diamondoids are NEA materials, consistent with the recent diffusion Monte Carlo (DMC) calculations (5). Moreover, the calculated DMC band gap, about 7 eV for tetramantane (5), is also consistent with the band gap estimated from our photoemission spectra, 6 to 8 eV (25). As further evidence of NEA, we evaporated slightly potassium (K) metal onto the SAM sample. In the PES spectrum of a K-covered [121]tetramantane-6-thiol SAM on a Ag substrate, the sharp peak retains its high intensity and occurs at the same energy position as in the PES spectrum

without K (fig. S4). This is another indication of NEA because K deposition onto a positive electron affinity semiconductor will lead to a shift of the low-kinetic energy cutoff and strong enhancement of the secondary electron background.

On a typical NEA surface, electrons excited into unoccupied states relax to the bottom of the conduction band as a result of inelastic scattering, a process normally referred to as the secondary cascade. A number of secondary electrons will then accumulate at the bottom of the conduction band. For a surface with positive electron affinity (as occurs in almost all untreated semiconductor surfaces), these accumulated electrons cannot escape. For an NEA surface, these accumulated electrons can be emitted directly because the vacuum level lies below the bottom of conduction band. As a result, a peak will be observed at the low-kinetic energy threshold in PES (4, 17–19, 23, 24).

However, on diamondoid SAM surfaces, there is only a single layer of diamondoid molecules. The detailed mechanism responsible for the highly monochromatic emission is unknown at this stage. Naïvely, one may consider that photoexcited electrons lose energy by creating phonons in the molecules, but this would likely lead to the destruction of the molecules. A plausible scenario is that most of the photoexcited electrons come from the substrate. These electrons first thermalize in the metal, producing many more low-energy electrons. Electrons with energies above the diamondoid conduction-band minimum may get transferred to diamondoid molecules, reach the bottom of the conduction band by creating phonons, and get emitted. This proposal is shown schematically in Fig. 4. Another difference between our results and those of other typical NEA systems (4, 17–19, 23, 24) is that our data show a spike in the spectra rather an exponential rise of the secondary tail toward the threshold, suggesting that a single energy level, resulting from the molecular nature of nanometer-sized diamondoids, and/or a strong resonance process are involved.

Our results suggest that diamondoid monolayers may have promising utility. Not only can functionalized diamondoids be easily grown into large area SAMs with NEA properties, they also naturally circumvent the long-standing electron-conductivity issues encountered for wide-gap bulk NEA semiconductors (4, 26). On a diamondoid SAM surface, electron conduction from the electron reservoir (metal substrates) to the emission surface is through a single molecule, which successfully avoids the low-conductivity problem and enhances the electron emission. Additionally, the possibility of different functionalizations (3, 4) allows one to optimize the NEA and other properties of diamondoids. Although many technical issues need to be addressed before diamondoid SAMs can be used as electron emitters, diamondoids provide intrinsic advantages over bulk materials because of their special molecular characteristics—for example, narrow energy distribution of the electronic states.

References and Notes

- J. E. Dahl, S. G. Liu, R. M. K. Carlson, *Science* **299**, 96 (2003).
- B. A. Tkachenko *et al.*, *Org. Lett.* **8**, 1767 (2006).
- P. R. Schreiner *et al.*, *J. Org. Chem.* **71**, 8532 (2006).
- A. Paoletti, A. Tucciarone, Eds., *The Physics of Diamond*, Proceedings of the International School of Physics Enrico Fermi (IOS Press, Amsterdam, 1997).
- N. D. Drummond, A. J. Williamson, R. J. Needs, G. Galli, *Phys. Rev. Lett.* **95**, 096801 (2005).
- Materials and methods are available as supporting material on Science Online.
- A. Ulman, *Chem. Rev.* **96**, 1533 (1996).
- J. Stöhr, *NEXAFS Spectroscopy* (Springer, Berlin, 1992).
- G. Hähner, *Chem. Soc. Rev.* **35**, 1244 (2006).
- M. Zharnikov, M. Grunze, *J. Phys. Condens. Matter* **13**, 11333 (2001).
- T. M. Willey *et al.*, *Phys. Rev. Lett.* **95**, 113401 (2005).
- T. M. Willey *et al.*, *Phys. Rev. B* **74**, 205432 (2006).
- P. E. Laibinis *et al.*, *J. Am. Chem. Soc.* **113**, 7152 (1991).
- A. Shaporenko *et al.*, *Langmuir* **21**, 4370 (2005).
- J. C. Love *et al.*, *Chem. Rev.* **105**, 1103 (2005).
- D. G. Castner, K. Hinds, D. W. Grainger, *Langmuir* **12**, 5083 (1996).
- F. J. Himpsel, J. A. Knapp, J. A. VanVechten, D. E. Eastman, *Phys. Rev. B* **20**, 624 (1979).
- B. B. Pate, *Surf. Sci.* **165**, 83 (1986).
- J. van der Weide, R. J. Nemanich, *Appl. Phys. Lett.* **62**, 1878 (1993).
- W. L. Yang *et al.*, *Science* **300**, 303 (2003).
- C. D. Bain *et al.*, *J. Am. Chem. Soc.* **111**, 321 (1989).
- The lack of a strong secondary electron component on the annealed sample may indicate that the transmission efficiency of the spectrometer is poor at low kinetic energies. This suggests that the peak from SAM surface could have been even stronger. Artificial effects on the peak have been ruled out by testing with different bias voltages.
- L. W. James, J. L. Moll, *Phys. Rev.* **183**, 740 (1969).
- R. C. Eden, J. L. Moll, W. E. Spicer, *Phys. Rev. Lett.* **18**, 597 (1967).
- For NEA materials, the difference between photoemission spectral width and the excitation energy should match the band-gap value (4, 17–19). Although there is no precise gap value reported for [121]tetramantane-6-thiol, and it is difficult to define a precise photoemission spectral width of an insulating monolayer system (owing to the difficulty in determining the spectral onset), the estimate obtained from our spectra is consistent with the DMC calculation (5), considering that the thiol groups are likely to change the gap value by only a few tenths of an electron volt.
- R. L. Bell, *Negative Electron Affinity Devices* (Clarendon, Oxford, 1973).
- We acknowledge helpful discussions with Z. Liu, D.-H. Lee, and H. Padmore. W.L.Y. thanks Y. Y. Wang for sharing information on diamondoid film deposition and J. Pepper and S. DiMaggio for technical support. The work at Stanford Synchrotron Radiation Laboratory and the Advanced Light Source is supported by the U.S. Department of Energy, Office of Basic Energy Science, Division of Material Science, under contracts DE-FG03-01ER45929-A001 and DE-AC03-76SF00515, respectively. The work at Stanford is also supported by Chevron through the Stanford-Chevron Program on Diamondoid Nano-Science.

Supporting Online Material

www.sciencemag.org/cgi/content/full/316/5830/1460/DC1
Materials and Methods
Figs. S1 to S4
References

27 February 2007; accepted 30 April 2007
10.1126/science.1141811

Coherence Dynamics in Photosynthesis: Protein Protection of Excitonic Coherence

Hohjai Lee, Yuan-Chung Cheng, Graham R. Fleming*

The role of quantum coherence in promoting the efficiency of the initial stages of photosynthesis is an open and intriguing question. We performed a two-color photon echo experiment on a bacterial reaction center that enabled direct visualization of the coherence dynamics in the reaction center. The data revealed long-lasting coherence between two electronic states that are formed by mixing of the bacteriochlorophyll and accessory bacteriochlorophyll excited states. This coherence can only be explained by strong correlation between the protein-induced fluctuations in the transition energy of neighboring chromophores. Our results suggest that correlated protein environments preserve electronic coherence in photosynthetic complexes and allow the excitation to move coherently in space, enabling highly efficient energy harvesting and trapping in photosynthesis.

Highly efficient solar energy harvesting and trapping in photosynthesis relies on sophisticated molecular machinery built from pigment-protein complexes (1, 2). Although the pathways and time scales of excitation energy

transfers within and among these photosynthetic complexes are well studied, less is known about the precise mechanism responsible for the energy transfer. In particular, to what extent quantum coherence contributes to the efficiency of energy transfer is largely unknown. Only recently have nonlinear optical spectroscopy and theoretical modeling started to reveal that coherences between electronic excitonic states can have a substantial impact on excitation energy transfer in photosynthetic systems (2–4). For example,

Department of Chemistry and QB3 Institute, University of California, Berkeley and Physical Bioscience Division, Lawrence Berkeley National Laboratory, Berkeley, CA 94720, USA.

*To whom correspondence should be addressed. E-mail: GRFleming@lbl.gov

Engel *et al.* have demonstrated using two-dimensional (2D) electronic spectroscopy that surprisingly long-lived (>660 fs) quantum coherences between excitonic states play an important role in the dynamics of energy transfer in photosynthetic complexes—i.e., the energy transfer is described by wavelike coherent motion instead of incoherent hopping (4).

To understand the origins of such long-lived coherences and the role of the protein matrix in its preservation, an experiment specifically designed to monitor electronic coherences between excited states is required. Here, we describe a two-color electronic coherence photon echo experiment (2CECPE) that produces a direct probe of electronic coherences between two exciton states. We applied the method to the coherence between bacteriopheophytin and accessory bacteriochlorophyll in the purple bacteria reaction center (RC). The measurement quantifies dephasing dynamics in the system and provides strong evidence that the collective long-range electrostatic response of the protein environment to the electronic excitations is responsible for the long-lasting quantum coherence. In other words, the protein environment protects electronic coherences and plays a role in the optimization of excitation energy transfer in photosynthetic complexes.

The RC from the photosynthetic purple bacterium *Rhodospirillum rubrum* includes a bacteriochlorophyll dimer called the special pair (P) in the center, an accessory bacteriochlorophyll flanking P on each side (BChl; B_L and B_M, for the L and M peptides, respectively), and a bacteriopheophytin (BPhy; H_L and H_M for the L and M peptides, respectively) next to each BChl (5). (We use H and B to denote excitonic states whose major contributions are from monomeric BPhy and accessory BChl in the RC, respectively.) In addition to electron transfer with near-unity efficiency (6), energy transfer occurs between the excitonically coupled chromophores—for example, from H to B in about 100 fs and from B to P in about 150 fs—in the isolated RC (7–10). In our experiments, the primary electron donor (P) is chemically oxidized by K₃Fe(CN)₆ (11), which blocks electron transfer from P to H_L, but does not affect the dynamics of energy transfer (8). This modification eliminates interference from the charge-transfer dynamics. The absorption spectrum of the P-oxidized RC at 77 K (Fig. 1A) shows the H band at 750 nm and the B band at 800 nm.

In our 2CECPE (11) (Fig. 1B), three ~40-fs laser pulses interact with the sample and generate a signal field in the phase-matched direction k_s . The first two pulses have different colors and are respectively tuned for resonant excitation of the H transition at 750 nm and the B transition at 800 nm (Fig. 1A). This is different from conventional two-color three-pulse photon echo technique in which the first two pulses have the same color (12). In our experiment, the first pulse (750 nm) creates an optical coherence

(electronic superposition) between the ground state and the H excitonic state ($|g\rangle\langle H|$ coherence). The coherence evolves for time delay t_1 until the second pulse (800 nm) interacts with the sample to form a coherence between B and H ($|B\rangle\langle H|$ coherence) that evolves for a time t_2 . Finally, the third pulse (750 nm) interacts with the system to generate a photon echo signal if, and only if, B and H are mixed. The integrated intensity of the echo signal is recorded at different delay times t_1 and t_2 . The central idea of the experiment is that if two chromophores are coupled and create two exciton bands (H and B in this case) in the absorption spectrum, then excitation resonant with one transition ($|g\rangle\langle H|$), followed by excitation resonant with the other ($|g\rangle\langle B|$) converts the initial coherence ($|g\rangle\langle H|$) into a coherence of the two exciton bands ($|B\rangle\langle H|$). This experiment is distinct from conventional two-color three-pulse photon echo measurements because different colors in the first two pulses are used to optically select the contributions to the third-order response function that arise from coherence pathways involving electronic superposition between two exciton states in the t_2 period. Because the system is in a coherence state in time t_2 , population dynamics only contribute to dephasing and do not generate additional echo signals; therefore, this technique is specifically sensitive to the coherence dynamics and provides a probe for the protein environment of the chromophores. A similar pulse ordering was applied in dual-frequency 2D infrared spectroscopy to study vibrational coherence transfer and mode couplings (13, 14).

The 2CECPE signals for the RC as a function of t_1 and t_2 measured at 77 K and 180 K are shown in Fig. 2, A and B, respectively. These figures provide a 2D representation of the system, which propagates as a $|g\rangle\langle H|$ coherence during the t_1 period and as a $|B\rangle\langle H|$ coherence during the t_2 period. The result is a map showing the dephasing dynamics of the $|g\rangle\langle H|$ coherence along the t_1 axis and the dynamics of the $|B\rangle\langle H|$ coherence along the t_2 axis. Clearly, the decay of the $|g\rangle\langle H|$ coherence is much faster than the decay of the $|B\rangle\langle H|$ coherence. Moreover, following the black curve that connects the maximum of integrated echo signal at fixed t_2 , we see that the signals exhibit a sawtooth-shaped beating pattern that persists for longer than $t_2 > 400$ fs. This oscillatory behavior is not from excitonic beating, given that we detect signal intensities in which the oscillatory phase factor vanishes; instead, this beating indicates electronic coupling to vibrational modes. Notably, the pattern is also peculiarly slanted along the antidiagonal direction; this slant arises because the vibrational coherence is induced by the first laser pulse and propagates in time $t_1 + t_2$, making the peaks of the beats parallel to the antidiagonal ($t_1 + t_2$ is fixed). The signals show substantial peak shift [i.e., shift from $t_1 = 0$ (12)], indicating correlation of the excitation energies between the H and B transitions (12).

To analyze the $|B\rangle\langle H|$ coherence dynamics, we plotted the integrated signal at $t_1 = 30$ fs (across the maxima of the first beat) as a function of t_2 (Fig. 3). Clearly, the dephasing is enhanced at higher temperature, as expected. The decay of the echo signal as a function of t_2 is not described by a single exponential decay because of its highly non-Markovian nature and the vibrational modulation. A Gaussian-cosine fit of the signal shows that the main component of the coherence signal decays with a Gaussian decay time (τ_g) of 440 and 310 fs at 77 and 180 K, respectively (eq. S1 and fig. S1). These dephasing times are substantially longer than the experimentally estimated excitation energy transfer time scale of about 250 fs from H to B to P⁺ (8). The surprisingly long-lived $|B\rangle\langle H|$ coherence indicates that the excitation energy transfer in the RC cannot be described by Förster theory, which neglects the coherence between donor and acceptor states (15). In addition, the decay of the $|g\rangle\langle H|$ coherence is much faster than the decay of the $|B\rangle\langle H|$ coherence. Considering that the dephasing of the $|g\rangle\langle H|$ coherence is caused by the transition energy fluctuations on H, whereas the dephasing of the $|B\rangle\langle H|$ coherence is due to the fluctuations on the gap between H and B transition energies, the transition energy fluctuations on B and H must be strongly correlated, because in-phase energy fluctuations do not destroy coherence. Such a strong correlation can arise for two possible reasons: strong electronic coupling between B and H and/or strong correlation between nuclear modes that modulate transition frequency fluctuations of localized BChl and

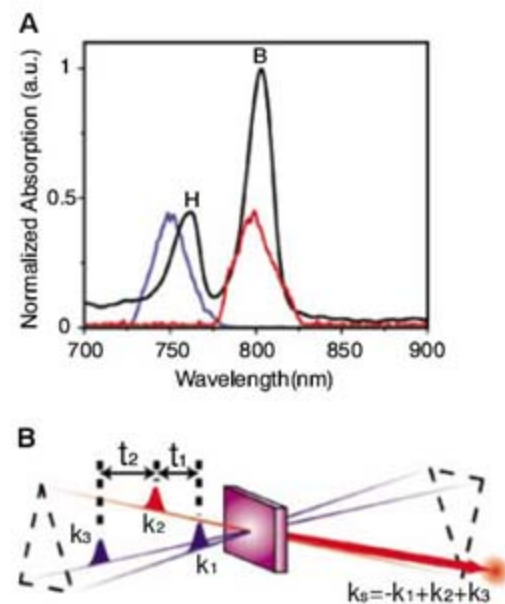


Fig. 1. The 2CECPE experiment. (A) The 77 K absorption spectrum (black) of the P-oxidized RC from the photosynthetic purple bacterium *R. sphaeroides* and the spectral profiles of the ~40-fs laser pulses (blue, 750 nm; red, 800 nm) used in the experiment. (B) The pulse sequence for the 2CECPE experiment. We detect the integrated intensity in the phase-matched direction $k_s = -k_1 + k_2 + k_3$. a.u., arbitrary units.

BPhy excitations. Our theoretical analysis found that strong electronic coupling alone cannot reproduce the sawtooth pattern and a dephasing time as long as that observed (11). Instead, cross-correlation between nuclear modes modulating the energy levels of localized BChl and BPhy excitations is required.

We modeled the 2CECPE signals using impulsive limit third-order response functions for a coupled heterodimer based on the transition frequency correlation functions for each localized excitation (11, 16). The model correlation functions contain a sum of a Gaussian component representing solvent reorganization and a constant term representing the inhomogeneous static contribution:

$$C_i(t) = \langle \Delta\omega_i^2 \rangle \exp(-t^2/\tau_i^2) + \Delta_i^2 \quad (1)$$

where $\langle \Delta\omega_i^2 \rangle^{1/2}$ is the fluctuation amplitude that is determined by the reorganization energy λ , τ is the bath relaxation time, Δ is the standard deviation of Gaussian static distribution, and $i = h, b$, and hb denote the localized BPhy, BChl excitations, and the cross-correlation between them, respectively. For $C_h(t)$ and $C_b(t)$, we adopted parameters established by previous photon echo experiments on the neutral RC and by quantum chemistry calculations (17–20). For simplicity, we used a single coefficient c to describe the cross-correlation and assume $\lambda_{hb} = c \cdot \sqrt{\lambda_h \lambda_b}$ and $\Delta_{hb}^2 = c \cdot \Delta_h \Delta_b$. The cross-correlation coefficient c represents the extent to which nuclear motions modulating the transition frequencies of localized BPhy and BChl excitations are correlated with

each other. With $c = 0.9$ and the addition of a vibrational mode coupled to the localized BPhy excitation ($\omega = 250 \text{ cm}^{-1}$; Huang-Rhys factor $S = 0.4$; damping time $> 0.6 \text{ ps}$; phase shift 0.28 rad), the model semiquantitatively reproduces the measurements at 77 and 180 K simultaneously; a c value of 0.6 substantially diminishes agreement with experiment (Figs. 2 and 3). Adding more terms to the model correlation functions improves the fit to experiments, but does not change any conclusions.

A c value near unity implies that nuclear modes coupled to H and B exhibit almost identical motions immediately after excitation. In other words, the two chromophores, H and B, are effectively embedded in the same protein environment and feel a similar short-time Gaussian component of their energy-level fluctuations. Most likely, this short-time component is the electrostatic response of the protein environment to the electronic excitations. Molecular dynamics simulations of the RC support this conclusion and show that interactions with the solvent environment (protein and water), rather than the intramolecular contributions, dominate the transition energy fluctuations of the P dimer excited state (21).

Theories for excitation energy transfer in pigment-protein complexes usually assume an independent bath for each of the individual chromophores (1–3, 15, 22, 23). However, our result suggests that in densely packed pigment-protein complexes, the assumption of independent bath environments for each site is not correct. Indeed, a previous molecular dynamics simulation on the

RC of *Rhodospseudomonas viridis* also showed that nuclear motions of adjacent chromophores are strongly correlated (24). Given that closely packed pigment-protein complexes are a ubiquitous configuration for efficient energy harvesting and trapping in photosynthetic organisms, the long-range correlated fluctuations indicated by our results are unlikely to be unique.

What are the likely consequences of long-lived electronic coherence in the RC? First, such coherence enables the excitation to move rapidly and reversibly in space, allowing a very efficient search for the energetic trap, in this case the primary electron donor, P. The almost complete correlation of the H and B fluctuations (on the few hundred-femtosecond time scale) and the likely significant correlation of the fluctuations of both exciton states of P with those of B will also enable bath-induced coherence transfers between the various pairs of excitons (25–27). We suggest that the overall effect of the protection of electronic coherence is to substantially enhance the energy transfer efficiency for a given set of electronic couplings over that obtainable when electronic dephasing is fast compared with transfer times.

It will be important to confirm this proposal by carrying out experiments similar to the one described here, but with excitation wavelengths resonant with B and P and with H and P. The

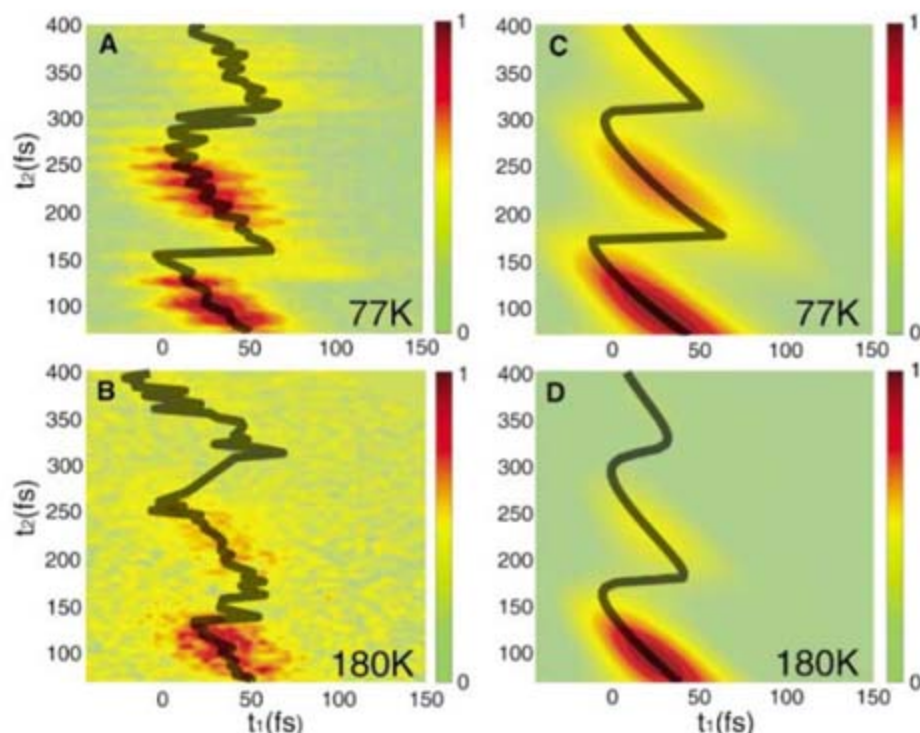


Fig. 2. Two-dimensional maps of experimental (A and B) and simulated (C and D) integrated echo signals as a function of the two delay times, t_1 and t_2 , from the RC. The black lines follow the maximum of the echo signal at a given t_2 . The data at $t_2 < 75 \text{ fs}$ are not shown because the conventional two-color three-pulse photon echo signal (750–750–800 nm) overwhelms the 2CECPE signal in this region, due to the pulse overlap effect.

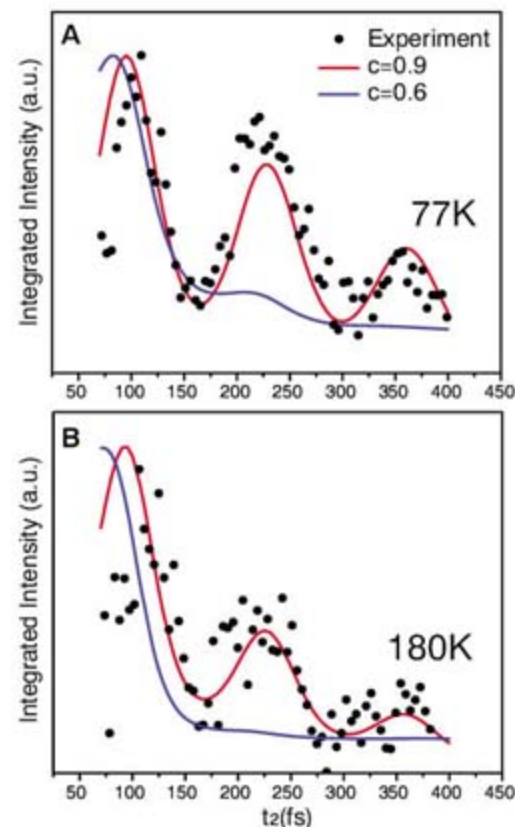


Fig. 3. Integrated echo signals as a function of t_2 at $t_1 = 30 \text{ fs}$. Because the system evolves as a coherence between the H and B excitons during the t_2 period, this plot represents the dephasing dynamics of the |B>|H> coherence. Measurements at 77 K (A) and 180 K (B) are shown in solid circles, and the theoretical curves are shown in red ($c = 0.9$) or blue ($c = 0.6$) lines. a.u., arbitrary units.

recent results of Engel *et al.* on the Fenna-Matthew-Olson complex of green sulfur bacteria also suggest strong correlations between the fluctuations of the neighboring one-exciton states of the complex (4). Clearly, further studies are required before it can be stated that correlated fluctuations and the consequent protection of electronic coherence is a general feature of photosynthetic pigment-protein complexes, but it seems clear that any accurate description of the dynamics (and design principles) of these systems will require proper consideration of both quantum coherences and long-range system-bath interactions (3, 22, 23).

We close by briefly comparing the present technique with existing experimental methods. In principle, 2D electronic spectroscopy (4, 28, 29) and pump-probe anisotropy spectroscopy (10, 23, 30) both contain information about coherence dynamics in the form of quantum beatings. However, interferences from other coherence states and population relaxation can create a complicated beating pattern that makes a quantitative analysis of coherence dynamics in the 2D spectrum or an anisotropy decay difficult. In this regard, the 2CECPE technique provides a unique tool that can resonantly select third-order response contributions from a specific coherence pathway and should lead to a much-improved understanding of coherence dynamics and the protein fluctuations that govern these dynamics.

References and Notes

- R. E. Blankenship, *Molecular Mechanisms of Photosynthesis* (Blackwell Science, Oxford, 2002).
- R. van Grondelle, V. I. Novoderezhkin, *Phys. Chem. Chem. Phys.* **8**, 793 (2006).
- O. Kühn, V. Sundström, T. Pullerits, *Chem. Phys.* **275**, 15 (2002).
- G. S. Engel *et al.*, *Nature* **446**, 782 (2007).
- U. Ermler, G. Fritzsche, S. K. Buchanan, H. Michel, *Structure* **2**, 925 (1994).
- C. A. Wraight, R. K. Clayton, *Biochim. Biophys. Acta* **333**, 246 (1973).
- R. J. Stanley, B. King, S. G. Boxer, *J. Phys. Chem.* **100**, 12052 (1996).
- J. A. Jackson *et al.*, *J. Phys. Chem. B* **101**, 5747 (1997).
- M. H. Vos, J. Breton, J.-L. Martin, *J. Phys. Chem. B* **101**, 9820 (1997).
- D. C. Arnett, C. C. Moser, P. L. Dutton, N. F. Scherer, *J. Phys. Chem. B* **103**, 2014 (1999).
- Materials and methods are available as supporting material on Science Online.
- R. Agarwal, B. S. Prall, A. H. Rizvi, M. Yang, G. R. Fleming, *J. Chem. Phys.* **116**, 6243 (2002).
- M. A. Rickard, A. V. Pakoulev, K. Kornau, N. A. Mathew, J. C. Wright, *J. Phys. Chem. A* **110**, 11384 (2006).
- I. V. Rubtsov, J. Wang, R. M. Hochstrasser, *Proc. Natl. Acad. Sci. U.S.A.* **100**, 5601 (2003).
- S. J. Jang, M. D. Newton, R. J. Silbey, *Phys. Rev. Lett.* **92**, 218301 (2004).
- T. Meier, V. Chernyak, S. Mukamel, *J. Chem. Phys.* **107**, 8759 (1997).
- M. L. Groot, J. Y. Yu, R. Agarwal, J. R. Norris, G. R. Fleming, *J. Phys. Chem. B* **102**, 5923 (1998).
- X. J. Jordanides, G. D. Scholes, W. A. Shapley, J. R. Reimers, G. R. Fleming, *J. Phys. Chem. B* **108**, 1753 (2004).
- D. Y. Parkinson, H. Lee, G. R. Fleming, *J. Phys. Chem. B* **10.1021/jp070029q** (2007).
- We used $\lambda_a = 50 \text{ cm}^{-1}$, $\lambda_b = 80 \text{ cm}^{-1}$, $\tau_h = \tau_b = 60 \text{ fs}$, and $\Delta_a = \Delta_b = 20 \text{ cm}^{-1}$, and we assumed the electronic coupling $J = 220 \text{ cm}^{-1}$ and the gap between excitonic H and B states is 680 cm^{-1} ; these values are well within the range suggested by other theoretical studies and our recent experiments (16–19).
- M. Souaille, M. Marchi, *J. Am. Chem. Soc.* **119**, 3948 (1997).
- T. Renger, V. May, O. Kühn, *Phys. Rep.* **343**, 137 (2001).
- V. Novoderezhkin, M. Wendling, R. van Grondelle, *J. Phys. Chem. B* **107**, 11534 (2003).
- H. Treutlein *et al.*, *Proc. Natl. Acad. Sci. U.S.A.* **89**, 75 (1992).
- P. de Bree, D. A. Wiersma, *J. Chem. Phys.* **70**, 790 (1979).
- Y. Ohtsuki, Y. Fujimura, *J. Chem. Phys.* **91**, 3903 (1989).
- J. M. Jean, G. R. Fleming, *J. Chem. Phys.* **103**, 2092 (1995).
- T. Brixner, T. Mančal, I. V. Stiopkin, G. R. Fleming, *J. Chem. Phys.* **121**, 4221 (2004).
- A. V. Pislakov, T. Mančal, G. R. Fleming, *J. Chem. Phys.* **124**, 234505 (2006).
- K. Wynne, R. M. Hochstrasser, *Chem. Phys.* **171**, 179 (1993).
- This work was supported by the Office of Basic Energy Sciences, Chemical Sciences Division, U.S. Department of Energy (contract DE-AC03-76SF00098). We thank S. G. Boxer for *R. sphaeroides* samples; B. S. Prall and D. Y. Parkinson for valuable discussions; and E. A. Berry, L. S. Huang, and N. G. Pon for help with sample preparation.

Supporting Online Material

www.sciencemag.org/cgi/content/full/316/5830/1462/DC1
Materials and Methods
Figs. S1 to S2
References

6 March 2007; accepted 26 April 2007
10.1126/science.1142188

Stepwise Quenching of Exciton Fluorescence in Carbon Nanotubes by Single-Molecule Reactions

Laurent Cognet,^{1,2*} Dmitri A. Tsyboulski,^{2†} John-David R. Rocha,^{2†} Condell D. Doyle,² James M. Tour,² R. Bruce Weisman^{2*}

Single-molecule chemical reactions with individual single-walled carbon nanotubes were observed through near-infrared photoluminescence microscopy. The emission intensity within distinct submicrometer segments of single nanotubes changed in discrete steps after exposure to acid, base, or diazonium reactants. The steps were uncorrelated in space and time and reflected the quenching of mobile excitons at localized sites of reversible or irreversible chemical attack. Analysis of step amplitudes revealed an exciton diffusional range of about 90 nanometers, independent of nanotube structure. Each exciton visited about 10,000 atomic sites during its lifetime, providing highly efficient sensing of local chemical and physical perturbations.

Optical excitation of semiconducting single-walled carbon nanotubes (SWNTs) generates relatively strongly bound excitons whose spatial dimensions are predicted to be a few nanometers (1–3). Experimental evidence of efficient exciton-exciton annihilation in nanotubes indicates that SWNT excitons have substantial mobility along the tube axis (4–6). However, the extent of this mobility is still experimentally and theoretically uncertain. A notable related effect is the strong suppression of photoluminescence (PL) when SWNT sidewalls

are perturbed by chemical reactions (7–9). This quenching phenomenon has hampered the use of covalently derivatized SWNTs as near-infrared (near-IR) fluorophores.

We report the use of single-nanotube microscopy to detect stepwise changes in SWNT PL intensity within segments of individual nanotubes while they are exposed to chemical reactants. These stepwise changes in PL intensity are caused by reactions of single molecules with one nanotube. Since the pioneering low-temperature experiments of Orrit and Moemer, single-molecule

spectroscopy has proven to be a powerful tool that bypasses ensemble averaging in the study of static and dynamic nano-objects in various environments (10, 11). Single-molecule approaches are especially appealing for SWNT fundamental studies and applications (12–14) because the bulk samples are highly heterogeneous. In the present work, the magnitudes of PL intensity steps caused by single-molecule reactions reveals that the exciton excursion range in highly luminescent SWNTs is ~90 nm and is essentially independent of nanotube structure. This room-temperature excitonic motion is deduced to be diffusional. Because each nanotube exciton visits a very large number of atomic sites during its lifetime, PL quenching provides an ultrasensitive method for sensing and studying certain types of chemical reactions with nanotube sidewalls at the single-molecule level.

Our studies required highly luminescent and relatively long nanotubes that were immobilized yet accessible to added reactant solutions. We therefore used very brief tip ultrasonication to

¹Centre de Physique Moléculaire Optique et Hertzienne, Université Bordeaux 1, and CNRS, Talence F-33405, France.

²Department of Chemistry, Center for Biological and Environmental Nanotechnology, and R. E. Smalley Institute for Nanoscale Science and Technology, Rice University, Houston, TX 77005, USA.

*To whom correspondence should be addressed. E-mail: lcognet@u-bordeaux1.fr (L.C.); weisman@rice.edu (R.B.W.)
†These authors contributed equally to this work.

disperse raw high-pressure CO (HiPco) SWNTs in aqueous sodium dodecylbenzenesulfonate (SDBS) surfactant before mixing the dilute suspension with a melted agarose gel preparation (15). Aqueous gels are commonly used in molecular biology to provide an inert immobilizing environment and have previously been applied in single-molecule optical measurements (16). We captured near-IR fluorescence images of single nanotubes with a wide-field inverted microscope modified to include laser excitation and a low-noise InGaAs camera (14). Individual SWNTs a few micrometers in length were easily identified in these images, and some of them displayed uniform and high PL intensity (Fig. 1A). The (n,m) structural assignment of each studied tube was deduced from the peak wavelength of its narrow Lorentzian emission spectrum (17), as measured with a dedicated spectrograph and multichannel near-IR detector (Fig. 1B). In this study, we selected the brightest nanotubes present in the weakly sonicated samples. We believe that these selected nanotubes have low defect densities and nonradiative relaxation rates that are dominated by intrinsic processes. Most of these nanotubes displayed PL that varied linearly at the excitation intensities used here and remained stable for tens of minutes under continuous illumination (Fig. 1, B and C). We used low laser intensities (~ 100 W/cm²) to avoid exciton-exciton annihilation effects that would shorten the exciton lifetime and reduce the exciton's excursion range (4–7). Furthermore, we verified that the nanotubes studied here showed

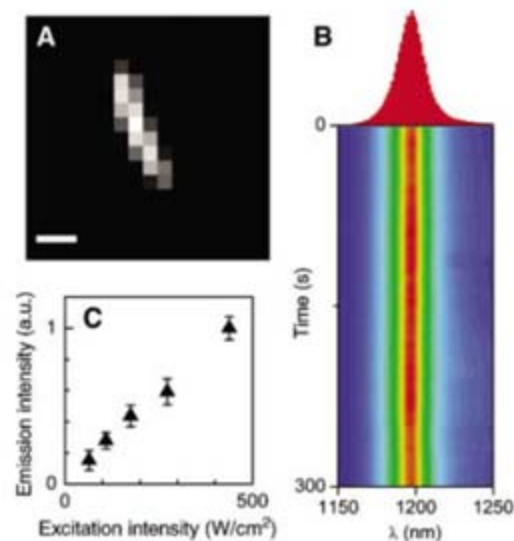


Fig. 1. Fluorescence measurements on an individual SWNT immobilized in agarose gel. (A) Image of an (11,3) SWNT excited at 100 W/cm². Scale bar, 1 μ m; the intensity scale is linear from 0 (black) to 45,000 camera counts (white). (B) Spectrum of the same nanotube (top) and color-coded contour plot (bottom) showing the stability of spectra taken at 5-s intervals for 300 s. (C) Luminescence intensity from the same nanotube as a function of excitation intensity. Linearity up to 500 W/cm² indicates that no multiexciton processes occur at 100 W/cm², which is the excitation intensity used in this study.

no detectable spectral shifts, spectral broadening, or change in emission intensity during the typical duration of our experiments (Fig. 1B). Finally, we confirmed that the emission spectra of SWNTs embedded in agarose gels matched those of SWNTs in fluid surfactant suspension.

To initiate chemical reactions, we placed a 10- μ l drop of reactant solution on the edge of the 20 mm by 20 mm sample gel while recording fluorescence images of a specific nanotube with stable and spatially uniform emission (fig. S1). Two reactants were used. One was sulfuric acid (0.05 M), which causes pH-dependent, reversible quenching of SWNT fluorescence (7, 8, 18). The other was 4-chlorobenzenediazonium tetrafluoroborate (1 mg/ml in water), which is known to give irreversible covalent derivatization of carbon atoms on the nanotube sidewall (19). We recorded fluorescence image sequences at an 18-Hz frame rate and plotted the total intensity within selected 2×2 pixel regions to obtain PL intensity traces. The chosen spatial binning region (4 pixels) corresponded to 670 nm by 670 nm, which is essentially the diffraction limit at the near-IR wavelengths.

The PL intensity trace from a 670-nm segment of an individual (8,6) nanotube after exposure to sulfuric acid is shown in Fig. 2A. That nanotube's luminescence spectrum is plotted in Fig. 2B. Coarsely, the PL time trace displays an exponential decay form. However, closer examination reveals a series of strikingly distinct steps between well-defined intensity levels, rather than a continuous decrease (Fig. 2A, inset). Moreover, the luminescence shows upward as well as downward steps. To analyze the distribution of

step amplitudes, we compiled a histogram for the first 108-s period, showing signal differences (δI) between successive image frames (Fig. 2C). Apart from the large main peak near zero, whose width arises mainly from signal noise, there are four distinct side bands distributed symmetrically around zero. These side bands are the signature of specific step amplitudes. The inner two (labeled +1 and -1) correspond to positive and negative steps of the same unit intensity, whereas the outer two (+2 and -2) correspond to double-amplitude steps. The presence of discrete (quantized) intensity changes is confirmed by the precisely linear relation linking the amplitudes of these intensity steps (Fig. 2D).

We attribute the observed discrete intensity steps to individual protonation reactions at the nanotube surface. The -1 and -2 steps would arise, respectively, from one or two independent sidewall reactions occurring within the 54-ms sampling interval, whereas the +1 and +2 steps would arise from the reverse chemical processes. The mechanism through which acids quench nanotube luminescence has been described as a protonation at the sidewall of the nanotubes (7, 8, 18). In this scheme, a hole is injected into the nanotube π -system near the protonation site. If an exciton encounters such a chemically induced hole before it radiatively recombines, the exciton's luminescence will be efficiently quenched through nonradiative Auger processes (6).

Because the excitons have a limited excursion range, only a fraction of those generated within an observed 670-nm segment will be quenched by a single protonation-induced hole. If the density of such holes is low, then each one causes the

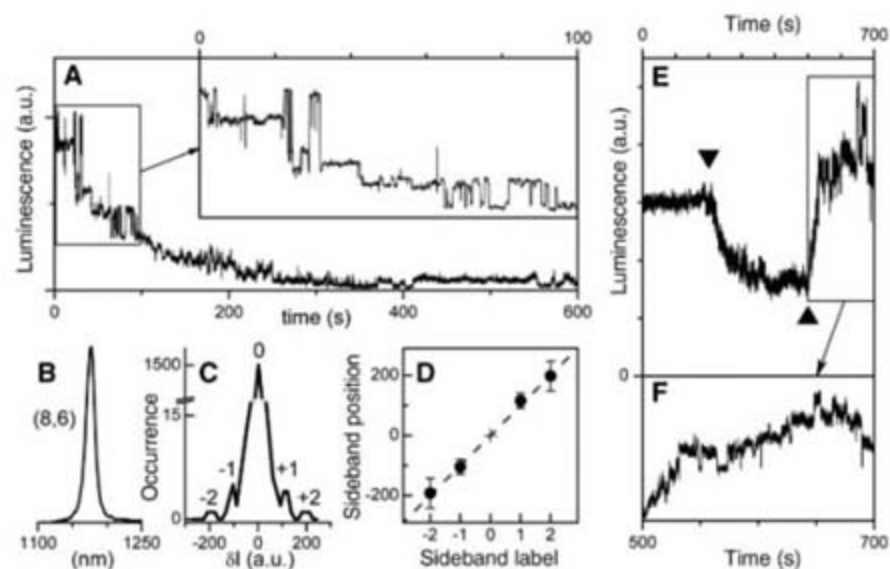


Fig. 2. Reversible stepwise quenching of individual SWNTs by acid. (A) Luminescence intensity of a diffraction-limited segment of an individual (8,6) SWNT after addition of acid. Inset shows an expansion of the first 100-s period, revealing well-defined reversible steps. (B) Near-IR emission spectrum of this SWNT, showing a single Lorentzian peak. (C) Histogram constructed from the data in the inset of (A), showing the distribution of changes in luminescence signal (δI) between successive 50-ms frames. Four symmetrically located side bands are evident at well-defined δI values. (D) Sideband peak positions as a function of sideband label. The linear relationship indicates that the side bands correspond to discrete protonation and deprotonation steps (see text). (E) Luminescence signal of a diffraction-limited segment of an individual (7,6) SWNT upon successive addition of acid (▼) and base (▲). Luminescence recovery is observed after base addition. (F) Expanded inset from (E) showing reversible steps in the recovery period.

same amount of quenching (corresponding to the observed -1 step amplitude), and each deprotonation restores the same amount of luminescence (the observed $+1$ step amplitude). However, when the typical distance between quenching sites becomes shorter or comparable to the exciton excursion range, the quenching impact of additional sites is reduced, giving smaller and eventually unresolved steps, as seen at later times in Fig. 2A.

To confirm that the observed stochastic stepwise quenching arises from reversible protonation, we added $\sim 10 \mu\text{l}$ of 1 M NaOH to nanotube samples that had previously been quenched by acid addition. The inverted triangle in Fig. 2E marks the point of acid addition, and the standard triangle marks the point of base addition. The period of luminescence restoration is expanded in Fig. 2F, which shows the expected stochastic stepwise intensity changes. Statistical analysis of upward and downward steps in a medium of known pH can in principle provide the $\text{p}K_a$ of the protonated nanotube. However, we could not perform this analysis on our data because of time-dependent pH gradients in the sample. Large intensity fluctuations were observed after luminescence was restored by base addition. We attribute this behavior to local pH fluctuations near the nanotube within the agarose pores after the successive addition of acid and base without active mixing. Finally, the higher intensities seen in Fig. 2E after restoration likely reflect a higher final pH level at the nanotube (18).

To compare these exciton-quenching effects with those caused by an irreversible chemical

reaction, we performed similar measurements on samples exposed to diazonium salts (Fig. 3) (20). These traces also display distinct steps in luminescence intensity, but the great majority of the steps are negative ($>95\%$), indicating a mainly irreversible process (9). Adjacent diffraction-limited segments within a single nanotube exhibited very different dynamics, with little or no correlation between the time positions of the steps (compare each set of red and black traces in Fig. 3, A to C). Similar spatially uncorrelated behavior in acid quenching is vividly illustrated in movie S1. This observation demonstrates that the mean excursion range of excitons must be smaller than our optical resolution of 670 nm. The same conclusion can be drawn from the localized PL in bent nanotubes excited by linearly polarized light (14) (fig. S2).

Comparison of the PL time traces within each frame of Fig. 3, A to C, reveals that for different segments of one nanotube, the first few step heights are integer multiples of the same unit intensity change Δ (regions marked by single asterisks). This stepwise quenching pattern leads to emission intensity plateaus that match between distinct segments of the same tube. As was observed for acid quenching, the steps have identical amplitudes at low densities of quenching sites, and they have gradually smaller amplitudes at longer times when the typical distance between quenching sites becomes shorter than or comparable to the exciton excursion range. However, in contrast to the reversible protonation reaction of acid quenching, the single-molecule diazonium salt reactions are essentially irreversible. Here,

the chlorobenzenediazonium ion (or its diazotate dimeric product) is thought to first adsorb onto the surface of a nanotube, forming a charge transfer complex. The complex then irreversibly decomposes to form a covalent bond with the nanotube surface (9, 21).

We presume that either of these nanotube perturbations can cause efficient exciton non-radiative decay. A mechanism for luminescence quenching by sidewall derivatization is suggested by scanning tunneling spectroscopy results on nanotubes covalently functionalized with amido groups, obtained with 10-nm resolution. The semiconducting energy gap was locally filled at the derivatization site (22). Excitons encountering such electronic perturbations should undergo efficient nonradiative recombination.

For each nanotube studied, repeatable values of Δ are obtained at early stages of the reaction when only a few independent sites have been derivatized within the observed diffraction-limited segment. We found that Δ values matched for separate segments in a single nanotube (Fig. 3, A to C). As for the minor variations in intensity step heights found at early stages of the reaction, we attribute these to the finite length of the diffraction-limited segment, because quenching events near the edge of the region produce smaller steps. Several simultaneous steps sometimes occurred within a single 54-ms frame (Fig. 3, A and B). This behavior probably results from nonuniform dilution of reactants in the submicrometer pores of the agarose gels, exposing the nanotube segments to large local concentration fluctuations.

Normalizing Δ by the initial luminescence intensity I gives a ratio representing the probability that a mobile exciton within the nanotube segment encounters a chemical reaction site during its lifetime. This probability also represents the fraction of the nanotube length explored by an exciton. The average exciton excursion range Λ is therefore simply given by $(\Delta/I) \times L$, where L is the observed segment length. For $L = 670$ nm, we measured Λ values for 19 different highly luminescent SWNTs. The resulting distribution is strikingly narrow, with a mean value of 91 nm (Fig. 4A). The small dispersion found for Λ values suggests that Λ does not depend strongly on nanotube structure. We plotted Λ values measured for 11 different (n,m) species (23) as a function of SWNT diameter (Fig. 4B) and found no systematic variation of exciton excursion range with diameter (for the range studied, 0.7 to 1.1 nm) or with chiral angle.

As mentioned above, our determination of Λ assumes that the local perturbation induced by a reaction sufficiently modifies the electronic structure of these bright tubes (22) to completely quench excitons at that site. If this quenching probability P is in fact less than 1, then Λ would be given by $90 \text{ nm}/P$ (but could not exceed 670 nm). However, several observations support the estimate of $P = 1$. The results are independent of nanotube structure, the normalized initial step

Fig. 3. Irreversible localized quenching of individual SWNTs with 4-chlorobenzenediazonium tetrafluoroborate. Luminescence quenching of diffraction-limited segments of individual SWNTs is shown for (8,3) (A), (8,6) (B), and (11,1) (C) species upon addition of the diazonium salt solution. Irreversible intensity steps are observed. Each asterisk marks an elementary unit step. In each frame, the red (lower) and black (upper) traces correspond to adjacent segments (each 670 nm in length) of the same nanotube. The black traces have been shifted upward by one unit step for clarity.

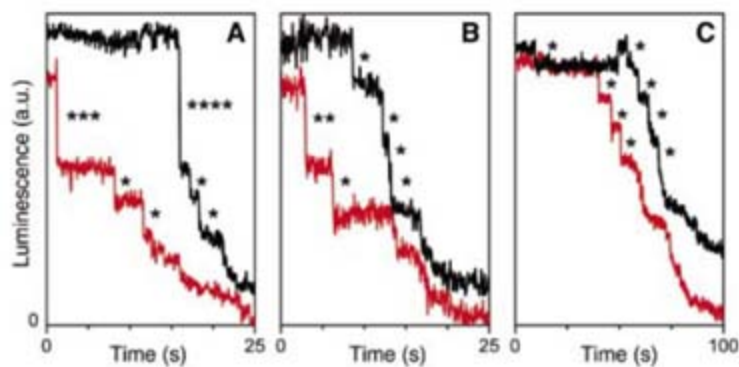
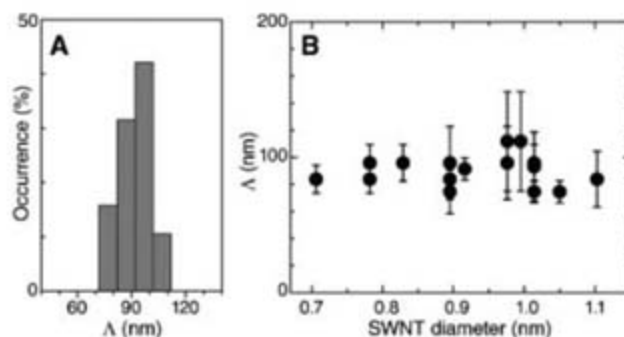


Fig. 4. Exciton excursion range (Λ) measured for various SWNTs. (A) Distribution ($n = 19$) of Λ values deduced from elementary step amplitudes (see text). (B) Plot of Λ values as a function of SWNT diameter.



amplitudes are consistent for acid quenching and diazonium salt quenching, and Auger quenching of excitons is known to be efficient.

Is the exciton motion ballistic or diffusional? For the bright emissive SWNTs studied here, we assume an exciton recombination lifetime $\tau = 100$ ps, which is among the larger values reported from time-resolved spectroscopy (24, 25). If the motion is ballistic, then the exciton's kinetic energy would be given by

$$E_{\text{ballistic}} = \frac{1}{2} m_{\text{exciton}}^* \left(\frac{\Lambda}{\tau} \right)^2 \quad (1)$$

where m_{exciton}^* is the exciton effective mass. Using an estimated m_{exciton}^* of $\sim 0.1 m_e$ (1, 26), we obtain $E_{\text{ballistic}} \sim 10^{-7}$ eV. This value is orders of magnitude lower than the 0.012 eV ($\sim k_B T$) expected from rapid thermalization induced by the exciton-phonon coupling evident in SWNT spectroscopy (27). We conclude that the excitonic motion is instead diffusional, in agreement with a recent investigation on bulk samples (28). The corresponding diffusion coefficient for the exciton one-dimensional random walk is then given as $D = \Lambda^2/2\tau \sim 0.4 \text{ cm}^2 \text{ s}^{-1}$.

This value lies more than two orders of magnitude below a prior tentative estimate that was indirectly deduced from transient absorption experiments on ensembles of short SWNTs in annealed dried films (29). The exciton diffusion coefficient measured here for highly luminescent individual SWNTs may be used to interpret the $\sim 150 \text{ cm}^{-1}$ Lorentzian line widths observed in emission spectroscopy of room-temperature SWNTs (see Figs. 1B and 2B). These widths arise from dephasing that is far more rapid (70 fs) than the ~ 100 -ps exciton population lifetime τ .

If dephasing instead occurs by diffusional hopping of the exciton along the tube axis, then

the hopping step length d_{hop} can be estimated from the relation $D = d_{\text{hop}}^2/2\tau_{\text{hop}}$, where τ_{hop} represents the interval between hops, identified as the 70-fs dephasing time. This approach gives a hopping step length of ~ 2 nm, which closely matches theoretical estimates of the exciton size (1–3). We propose that the emission linewidth may originate from thermally assisted short-range hopping of excitons along the nanotube axis. At cryogenic temperatures, suppression of this hopping would then remove the major source of line broadening and would account for markedly narrower spectral features (30).

If efficient exciton quenching occurs not only at chemical derivatization sites but also at the ends of cut nanotubes, our value of the exciton diffusion range Λ naturally explains the strong reduction in PL reported for SWNTs shorter than ~ 100 nm (31). More generally, the measured diffusion range implies that one exciton will visit $\sim 10^4$ carbon atoms during its lifetime. Thus, PL becomes remarkably sensitive to certain sidewall electronic perturbations, which may include chemical derivatizations and defects introduced during nanotube processing. PL may then prove useful for detecting local pH gradients in restricted environments, such as microfluidic channels or organelles inside biological cells.

References and Notes

1. T. G. Pedersen, *Phys. Rev. B* **67**, 073401 (2003).
2. V. Perebeinos, J. Tersoff, Ph. Avouris, *Phys. Rev. Lett.* **92**, 257402 (2004).
3. C. D. Spataru et al., *Phys. Rev. Lett.* **92**, 077402 (2004).
4. J. Chen et al., *Science* **310**, 1171 (2005).
5. Y.-Z. Ma et al., *Phys. Rev. Lett.* **94**, 157402 (2005).
6. F. Wang et al., *Phys. Rev. B* **70**, 241403R (2004).
7. M. O'Connell et al., *Science* **297**, 593 (2002).
8. M. S. Strano et al., *J. Phys. Chem. B* **107**, 6979 (2003).
9. M. L. Usrey, E. S. Lippmann, M. S. Strano, *J. Am. Chem. Soc.* **127**, 16129 (2005).
10. W. E. Moerner, M. Orrit, *Science* **283**, 1670 (1999).
11. L. Cognet et al., *Sci. STKE* **2006**, pe13 (2006).

12. A. Hartschuh et al., *Science* **301**, 1354 (2003).
13. J. Lefebvre et al., *Phys. Rev. B* **69**, 075403 (2004).
14. D. A. Tsyboutski, S. M. Bachilo, R. B. Weisman, *Nano Lett.* **5**, 975 (2005).
15. See supporting material on Science Online.
16. R. M. Dickson et al., *Science* **274**, 966 (1996).
17. S. M. Bachilo et al., *Science* **298**, 2361 (2002).
18. G. Dukovic et al., *J. Am. Chem. Soc.* **126**, 15269 (2004).
19. M. S. Strano et al., *Science* **301**, 1519 (2003).
20. J. L. Bahr et al., *J. Am. Chem. Soc.* **123**, 6536 (2001).
21. C. A. Dyke et al., *Synlett* **2004**, 155 (2004).
22. D. Bonifazi et al., *Nano Lett.* **6**, 1408 (2006).
23. The studied SWNT species were (7,3), (7,5), (7,6), (8,3), (8,6), (9,5), (9,7), (10,5), (12,1), (11,1), and (11,3).
24. A. Hagen et al., *Phys. Rev. Lett.* **95**, 197401 (2005).
25. M. Jones et al., *Nano Lett.* **7**, 300 (2007).
26. C. D. Spataru et al., *Phys. Rev. Lett.* **95**, 247402 (2005).
27. M. S. Dresselhaus, G. Dresselhaus, Ph. Avouris, *Carbon Nanotubes: Synthesis, Structure, Properties, and Applications* (Springer-Verlag, New York, 2001).
28. R. M. Russo et al., *Phys. Rev. B* **74**, 041405 (2006).
29. O. J. Korowanka et al., *Phys. Rev. Lett.* **92**, 017403 (2004).
30. H. Htoon et al., *Phys. Rev. Lett.* **93**, 027401 (2004).
31. D. A. Heller et al., *J. Am. Chem. Soc.* **126**, 14567 (2004).
32. Supported by the Fulbright Foundation and Delegation Generale pour l'Armement (DGA) grant ERE060016 (L.C.), Welch Foundation postdoctoral fellowship L-C-0004 (D.A.T.), the Rice-Houston Alliances for Graduate Education in the Professoriate (AGEP) program (NSF Cooperative HRD-0450363) (J.D.R.R.), NSF grant CHE-0314270, NSF Center for Biological and Environmental Nanotechnology grant EEC-0647452, Welch Foundation grant C-0807, NASA grant JSC-NNJ06HC25G, and Applied NanoFluorescence LLC. We thank J. T. Willerson, S. W. Casscells III, and J. L. Conyers for instrumentation support.

Supporting Online Material

www.sciencemag.org/cgi/content/full/316/5830/1465/DC1

Materials and Methods

Figs. S1 to S2

Movie S1

References

14 February 2007; accepted 23 April 2007

10.1126/science.1141316

Seismic Evidence for Deep-Water Transportation in the Mantle

Hitoshi Kawakatsu* and Shingo Watada

We report seismic evidence for the transportation of water into the deep mantle in the subduction zone beneath northeastern Japan. Our data indicate that water is released from the hydrated oceanic crust at shallow depths (≤ 100 kilometers) and then forms a channel of hydrated mantle material on top of the subducting plate that is the pathway for water into the deep mantle. Our result provides direct evidence that shows how water is transported from the ocean to the deep mantle in a cold subduction zone environment.

Water in the mantle is expected to play essential roles in various notable problems of geodynamics, such as the generation of arc volcanism (1), lubrication of the subduction zone plate interface that may trigger large earthquakes (2), and control of mantle rheology (3). How water is transported into the mantle, however, has not been clear, except that it

is generally believed that subducting hydrated oceanic crust is the major carrier, preventing Earth scientists from accurately estimating the overall water circulation budget of the Earth system (4).

Beneath northeastern Japan, the old Pacific plate is subducting along the Japan trench. Owing partly to the favorable subduction geometry,

as well as the dense and well-maintained seismic network there, it is the most detail-studied subduction zone on the planet, and a number of discoveries of subduction processes have been made there. In recent years, these have included the finding of a double seismic zone (5); detailed mapping of a low-velocity area in the mantle wedge that possibly corresponds to a pathway of magmatic melt migration responsible for arc volcanism (6–8); fingerlike distribution of active volcanoes (9, 10); and a transition from the trench-parallel to trench-normal seismic anisotropy (11). On the basis of these findings, we now have a much better understanding of the detailed mechanics of subduction. However, if we consider a subduction zone as a place of material consumption (subduction of the oceanic plate)

Earthquake Research Institute, University of Tokyo, 1-1-1 Yayoi, Bunkyo-ku, Tokyo 113-0032, Japan.

*To whom correspondence should be addressed. E-mail: hitosi@eri.u-tokyo.ac.jp

and production (generation of arc volcanism), understanding of the essential element—how water is transported into the mantle—is still not resolved.

Water exists in oceanic crust as various hydrous minerals. When the oceanic plate subducts at the trench, the hydrated crust carries water with it in the form of hydrous meta-basalt [e.g., blueschist (12)]. The presence of hydrous minerals in the oceanic crust reduces the seismic velocity to considerably less than the velocity of the surrounding mantle (13, 14), and evidence for this has been detected in different subduction environments as a low-velocity layer near the top surface of the subducting plate (15, 16). It is experimentally established that those hydrous minerals become unstable at pressure and temperature conditions characteristic of a shallow subduction zone (~50-km depth) and are dehydrated to become anhydrous eclogitic oceanic crust. This dehydration process is expected to occur at depths of ~50 to ~150 km in a cold subduction environment such as exists beneath northeast Japan (14, 17), and expelled free water should move directly upward due to buoyancy into the mantle wedge. Because the presence of water substantially lowers the melting temperature of the mantle peridotite, it is generally believed that this water eventually triggers the mantle melting to generate island arc volcanism (1). What is not resolved is how and where this process occurs in the mantle wedge.

On the basis of seismic tomography and a numerical simulation, Iwamori and Zhao (17) suggested that free water in the mantle wedge metamorphoses (or hydrates) the mantle peridotite into hydrous serpentinite, and the serpentinitized mantle is dragged downward parallel to the direction of the slab subduction, forming a thin serpentinite layer along the top surface of the subducting slab. The postulated serpentinite layer may be the pathway by which substantial amounts of water are transported into the deep mantle (4). It is, however, difficult to resolve the existence of such a layer by seismic transmission tomography, owing to the low sensitivity of this method. The scattered seismic wavefield, by contrast, is sensitive to local velocity changes and thus has the potential to resolve thin layers.

We reconstructed such a scattered seismic wave field to image the reflectivity profile beneath northeast Japan (Fig. 1). We used the receiver function (RF) technique (18–20) and obtained the data from the Japanese Hi-net seismic array (21) [see Supporting Online Material (SOM)]. The RF images (Fig. 1 and fig. S1) show clear images of the top part of the subducting Pacific plate: The oceanic Moho is mapped continuously parallel to the upper plane of the double seismic zone (5) as positive RFs (red in the figure, representing the velocity increase with depth). Above this feature, a strong velocity decrease (negative RFs, blue), due to the presence of the hydrous oceanic crust, is observed. The strength of the negative RFs is reduced

drastically at depths of 50 to 90 km (Fig. 2), where the hydrous minerals are expected to dehydrate. The seismic velocity of the hydrous oceanic crust is much slower than that of the surrounding mantle, whereas that of the anhydrous eclogitic crust is seismically indistinguishable (13). Thus, the degree of dehydration would strongly control the reflectivity at the top part of the slab, and our images are in good agreement with existing models of the oceanic crust dehydration (14, 17). We therefore conclude that this reduction of the RF amplitudes provides direct evidence for the dehydration of subducted oceanic crust at this depth range.

At a depth of ~90 km, where strong negative RFs disappear, positive RFs emerge parallel to the dip of the subducting plate (pink line in Fig. 1B). Because the positive RF corresponding to the oceanic Moho (red line) continues to just below this feature, it cannot be the oceanic Moho itself displaced upward due to the effect of some unmodeled structure. A positive RF is a signature

of a velocity increase, and thus the observed feature indicates that the seismic velocity is slower above the top of the subducting plate. The similarity between our RF image and the numerically predicted water content in the mantle wedge (Fig. 3A) allows us to interpret the image as follows (Fig. 3B): The dehydration of the oceanic crust causes its velocity to increase, whereas the serpentinization of the mantle wedge peridotite by the expelled water causes the velocity there to decrease. As this process continues to deep subduction, there is a depth at which the seismic velocity of serpentinitized mantle wedge becomes slower than that of the oceanic crust underneath; below this depth, both the top and bottom sides of the oceanic crust show a velocity increase with depth and are imaged as positive RFs, as observed in Fig. 1A. The top part of the serpentinitized low-velocity layer is not imaged in Fig. 1A, possibly reflecting a more gradual boundary due to the diffusive nature of the hydration/dehydration process (22).

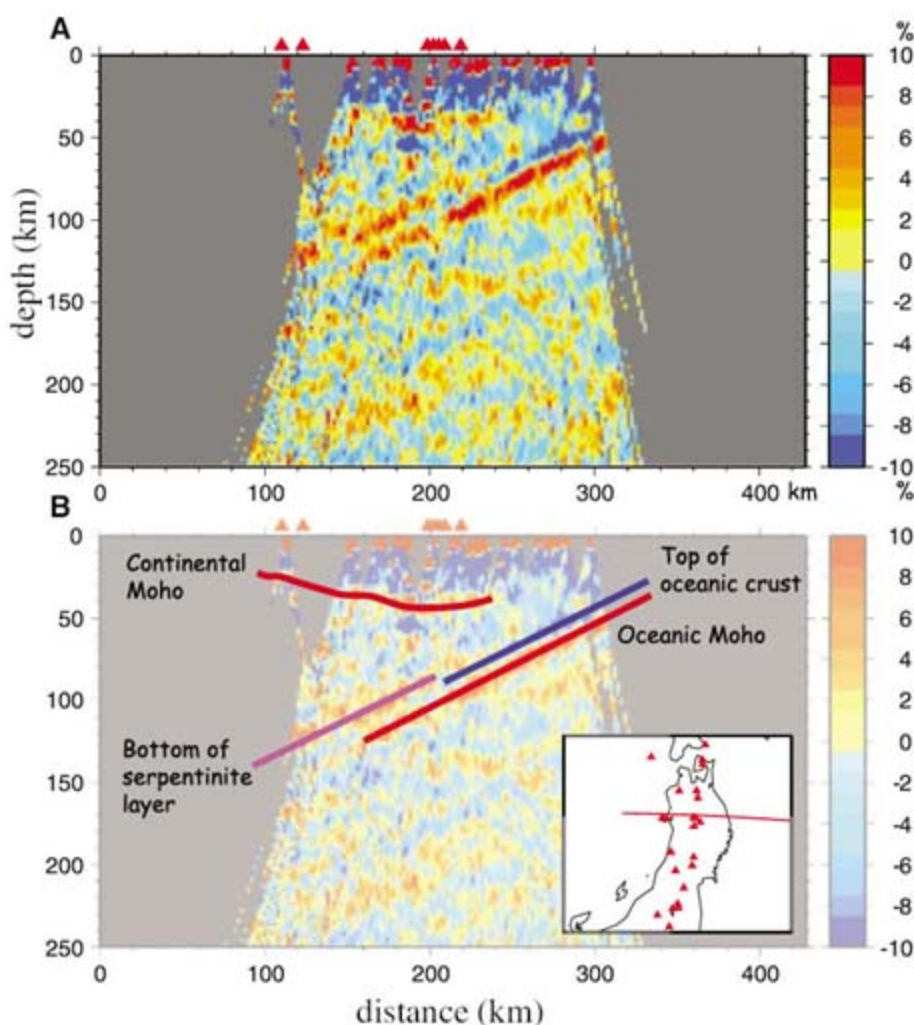


Fig. 1. The reflectivity profile beneath northeast Japan. **(A)** Reflectivities given by RFs are measures of local *S*-wave velocity jumps, because a *P*-to-*S* seismic wave conversion is sensitive to the *S*-wave velocity change. Red and blue colors correspond to velocity increase and decrease with depth, respectively. The color scale is given in terms of an equivalent *S*-wave velocity change (in percent) at a first-order discontinuity. **(B)** Interpretation of the image is overlaid on top of the reflectivity profile in **(A)**. The continental Moho is not imaged well because of the frequency range used for the analysis. (Inset) A map of northeast Japan. The red line delineates where the 100-km-wide cross section is made. Red triangles indicate volcanoes active in the past 10,000 years (Smithsonian Institution, Global Volcanism Program) and are also plotted on the top of the cross sections.

Fig. 2. Amplitude variation of the imaged reflectivity peaks. Peak values of the reflectivities of the interpreted images (along the red and blue lines in Fig. 1B) of three sections (Fig. 1A and fig. S1, D and F) are shown as a function of depth. Open and closed symbols correspond to the red and blue images, respectively, in Fig. 1. The reflectivity values are given in terms of the equivalent *S*-wave velocity increase. The amplitude (or magnitude) of the negative reflectivities decreases with depth, whereas that of the positive ones stays almost constant down to a depth of ~100 km and then becomes weak. A low velocity of ~13% is consistent with the existence of a fully hydrated oceanic crust (blueschist) (29).

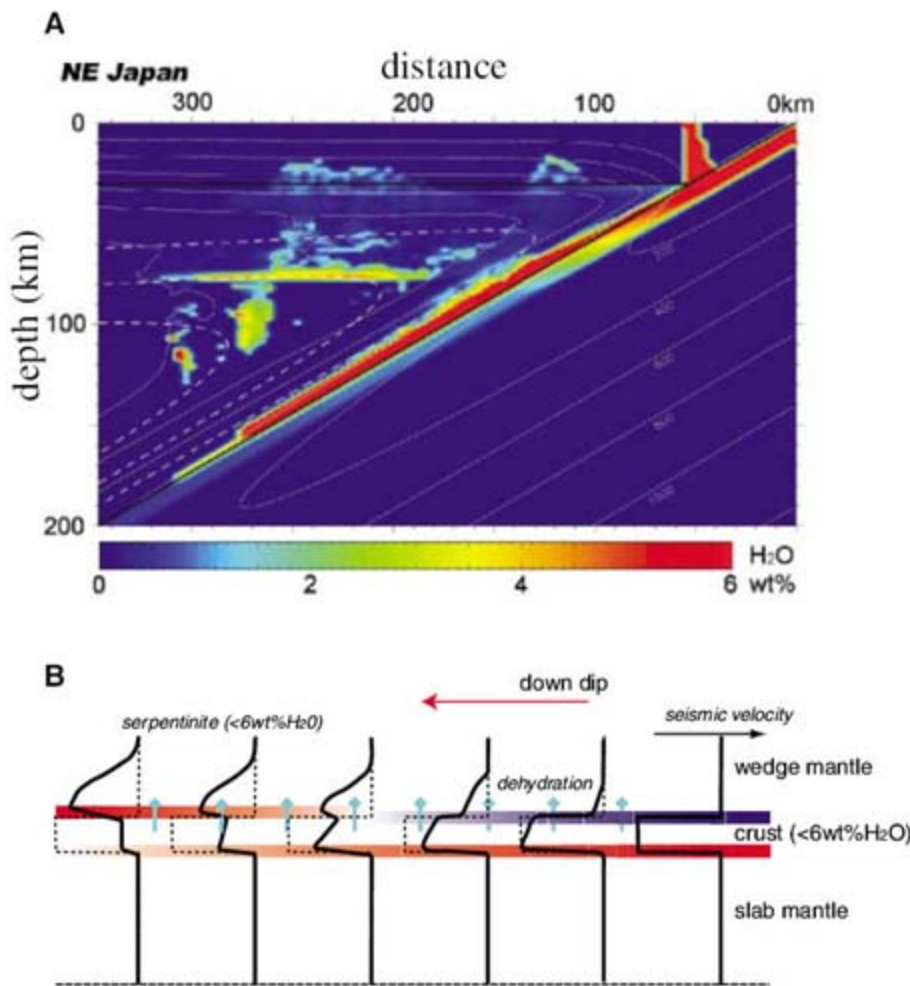
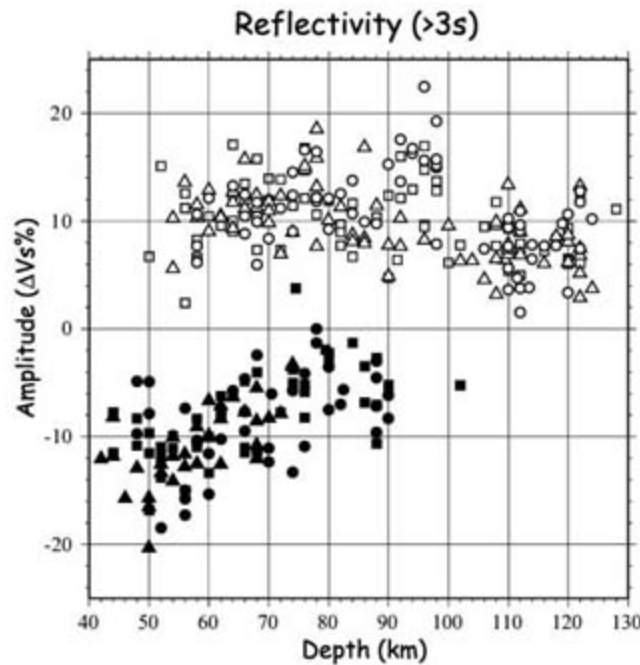


Fig. 3. Interpretation of the reflectivity profile in terms of the water transportation in the mantle wedge. (A) A numerical simulation of the water transportation beneath northeast Japan (4). Bright colors indicate a high concentration of water. The water in the hydrated oceanic crust [shallow (<50 km) dipping red layer] is expelled to serpentinize the mantle wedge, which is dragged downward on top of the subducting plate to form a serpentinite layer (deeper dipping red layer). (B) A schematic model for the effect of crustal dehydration on the seismic velocity near the top of the subducting plate. Seismic-velocity profiles (black lines) perpendicular to the slab surface are given at different down-dip distances. Red and blue colors show the expected reflectivities in a manner similar to that for the reflectivity profile (Fig. 1). Light blue arrows indicate the dehydration process. The slab surface is rotated to become horizontal.

The accurate relative location of RF images to seismicity and tomographic images of the same region is essential for our interpretation, but the RF image (Fig. 1) does not allow such a direct comparison because the effect of the dipping interface dislocates the image. Instead, we use a dip-corrected RF image (see SOM) for such a comparison (Fig. 4A). Two important observations may be made. First, most of the earthquakes in the upper plane of the double seismic zone are located above or near the peak of the positive RFs, and thus occur in the oceanic crust (or near the oceanic Moho); second, the positive RFs interpreted as the bottom of the serpentinite layer are located substantially deeper than the strong low-velocity region in the mantle wedge, which apparently corresponds to the melt pathway for the arc volcanism (8), and thus are unlikely to be directly related to this feature.

The presence of a low-velocity layer near the top part of the subducting plate has been observed in some subduction zones (15, 16, 23–25) and often interpreted as a subducted hydrated oceanic crust (13, 15). Our observation sheds new light on how we interpret those low-velocity structures. Assuming that the amount of water roughly determines the seismic-velocity reduction in both crust and mantle and that most of the expelled water serpentinizes the mantle, the depth at which the top of the oceanic crust loses its illumination may roughly correspond to a depth at which about half of the water in the crust is dehydrated [completion of blueschist dehydration (14), ~90-km depth]. As the dehydration continues further, the oceanic Moho also loses its illumination (~125-km depth), indicating that most of the water in the oceanic crust is dehydrated. Below this depth, the bottom of the serpentinite layer dominates the reflectivity profile until the depth at which serpentine itself becomes unstable, thereby releasing water upward to trigger melting in the wedge (4) (130- to 150-km depth, Fig. 4). If the temperature of this region is cold enough, another hydrous mineral, phase-A, may further bring water down to a depth greater than 300 km (4); this phase-A layer on the top of the slab should show a velocity profile similar to that of the serpentinite layer in Fig. 3B, except that the signature is weaker after the serpentine dehydration. Such a structure had been observed in the deeper portion (250- to 400-km depth) beneath central Japan (23) as a sharp velocity increase at the top surface of the subducting slab. This feature was originally attributed to the partial melting of the wedge mantle (23) and, more recently, to the low-velocity due to the oceanic crust (15). In the context of the present work, we attribute it to the hydrated mantle wedge as a continuation of the serpentinite layer, as suggested above. Furumura and Kennett (26) recently showed that the suggested persistent deep (100 to 250 km) low-velocity crustal layer (15, 24) is not required from seismic waveform data beneath Japan. Indeed, a reflectivity profile

corresponding to a velocity increase subparallel to the deep-slab seismicity is observed down to ~400 km, just above the 410-km discontinuity beneath central Japan (27). The schematic model (Fig. 4B) is qualitatively consistent with most of the seismic observations so far made beneath northeast and central Japan (15, 23, 26, 28) and may possibly explain the depth variation of the reflectivity at the slab surface (13). It brings many individual observations together in a single framework that is consistent with petrological (1) and geodynamical (4, 14, 17) arguments. Thus, our result provides convincing seismic evidence to delineate how water is transported into the deep mantle within the mantle wedge in a cold subduction environment.

The amplitudes of the reflectivity profile of both sides of the oceanic crust at shallow depths (~50 km) are large and consistent with the exist-

tence of a fully hydrated oceanic crust (Fig. 2) that may contain ~6 weight % H₂O (4, 14). To produce the RF signature corresponding to the bottom of the serpentinite layer as observed (Fig. 1), a large amount of the water expelled from the oceanic crust by dehydration must be used to serpentinite the wedge mantle. Consequently, a substantial amount (several wt %) of water must be transported to depths of ~130 to 150 km through this channel. How much deeper and how much water is transported through this channel are important questions that must be answered to quantify the water circulation budget in the subduction zone. Waveform analyses of broadband data of reflected and converted waves at the top of the slab below ~150-km depth may provide answers to these questions, eventually allowing us to estimate the overall water circulation budget in the Earth system (4).

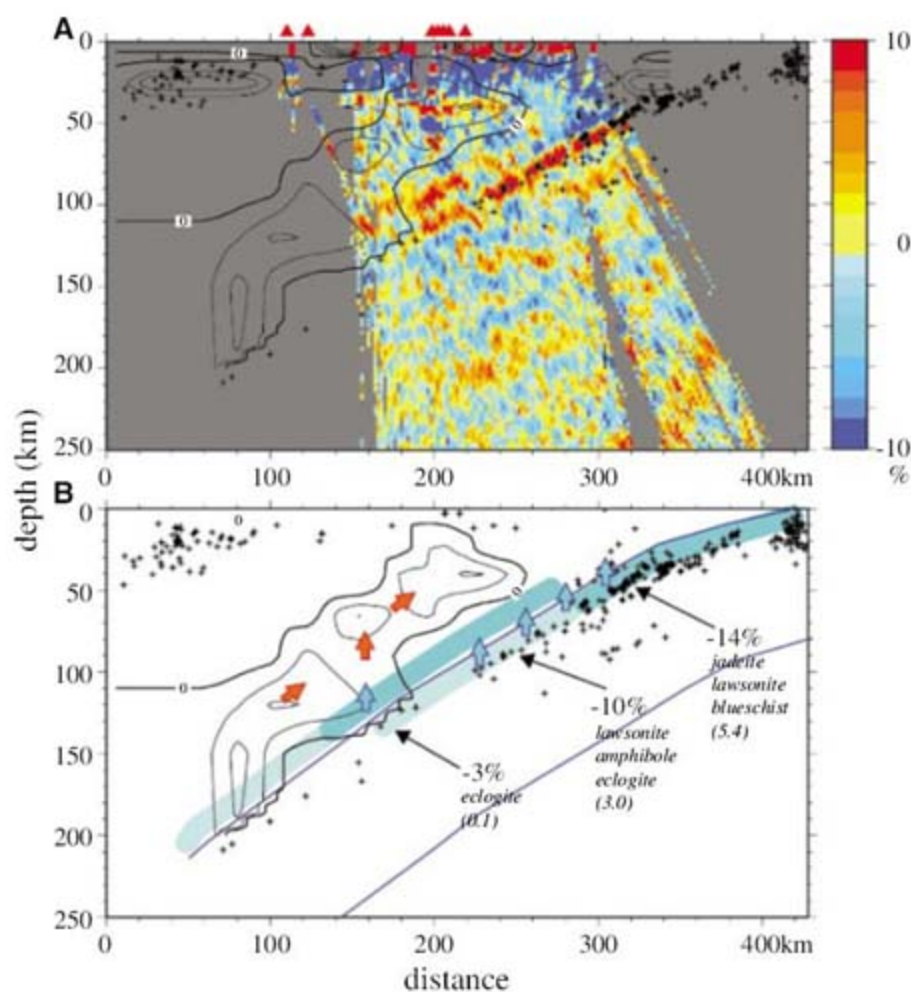


Fig. 4. Integrated seismic images beneath the Tohoku subduction zone and a schematic model for the water transportation. (A) The dip-corrected reflectivity image of Fig. 1A is compared with the tomographic image (7) and the seismicity (magnitude larger than 3) reported by the Japan Meteorological Agency. The S-wave tomographic image above the subducting slab is given by contours with 3% velocity-change intervals. The thick solid contours give the average velocity. Thin contours in the mantle wedge correspond to the low-velocity regions. Plus signs indicate earthquakes. Red triangles are the same as in Fig. 1. (B) The pathway of water transportation postulated by Iwamori [(4); see also (30)] is schematically illustrated by light blue and red colors for nonmagmatic and magmatic paths, respectively. Negative percentages give the S-wave velocities of fully hydrated oceanic crust relative to those of the slab-mantle estimated by Hacker and Abers (29) (also given are the names of the stable crustal rock facies, and wt % H₂O in parentheses). The plate boundaries of the subducting slab are shown schematically as blue lines. Earthquakes and contours of the low-velocity region in the mantle wedge of Fig. 4A are also shown.

References and Notes

1. Y. Tatsumi, *J. Geophys. Res.* **94**, 4697 (1989).
2. M. E. Magee, M. D. Zoback, *Geology* **21**, 809 (1993).
3. S. Karato, in *Geophys. Monogr.* **138** (American Geophysical Union, Washington, DC, 2003), pp. 135–152.
4. H. Iwamori, *Chem. Geol.* **239**, 182 (2007).
5. A. Hasegawa, N. Umino, A. Takagi, *Tectonophysics* **47**, 43 (1978).
6. D. Zhao, A. Hasegawa, S. Horiuchi, *J. Geophys. Res.* **97**, 19909 (1992).
7. J. Nakajima, T. Matsuzawa, A. Hasegawa, D. Zhao, *J. Geophys. Res.* **106**, 21843 (2001).
8. J. Nakajima, Y. Takei, A. Hasegawa, *Earth Planet. Sci. Lett.* **234**, 59 (2005).
9. Y. Tamura, Y. Tatsumi, D. Zhao, Y. Kido, H. Shukuno, *Earth Planet. Sci. Lett.* **197**, 105 (2002).
10. S. Honda, T. Yoshida, *Geochim. Geophys. Geosyst.* **6**, Q01002 10.1029/2004GC000785 (2005).
11. J. Nakajima, A. Hasegawa, *Earth Planet. Sci. Lett.* **225**, 365 (2004).
12. S. M. Peacock, *Geol. Soc. Am. Bull.* **105**, 684 (1993).
13. G. R. Helffrich, in *Geophys. Monogr.* **96** (American Geophysical Union, Washington, DC, 1996), pp. 215–222.
14. B. R. Hacker, S. M. Peacock, G. A. Abers, S. D. Holloway, *J. Geophys. Res.* **108**, 2030 10.1029/2001JB001129 (2003).
15. T. Matsuzawa, N. Umino, A. Hasegawa, A. Takagi, *Geophys. J. R. Astron. Soc.* **86**, 767 (1986).
16. X. Yuan et al., *Nature* **408**, 958 (2000).
17. H. Iwamori, D. Zhao, *Geophys. Res. Lett.* **27**, 425 (2000).
18. L. P. Vinnik, *Phys. Earth Planet. Int.* **15**, 39 (1977).
19. C. A. Langston, *J. Geophys. Res.* **84**, 4749 (1979).
20. C. J. Ammon, *Bull. Seismol. Soc. Am.* **81**, 2504 (1991).
21. K. Obara, K. Kasahara, S. Hori, Y. Okada, *Rev. Sci. Instrum.* **76**, 021301 10.1063/1.1854197 (2005).
22. The bottom of the serpentinite layer appears to be also slightly diffusive because it is not resolved in the higher-frequency image (SOM). If serpentinitization of the mantle peridotite occurs in an equilibrium manner, this boundary may be expected to be sharp. Our result, however, does not support this scenario. The detailed mechanism of water transportation in the mantle wedge is poorly known, and some additional factor appears to be necessary to fully explain our observation.
23. H. Okada, *J. Phys. Earth* **27** (suppl.), 553 (1979).
24. G. A. Abers, *Earth Planet. Sci. Lett.* **176**, 323 (2000).
25. A. Ferris, G. A. Abers, D. H. Christensen, E. Veenstra, *Earth Planet. Sci. Lett.* **214**, 575 (2003).
26. T. Furumura, B. L. N. Kennett, *J. Geophys. Res.* **110**, B10302 (2005).
27. H. Kawakatsu, S. Watada, *EOS Trans. AGU* **86** (Fall Meet. Suppl.), abstract D141A (2005).
28. S. Kita, J. Nakajima, T. Matsuzawa, A. Hasegawa, *Geophys. Res. Lett.* **33**, L24310 (2006).
29. B. R. Hacker, G. A. Abers, *Geochim. Geophys. Geosyst.* **5**, Q01005 (2004).
30. A. Hasegawa, J. Nakajima, in *Geophys. Monogr.* **150** (American Geophysical Union, Washington, DC, 2004), pp. 81–94.
31. We thank H. Iwamori and C. Bina for discussions and J. Nakajima for the tomographic model. An anonymous reviewer provided useful comments. This research was supported by the Japan Society for the Promotion of Science and by the Ministry of Education, Culture, Sports, Science and Technology of Japan.

Supporting Online Material

www.sciencemag.org/cgi/content/full/316/5830/1468/DC1

SOM Text

Fig. S1

References

5 February 2007; accepted 12 April 2007
10.1126/science.1140855

Global Prevalence of Double Benioff Zones

Michael R. Brudzinski,^{1*} Clifford H. Thurber,² Bradley R. Hacker,³ E. Robert Engdahl⁴

Double Benioff zones provide opportunities for insight into seismogenesis because the underlying mechanism must explain two layers of deep earthquakes and the separation between them. We characterize layer separation inside subducting plates with a coordinate rotation to calculate the slab-normal distribution of earthquakes. Benchmark tests on well-established examples confirm that layer separation is accurately quantified with global seismicity catalogs alone. Global analysis reveals double Benioff zones in 30 segments, including all 16 subduction zones investigated, with varying subducting plate ages and stress orientations, which implies that they are inherent in subducting plates. Layer separation increases with age and is more consistent with dehydration of antigorite than chlorite.

Despite the passage of nearly 30 years since the discovery of double Benioff zones (DBZs) (*1*), the nature of these parallel planes of seismicity in a subducting plate remains enigmatic (*2–5*). Benioff zones represent internal deformation of actively sinking lithosphere as inclined zones of seismicity connecting shallow earthquakes near the trench with earthquakes deep in the mantle. The mechanism for any seismicity below ~70-km depth is a matter of ongoing debate because of the need to overcome high confining pressure that would otherwise prohibit the sudden release of strain as earthquakes [e.g., (*6*)]. The existence of DBZs presents an important opportunity for gaining insight into earthquakes at intermediate depths of 70 to 300 km, because a hypothesis for such seismogenesis must explain the presence of the two layers and the separation between them. In general terms, earthquakes require two conditions: the presence of sufficient deviatoric stress to generate shear deformation and an adequate mechanism to store and release strain in a seismogenic way. Proposed mechanisms for triggering intermediate-depth seismogenesis that may account for DBZs center around dehydration of hydrothermally altered oceanic lithosphere, with a variety of hydrated rocks being suggested as contributors (e.g., serpentine, chlorite, and gabbro) (*5, 7–13*). Likewise, several mechanisms have been proposed to explain the stress conditions in DBZs, including unbending of the slab [e.g., (*14, 15*)], thermoelastic stress [e.g., (*16*)], and sagging of the plate [e.g., (*17*)]. An open question that would provide a key constraint on models for seismogenesis is: Are DBZs common in subduction zones globally as a result of a ubiquitous mechanism, or are they rare because of special

conditions present in only a few situations? This study provides a preliminary answer to this question: DBZs are relatively widespread.

DBZs have been most successfully characterized in regions where local seismic networks provide adequate coverage to yield relatively high-precision earthquake hypocenters (*18–23*). We can use such locally “calibrated” DBZs to test the ability of global seismicity catalogs to identify the presence of DBZs and estimate the layer separation. Despite increased location scatter in global catalogs compared with local-network catalogs, a benchmark test described below indicates that global catalogs are sufficient for characterizing DBZs. In this study, we investigated (i) whether DBZs are prevalent globally and (ii) potential relationships between DBZ layer separation and subducting-plate properties, with special attention to thermal parameters (Fig. 1). The overall prevalence and regularity of DBZs on a global basis will

characterize the conditions at depth, both seismic and petrologic, that reveal how a plate evolves after subduction.

We have developed a straightforward method for determining the separation between layers of a DBZ that can also assess the existence of a DBZ. This technique determines the distribution of events in the slab-normal direction for a given slab segment such that seismic layers appear as peaks in earthquake histograms. We use the dip test to establish whether the distribution is multimodal (*24*); if it is, we calculate the separation between modes and the associated uncertainty using a multiple Gaussian fit (*25*). Further details on data and analysis are in the Supporting Online Material.

To evaluate the performance of our method for determining DBZ separation with the slab-normal distribution, we applied the technique to what is arguably the best-characterized DBZ—northeastern Japan—using hypocenters relocated with the advanced double-difference tomography method and local network data (*19*). In this case, DBZ separation was easily seen before coordinate rotation due to high-precision event locations (Fig. 2A, top panel), and it has been established to be ~30 km (*1, 19*). After rotation of the events into down-dip and slab-normal directions (Fig. 2A, bottom), we found that the distribution is bimodal at >99.99% confidence level ($P < 0.0001$) and that the peak-to-peak separation is 31 km.

Having established that the technique can reproduce a DBZ spacing with precisely located events, we compared results for northeastern Japan using the global hypocentral catalogs of Engdahl *et al.* (EHB) (*26, 27*, and subsequent updates) and the Preliminary Determination of

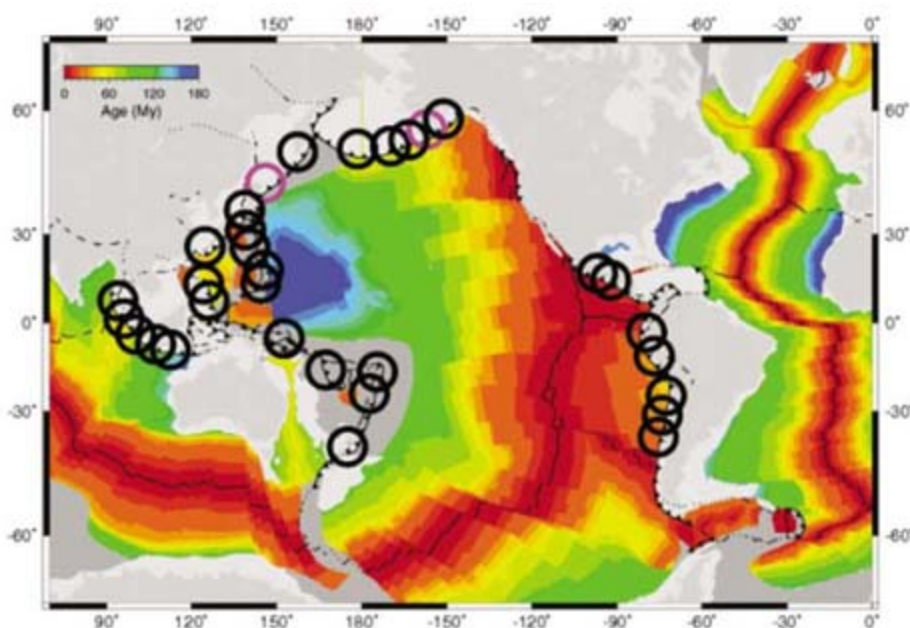
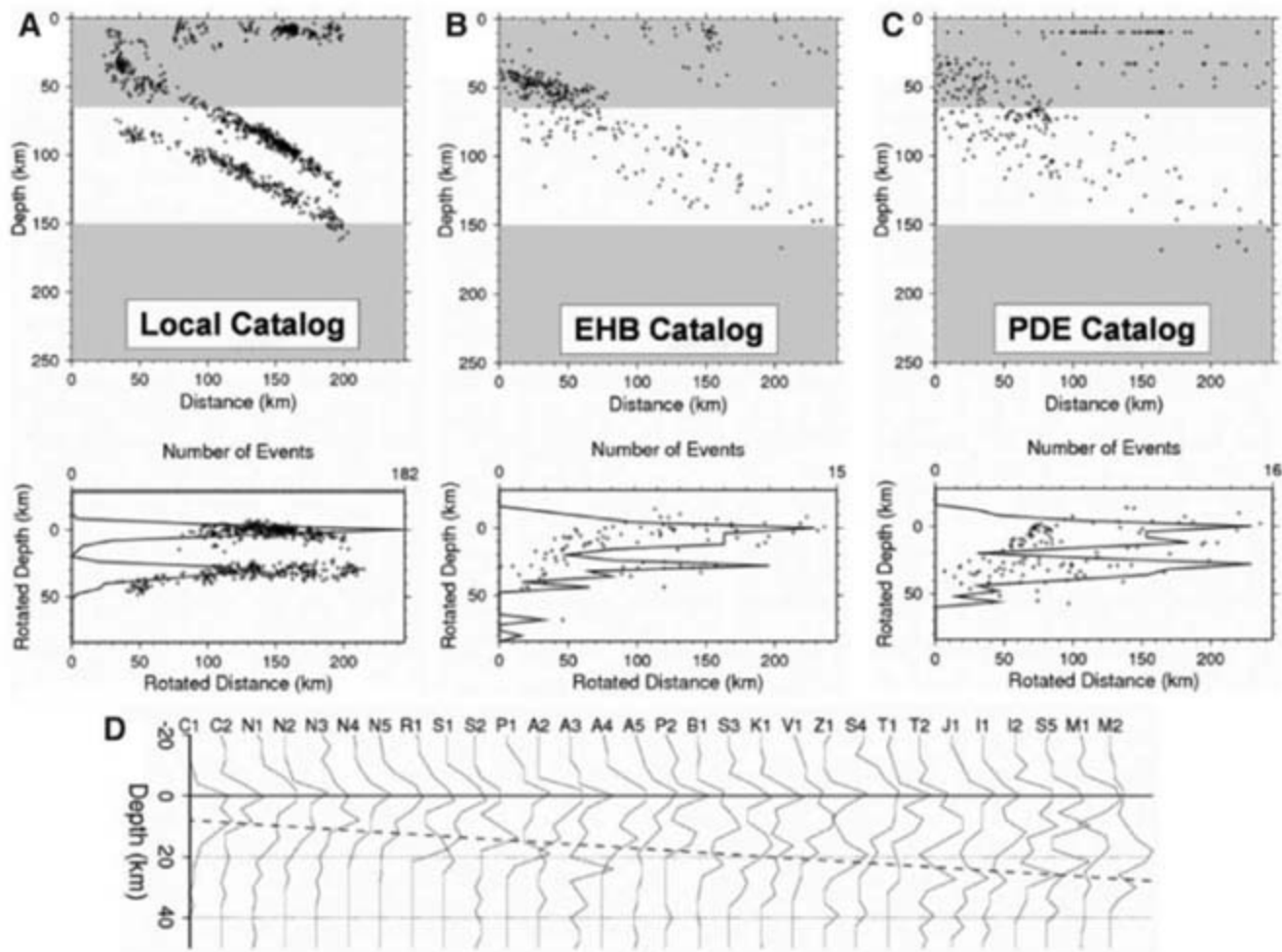


Fig. 1. Subduction-zone segments analyzed, with color scale illustrating seafloor age (*28*) before being consumed at trenches (barbed lines). Black circles indicate areas with a multimodal distribution of events in the slab-normal direction (pink circles indicate cases with confidence < 95%), demonstrating that DBZs are globally prevalent.

¹Geology Department, Miami University, Oxford, OH 45056, USA. ²Department of Geology and Geophysics, University of Wisconsin, Madison, WI 53706, USA. ³Department of Earth Science, University of California, Santa Barbara, CA 93106, USA. ⁴Department of Physics, University of Colorado, Boulder, CO 80309, USA.

*To whom correspondence should be addressed. E-mail: brudzimr@muohio.edu

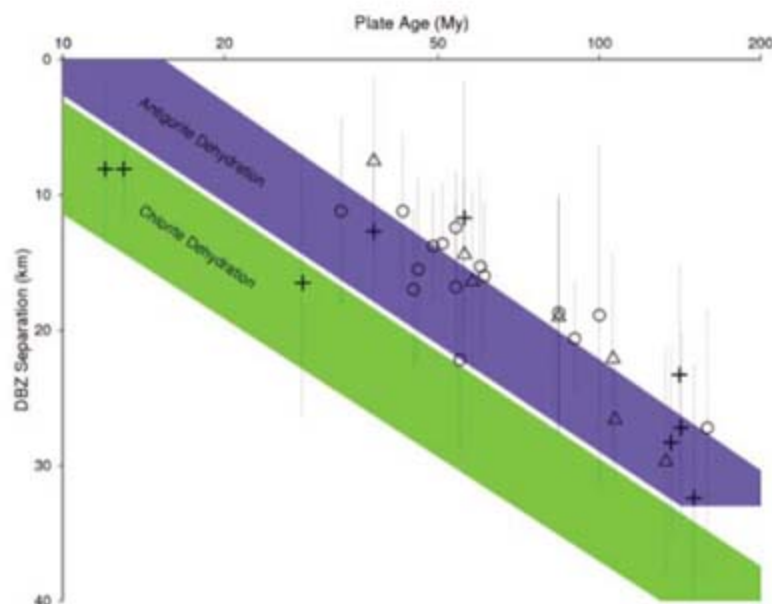
Fig. 2. Analysis of DBZ separation using slab-normal distributions. (A) Results for north-eastern Japan using relocated, local-network hypocenters (19). Top panel shows events (crosses) in typical cross-section view (gray areas not analyzed), and bottom panel shows events after rotation into down-dip and slab-normal locations. This provides the benchmark for comparison with results using global hypocentral catalogs of (B) EHB (26, 27) and (C) PDE. Similar estimates of DBZ separation among the three data sets at several other subduction zones confirm that global catalogs are sufficient to characterize DBZs. (D) Histograms showing slab-normal distribution of EHB events for all segments analyzed, sorted by subducting plate age. DBZ separation is estimated by multiple Gaussian fits shown in green, and dashed linear best fit highlights a significant increase with age.



Epicenters (PDE). The catalogs are constructed only from hypocenters determined using globally reported arrival times and do not include hypocenter solutions from dense local networks. In these cases, the DBZ separation is more difficult to see in a typical cross-sectional view because of the increased scatter in event location and depth, presumably due to the increased effects of subduction zone lateral heterogeneity on global arrival-time data combined with arrival-time pick inaccuracy (Fig. 2, B and C, top). Nevertheless, the slab-normal distribution after coordinate rotation shows two prominent peaks (Fig. 2, B and C, bottom), the dip test for multimodality is easily satisfied ($P < 0.01$), and the separations between the Gaussian peak fits are 30 km for EHB and 29 km for PDE.

Comparing the EHB catalog and other available local network locations, we found excellent agreement for the DBZ separation (18, 20, 21, 23). For example, in the case of New Zealand (22), we determined the slab-normal distribution of EHB and local catalog data, finding DBZ separations of 21 km for each. With the successful benchmark tests in hand, our method allows a new global investigation of DBZ prevalence and patterns in the DBZ separation. We investigated 16 different subduction zones (Alaska, Aleutians, Central Amer-

Fig. 3. DBZ separation versus subducting plate age for each segment analyzed, including 1-SD uncertainties from Gaussian fits. Predictions of DBZ separation due to the lower zone resulting from ultimate dehydration of antigorite (blue) and chlorite (green) are shown based on Hacker *et al.* (9). Antigorite dehydration is consistent with all observed DBZ separations, whereas chlorite dehydration might explain only a few cases. Separations are not correlated with stress orientations, shown as triangles for typical down-dip compression overlying down-dip extension, circles for a different pattern, and crosses when the pattern is unknown.



ica, Kurile-Kamchatka, Izu-Bonin, Japan, Mariana, Nazca, New Britain, New Hebrides, New Zealand, Philippines, Ryukyu, Sumatra, Sunda, and Tonga) that account for a range of subducting plate ages [~10 to 160 million years (My)] (Fig. 1) (28) and slab dips (~0 to 70°) (table S1).

After constructing histograms for the slab-normal distribution of events in the EHB catalog for each region (Fig. 2D), we found 30 different segments that have a bimodal or trimodal distribution that fulfills the dip test for multimodality (table S1). When the results for slab-normal dis-

tribution of events are sorted by age of subducting plate (Fig. 2D), the DBZ separation reveals a significant increase with plate age, from ~8 km for a ~12-My-old slab up to ~30 km for a ~160-My-old slab. A linear estimate for the DBZ separation versus age relationship is ~0.14 km/My, but the data can also be fit with a log-linear relationship.

Every subduction zone studied has at least one segment with a DBZ (Fig. 1), suggesting that DBZs are ubiquitous features. However, our method was not able to identify a DBZ in every section of every subduction zone. This is mainly due to difficulties constructing cross sections in areas with less seismicity, where wider cross sections raise problems with trench curvature or changes in slab dip. Two clear cross sections that did not meet the dip test for multimodality in Kurile-Kamchatka and Eastern Aleutians have been reported as transitions from a DBZ to a single Benioff zone, interpreted as situations where stresses are reduced (4, 29). Moving from northeast to southwest in Kurile-Kamchatka, the decreasing compressive stress transmitted from greater depth is thought to control changes from single compressive zone to DBZ to single extensive zone.

Further evidence for the variable stress regime in DBZs globally can be seen in a survey of reported focal mechanisms (table S1), with several DBZs showing patterns different from the conventional compressive upper layer and extensive lower layer (1) (Fig. 3). This places new constraints on models for the source of stress in DBZs, which leads us to question the viability of each of the proposed models (thermoelastic, slab unbending, and sagging plate), which may have difficulty generating sufficient levels of stress for the wide range of slab temperatures, configurations, and focal mechanisms. The systematic variation in layer separation with plate age despite variations in stress orientations also suggests that the trend in layer separations is not controlled by intraplate stresses. Instead, the discovery of DBZs over a wide range of ages and focal mechanisms indicates that the conditions for seismogenesis can be met in two separate layers within plates at intermediate depths regardless of the slab thermal state and stress orientation. Thus, the triggering mechanism does not result from an unusual set of circumstances, but must be common in subduction zones.

The triggering mechanism for DBZs has typically been interpreted as due to the thermal-petrological evolution of the subducting plate [e.g., (9)]. One proposed mechanism for intermediate-depth seismogenesis that may account for DBZs is the breakdown of hydrous phases to produce a free fluid—and therefore zero effective pressure—allowing brittle faulting (e.g., 7, 13, 30, 31) (32). A variety of hydrous minerals have been suggested as contributors, with metamorphosed basalt near the top of the plate being the pri-

mary candidate for the upper zone of seismicity (5, 9–11, 19). Recently, the upper zone beneath northern Japan has been proposed to consist of two thin layers of seismicity with different focal mechanisms separated by a few kilometers (33). Although the global database used here is likely insufficient to see such a triple seismic zone, there are a few segments in this study (i.e., J1, T1, and T2) where a trimodal solution with a small separation between peaks in the upper layer provides a better fit than a bimodal solution.

Petrologic candidates that might explain the lower zone of DBZ seismicity as the result of dehydration include antigorite (12) and chlorite (9) in hydrous peridotite (34). The chlorite-dehydration reaction occurs at higher temperatures of 700 to 800°C (deeper within the plate), so the dipping seismic zone associated with this reaction would occur up to 10 km below that associated with antigorite dehydration at 600 to 650°C, generating a larger DBZ separation (9). Given this difference between the two dehydration reactions, we compared the results for DBZ separation versus subducting plate age found in this study with separations predicted for the dehydration of antigorite and chlorite based on the thermal-petrological models of Hacker *et al.* (9) (Fig. 3). Antigorite dehydration is consistent with all the observed DBZ separations, whereas chlorite dehydration can explain only a few cases. Given the variation of stress orientations in DBZs of our study areas, the lack of larger separations that would indicate chlorite dehydration is not due to stress limitations. This implies that the lower zone of earthquakes at intermediate depths is most likely associated with fluid released from antigorite breakdown. Given that serpentized peridotite can store several times more water than chlorite-bearing peridotite (9), the amount of fluid released may be a key factor in generating earthquakes, which could be used to evaluate the seismogenic potential of other dehydration reactions [or perhaps phase changes that result in fluid-like material (35)].

Regardless of whether our inference about antigorite breakdown is correct, our finding that DBZs are found in all subduction zones worldwide requires that any triggering mechanism to explain DBZ seismicity (and hence intermediate-depth earthquakes in general) must be present in all subduction zones regardless of plate age, convergence rate, or stress orientation.

References and Notes

1. A. Hasegawa, N. Umino, A. Takagi, *Geophys. J. R. Astron. Soc.* **54**, 281 (1978).
2. G. A. Abers, in *Subduction: Top to Bottom*, G. E. Behout *et al.*, Eds. (American Geophysical Union Geophysical Monograph, 1996), vol. 96, pp. 223–228.
3. K. Fujita, H. Kanamori, *Geophys. J. R. Astron. Soc.* **66**, 131 (1981).
4. H. Kao, W.-P. Chen, *J. Geophys. Res.* **99**, 6913 (1994).
5. T. Yamasaki, T. Seno, *J. Geophys. Res.* **108**, 10.1029/2002JB001918 (2003).

6. C. H. Scholz, *Mechanics of Earthquakes and Faulting* (Cambridge Univ. Press, Cambridge, 1990).
7. H. Jung, H. W. Green, L. F. Dobrzynetskiy, *Nature* **428**, 545 (2004).
8. B. R. Hacker, G. A. Abers, S. M. Peacock, *J. Geophys. Res.* **108**, 2029 (2003).
9. B. R. Hacker, S. M. Peacock, G. A. Abers, S. D. Holloway, *J. Geophys. Res.* **108**, 2030 (2003).
10. S. H. Kirby, E. R. Engdahl, R. P. Denlinger, in *Subduction Top to Bottom* (American Geophysical Union, Washington, DC, 1996), vol. 96, pp. 195–214.
11. D. M. Kerrick, J. A. D. Connolly, *Earth Planet. Sci. Lett.* **189**, 19 (2001).
12. S. M. Peacock, *Geology* **29**, 299 (2001).
13. D. P. Dobson, P. G. Meredith, S. A. Boon, *Science* **298**, 1407 (2002).
14. B. L. Isacks, M. Barazangi, Eds., *Geometry of Benioff Zones: Lateral Segmentation and Downwards Bending of the Subducted Lithosphere*, vol. 1 (American Geophysical Union, Washington, DC, 1977), pp. 99–114.
15. E. R. Engdahl, C. H. Scholz, *Geophys. Res. Lett.* **4**, 473 (1977).
16. H. Hamaguchi, K. Goto, Z. Suzuki, *J. Phys. Earth* **31**, 329 (1983).
17. N. H. Sleep, *J. Geophys. Res.* **84**, 4565 (1979).
18. G. A. Abers, *Geophys. Res. Lett.* **19**, 2019 (1992).
19. H. J. Zhang *et al.*, *Geology* **32**, 361 (2004).
20. N. A. Ratchkovsky, J. Pujol, N. N. Biswas, *Tectonophysics* **281**, 163 (1997).
21. A. Rietbrock, F. Waldhauser, *Geophys. Res. Lett.* **31**, L10608, 10.1029/2004GL019610 (2004).
22. W. X. Du, C. H. Thurber, M. Reyners, D. Eberhart-Phillips, H. J. Zhang, *Geophys. J. Int.* **158**, 1088 (2004).
23. H. Kao, R. J. Rau, *J. Geophys. Res.* **104**, 1015 (1999).
24. J. A. Hartigan, P. M. Hartigan, *Ann. Stat.* **13**, 70 (1985).
25. W. Menke, *Geophysical Data Analysis: Discrete Inverse Theory* (Academic Press, New York, ed. 2, 1989), pp. 289.
26. E. R. Engdahl, R. D. van der Hilst, R. P. Buland, *Bull. Seismol. Soc. Am.* **88**, 722 (1998).
27. E. R. Engdahl, A. Villasenor, in *International Handbook of Earthquake and Engineering Seismology, Part A*, W. H. K. Lee, H. Kanamori, P. C. Jennings, C. Kisslinger, Eds. (Academic Press, Amsterdam, 2002), chap. 41, pp. 665–690.
28. R. D. Müller, W. R. Roest, J.-Y. Royer, L. M. Gahagan, J. G. Sclater, *J. Geophys. Res.* **102**, 3211 (1997).
29. K. W. Hudnut, J. J. Taber, *Geophys. Res. Lett.* **14**, 143 (1987).
30. C. B. Raleigh, M. S. Paterson, *J. Geophys. Res.* **70**, 3965 (1965).
31. S. Kirby, *Rev. Geophys.* **33**, 287 (1995).
32. "Dehydration embrittlement" is a special case of this process in which embrittlement occurs at the site of dehydration and immediately at the time of dehydration.
33. T. Igarashi, T. Matsuzawa, N. Umino, A. Hasegawa, *J. Geophys. Res.* **106**, 2177 (2001).
34. Hydration of the slab mantle may occur by outer-rise normal faulting (11) or by upward fluid flow within a dipping slab (8).
35. H. W. Green II, Y. Zhou, *Tectonophysics* **256**, 39 (1996).
36. This material is based on work supported by the National Science Foundation under grants EAR-0337495 (U.W.), EAR-0542253 (M.U.), and EAR-0215641 (U.C.S.B.). We thank M. Hughes for statistical guidance and H. DeShon, S. Kirby, and H. Zhang for helpful discussions.

Supporting Online Material

www.sciencemag.org/cgi/content/full/316/5830/1472/DC1
Methods
SOM Text
Table S1
References

22 December 2006; accepted 24 April 2007
10.1126/science.1139204

A Meta-Analysis of Effects of Bt Cotton and Maize on Nontarget Invertebrates

Michelle Marvier,^{1*} Chanel McCreedy,¹ James Regetz,² Peter Kareiva^{1,3}

Although scores of experiments have examined the ecological consequences of transgenic *Bacillus thuringiensis* (Bt) crops, debates continue regarding the nontarget impacts of this technology. Quantitative reviews of existing studies are crucial for better gauging risks and improving future risk assessments. To encourage evidence-based risk analyses, we constructed a searchable database for nontarget effects of Bt crops. A meta-analysis of 42 field experiments indicates that nontarget invertebrates are generally more abundant in Bt cotton and Bt maize fields than in nontransgenic fields managed with insecticides. However, in comparison with insecticide-free control fields, certain nontarget taxa are less abundant in Bt fields.

Public debate regarding risks and benefits of genetically modified (GM) crops continues unabated (1–5). One reason for the unrelenting controversy is that disagreements about new technologies often have little to do with scientific uncertainty but instead arise from differing personal values and differing levels of trust in public institutions (6, 7). However, in the case of GM crops, scientific analyses have also been deficient (4). In particular, many experiments used to test the environmental safety of GM crops were poorly replicated, were of short duration, and/or assessed only a few of the possible response variables (8). Much could be learned and perhaps some debates settled if there were credible quantitative analyses of the numerous experiments that have contrasted the ecological impact of GM crops with those of control treatments involving non-GM varieties.

Here, we describe a meta-analysis of field studies involving *Bacillus thuringiensis* (Bt) crops, which represent the predominant modification entailing the novel production of pesticidal substances (Cry proteins) in crop plants. The incorporation of bacterial-derived *cry* genes into plants means that a wide variety of species are exposed, on a relatively continuous basis, to pesticidal Cry proteins. We restricted our analyses to lepidopteran-resistant cotton expressing Cry1Ac protein, lepidopteran-resistant maize expressing Cry1Ab protein, and coleopteran-resistant maize expressing Cry3Bb protein, because the aggregate collection of field experiments assessing these Bt crops is large enough to draw some compelling conclusions (9–11).

The standard approach to assessing nontarget effects entails measurements of abundance, survival, or growth of nontarget species

when exposed to a GM variety versus when exposed to the same or similar variety lacking the genetic modification. We focused on field studies, and the response variable we analyzed is the abundance of nontarget invertebrates, sampled in a variety of ways. For each experiment, we recorded many attributes, including locations, durations, plot sizes, and sample sizes (12) (table S2). Experiments relied on two different types of control treatments, each reflecting a different philosophy of risk assessment: (i) controls entailing non-GM varieties grown under identical conditions but treated with insecticides and (ii) controls entailing non-GM varieties grown under identical conditions and with no insecticides applied. A third type of comparison, in which both Bt and control plants were treated with insecticides, was occasionally used.

We report a weighted mean effect size, Hedges' *d*, calculated as the difference between the means of the Bt and the control treatments divided by the pooled standard deviation and weighted by the reciprocal of sampling variance. Negative values indicate lower abundance (whereas positive values indicate higher abundance) in Bt plots compared with abundance in control plots.

The mean abundance of all nontarget invertebrate groups lumped together is significantly reduced in Cry1Ac cotton fields compared with mean abundance in non-GM, insecticide-free fields [Fig. 1A, white bars; 95% confidence intervals (CI) do not overlap with $d = 0$]. However, the abundance of nontarget invertebrates is significantly higher in Bt cotton compared with that of control fields sprayed with insecticides (Fig. 1A, hatched bars). There was no significant difference in the abundance of nontarget invertebrates for studies where both the Bt and the control fields were treated with insecticides (Fig. 1A; gray bars). Thus, the different types of experimental comparison revealed significantly different effects of Bt crops [Fig. 1A, left; between-groups heterogeneity (Q_b) = 49.96; degrees of freedom (df) = 2; $P < 0.001$]. Results were qual-

itatively similar when analyses were restricted to the related transgenic events MON531 and MON757 (Fig. 1A, right).

For all Cry1Ab maize events, the overall mean abundance of nontarget invertebrates was significantly lower in Bt compared with that in control fields that lacked insecticide applications (Fig. 1B; leftmost white bar). However, the mean abundance of nontarget invertebrates was greater in Cry1Ab maize than in non-GM maize sprayed with pyrethroid insecticides (Fig. 1B; leftmost hatched bar).

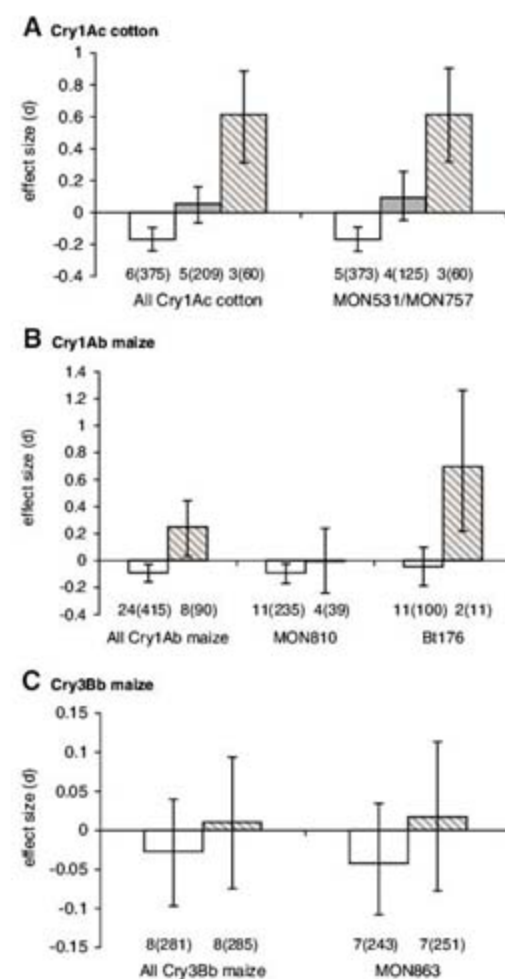


Fig. 1. Meta-analysis of field studies assessing abundance of nontarget invertebrate species for (A) lepidopteran-resistant Cry1Ac cotton, (B) lepidopteran-resistant Cry1Ab maize, and (C) coleopteran-resistant Cry3Bb maize. Effect size is Hedges' *d*, and error bars represent bias-corrected 95% CI. Values below each bar indicate the number of different papers or reports and, in parentheses, the number of lines of data summarized (each line of data represents a comparison of a group's average abundance in a Bt versus control treatment). White bars compare the abundance of nontarget invertebrates in Bt and non-GM varieties, without insecticide applications. Gray bars compare the abundance of nontarget invertebrates in Bt and non-GM varieties, both treated with insecticides. Hatched bars compare the abundance of nontarget invertebrates in insecticide-free Bt varieties versus non-GM varieties managed with applications of [(A)] any chemical insecticide and [(B) and (C)] pyrethroids.

¹Environmental Studies Institute, Santa Clara University, Santa Clara, CA 95053, USA. ²National Center for Ecological Analysis and Synthesis (NCEAS), University of California at Santa Barbara, 735 State Street, Suite 300, Santa Barbara, CA 93101, USA. ³The Nature Conservancy, 4722 Latona Avenue NE, Seattle, WA 98105, USA.

*To whom correspondence should be addressed. E-mail: mmarvier@scu.edu

Effects measured by using these two different types of control treatments differed significantly (e.g., Fig. 1B, left pair of bars; $Q_b = 19.36$; $df = 2$; $P < 0.001$). Qualitatively different patterns emerged when analyses were restricted to single transgenic events. For MON810, effect sizes measured using controls with versus without insecticides did not significantly differ (Fig. 1B, middle bars; $Q_b = 0.71$; $df = 2$; $P = 0.39$). For Bt176, the two control types yielded significantly different effects (Fig. 1B, right bars; $Q_b = 9.41$; $df = 2$; $P = 0.012$), but there was no significant reduction in abundance observed with the insecticide-free controls (white bar, 95% CI overlaps with $d = 0$).

For Cry3Bb maize, the mean abundance of nontarget invertebrates was not significantly different in Bt fields compared to abundance in non-GM maize either with or without pyrethroid applications (Fig. 1C; for the left pair of bars, $Q_b = 0.37$ and $P = 0.51$). This same pattern held when analyses were restricted to event MON863.

The general indication of our analyses is that if agriculture with insecticide applications is the standard of comparison and if adoption of Bt crops truly reduces insecticide applications, then Bt crops may increase the abundance of nontarget invertebrates overall. Alternatively, if the comparison is made to farming systems without insecticides, some nontarget groups are significantly less abundant in Bt than in control fields (Fig. 2). Not surprisingly, the mean abundance of nontarget lepidopterans is significantly reduced in Cry1Ac cotton (Fig. 2A), which targets related lepidopteran pests. There were insufficient data to test this question in Cry1Ab maize. However, the mean abundance of nontarget coleopterans does not appear to be reduced in coleopteran-resistant Cry3Bb maize (Fig. 2C).

Coleopterans and hemipterans appear to be slightly less common in Cry1Ac cotton than non-GM, insecticide-free cotton (Fig. 2A). Although these groups both include a wide variety of functional groups (herbivores, predators, detritivores, etc.), we found no indication that some functional groups exhibit stronger effect sizes than others [see Supporting Online Material (SOM) text for additional details]. Lastly, hymenopterans are less common on average in Cry1Ab and Cry3Bb maize compared with hymenopterans in non-GM, insecticide-free controls (Fig. 2, B and C, respectively). For the Cry1Ab comparison, data on hymenopterans mostly comprised parasitic wasps of the braconidae and ichneumonidae. For Cry3Bb maize, data included parasitic wasps and ants. It is unclear whether the reduced abundance of these groups (coleopterans, hemipterans, and hymenopterans) is due to direct toxicity or is a response to reduced availability of prey in Bt crops. A significant reduction of collembolans in Cry1Ab maize is based on too few observations to be credible at this point (Fig. 2B).

To investigate the sensitivity of our findings to how we designed our comparisons, we performed additional analyses with use of several different subsets of experimental comparisons as the foundation (12). For example, we used only studies in peer-reviewed journals or only studies that identified invertebrate taxa to at least the level of family. With only minor exceptions, results using these alternative queries were qualitatively similar to those reported here (SOM text).

To facilitate additional syntheses, we have created a publicly accessible, searchable database, detailing methods and results of lab and field studies examining nontarget invertebrates and Bt crops (<http://delphi.nceas.ucsb.edu/btcrops/>). While assembling this database, we found numerous studies that did

not report measures of variance to accompany treatment means (40% of 64 reports of field studies), did not clearly present the sample size (20%), or improperly used subsamples to calculate measures of variance (22%). By corresponding with authors, we were often able to resolve these issues. If regulatory agencies were to require researchers to enter details regarding their study methods and results into a similar database, it would be easy to spot omitted information and postpone approval of pesticidal crops until complete records were submitted.

Our analyses provide some support to the claim that GM plants can reduce environmentally undesirable aspects of agriculture, particularly the nontarget impacts of insecticides. However, we examined only one type of genetic modification, and most of the underlying studies entailed controlled field experiments with small spatial scales as opposed to actual farming systems, where continued insecticide use sometimes occurs with Bt crops. Secondly, the conclusion that adoption of Bt cotton or maize may entail ecological benefits assumes a baseline condition of insecticide applications. In reality, both types of control treatment reflect farming practices: in 2005, insecticides were applied to 23% of maize acreage cultivated in 19 states surveyed by the U.S. Department of Agriculture (USDA) (13). Moreover, the vast majority of Bt maize acreage comprises varieties used for silage or processed foods (e.g., corn syrup) for which insecticide use has typically been limited. Insecticides are more commonly used in cotton production, with 71% of surveyed cotton acreage treated in 2005 (13).

Studies such as those synthesized here investigate whether changes in invertebrate abundance are statistically significant. Whereas the lack of a difference is generally considered a signal of environmental safety, it is harder to interpret whether statistically sig-

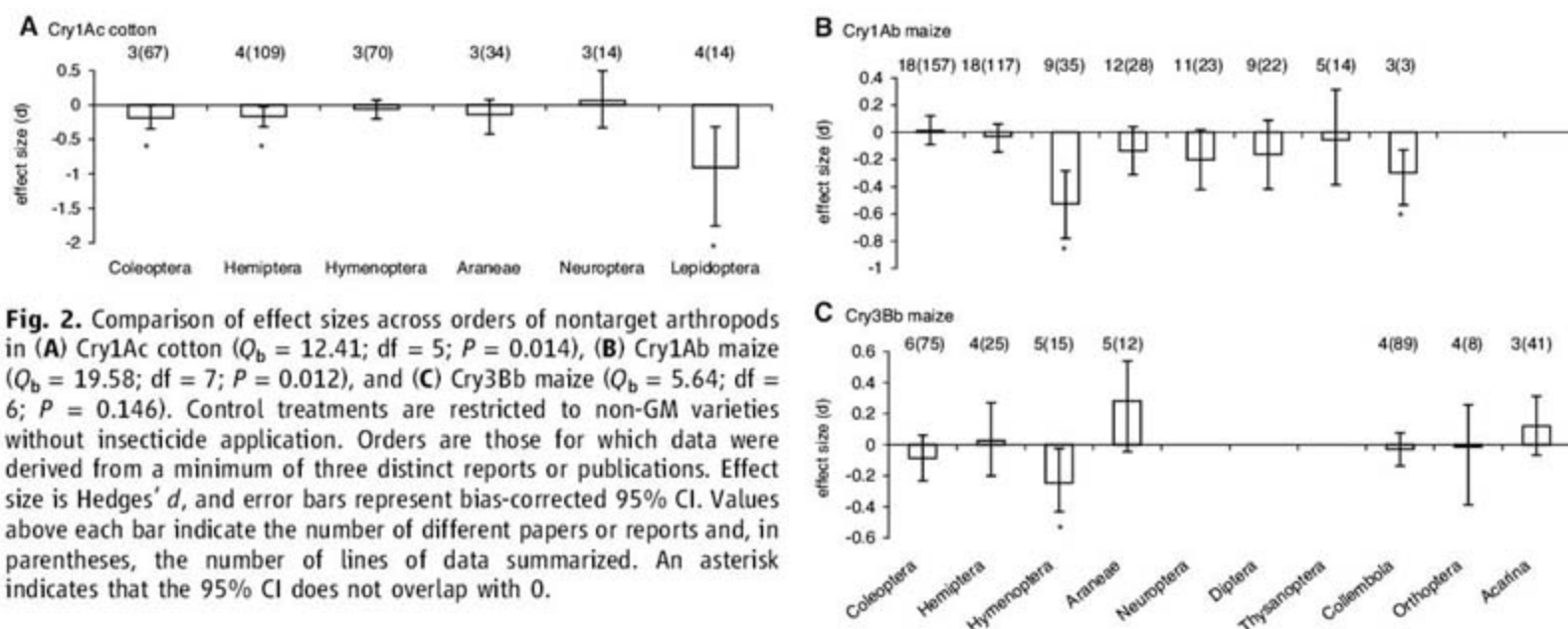


Fig. 2. Comparison of effect sizes across orders of nontarget arthropods in (A) Cry1Ac cotton ($Q_b = 12.41$; $df = 5$; $P = 0.014$), (B) Cry1Ab maize ($Q_b = 19.58$; $df = 7$; $P = 0.012$), and (C) Cry3Bb maize ($Q_b = 5.64$; $df = 6$; $P = 0.146$). Control treatments are restricted to non-GM varieties without insecticide application. Orders are those for which data were derived from a minimum of three distinct reports or publications. Effect size is Hedges' d , and error bars represent bias-corrected 95% CI. Values above each bar indicate the number of different papers or reports and, in parentheses, the number of lines of data summarized. An asterisk indicates that the 95% CI does not overlap with 0.

nificant differences in abundance translate into ecologically important changes. Regardless of one's philosophical perspective on risk assessment for GM crops, enough experimental data has accumulated to begin drawing empirically based conclusions, as opposed to arguing on the basis of anecdote or hand-picked examples.

References and Notes

1. B. Breckling, R. Verhoeven, Eds., *Risk Hazard Damage: Specification of Criteria to Assess Environmental Impact of Genetically Modified Organisms* (Natuschutz und Biologische Vielfalt, Bonn, Germany, 2004), vol. 1, p. 256.
2. L. L. Wolfenbarger, P. R. Phifer, *Science* **290**, 2088 (2000).

3. H. Torgersen, *EMBO Rep.* **5**, 517 (2004).
4. A. A. Snow *et al.*, *Ecol. Appl.* **15**, 377 (2005).
5. D. A. Andow, C. Zwanen, *Ecol. Lett.* **9**, 196 (2006).
6. P. Slovic, *Risk Anal.* **19**, 689 (1999).
7. P. Sturgis, H. Cooper, C. Fife-schaw, *New Genet. Soc.* **24**, 31 (2005).
8. M. A. Marvier, *Ecol. Appl.* **12**, 1119 (2002).
9. G. L. Lövei, S. Arpaia, *Entomol. Exp. Appl.* **114**, 1 (2005).
10. J. Romeis, M. Meissle, F. Bigler, *Nat. Biotechnol.* **24**, 63 (2006).
11. B. W. Clark, T. A. Phillips, J. R. Coats, *J. Agric. Food Chem.* **53**, 4643 (2005).
12. Materials and methods are available as supporting material on Science Online.
13. USDA, *Agricultural Chemical Usage 2005 Field Crops Summary* (National Agricultural Statistics Service, USDA, Washington, DC, 2006).

14. This research was funded by Environmental Protection Agency grant CR-832147-01. Thanks to the many researchers who verified information and provided additional details, especially those who shared their raw data, and to the NCEAS for hosting the Bt crop nontarget effects database.

Supporting Online Material

www.sciencemag.org/cgi/content/full/316/5830/1475/DC1

Materials and Methods

SOM Text

Tables S1 and S2

References

Data

22 December 2006; accepted 30 April 2007

10.1126/science.1139208

An Ancient Mechanism Controls the Development of Cells with a Rooting Function in Land Plants

Benoît Menand,¹ Keke Yi,^{1,2} Stefan Jouannic,^{1*} Laurent Hoffmann,^{1†} Eoin Ryan,¹ Paul Linstead,¹ Didier G. Schaefer,^{3‡} Liam Dolan^{1§}

Root hairs and rhizoids are cells with rooting functions in land plants. We describe two basic helix-loop-helix transcription factors that control root hair development in the sporophyte ($2n$) of the angiosperm *Arabidopsis thaliana* and rhizoid development in the gametophytes (n) of the bryophyte *Physcomitrella patens*. The phylogeny of land plants supports the hypothesis that early land plants were bryophyte-like and possessed a dominant gametophyte and later the sporophyte rose to dominance. If this hypothesis is correct, our data suggest that the increase in morphological complexity of the sporophyte body in the Paleozoic resulted at least in part from the recruitment of regulatory genes from gametophyte to sporophyte.

The invasion of land by plants in the Paleozoic was accompanied by marked changes in plant structure and life cycle and resulted in diversification of terrestrial ecosystems and pronounced climate change (1–3). One of the most important transformations that occurred during the first 100 million

years after plants colonized the land was the rise to dominance of the diploid phase (sporophyte) of the life cycle (the land-plant life cycle comprises independent haploid and diploid organisms). The phylogenetic relationship among green algae and land plants suggests that the haploid phase (gametophyte) was morphologically more complex than the smaller diploid phase (sporophyte) in the earliest land plants (4). This changed over a period of ~100 million years to a situation in which the diploid phase became larger and more morphologically complex (4). This rise to dominance of the diploid phase of the life cycle was accompanied by an enormous increase in morphological diversity evident in Devonian floras and has persisted to the present day, when the land floras are largely dominated by diploid plants (3). To date, we have little understanding of the genetic basis of such a metamorphosis of the land plant body. The characterization of the function of regulatory genes such as *LEAFY (LFY)* in both bryophytes and angiosperms suggests that the increase in sporophyte diversity was brought about through the

modification of the activities of sporophyte-specific genes with sporophyte-specific functions (5). Here we show that genes that specifically promote the development of root hairs in diploid sporophytes of angiosperms also control the development of cells with similar functions in the haploid gametophytes of mosses. This suggests that genes with gametophyte functions in ancestral land plants were recruited to function in the sporophyte during the metamorphosis of the land plant body.

Root hairs are highly polarized cells that increase the surface area of the plant that is in contact with the growth substrate. They play important roles in nutrient acquisition and anchorage in those land plants that have roots (6, 7). The *Arabidopsis thaliana* root epidermis is organized in alternate rows of hair-forming cells (H cells) that produce a tip-growing protuberance (root hairs) and rows of non-hair cells (N cells) that remain hairless. *AtRHD6 (ROOT HAIR DEFECTIVE 6)* positively regulates the development of H cells—*Atrhd6* mutants develop few root hairs (Fig. 1A) (8). We cloned *AtRHD6* using an enhancer trap line (*Atrhd6-2*) in which the *GUS* reporter gene is expressed in H cells but not in N cells (Fig. 1, C and D, and fig. S1). *AtRHD6* encodes the basic-helix-loop-helix (bHLH) transcription factor At1g66470 (9). The identification of another independent allele (*Atrhd6-3*) with a similar phenotype and the complementation of the *Atrhd6-3* mutation with a whole gene *AtRHD6p::GFP:AtRHD6* translational fusion with the GREEN FLUORESCENT PROTEIN (GFP) confirmed that the defect in root hair development observed in this mutant is due to mutation of *At1g66470* (Fig. 1A). This complementing *AtRHD6p::GFP:AtRHD6* fusion indicates that *AtRHD6* protein accumulates in H-cell nuclei in the meristem and elongation zones (Fig. 1B) but disappears before the emergence of the root hair (data not shown). The spatial pattern of N cells and H cells in the *A. thaliana* root epidermis is controlled by a transcriptional network including the posi-

¹Department of Cell and Developmental Biology, John Innes Centre, Norwich NR47UH, UK. ²State Key Laboratory of Plant Physiology and Biochemistry, College of Life Science, Zhejiang University, Hangzhou, 310058, P. R. China. ³Département de Biologie Moléculaire Végétale, Université de Lausanne, CH-1015 Lausanne, Switzerland.

*Present address: Institut de Recherche pour le Développement, UMR 1098 Biologie du Développement des Espèces Pérennes Cultivées, 911 avenue Agropolis, F-34394 Montpellier Cedex 5, France.

†Present address: UMR CNRS/UPS 5546, Surfaces Cellulaires et Signalisation chez les Végétaux, Pôle de Biotechnologies végétales, 24 chemin de Borde-Rouge, F-31326 Castanet-Tolosan, France.

‡Present address: Institut Jean-Pierre Bourgin, Station de Génétique et Amélioration des Plantes, Institut National de la Recherche Agronomique Versailles, Route de Saint Cyr, F-78000 Versailles, France.

§To whom correspondence should be addressed. E-mail: liam.dolan@bbsrc.ac.uk

tive regulator of H-cell identity *CPC* and the negative regulators of H-cell identity *WER*, *TTG*, and *GL2* (10). To determine if *Atrhd6* is regulated by these genes, we analyzed the promoter activity of the *Atrhd6-2* enhancer trap in different mutant backgrounds. While the *Atrhd6-2* enhancer trap expresses GUS in cells in the H position, this expression spreads to the cells in the N position in the *wer*, *ttg*, and *gl2* mutant backgrounds, indicating that *WER*, *TTG*, and *GL2* negatively regulate transcription of *Atrhd6* in the N position (Fig. 1D). No expression was observed in the *cpc* mutant, indicating that *CPC* positively regulates *Atrhd6* expression (Fig. 1D). Thus, *Atrhd6* controls the development of root hair cells and acts downstream of the genes involved in epidermal pattern formation.

ATRHD6 is a member of subfamily VIIIc of bHLH transcription factors that comprises five other members (9, 11). One of these genes, *At5g37800*, hereafter named *RHD SIX-LIKE1* (*AtRSL1*), is very similar to *Atrhd6*, suggesting that these two genes derive from a relatively recent duplication event (9). This suggests that *Atrhd6* and *AtRSL1* might have redundant functions. To determine if *AtRSL1* is also required for root hair development, we identified a line (*Atrsl1-1*) carrying a complete loss-of-function mutation in the *AtRSL1* gene and created the *Atrhd6-3 Attrsl1-1* double mutant (fig. S1). Because no new phenotypes were observed when these mutants were grown in our standard growth conditions, we grew them on the surface of cellophane disks, where small numbers of root hairs develop in the *Atrhd6-3* single mutant (Fig. 2A). Plants homozygous for the *Atrsl1-1* mutation had wild-type root hair morphology when grown on cellophane disks (Fig. 2A). However, the *Atrhd6-3 Attrsl1-1* double mutant did not develop root hairs, indicating that *Atrhd6* and *AtRSL1* have partially redundant functions in root hair development (Fig. 2A). *Atrhd6-3 Attrsl1-1* double-mutant plants carrying the genomic construct *AtRSL1p::GFP::AtRSL1* displayed the *Atrhd6-3* mutant phenotype, confirming that the extreme hairless phenotype of the *Atrhd6-3 Attrsl1-1* double mutant is the result of a loss of function of both *Atrhd6* and *AtRSL1* genes (Fig. 2A). The complementing GFP::AtRSL1 fusion protein accumulates in hair cell nuclei in the meristem and elongation zones, indicating that *Atrhd6* and *AtRSL1* have similar expression patterns (Fig. 2B). These data indicate that *Atrhd6* and *AtRSL1* act together to positively regulate root hair development. To determine if *Atrhd6* and *AtRSL1* are required for the development of the only other tip-growing cell in flowering plants, the pollen tube, we characterized the phenotypes of pollen tubes in *Atrhd6-3*, *Atrsl1-1*, and *Atrhd6-3 Attrsl1-1* mutants both in vitro and in vivo. We detected neither a defect in pollen tube growth nor in the segregation of mutant alleles in the F₂ progeny

of backcrosses to wild type (fig. S2). No other defective phenotype was detected in any other part of *Atrhd6-3*, *Atrsl1-1*, or *Atrhd6-3 Attrsl1-1*

mutants. Together these data indicate that *Atrhd6* and *AtRSL1* are bHLH transcription factors that are specifically required for the

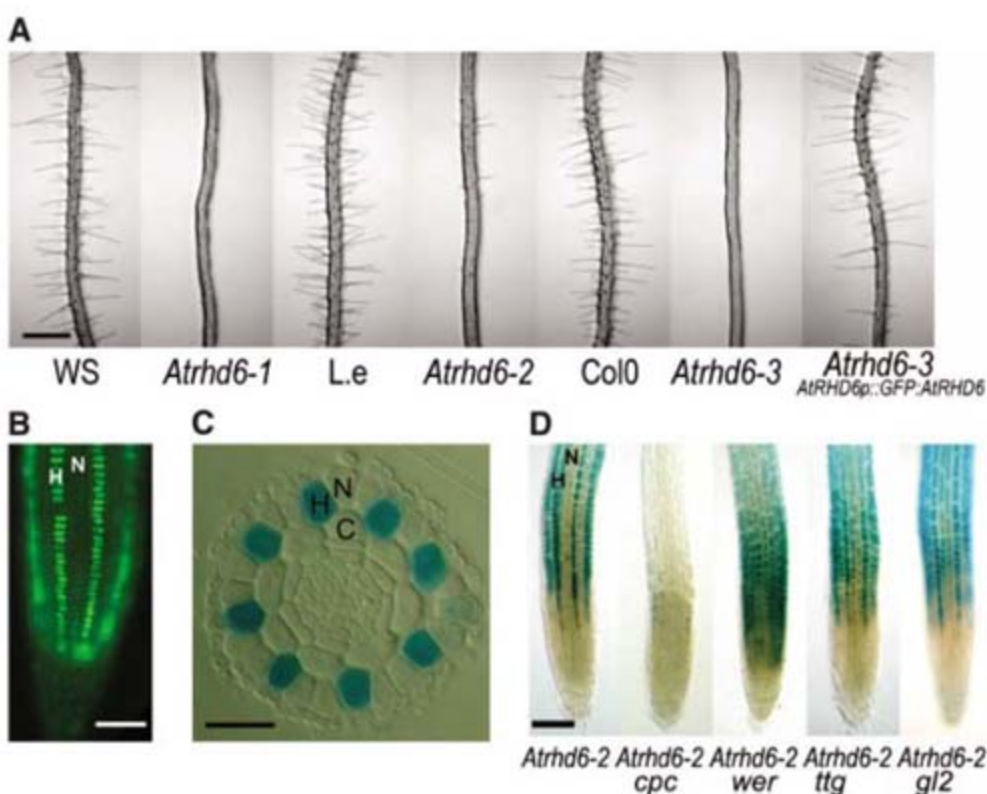


Fig. 1. *Atrhd6* is a positive regulator of root hair development in *A. thaliana*. (A) Roots of *Atrhd6-1*, *Atrhd6-2*, and *Atrhd6-3* mutants with their respective wild-type ecotype (WS, Wassilewskija; Col0, Columbia 0; L.e., *Landsburg erecta*) and complementation of the *Atrhd6-3* mutant with a genomic *Atrhd6p::GFP::Atrhd6* fusion. (B) Fluorescent image of the genomic *Atrhd6p::GFP::Atrhd6* fusion in the *Atrhd6-3* background showing *ATRHD6* protein in hair cells nuclei. (C) Expression of the *Atrhd6-2* enhancer trap *GUS* gene in root cross section. (D) Whole-mount longitudinal view of the expression of the enhancer trap *GUS* gene in *Atrhd6-2* and in different backgrounds (*cpc*, *wer*, *ttg1*, and *gl2*). H, hair cell; N, non-hair cells; C, cortex. Scales bars, 500 μ m (A), 50 μ m (B), 25 μ m (C), and 100 μ m (D).

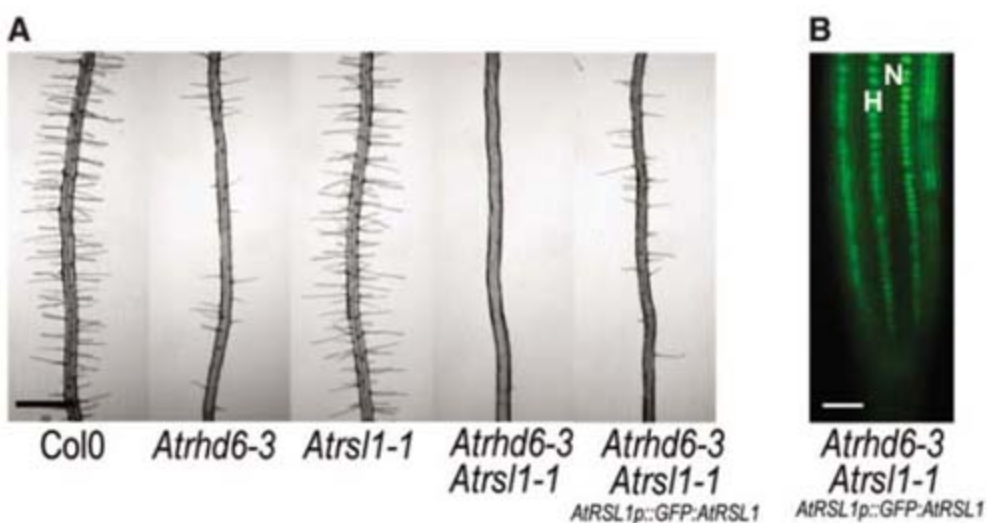


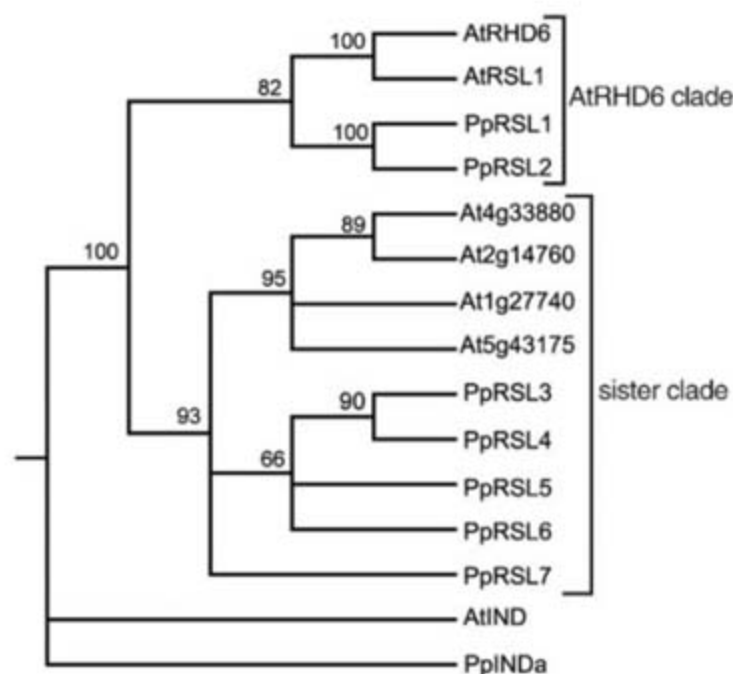
Fig. 2. *AtRSL1* positively regulates root hairs development in *A. thaliana*. (A) Roots of WT, *Atrhd6-3* single mutant, *Attrsl1-1* single mutant, *Atrhd6-3 Attrsl1-1* double mutant, and *Atrhd6-3 Attrsl1-1* double mutant bearing the *AtRSL1p::GFP::AtRSL1* transgene. Plants were grown on MS media with sucrose overlaid with a cellophane disk to increase root hair production in the *Atrhd6-3* mutant. (B) Fluorescent image of the genomic *AtRSL1p::GFP::AtRSL1* fusion in the *Atrhd6-3 Attrsl1-1* background showing *AtRSL1* protein in hair cells nuclei. H, hair cell; N, non-hair cells. Scale bars, 500 μ m (A) and 50 μ m (B).

development of root hairs and act downstream of the genes that regulate epidermal pattern formation in the flowering plant *A. thaliana*.

The most ancestral grade of land plants are the bryophytes—the earliest microfossils of land plants from the middle Ordovician (~475 million years ago) have bryophyte characteristics (12). Bryophytes do not have roots but possess tip-growing cells that are morphologically similar to root hairs and fulfill rooting functions. In mosses, caulonemal cells increase the surface area of the filamentous protonema tissue in contact with the substrate and rhizoids anchor the leafy gametophore to their growth substrate (13, 14); both cell types are hypothesized to be involved in nutrient acquisition (13). However, rhizoids and caulonema develop from the gametophyte of mosses, whereas root hairs develop from the sporophyte of modern vascular plants. Thus, according to the current view that land plants evolved by the intercalation of a sporophytic generation from a haplontic algal ancestor followed by the progressive increase of size and complexity of the sporophyte in parallel to a reduction of the gametophyte (4, 15), neither rhizoids nor caulonema are homologous to root hairs. To determine if the developmental mechanism that controls the development of root hairs in angiosperms also controls the development of nonhomologous tip-growing cells with a rooting function in bryophytes, we identified *RHD6-LIKE* genes from the moss *Physcomitrella patens*. We identified seven members of the *AtRHD6* subfamily of bHLH genes from the publicly available *P. patens* genomic sequence (<http://moss.nibb.ac.jp/>), suggesting that these genes have been conserved through the land plant evolution. These were designated *Physcomitrella patens RHD SIX-LIKE 1* to 7 (*PpRSL1* to *PpRSL7*). To analyze the relationship between *P. patens* and *A. thaliana* *RSL* genes, we constructed trees by maximum parsimony. A strict consensus tree shows that *AtRHD6*, *AtRSL1*, and the two *P. patens* genes *PpRSL1* and *PpRSL2* are closely related and together form a monophyletic clade (*AtRHD6* clade) that is sister to the clade comprising all the other members of the subfamily (*sister clade*) (Fig. 3 and fig. S3). This indicates that the *AtRHD6* clade evolved before the separation of the bryophytes and the vascular plants from a common ancestor.

To characterize the function of the *RHD6-LIKE* genes in moss, we constructed deletion mutants that lacked the function of *PpRSL1* and *PpRSL2* genes and determined whether they developed morphological defects. Three independent RNA null mutants with single insertions into the *PpRSL1* and *PpRSL2* genes were made. Double mutants with single insertions into both genes were also generated (fig. S4). The phenotypes of each of these mutants were then analyzed. A haploid protonema develops upon germination of a wild-type *P.*

Fig. 3. Relationship between *RHD6-LIKE* proteins from *A. thaliana* and *P. patens*. The tree is a strict consensus tree of 12 most parsimonious trees generated with the alignment of bHLH domains amino acids sequences shown in fig. S3. The *A. thaliana* genes used are the members of bHLH subfamily VIIIc, except *AtIND* (*INDEHISCENT*)/*At4g00120*, which was used as out-group and belongs to the bHLH subfamily VIIIb (9, 11, 21). *P. patens* *PpRSL 1* to 7 sequences were obtained by BLAST of the *P. patens* genomic sequence. *PpIND1* is a *P. patens* sequence similar to *AtIND* and a putative member of family VIIIb in *P. patens*. Numbers are bootstrap values and indicates an 82% level of confidence for the occurrence of the *AtRHD6* clade. The brackets indicate the *AtRHD6* clade and the sister clade.



P. patens. Numbers are bootstrap values and indicates an 82% level of confidence for the occurrence of the *AtRHD6* clade. The brackets indicate the *AtRHD6* clade and the sister clade.

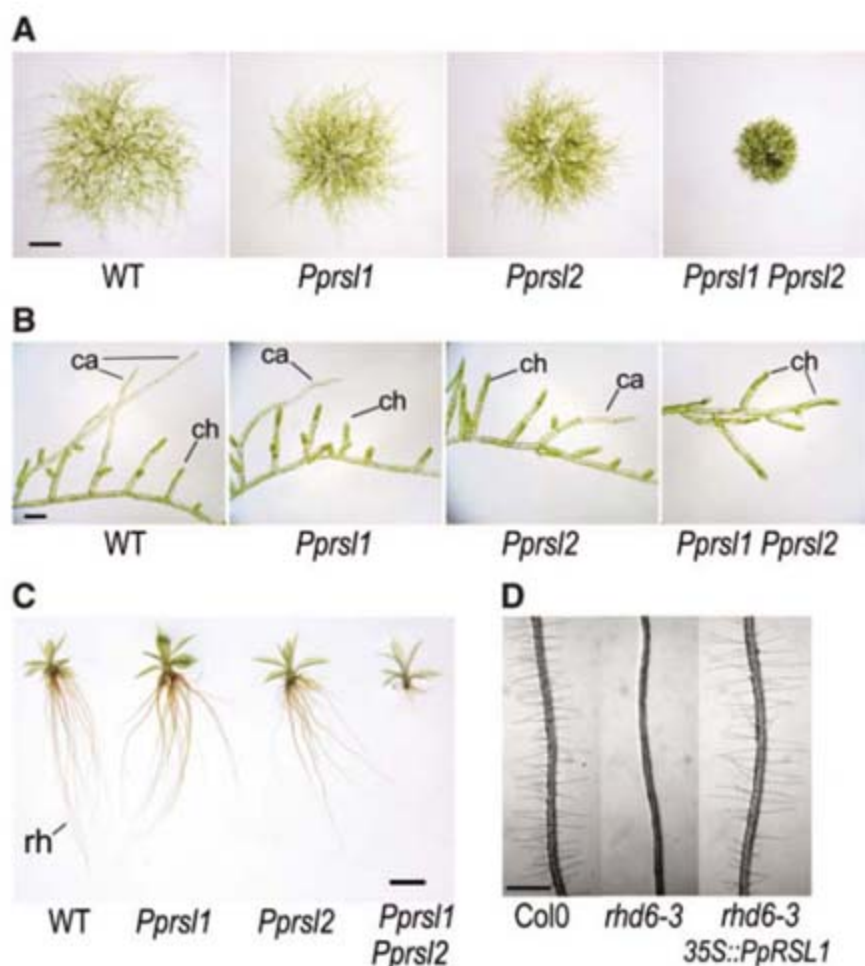


Fig. 4. *PpRSL1* and *PpRSL2* positively control the development of caulonemal cells and rhizoids in *P. patens*, and *PpRSL1* and *AtRHD6* have a conserved molecular function. (A and B) Eighteen-day-old protonema from WT, *PpRsl1*, and *PpRsl2* single mutants, and *PpRsl1 PpRsl2* double mutant, were grown from spores on 0.8% agar. (A) Whole protonema growing from a single spore. (B) Dissected filaments from protonema shown in (A). (C) Isolated 1-month-old gametophores. (D) Roots of the *A. thaliana Atrhd6-3* mutant carrying the *35S::PpRSL1* transgene compared to WT and *Atrhd6-3* roots. ca, caulonemal cell; ch, chloronemal cell; rh, rhizoid. Scale bars, 1 mm (A), 100 μ m (B), 1 mm (C), and 500 μ m (D).

patens spore (13). This filamentous tissue comprises two cell types, the chloronema and the caulonema (Fig. 4, A and B). Chloronemal cells contain large chloroplasts and grow by a slow tip-growth mechanism (16). Caulonemal cells are more elongated, contain few smaller chloroplasts, grow by rapid tip growth, and are involved in the colonization of the substrate. Leafy gametophores usually develop from caulonema and are anchored to their substrate by tip-growing multicellular rhizoids that are morphologically similar to caulonema (Fig. 4C). The *Pprsl1* and *Pprsl2* single mutants have slightly smaller and greener protonema cultures than the wild type (WT), and this phenotype is much stronger in the *Pprsl1 Pprsl2* double mutant, which produces small dark-green protonema (Fig. 4A). *Pprsl1* and *Pprsl2* single mutants produce fewer caulonemal cells than the WT, indicating that the greener protonema phenotype is the result of a defect in the development of caulonemal cells (Fig. 4B). No caulonemal cells develop in the *Pprsl1 Pprsl2* double mutant, and the protonema of this mutant consists of chloronemal cells only (Fig. 4B). In wild-type plants gametophores develop from caulonema, but in the *Pprsl1 Pprsl2* double mutants the gametophores develop from chloronema, as previously observed in another caulonema-defective mutant (17). The gametophores of the *Pprsl1 Pprsl2* double mutant develop few very short rhizoids (Fig. 4C). No other defective phenotypes were detected in the chloronema, in the leafy part of the gametophore, or in the sporophyte in the single or double mutants. This indicates that *PpRSL1* and *PpRSL2* together regulate the development of caulonemal cells and rhizoids in the moss gametophyte. The lack of a defect in chloronemal cells, which are the other tip-growing cells that develop in moss (16), in the *Pprsl1 Pprsl2* double mutant shows that, as in *A. thaliana*, these genes are not general regulators of tip growth. Instead it suggests that they function specifically to regulate the development of cells with rooting functions such as caulonemal cells and rhizoids. To determine if protein function is conserved across the land plants, we performed a cross-species complementation experiment. Expression of *PpRSL1* under the cauliflower mosaic virus (CaMV) 35S promoter in the *Atrhd6-3* mutant resulted in the formation of wild-type root hairs (Fig. 4D). Thus, the moss *PpRSL1* gene can substitute for loss of *Atrhd6* function in *A. thaliana*. This indicates that the molecular function of *PpRSL1* and *Atrhd6* has been conserved since the divergence of seed plants and mosses from a common ancestor and suggests that the same molecular mechanism controls the development of *A. thaliana* root hairs and *P. patens* caulonema and rhizoids.

We have shown that closely related transcription factors control the development of

root hairs and rhizoids in the seed plant sporophyte and the bryophyte gametophyte, respectively. The demonstration of the existence and function of these genes in plants derived from the earliest colonizers of the land (bryophytes) indicates that an ancient common mechanism controls the development of these two nonhomologous cell types. The *RHD6-LIKE* genes will have been important for the invasion of land by plants because they control the development of structures required for anchorage to the terrestrial substrate and nutrient acquisition. The observation that rhizoids have been found on some of the oldest land-plant fossils is consistent with this view (18–20).

Our demonstration that *RHD6*-related genes function in both bryophytes and angiosperms in the development of rhizoids and root hairs, respectively, suggests a mechanism to explain the increased morphological and cellular diversity of the sporophyte in the land plants derived from bryophyte ancestors. Our results suggest that *RHD6-LIKE* genes functioned in the haploid generation (gametophyte) of these early land plants that had a bryophyte-like life cycle (18), where they controlled the formation of cells with a rooting function. Then, during the subsequent radiation of the land plants, these genes were deployed in the development of the diploid generation (sporophyte) of the nonbryophyte land plants, where they controlled the development of rhizoids and root hairs. Here we propose a general model for the increase in morphological diversity of the land-plant sporophyte based on these findings. We suggest that some of the genes that controlled the development of the bryophyte haploid body were recruited by the diploid phase in their descendants, where they provided part of the genetic mechanism for the increased morphological and cellular diversity of the sporophyte. Thus, the recruitment of genes from haploid to diploid phases of the life cycle, in concert with the modification of function of sporophyte-specific genes, such as *LFY* (5), is a mechanism that may account for the explosion in morphological diversity of the diploid stage of the life cycle (sporophyte) that occurred in the middle Palaeozoic when green plants colonized the continental surfaces of the planet (3). The full extent of the recruitment of genes from the haploid to the diploid phases during the colonization of the land will be quantified through future comparative analysis of gene function in bryophytes and angiosperms. The discovery and description of more bryophyte fossils from the middle Paleozoic is necessary to unequivocally define the nature of early land-plant life histories. This is important because although it is likely that the earliest land plants had bryophyte-like life cycles, there is still a possibility that their life cycles were unlike those of modern bryophytes.

Only through the combination of paleobotanical and developmental genetic approaches will we understand the mechanism by which the land plant body developed over 400 million years ago.

References and Notes

1. R. A. Berner, in *Plants Invade the Land*, P. Gensel, D. Edwards, Eds. (Columbia Univ. Press, New York, 2001), pp. 173–178.
2. P. Kenrick, P. R. Crane, *Nature* **389**, 33 (1997).
3. P. Kenrick, P. Davis, *Fossil Plants* (The Natural History Museum, London, 2004).
4. L. E. Graham, M. E. Cook, J. S. Busse, *Proc. Natl. Acad. Sci. U.S.A.* **97**, 4535 (2000).
5. T. Tanahashi, N. Sumikawa, M. Kato, M. Hasebe, *Development* **132**, 1727 (2005).
6. R. J. Carol, L. Dolan, *Philos. Trans. R. Soc. London B Biol. Sci.* **357**, 815 (2002).
7. T. S. Gahoonia, D. Care, N. E. Nielsen, *Plant Soil* **191**, 181 (1997).
8. J. D. Masucci, J. W. Schiefelbein, *Plant Physiol.* **106**, 1335 (1994).
9. M. A. Heim et al., *Mol. Biol. Evol.* **20**, 735 (2003).
10. J. Schiefelbein, *Curr. Opin. Plant Biol.* **6**, 74 (2003).
11. P. C. Bailey et al., *Plant Cell* **15**, 2497 (2003).
12. C. H. Wellman, P. L. Osterloff, U. Mohiuddin, *Nature* **425**, 282 (2003).
13. J. G. Duckett, A. M. Schmid, R. Ligrone, in *Bryology for the Twenty-First Century*, J. W. Bates, N. W. Ashton, J. G. Duckett, Eds. (British Bryological Society, Leeds, UK, 1998), pp. 223–245.
14. K. Sakakibara et al., *Development* **130**, 4835 (2003).
15. W. H. Blackwell, *Bot. Rev.* **69**, 125 (2003).
16. B. Menand, G. Calder, L. Dolan, *J. Exp. Bot.* **58**, 1843 (2007).
17. M. Thelander, T. Olsson, H. Ronne, *J. Exp. Bot.* **56**, 653 (2005).
18. D. Edwards, J. G. Duckett, J. B. Richardson, *Nature* **374**, 635 (1995).
19. H. Kerp, H. Hass, V. Mosbrugger, in *Plants Invade the Land*, P. Gensel, D. Edwards, Eds. (Columbia Univ. Press, New York, 2001), pp. 52–82.
20. H. Kerp, N. H. Trewhin, H. Hass, *Trans. R. Soc. Edinb. Earth Sci.* **94**, 411 (2004).
21. S. J. Liljgren et al., *Cell* **116**, 843 (2004).
22. This research is funded by a grant from the Natural Environment Research Council (Ne/c510732/1) and Human Frontier Science Program Organization (HFSPO) (to L.D.), and a grant-in-aid from the Biotechnology and Biological Sciences Research Council to the John Innes Centre. B.M. and S.J. were funded by the European Molecular Biology Organization (EMBO) and Marie Curie Fellowships (EMBO ALTF 89-2002 and Marie Curie HPMF-CT-2002-01935 to B.M.). E.R. was supported by a Marie Curie Fellowship. L.H. is funded by the Marie Curie TIPNET network. K.Y. is partially supported by a Joint Scholarship between the University of East Anglia and China Scholarship Council and HFSPO (RGP0012/2005-C). We are grateful to E. Moylan and J. Harrison for advice in using PAUP*. We also thank J. Doonan, N. Harberd, M. Pernas-Ochoa, S. Takeda, and Y. Yasumura for critical comments on the manuscript and N. Pires for help with BLAST of the *P. patens* genome. We thank J. Langdale and P. Kenrick for invaluable discussions and J. Duckett for teaching us moss morphology.

Supporting Online Material

www.sciencemag.org/cgi/content/full/316/5830/1477/DC1
Materials and Methods

Figs. S1 to S5
References

16 March 2007; accepted 8 May 2007
10.1126/science.1142618

Polony Multiplex Analysis of Gene Expression (PMAGE) in Mouse Hypertrophic Cardiomyopathy

Jae Bum Kim,^{1,2*} Gregory J. Porreca,^{2*} Lei Song,² Steven C. Greenway,² Joshua M. Gorham,² George M. Church,² Christine E. Seidman,^{1,2,3†} J. G. Seidman^{2†}

We describe a sensitive mRNA profiling technology, PMAGE (for “polony multiplex analysis of gene expression”), which detects messenger RNAs (mRNAs) as rare as one transcript per three cells. PMAGE incorporates an improved ligation-based method to sequence 14-nucleotide tags derived from individual mRNA molecules. One sequence tag from each mRNA molecule is amplified onto a separate 1-micrometer bead, denoted as a polymerase colony or polony, and about 5 million polonies are arrayed in a flow cell for parallel sequencing. Using PMAGE, we identified early transcriptional changes that preceded pathological manifestations of hypertrophic cardiomyopathy in mice carrying a disease-causing mutation. PMAGE provided a comprehensive profile of cardiac mRNAs, including low-abundance mRNAs encoding signaling molecules and transcription factors that are likely to participate in disease pathogenesis.

One of the central goals in cell biology is to define the complete repertoire of RNA transcripts that drive essential physiologic processes and to understand how transcription changes with pathology. Several powerful technologies are available to study large-scale transcriptional changes, including microarrays and serial analysis of gene expression (SAGE) (1–3). However, these technologies have limitations that preclude comprehensive interrogation of gene expression. For example, microarray-based approaches have a limited ability to detect low-abundance RNAs and they can produce misleading results owing to cross-hybridization (4). Because SAGE involves dideoxy sequencing of concatenated cDNA ditags, this approach provides the statistical rigor of digital quantification and addresses some of the limitations associated with hybridization-based platforms (5). In practice however, the cost of SAGE experiments limits sampling depth, which diminishes sensitivity for interrogation of rare transcripts.

To obtain comprehensive mRNA profiles that include rare and potentially important transcripts expressed at levels as low as <1 copy per cell, we developed polony multiplex analysis of gene expression (PMAGE) (6). This method permits accurate quantitative assessment of mRNA expression because individual cDNA molecules are directly subjected to sequencing without antecedent library amplification, concatenation, or subcloning. In PMAGE, individual cDNA template molecules are clonally amplified onto each polony bead in millions of parallel, compartmen-

talized droplets formed in a water-in-oil emulsion (7). Polony sequence-by-ligation (SBL) (8) is used to provide an accurate, inexpensive, and multiplexed platform for high-throughput DNA tag sequencing. SBL takes advantage of the high discriminatory power of DNA ligase to iteratively label each bead with a fluorophore encoding the identity of a base within the template. Microscopy-based detection of fluorescence ligation events permits the assessment of as many as 5 million cDNA molecules per run, and digital quantification of tag data accommodates rigorous statistical analysis over a broad dynamic range of mRNA expression.

The critical first step in PMAGE is the manufacture of tag libraries (Fig. 1A). Double-stranded cDNA is synthesized from total RNA and bound to oligo(dT) ferromagnetic beads. cDNAs are then cleaved with an anchor endonuclease, Nla III, leaving a 4-base pair (bp) 3' overhang, which is ligated to an adapter containing an *Acu* I type II endonuclease recognition site. Digestion with *Acu* I cleaves 16 bases from the nonpalindromic recognition sequence and releases the adapter with its 10-bp cDNA sequence tag (plus a 4-base CATG anchor sequence) (fig. S1). The tag is subsequently ligated to a reverse adapter containing a 2-bp 3' degenerate overhang. From the total RNA, 10 μ g generates sufficient library template, in principle, to perform up to 90 experiments, each with >4 million polonies [supporting online material (SOM), note S1]. This method of *in vitro* library construction ensures a faithful representation of mRNA levels because each mRNA molecule is converted into one cDNA template and one polony.

Because PMAGE requires a highly accurate sequencing methodology, we improved upon polony SBL, which has a median raw sequencing accuracy of 99.7% for reads placed against a reference genome (8). We optimized the performance of polony SBL through five specific modifications [detailed in SOM, figs. S2 to S5,

and notes S1 to S4]. The polony beads were bound directly to glass rather than embedded in an acrylamide matrix (Fig. 1B and SOM, note S2), allowing an arraying density two or three times that of SBL. This modification allowed beads to coat the gel-less glass surface as a monolayer in a single focal plane (Fig. 1C), which improved microscopy-based imaging, data yield, and signal coherence (fig. S5).

To assess the utility of PMAGE for obtaining comprehensive transcriptional profiles, we studied mouse myocardial tissues. Cardiac tissue poses a challenge for detection of rare transcripts, because of the heterogeneity of resident cell types and the considerable abundance of mRNAs encoding sarcomere and mitochondrial proteins (fig. S6). We constructed two PMAGE libraries from cardiac left ventricles of 8-week-old mice; one library was derived from wild-type mice, the other from α MHC^{403/+} littermates that carry an R403Q missense mutation (in which glutamine replaces arginine at codon 403) in one allele of the endogenous cardiac α -myosin heavy-chain gene. R403Q is orthologous to a human mutation that causes hypertrophic cardiomyopathy (HCM). α MHC^{403/+} mice recapitulate human HCM (9) with development of cardiac pathology after 25 weeks of age. We studied young mutant mice (denoted as prehypertrophic), to identify early transcriptional changes involved in triggering hypertrophy, increased myocardial fibrosis, and other protean manifestations of HCM. For comparison, we constructed SAGE libraries (10) from the same RNAs.

We produced PMAGE libraries from normal and mutant tissue using different primer-bound beads, so that both libraries could be loaded onto the same array and sequenced simultaneously. Primers bound to each set of beads contained a unique oligonucleotide sequence, which allowed data from the two libraries to be distinguished by hybridization analysis (Figs. 1, D and E, and SOM, notes S1 and S3). The two PMAGE libraries were assembled into one array consisting of 53.8 million beads (that included polonies and beads without tags). About 5.5 million polony beads (~10%) met criteria for containing clonal and well-amplified cDNA tags. Sequence reads from ~4.7 million polonies (~86%) yielded 14-bp tags, which is consistent with the predicted cleavage behavior of *Acu* I (fig. S1).

Sequencing errors in abundant tags are a source for false-positive detection of rare transcripts. To minimize this error, we implemented an approach similar to the strategy used to evaluate ~3.5 million human SAGE tags in a meta-analysis of 84 published SAGE libraries (11). The sequence of each PMAGE tag was compared with all other tags in the library for potential error-derived substitutions. If criteria were met for sequencing error (SOM, note S4), the tag was excluded. This correction removed 278,955 tags from 4.7 million PMAGE tags. We also excluded single-copy PMAGE tags (59,302) from the combined libraries, on the assumption that

¹Cardiovascular Division, Brigham and Women's Hospital, Boston, MA 02115, USA. ²Department of Genetics, Harvard Medical School, Boston, MA 02115, USA. ³Howard Hughes Medical Institute, Harvard Medical School, Boston, MA 02115, USA.

*These authors contributed equally to this work.

†To whom correspondence should be addressed. E-mail: seidman@genetics.med.harvard.edu (J.G.S.); cseidman@genetics.med.harvard.edu (C.E.S.)

random errors were more likely to generate singleton tags. If we assume that all excluded tags reflected sequencing errors, the maximum calculated tag error rate for PMAGE was 7.1%, a value that compared favorably with reported tag error rates (6.8 to 9.4%) from dideoxy sequencing of SAGE libraries (2, 11). The final yield was 4,402,432 filtered PMAGE tags, with roughly equal yields for the normal and mutant libraries (Table 1). The full lists of differentially expressed PMAGE tags (table S1), UniGene clusters (table S2), and transcription factors (table S3) are provided as SOM (descriptions in note S4).

Technical replicates of a PMAGE library were highly reproducible ($R = 0.9986$; fig. S7), which compared favorably with previously published data on SAGE ($R^2 = 0.96$, $R \sim 0.98$) (12). Base composition in PMAGE data did not

reveal noticeable base bias, and distributions did not deviate from expected (fig. S8). Comparison of tag counts in SAGE and PMAGE libraries constructed from the same RNA were highly correlated ($R = 0.8876$), which provided an independent validation of PMAGE data (Fig. 2A). However, data yields were markedly different between these two technologies (Table 1 and fig. S6). Using PMAGE, we sequenced more total tags by a factor of 31 than with SAGE, which included four times as many unique tags, and we identified twice as many genes as in SAGE. PMAGE identified expression of more than 10,000 genes that were undetected by SAGE.

Analyses of >2 million PMAGE tags per library provided sufficient sampling depth to capture rare transcripts (fig. S9) and to provide redundant coverage of the estimated 300,000

transcripts per cell (13). PMAGE data demonstrated a wide dynamic range in cardiac mRNA expression, with transcript counts ranging from 0.3 tags per cell [e.g., *Vgll2* (vestigial-like-2 homolog), (Table 2)] to ~29,000 tags per cell [e.g., cytochrome c oxidase III (fig. S6)]. Among 68,762 unique tags in the wild-type PMAGE library, 447 were expressed at >60 copies per cell and accounted for 65% of all mRNA molecules. Of the unique tags, 99% were expressed at low abundance (<60 copies per cell). Among 1337 transcription factors identified in the wild-type left ventricle PMAGE library (SOM, note S4), only 13 were present at >60 copies per cell; the remainder were expressed at low abundance.

The comparison of PMAGE profiles from wild-type and prehypertrophic $\alpha\text{MHC}^{403/+}$ left ventricles (Fig. 2B) demonstrated a surprisingly

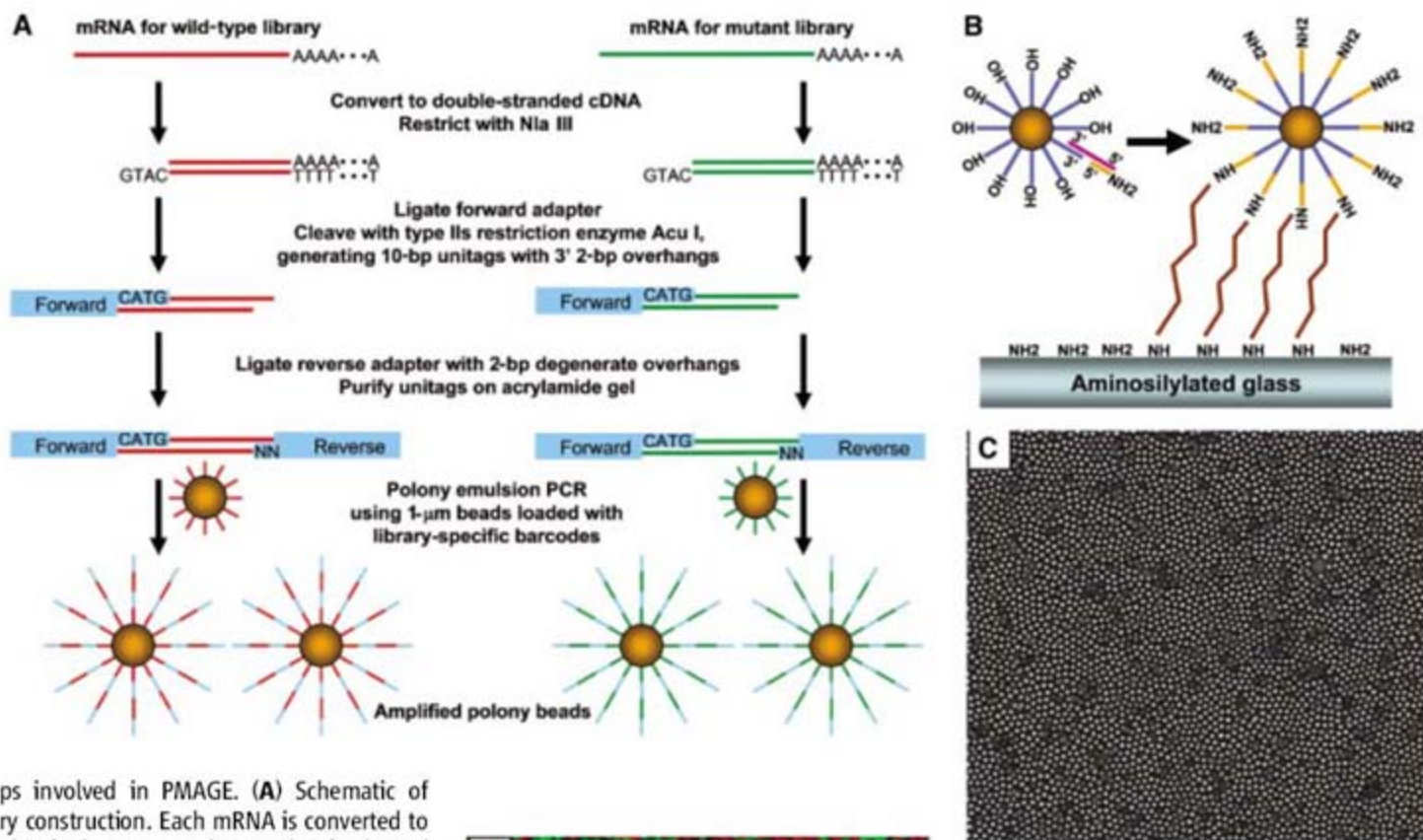


Fig. 1. Steps involved in PMAGE. (A) Schematic of PMAGE library construction. Each mRNA is converted to cDNA molecules (red orange and green bars), cleaved with anchor endonuclease, ligated to forward adapters, cleaved with tagging enzyme *Acu* I, ligated with reverse adapters, and amplified onto beads carrying primers with sequences that match the forward adapters. With emulsion PCR, each polony bead carries clonal molecules encoding one cDNA tag. (B) Polony bead capping and attachment to glass slide. Polony beads carry DNA templates (blue bars) that have terminal 3' OH groups. 3' Termini are capped by ligation, by using annealed bridging primers (purple bar), with oligonucleotides that contain 3' amines (yellow orange bars). 3' Amines on polony beads are cross-linked to aminosilylated glass with amino-ester bridges (jagged lines) (SOM, note S2), providing a gel-less milieu for sequence chemistry. (C) Bright-field image of the cardiac PMAGE library arrayed in a dense monolayer on a glass slide (each spherical object is a 1- μm polony bead). This gel-less platform enhances access to sequencing reagents and provides a single focal plane for microscopy-based imaging during polony sequencing. (D) Pseudofluorescence imaging of wild-type

(red) and $\alpha\text{MHC}^{403/+}$ (green) polonies in a PMAGE sequencing array hybridized with library-specific fluorescence oligonucleotides (SOM, notes S2 and S3). (E) A fluorescence intensity plot of 10,000 polonies parsed into the wild-type (Cy3) and $\alpha\text{MHC}^{403/+}$ (Cy5) libraries that were simultaneously sequenced.

large number of differentially expressed mRNAs, given the absence of overt pathology in mutant hearts. There were 1486 unique PMAGE tags, corresponding to 706 genes, that were significantly up-regulated or down-regulated ($P < 0.01$) in the prehypertrophic ventricle (SOM, note S4 and tables S1 and S2). These widespread changes affected components in pathways involved in myocardial excitation-contraction coupling, Ca^{++}

homeostasis, and energy metabolism (fig. S11). The vast majority of these differentially regulated transcripts escaped detection by SAGE, which identified only 53 genes with significantly ($P < 0.01$) altered expression.

We assessed 20 genes that PMAGE identified as both low abundance (54 to <0.3 per cell) and differentially expressed in prehypertrophic $\alpha MHC^{403/+}$ hearts. Real-time reverse

transcription polymerase chain reaction (RT-PCR) confirmed PMAGE results for 19 of 20 genes (fig. S10 and Table 2). Some of these genes [e.g., *Nfkbie* (nuclear factor kappa light polypeptide gene enhancer in B cells inhibitor epsilon *Nr1h3* (nuclear receptor subfamily 1, group h, member 3), and the gene for the retinoid-responsive nuclear hormone receptor *LXR α* (liver X receptor α)] have unknown roles in HCM pathogenesis, whereas other genes encode proteins that may stimulate the protean manifestations of HCM: myocyte enlargement, increased cardiac fibrosis, and abnormal calcium homeostasis (14). *Hod* (homeobox-only protein), *Hand2* (hand and neural crest derivatives 2), *Vgll2*, and *Egr3* (early growth response-3) are transcriptional regulators implicated in myocyte specification and growth during development (15–19). Differential expression of these transcripts in prehypertrophic $\alpha MHC^{403/+}$ hearts may indi-

Table 1. Cardiac left ventricular PMAGE and SAGE libraries. Total tags are filtered tag counts. PMAGE libraries were filtered to exclude tags with potential sequence errors (SOM, note S4) and singleton tags from the combined dataset. SAGE libraries were filtered to exclude linker sequences. Unique tags assigned to the same UniGene cluster or gene symbol were combined into one vector.

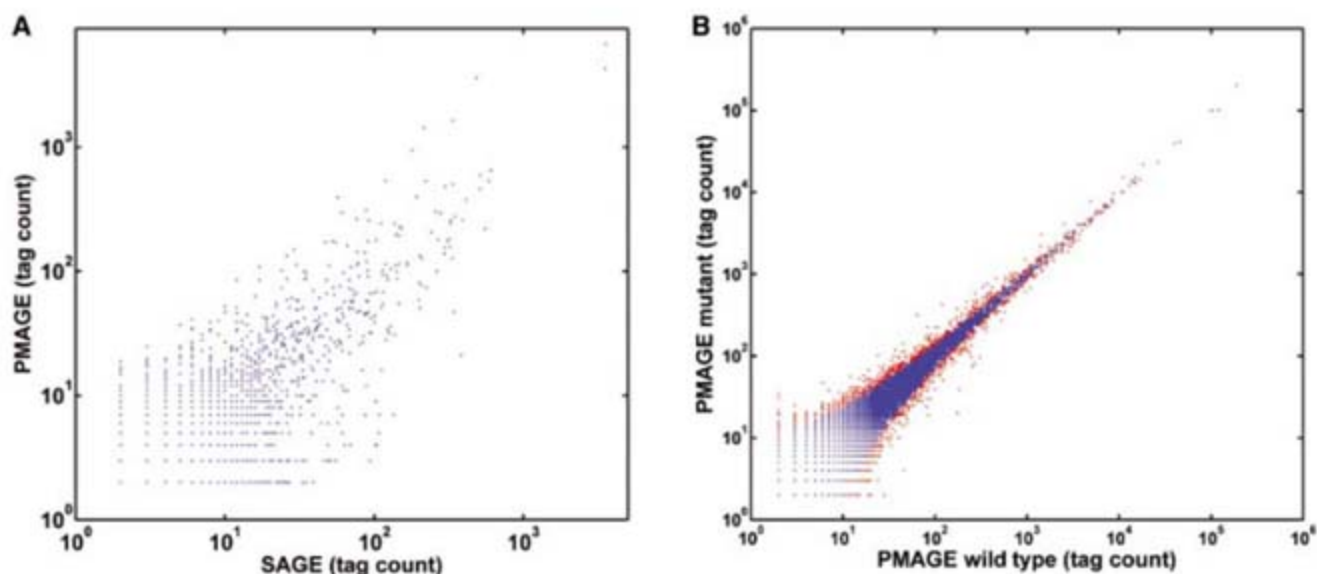
	PMAGE		SAGE	
	Wild type	$\alpha MHC^{403/+}$	Wild type	$\alpha MHC^{403/+}$
Total tags	2,042,192	2,360,240	70,731	69,268
Unique tags	68,762	72,143	17,896	18,412
Unique genes	17,931	18,311	7,783	8,027

Table 2. Examples of low-abundance transcripts with changed expression in prehypertrophic $\alpha MHC^{403/+}$ hearts. Low-abundance genes (<60 copies per cell) are listed in order of decreasing transcript abundance in the wild-type left ventricle. *Nppa*, an established hypertrophy-regulated gene that encodes atrial natriuretic peptide (30), is the only transcript among these 12 genes that was

detected by SAGE as differentially expressed. Tag counts are followed by calculated transcript copies per cell (provided in parentheses). PMAGE tag counts were normalized to 2 million tags per library; actual SAGE tag counts are presented. Differential expression of each gene was confirmed by quantitative RT-PCR (fig. S10).

Gene symbol	PMAGE			SAGE		
	Wild type	$\alpha MHC^{403/+}$	<i>P</i> value	Wild type	$\alpha MHC^{403/+}$	<i>P</i> value
<i>Hod</i>	357 (54)	255 (38)	3.25E-05	6 (25)	1 (4)	n.s.
<i>Hand2</i>	342 (51)	282 (42)	1.52E-02	16 (68)	21 (91)	n.s.
<i>Abcc9</i>	302 (45)	103 (15)	4.88E-24	9 (38)	4 (17)	n.s.
<i>Ctgf</i>	233 (35)	476 (71)	4.17E-20	14 (59)	23 (100)	n.s.
<i>Nppa</i>	183 (27)	744 (112)	8.76E-81	15 (64)	66 (286)	2.91E-09
<i>Sln</i>	183 (27)	39 (6)	8.84E-24	2 (8)	0 (0)	n.s.
<i>Postn</i>	43 (6)	132 (20)	7.41E-12	1 (4)	3 (13)	n.s.
<i>Tgfbβ1</i>	19 (3)	41 (6)	4.56E-03	0 (0)	0 (0)	n.s.
<i>Nr1h3</i>	2 (0.3)	12 (2)	7.47E-03	2 (8)	1 (4)	n.s.
<i>Vgll2</i>	2 (0.3)	12 (2)	7.47E-03	0 (0)	0 (0)	n.s.
<i>Nfkbie</i>	1 (0.2)	11 (2)	3.46E-03	1 (4)	0 (0)	n.s.
<i>Egr3</i>	0 (0)	7 (1)	7.88E-03	0 (0)	0 (0)	n.s.

Fig. 2. PMAGE accurately detects mRNA abundance and differentially expressed transcripts. **(A)** Scatter plot (logarithmic scale) of tags in wild-type left ventricular SAGE (total tag count, 70,731) and PMAGE (normalized to a total count of 70,731) libraries derived from the same RNA. All tags with counts ≥ 1 copy were compared. $R = 0.8858$. **(B)** Scatter plot (logarithmic scale) of PMAGE tag abundances (normalized to total count of 2 million tags per library) from wild-type and $\alpha MHC^{403/+}$ hearts (blue dots $P \geq 0.01$, red dots $P < 0.01$). $R = 0.9950$.



cate that these molecules also function in early growth responses to sarcomere dysfunction.

Myocardial fibrosis is characteristic of advanced HCM pathology and contributes to impaired cardiac relaxation, heart failure, arrhythmias, and sudden death (20, 21). The increased expression of *Tgfb1* (transforming growth factor- β 1), *Ctgf* (connective tissue growth factor) and *Postn* (periostin), potent regulators of fibrosis and collagen deposition (22–24), in prehypertrophic ventricles indicates early activation of this pathway, which raises the possibility that fibrosis is not an advanced secondary phenomenon, but a primary contributor to myocardial dysfunction.

Impaired relaxation is the fundamental physiologic abnormality in HCM (25). Cardiac relaxation and contraction reflects Ca^{++} cycling between the sarcoplasmic reticulum and the sarcomere in cardiomyocytes. Ca^{++} uptake into the sarcoplasmic reticulum occurs via sarcoplasmic reticulum Ca^{++} transport adenosine triphosphatase (ATPase) (SERCA2a/Atp2a2), which is regulated by phospholamban (Pln) and sarcolipin (Sln) (26). Transcripts encoding each of these proteins were significantly decreased in prehypertrophic hearts (fig. S11), which may directly account for the early impairment in cardiac relaxation previously observed in this model (27). Down-regulation of *Abcc9* [adenosine triphosphate (ATP)-binding cassette subfamily C member 9], which encodes SUR2, suggested another mechanism for Ca^{++} imbalance in prehypertrophic hearts. SUR2 is the ATPase-regulatory subunit of the inwardly rectifying cardiac K_{ATP} channel, which balances Ca^{++} homeostasis with energetic demands (28); *Abcc9*-null mice develop arrhythmias and myocardial calcium overload (29).

Notably, PMAGE also revealed significant ($P < 0.01$) differences in the expression of genes encoding 29 transcription factors between wild-type and prehypertrophic α MHC^{403/+} hearts (table S3). The biologic processes evoked by these molecules are likely to be considerable. By interrogating the temporal and spatial expression of these transcription factors, we can potentially dissect the networks activated in this cardiomyopathy, which, in turn, should help identify new molecular targets for therapeutic intervention.

In summary, PMAGE profiling provided reproducible, large-scale transcript identification, with sequence accuracy comparable to SAGE, and greater sensitivity for quantification of rare transcripts. We estimate that sampling ~2 million tags provides comprehensive assessment of most mRNAs (fig. S9); nevertheless, the current PMAGE platform has the capacity to read more than 4 million tags per experiment. Thus, PMAGE can be used for very deep sampling of one library or analyses of multiple libraries simultaneously by adapting polony beads that contain unique sequence identifiers. PMAGE offers several advantages over other currently available transcription profiling methods at a potentially lower cost (fig. S12). We anticipate that PMAGE studies will help further define mRNA regula-

tory networks that orchestrate critical cellular processes in healthy and diseased tissues.

References and Notes

- G. A. Churchill, *Nat. Genet.* **32** (suppl.), 490 (2002).
- V. E. Velculescu et al., *Cell* **88**, 243 (1997).
- M. J. Holland, *J. Biol. Chem.* **277**, 14363 (2002).
- S. Draghici, P. Khatri, A. C. Eklund, Z. Szallasi, *Trends Genet.* **22**, 101 (2006).
- S. Audic, J. M. Claverie, *Genome Res.* **7**, 986 (1997).
- Materials and methods are available as supporting material on Science Online.
- D. Dressman, H. Yan, G. Traverso, K. W. Kinzler, B. Vogelstein, *Proc. Natl. Acad. Sci. U.S.A.* **100**, 8817 (2003).
- J. Shendure et al., *Science* **309**, 1728 (2005).
- A. A. Geisterfer-Lowrance et al., *Science* **272**, 731 (1996).
- S. Blackshaw, J. B. Kim, B. St. Croix, K. Polyak, in *Current Protocols in Molecular Biology*, F. M. Ausubel, Ed. (Greene Publishing Associates and Wiley-Interscience, New York, 2002), pp. v (loose leaf).
- V. E. Velculescu et al., *Nat. Genet.* **23**, 387 (1999).
- S. Diné et al., *Nucleic Acids Res.* **33**, e26 (2005).
- N. D. Hastie, J. O. Bishop, *Cell* **9**, 761 (1976).
- J. G. Seidman, C. Seidman, *Cell* **104**, 557 (2001).
- F. Chen et al., *Cell* **110**, 713 (2002).
- C. H. Shin et al., *Cell* **110**, 725 (2002).
- D. Srivastava, P. Cserjesi, E. N. Olson, *Science* **270**, 1995 (1995).
- T. Maeda, D. L. Chapman, A. F. Stewart, *J. Biol. Chem.* **277**, 48889 (2002).

- Y. Albert et al., *J. Cell Biol.* **169**, 257 (2005).
- A. M. Varnava, P. M. Elliott, N. Mahon, M. J. Davies, W. J. McKenna, *Am. J. Cardiol.* **88**, 275 (2001).
- K. M. Harris et al., *Circulation* **114**, 216 (2006).
- P. J. Lijnen, V. V. Petrov, R. H. Fagard, *Mol. Genet. Metab.* **71**, 418 (2000).
- M. S. Ahmed et al., *J. Mol. Cell. Cardiol.* **36**, 393 (2004).
- R. A. Norris et al., *J. Cell. Biochem.* **101**, 695 (2007).
- B. J. Maron, *JAMA* **287**, 1308 (2002).
- M. Asahi et al., *Proc. Natl. Acad. Sci. U.S.A.* **101**, 9199 (2004).
- D. Georgakopoulos et al., *Nat. Med.* **5**, 327 (1999).
- M. Bienengraeber et al., *Nat. Genet.* **36**, 382 (2004).
- L. V. Zingman et al., *Proc. Natl. Acad. Sci. U.S.A.* **99**, 13278 (2002).
- R. T. Lee et al., *J. Clin. Invest.* **81**, 431 (1988).
- We thank J. Shendure, S. Barr, S. DePalma, M. Maida, P. Teekakirikul, S. Blackshaw, Z. Arany, J. Loscalzo, and B. Vogelstein for advice and technical assistance. Funded by grants from NIH and Howard Hughes Medical Institute.

Supporting Online Material

www.sciencemag.org/cgi/content/full/316/5830/1481/DC1
Materials and Methods
Figs. S1 to S12
Tables S1 to S3
References

8 November 2006; accepted 3 May 2007
10.1126/science.1137325

RNA Maps Reveal New RNA Classes and a Possible Function for Pervasive Transcription

Philipp Kapranov,¹ Jill Cheng,¹ Sujit Dike,¹ David A. Nix,¹ Radharani Duttgupta,¹ Aaron T. Willingham,¹ Peter F. Stadler,² Jana Hertel,² Jörg Hackermüller,³ Ivo L. Hofacker,⁴ Ian Bell,¹ Evelyn Cheung,¹ Jorg Drenkow,¹ Erica Dumais,¹ Sandeep Patel,¹ Gregg Helt,¹ Madhavan Ganesh,¹ Srinka Ghosh,¹ Antonio Piccolboni,¹ Victor Sementchenko,¹ Hari Tammana,¹ Thomas R. Gingeras^{1*}

Significant fractions of eukaryotic genomes give rise to RNA, much of which is unannotated and has reduced protein-coding potential. The genomic origins and the associations of human nuclear and cytosolic polyadenylated RNAs longer than 200 nucleotides (nt) and whole-cell RNAs less than 200 nt were investigated in this genome-wide study. Subcellular addresses for nucleotides present in detected RNAs were assigned, and their potential processing into short RNAs was investigated. Taken together, these observations suggest a novel role for some unannotated RNAs as primary transcripts for the production of short RNAs. Three potentially functional classes of RNAs have been identified, two of which are syntenically conserved and correlate with the expression state of protein-coding genes. These data support a highly interleaved organization of the human transcriptome.

A large fraction of the noncoding part of a eukaryotic genome is used to make RNA that is sufficiently stable in a cell to be detected by different technological approaches (1–4). The biological significance of this pervasive transcription is unclear and controversial. One possibility is that only very short regions of such unannotated RNA are biologically relevant (5). In-depth characterization of RNAs as to their subcellular compartmentalization, size, modifications, and genomic origins can potentially provide clues to their functions. This study reports two general observations derived from

the maps of nuclear and cytosolic polyadenylated [poly(A)⁺] RNAs longer than 200 nucleotides (nt) (long RNAs, lRNAs) and whole-cell RNAs less than 200 nt (short RNAs, sRNAs) over the entire nonrepetitive portion of the human ge-

¹Affymetrix Laboratory, Affymetrix, Inc., 3420 Central Expressway, Santa Clara, CA, 95051, USA. ²University of Leipzig, Department of Computer Science, Leipzig, Germany. ³Fraunhofer Institute for Cell Therapy and Immunology, Leipzig, Germany. ⁴Institute for Theoretical Chemistry, University of Vienna, Austria.

*To whom correspondence should be addressed. E-mail: tom.gingeras@affymetrix.com

nome. First, the potential biological function of an appreciable portion of long unannotated transcripts is to serve as precursors for sRNAs. Second, these maps reveal three classes of RNAs that have specific genomic localization at gene boundaries. Biological relevance of these classes of RNAs is supported by strong correlation with the expression state of genes they associate with, as well as their syntenic conservation between human and mouse.

The complexity of steady-state RNA populations was profiled by using tiling arrays at 5-nt resolution to detect transcribed regions in the human genome (6, 7). Overall, we found the extent and general properties of the IRNA portion of the human transcriptome to be similar to our earlier study (7). Patterns of annotated and unannotated transcription were similar among cell lines and within subcellular compartments (fig. S1, A to J, and table S2, A and B). About 64% of detected poly(A)⁺ transcription (nucleus and cytosol) did not align with annotations (fig. S1N) (7). Of the 265,237 annotated exons, 80% were expressed in at least one cell line (fig. S2).

A total of 1.1% of the interrogated genome is covered by transcribed fragments (transfrags) representing sRNAs (summarized in table S1 and S2C, figs. S3 and S4). sRNA transfrags have a nonrandom association with genomic features, including EvoFold structure predictions (figs. S5 and S7 and table S1B). In addition, a tendency for some to map antisense to splice junctions was also found. sRNAs were found in intronic, intergenic, and annotated regions (fig. S4). Unannotated sRNAs were verified by Northern blots (table S3 and fig. S6) and real-time reverse transcription polymerase chain reaction (table S3), with an overall verification rate of ~70% (7).

Maps of sRNAs and IRNAs from different subcellular compartments can be further used to provide a virtual "genealogy" describing origins of particular classes of RNAs (Fig. 1 and table S4). A total of 12.7% of all interrogated nucleotides can be detected as composing IRNAs or sRNAs in HeLa or HepG2 cell lines. One-third of this total (33.2%) is exclusively observed in the nucleus as IRNAs and overlapping sRNAs (Fig. 1A). Another 15.1% is exclusively found as cytosolic IRNAs and overlapping sRNAs. A total of 46.3% of the sequences detected are found in both the nucleus and cytosol (Fig. 1A). Finally, 5.3% of the nucleotides were detected in sRNA transfrags exclusively.

The origin of 79.6% of all transcribed bases can be mapped back to the nucleus as IRNAs with 15.1% found only in cytosol (Fig. 1B). About 41.8% of the sequences seem to remain exclusively in the nucleus; the remainder is transported into the cytosol. Furthermore, 3.1% of the exclusively nuclear IRNA sequences and 6.6% of the nuclear sequences transported into the cytosol overlap sRNA sequences, which suggests that ~40% of the latter may be processed from long nuclear transcripts (Fig. 1B and table S4).

About one-fifth of sRNAs transfrags, 20.9% (HepG2) and 18.4% (HeLa), were identified as evolutionarily conserved. The PhastCons scores (7) associated with sRNAs are significantly enriched in conserved sequences (P value 2.2×10^{-16} , Wilcoxon nonparametric test) over random (fig. S8, A and B), which points to the possible biological relevance of these transcripts (Fig. 2A). There is also a statistically significant concordance ($P < 0.01$, permutation test) observed between the locations of sRNA and nuclear IRNA transfrags. A total of 13% (HepG2)

and 9% (HeLa) nuclear IRNA transfrags overlap sRNAs. Conversely, 44% and 31% of sRNA transfrags overlap with nuclear IRNA transfrags. Such an association is potentially confounded by the elevated G-C composition of these regions (7). To explore this further, we divided the transfrags obtained from nuclear IRNA into those that do and do not overlap sRNA transfrags (Fig. 2B). Mean PhastCons scores for the IRNA transfrags that do overlap with sRNAs are significantly higher than such of the transfrags that do not (Fig. 2C and table S5). For IRNA transfrags overlapping sRNAs, a total of 23.9% (HepG2) and 26.2% (HeLa) exhibit PhastCons scores equivalent or higher than the average score observed for annotations (Fig. 2D). The conservation of the nuclear IRNA transfrags often extends beyond a sRNA transfrag it overlaps (Fig. 2B), indicating that other sequences outside of the overlapping regions may be important, reminiscent of the extended conservation seen in the miRNA precursors (8).

Taken together, these data suggest a possible product-precursor relation between overlapping transfrags derived from IRNAs and sRNAs, underscored by the enrichment of evolutionarily conserved sequences in genomic regions found transcribed in both IRNAs and sRNAs. Conservatively, 3.1% of HepG2 and 2.4% of HeLa nuclear IRNA transfrags may be parts of precursors of sRNAs. The full extent of transcription, which may serve as precursors of sRNA, could, however, be much larger, because IRNA transfrags that directly overlap sRNAs are almost certainly connected to other transfrags in a precursor transcript. Thus, any given IRNA transfrag can be an order of magnitude smaller than the IRNA transcript it represents.

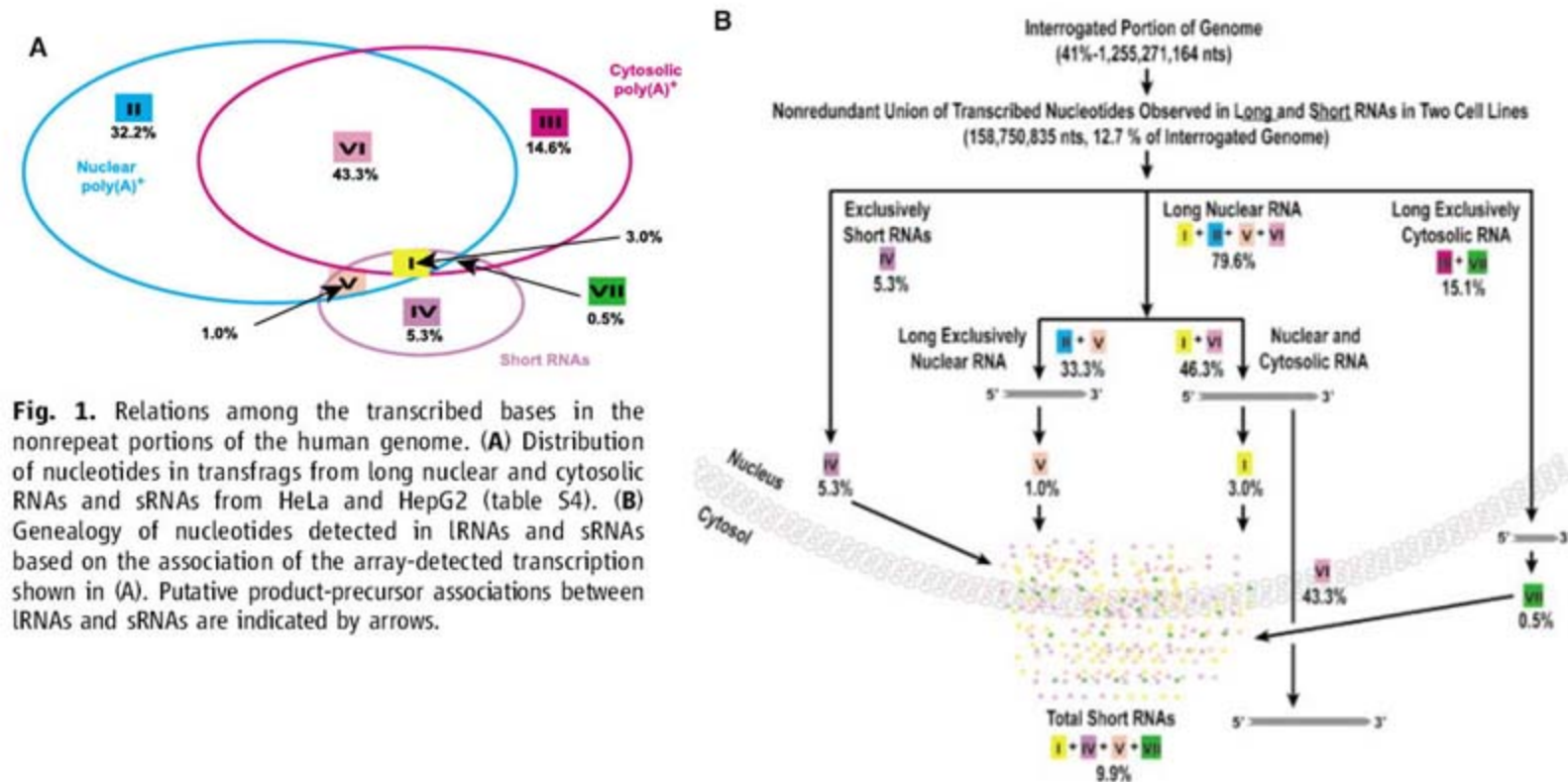


Fig. 1. Relations among the transcribed bases in the nonrepeat portions of the human genome. **(A)** Distribution of nucleotides in transfrags from long nuclear and cytosolic RNAs and sRNAs from HeLa and HepG2 (table S4). **(B)** Genealogy of nucleotides detected in IRNAs and sRNAs based on the association of the array-detected transcription shown in (A). Putative product-precursor associations between IRNAs and sRNAs are indicated by arrows.

sRNA mapping and sequence conservation analysis (fig. S8C) indicate that sRNAs cluster at the 5' and 3' of genes (Fig. 3). We denote these classes of sRNAs "promoter-associated sRNAs" (PASRs) and "termini-associated sRNAs" (TASRs). The occurrence of sRNAs centers around 5' or 3' termini and is statistically significant compared with G-C-matched random regions (Fig. 3, B and C, and table S1). Northern hybridization analysis revealed that PASRs and TASRs can vary in length (22 to 200 nt), with one prominent class of PASRs with lengths of ~26, 38, and 50 nt (Fig. 3, B and C, and figs. S9 and S12 and tables S6 and S7). PASRs were expressed at levels similar to those of the protein-coding genes they overlap (7).

Several characteristics of both PASRs and TASRs support the biological significance of these sRNAs. As explained below, gene expression correlates with the density of PASRs, and PASRs associate with other lRNAs at the 5' boundaries of genes. Also, expressed PASRs are syntenic with mouse.

The correlation of gene expression with the density of PASRs (Fig. 3D) is similar to a trend seen for antisense TASRs (fig. S10, A and B). Overall, 44.6 and 43.8% of genes found to be expressed in cytosol or nucleus have PASR association. Another 11.8 and 18.1% of genes had signal only in the first exon in cytosolic or nuclear RNAs, respectively. Almost half of those are observed to have PASRs (fig. S10, C and D). Conversely, for ~80% of silent genes (<10% of exons detected), no PASRs were observed.

A third class of RNAs is the long transcripts that overlap 5' boundaries of protein-coding genes but do not include most of the other exons. This is exemplified by genes that show signal only in their first exons (Fig. 3A). To characterize these promoter-associated lRNAs (PALRs), we performed 5' and 3' RACE analysis (rapid amplification of cDNA ends) followed by hybridization to tiling arrays (fig. S11). These experiments revealed that transcripts overlapping the promoter and the first exon and intron regions, ranging in length from hundreds of base pairs to

more than 1 kb, are made and map to the same genomic regions as PASRs.

We constructed sRNA maps in two syntenic regions of the human and mouse genomes (*IL4R* cytokine cluster and four *Hox* loci) using mouse STO and R1 and human HepG2 and HeLa cell lines (7). Both species-specific and conserved PASRs and TASRs were found, with ~39% of PASR sequences and 35% of TASR sequences mapping into syntenically conserved regions (Fig. 4A). Genomic regions shared by the PASR (HMSY19) at the 5' boundaries of the *Hox* D9 and the TASR (HMSY5) in the 3' termini of *Hox*D10 genes of both species are illustrated in Fig. 4. The sizes of PASRs and TASRs are similar for mouse and human cell lines (fig. S13 and table S8).

We have found that ~10% of detected transcription is present in sRNA sequences (ranging from 22 to 200 nt in length). The distribution of these sRNAs is not uniform across the genome, because sRNAs are more frequent among genes than in intergenic regions. Further-

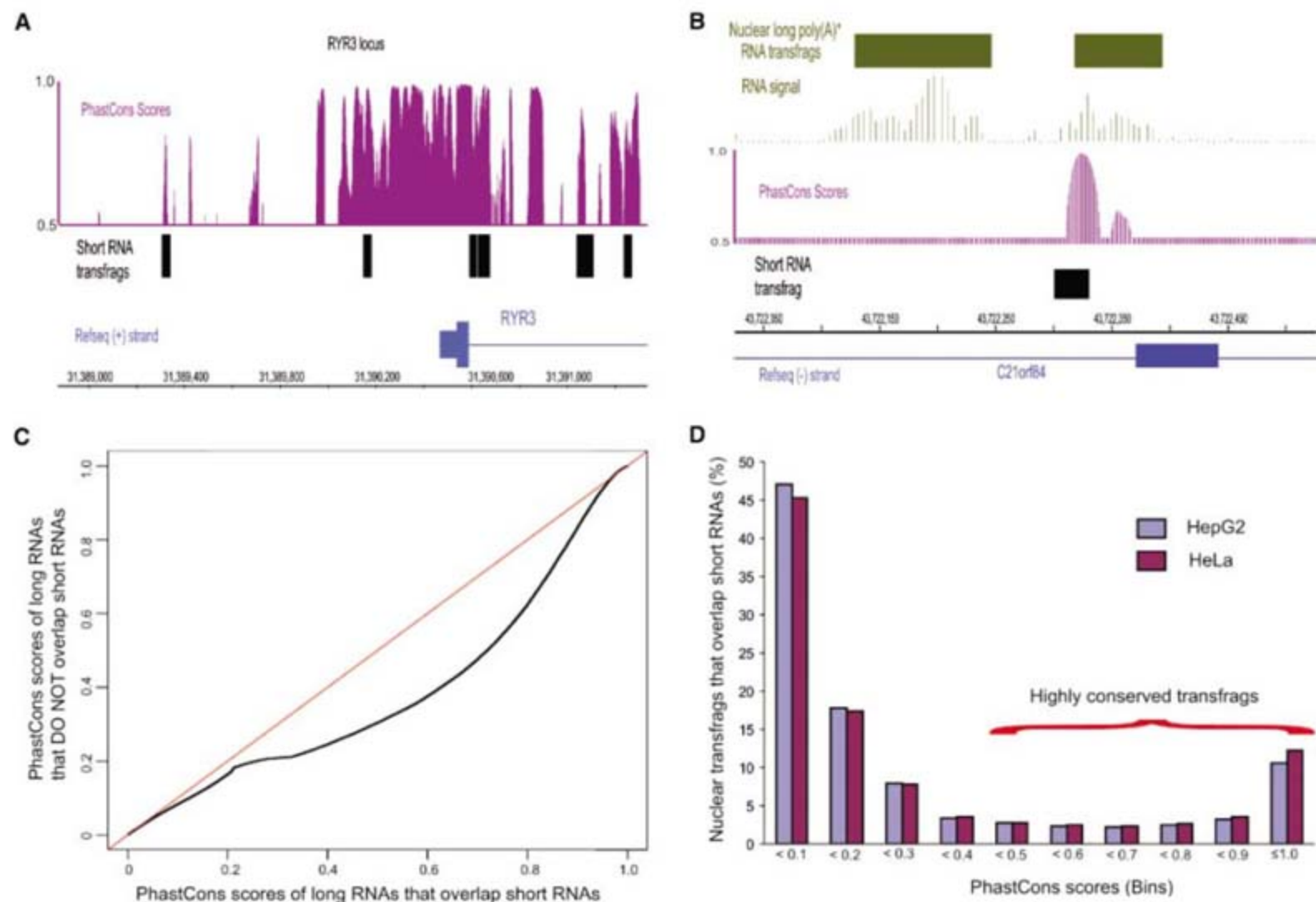


Fig. 2. Sequence conservation analysis of short and long nuclear RNA (7). **(A)** Conserved sRNAs surrounding the first exon of *RYR3* gene. **(B)** Long nuclear transfrag that overlaps sRNA is more conserved than adjacent lRNA transfrag that does not. **(C)** Quantile-quantile plot of PhastCons scores of long nuclear transfrags that do (x axis) and do not (y axis) overlap sRNAs. For any given

point on the curve, an equal proportion of each "quantile distribution" occurs at this juncture. **(D)** Distribution of PhastCons scores of long nuclear transfrags that overlap sRNAs, binned on the basis of PhastCons scores (x axis), versus percentage of transfrags in each bin (y axis). Highly conserved transfrags (scores > 0.4) are indicated.

more, sRNA transfrags overlap a collection of IRNA transfrags that are significantly enriched in conserved sequences. Taken together, these data suggest that these IRNA transfrags potentially represent parts of nuclear primary transcripts that encode conserved functional sRNAs.

Several other observations are also derived from these mapping data. First, an appreciable fraction of protein-coding genes have expression only in the first exon and intron. This suggests that transcription may have two different states that are characterized by the lengths of transcripts made from the transcriptional start site of gene locus. Second, the fate of the transcripts derived from a particular detected transcribed region could be predicted on the basis of their retention in the

nucleus, transport into cytosol, or processing into sRNAs. Overall, these RNA maps provide a virtual genealogy of RNAs (Fig. 1B). Third, PASRs often align within the boundaries of some of the PALRs. The genomic loci and boundaries of PASRs appear to be well conserved in two human cell lines and, in some cases, between mouse and human cells; this may indicate that there could be common processing signals used to create them. Fourth, the ends of almost half of human protein-coding genes were found to be bracketed by PASRs and TASRs. Given that large regions (i.e., >1 kb) are contained in the sequences covered by the sRNAs, the functional roles of these sRNAs may involve broad domains consistent with involvement in chromatin alterations.

Other recent studies also report the presence of multiple transcripts at the 5' boundaries of genes (9), including unstable lRNAs postulated to be involved in regulation of gene expression (10, 11). Thus, these results suggest a model of genome organization where protein-coding genes are at the center of a complex network of overlapping sense and antisense lRNA transcription, with interleaved sRNAs often marking their boundaries and correlating with their expression state (fig. S14). Our studies also highlight a possible important biological function for a portion of unannotated nuclear transcription as possible precursors for sRNAs. Such interleaved transcription produces a variety of non-protein coding sRNA and lRNA species that offer cis- and trans-regulatory potential (12–14).

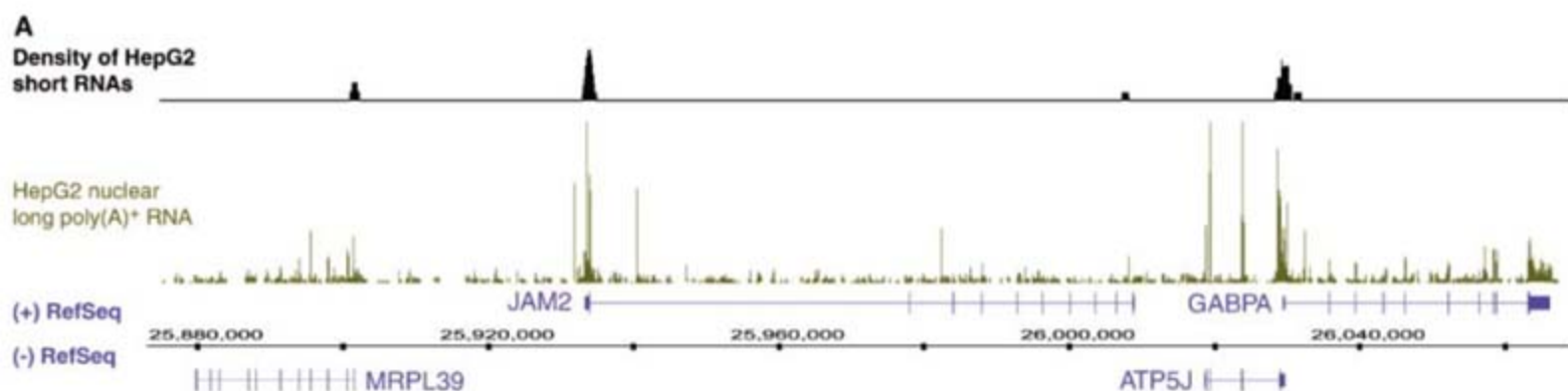
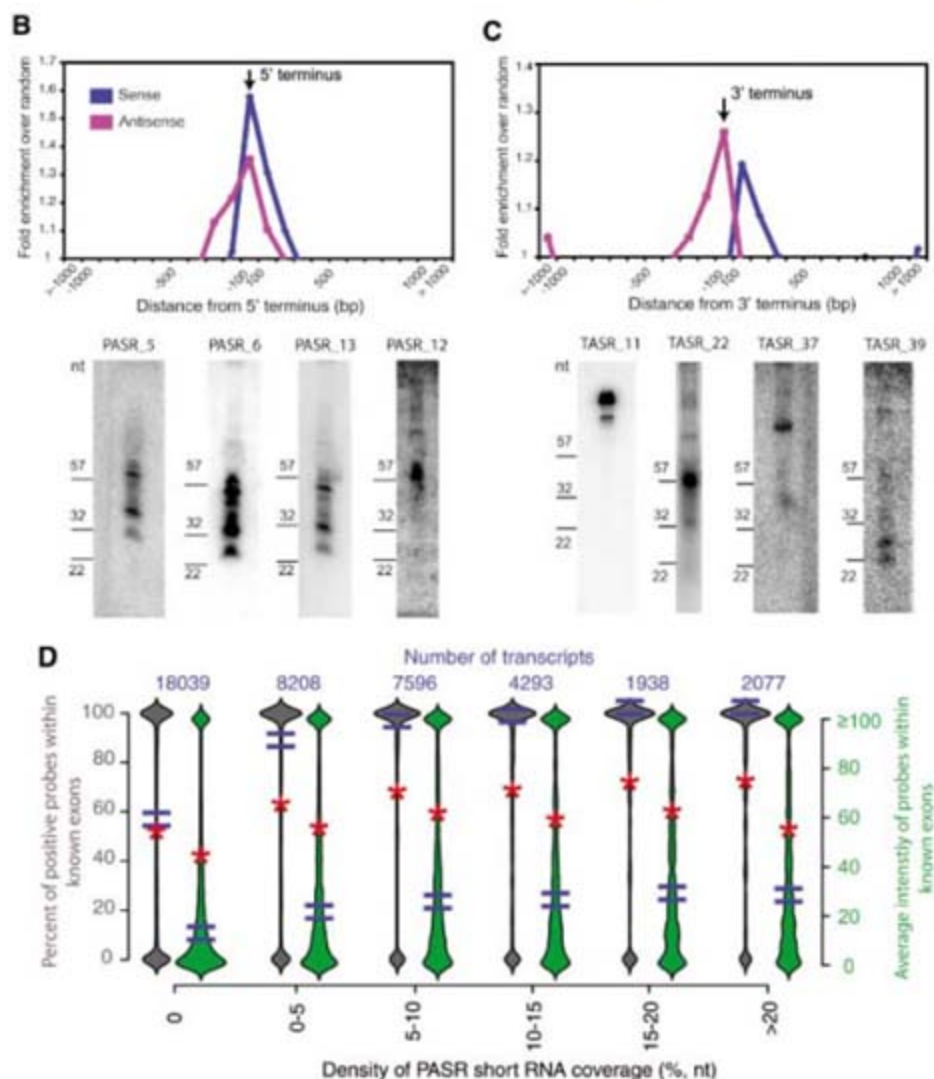


Fig. 3. sRNAs are enriched at boundaries of transcripts. (A) Smoothed density of sRNAs and the map of long nuclear RNA from HepG2 are shown for a region of chromosome 21. (B and C) Association of sRNAs with 5' and 3' boundaries of annotated transcripts is enriched compared with a set of random regions with matched G-C-content. The fold enrichment over random is plotted as a function of a distance from the 5' or 3' termini for sRNAs on the same ("sense") or opposite ("antisense") strand as the annotations. Examples of Northern blots for PASRs and TASRs are shown below. (B) PASRs; (C) TASRs. (D) A positive correlation between the density of PASRs and the expression level of the associated genes. Violin plots illustrate the frequency distribution of measured expression levels for bins of genes (7). The median and mean expression levels for each bin are indicated by "=" and "*", respectively. The numbers on top indicate the number of genes in each bin.



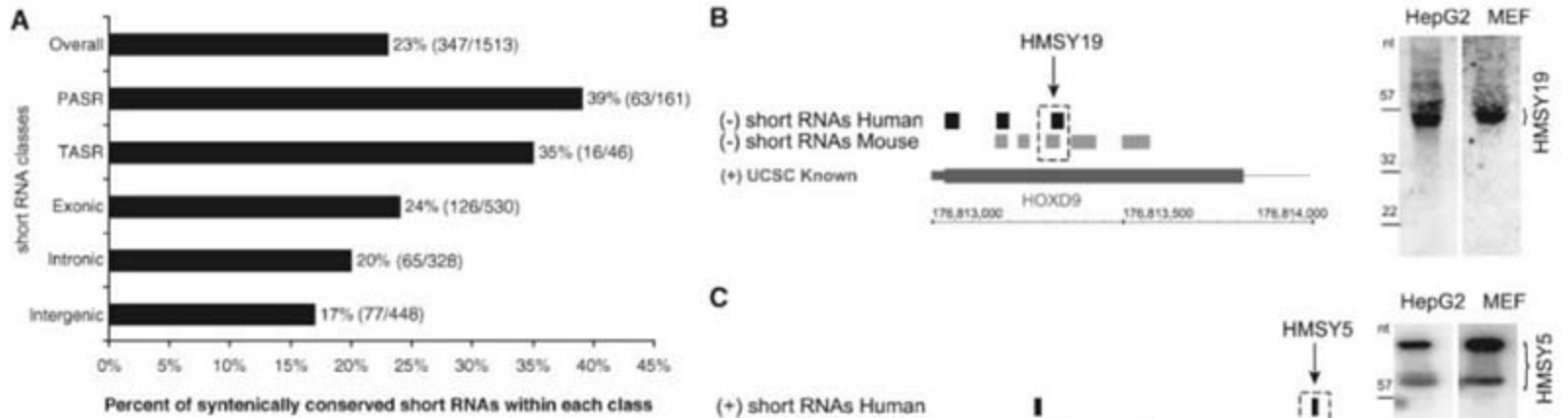


Fig. 4. (A) Distribution of syntenically conserved sRNAs. The fractions of sRNAs in each class (ordinate) found in a syntenic location in both species are shown as percentages of the total number of sRNAs in the class. (B and C) Characterization of syntenically conserved PASRs (B) and TASRs (C). Combined maps of syntenic sRNAs from HeLa and HepG2 human cell lines (black) and R1mES and MEF mouse cell lines (gray) are shown. Syntenic PASR HMSY19 and TASR HMSY5 are shown on either top (+) or bottom (–) strands. Northern blots show HMSY19 and HMSY5 in both species with comparable sizes.

References and Notes

1. J. Cheng *et al.*, *Science* **308**, 1149 (2005).
2. ENCODE-Project-Consortium, in preparation.
3. P. Kapranov *et al.*, *Science* **296**, 916 (2002).
4. A. T. Willingham, T. R. Gingeras, *Cell* **125**, 1215 (2006).
5. J. Ponjavic, C. P. Ponting, G. Lunter, *Genome Res.* **17**, 556 (2007).
6. Data available at http://transcriptome.affymetrix.com/hs_whole_genome; www.ncbi.nlm.nih.gov/geo/; <http://genome.ucsc.edu/>.
7. Materials and methods are available as supporting material on *Science Online*.
8. U. Ohler, S. Yekta, L. P. Lim, D. P. Bartel, C. B. Burge, *RNA* **10**, 1309 (2004).
9. P. Carninci *et al.*, *Nat. Genet.* **38**, 626 (2006).
10. C. A. Davis, M. Ares Jr., *Proc. Natl. Acad. Sci. U.S.A.* **103**, 3262 (2006).
11. I. Martianov, A. Ramadass, A. Serra Barros, N. Chow, A. Akoulitchev, *Nature* **445**, 666 (2007).
12. R. J. Britten, E. H. Davidson, *Science* **165**, 349 (1969).
13. F. Jacob, J. Monod, *J. Mol. Biol.* **3**, 318 (1961).
14. J. S. Mattick, *Curr. Opin. Genet. Dev.* **4**, 823 (1994).
15. We thank M. Mittmann, D. Le, and E. Schell for design of tiling arrays; K. Kole, D. Barone, and C. Chen for their help with direct RNA labeling; G. Hannon, K. Fejes-Toth, D. Gerhard, and K. Nussbacher for technical discussion and assistance in manuscript preparation; Mt. Sinai Hospital and A. Nagy, R. Nagy, W. Abramow-Newerly, J. Rossant, and J. Roder for procurement of the R1mES cell line; and M. Brown and D. Menke at Stanford for help in preparation of mouse embryo fibroblasts. This project has been funded in part with funds from the National Cancer Institute, NIH, under contract no. N01-CO-12400 and from the National Human Genome Research

Institute, NIH, under grant no. U01HG003147, and by Affymetrix, Inc. The data discussed in this publication have been deposited in National Center for Biotechnology Information's Gene Expression Omnibus (GEO, www.ncbi.nlm.nih.gov/geo/) and are accessible through GEO Series accession number GSE-7576.

Supporting Online Material

www.sciencemag.org/cgi/content/full/1138341/DC1
 Materials and Methods
 Figs. S1 to S14
 Tables S1 to S8
 References

4 December 2006; accepted 24 April 2007
 Published online 17 May 2007;
10.1126/science.1138341
 Include this information when citing this paper.

A Common Allele on Chromosome 9 Associated with Coronary Heart Disease

Ruth McPherson,^{1*†} Alexander Pertsemlidis,^{2*} Nihan Kavaslar,¹ Alexandre Stewart,¹ Robert Roberts,¹ David R. Cox,³ David A. Hinds,³ Len A. Pennacchio,^{4,5} Anne Tybjaerg-Hansen,⁶ Aaron R. Folsom,⁷ Eric Boerwinkle,⁸ Helen H. Hobbs,^{2,9} Jonathan C. Cohen^{2,10†}

Coronary heart disease (CHD) is a major cause of death in Western countries. We used genome-wide association scanning to identify a 58-kilobase interval on chromosome 9p21 that was consistently associated with CHD in six independent samples (more than 23,000 participants) from four Caucasian populations. This interval, which is located near the *CDKN2A* and *CDKN2B* genes, contains no annotated genes and is not associated with established CHD risk factors such as plasma lipoproteins, hypertension, or diabetes. Homozygotes for the risk allele make up 20 to 25% of Caucasians and have a ~30 to 40% increased risk of CHD.

Coronary heart disease (CHD) is the single greatest cause of death worldwide (1, 2). Although CHD is highly heritable, the DNA sequence variations that confer cardiovascular risk remain largely unknown. To identify sequence variants associated with CHD, we undertook a genome-wide association study using 100,000 single-nucleotide polymorphisms

(SNPs). To minimize false positive associations without unduly sacrificing statistical power, we designed the study to comprise three sequential case-control comparisons performed at a nominal significance threshold of $P < 0.025$ (Fig. 1). For the initial genome-wide scan, cases and controls were Caucasian men and women from Ottawa, Canada who participated in the Ottawa Heart

Study (OHS). Cases had severe, premature CHD with a documented onset before the age of 60 years and culminating in coronary artery revascularization (table S1). To limit confounding by factors that strongly predispose to premature CHD, we excluded individuals with diabetes or plasma cholesterol levels consistent with mono-

¹Division of Cardiology, University of Ottawa Heart Institute, Ottawa K1Y4W7, Canada. ²Donald W. Reynolds Cardiovascular Clinical Research Center and the Eugene McDermott Center for Human Growth and Development, University of Texas Southwestern Medical Center, Dallas, TX 75390, USA. ³Perlegen Sciences, Mountain View, CA 94043, USA. ⁴Genomics Division, Lawrence Berkeley National Laboratory, Berkeley, CA 94720, USA. ⁵U.S. Department of Energy Joint Genome Institute, Walnut Creek, CA 94598, USA. ⁶Department of Clinical Biochemistry, Rigshospitalet, Copenhagen University Hospital, Copenhagen DK-2100, Denmark. ⁷Division of Epidemiology and Community Health, University of Minnesota, Minneapolis, MN 55454, USA. ⁸Human Genetics Center and Institute for Molecular Medicine, University of Texas Health Science Center, Houston, TX 77030, USA. ⁹Howard Hughes Medical Institute at the University of Texas Southwestern Medical Center, Dallas, TX 75390, USA. ¹⁰Center for Human Nutrition at the University of Texas Southwestern Medical Center, Dallas, TX 75390, USA.

*These authors contributed equally to this work.
 †To whom correspondence should be addressed. E-mail: jonathan.cohen@utsouthwestern.edu (J.C.C.); rmcpherson@ottawaheart.ca (R.M.)

genic hypercholesterolemia (>280 mg/dL). Controls were healthy Caucasian men (>65 years) and women (>70 years) from Ottawa who had no symptoms or history of CHD (table S1).

Custom oligonucleotide arrays (3) were used to assay 100,000 SNPs arranged at ~30-kb intervals throughout the genome in 322 cases and 312 controls (data set designated as OHS-1). Of these, 9636 SNPs deviated strongly from Hardy-Weinberg equilibrium ($P < 0.001$) or did not meet quality-control criteria (3), and 17,500 were subpolymorphic (minor allele frequency < 1%) in the sample. The remaining 72,864 SNPs were entered into the analysis, and 2586 were associated with CHD at a nominal significance threshold of 0.025 (table S2). These 2586 SNPs were genotyped in an independent sample of 311 cases and 326 controls from Ottawa (OHS-2) using the same criteria as OHS-1 (table S1). Of these, 50 were associated with CHD at a nominal

significance threshold of 0.025, with the same direction of effect (table S2).

To limit attrition of true positive associations due to inadequate statistical power, we performed the third case-control comparison in a much larger prospective study of CHD risk, the Atherosclerosis Risk in Communities (ARIC) study, which enrolled and followed 11,478 Caucasians (4). Only 2 of the 50 SNPs identified in the Ottawa cohorts were significantly associated with incident CHD in the ARIC population (table S2). These two SNPs, rs10757274 and rs2383206, were located within 20 kb of each other on chromosome 9p21 and were in strong linkage disequilibrium ($r^2 = 0.89$).

To validate the association between rs10757274 and rs2383206 and CHD, we assayed both SNPs in three additional independent cohorts: the Copenhagen City Heart Study (CCHS), a prospective study of ischemic heart disease in 10,578 Danish men and women (5); the Dallas

Heart Study (DHS), a population-based probability sample of Dallas County residents (6); and a third sample of 647 cases and 847 controls from the Ottawa Heart Study population (OHS-3). In the CCHS, cases were participants who experienced an ischemic cardiovascular event during the 20-year follow-up period, whereas controls were those who did not develop CHD over the same time interval. In the DHS, cases and controls were defined by using electron-beam computer tomography to measure coronary artery calcium, an index of coronary atherosclerosis (7). In OHS-3, cases were participants that had documented CHD before the age of 55 (men) or 65 (women) years, whereas controls were men aged > 65 years and women aged > 70 years who did not have symptoms of CHD (table S1). In all three validation studies, both SNPs were significantly associated with CHD (Table 1).

The magnitude of CHD risk associated with the risk allele was determined by Cox proportional-hazards modeling in the ARIC and CCHS cohorts. The hazard ratios associated with the risk alleles were comparable in the two populations and indicated a graded increase in risk from noncarriers to heterozygotes to homozygotes (Table 2). The two SNPs (rs10757274 and rs2383206) define an allele that was associated with an ~15 to 20% increase in risk in the 50% of individuals who were heterozygous for the allele and an ~30 to 40% increase in CHD in the 25% of Caucasians who were homozygous for the allele. The population attributable risk associated with the risk allele was 12.5 to 15% in the ARIC population and 10 to 13% in the CCHS cohort.

The mechanistic basis for the association between the risk allele defined by rs10757274 and rs2383206 and CHD is not known. The allele may increase the development of atherosclerotic plaques, promote thrombogenesis, or increase the tendency of atherosclerotic plaques to rupture. The finding that the risk allele was associated with coronary artery calcification in the DHS and with severe premature atherosclerosis in OHS-1 suggests that it promotes CHD by increasing the atherosclerotic burden. The risk allele was not associated with any of the major risk factors for atherosclerosis in ARIC or CCHS (tables S3 and S4), and the association remained significant in models that considered multiple

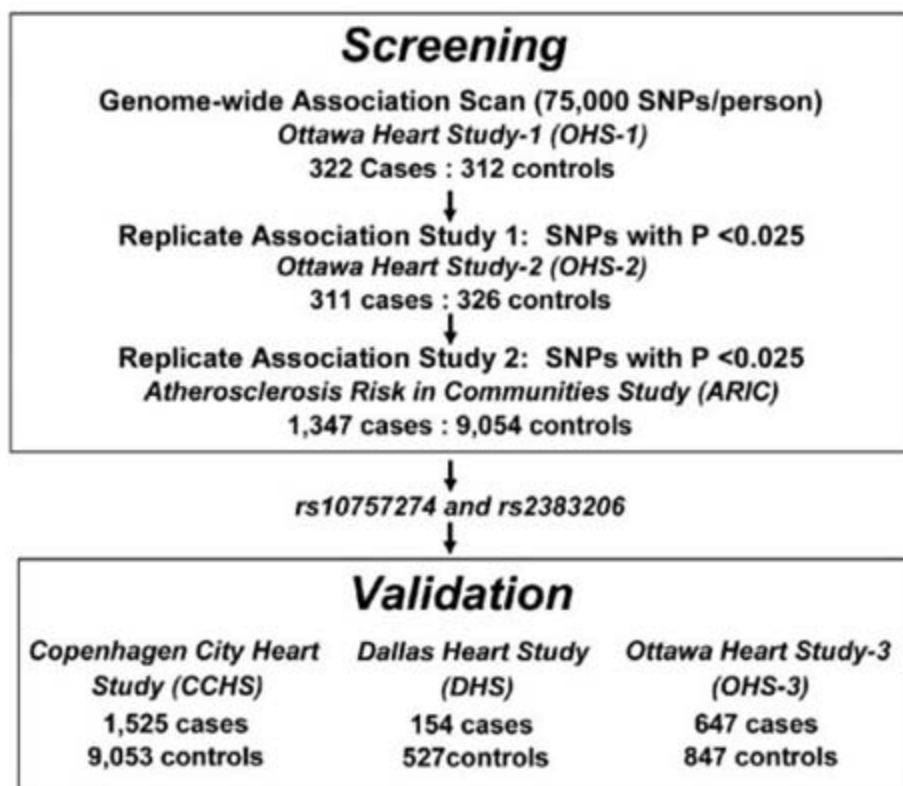


Fig. 1. Study design for identification and validation of sequence variants associated with CHD. Assuming independence, the probability of any single SNP achieving a nominal significance level of 0.025 in all three studies with the associations being in the same direction was 3.9×10^{-6} ($0.025^3 \times 0.5^2$); thus, none of the 100,000 SNPs would be expected by chance to replicate consistently in all three comparisons.

Table 1. Association between SNPs rs10757274 and rs2383206 and CHD. Values are numbers of individuals in each genotype group. P values were calculated by χ^2 tests on allele counts. HW, Hardy-Weinberg equilibrium.

	rs10757274						χ^2 P	HW P	rs2383206						χ^2 P	HW P
	Controls			Cases					Controls			Cases				
	AA	AG	GG	AA	AG	GG			AA	AG	GG	AA	AG	GG		
OHS-1	85	149	78	49	148	125	3.7×10^{-6}	0.08	77	147	88	45	140	137	6.7×10^{-6}	0.19
OHS-2	85	161	80	56	140	108	0.0009	0.4	80	160	86	50	141	113	0.0008	0.34
ARIC	2063	3822	1858	230	525	282	0.004	0.11	2140	4161	2231	230	600	324	0.0007	0.21
CCHS	2752	4543	1758	393	792	340	0.0004	0.56	2489	4583	1981	372	782	371	0.016	0.58
DHS	147	258	122	27	85	42	0.025	0.99	131	258	138	24	84	46	0.045	0.95
OHS-3	228	418	201	121	333	193	0.0003	0.96	197	416	229	115	327	209	0.011	0.98

Table 2. Risk of CHD as a function of rs10757274 and rs2383206 in the ARIC study and the CCHS. ARIC expected event values are based on the log-rank test. ARIC incidence rates are measured in number of events per 10,000 person years of followup. Ranges in parentheses indicate 95% confidence interval.

	ARIC study					CCHS				
	<i>n</i> (%)	Number of events Observed	Expected	Incidence	Hazard ratio	<i>n</i> (%)	Number of events Observed	Expected	Incidence	Hazard ratio
<i>rs10757274</i>										
AA	2293 (26)	255*	295	79 (70–89)	1	3145 (30)	393‡	473	61 (55–68)	1
AG	4347 (50)	564	553	93 (86–101)	1.18 (1.02–1.37)	5335 (50)	792	755	73 (68–79)	1.26 (1.12–1.42)
GG	2140 (24)	298	269	101 (90–114)	1.29 (1.09–1.52)	2098 (20)	340	296	80 (72–89)	1.38 (1.19–1.60)
<i>rs2383206</i>										
AA	2370 (25)	259†	310	78 (69–88)	1	2,861 (27)	372§	425	64 (58–71)	1
AG	4761 (49)	643	610	97 (90–105)	1.26 (1.09–1.46)	5,365 (51)	782	772	72 (67–77)	1.16 (1.02–1.31)
GG	2555 (26)	345	327	97 (88–108)	1.26 (1.07–1.48)	2,352 (22)	371	327	78 (71–87)	1.29 (1.12–1.50)

* $P < 0.0111$. † $P < 0.0041$. ‡ $P < 0.00001$. § $P < 0.005$.

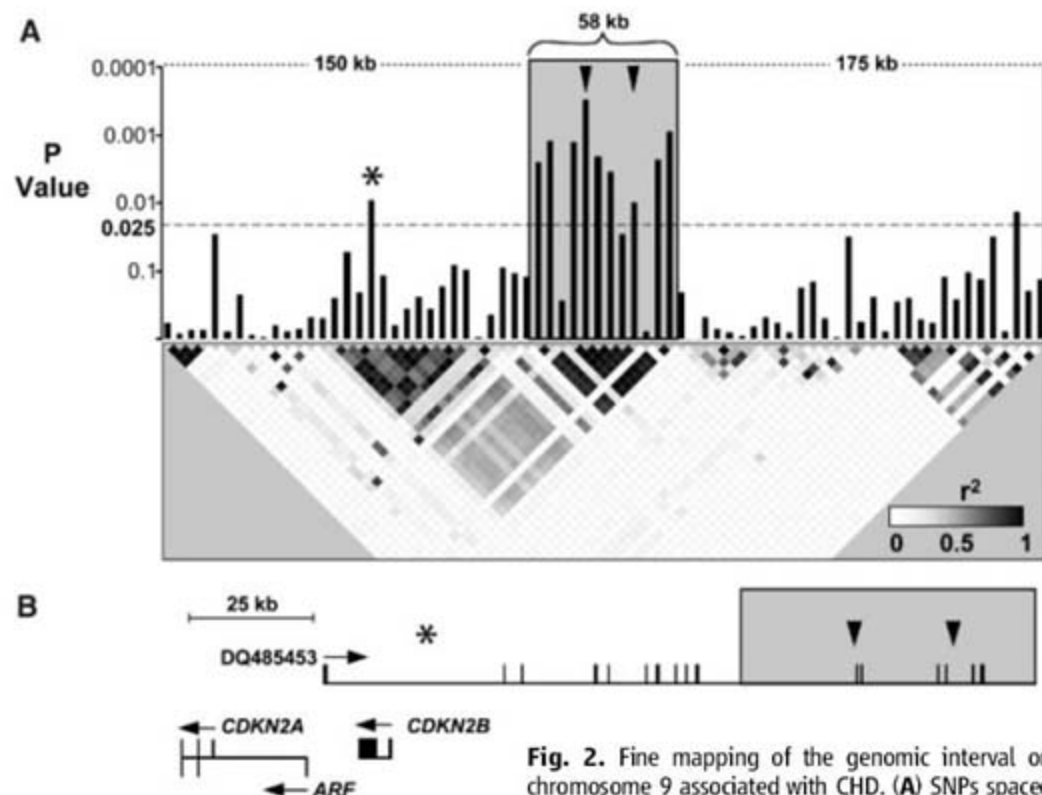


Fig. 2. Fine mapping of the genomic interval on chromosome 9 associated with CHD. (A) SNPs spaced ~5 kb apart in the interval extending 175 kb upstream and downstream of rs10757274 and rs2383206 were assayed in 500 cases and 500 controls from the OHS population with GeneChip Human Mapping 500K Array Sets (Affymetrix, Santa Clara, CA). Bars represent P values (determined with χ^2 tests) for differences in allele frequency between cases and controls. Arrowheads indicate rs10757274 and rs2383206. The asterisk represents rs518394. The risk interval is indicated with a gray box. The linkage disequilibrium map indicates pairwise r^2 values. Blocks are shaded on a continuous scale, where white represents an r^2 of 0 and black represents an r^2 of 1. (B) Physical map of the region showing the location of the risk interval (gray box) relative to the noncoding RNA DQ485453 and adjacent genes *CDKN2A*, *ARF*, and *CDKN2B*. Arrowheads indicate rs10757274 and rs2383206, and the asterisk represents rs518394 [see (A)].

possible confounding covariates (including age, gender, plasma lipid levels, blood pressure, diabetes, and plasma C-reactive protein concentrations; table S3). These analyses suggest that the effect of the chromosome 9 risk allele on CHD was not mediated by any of the established risk factors for cardiovascular disease.

To fine-map the locus associated with CHD, we assayed SNPs spaced at ~5-kb intervals across the region extending 175 kb upstream and downstream of rs10757274 and

rs2383206 in 500 cases and 500 controls from OHS-2 and OHS-3. Eight additional SNPs at the locus spanning a 58-kb region (extending from 22,062,301 to 22,120,389) were significantly associated with CHD (Fig. 2). All eight were in strong linkage disequilibrium with each other and with rs10757274 and rs2383206. The region demarcated by these SNPs was flanked on both sides by ~50-kb regions in which none of the 30 SNPs tested were associated with CHD. Two of 65 SNPs in the 350-kb region surrounding the

58-kb risk locus were associated with CHD at the nominal significance threshold, but neither was in strong linkage disequilibrium with rs10757274 and rs2383206. These data indicate that the risk allele comprises a single haplotype that spans ~58 kb.

Inspection of the UCSC Genome Browser (<http://genome.ucsc.edu>) and BLAST searches against the National Center for Biotechnology Information (NCBI) (www.ncbi.nlm.nih.gov/blast) nr (nonredundant) nucleotide sequence database revealed no annotated genes or microRNAs within the 58-kb interval. A number of spliced expressed sequence tags (ESTs) map within the interval, but none contained an open reading frame that extends more than a few amino acids. Resequencing of the 58-kb interval in two homozygotes for the risk allele and one homozygote for the reference allele revealed 66 polymorphisms (SNPs plus small insertions or deletions), of which 35 were specific to the risk allele (table S5). Only one of these variants, a copy number variation in a run of nine consecutive CAT repeats (extending from nucleotide 22110787 to 22110814, NCBI build 36.1) mapped to a spliced transcript (BI765545) that appears to be part of a large noncoding RNA of unknown function (8). Polymerase chain reaction (PCR) amplification of cDNAs confirmed expression of the transcript in placenta and transformed lymphocytes (fig. S1). It is possible that variation in the expression or function of this transcript may be associated with risk of CHD.

Alternatively the risk allele may alter a regulatory element that affects the expression of a gene (or genes) located outside of the 58-kb interval. Cross-species sequence alignments revealed several conserved segments within the 58-kb interval that may contain such regulatory elements (fig. S2). It is also possible that the risk allele extends beyond the 58-kb interval defined in this study and that the functional sequence variants that confer risk of CHD are located outside of the interval. Resequencing the coding regions of the two genes most proximal to the risk locus, *CDKN2A* and *CDKN2B*, revealed only a single variant (Ala¹⁵⁸→Ser¹⁵⁸ in *CDKN2A*) that was present in 6 of the 96 individuals examined and is thus unlikely to explain the CHD risk

associated with the locus. The localization of the risk locus to a region devoid of known genes implicates a previously unrecognized gene or regulatory element that can substantially affect CHD independently of established risk factors. Further studies will be required to elucidate the mechanism by which the locus modulates CHD risk.

Comparison of the Yoruba and Centre d'Etude du Polymorphisme Humain (CEPH) data from the International HapMap Project (www.hapmap.org) revealed notable ethnic differences in allele frequencies in the risk interval (table S6). Of the 10 alleles that were significantly associated with CHD in whites, 3 were virtually absent from the Yoruba population, and 6 others were much less common. Both rs10757274 and rs2383206 were present at appreciable frequencies among African-Americans in ARIC and DHS, but neither SNP was associated with CHD in either population (table S7). The apparent ethnic differences in association between these SNPs and CHD in ARIC may reflect differences in statistical power in ARIC but cannot explain the ethnic differences observed in DHS, where African-Americans are the largest group. Accordingly, it seems more likely that the functional sequence variants associated with the risk allele in whites are less common in African-Americans. This notion is consistent with our finding that the frequencies of several alleles associated with CHD risk factors differ widely among ethnic groups (9–11). Comprehensive analysis of the locus in African-Americans may allow further refinement of the risk interval.

The results of this study illustrate both the perils and the promise of whole-genome association. The initial scan and the first replicate screen both generated substantially more SNPs that achieved the prespecified significance threshold than would be predicted by chance alone, as indicated by permutation testing (table S2). Yet only two of these SNPs (comprising one allele) survived further replication, despite the use of a large sample (i.e., ARIC) with high statistical power. This finding highlights the necessity for adequate replication to protect against artifacts that may occur because of population stratification, multiple testing, or other factors to which whole-genome association studies are particularly susceptible. The consistent replication of the chromosome 9 risk allele in six independent study samples indicates that the approach can be productively applied to conditions as complex as CHD, which is known to be influenced by a variety of environmental and genetic factors (12). Furthermore, analysis of 50 randomly selected regions of 500 kb each indicated that the 72,864 informative SNPs used in the initial scan provided 30 to 40% of the power that would be obtained by assaying all phase II Hapmap SNPs. Therefore, scans with denser SNP panels and larger sample sizes may reveal further loci associated with CHD risk.

References and Notes

1. C. J. Murray, A. D. Lopez, *Lancet* **349**, 1436 (1997).
2. C. D. Mathers, D. Loncar, *PLoS Med.* **3**, e442 (2006).
3. S. F. Saccone et al., *Hum. Mol. Genet.* **16**, 36 (2007).
4. The ARIC Study Investigators, *Am. J. Epidemiol.* **129**, 687 (1989).

5. P. Schnohr, G. Jensen, H. Scharling, M. Appleyard, *Eur. Heart J.* **3** (suppl. H), H1 (2001).
6. R. G. Victor et al., *Am. J. Cardiol.* **93**, 1473 (2004).
7. A. S. Agatston et al., *J. Am. Coll. Cardiol.* **15**, 827 (1990).
8. E. Pasmant et al., *Cancer Res.* **67**, 1 (2007).
9. J. C. Cohen et al., *Proc. Natl. Acad. Sci. U.S.A.* **103**, 1810 (2006).
10. J. C. Cohen, E. Boerwinkle, T. H. Mosley, H. H. Hobbs, *N. Engl. J. Med.* **354**, 34 (2006).
11. S. Romeo et al., *Nat. Genet.* **39**, 513 (2007).
12. National Cholesterol Education Program (NCEP) Expert Panel on Detection, Evaluation, and Treatment of High Blood Cholesterol in Adults (Adult Treatment Panel III), *Circulation* **106**, 3143 (2002).
13. We thank T. Hyatt, H. Doelle, T. Naing, L. Nie, K. Moller Rasmussen, M. Refstrup, W. S. Schackwitz, J. Martin, and A. Ustaszewska for excellent technical assistance and J. Schageman, C. Lee, K. Lawson, and K. Williams for statistical analyses. We are indebted to the staff and participants of the OHS, the DHS, the ARIC study, and the CCHS for their important contributions. Supported by grants from Foundation Le Ducq, the Donald W. Reynolds Foundation, NIH (HL-082896), the National Heart, Lung, and Blood Institute Program for Genomic Applications (no. HL-066681), the U.S. Department of Energy (contract no. DE-AC02-05CH11231), the Canadian Institutes of Health Research (no. 44360), the Canadian Foundation for Innovation, the Heart and Stroke Foundation of Ontario (no. NA-5413) the Danish Medical Research Council, the Danish Heart Foundation, and the Research Fund at Rigshospitalet, Copenhagen University Hospital. D.R.C. and D.A.H. have equity interest in Perlegen Sciences.

Supporting Online Material

www.sciencemag.org/cgi/content/full/1142447/DC1

Materials and Methods

Figs. S1 and S2

Tables S1 to S7

12 March 2007; accepted 24 April 2007

Published online 3 May 2007;

10.1126/science.1142447

Include this information when citing this paper.

A Common Variant on Chromosome 9p21 Affects the Risk of Myocardial Infarction

Anna Helgadóttir,^{1*} Gudmar Thorleifsson,^{1*} Andrei Manolescu,^{1*} Solveig Gretarsdóttir,¹ Thorarinn Blondal,¹ Aslaug Jonasdóttir,¹ Adalbjorg Jonasdóttir,¹ Asgeir Sigurdsson,¹ Adam Baker,¹ Arnar Palsson,¹ Gisli Masson,¹ Daniel F. Gudbjartsson,¹ Kristinn P. Magnusson,¹ Karl Andersen,² Allan I. Levey,³ Valgerdur M. Backman,¹ Sigurborg Matthiasdóttir,¹ Thorbjorg Jonsdóttir,¹ Stefan Palsson,¹ Helga Einarsdóttir,¹ Steinunn Gunnarsdóttir,¹ Arnaldur Gylfason,¹ Viola Vaccarino,³ W. Craig Hooper,³ Muredach P. Reilly,⁴ Christopher B. Granger,⁵ Harland Austin,³ Daniel J. Rader,⁴ Svati H. Shah,⁵ Arshed A. Quyyumi,³ Jeffrey R. Gulcher,¹ Gudmundur Thorgeirsson,² Unnur Thorsteinsdóttir,¹ Augustine Kong,^{1†} Kari Stefansson^{1†}

The global endemic of cardiovascular diseases calls for improved risk assessment and treatment. Here, we describe an association between myocardial infarction (MI) and a common sequence variant on chromosome 9p21. This study included a total of 4587 cases and 12,767 controls. The identified variant, adjacent to the tumor suppressor genes *CDKN2A* and *CDKN2B*, was associated with the disease with high significance. Approximately 21% of individuals in the population are homozygous for this variant, and their estimated risk of suffering myocardial infarction is 1.64 times as great as that of noncarriers. The corresponding risk is 2.02 times as great for early-onset cases. The population attributable risk is 21% for MI in general and 31% for early-onset cases.

Coronary artery disease (CAD), including acute myocardial infarction (MI), is the leading cause of death worldwide (1). Identifi-

cation of the underlying genetic architecture of heart disease may provide improved risk assessment and better measures for prevention and treatment.

To this end, we conducted a genome-wide association study on Icelandic patients with MI, using the Illumina Hap300 chip. After quality filtering, 305,953 single-nucleotide polymorphisms (SNPs) were tested for association with MI in a sample of 1607 cases, with age at onset before 70 in males and before 75 in females; 6728 patients without a history of CAD were used as controls (2). The results were adjusted for relatedness between individuals and potential population stratification with the use of a method of genomic control (3). Although none of the SNPs were significant after adjusting for the number of tests performed, more signals with *P* values of less than 10^{-5} were observed than expected by chance (fig. S1). Hence, we further explored the SNPs with *P* values that were closest to genome-wide significance.

The strongest association with MI was observed with three correlated SNPs—rs1333040,

¹deCODE genetics, Sturlugata 8, IS-101 Reykjavik, Iceland.

²Landspítali University Hospital, Reykjavik, Iceland.

³Emory University School of Medicine, Atlanta, GA 30322, USA.

⁴University of Pennsylvania School of Medicine, Philadelphia, PA 19104, USA.

⁵Duke University School of Medicine, Durham, NC 27710, USA.

*These authors contributed equally to this work.

†To whom correspondence should be addressed. E-mail: augustine.kong@decode.is (A.K.); kstefans@decode.is (K.S.)

rs2383207, and rs10116277. Each had an odds ratio (OR) around 1.22 for the risk allele and a *P* value of approximately 1×10^{-6} (table S1). All three SNPs are located within a 190-kb linkage disequilibrium (LD) block on chromosome 9p21 (fig. S2). Apart from these 3 SNPs, 11 other SNPs in the same LD block showed nominally significant association with MI. The associations with these SNPs tended to become weaker after accounting for the association with the three SNPs mentioned above (table S1). After adjustment, a few remained nominally significant ($P < 0.05$), but none had a $P < 0.01$.

To replicate the observed associations, we genotyped the three SNPs—rs1333040, rs2383207 and rs10116277—in an additional 665 Icelandic MI cases and 3533 controls, and in three case-control sample sets of European descent from three cities from the United States: Philadelphia, Atlanta, and Durham (2). For consistency, we used the same age-at-onset criteria in the association analysis as for the discovery group. The association with MI was replicated with significance in all four groups (table S2). When we combined the replication sets using a Mantel-Haenszel model (4), all three SNPs showed highly significant association with MI ($P < 1 \times 10^{-8}$), with ORs comparable to those observed in the Icelandic discovery samples. When all groups were combined, rs2383207 showed the most-significant association ($P = 2.0 \times 10^{-16}$), with an OR of 1.25 [95% confidence interval (CI) 1.18 to 1.31] for the risk allele G. Notably, rs2383207 and rs10116277 are highly correlated ($r^2 = 0.90$) and their effects could not be reliably distinguished from each other in these data. The SNP rs1333040 is also substantially correlated with rs2383207 and rs10116277 ($r^2 = 0.57$ and 0.67 , respectively). In an attempt to refine this association signal, we identified the SNPs that are substantially correlated with rs2383207 ($r^2 > 0.5$) based on the Hapmap CEU data and that are not part of the Illumina Hap300 chip. Among the 36 such SNPs, we selected 8 to be genotyped. Each of the 36 SNPs was either one of the eight or had a very good surrogate among them ($r^2 > 0.90$) (table S7). With data from all case-control groups combined, allele G of the refinement SNP rs10757278 showed the strongest association with the disease (OR = 1.28, $P = 1.2 \times 10^{-20}$; Table 1 and table S2). Furthermore, whereas rs2383207 was no longer significant after adjusting for rs10757278 ($P = 0.25$), rs10757278 remained significant with adjustment for rs2383207 ($P = 2.0 \times 10^{-5}$). Among the SNPs in this region that showed very significant association with the disease when tested individually, none was significant after adjustment for rs10757278 with the exception of the refinement SNP rs1333046, which was marginally significant ($P = 0.044$) with adjustment (table S8). Henceforth, for simplicity of presentation, we focused on the most significant SNP, rs10757278. Additional results for other SNPs in the region are provided in tables S2 to S6.

Table 1. Association results for rs2383207 (G) and rs10757278 (G), in 9p21 in Iceland and the United States. Results are shown for the initial Icelandic discovery MI case-control group (Iceland A), an independent Icelandic replication group (Iceland B), and for the three U.S. replication groups of European descent. Also included are the results for the MI case-control groups combined. Study population includes the number of MI cases (*n*) and controls (*m*). To combine the Icelandic cohorts, we analyzed them together and adjusted the results for relatedness in the combined group. For the combined groups, we calculated OR and *P* value using a Mantel-Haenszel model, and the frequency in cases and controls is a simple average over the frequency in the individual groups. When combining Icelandic and U.S. groups, the frequency in cases and controls is the average over the two populations.

Study population (<i>n/m</i>) Variant (allele)	Frequency		OR (95% CI)	<i>P</i>
	Controls	Cases		
Iceland A (1607/6728)				
rs2383207 (G)	0.455	0.506	1.22 (1.13–1.33)	1.4×10^{-6}
rs10757278 (G)	0.434	0.489	1.25 (1.15–1.36)	1.5×10^{-7}
Iceland B (665/3533)				
rs2383207 (G)	0.462	0.525	1.29 (1.15–1.45)	2.6×10^{-5}
rs10757278 (G)	0.436	0.503	1.31 (1.16–1.47)	1.4×10^{-5}
Atlanta (596/1284)				
rs2383207 (G)	0.541	0.593	1.23 (1.07–1.42)	3.0×10^{-3}
rs10757278 (G)	0.484	0.551	1.31 (1.14–1.50)	1.5×10^{-4}
Philadelphia (582/504)				
rs2383207 (G)	0.524	0.602	1.37 (1.16–1.63)	2.6×10^{-4}
rs10757278 (G)	0.470	0.550	1.38 (1.17–1.64)	1.9×10^{-4}
Durham (1137/718)				
rs2383207 (G)	0.513	0.559	1.20 (1.05–1.37)	6.0×10^{-3}
rs10757278 (G)	0.460	0.521	1.28 (1.12–1.46)	2.7×10^{-4}
Combined				
Iceland (2272/10,261)				
rs2383207 (G)	0.458	0.511	1.24 (1.16–1.33)	3.3×10^{-10}
rs10757278 (G)	0.435	0.493	1.26 (1.18–1.35)	5.3×10^{-12}
U.S. groups (2315/2506)				
rs2383207 (G)	0.526	0.585	1.25 (1.15–1.36)	1.1×10^{-7}
rs10757278 (G)	0.471	0.541	1.31 (1.21–1.43)	1.5×10^{-10}
Replication groups (2980/6039)				
rs2383207 (G)	0.494	0.555	1.27 (1.18–1.36)	1.4×10^{-11}
rs10757278 (G)	0.454	0.522	1.31 (1.22–1.40)	1.0×10^{-14}
All groups (4587/12,767)				
rs2383207 (G)	0.492	0.548	1.25 (1.18–1.31)	2.0×10^{-16}
rs10757278 (G)	0.453	0.517	1.28 (1.22–1.35)	1.2×10^{-20}

Table 2. Genotype-specific OR for the risk allele of rs10757278. The risk for heterozygous carriers (OX) and homozygous carriers (XX) is compared with the risk for noncarriers (OO), together with 95% CI and the population attributable risk (PAR). The lower part of the table includes the corresponding values when the analysis is restricted to early-onset MI cases. Study population includes the number of MI cases (*n*) and controls (*m*). For the Icelandic groups, *P* values and OR were adjusted for relatedness using simulations.

Study population (<i>n/m</i>) Variant (allele)	Genotype-specific OR			PAR
	OO	OX (95% CI)	XX (95% CI)	
Iceland (2272/10,261)				
rs10757278 (G)	1	1.25 (1.12–1.39)	1.58 (1.38–1.81)	0.19
U.S. groups (2315/2506)				
rs10757278 (G)	1	1.28 (1.14–1.45)	1.72 (1.45–2.03)	0.23
All groups (4587/12,767)				
rs10757278 (G)	1	1.26 (1.16–1.36)	1.64 (1.47–1.82)	0.21
<i>Early-onset MI (<50 for males; <60 for females)</i>				
Iceland (621/10,261)				
rs10757278 (G)	1	1.38 (1.13–1.69)	1.94 (1.53–2.46)	0.27
U.S. groups (1080/2506)				
rs10757278 (G)	1	1.56 (1.32–1.85)	2.08 (1.69–2.58)	0.34
All groups (1701/12,767)				
rs10757278 (G)	1	1.49 (1.31–1.69)	2.02 (1.72–2.36)	0.31

Table 3. Association of the G allele of rs10757278 with CAD. The association results are shown for CAD, both including and excluding known MI cases. Results are shown for the Icelandic case-control group (except for the initial discovery group individuals, which have been excluded both from cases and controls), for two of the U.S. groups, and for the groups combined.

Study population (<i>n1/n2/m</i>) Variant (allele)	Control frequency	All CAD cases			Excluding MI cases		
		Case frequency	OR (95% CI)	<i>P</i>	Case frequency	OR (95% CI)	<i>P</i>
Iceland (1563/773/3533) rs10757278 (G)	0.439	0.496	1.26 (1.15–1.37)	1.9×10^{-7}	0.490	1.22 (1.09–1.37)	5.0×10^{-4}
Atlanta (724/128/1284) rs10757278 (G)	0.484	0.552	1.31 (1.15–1.50)	3.6×10^{-5}	0.557	1.34 (1.04–1.73)	2.6×10^{-2}
Philadelphia (709/126/504) rs10757278 (G)	0.470	0.547	1.36 (1.16–1.60)	1.9×10^{-4}	0.528	1.26 (0.96–1.66)	1.0×10^{-1}
Combined							
U.S. groups (1433/254/1788) rs10757278 (G)	0.477	0.550	1.33 (1.20–1.47)	2.7×10^{-8}	0.542	1.30 (1.08–1.57)	5.9×10^{-3}
All groups (2996/1027/5321) rs10757278 (G)	0.458	0.523	1.29 (1.21–1.38)	3.6×10^{-14}	0.525	1.24 (1.13–1.37)	1.1×10^{-5}

To investigate the mode of inheritance in more detail, we computed genotype-specific ORs for rs10757278. With results from all groups combined, relative to noncarriers, the ORs for heterozygous and homozygous carriers of the risk allele G were 1.26 and 1.64, respectively (Table 2). Assuming a frequency of 45.3% for the allele, the average of the frequencies in Iceland and the United States, the corresponding population attributable risk is 21%.

Because the impact of genetic factors on CAD has been shown to be greater at early ages (5), we investigated the correlation of allele G of rs10757278 to age at onset of MI. In this analysis, we used all cases with a known age at onset, including those who had onset after the age of 70 or 75 for males and females, respectively. This added a total of 973 cases to the study groups compared with the number of cases used in the case-control analyses. Regressing the age at onset on the number of risk alleles showed that, for each copy of the risk allele, the age at onset of MI was on average reduced by approximately 1 year ($P = 2.9 \times 10^{-7}$) (table S4). Alternatively, restricting the case-control analysis to early-onset MI, defined as an MI before the age of 50 for males and before the age of 60 for females, the allelic OR for rs10757278 G in all groups combined increased to 1.42 (95% CI 1.31 to 1.53) (table S5). Relative to noncarriers, genotype-specific OR for early-onset MI is 1.49 and 2.02 for heterozygous and homozygous carriers of the risk allele, respectively (Table 2).

Having established that allele G of rs10757278 is associated with MI, we explored its impact on the broader phenotype of CAD (Table 3). To eliminate bias that could have arisen from the selection of the most-significant variants in the initial genome-wide study, the cases and controls from the Icelandic discovery group (Iceland A) were not included here. If the Icelandic group had been included, there would have been little change to the estimated effects, but the results would have

become more significant due to the larger sample sizes. Also, the group from Durham did not have CAD cases without MI. As expected, rs10757278 was associated with CAD with high significance (OR = 1.29, $P = 3.6 \times 10^{-14}$ for the groups combined). After removal of MI cases from the analyses, the associations remained significant for the groups from Iceland and Atlanta but not for the Philadelphia group. Combining results from the three groups gave an OR of 1.24 ($P = 0.000011$).

The variants on chromosome 9p21 associated with MI are located in an LD block that contains the *CDKN2A* and *CDKN2B* genes. The proteins encoded by these genes—called p16^{INK4a}, ARF, and p15^{INK4b}—play a critical role in regulating cell proliferation, cell aging and senescence, and apoptosis in many cell types (6). These are all important features of atherogenesis, the underlying cause of MI and CAD (7, 8). Sequencing of 93 early-onset MI patients across exons, exon-intron junctions, and regulatory regions of *CDKN2A* and *CDKN2B* did not reveal obvious candidates for functional variants or other variants that could account for the observed association with rs10757278 (tables S11 and S12). In addition to *CDKN2A* and *CDKN2B* genes, the LD block contains two exons of the mRNA transcript AF109294, a hypothetical methylthioadenosine phosphorylase fusion protein mRNA, and several expressed sequence tags that are expressed in various tissues (2). The functional relevance of the variants of this genomic region to MI and CAD remains to be elucidated.

We show that a common genetic variant located in the vicinity of the tumor suppressor genes *CDKN2A* and *CDKN2B* on chromosome 9p21 associates with MI. This is the first common variant discovered to consistently confer substantial risk (OR > 1.20) of MI in multiple case-control groups of European descent. Due to its high frequency, the population attributable risk of

the variant is approximately 21% for MI in general and approximately 31% for early-onset cases, which is substantial from a public health point of view. However, as the relative risks are not extremely high, it explains only a small fraction of the familial clustering of the disease and would not generate large linkage scores. Hence, other susceptibility variants remain to be identified and some could be located in candidate regions identified by genome-wide linkage scans (9–11). There is evidence to suggest that the variants identified here could increase the risk of CAD in general in addition to their impact on MI, an observation that warrants further investigation. The mechanism whereby the genetic variants exert their effects in the pathogenesis of MI remains to be elucidated.

References and Notes

1. T. Thom *et al.*, *Circulation* **113**, e85 (2006).
2. Materials and methods are available as supporting material on Science Online.
3. B. Devlin, K. Roeder, *Biometrics* **55**, 997 (1999).
4. N. Mantel, W. Haenszel, *J. Natl. Cancer Inst.* **22**, 719 (1959).
5. S. Zdravkovic *et al.*, *J. Intern. Med.* **252**, 247 (2002).
6. W. Y. Kim, N. E. Sharpless, *Cell* **127**, 265 (2006).
7. A. J. Lusis, *Nature* **407**, 233 (2000).
8. T. Minamino, I. Komuro, *Circ. Res.* **100**, 15 (2007).
9. E. Zintzaras, G. Kitsios, *J. Hum. Genet.* **51**, 1015 (2006).
10. Q. Wang *et al.*, *Am. J. Hum. Genet.* **74**, 262 (2004).
11. N. J. Samani *et al.*, *Am. J. Hum. Genet.* **77**, 1011 (2005).
12. We thank the participants whose contribution made this study possible, the nurses at the Icelandic Heart Association, and personnel at the deCODE core facilities. The authors from deCODE genetics declare competing financial interests. deCODE genetics has applied for a patent related to this work.

Supporting Online Material

www.sciencemag.org/cgi/content/full/1142842/DC1

Materials and Methods

SOM Text

Figs. S1 and S2

Tables S1 to S13

References

21 March 2007; accepted 26 April 2007

Published online 3 May 2007;

10.1126/science.1142842

Include this information when citing this paper.

Attenuation of Allergic Contact Dermatitis Through the Endocannabinoid System

Meliha Karsak,^{1*} Evelyn Gaffal,^{2*} Rahul Date,¹ Lihua Wang-Eckhardt,³ Jennifer Rehnelt,¹ Stefania Petrosino,⁴ Katarzyna Starowicz,⁴ Regina Steuder,² Eberhard Schlicker,⁵ Benjamin Cravatt,⁶ Raphael Mechoulam,⁷ Reinhard Buettner,⁸ Sabine Werner,⁹ Vincenzo Di Marzo,⁴ Thomas Tüting,^{2†} Andreas Zimmer^{1†}

Allergic contact dermatitis affects about 5% of men and 11% of women in industrialized countries and is one of the leading causes for occupational diseases. In an animal model for cutaneous contact hypersensitivity, we show that mice lacking both known cannabinoid receptors display exacerbated allergic inflammation. In contrast, fatty acid amide hydrolase-deficient mice, which have increased levels of the endocannabinoid anandamide, displayed reduced allergic responses in the skin. Cannabinoid receptor antagonists exacerbated allergic inflammation, whereas receptor agonists attenuated inflammation. These results demonstrate a protective role of the endocannabinoid system in contact allergy in the skin and suggest a target for therapeutic intervention.

Allergic contact dermatitis is characterized by a loss of immunological tolerance toward small allergenic molecules (haptens). The allergen or hapten first penetrates the epidermis and is taken up by skin dendritic cells, which migrate to the draining lymph nodes and present haptenated peptide or major histocompatibility complexes (MHC) to naïve antigen-specific T lymphocytes. Upon repeated allergen contact, an inflammatory response is elicited by the recruitment of antigen-specific effector T cells to the skin and the subsequent production of inflammatory cytokines and chemokines (1). Cannabinoid receptors CB1 and CB2 are heterotrimeric GTP-binding protein (G protein)-coupled receptors, which are activated by the cannabinoid Δ^9 -tetrahydrocannabinol (Δ^9 -THC), as well as by endocannabinoids such as arachidonylethanolamide (anandamide or AEA) or 2-arachidonoylglycerol (2-AG) (2). Both cannabinoid receptors are present on keratinocytes in the epidermis, which also express enzymes involved in the synthesis and degradation of endocannabinoids (3, 4).

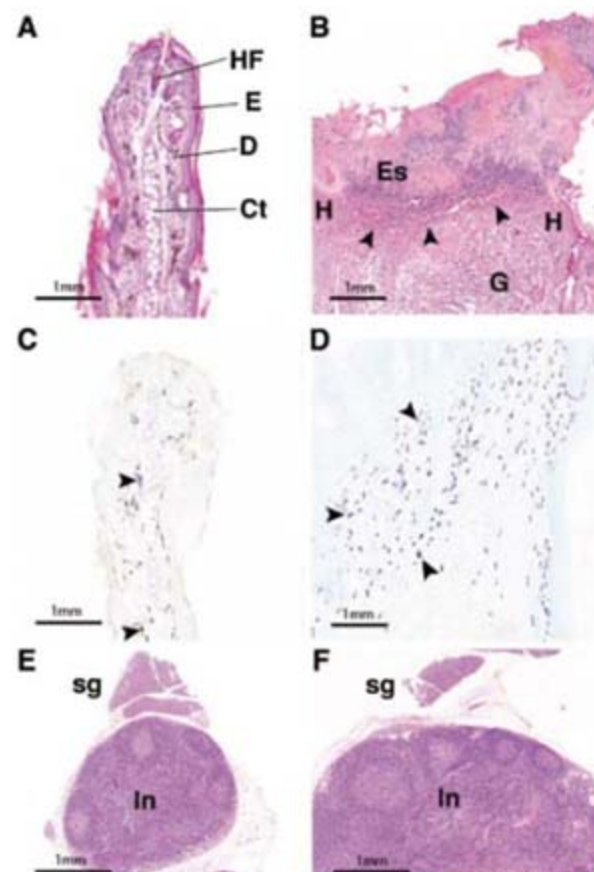
Although nickel-containing ear tags are generally well tolerated by individuals in our mouse

colony (5), we observed that mice lacking both cannabinoid CB1 and CB2 receptors [CB1 receptor-deficient ($Cnr1^{-/-}$) and CB2 receptor-deficient ($Cnr2^{-/-}$) mice] (6, 7) frequently scratch their ear tags, leading to severe ulcerations in the head and neck regions (Fig. 1, A and B, and fig. S1). Because localized necrotic lesions initially developed around the ear tag, we first considered that impaired wound healing might be the potential primary cause for the skin lesions.

Fig. 1. Histological views of $Cnr1^{-/-}/Cnr2^{-/-}$ mouse ears. Clips with high nickel content cause chronic ear ulceration in $Cnr1^{-/-}/Cnr2^{-/-}$ mice (fig. S1). (A) Hematoxylin and eosin (H&E)-stained sections of ear tissue from healthy $Cnr1^{+/+}/Cnr2^{+/+}$ mice with normal size and histology. Ct, cartilage; D, dermis; E, epidermis; HF, hair follicle. (B) H&E-stained sections of ulcerated ear tissue from $Cnr1^{-/-}/Cnr2^{-/-}$ mice carrying nickel ear tags. Arrowheads point to keratinocytes on the re-epithelized body of the wound. The eschar (Es), the strong hyperproliferative epithelium (H), and the granulation tissue (G) are indicated. (C) Toluidine blue-stained sections of ear tissue from healthy $Cnr1^{+/+}/Cnr2^{+/+}$ mice showing few metachromatic mast cells (arrowheads). (D) Toluidine blue-stained sections of ulcerated ear tissue from $Cnr1^{-/-}/Cnr2^{-/-}$ mice carrying nickel tags with intense infiltration of mast cells (arrowheads). (E) H&E-stained sections of lymph nodes from healthy $Cnr1^{+/+}/Cnr2^{+/+}$ mice. In, lymph node; sg, salivary gland. (F) H&E-stained sections of lymph nodes from $Cnr1^{-/-}/Cnr2^{-/-}$ mice carrying nickel ear tags with reactive enlargement and lymphadenitis of preauricular lymph nodes. The preauricular salivary glands located next to the lymph nodes are the same size in $Cnr1^{-/-}/Cnr2^{-/-}$ mice without (E) and with (F) ear ulceration and serve as an internal standard.

However, experiments to test the wound healing ability revealed no measurable difference between wild-type (WT) and $Cnr1^{-/-}/Cnr2^{-/-}$ double-knockout (DKO) mice (5, 8) (fig. S2). We also noted that skin ulcerations appeared to be particularly prominent in mice with tags containing high nickel content (65 to 70%). In these cases, skin ulcerations were observed in 88 out of 304 $Cnr1^{-/-}/Cnr2^{-/-}$ DKO mice (29%), but were not observed in single $Cnr1^{-/-}$ or $Cnr2^{-/-}$ knockouts or in any other mouse strain. Furthermore, no ulcerations were noted in mice with pure brass tags (fig. S1). Subsequent histopathological analyses of ulcerated ear tissue revealed intense infiltration of mast cells in close proximity to the ulcers (Fig. 1, C and D), suggesting that an allergic reaction might be involved in the pathology seen in $Cnr1^{-/-}/Cnr2^{-/-}$ DKO mice. Consistently, the regional preauricular and submental lymph nodes (Fig. 1, E and F) were swollen, reaching a diameter of 51 ± 2.4 mm in comparison with 20.5 ± 1.9 mm in healthy $Cnr1^{+/+}/Cnr2^{+/+}$ mice, as a result of mixed follicular and interfollicular lymphatic hyperplasia.

We therefore considered the possibility that an increase in allergic responses might exist in knockout (KO) mice. To test this hypothesis, we evaluated cutaneous contact hypersensitivity (CHS) in $Cnr1^{-/-}/Cnr2^{-/-}$ animals using the obligate contact allergen 2,4-dinitrofluorobenzene (DNFB), which generates a specific cutaneous T cell-mediated allergic response upon repeated allergen contact (9). A marked increase in allergic



¹Department of Molecular Psychiatry, University of Bonn, Germany. ²Laboratory of Experimental Dermatology, Department of Dermatology, University of Bonn, Germany. ³Life & Brain GmbH, Bonn, Germany. ⁴Endocannabinoid Research Group, Institute of Biomolecular Chemistry, Consiglio Nazionale delle Ricerche, Pozzuoli (Napoli), Italy. ⁵Institute of Pharmacology and Toxicology, University of Bonn, Germany. ⁶The Skaggs Institute for Chemical Biology and Departments of Cell Biology and Chemistry, The Scripps Research Institute, La Jolla, CA, USA. ⁷Department of Medicinal Chemistry and Natural Products, The Hebrew University of Jerusalem, Israel. ⁸Department of Pathology, University of Bonn, Germany. ⁹Institute of Cell Biology, Eidgenössische Technische Hochschule, Zurich, Switzerland.

*These authors contributed equally to this work.

†To whom correspondence should be addressed. E-mail: a.zimmer@uni-bonn.de (A.Z.); thomas.tueing@ukb.uni-bonn.de (T.T.)

responses was apparent in $Cnr1^{-/-}/Cnr2^{-/-}$ mice as compared with WT controls (Fig. 2A). The difference was particularly prominent 48 hours after the second and the third DNFB challenge. Infiltration of the skin with Gr-1⁺ granulocytes was increased in the ears of DNFB-exposed $Cnr1^{-/-}/Cnr2^{-/-}$ mice, as compared with WT animals (fig. S3), and correlated with a higher myeloperoxidase activity, which is indicative of enhanced neutrophil recruitment (10, 11). Furthermore, we found an increased number of MHC II⁺ antigen-presenting cells in $Cnr1^{-/-}/Cnr2^{-/-}$ mice. Upon examination of mice with a single deletion of either CB1 or CB2 receptors, we observed a similarly pronounced increase of allergic ear swelling (Fig. 2B), suggesting a nonredundant role for each cannabinoid receptor in the allergic response to DNFB. This finding would also suggest that the

response to the milder stimulus originating from the nickel ear tag was only detectable in mice lacking both receptors.

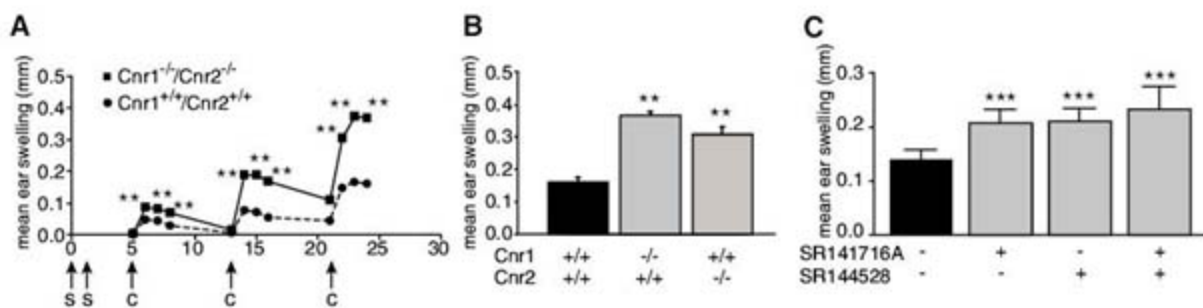
In order to obtain independent evidence for a role of the CB1 and CB2 receptors in the regulation of CHS, we examined WT mice after administration of the CB1 receptor antagonist SR141716A (Rimonabant) and the CB2 receptor antagonist SR144528, respectively. After the induction of CHS, animals received three injections of the corresponding antagonist 30 min before and after each challenge. In these cases, ear swelling was significantly increased in treated mice as compared with control mice (Fig. 2C), further supporting the role of both receptors in CHS. In contrast, however, acute oral or topical administration of the CB2 receptor antagonists appeared to ameliorate inflammatory skin responses (12, 13),

thus suggesting that CB2 antagonism may be initially beneficial but detrimental upon chronic blockade.

To explore this issue more carefully, we investigated the synthesis of endogenous cannabinoids and the expression of cannabinoid receptors during experimental contact allergy studies. After DNFB treatment, the levels of 2-AG increased in the DNFB-treated ears of WT controls and to an even larger extent in the ears of $Cnr1^{-/-}/Cnr2^{-/-}$ mice (Fig. 3A), whereas AEA production was strongly induced in both genotypes. Endocannabinoids may have been overproduced in KO animals as a result of the lack of communication between receptors and ligands (14) or as a further consequence of the exacerbated allergic response. Keratinocytes are known to express CB1 receptors (4), although the expression of CB2 on these

Fig. 2. Contact allergy in cannabinoid receptor-deficient mice.

(A) $Cnr1^{-/-}/Cnr2^{-/-}$ and $Cnr1^{+/+}/Cnr2^{+/+}$ mice were sensitized (indicated by "s") with DNFB on the shaved abdomen. On day 5, mice were challenged (indicated by "c") with DNFB on the right ear. A second and third challenge was performed on day 13 and 21. Shown is the mean ear swelling over time \pm SEM



of a representative experiment with nine mice per group. Statistical significance was evaluated with the Wilcoxon-Mann-Whitney two-sample test (** $P < 0.01$). This experiment was independently repeated four times with similar results. (B) $Cnr1^{-/-}/Cnr2^{+/+}$, $Cnr1^{+/+}/Cnr2^{-/-}$, and $Cnr1^{-/-}/Cnr2^{+/+}$ mice were sensitized as described in (A). Ear swelling 48 hours after the third challenge of a representative experiment with eight mice per group is shown. Similar results were

obtained in four independent experiments with a total of 23 mice (** $P < 0.01$). (C) Contact allergic response in C57BL/6 mice after treatment with the indicated CB receptor antagonists. Ear swelling 48 hours after the second challenge of a representative experiment with 10 mice per group is shown. Similar results were obtained in four independent experiments with a total of 25 mice (** $P < 0.001$). Error bars in (B) and (C) indicate SEM.

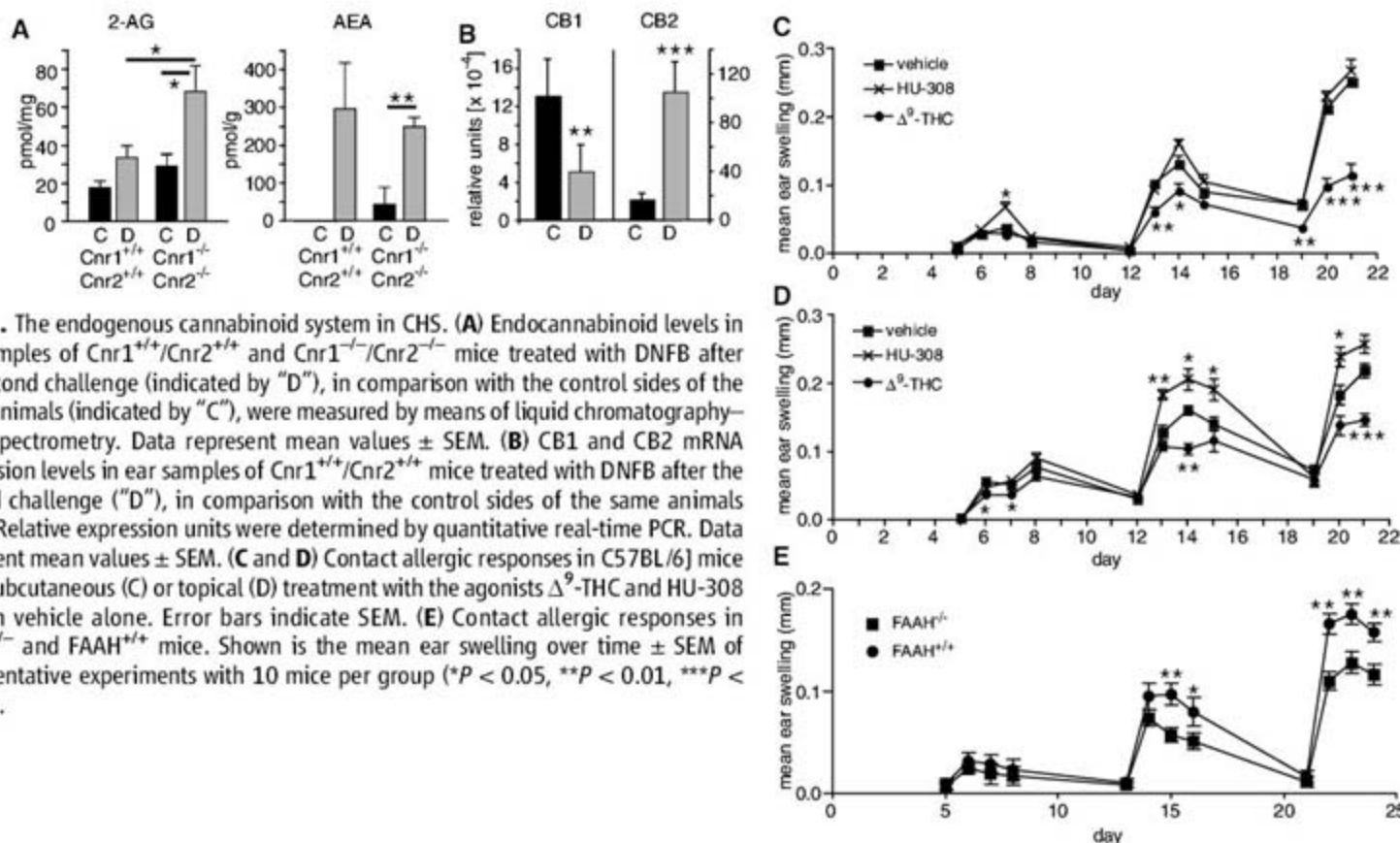


Fig. 3. The endogenous cannabinoid system in CHS. (A) Endocannabinoid levels in ear samples of $Cnr1^{+/+}/Cnr2^{+/+}$ and $Cnr1^{-/-}/Cnr2^{-/-}$ mice treated with DNFB after the second challenge (indicated by "D"), in comparison with the control sides of the same animals (indicated by "C"), were measured by means of liquid chromatography-mass spectrometry. Data represent mean values \pm SEM. (B) CB1 and CB2 mRNA expression levels in ear samples of $Cnr1^{+/+}/Cnr2^{+/+}$ mice treated with DNFB after the second challenge ("D"), in comparison with the control sides of the same animals ("C"). Relative expression units were determined by quantitative real-time PCR. Data represent mean values \pm SEM. (C and D) Contact allergic responses in C57BL/6 mice after subcutaneous (C) or topical (D) treatment with the agonists Δ^9 -THC and HU-308 or with vehicle alone. Error bars indicate SEM. (E) Contact allergic responses in $FAAH^{-/-}$ and $FAAH^{+/+}$ mice. Shown is the mean ear swelling over time \pm SEM of representative experiments with 10 mice per group (* $P < 0.05$, ** $P < 0.01$, *** $P < 0.001$).

cells has been debated (3, 12, 15). We could identify both receptor mRNAs in human HaCat keratinocytes (fig. S4). CB1 receptor mRNA was down-regulated in HaCat cells that had been stimulated for 24 hours with polyinosinic-polycytidylic acid and also in DNFB-exposed ears, whereas CB2 mRNA and protein expression was up-regulated in both cases (Fig. 3B and fig. S4). Taken together, these findings indicate that DNFB-induced CHS caused an activation of the endocannabinoid system in the skin and imbalanced expression of both receptors.

Because our data indicate that activation of the endocannabinoid system may function to dampen the CHS response, we considered the possibility that administration of cannabinoids such as Δ^9 -THC might attenuate CHS in WT animals. Therefore, after CHS was induced, we injected mice with Δ^9 -THC (5 mg per kilogram of body weight, administered subcutaneously) 30 min before, as well as 24 and 48 hours after, DNFB challenge. Indeed, Δ^9 -THC significantly decreased ear swelling (Fig. 3C) and reduced the recruitment of Gr-1⁺ granulocytes in comparison with swelling and granulocyte recruitment in untreated mice [vehicle: 483 ± 62 Gr-1⁺ cells per high power field (HPF) versus 200 ± 50 Gr-1⁺ cells per HPF in subcutaneous THC treatment]. A similar therapeutic effect of Δ^9 -THC was observed after topical application of 30 μ g of Δ^9 -THC 30 min before, as well as 24 and 48 hours after, DNFB administration (Fig. 3D). In contrast, the CB2-specific agonist HU-308 either showed no efficacy or even increased the allergic response after subcutaneous or topical application (Fig. 3, C and D) (13). It has recently been shown that leukocyte chemotaxis is inhibited by the CB2 receptor inverse agonist *N*-[1(S)-[4-[[4-

methoxy-2-[(4-methoxyphenyl)sulfonyl]phenyl]-sulfonyl]phenyl]ethyl]methanesulfonamide (Sch. 336) and, thus, HU-308 administration to the inflamed ear may have further increased leukocyte infiltration (16).

Because endocannabinoid levels were regulated in DNFB-treated ears and Δ^9 -THC had a beneficial effect on CHS, we asked whether mice having higher endocannabinoid levels would show altered allergic responses after DNFB treatment. Therefore, we analyzed the allergic reaction in mice lacking the enzyme fatty acid amide hydrolase (FAAH), which have augmented anandamide levels (17). As shown in Fig. 3E, we found a significantly decreased allergic response in FAAH KO mice after the second and third DNFB challenge when compared with the response in WT mice. Similar to our results, mice with only peripherally elevated fatty acid amides showed a reduced inflammation in the carrageenan foot-pad model (18). All data indicate that the anti-inflammatory responses were peripheral, rather than central, and that FAAH inhibitors are a potential therapeutic approach for inflammation (and a potentially useful alternative to direct CB1/CB2 agonists).

In order to gain insight into the molecular mechanism that may contribute to the increased magnitude of CHS in cannabinoid receptor-deficient mice, we performed a series of microarray experiments with RNA isolated from DNFB-treated ears of *Cnr1*^{-/-}/*Cnr2*^{-/-} and *Cnr1*^{+/+}/*Cnr2*^{+/+} mice, as well as from the untreated ears of control mice. In all, 830 probe sets were differentially expressed between control and DNFB-treated ears, of which 674 were up-regulated and only 156 were down-regulated. We grouped the probe sets by using gene ontology (GO) annotation

(19, 20) (Fig. 4A). Immune-related probe sets represented the largest group of differentially expressed genes (40 down-regulated and 117 up-regulated probe sets). Notably, large numbers of chemokine C-C and C-X-C motif ligands (21) and receptors were found in the up-regulated group (table S1) and represented 22% of the immune-related probe sets (table S2). Fifty-four genes were differentially expressed in DNFB-treated whole-ear specimens of *Cnr1*^{+/+}/*Cnr2*^{+/+} mice versus those of *Cnr1*^{-/-}/*Cnr2*^{-/-} mice (fig. S5). The only chemokine gene transcript in this group was monocyte chemoattractant protein 2 (MCP-2)/chemokine (C-C motif) ligand 8 (CCL8). Using real-time reverse transcription polymerase chain reaction (RT-PCR) and in situ hybridization, we confirmed the differential expression of MCP-2/CCL8 mRNA in keratinocytes (Fig. 4, B and C). Further in vitro experiments showed dynamic regulation of MCP-2/CCL8 production in activated keratinocytes through cannabinoid agonists (fig. S6). MCP-2/CCL8 is a member of the MCP family, which has been shown to play a major role in the recruitment of macrophages, activated lymphocytes, and mast cells into inflammatory sites (22, 23). Taken together, our results suggest that the endocannabinoid system regulates allergic inflammation through a modulation of the chemokine system.

The observation that the endocannabinoid system is activated in a model of CHS, together with the fact that genetic deletion or pharmacologic blockade of CB receptors enhanced contact allergic inflammation, whereas stimulation of CB receptors reduced such inflammation, strongly suggests that the endocannabinoid system serves to attenuate the inflammatory re-

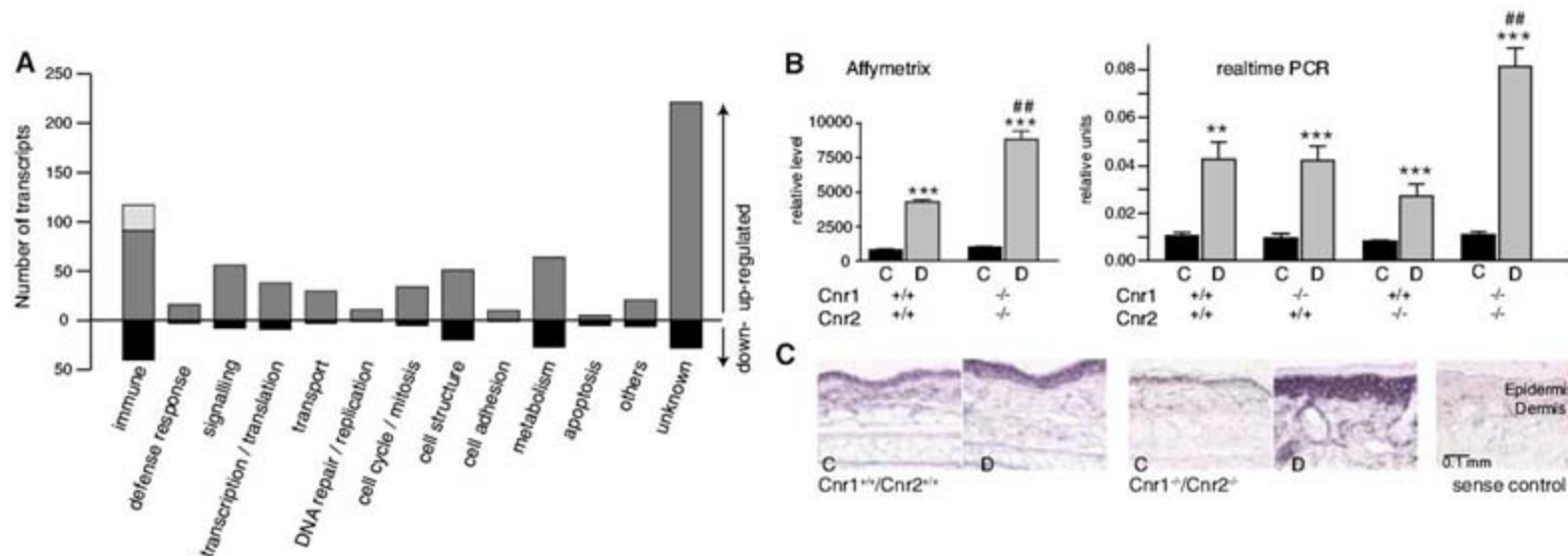


Fig. 4. Gene expression analysis. (A) Microarray analysis of ear samples of *Cnr1*^{+/+}/*Cnr2*^{+/+} and *Cnr1*^{-/-}/*Cnr2*^{-/-} mice treated with DNFB 48 hours after the second challenge ("D") in comparison with the control sides of the same animals ("C") revealed 674 up-regulated and 156 down-regulated probe sets in response to the treatment. Grouping was performed by GO annotation. Chemokine C-C motif and C-X-C motif ligands and receptors in the up-regulated group are presented in light gray in the column of immune-related genes. (B) Transcripts for the chemokine MCP-

2/CCL8 in DNFB-treated ears of *Cnr1*^{+/+}/*Cnr2*^{+/+} and *Cnr1*^{-/-}/*Cnr2*^{-/-} mice resulting from microarray expression study (left panel) and real-time RT-PCR quantification (right panel). Shown are representative results of three independent experiments (***P* < 0.01, ###*P* < 0.01, ****P* < 0.001). Error bars indicate SEM. (C) In situ hybridization with the use of a digoxigenin-labeled probe for MCP-2/CCL8 in ear tissue of DNFB-treated and control ears from *Cnr1*^{+/+}/*Cnr2*^{+/+} and *Cnr1*^{-/-}/*Cnr2*^{-/-} mice. The sense probe showed no staining.

sponse in cutaneous CHS. The finding that topical application of Δ^9 -THC reduced allergic inflammation points to the promising potential of developing pharmacological treatments (24) with the use of selective CB receptor agonists or FAAH inhibitors.

References and Notes

1. S. Grabbe, T. Schwarz, *Immunol. Today* **19**, 37 (1998).
2. T. Bisogno, A. Ligresti, V. Di Marzo, *Pharmacol. Biochem. Behav.* **81**, 224 (2005).
3. M. M. Ibrahim et al., *Proc. Natl. Acad. Sci. U.S.A.* **102**, 3093 (2005).
4. M. Maccarrone et al., *J. Biol. Chem.* **278**, 33896 (2003).
5. Materials and methods are available as supporting material on Science Online.
6. A. Zimmer, A. M. Zimmer, A. G. Hohmann, M. Herkenham, T. I. Bonner, *Proc. Natl. Acad. Sci. U.S.A.* **96**, 5780 (1999).
7. N. E. Buckley et al., *Eur. J. Pharmacol.* **396**, 141 (2000).
8. S. Werner et al., *Science* **266**, 819 (1994).
9. J. Knop, R. Stremmer, C. Neumann, E. De Maeyer, E. Macher, *Nature* **296**, 757 (1982).
10. R. I. Lehrer, J. Hanifin, M. J. Cline, *Nature* **223**, 78 (1969).
11. C. Nathan, *Nat. Rev. Immunol.* **6**, 173 (2006).
12. S. Oka et al., *J. Immunol.* **177**, 8796 (2006).
13. Y. Ueda, N. Miyagawa, T. Matsui, T. Kaya, H. Iwamura, *Eur. J. Pharmacol.* **520**, 164 (2005).
14. V. Di Marzo et al., *J. Neurochem.* **75**, 2434 (2000).
15. S. Stander, M. Schmelz, D. Metzke, T. Luger, R. Rukwied, *J. Dermatol. Sci.* **38**, 177 (2005).
16. C. A. Lunn et al., *J. Pharmacol. Exp. Ther.* **316**, 780 (2006).
17. B. F. Cravatt et al., *Proc. Natl. Acad. Sci. U.S.A.* **98**, 9371 (2001).
18. B. F. Cravatt et al., *Proc. Natl. Acad. Sci. U.S.A.* **101**, 10821 (2004).
19. J. S. Lee, G. Katari, R. Sachidanandam, *BMC Bioinform.* **6**, 189 (2005).
20. M. Ashburner et al., *Nat. Genet.* **25**, 25 (2000).
21. M. F. Bachmann, M. Kopf, B. J. Marsland, *Nat. Rev. Immunol.* **6**, 159 (2006).
22. A. de Paulis et al., *Int. Arch. Allergy Immunol.* **124**, 146 (2001).
23. D. D. Taub et al., *J. Clin. Invest.* **95**, 1370 (1995).
24. T. W. Klein, *Nat. Rev. Immunol.* **5**, 400 (2005).
25. This work was supported by grants from the Deutsche Forschungsgemeinschaft [SFB645 and GRK804 (to M.K. and A.Z.) and Tu90/5-1 (to T.T.)], by a Bonfor stipend to E.G., and a grant from Epitech S.r.l. to V.D.M. We thank M. Krampert for her help in wound healing experiments, L. Cristino for her help with immunohistochemistry, and J. Essig, A. Zimmer, E. Erxlebe, and I. Heim for technical assistance.

Supporting Online Material

www.sciencemag.org/cgi/content/full/316/5830/1494/DC1

Materials and Methods

Figs. S1 to S6

Tables S1 and S2

References

8 March 2007; accepted 4 May 2007

10.1126/science.1142265

Genome-Wide Mapping of in Vivo Protein-DNA Interactions

David S. Johnson,^{1*} Ali Mortazavi,^{2*} Richard M. Myers,^{1†} Barbara Wold^{2,3†}

In vivo protein-DNA interactions connect each transcription factor with its direct targets to form a gene network scaffold. To map these protein-DNA interactions comprehensively across entire mammalian genomes, we developed a large-scale chromatin immunoprecipitation assay (ChIPSeq) based on direct ultrahigh-throughput DNA sequencing. This sequence census method was then used to map in vivo binding of the neuron-restrictive silencer factor (NRSF; also known as REST, for repressor element-1 silencing transcription factor) to 1946 locations in the human genome. The data display sharp resolution of binding position [± 50 base pairs (bp)], which facilitated our finding motifs and allowed us to identify noncanonical NRSF-binding motifs. These ChIPSeq data also have high sensitivity and specificity [ROC (receiver operator characteristic) area ≥ 0.96] and statistical confidence ($P < 10^{-4}$), properties that were important for inferring new candidate interactions. These include key transcription factors in the gene network that regulates pancreatic islet cell development.

Although much is known about transcription factor binding and action at specific genes, far less is known about the composition and function of entire factor-DNA interactomes, especially for organisms with large genomes. Now that human, mouse, and other large genomes have been sequenced, it is possible, in principle, to measure how any transcription factor is deployed across the entire genome for a given cell type and physiological condition. Such measurements are important for systems-level studies because they provide a global map of candidate gene network input connections. These direct physical interactions between transcription factors or cofactors and the

chromosome can be detected by chromatin immunoprecipitation (ChIP) (1). In ChIP experiments, an immune reagent specific for a DNA binding factor is used to enrich target DNA sites to which the factor was bound in the living cell. The enriched DNA sites are then identified and quantified.

For the gigabase-size genomes of vertebrates, it has been difficult to make ChIP measurements that combine high accuracy, whole-genome completeness, and high binding-site resolution. These data-quality and depth issues dictate whether primary gene network structure can be inferred with reasonable certainty and comprehensiveness, and how effectively the data can be used to discover binding-site motifs by computational methods. For these purposes, statistical robustness, sampling depth across the genome, absolute signal and signal-to-noise ratio must be good enough to detect nearly all in vivo binding locations for a regulator with minimal inclusion of false-positives. A further challenge in genomes large or small is to map factor-binding sites with high positional resolution. In addition to making com-

putational discovery of binding motifs feasible, this dictates the quality of regulatory site annotation relative to other gene anatomy landmarks, such as transcription start sites, enhancers, introns and exons, and conserved noncoding features (2). Finally, if high-quality protein-DNA interactome measurements can be performed routinely and at reasonable cost, it will open the way to detailed studies of interactome dynamics in response to specific signaling stimuli or genetic mutations. To address these issues, we turned to ultrahigh-throughput DNA sequencing to gain sampling power and applied size selection on immuno-enriched DNA to enhance positional resolution.

The ChIPSeq assay shown here differs from other large-scale ChIP methods such as ChIPArray, also called ChIPchip (3); ChIP-SAGE (SACO) (3); or ChIPPet (4) in design, data produced, and cost. The design is simple (Fig. 1A) and, unlike SACO or ChIPPet, it involves no plasmid library construction. Unlike microarray assays, the vast majority of single-copy sites in the genome is accessible for ChIPSeq assay (5), rather than a subset selected to be array features. For example, to sample with similar completeness by an Affymetrix-style microarray design, a nucleotide-by-nucleotide sliding window design of roughly 1 billion features per array would be needed for the nonrepeat portion of the human genome. In addition, ChIPSeq counts sequences and so avoids constraints imposed by array hybridization chemistry, such as base composition constraints related to T_m , the temperature at which 50% of double-stranded DNA or DNA-RNA hybrids is denatured; cross-hybridization; and secondary structure interference. Finally, ChIPSeq is feasible for any sequenced genome, rather than being restricted to species for which whole-genome tiling arrays have been produced.

ChIPSeq illustrates the power of new sequencing platforms, such as those from Solexa/Illumina and 454, to perform sequence census counting assays. The generic task in these applications is to identify and quantify the molecular

¹Department of Genetics, Stanford University School of Medicine, Stanford, CA, 94305-5120, USA. ²Biology Division, California Institute of Technology, Pasadena, CA 91125, USA. ³California Institute of Technology Beckman Institute, Pasadena, CA 91125, USA.

*These authors contributed equally to this work.

†To whom correspondence should be addressed. E-mail: woldb@its.caltech.edu (B.W.); myers@shgc.stanford.edu (R.M.M.)

contents of a nucleic acid sample whose genome of origin has been sequenced. The very large numbers of short individual sequence reads produced by these instruments (currently ~400,000 reads of 200 nucleotides (nt), or ~40 million reads of 25 nt, per instrument run, depending on the platform used) are extremely well suited to making direct digital measurements of the sequence content of a nucleic acid sample. By determining a short sequence read from each of many (10^5 to 10^7) randomly selected molecules from the sample and then informatically mapping each sequence read onto the reference genome, the identity of each starting molecule is learned, and its frequency in the sample is calculated. Desired levels of sensitivity and statistical certainty needed to detect rare molecular species can be achieved, in principle, by adjusting the total number of sequence reads. Sequence census assays do not require knowing in advance that a sequence is of interest as a promoter, enhancer, or RNA-coding domain, as most current microarray designs do. Below, we use the Solexa/Illumina platform, because high-read numbers contribute to high sensitivity and comprehensiveness in large genomes.

We used ChIPSeq to build a high-resolution interactome map for human neuron-restrictive silencer factor (NRSF; also known as REST, for repressor element-1 silencing transcription factor). This zinc finger repressor negatively regulates many neuronal genes in stem and progenitor cells and in nonneuronal cell types, such as the Jurkat T cell line studied here (6). A primary reason for selecting NRSF as a test case is that prior studies provide a large set of known "gold-standard" target genes, including more than 80 *in vivo* binding sites defined by ChIP-QPCR (quantitative real-time fluorescence polymerase chain reaction) (7). A subset of these genes has also been tested for regulatory function by transfection assays (8). In addition, the DNA motif bound by NRSF, called NRSE (also called RE1), is long (21 bp) and well-specified (8). This has led to a rich group of computational models for the site and for all its occurrences in the human genome (7, 9–11). These sites provide a framework of explicit predictions that can now be tested by measuring repressor binding globally. Finally, there is a high-quality monoclonal antibody (12) that recognizes NRSF efficiently in ChIP experiments (7).

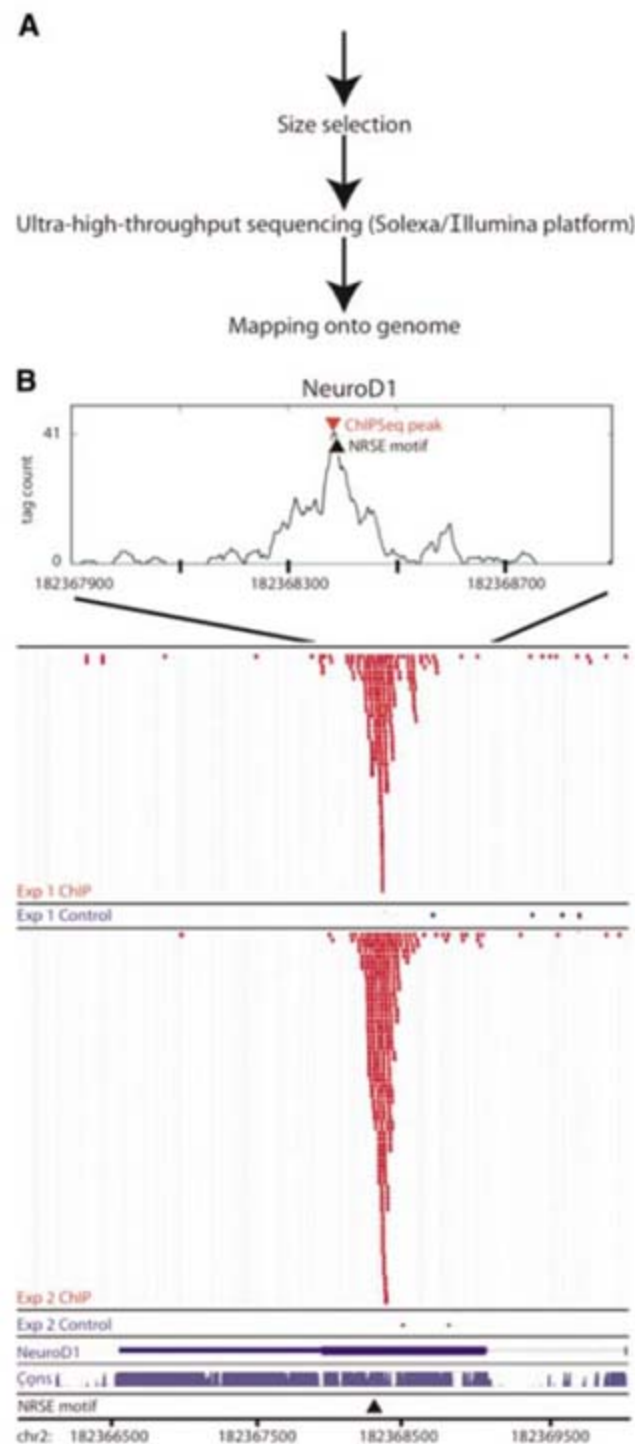
We prepared two DNA samples for each ChIPSeq experiment: an NRSF/REST-enriched ChIP sample and a companion control sample of the same fixed chromatin, but without immunoenrichment. In an effort to increase positional precision and to provide optimal substrate for the Solexa/Illumina sequencing platform, we introduced a size-selection step after cross-link reversal (Fig. 1A and fig. S2) (5). DNA sequencing of each sample was performed by the Solexa/Illumina protocol (13). Two to 5 million 25-nt sequence reads were produced per sample, of which about half mapped to single sites in the

human genome (table S1). Sequence reads that map to multiple sites in the genome were removed from subsequent analysis. This eliminates sequences in simple repeats, some complex repeats, and also 25-nt segments that are not unique by chance. The location of each remaining unique sequence read in the genome was recorded. To accommodate polymorphisms relative to the reference genome, up to two mismatches were allowed. The resulting sequence read distribution was processed with a ChIPSeq peak locator algorithm developed for this purpose (5). The algorithm finds a local concentration of sequence hits (a location cluster) and, within that location, calls a peak. We then required of these a minimum fivefold enrichment of sequence reads in the ChIP sample relative to the corresponding location in the control. Fivefold enrichment is a

conservative choice among enrichment thresholds commonly used in contemporary large-scale ChIP studies. A location that passed these criteria and also had 13 or more independent sequence reads (a threshold value selected based on the sensitivity and specificity analysis described below) was called an NRSF-positive binding event.

An example of primary ChIPSeq data from two independent experiments is shown in Fig. 1B for the *NEUROD1* locus. This positive signal, which has intermediate signal intensity and statistical certainty ($P = 8 \times 10^{-6}$), identifies a novel NRSF-binding target. The NRSF/REST sequence-tag distribution centers directly over the only canonical NRSE motif in a 4-kb region, which is located in the open reading frame of the *NEUROD1* gene. This site was called a

Fig. 1. ChIPSeq discovers NRSF/REST protein-DNA binding events with high resolution on a genome-wide scale. **(A)** Generalized scheme of ChIPSeq begins with ChIP, followed by size selection for recovered material (5), followed by standard preparation for Solexa/Illumina sequencing. An optional preamplification step after immuno-enrichment and before size selection can be inserted to work from smaller cell number input (used in experiment 2 below) (5). **(B)** Close-up view of ChIPSeq data mapped to a novel NRSF-binding site (NRSE; black arrowhead) located in the *NEUROD1* gene. Experiment 1 (no preamplification) and experiment 2 (with preamplification). Output from the peak-call algorithm is shown for this locus (red arrowhead), and corresponds closely with the sole NRSE in the *NEUROD* locus (black arrowhead).



ChIPSeq peak by the locator algorithm [open source available at (14)]. A previous study had implicated NRSF in repression of *NEUROD1*, but had failed to find a local site computationally. The authors theorized long-distance repression to explain the effect (15), but our results suggest a simpler explanation of a degenerate site within the *NEUROD1* gene itself. Over the entire primary data set (tables S2 and S3), the distribution of sequence-tag number per location ranged from the threshold value of 13 sequence tags to a maximum of 6718 tags at the highest signal (Fig. 2A and fig. S3). The two ChIPSeq experiments produced similar results (fig. S2), mapping 1946 shared enriched locations, most of which occur in or near 1020 genes.

NRSF-binding sites previously identified by QPCR or transfection assays (7, 8) plus a set of known negatives (5) were used to measure sensitivity (successful detection of true positives) and specificity (successful rejection of true neg-

atives) of the ChIPSeq assay. A ROC (receiver operator characteristic) analysis provides a way of measuring and graphically portraying sensitivity (fraction true positive on the y axis) versus specificity ($1 -$ the fraction of false-positives, displayed on the x axis) (Fig. 2B). Perfect sensitivity and specificity would produce an ROC curve that traces the y axis to a value of 1.0, which would extend across all possible x values to produce an area under the curve of 1.0. In contrast, entirely random classification by chance would produce an ROC area of ~ 0.5 . The observed ROC areas are high at 0.96 (shown) and 0.97 for the two independent experiments. The selected threshold of 13 sequence reads per region required for inclusion in the ChIPSeq interactome corresponds to a sensitivity of 87% and a specificity of 98%. We conclude that the ChIPSeq NRSF interactome measurements are accurate and, as suggested by P values (table S2), statistically robust. For rough comparison, a

recent ChIPPet study of the p53 interactome did not measure these parameters, but investigators estimated that less than 35% of the largest group of positive signals (Pet2 sites, which were defined by two paired end tags) are true sites, whereas the much more certain and smaller class (Pet3-and-above sites) likely misses more than half of true positives (4). In general, we expect that differences in immune reagent quality, epitope availability, and other aspects of design that affect all ChIP experiments, as well as interactome structure itself, will contribute to differences between studies.

We next assessed the precision of ChIPSeq site location relative to 771 computationally high-scoring NRSE motifs in the genome that also have positive ChIPSeq signals, by measuring the distance from the experimental ChIPSeq peak to the center of the computational NRSE sequence motif. In this group, 754 sites were ChIPSeq-positive in both experiments, and the center of a 21-bp NRSE motif was within ± 50 bp of the called ChIPSeq peak (5) for 94% of these (Fig. 2C). The resolution, which depends in part on size selection of sheared chromatin after immuno-enrichment (5), is much higher than is typical for ChIPchip or ChIP-SAGE (± 500 to 1000 bp) (3, 16).

How comprehensive are the NRSF ChIPSeq measurements? Several lines of evidence address this question. First, as shown in Fig. 2D, virtually all strong canonical NRSF motif instances across the human genome were detectably occupied. We defined strong sites as those having $\geq 90\%$ match to a previously developed motif model (a position-specific frequency matrix), which is based on evolutionarily conserved site instances across multiple mammalian genomes (5, 7). This high representation of detectable binding suggests that no strong sites were missed by undersampling. It also implies that all sites are accessible for NRSF/REST-binding in Jurkat cells, at least part-time in some individual cells, although the degree of accessibility might vary and may account for wide differences in the number of tags per site (Fig. 2A). Second, we observed ChIPSeq-positive signals for sites previously studied in detail by transfection analysis (8), and they correspond to a wide range of ChIPSeq signals, with all but one scoring positive in both ChIPSeq experiments. Taken together with the sensitivity results (Fig. 2B), these observations suggest that the NRSF/REST interactome measurements are genome-comprehensive and have been sampled deeply enough to include most sites known by any other criteria to be biologically active, even if relatively weakly. This level of genome completeness is attributable to the depth of Solexa/Illumina sequence sampling and is substantially greater than in prior studies of the adenosine 3',5'-monophosphate (cAMP) response element-binding protein (CREB) interactome measured by SACO (3) and the p53 interactome measured by ChIPPet (4).

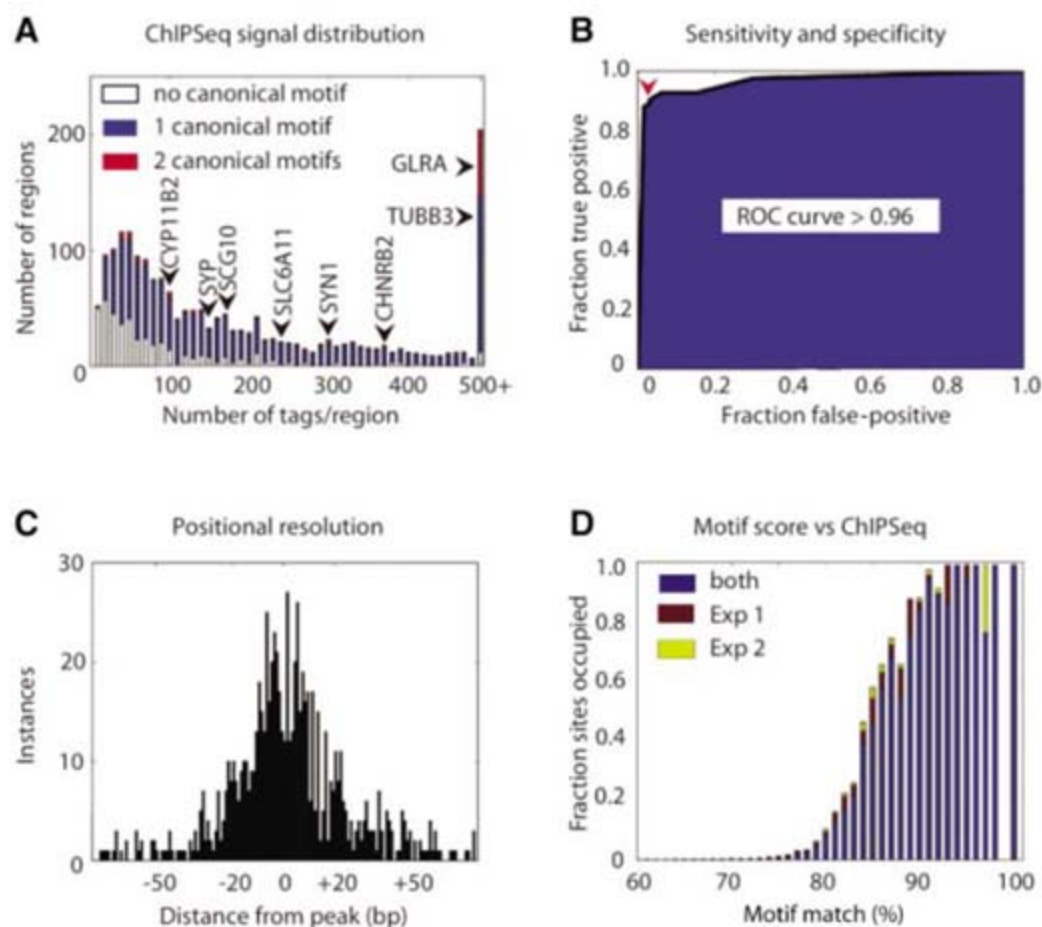


Fig. 2. (A) Histogram of all ChIPSeq-positive regions, as a function of sequence read number, that map within that region; zero (white), one (blue), or two or more (red) canonical motif instances defined as those scoring $\geq 70\%$ match to the position-specific frequency matrix (PSFM) model of the NRSF-binding site (7). (B) ROC analysis with area under the curve >0.96 for experiment 2 (shown) and >0.97 for experiment 1. This measures the performance of ChIPSeq in detecting previously validated true positives (83) and true negatives (130), as described in the text and (5). The threshold used for subsequent analysis corresponds to 87% and specificity 98%, as indicated by the arrowhead. ChIPSeq false-negatives corresponded to the lowest QPCR-positive validation values. (C) Distribution of the distance from the center of 771 high-scoring canonical NRSE motifs [84% or higher match to the PSFM motif model (7)] in ChIPSeq-enriched regions (experiment 1). In this example, 46% of peaks fall within the boundaries of NRSE (here, $+10$ to -10 bp), and 94% of the canonical NRSEs fall within 50 bp of the called experimental peak. (D) Site occupancy detected by ChIPSeq for NRSE motifs in Jurkat cells as a function of PSFM score (7).

We next asked whether NRSF binding in or near promoters is correlated with low levels of transcription, as expected for a transcriptional repressor. To answer this question, we looked for high-confidence promoter predictions (5) that occur within 1 kb of a ChIPSeq peak. We then assessed genome-wide transcript levels in Jurkat cells by hybridizing labeled RNA to Illumina RefSeq8 Sentrix arrays. The subset of 230 transcripts corresponding to promoters near NRSF-binding sites had significantly lower ($P = 1 \times 10^{-11}$) transcript signals than the full set of 20,589 transcripts (fig. S5). This argues that NRSF binding near promoters is significantly associated with transcriptional repression in these cells.

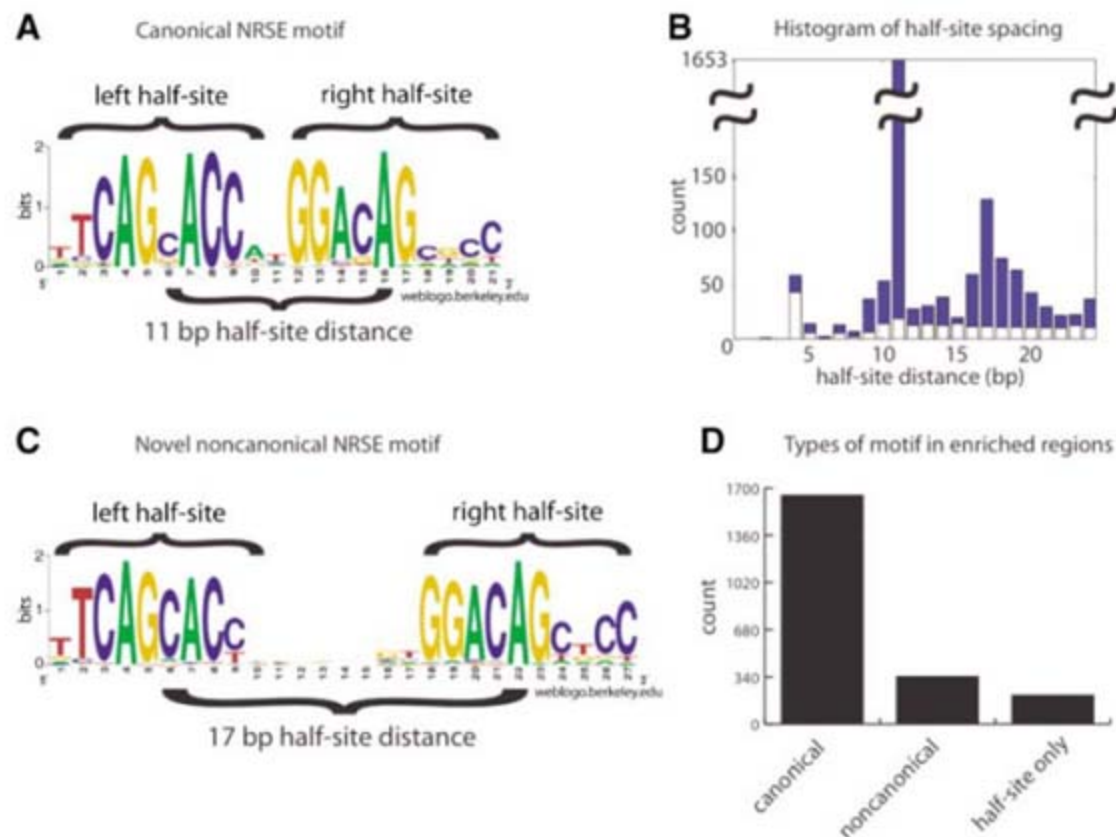
The positional resolution and low number of false-positives in these experiments can greatly facilitate motif-finding algorithms. The effect is to elevate the frequency of occurrence of true motifs within the input DNA relative to background sequences. This can improve signal-to-noise and also greatly reduce the run times for many algorithms. Much is known about the canonical NRSF-binding site (NRSE motif) (7, 10, 17), and this allowed us to ask if that site emerges when a sample of the experimental interactome peak domains are used. We first applied the motif-finding algorithm MEME (18) to all sites in the top 10% of signal intensity (100-bp segments from 198 regions having 500 reads or more). MEME returned the full previously known motif (table S4). Single or multiple matches to this canonical motif, using a 70% match threshold, account for 75% of all ChIPSeq regions mapped in this study.

We next focused attention on those remaining ChIPSeq-positive regions that have 300 or more ChIPSeq reads, yet have no canonical motif match. There are 22 such locations, and when they were run in MEME, only two candidate motifs stood out (table S5). By inspection, the large canonical NRSF-binding motif of 21 bp is naturally subdivided into two prominent, nonidentical, nonpalindromic half sites (Fig. 3A). The two motifs from the MEME search correspond directly to the separate left and right sides of the canonical motif. We next asked if these motifs occur at other ChIPSeq-binding locations and if they are organized in any discernible pattern. A distinctive pattern was discovered within 50 bp of many ChIPSeq peaks, in which left and right half-site motifs are separated by additional "spacer" sequence that increases the center-to-center distance from the canonical 11 bp to 16 to 19 bp, or decreases it by 1 bp to 10 bp (Fig. 3B and fig. S6). Thus, the canonical site has two central positions that have no sequence specificity, and the noncanonical group is similarly oriented but has increased the separation distance by an additional 5 to 9 bp (Fig. 3C). These linked half sites, oriented with respect to each other in the same way as in the canonical site, occur in NRSF ChIPSeq binding domains in a statistically significant manner relative to random sequence windows in the genome ($\chi^2 = 1309$ for the half-site distance of 17, P value of 0) and account for 197 regions lacking a canonical motif (Fig. 3B and fig. S4). We also found that some binding locations have multiple clustered occurrences of noncanonical motif(s) along with a canonical one.

There are no structural data available for NRSF, so we cannot relate this new family of binding-site motifs to a known DNA binding structure. However, the protein has eight zinc fingers in its DNA binding domain, and other C2H2 zinc finger proteins such as Zif268 bind DNA with three fingers per 10-bp turn, but they show considerable strain when binding with six fingers (19). This makes simultaneous binding of one molecule of NRSF to these noncanonical half-site configurations plausible, but it is also possible that the protein is bound to only one half site at a time by using a subset of its fingers in these cases. It will be interesting to learn if there are other functional and molecular characteristics that set these sites apart. For example, do the different NRSF co-repressors differ in their interactions at noncanonical sites compared with canonical ones (20, 21)?

We also asked whether half sites are significantly enriched in our ChIPSeq neighborhoods, without regard to orientation or spacing, relative to expectations based on their occurrence in the genomes, and found that these regions are greatly enriched for left-side half sites ($\chi^2 = 3070$) and right-side half sites ($\chi^2 = 11,674$). This range of configurations, from concentrated half sites to the noncanonical 16- to 19-bp-spaced left and right sites, to the canonical 11-bp-spaced full site, is quite striking. Significant NRSF binding occurs in vivo, according to our data, at all three kinds of loci. Because the half sites are much shorter than the full 21-bp NRSE motif, they also occur widely over the genome, presumably mainly by chance. This would mean that there is a rich pool of

Fig. 3. (A) Canonical NRSF-binding motif WebLogo (26). Its left and right half sites have a center-to-center distance of 11 bp. (B) Histogram of half-site distances in ChIPSeq-enriched regions, showing the observed (blue) and expected (white) counts (based on frequency in the genome). In addition to the expected canonical peak at distance 11 bp, there is also significant enrichment of half sites with noncanonical distances of 16 to 20 bp. (C) WebLogo of noncanonical NRSE with half-site distance of 17, showing the lack of conservation in the spacer nucleotides. (D) The 2214 NRSF-binding motifs predicted in the 1946 ChIPSeq-positive regions that contain canonical, noncanonical, or only half-site motifs.



possible binding sites from which higher affinity canonical sites could be gradually made and tested in evolution, as suggested previously (10). However, these sites were considered unlikely to interact with NRSF specifically (10), whereas, within the noncanonical motif family we define here, sites bind on their own, especially when clustered (fig. S6). This suggests a plausible multistep path by which the

target-site repertoire could evolve, beginning with clustered partial sites, passing through an intermediate and more specific orientation and spacing (the 10- or 16- to 19-bp-spaced family here), and eventually becoming refined into the canonical site (the 11-bp-spaced classic binding motif). Because there are more than 500 multi-zinc finger transcription factors encoded in the genome (22), many of which are evolving

rapidly in humans and mice, this strategy might be used by other members of the zinc finger family.

We found that genes encoding 110 transcription factors, 22 microRNAs, and five splicing regulators were occupied by NRSF. NRSEs occur prominently in introns (table S6), including a noncanonical site ($P = 4 \times 10^{-5}$) located about 500 bp downstream of the transcription start site of the *NRSF* gene itself, which suggests the possibility of negative autoregulatory feedback. We also found, as expected, that NRSF-bound loci are highly enriched in gene ontology (GO) terms related to neurons and their development (Fig. 4A). The enrichment for the experimentally determined sites exceeded that achieved for any computationally predicted target gene cohort. Synaptic transmission and nervous system development rank in the top three GO terms among 6000, with P values for overrepresentation of the NRSF target genes of 10^{-24} and 10^{-17} (5) (Fig. 4A). This group includes a set of transcription factors that have not previously been suggested as NRSF targets, but are known to be critical in the gene network that drives islet cell development in the pancreas. The transcription factors *NEUROD1/BETA2*, hepatocyte nuclear factors *HNF4a* and *HNF6/Onecut1*, and *Hes1* were all detected here for the first time as *in vivo* binding targets of NRSF, and together with *Neurogenin3*, which is a previously identified target (7), they are positioned critically in the regulatory network that controls pancreatic β cell development (Fig. 4B) (23). Although *in vivo* binding does not ensure NRSF repression activity, these regulators are known to function as positive drivers of pancreatic neuroendocrine development. If NRSF repression is active at all these sites, as might be the case in progenitor cells, the circuit would be effectively blocked. In this hypothesis, NRSF acts as a permissivity factor gating entry into and progress through the developmental pathway.

These pancreatic network sites are among the more modest ChIPSeq signals, ranging from 55 sequence reads for *HNF6* to 202 sequence reads for *NeuroD1*, values that are comfortably above the significance threshold of 13 (set on the basis of sensitivity/specificity considerations and known regulatory targets of Fig. 2, A and B), yet they fall in the bottom quartile. Thus, these ChIPSeq data were statistically robust enough to map parts of this gene network that might otherwise have gone undetected or been highly uncertain (Fig. 2A and fig. S3). There are precedents in other systems that show that relatively weak sites are biologically important, specifically because they are, in the biochemical binding sense, suboptimal. For example, in *Caenorhabditis elegans*, the *Pha4/FoxA* factor is the key activator of a large interactome, and a subset of target genes has suboptimal sequences and numbers of sites (24). In that system, when binding is suboptimal, it is believed

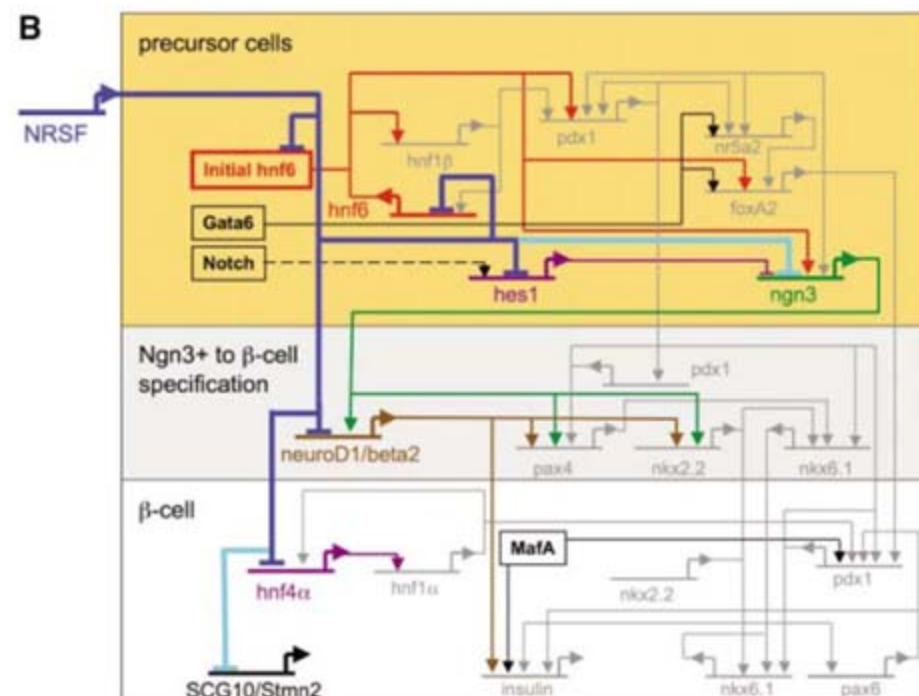
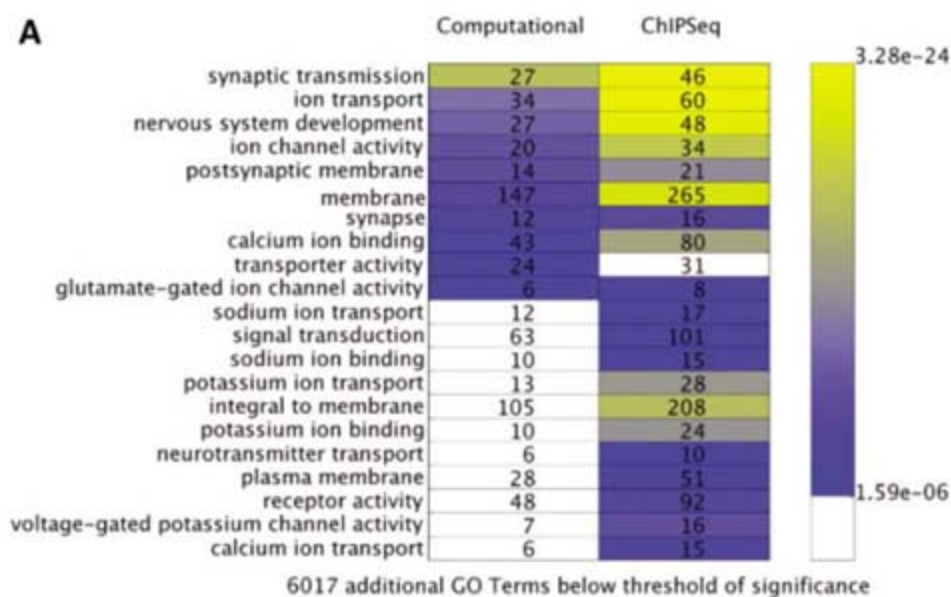


Fig. 4. (A) Gene ontology (GO) analysis of the computationally predicted cohort of NRSF target genes [genes scoring as $\geq 84\%$ match to the previously developed computational model for the NRSE motif (7)] compared with ChIPSeq-positive genes (right). P values for enrichment of GO terms above the significance threshold of 1.59×10^{-6} , which accounts for multiple hypothesis testing (7), are indicated by the color scale; GO terms below the significance threshold are in white boxes. ChIPSeq NRSE target genes are most enriched in synaptic transmission, nervous system development, and ion channel-activity functions (tables S1 and S2). (B) ChIPSeq data identified new candidate connections (blue) between NRSF and members of the pancreatic islet β cell-specification gene regulatory network [adapted from (23)]. Key transcription factors bound by NRSF, including *ngn3* and *neuroD1*, occupy positions high in the network that govern network activation and progression. ChIPSeq data also confirmed previously known NRSF targets (cyan) that include terminal differentiation genes such as *SCG10/stmn2* (25).

to help program the temporal order of action during development, with poor binders turning on at later times in the developmental progression, when *Pha4* levels are highest. By analogy, the regulators that govern the pancreatic network may be released from NRSF repression relatively early in down-regulation of the repressor to create a permissive state that must be established before the neuroendocrine development program is launched. Also following this logic, *SCG10/Stmn2* is a classic NRSF target gene that is expressed later in development in differentiated islet cells, and it displayed relatively higher ChIPSeq tag scores than most of the transcription factors that are positioned higher and earlier in the network. Independent evidence suggests that *SCG10/Stmn2* expression depends on relief from NRSF-mediated repression in islet cells (25). Targets of the regulatory class highlighted here (Fig. 4B) can also participate in positive autoregulatory and cross-regulatory interactions that we expect would stabilize and push forward the circuit once it begins (23). This makes a "protective" repressor, active in nonpancreatic cell types or progenitor cells, an attractive piece of regulatory logic.

The initial picture we have of the experimentally determined NRSF/REST interactome has been drawn for one cell type (Jurkat T cell line), and T cells express this factor at relatively high levels. In this cell environment, the interactome is composed of three broad classes of target loci with respect to binding motifs. First are loci defined by near-optimal canonical motifs, and virtually all of these bound the factor detectably *in vivo*. This suggests that for biochemically optimal sites, there is sufficient chromatin access and high enough DNA affinity to establish measurable occupancy, although the strength of the ChIPSeq signal among these sites varied over wide range. Second are loci containing instances of the noncanonical motif family (Fig. 3) or sites that are weaker matches to the canonical 21-bp site. Binding of sites in this class could not be predicted solely on the basis of their motif sequence. Several hundred instances showed significant binding, whereas thousands of others in this group had no detectable ChIPSeq signal. Binding-motif properties we do not yet appreciate, differential

chromatin access, or epitope exposure for subset of NRSF-containing complexes might discriminate the minority ChIP-positives in this group from the majority that are nonbinding. These observations argue that global experimental data are needed to discriminate motif instances occupied *in vivo* from many others that appear similar in motif quality, but are not similarly occupied, even for a factor like NRSF/REST, which has a well-specified binding-motif family. Finally, there is a third small, but interesting, class that binds NRSF/REST reproducibly, and in some cases quite robustly, but lacks any identifiable NRSE motif except for the presence of half sites (tables S2 and S7). It is uncertain if these are explained by their half-site content, because they make up a tiny minority of loci with superficially similar half-site content. This raises the possibility that NRSF/REST might associate indirectly, rather than directly, with a limited number of specific chromosomal locations.

ChIPSeq, as performed here, is relatively cost-effective; Solexa/Illumina platform sequencing costs per experiment are currently about half that of the most comprehensive human whole-genome tiling arrays. ChIPSeq sampling that is 10 to 20 times deeper than was used here is plausible now, within the general range of microarray costs, and this capacity may be needed for interactomes having many more sites per genome than NRSF. For example, it is possible that some widely used transcription cofactors or chromatin remodeling complexes might have on the order of 10^4 to 10^5 true-positive sites distributed over a wide dynamic range of occupancy levels, and such interactome structures will require correspondingly deeper sequence sampling. Other ultrahigh-throughput sequencing platforms, such as the one from 454 Life Sciences, could also be used to assay ChIP products, but whatever sequencing platform is used, our results indicate that read number capacity and input ChIP DNA size are key parameters.

References and Notes

1. T. H. Kim, B. Ren, *Annu. Rev. Genom. Hum. Genet.* **7**, 81 (2006).
2. ENCODE Project Consortium, *Science* **306**, 636 (2004).
3. S. Impey *et al.*, *Cell* **119**, 1041 (2004).
4. C. L. Wei *et al.*, *Cell* **124**, 207 (2006).

5. Materials and methods are available as supporting material on Science Online.
6. N. Ballas, G. Mandel, *Curr. Opin. Neurobiol.* **15**, 500 (2005).
7. A. Mortazavi, E. C. Thompson, S. T. Garcia, R. M. Myers, B. Wold, *Genome Res.* **16**, 1208 (2006).
8. C. J. Schoenherr, A. J. Paquette, D. J. Anderson, *Proc. Natl. Acad. Sci. U.S.A.* **93**, 9881 (1996).
9. A. W. Bruce *et al.*, *Proc. Natl. Acad. Sci. U.S.A.* **101**, 10458 (2004).
10. C. Zhang *et al.*, *Nucleic Acids Res.* **34**, 2238 (2006).
11. J. Wu, X. Xie, *Genome Biol.* **7**, R85 (2006).
12. Z. F. Chen, A. J. Paquette, D. J. Anderson, *Nat. Genet.* **20**, 136 (1998).
13. Solexa sequencing technology, www.illumina.com/pages/ilmn?ID=203.
14. ChIPSeq peak finder, available at <http://woldlab.caltech.edu>.
15. V. V. Lunyak *et al.*, *Science* **298**, 1747 (2002).
16. S. Cawley *et al.*, *Cell* **116**, 499 (2004).
17. N. C. Jones, P. A. Pevzner, *Bioinformatics* **22**, e236 (2006).
18. T. L. Bailey, C. Elkan, *Mach. Learn.* **21**, 51 (1995).
19. E. Peisach, C. O. Pabo, *J. Mol. Biol.* **330**, 1 (2003).
20. N. Ballas, C. Grunseich, D. D. Lu, J. C. Speh, G. Mandel, *Cell* **121**, 645 (2005).
21. M. Yeo *et al.*, *Science* **307**, 596 (2005).
22. S. Huntley *et al.*, *Genome Res.* **16**, 669 (2006).
23. E. H. Davidson, *The Regulatory Genome: Gene Regulatory Networks in Development and Evolution* (Academic Press/Elsevier, San Diego, CA, 2006).
24. J. Gaudet, S. E. Mango, *Science* **295**, 821 (2002).
25. F. Atouf, P. Czernichow, R. Scharfmann, *J. Biol. Chem.* **272**, 1929 (1997).
26. Web-based sequence logo generating application; Weblogo.berkeley.edu.
27. We thank G. Schroth and his group at Solexa/Illumina, Inc., for access to the sequencing platform, without which this work would not have been possible. We thank B. Anton, L. Nguyen, C. Medina, and L. Tsavaler for outstanding experimental work and K. F. McCue for invaluable counsel on statistical analyses. We are grateful to D. Anderson of Caltech for the gift of monoclonal antibody against NRSF. This work was supported by NIH grant U01 HG003162 to R.M.M. with a supplement to B.W. and by a grant from the Caltech Beckman Institute. A.M. was supported by NIH/National Research Service Award 5T32GM07616; B.W. by a Bren Chair endowment at Caltech, and R.M.M. by the Stanford W. Ascherman Chair endowment at Stanford University.

Supporting Online Material

www.sciencemag.org/cgi/content/full/1141319/DC1
Materials and Methods
Figs. S1 to S6
Tables S1 to S7
References

14 February 2007; accepted 26 April 2007
Published online 31 May 2007;
10.1126/science.1141319
Include this information when citing this paper.

EUV Light Source

Model 642 is an extreme ultraviolet (EUV) light source similar to sealed x-ray tubes. It makes use of a filament to produce electrons that are accelerated toward a target by high voltage. The interaction of the electrons as they impact the solid target (anode) causes excitation of the atomic inner shells with subsequent decay and emission. The output emission spectrum of the source follows the target anode material valence band structure. The model 642 source is not a sealed tube so users can exchange anodes in order to produce desired wavelengths, for example, boron for 6.7 nm, silicon for 13.5 nm, and aluminum for 17.1 nm. Many different anodes have been characterized and are available for purchase as accessories. The 642 also features two symmetrical output beams. It is useful for sample/reference comparison in a variety of test setups. The model 642 is stable, the output is debris-free, and the source is compact and controllable.

McPherson For information 800-255-1055 www.McPhersonInc.com



Neural Progenitor Cell Lines

The ReNcell product line of human immortalized neural somatic stem cell lines offers a convenient solution for scientists needing reproducible results with neurons easily derived from human cells. These progenitor cells are particularly useful in drug discovery applications, where the development of these pathways can be monitored during screening. The product line consists of two cell lines of immortalized human neural progenitor cells and media for the maintenance, expansion, and freezing of the cells. The cell lines and media are available either individually or as a kit.

Millipore For information 800-548-7853 www.millipore.com

Electronic Pipettors

New Excel Electronic Pipettors require little force for operation and offer various options for fast completion of pipetting tasks. Designed with ergonomics and efficiency in mind, they are available in single-channel, eight-channel, and 12-channel versions. In addition to standard mode for pipetting single volumes, the Excel pipettors can be set for repeat pipetting, sequential pipetting, automatic mixing, and serial dilutions. Each pipettor is supplied with a rechargeable lithium ion battery and charger.

Labnet International.
For information 888-522-6381
www.labnetlink.com

Protein Modification Software

Modiro, The PTM-Explorer, automates the identification of posttranslational modifications (PTMs) of proteins to provide more comprehensive information while reducing the time for analysis. PTMs modulate the activity of most proteins, and analysis of these modifications has become increasingly important for drug discovery and development. Modiro analyzes thou-

sands of mass spectrometry profiles in parallel to identify unknown mass shifts, sequence errors, and unspecific enzymatic cleavage of amino acids in high throughput. In a single step, Modiro enables these variances to be clearly visualized and evaluated via a unique interface. The analysis of many spectra in parallel, together with Modiro's analysis interface, provides a faster, more complete characterization of the protein than previously possible.

Protagen.
For information +49 (0) 231 9742 6300
www.protagen.de

Labeled Secondary Antibodies

High-quality, labeled secondary antibodies are available for use in single-labeling and double-labeling experiments, fluorescence-activated cell sorting, enzyme-linked immunoadsorbent assays, detection assays, and protein immunoblotting applications. This series of antibodies is available either unconjugated or conjugated to an enzyme, biotin, or fluorophore.

Millipore.
For information 800-548-7853
www.millipore.com

Stem Cell Identification Tool

The Aldefluor fluorescent reagent system offers a novel approach to the identification, evaluation, and isolation of stem and progenitor cells based on their expression of the enzyme, aldehyde dehydrogenase (ALDH), rather than cell surface phenotype. The system identifies only viable cells with an intact cellular membrane. There is no need for antibody staining and it is nontoxic both in vivo and in vitro. It can be used with cryopreserved or fresh samples, and is optimized for human bone marrow, umbilical cord blood, apheresis, and peripheral blood. It is adaptable for use with other species and cell types, including tumor cells. It detects stem and progenitor

cells in multiple lineages, including hematopoietic, mesenchymal, endothelial, and neural.

StemCell Technologies.
For information 800-667-0322
www.stemcell.com

Agarose Coupling Kits

The Hook Agarose Coupling Kits are available for the coupling of proteins and peptides to agarose resin for diverse research applications. Researchers have the option of obtaining individual reagents or complete kits with all the necessary reagents. The kits are suitable for preparing affinity columns and resins for the purification of antibodies or interacting proteins.

G-Biosciences/Genotech.
For information 800-628-7730
www.GBiosciences.com

Sterile Plates for Cell Growth

BactiGrowth plates offer a contamination-free deep-well microplate optimized for high-yield growth of bacteria, yeast, and mammalian or insect cell lines. Produced under class 10,000 clean-room conditions from ultra-pure grade polypropylene, BactiGrowth plates contain no contaminants to leach out and affect bacterial or cell growth. BactiGrowth plates are available in a choice of well formats (24-, 96-, and 384-well) and well volumes from 300 μ l to 10 μ l per well to suit most cellular growth applications.

Porvair Sciences.
For information +44 1932 240255
www.porvair-sciences.com

Newly offered instrumentation, apparatus, and laboratory materials of interest to researchers in all disciplines in academic, industrial, and government organizations are featured in this space. Emphasis is given to purpose, chief characteristics, and availability of products and materials. Endorsement by *Science* or AAAS of any products or materials mentioned is not implied. Additional information may be obtained from the manufacturer or supplier.

Classified Advertising



From life on Mars
to life sciences

For full advertising details, go to
www.sciencecareers.org and click on
For Advertisers, or call one of our representatives.

United States & Canada

E-mail: advertise@sciencecareers.org
Fax: 202-289-6742

IAN KING Recruitment Sales Manager
Phone: 202-326-6528

NICHOLAS HINTIBIDZE
West Academic
Phone: 202-326-6533

DARYL ANDERSON
Midwest/Canada Academic
Phone: 202-326-6543

ALLISON MILLAR
Industry/Northeast Academic
Phone: 202-326-6572

TINA BURKS
Southeast Academic
Phone: 202-326-6577

Europe & International

E-mail: ads@science-int.co.uk
Fax: +44 (0) 1223 326532

TRACY HOLMES Sales Manager
Phone: +44 (0) 1223 326525

CHRISTINA HARRISON
Phone: +44 (0) 1223 326510

ALEX PALMER
Phone: +44 (0) 1223 326527

LOUISE MOORE
Phone: +44 (0) 1223 326528

Japan

JASON HANNAFORD
Phone: +81 (0) 52-757-5360
E-mail: jhannaford@sciencemag.jp
Fax: +81 (0) 52-757-5361

To subscribe to Science:
In U.S./Canada call 202-326-6417 or 1-800-731-4939
In the rest of the world call +44 (0) 1223-326-515

Science makes every effort to screen its ads for offensive and/or discriminatory language in accordance with U.S. and non-U.S. law. Since we are an international journal, you may see ads from non-U.S. countries that request applications from specific demographic groups. Since U.S. law does not apply to other countries we try to accommodate recruiting practices of other countries. However, we encourage our readers to alert us to any ads that they feel are discriminatory or offensive.

ScienceCareers.org

We know science



POSITIONS OPEN

**GROUP LEADER POSITION, BREAST
CANCER/MOLECULAR ONCOLOGY**
British Columbia Cancer Agency Research Centre
Vancouver, British Columbia, Canada

A junior Group Leader position is available immediately for an investigator to join the Molecular Oncology/Breast Program at the British Columbia Cancer Agency Research Centre ([website: http://www.bccrc.ca](http://www.bccrc.ca)). The Molecular Oncology Department is housed within a recently opened 250,000 square-foot research facility that houses 50 principal investigators and state-of-the-art facilities for mouse genetics, imaging, flow cytometry, genomics, molecular pathology, and high throughput screening.

The Department is seeking a young investigator with research interests in any aspect of quantitative biology applicable to breast cancer, to complement existing strengths in molecular pathology, cell biology, tumour genetics, mouse genetics, and high throughput siRNA screening. Applicants will have excellent communication skills and will be expected to contribute towards teaching medical students and/or graduate students.

Initial salary support for up to five years and a startup package will be available, and qualified candidates will be eligible for an **ASSISTANT PROFESSOR** level appointment at the University of British Columbia. Applicants should submit curriculum vitae, three letters of reference, and a three-page summary of a research proposal to **Jenny Cromarty** (e-mail: jcromarty@bccrc.ca). Informal enquires may be directed to the **Department Head, Dr. Samuel Aparicio** (e-mail: saparicio@bccrc.ca).

University of British Columbia and BCCRC hire on the basis of merit and are committed to employment equity. We encourage all qualified persons to apply; however Canadians and permanent residents of Canada will be given priority.

Closing date for applications: August 2007.

**ANTICIPATED ASSISTANT or
ASSOCIATE PROFESSOR
(Tenure Track)**
Comparative Biomedical Sciences

Department with numerous funded investigators in cell and molecular biology (including cancer biology) seeks a faculty person in cancer-related research. Required qualifications: Ph.D. or equivalent degree in biological/biomedical sciences or related field; postdoctoral experience; research background in the cell/molecular biology of cancer; ability to teach in the graduate and professional program; have (or will have) extramural funding. Additional qualifications desired: gene or stem cell therapy research experience. Responsibilities: establishes and maintains an extramurally funded research program in cancer-related research; participates in the graduate program and in teaching. Salary and rank will be commensurate with qualifications. An offer of employment is contingent on a satisfactory pre-employment background check. Application deadline is July 31, 2007, or until candidate is selected. Submit letter of application and resume (including e-mail address) to:

Dr. Shulin Li, Associate Professor
Department of Comparative Biomedical Sciences
School of Veterinary Medicine
Louisiana State University
Reference: #027360
Baton Rouge, LA 70803
Telephone: 225-578-9758
E-mail: sli@vetmed.lsu.edu

LSU is an Equal Opportunity/Equal Access Employer.

**RESEARCH HEALTH SCIENTIST, Saint
Louis VA Medical Center.** Three-year term position focusing on malaria. Review published scientific literature, prepare research protocols, design experiments, independently collect and evaluate research data, and prepare manuscripts and grant applications for submission to appropriate journals and national granting agencies. To apply, contact **Alice Taylor**, telephone: 314-894-6620. For additional information about the position, contact **Dr. Coy Fitch**, telephone: 314-289-7030. *Equal Opportunity Employer.*

POSITIONS OPEN

VISITING ASSISTANT PROFESSOR
Ecology and Evolutionary Biology
Tulane University

The Department of Ecology and Evolutionary Biology at Tulane University is accepting applications for the position of Visiting Assistant Professor (two appointments) during the 2007-2008 academic year. Each appointment will involve the equivalent of a three-course load each semester. Teaching assignments will include lecture courses and freshman laboratories. The salary is competitive and benefits are included. Applications should include a statement of interest (including teaching philosophy and courses one could teach), curriculum vitae, and three letters of recommendation that specifically address teaching experience and capabilities. Send application materials via e-mail: jbattis@tulane.edu and by mail to: **Visiting Assistant Professor Search, Department of Ecology and Evolutionary Biology, Tulane University, New Orleans, LA 70118**. Review of applications will begin 15 June 2007, and the search will remain open until the positions are filled. *Tulane University is an Affirmative Action/Equal Employment Opportunity Employer.*

The Department of Veterinary Physiology and Pharmacology, College of Veterinary Medicine and Biomedical Sciences, Texas A&M University, announces the availability of a **TENURE-TRACK FACULTY POSITION** (open rank). We seek an individual whose area of research focuses on endocrine regulation of the cardiovascular system or processes/disease conditions that directly involve both endocrine function and the cardiovascular system. Preference will be given to applicants whose research questions exhibit bench-to-bedside relevance and the ability to potentially collaborate with departmental faculty with related research interests. Opportunities exist to collaborate with faculty in the Colleges of Agriculture and Life Science, Engineering, Medicine, Science and Veterinary Medicine and the DeBakey Institute for Comparative Cardiovascular Science and Biomedical Devices. A strong research program and evidence of a commitment to excellence in teaching are required. Departmental faculty and their interests can be identified at [website: http://www.cvm.tamu.edu/vtpp](http://www.cvm.tamu.edu/vtpp). Evaluation of applications will begin July 1, 2007, and continue until the position is filled. Candidates should send curriculum vitae, letter of application, and names and addresses of three references to:

Dr. Timothy A. Cudd
Department of Veterinary Physiology and
Pharmacology
Texas A&M University
College Station, TX 77843-4466
Telephone: 979-862-1972, fax: 979-845-6544
E-mail: tcudd@cvm.tamu.edu

Texas A&M University is an Equal Opportunity Employer/Educator.

The Appalachian Laboratory, University of Maryland Center for Environmental Science (UMCES) invites applications for a tenure-track position to collaborate with UMCES faculty on issues concerned with the impact of climate change on terrestrial and/or aquatic ecosystems. Applicants must have completed a Ph.D. and have demonstrated an ability to generate external research funding. This appointment will be at the **ASSISTANT or ASSOCIATE PROFESSOR** level depending on applicant's qualifications. Send application materials (see [website: http://www.al.umces.edu/about/employment.htm](http://www.al.umces.edu/about/employment.htm) for details) to: **Climate Search Chair, Appalachian Laboratory, University of Maryland Center for Environmental Science, 301 Braddock Road, Frostburg, MD 21532**. Review of applications will begin September 1, 2007, and will continue until the position is filled. *UMCES is an Affirmative Action/Equal Opportunity Employer.*

North Carolina: Opportunity and Community

By Emma Hitt

Trees, tees, and Ph.D.s” is the phrase locals use to portray North Carolina’s Research Triangle Park (RTP), an 8-mile by 2-mile area bordered by Chapel Hill, Raleigh, and Durham. The area does, in fact, boast one of the highest per capita concentrations of Ph.D.s. Only the street-level concrete signs reveal the region’s foremost function; the peaceful, tree-lined roads winding through rolling hills are more in keeping with the scenery of a nature reserve than that of a hotbed of scientific research.

One should not underestimate the area, however. The entire state of North Carolina ranks third in the nation, behind Boston and California, for its number of biotechnology companies, according to Ernst and Young’s 2006 Industry Survey, and nearly 400 bioscience companies—albeit hidden behind pine trees—are headquartered or have operations in the state. The RTP itself is the largest planned research park in the world and contains more than 150 companies (132 R&D-related), employing about 40,000 people, and continues to expand, unbounded by geographical limits.

Research Focus

The effort to transform the Raleigh-Durham region—and also the entire state of North Carolina—into a technology and research leader began in the 1950s. RTP, the focal point of that effort, opened in 1959, with its first tenant, Research Triangle International, now the nation’s second largest independent nonprofit research organization. The region is also home to several biomanufacturing and pharmaceutical plants including Merck, GlaxoSmithKline (GSK), Wyeth, and Novartis as well as one of the largest concentrations of contract research organizations in the world.

Pharmaceutical and biopharmaceutical R&D is the leading industry in the area. In addition, three of the world’s largest agribusiness companies—Bayer CropScience, Syngenta Biotechnology, and BASF Corp.—have headquarters in the region. Other clusters of industry include biological agents and infectious diseases, analytical instrumentation, nanoscale technologies, and informatics. The area also accommodates a smattering of high-tech companies, including IBM, SAS, Cisco, and Nortel.

“We conduct our fair share of true academic and industrial research, but an area of science that is focused on here perhaps more than in other research-intensive areas is bioprocess science—the actual production and manufacture of biological therapeutics,” says **Maria Rapoza**, vice president of science and technology for the North Carolina Biotechnology Center, a government-sponsored organization dedicated to developing the biotechnology industry here. “It’s an exciting and lucrative area of opportunity for Ph.D.-level scientists,” she adds.

Growth in Industry

Opportunities for scientists in industry, at companies both small and large, abound. Biolex Therapeutics, a small company (just over 100 employees), is developing and commercializing therapeutic proteins based on its proprietary LEX System, an expression system that enables the production of hard-to-make proteins and the optimization of monoclonal antibodies. “We are not only researching but also developing drugs,” says **Jan Turek**, CEO of Biolex, “and the development of these drugs requires people who have experience in both clinical drug development as well as the manufacturing of those drugs.”

On a larger scale, GlaxoSmithKline (GSK), which has about 5,000 employees, is hiring scientists with expertise in a number of different disciplines, including medicinal chemistry, biostatistics and bioinformatics, toxicology, pharmaceutical development, medical genetics, and clinical pharmacology, says GSK spokesperson **Robert P. Sutton**. Likewise, Talecris Biotherapeutics is hiring in all areas of the organization, “from science and R&D to [continued](#) »



“It’s an exciting and lucrative area of opportunity here for Ph.D.-level scientists.”



From Top: **Maria Rapoza**; **Dr. Giles Shih**, President of BioResource International, is using biotechnology to develop natural feed additive enzymes for poultry diets; **North Carolina Biotechnology Center**

UPCOMING FEATURES

International Careers Report: UK and Ireland — June 22

Careers in Chemistry — August 10

Postdoc Scientist Survey — August 31

Regional Focus: North Carolina

“We have a number of different mechanisms available to continue to keep this as an exciting and dynamic environment for research.”

—Larry Reiter



finance and manufacturing,” notes spokesperson **Lacy McMahon**. The growth at Talecris shows no signs of slowing down, says McMahon. “We added over 900 employees last year through an acquisition and hired several more on top of that, and we will be hiring more people next year as well.”

By all accounts, the growth of the region is extensive. Within the last three years, 90,000 new jobs have been added to the 13-county region surrounding RTP, according to the Research Triangle Regional Partnership. Recent biopharmaceutical additions to the area include a \$100 million expansion of the operations of Quintiles Transnational. In addition, both Novartis and Merck are building vaccine manufacturing plants costing upwards of \$200 million. Major planned expansions have also been announced by Wyeth, Novo Nordisk, GSK, and other companies. Fueling some of the growth are tax credits available for the purposes of job creation and property purchases as well as state-funded industrial training for workers at local community colleges, which make the area an attractive destination for companies.

Local Government Agencies

RTP is also home to two major US government health and environmental agencies: the National Institute of Environmental Health Sciences (NIEHS) and the Environmental Protection Agency (EPA), making the area the largest concentration of environmental sciences research in the world.

The EPA, perched on the side of a lake, directly opposite the NIEHS, has an army of over 2,000 scientists strongly focused on scientific research. “Many people and businesses attribute policy-making and regulation of pollution to the EPA,” notes EPA spokesperson **Cynthia Yu**. “But our focus here is more on improving the environment through scientific research so that informed, evidence-based decisions can be made.”

Across the lake, the NIEHS is planning its first outpatient clinical research unit to help bridge the gap between bench science and patient care and which will provide training opportunities, especially for physician scientists. According to **Perry Blackshear**, director of clinical research at NIEHS, the unit will include a modular building of around 11,000 square feet where patients can have blood, urine, and other samples taken and can be assessed for a variety of environmental exposures. He says the agency is actively seeking tenure-track M.D./Ph.D. scientists to work in the clinical research unit.

Notably, the EPA and the NIEHS ranked third and seventh, respectively, in a 2007 survey of best places to work for postdocs, conducted by *The Scientist*. The rankings took into account several factors, including training and access to state-of-the-art technology, availability of benefits such as health care, and starting salary. Starting salaries at the NIEHS and EPA are \$42,000 to \$65,000 and \$45,106 to \$85,037, respectively, while the average annual salary of RTP employees overall is about \$56,000.

Collaborative Efforts

A strong collaboration exists between industry, government, and the local universities in the area. “Having the opportunity to collaborate with a community of scientists is a real advantage,” says postdoctoral trainee **Jamie DeWitt**, with the EPA’s National Health and Environmental Effects Research Laboratory (NHEERL). “There’s a scientist doing something of everything down here—you can explore any type of science you want.” DeWitt also points out that the scientists at EPA communicate regularly with scientists at NIEHS and work closely with industry.

The immediate area surrounding RTP is home to three major universities: Duke, University of North Carolina (UNC) at Chapel Hill, and North Carolina State University. NC State is the largest school in the region, with an enrollment of nearly 30,000 students, and was ranked by MIT Technology Review as No. 12 in a national survey of technology-transfer strength, a measure, among other things, of the number of patents issued.

RTP becomes the logical home to much of the technology spawned at local universities. The technology produced by Biolex, for example, was initiated at NC State. “Obviously since our technology came from one of the major universities here, it made sense for the company to establish its business nearby,” notes Turek. “This region is well known for its universities, so the ability to attract strong, research-oriented people has not been a challenge,” he adds.

According to **Marcia Harris**, director of University Career Services with UNC-Chapel Hill, a number of advantages exist for UNC students due to the presence of multiple employers as well as professional associations and other universities. “The students here have a lot of resources available to them.” Harris estimates that about a third of graduating Master’s and Ph.D. students from UNC remain in the immediate area after graduating.

Talecris and GSK both say the universities provide an important resource in terms of conducting research and as a source of qualified people. The proximity of research universities ranked as the Triangle’s greatest strength while the availability and retention of top technical, nontechnical, and management talent registered as the most significant concern, according to one 2007 survey of RTP bio-science entrepreneurs.

Larry Reiter, director of the National Exposure Research Laboratory (NERL) at the EPA, also points out that in addition to federal postdoctoral research programs at his institution, the EPA has developed cooperative training agreements with UNC, Duke, and others, allowing predoctoral students to do their thesis research under scientists at EPA. “We also bring in faculty members from universities that are interested in doing a sabbatical and working in our labs for up to two years. So, we have a number of different mechanisms available to continue to keep this as an exciting and dynamic environment for research,” he says.

Likewise, the NIEHS offers its Summers of Discovery Program, a full-time, 8- to 12-week program during May to September, open to teachers and college faculty, graduate, undergraduate, and high-school students, which according to Blackshear, is a “good way to test out working at the institution.”

Seeding Science

While the RTP remains the focal point of scientific research in the area, smaller annexes are beginning to colonize [continued »](#)

2008 Grant Programs for Physician-Scientists

**BURROUGHS
WELLCOME
FUND** 

919.991.5100
www.bwfund.org

The Burroughs Wellcome Fund is an independent private foundation dedicated to advancing the biomedical sciences by supporting research and other scientific and educational activities.

2008 Clinical Scientist Awards in Translational Reserach

Deadline: August 15, 2007

\$750,000 over five years for established physician-scientists

- Candidates must have an M.D. or M.D.-Ph.D. degree, hold an appointment or joint appointment in a subspecialty of clinical medicine, and hold a current license to practice medicine in the U.S. or Canada.
- Candidates must be academic investigators at the assistant professor or early associate professor level, holding a tenure-track or equivalent position at the time of application.
- BWF is interested particularly in supporting investigators who will bring novel ideas and new approaches to translational research.
- Degree-granting institutions in the United States and Canada may nominate from two to four candidates.

Career Awards for Medical Scientists

Deadline: October 1, 2007

\$700,000 over five years for established physician-scientists

- Candidates should have an M.D., D.D.S., D.V.M., Pharm.D., or equivalent clinical degree.
- Proposals must be in the area of basic biomedical, disease oriented, translational, or molecular, genetic, or pharmacological epidemiology research. Proposals that are in the area of epidemiology should contact BWF to determine the eligibility of the proposal. Proposals in health services research or involving large-scale clinical trials are ineligible.
- BWF encourages proposals in reproductive science.
- Candidates must have at least two years of research experience and be in a mentored position at the time of application.
- The award must be taken at a degree-granting institution in the United States or Canada.
- During the award period, at least 75 percent of the awardee's time must be devoted to research-related activities.

Complete program information, eligibility guidelines, and application forms are available on BWF's website at www.bwfund.org.

Regional Focus: North Carolina



BASF Corp.
www.basf.com

Bayer Crop Science
www.bayercropscience.com

Biolex Therapeutics
www.biolex.com

Cisco
www.cisco.com

Duke University
www.duke.edu

GlaxoSmithKline
www.gsk.com

IBM
www.ibm.com

Merck
www.merck.com

National Exposure Research Laboratory
www.epa.gov/nerl

**National Health and Environmental
 Effects Research Laboratory**
www.epa.gov/nheerl

Nortel
www.nortel.com

North Carolina Biotechnology Center
www.ncbiotech.org

North Carolina Research Campus
www.ncresearchcampus.net

North Carolina State University
www.ncsu.edu/

Novartis
www.novartis.com

Novo Nordisk
www.novonordisk.com

Quintiles Transnational
www.quintiles.com

SAS
www.sas.com

Syngenta Biotechnology
www.tmri.org

Talecris Biotherapeutics
talecris.com

University of North Carolina at Chapel Hill
www.unc.edu/

US Environmental Protection Agency (EPA)
www.epa.gov

**US National Institute of Environmental
 Health Sciences**
www.niehs.nih.gov

Wyeth
www.wyeth.com

around the state. Another emerging area, about 100 miles to the west of RTP, is the Piedmont Triad (Greensboro, Winston-Salem, and High Point). "The activity in the RTP region is the fruit of over 20 years of investments," says **Kathleen Kennedy**, vice president of education and training with the North Carolina Biotechnology Center. "We hope to start that again and clone this type of development in other regions around North Carolina," she says.

An intriguing story is the North Carolina Research Campus (NCRC) in Kannapolis, a small town just north of Charlotte, on Interstate 85 and a few miles south of the Piedmont Triad. In July 2003, the town of Kannapolis became the epicenter of the largest mass layoff in North Carolina's history, when a Pillowtex Corporation plant was affected by a general slowdown of the state's textile industry; 4,800 workers lost their livelihood. But in December 2005, Rupert Murdock, owner of Dole Food Company, donated \$1 billion to establish the research campus there. The NCRC, now under construction, will be devoted to the study of nutrition, crop development, produce development, and the genomics of nutrition, and will include 350-acres of state-of-the-art laboratory space. Duke, UNC, NC State, and others all will have laboratories on the planned multibuilding campus.

"Extensive opportunities for the training of residents, including laid off workers, will continue to be available so that they can prepare for employment at the NCRC; the NC Community College System will have a training center on the Kannapolis NCRC campus for precisely this purpose," notes NC Biotech's Kennedy. "My guess is that the NCRC will change the shape of economic development in that region north of Charlotte and will help stimulate the development of research areas along the I-85 corridor," she adds.

Another research focus of the area is marine biology, scattered along the state's 300-mile-long coastline. "Many people are unaware of the wealth of marine research that is here in North Carolina," says NC Biotech's Rapoza. "We really have the equivalent of Woods Hole here—it's just spread over a number of different marine labs and institutes." Duke University's marine lab, for example, is located in coastal Beaufort and offers a year-round curriculum for undergraduates as well as research facilities for postdocs and faculty.

An Agreeable Life

A number of lifestyle factors make the area attractive to many people seeking to relocate, and the region has ranked high on a number of "best-of" lists. Raleigh-Cary was ranked as the No. 1 Best US City for Jobs by *Forbes* in February 2007, and Raleigh was ranked No. 4 among the Best Places to Live by *Money* in 2006. The cost of living relative to other biotechnology hubs is particularly attractive, with an index score of 97.1 for the area, compared with 100 for the nation as a whole, 138 for Boston, and 173 for San Francisco.

"The housing prices are much more moderate as compared to the Northeast or the West Coast, and it's a great place to raise families; the beaches are beautiful and only two hours away," Turek says. "Everyone that we've brought to Biolex—from San Diego, from the Northeast—really loves it."

"Employees here tend to like the fact that we're not a big cosmopolitan area," says GSK's Sutton. "On the way to work you see trees and vegetation, not skyscrapers, and this tends to be a drawing card for the colleagues I work with." Blackshear with the NIEHS agrees that the area is a "fantastic" place for raising families, and provides numerous job opportunities for spouses. "Those of us who have lived here for a while love living here," he says.

However, the same qualities that make the area a great place to live, also give rise to an important potential negative that could make or break the living experience for some. That quality is an undeniable smaller-town feel. While the community is, by all accounts, a cosmopolitan area replete with most of the offerings of a big city, the cities are, in fact, small. The most populous city in the state is Charlotte, with about 700,000 people, and the numbers decline from there. Blackshear relayed the story of a potential recruit to the NIEHS who came from a major East Coast city and spent the entire day looking at real estate with his wife. At dinner, the recruit's wife asked, "This place is fine, but is there a city anywhere around here?" To which the most accurate response might be "maybe—have you tried looking behind the trees?"

Emma Hitt is a freelance medical and science writer residing in Marietta, Georgia.

Appalachian[®]

STATE UNIVERSITY

FOUNDING DIRECTOR Research Institute for Environment, Energy, and Economics

Appalachian State University invites applications and nominations for the position of **Founding Director of the Research Institute for Environment, Energy, and Economics**, with a starting date as early as 1 January 2008. The Founding Director will report to the Provost, and work with various constituencies in all colleges and schools at Appalachian. Qualifications for this position include:

- Significant academic and research credentials in one or more of the Institute's core areas or in a closely related discipline.
- Senior-level administrative experience, preferably in an academic setting or research center or institute.
- Success in managing research by multidisciplinary teams in the relevant areas.
- Significant track record of external funding from state, federal and private sources for research in environment, energy, and/or economics. Success in assisting others to secure funding for multidisciplinary research.
- Effective interaction with public, political and academic audiences.

Appalachian faculty have built a reputation for solid basic and applied research, education, and public programming in environment, energy, and economics. In addition, Appalachian offers related graduate programs in biology, physics, public administration, and technology, and undergraduate programs in chemistry, economics, geology, sustainable development, appropriate technology, and building science. The University is committed to strengthening these areas of excellence by developing the Research Institute for Environment, Energy, and Economics to encourage and coordinate basic and applied research, emphasize the University's commitment to energy and environmental studies, and facilitate educational and community outreach programs. With a formal focus on environment, energy, and economics, the Institute will facilitate research that brings together faculty and students whose interests lie at the intersections between and among these areas.

Appalachian State University (www.appstate.edu) is a member institution of the University of North Carolina System. Located in Boone, North Carolina, Appalachian has approximately 15,000 students in undergraduate and graduate programs at the Boone campus and several distance education sites. Information about the proposed Institute and about University activities in energy and the environment is available at www.web.appstate.edu/research/.

Applicants are invited to send a letter of application, a current c.v., and contact information of five references. Completed applications in pdf or paper should be sent to resdirector@appstate.edu with "Institute Director Search" in the subject line, or to **Institute Director Search, Cratis D. Williams Graduate School, Box 32068, Appalachian State University, Boone, NC 28608**. Application review begins on **2 July 2007**, continuing until the position is filled.

Appalachian State University is an Equal Opportunity Employer. Women and minorities are strongly encouraged to apply.



North Carolina Central University (NCCU) has established the Bio-manufacturing Research Institute and Technology Enterprise (BRITE) Center of Excellence. BRITE will provide the pharmaceutical and biomanufacturing industry with skilled scientists who are prepared to pursue careers in biopharmaceutical science and management. The Golden Leaf Foundation Inc. has provided a grant of \$20.1 million for the construction of the BRITE facility. The 52,000 square foot state-of-art facility is currently under construction, and scheduled to be completed by March, 2008. In 2005, the Golden Leaf Foundation Inc awarded BRITE for additional \$1.5 million for laboratory equipment. In 2005-2006, BRITE has purchased \$4.6 million dollars laboratory equipment including 500 MHz NMR, Imaging station for high content screens, FACS, TOF-MS.

As a component of the North Carolina Biomanufacturing and Pharmaceutical Training Consortium, BRITE will offer education program in biotechnology and biomanufacturing at the B.S., M.S. and Ph.D. levels in Pharmaceutical Sciences. This new degree program associated with BRITE at NCCU will enroll students in B.S. and M.S. degrees in fall, 2007 and followed by a Ph.D. degree program currently in preparation. The graduate program will consist faculty members from BRITE, Biology, Chemistry and other science related departments at NCCU.

Department Chair: Pharmaceutical Sciences currently seeks an internationally recognized scientific leader as Professor and Chair of the Department of Pharmaceutical Sciences. This new institute has research programs related to drug discovery and drug manufacturing process. The detail research strength can be viewed at <http://brite.nccu.edu>. NCCU is one of the 16 state funded universities.

The new chair will have the opportunity to lead and expand this new department. Applicant must have a distinguished record of extramural funding, strong leadership, and administrative skills and should promote alliances with other institutes within and outside NCCU to stimulate research with translational implications in various therapeutic areas. The successful candidate must also be committed to undergraduate and graduate education, supporting the use of innovative educational technologies.

Other tenure-track faculty positions are available at all levels: The successful candidate will be expected to direct an independent research program supported by extramural funding, participate in graduate training, teach graduate and undergraduate students and provide service to the community. Candidates with research interests in molecular aspects of signal transduction and model organisms in disease status that leads to drug discovery are especially encouraged to apply.

Tenure-track positions at NCCU's Kannapolis Campus, Kannapolis, NC: Applications are invited for tenure-track Assistant or Associate Professor positions at North Carolina Central University's newly created research programs located in the UNC Human Nutrition Institute on the North Carolina Research Campus (NCRC) at Kannapolis, NC. To learn more about NCRC, please visit www.ncresearchcampus.net. The successful candidates will be appointed to faculty positions in NCCU's Pharmaceutical Sciences at BRITE in the following areas:

1. Medicinal Chemistry involves in organic synthesis, structure activity relationship (SAR) analysis and chemical library design. Experience of working in the drug design is a plus.
2. Transgenic plant using molecular biology to create functional foods will be the focus of research.

Other instructor and research associate positions are available at Ph.D, M.S. and B.S. levels.

All tenure track faculty positions are 12-month appointments starting on July 1 academic year. Review of applicants will begin immediately and will continue until the position is filled. Applicants should submit by mail or email *curriculum vitae*, a description of research interests, and contact information for three references to: **Search Committee, c/o Administrative Officer, BRITE, North Carolina Central University, 1801 Fayetteville Street, Durham, NC 27707; Email: sjordan@nccu.edu.**

NCCU is an Affirmative Action/Equal Opportunity Employer. Minorities and women are encouraged to apply.

FOCUS ON NORTH CAROLINA



THE UNIVERSITY OF NORTH CAROLINA

GREENSBORO

North Carolina A&T
State University

Founding Dean, Joint School of Nanoscience and Nanoengineering

The University of North Carolina at Greensboro and North Carolina Agricultural & Technical State University invite applications and nominations for the position of Dean of a new Joint School of Nanoscience and Nanoengineering (JSNN). The JSNN is a collaborative enterprise between the two Universities and will be housed in a new state-of-the-art facility at the Gateway University Research Park in Greensboro.

We seek a visionary scientist with strong research credentials, a history of success in attracting outside funding, experience with technology transfer, and a record of accomplishment in developing and managing complex interdisciplinary programs. A Ph.D. in a scientific, mathematical, or engineering discipline with significant research contributions in nanoscience or nanoengineering is required. At least five years of administrative experience in an academic research environment is preferred, although exceptional candidates with non-academic backgrounds will be given serious consideration.

Please submit nominations and applications electronically to the Search Committee for Dean of the JSNN at maplater@ncat.edu. Applications (which will be kept confidential on request) must include an Administrative and Faculty Employment Application (found at <http://facultypages.ncat.edu/hr/>), letter of interest, curriculum vitae, and names and contact information for five references. Inquiries may be directed to either of the Co-Chairs of the Search Committee: Michael A. Plater, Dean, College of Arts & Sciences, NCAT (maplater@ncat.edu) or Timothy D. Johnston, Dean, College of Arts & Sciences, UNCG (johnston@uncg.edu).

Screening of applications begins July 10, 2007, and continues until the position is filled.

For more information visit: <http://facultypages.ncat.edu/hr/>

North Carolina A&T State University and The University of North Carolina Greensboro are AA/EEO employers.

POSITIONS OPEN

RESEARCH PROFESSOR
DRUG DISCOVERYUNIVERSITY OF
PENNSYLVANIA
SCHOOL OF MEDICINE

The Department of Pathology and Laboratory Medicine at the University of Pennsylvania's School of Medicine seeks candidates for a Full Professor position in the non-tenure research track. Applicants must have a Ph.D. or equivalent degree and have demonstrated excellent qualifications in Research.

Candidates must have biotechnology/pharmaceutical research experience in drug discovery, especially related to targets for neurodegenerative diseases, as well as the ability to develop an independent research program in this area.

The University of Pennsylvania is an equal opportunity, affirmative action employer. Women and minority candidates are strongly encouraged to apply.

Please submit curriculum vitae, a letter of interest, 3 reference letters, and a statement of research interests to:

Cyndi MacLeon
University of Pennsylvania
Sch. Med., Dept. of Path. and Lab. Med.
Maloney 3, HUP, 3600 Spruce Street
Phila., PA 19104-4283. fax 215-349-5909
macleon@mail.med.upenn.edu

[http://pathology.uphs.upenn.edu/
Faculty/faculty_jobs.aspx](http://pathology.uphs.upenn.edu/Faculty/faculty_jobs.aspx)

FOCUS ON NORTH CAROLINA



James E. Shepard, President

ASSISTANT/ASSOCIATE
PROFESSOR
NCCU Program in Human Nutrition

Applications are invited for tenure-track Assistant or Associate Professor positions at North Carolina Central University's newly created research programs located in the UNC Human Nutrition Institute on the North Carolina Research Campus (NCRC) at Kannapolis, NC. To learn more about NCRC, please visit www.ncresearchcampus.net. The successful candidates will be appointed to faculty positions in NCCU's Julius L. Chambers Biomedical/ Biotechnology Research Institute (BBRI) in the following two areas:

1. Transgenic zebrafish modeling to study the effects of natural products or drugs on organ development. Preference will be given to individuals whose research focuses on nervous system, cardiovascular, or GI function.
2. Mechanism-based cancer prevention using dietary or pharmaceutical agents. Preference will be given to individuals whose research focuses on oro-esophageal cancer using genetically modified animal models.

The successful candidates will be expected to: establish extramurally funded research programs; collaborate with other North Carolina Research Campus investigators studying nutrigenomics; and train graduate students in their fields of expertise. Applicants must hold a Ph.D. and/or M.D., and have a record of research productivity.

Review of applicants will begin immediately and will continue until the position is filled. Applicants should submit by mail or email *curriculum vitae*, a description of research interests, and contact information for three references to: **Connie Key, Julius L. Chambers Biomedical/Biotechnology Research Institute, North Carolina Central University, 700 George Street, Durham, NC 27707, Email: chkey@nccu.edu**. For more information about the BBRI and NCCU visit <http://www.nccu.edu/BBRI>.

North Carolina Central University is a constituent institution of the University of North Carolina System and an Equal Opportunity, Affirmative Action Employer. NCCU complies with the Immigration Reform and Control Act of 1986.

POSITIONS OPEN

OTOLARYNGOLOGIST

The Section of Otolaryngology - Head and Neck Surgery at Dartmouth-Hitchcock Medical Center seeks a board certified or board eligible Otolaryngologist for a full-time faculty position. The candidate should possess an interest in an academic career and in the education of medical students and residents. This position will combine a general otolaryngology with a subspecialty practice in otology or pediatric otolaryngology. Fellowship training in otology/ neurotology or pediatric otolaryngology is desirable. Research interests will be encouraged. Academic rank will be commensurate with qualifications and experience.

Interested applicants are encouraged to send letters of inquiry and CV to:

Daniel Morrison, MD, Chairman
Section of Otolaryngology - Head & Neck Surgery
Dartmouth-Hitchcock Medical Center
One Medical Center Drive
Lebanon, NH 03756
Telephone: 603-650-8123

DARTMOUTH-HITCHCOCK
MEDICAL CENTER

Dartmouth-Hitchcock Medical Center is an affirmative action/equal opportunity employer and is especially interested in identifying female and minority candidates.

www.DHMC.org



Tenure-Track Positions Liver Diseases Branch

New Research Initiative – Fatty Liver Disease & Obesity - Tenure Track Position:

The Liver Diseases Branch of the National Institute of Diabetes and Digestive and Kidney Diseases (NIDDK), National Institutes of Health (NIH) invites applications for one tenure track position from scientists interested in basic and/or clinical research involving non-alcoholic fatty liver disease and metabolic syndrome. Specific areas of research interest include pathogenesis and mechanism of metabolic derangement in non-alcoholic fatty liver disease and its pathophysiological link to insulin resistance and obesity. Priority will be given to applicants at the Assistant Professor level in traditional universities or those finishing their post-doctoral/fellowship positions.

New Research Initiative – Liver Stem Cells - Tenure Track Position:

The Liver Diseases Branch of the National Institute of Diabetes and Digestive and Kidney Diseases (NIDDK), National Institutes of Health (NIH) invites applications for one tenure track position from scientists interested in basic and/or clinical research involving mammalian adult stem cells. Specific areas of research interest include functional differentiation and mechanism of development of adult tissue-derived stem cells, especially those of the liver, and potential clinical application of stem cell therapy in liver diseases. Priority will be given to applicants at the Assistant Professor level in traditional universities or those finishing their post-doctoral/fellowship positions.

The applicant must have a proven record of accomplishments and will be expected to propose and pursue an independent research program in one of these fields. The position offers unparalleled opportunities for interdisciplinary collaboration within NIDDK and throughout NIH. The Liver Diseases Branch of NIDDK is located on the main intramural campus of the NIH in Bethesda, Maryland, a suburb of Washington, D.C.

Interested applicants should send a Curriculum Vitae and list of publications, copies of three major publications, a summary of research accomplishments, a plan for future research, and three letters of recommendation to **Ms Michelle Brown, Search Committee, Liver Diseases Branch, NIDDK, Building 10-9B16, NIH, Bethesda, MD. 20892-1800.** Application deadline: **September 15, 2007.**



Tenure-Track Position Available

The National Institute on Alcohol Abuse and Alcoholism (NIAAA), a major research component of the National Institutes of Health (NIH) and the Department of Health and Human Services, is recruiting for an independent, tenure-track scientist to head the Section on Neuronal Structure within the Laboratory for Integrative Neuroscience of NIAAA.

Applicants should hold a Ph.D. and/or M.D. degree and have at least 3 years of post-doctoral research experience. This will be a tenure-track position. Research in this section will focus on neuronal morphology, structural plasticity and neuronal function in relation to development, addiction and neurological disorders. It is envisioned that the Section Chief will carry out studies measuring neuronal and synaptic morphology, intracellular neurophysiology, and intraneuronal calcium transients, using animal models of addiction, including alcohol addiction, and hereditary neurological disorders. Criteria for selection will include documented expertise in multiphoton microscopy and laser-based uncaging, quantitative measurement of subcellular morphology, intracellular calcium measurement and patch-clamp electrophysiology in brain slices, as well as an outstanding publication record. Facility in the use of techniques for manipulation of protein expression such as RNA interference and transgenic/gene-targeted mice is also a highly desirable component of the research in this section. Areas of preferred research emphasis include learning and memory/synaptic plasticity, neuronal development, neural mechanisms of addiction, and the morphological basis of neurological disorders. A joint appointment with the National Institute of Neurological Disorders and Stroke is available for suitable candidates. Interested candidates should submit a C.V., list of publications, a brief research proposal that reflects the applicant's research interests and proposal for establishing an independent research program, and names of three individuals who could be contacted for reference to: **Dr. Stephen R. Ikeda, Chair of Search Committee, NIAAA, 5625 Fishers Lane, Rm. TS-11A, MSC-9411, Bethesda, MD 20892-9411; (301) 443-2807; Fax (301) 480-0466.**

Applications must be received by **June 22, 2007.**

Postdoctoral, Research and Clinical Fellowships at the National Institutes of Health

www.training.nih.gov/pdopenings

www.training.nih.gov/clinopenings

Train at the bench, the bedside, or both

Office of Intramural Training and Education
Bethesda, Maryland 20892-0240
800.445.8283

University of Bergen

is a city university. Parts of the campus are in fact situated in the town centre. We have about 17,000 students and nearly 3000 employees. UiB is renowned for its research which holds a high European standard and we have three Centres of Excellence (CoE). The University of Bergen has a strong international profile which entails close co-operation with universities all over the world.



Professor in Marine Organismal Biology at the Department of Biology

The professor will work on marine invertebrates bridging the fields of evolutionary and developmental processes, systematics, phylogeny and evolutionary history using a combined approach accumulating data from many different fields. Start-up funding will be made available to help the successful candidate quickly becoming established in the position.

More at www.uib.no/stilling and <http://www.bio.uib.no/pages/home.php>.

Submit application in 5 copies, sorted into 5 bundles, to the Department of Biology, University of Bergen, PO Box 7803, NO-5020 Bergen, Norway, **by 18 June 2007.**

CICEPO 08



SLU (the Swedish University of Agricultural Sciences) develops learning and expertise in areas concerning our planet's living natural resources. www.slu.se

The Faculty of Natural Resources and Agricultural Sciences is the largest of the four faculties of SLU. Our area of activity covers a wide range of disciplines, spanning over agriculture, food and biotechnology to natural resources, environment and landscape planning. Our 18 departments are organised in four clusters.

The faculty office and most of our departments are located in Uppsala, 65 km north of Stockholm.

SLU (The Swedish University of Agricultural Sciences) hereby announces the vacancy of a

PROFESSORSHIP IN STRUCTURAL MOLECULAR BIOLOGY

at the Department of Molecular Biology, Uppsala, Sweden.

Ref no 1653/07

More detailed information concerning this position can be obtained from Professor Inger Andersson phone no +46 18 - 471 42 88, cell phone +46 (0)70 - 520 8101, fax no +46 18-536971, e-mail Inger.Andersson@molbio.slu.se The mission and activities of the department are found at <http://www.molbio.slu.se>

The complete announcement can be found at <http://personal.slu.se/job> as well as Appointment Procedures for SLU and a set of procedural directives pertaining to the application process. The outline used in these documents should be followed in the personal record/list of qualifications and publications.

An application, marked with the ref no should be submitted to the Registrar of SLU, P.O. Box 7070, SE-750 07 Uppsala, Sweden, **no later than July 06, 2007.** The application should be in English.

Associate Laboratory Director for Basic Energy Sciences

Brookhaven National Laboratory (BNL) is seeking candidates for the position of Associate Laboratory Director of its Basic Energy Science Directorate (BES). This Directorate is one of five science Directorates at the Laboratory and contains both major research and facility sectors, including Chemical Sciences, Condensed Matter Physics & Materials Sciences and the Center for Functional Nanomaterials (CFN) user research facility. The annual budget of the Directorate is about \$50 M with a staff of over 160.

The Associate Laboratory Director (ALD) is responsible for the scientific and managerial leadership of the Directorate. He/she reports to the Laboratory Director. The successful candidate must have a Ph.D. degree and a distinguished research career in the physical sciences accompanied by proven experience in the management of a mid-sized research effort. BNL is interested in candidates who will develop internationally leading programs that are aligned with the mission of the Department of Energy, and who will maintain and enhance a world-class scientific and technical staff. The ALD is the primary contact with BNL's programs and facility sponsors, principally the U.S. Department of Energy.

The ALD participates at the Director's level in the Laboratory-wide planning for new programs and user facilities and has line responsibility for safe and environmentally sound operation of his/her program. Recent areas of BES scientific focus include nanoscience, catalysis, strongly correlated and complex systems, interface of life and physical sciences, and photo/radiation chemistry & chemical dynamics. New programs are developing at the Laboratory level in renewable energy and energy efficiency. In the facilities sector, the focus will be on start up and transition to operations of the Center for Functional Nanomaterials as a major research and user facility with scientific thrusts in nanocatalysis, biological & soft nanomaterials and electronic materials, among others. The BES Directorate has, and will continue to play an important role in the development and use of BNL's National Synchrotron Light Source II. Emphasis will also be applied to coupling BES programs to those in the other BNL Directorates, including the Life Sciences and Energy, Environment and National Security.

BNL is a multi-disciplinary laboratory engaged in a broad scope of world-class basic and applied research in a highly stimulating and competitive science environment. It is managed by Brookhaven Science Associates under contract with the U.S. Department of Energy. Applications should be sent electronically to hempfling@bnl.gov, or by regular mail to William Hempfling, Human Resources Division, Brookhaven National Laboratory, Bldg. 400B, PO Box 5000, Upton, NY 11973-5000. BNL welcomes diversity and encourages applications from all qualified individuals.

BROOKHAVEN
NATIONAL LABORATORY
a passion for discovery.

www.bnl.gov



The European Molecular Biology Laboratory (EMBL) is an international research organisation with its Headquarters Laboratory in Heidelberg, Germany and four additional Units in Hinxton (the European Bioinformatics Institute, EBI), Grenoble, Hamburg, and Monterotondo. For our Outstation in Grenoble we have a vacancy for a

Team Leader

Synchrotron Methods for Structural Biology at EMBL, France

We are looking for a structural biologist who has a focus on advanced crystallographic methods and instrumentation, particularly with relation to synchrotron radiation. The appointed Team Leader will manage, together with the Head of Outstation, the long-term collaboration between the EMBL Grenoble Outstation and the European Synchrotron Radiation Facility (ESRF) concerning the development and operation of the automated protein crystallography beamlines. He/she will oversee the activities of the three existing EMBL beamline scientists currently responsible for the dedicated microfocus beamline ID23-2, the MAD beamline ID14-EH4 and the CRG beamline BM14 (co-operated with MRC-France) as well as a SAXS beamline scientist currently under recruitment. He/she will collaborate in particular with the Outstation Diffraction Instrumentation team led by Florent Cipriani, which has developed state-of-the-art sample handling equipment currently installed on all ESRF MX beamlines (microdiffractometer, sample changer, minikappa) and with the ESRF MX group led by Sean McSweeney. He/she will develop a research programme focused on advanced crystallographic methods and instrumentation coupled to structural biological problems or more generally on new synchrotron techniques that might have an impact in biology and which take advantage of the unique environment at the world-leading 3rd generation synchrotron site in Grenoble.

Further information on the position can be obtained from the Head of Grenoble Outstation Stephen Cusack (cusack@embl-grenoble.fr).

EMBL is an inclusive, equal opportunity employer offering attractive conditions and benefits appropriate to an international research organisation.

To apply, please email a curriculum vitae, three references and a concise description of research interests and future plans quoting ref. no. S/07/065 in the subject line, to: application@embl.de

www.embl.org



Scientist/Postdoctoral Position(s) in Progenitor Cell Biology

Opportunities exist to assume a lead role in Institute-, NIH- and corporate-sponsored investigations of: 1/ erythroid progenitor cell development (including novel Epo action modes and response factors); 2/ newly discovered tyrosine and S/T kinases with hematopoietic suppressor activities; and 3/ the nature (and action mechanisms) of niche-specific cell migration and adhesion factors involved in hematopoietic cell development.

Approaches include unique transgenic and knockout mouse models; systems for primary cell development ex vivo; transcriptome analyses and bioinformatics; and human CD34 cell & lentiviral RNAi systems. Opportunities also exist for participation in: studies of small molecule inhibitors & cytokine mimetics; human patient samples/studies; and graduate & undergraduate instruction. Resources include subsidized cores in: Progenitor Cell Separation and Analysis; Genomics & Bioinformatics; Transgenic mouse construction; Lenti- and retro-virus production; Confocal microscopy and cell imaging; DNA & protein sequencing; Histopathology; and high resolution MRI.

Benefits, salary and resources are nationally competitive and positions are within the laboratory of DM Wojchowski at the Maine Medical Center Research Institute (www.mmc.org). Please provide CV, statement of research interests, and professional reference contact information via your online application at www.mmc.org.

The MaineHealth Family, EOE



國家衛生研究院
National Health Research Institutes

The Director of Medical Engineering Division National Health Research Institutes (NHRI), Taiwan

Applicants and nominations are invited for the position of the Director of Medical Engineering Division at the National Health Research Institutes, Taiwan. The Director is responsible for supervision of all research programs within the Division, as well as research collaborations with other Divisions and institutions. The prospective candidate should have strong organizational, communicative, and interpersonal skills and ability to interact effectively with others at all levels inside and outside of NHRI. Applicants should have a doctoral degree in biomedical engineering or a closely related discipline, and have demonstrated a successful record in conducting a vigorous and independent research program in any of the broadly defined areas of biomedical engineering, include: biofluid mechanics, cellular and molecular biomechanics, biomaterials and functional tissue engineering, biological system modeling, molecular imaging, medical imaging and image guided surgery, robot-assisted surgery, and bioMEMS.

Applicants should also be familiar with the scientific and medical community in Taiwan, proficient in the Chinese language, and capable of working effectively in the research environment under current circumstances in Taiwan.

Applicants should send a complete curriculum vitae, three reprints of selected publications, a statement of research interests (two A4 pages or less), and names/addresses of five references to:

Search Committee for the Director of MED/NHRI, Department of Research Planning and Development, National Health Research Institutes, 35 Keyan Road, ZhuNan Town, Miaoli County 35053, Taiwan

The search will remain open until the position is filled. NHRI is an equal opportunity employer. Women and non-Taiwan citizens are encouraged to apply.

KATHOLIEKE UNIVERSITEIT
LEUVEN



Situated in Belgium in the heart of Europe, the Katholieke Universiteit Leuven (<http://www.kuleuven.be/english>) has a rich tradition of research and learning of almost six centuries, with a clear international orientation. The annual research budget is around 230 million euro, and the scientific staff counts over 5,300 researchers.

The Group of Science, Engineering and Technology at K.U.Leuven invites applications for 15 vacant academic positions at the level of professor or associate professor in:

- Differential Geometry
- Experimental Semiconductor Physics
- Structural Inorganic Chemistry
- Conformational Analysis
- Plant Systematics
- Rational Use of Electrical Energy
- Mathematical Engineering
- Industrial Biotechnology
- Process Intensification
- Energy in Buildings
- Building Materials and Construction Techniques
- Bacteriophage Genomics and Proteomics
- Design of Catalysts and Catalytic Reactors
- Economics and Policy of Natural Resources in Developing Countries
- Secure Software

In addition a limited number of research professorships is open for excellent candidates with a high-quality research programme.

Detailed descriptions of these profiles and information on how to apply can be found at <http://gexacte.kuleuven.be/vacancies/vacancies.htm>

The deadline for applications is **28 September 2007**.

For further information contact: **Els Lemmens, director of management Group Science, Engineering and Technology, K.U.Leuven, telephone +32 16 32 81 51, e-mail els.lemmens@gexacte.kuleuven.be**

Assistant, Associate or Full Professor Department of Dermatology University of California, Davis

The Department of Dermatology at UC Davis is seeking an experienced researcher for a state-funded tenured position. Candidates are expected to engage in research and teaching activities. The candidate should have an MD, PhD, or MD/PhD degree and a background that includes substantial time spent at an academic medical center with a strong extramurally funded research program. Preferential consideration will be given to those with a research background in inflammation, cancer, or tissue regeneration. Preferential consideration will also be given to those with clinical training in dermatology. The successful candidate will have demonstrated academic scholarship in the form of publications in major peer-reviewed journals and record of continued extramural research funding.

For full consideration, applications must be received by **July 31, 2007**. The position will remain open until filled through December 31, 2007.

If interested, please respond by sending a curriculum vitae and letter of inquiry to:

M. Yasner
Department of Dermatology
University of California, Davis
3301 C Street, Suite #1400
Sacramento, CA 95816

The University of California prohibits discrimination against or harassment of any person employed by or seeking employment with the University on the basis of race, color, national origin, religion, sex, physical or mental disability, medical condition (cancer-related) ancestry, marital status, age, sexual orientation, citizenship or status as a Vietnam-era veteran or special disabled veteran.



The Morehouse School of Medicine is seeking a Chair for its Department of Pharmacology. The successful candidate will be an outstanding nationally recognized scientist and academician, who will be responsible for continued development of the department and will guide its research and education missions. Candidates (Ph.D. or M.D.) with a strong record of research in any area of the pharmacological sciences will be considered. Excellent interpersonal skills, scientific leadership, and commitment to mentoring junior faculty are essential. Credentials appropriate for the rank of Professor are required. Areas of ongoing research foci within the department include cancer biology, cardiovascular pharmacology and neuroscience. Additional information is available at <http://web.msm.edu/Pharmacology/>. Opportunities for collaboration and program development within the institution are available through the Cardiovascular Research Institute, Center for Reproductive Science, Neuroscience Institute, Clinical Research Center, Cancer Biology Program, and other basic and clinical departments. The Department of Pharmacology contributes to the curriculum of the medical education program and to the training of graduate students through the interdisciplinary Ph.D. program in Biomedical Sciences.

Interested applicants should submit a curriculum vitae, names and contact information for at least three references, a statement of research interests and academic vision, and a summary of administrative experience either electronically (gwaymon@msm.edu) or by mail: **Dr. David R. Mann, Chair, Pharmacology Chair Search Committee, Room 317 Medical Education Building, Morehouse School of Medicine, 720 Westview Drive, SW, Atlanta, GA 30310**. Review of candidates will begin as applications are received and continue until the position is filled.

*The Morehouse School of Medicine is an Affirmative Action/
Equal Opportunity Employer.*



CENTRAL DRUG RESEARCH INSTITUTE
(Council of Scientific & Industrial Research)
Chattar Manzil Palace, P.O. Box 173, Lucknow-226 001 (India)

ADVERTISEMENT NO. 2/2007

Applications on the prescribed forms are invited from the persons of Indian nationality for the following posts in Central Drug Research Institute, Lucknow, India.

Scientist Gr. IV(3) : One post : (Scale of Pay : Rs. 12,000-375-16,500/-);

For Parasitology Division) Essential Qualification : 1st Class M.Sc. or equivalent in any branch of science with Ph.D. in Biochemistry and Molecular Biology of Parasites and atleast 4 years research experience in the area of Malaria Biochemistry and/or Immunology as evidenced by high quality of publications in high impact national/International journals. This is an independent group leader position where the candidate is required to undertake studies on development of newer drug targets and or novel therapeutic methods in the area of malaria.

Scientist Gr. IV(2) : Fifteen posts: Scale of Pay : Rs. 10000-325-15200/-)

Post No. 1 (for Pharmacology in the area of Biochemistry and Molecular Biology of Diabetes); **Post No. 2** (for Pharmacology in the area of Biochemistry and Molecular Biology of Lipid disorders); **Post No. 3** (for Pharmacology in the area of Cardio-vascular Pharmacology); **Post No. 4** (for Parasitology in the area of Biochemistry and Molecular Biology of Malaria); **Post No. 5** (for Microbiology in the area of Molecular Immunology); **Post No. 6** (for Microbiology in the area of virology); **Post No. 7** (for Pharmacokinetics in the area of drug metabolism & pharmacokinetics including development of bio-analytical methods as per regulatory requirements); **Post No. 8&9** (for Medicinal & Process Chemistry in the area of synthetic chemistry); **Post No. 10&11** (for Medicinal & Process Chemistry in the area of Natural Product Chemistry); **Post No. 12** [for Protein NMR (MSB)]; **Post No. 13** [for NMR (SAIF)]; **Post No. 14** [for Bioinformatics (MSB) in the area of Bioinformatics and computational biology] & **Post No. 15** : (For Toxicology in the broad area of toxicology/toxicogenomics.

For detailed information Website : <http://www.cdriindia.org/situationv.asp>
may be referred to.

"INTERIM QUERIES WILL NOT BE ENTERTAINED"



West Virginia University

ROBERT C. BYRD HEALTH SCIENCES CENTER

**Wyeth Research Scholar
Associate Professor or Professor
Director of Stroke/Cerebrovascular Research**

West Virginia University invites applications and nominations for the position of **Wyeth Research Scholar** and **Director of Stroke/Cerebrovascular Research**. The successful recruit will be expected to build a vigorous research program into the causes and prevention of stroke, including epidemiology, treatment of stroke and/or molecular mechanisms for repair of the damaged brain tissue. This research effort will complement an existing comprehensive clinical stroke program and help anchor a new Clinical and Translational Neuroscience Initiative organized through the **Center for Neuroscience** (<http://www.hsc.wvu.edu/wvuen/>), which is an integral part of a new Health Sciences Center Strategic Research Plan (SRP; *Science* 09/08/06, 313:1461).

The SRP includes faculty recruitment and expansion of research training for doctoral students and clinical fellows. The Director will be a member of the Center for Neuroscience and have an appointment as **Associate Professor** or **Professor** in the **Department of Neurology** (<http://www.hsc.wvu.edu/som/neurology>). Joint appointment in either the Department of Neurosurgery, Department of Emergency Medicine, or Department of Neurobiology and Anatomy is encouraged, pending training and research interests. The Director will receive research space, start-up funds, and a competitive salary. Recruitment of additional faculty is envisioned to develop a research team.

Candidates should have an MD and/or PhD degree, a strong record of funded research, transferable NIH R01 funding, and a commitment to mentoring graduate students and junior faculty. Translational and basic research is supported by existing core facilities that include the Center for Advanced Imaging (structural and functional MRI and PET/CT imaging) and Molecular Genetics Core units (Gene Array and Transgenic Rodent Facilities). Collaborative opportunities also exist with faculty in the Center for Cardiovascular Research (<http://www.hsc.wvu.edu/cires>).

West Virginia University is a land grant Carnegie-designated Doctoral/Research-Extensive institution with approximately 22,000 undergraduate and 5,500 graduate/professional students. The Health Sciences Center includes the Schools of Medicine, Pharmacy, Dentistry, and Nursing, each with health professional and graduate programs. Two new research buildings totaling 200,000 sq ft are currently under construction on the Health Sciences campus to accommodate our aggressive agenda for research growth. Relevant patient care facilities include a 460-bed University Hospital (Ruby Memorial) with a new, 80-bed addition, and an adjacent 70-bed psychiatric hospital (Chestnut Ridge). Morgantown is rated as one of the best small cities in the U.S. with affordable housing, excellent schools, a picturesque countryside, and many outdoor activities (<http://www.morgantown.com>).

Candidates should send a letter summarizing research interests and career goals, curriculum vitae and the names of three references, in confidence, either electronically (c/o sfinnegan@hsc.wvu.edu) or by mail to: **Dr. George Spirou, Stroke/Cerebrovascular Research Search Committee, WVU Health Sciences, PO Box 9304, Morgantown, WV 26506**. Review of applications will continue until the position is filled.

West Virginia University is an Affirmative Action/Equal Opportunity Employer.



**Faculty Position in Ocean Sensors
Scripps Institution of Oceanography
University of California, San Diego**

The Scripps Institution of Oceanography (SIO) (<http://scripps.ucsd.edu>) at the University of California, San Diego (UCSD) invites applications to fill one or more positions at the Assistant (tenure-track), Associate or Full Professor (tenured) levels in fields related to the research on, and development of, ocean sensors, with particular emphasis on sensors for biological and chemical variables. We seek an innovative individual who will establish a vigorous independent research program that complements established capabilities at Scripps.

The successful candidate will be expected to teach graduate level courses, and will be encouraged to participate in undergraduate teaching at UCSD. The position requires a Ph.D. degree and a competitive record of publication as well as evidence of the ability to conduct and fund an active research program and, for more senior candidates, of the ability to mentor graduate students and junior colleagues. The salary will depend on the experience of the successful applicant and will be based on the University of California pay scale.

Review of applications will begin **July 16, 2007**, and will continue until position(s) are filled. Applicants should submit their CV, a letter including descriptions of research interests and teaching interests/experience, a list of publications, immigration status, and the names of at least five potential referees, along with their complete institution address, email address, phone and fax numbers, to: **Chair, Ocean Sensors Search Committee, 0208, Scripps Institution of Oceanography, University of California at San Diego, La Jolla, CA 92093-0208, USA**. Please clearly label applications "Ocean Sensors Search". Applicants are welcome to include in their cover letter a personal statement summarizing their contributions to diversity.

UCSD is an Equal Opportunity Employer with a strong institutional commitment to excellence through diversity.

PostDoctoral Fellowship in Molecular Neurobiology ENDOCYTE Training Network

ENDOCYTE is a multidisciplinary Research and Training Network (RTN) funded by the 6th Framework Programme of the European Union. Members of the ENDOCYTE network are investigating the relevance of the intracellular routes of growth factor signalling for the regulation and diversification of growth factor function.

To complete this Network, the Consortium is seeking an enthusiastic and highly motivated PostDoctoral fellow to join the laboratory of M. Fainzilber at the Weizmann Institute of Science (Rehovot, Israel). For further information on research lines in the host laboratory please see http://www.weizmann.ac.il/Biological_Chemistry/scientist/Fainzilber/Fainzilber.html

For a full description of the project and further details of ENDOCYTE aims and training, please see <http://www.endocyte.ki.se>

Applications should be addressed to
mike.fainzilber@weizmann.ac.il



Chief, Endocrinology and Director, of the Diabetes Center

The Department of Medicine at Case Western Reserve University School of Medicine and University Hospitals Case Medical Center is seeking applicants for Chief, Division of Endocrinology and Director of the Diabetes and Obesity Center. The Division has 15 full-time faculty members providing patient care at University Hospitals Case Medical Center, the Cleveland Wade Park Veterans Administration Hospital, and outpatient satellite centers. The Division has current, robust basic, translational and clinical research programs. Its educational program includes University Hospitals Case Medical Center and the Wade Park Veterans Administration Hospital, with 5 fellows. The successful candidate will have an outstanding record of scholarly achievements, sustained extramural research funding, along with proven leadership, mentoring and administrative abilities. He/she should qualify for the rank of Professor with tenure at Case. A strong commitment to continuing to lead the Division in national prominence through building interdisciplinary programs as Diabetes and Obesity Center Director is expected.

Interested candidates should submit their curriculum vitae and a letter describing their research, teaching, service and administrative experience to: **Robert A. Salata, MD, Chair, Endocrinology Division and Director of the Diabetes and Obesity Center Chief Search Committee, Chief, Infectious Diseases, Department of Medicine, Case Western Reserve University, University Hospitals Case Medical Center, 11100 Euclid Ave., Cleveland, OH, 44106-5083.** Electronic format preferred to: robert.salata@case.edu.

Case Western Reserve University/University Hospitals Case Medical Center are Equal Opportunity/Affirmative Action Employers.

www.cardiff.ac.uk/jobs



Positions in Microbiology (2 posts) Cardiff School of Biosciences

Cardiff School of Biosciences, one of the largest bioscience departments in the UK, with an outstanding reputation for teaching and research, seeks to appoint up to 2 fully tenured positions in Microbiology within the full range from Lecturer to Professor.

We aim to recruit research active staff of the highest calibre who can contribute to the School's strategic ambitions and facilitate interdisciplinary collaboration within the research areas related to Microbiology within the School (see <http://www.cardiff.ac.uk/biosi/research>) and across the University.

Further details of the School's learning and teaching can be found at <http://www.cardiff.ac.uk/biosi/tl/index.html>

Salary:

Lecturer: £33799 - £39160 per annum (Grade 7) – Vacancy no. 369
Senior Lecturer: £40335 - £46758 per annum (Grade 8) – Vacancy no. 370
Professorial: Negotiable and nationally competitive within the Cardiff Professorial range – Vacancy no. 371

Informal enquiries can be made to the Head of School, Professor John Harwood at Harwood@cardiff.ac.uk or to the Head of the Microbiology Research Group, Professor Andrew Weightman at Weightman@cardiff.ac.uk

To work for an employer that values and promotes equality of opportunity, visit www.cardiff.ac.uk/jobs telephone + 44 (0) 29 2087 4017 or email vacancies@cardiff.ac.uk for an application form quoting the relevant vacancy number.

Please include full details of publications and research grant income (as relevant) and an indication of your research plans. A covering letter of application, setting out personal career aspirations and the post currently held by the applicant must be attached.

Closing date: 27 July 2007

Waseda Institute for Advanced Study Tenure Track Program

Waseda Institute for Advanced Study is currently recruiting researchers (fixed-term faculty) for the tenure track program outlined below.

■ Research Fields to be invited:

Computer Science :

Interaction, Parallel & Distributed Processing, Robotics

Modern Mechanical Engineering:

System Integration, Safety, Dependability, Robotics, Bioengineering, Environment

Civil and Environmental Engineering:

Sustainable Infrastructure, Disaster Prevention and Mitigation, Life Span System, Infrastructure and Area Management

Physics & Applied Physics:

Condensed Matter Physics, Photonics and Information Engineering, Mathematical and Statistical Physics, Astrophysics, Nuclear and Particle Physics, Biophysics

Applied Chemistry:

Energy Chemistry, Functional Materials Chemistry, Functional Materials Engineering

■ Period of appointment:

From November 1, 2007 (planned) to March 31, 2010

It can be renewed annually (up to a March 31, 2012 at the longest) depending upon the results of performance reviews. In FY2011, if the researcher is judged to be eligible following final appraisal, they will be employed as tenured (full-time) faculty from April 2012.

Applicants must have a doctorate or equivalent. However, it is desirable for the doctorate to have been obtained within 10 years of November 1, 2007. Further details and application forms can be obtained from our website: www.waseda.jp/wias/english

Contact: wias-info@list.waseda.jp

Applications should be sent to the following address:

Waseda Institute for Advanced Study
attention: Researcher Employment
1-6-1 Nishiwaseda, Shinjuku-ku,
Tokyo 169-8050, Japan

Closing Date: July 24, 2007
5pm (Japan time)

www.waseda.jp/wias



The European
Commission

The European Commission, Directorate General Joint Research Centre (JRC), is seeking to recruit (m/f):

DIRECTOR (grade AD14)

INSTITUTE FOR ENVIRONMENT AND SUSTAINABILITY IN ISPRA (JRC.H) (COM/2007/10050)

Official Journal n° C 126 A – 7 June 2007

We are the Joint Research Centre; our mission is to provide customer-driven scientific and technical support for the conception, development, implementation and monitoring of EU policies. JRC comprises 7 research institutes spread across 5 sites in Europe. We have a staff of 2,700 and an operating budget of € 300 M per annum; our core competence areas are food, chemical products and health; environment and sustainability; nuclear safety and security; and horizontal activities such as reference materials and measurements, techno-economic foresight, public security and anti-fraud.

We propose: a post of **Director of the Institute for Environment and Sustainability (JRC.H – ISPRA)**. The mission of the Institute for Environment and Sustainability (IES, <http://ies.jrc.ec.eu.int/>) is to provide scientific and technical support to EU policies for the protection of the environment contributing to a sustainable development in Europe. Its core activities are: Sustainable Use of Natural Resources; Sustainable Agriculture and Rural Development; Climate Change Mitigation and Adaptation; Environmental Risks and Natural Hazards; Sustainable Transport and Air Quality; Renewable Energies; Environmental Dimension of Development Cooperation; Environmental Information and Monitoring Systems.

The Director is responsible for the overall management of the Institute and has delegated financial and recruitment responsibilities for the complete budget and staff of their Institute. The Institute has some 450 staff and an annual budget of ca. € 40 million. The Director will be member of the JRC senior management team and contribute to the overall development and implementation of the JRC mission. He/she will in addition be expected to provide strategic orientation for and coordination of activities across the whole of the JRC related to environment and sustainability issues.

Applicants must: • be a national of one of the European Union Member States; • hold a university degree that gives access to undertake doctoral studies; • have at least 15 years' postgraduate professional experience at a level to which the qualifications referred to above give admission; at least 5 years of that professional experience must have been gained at high level management experience; • have a thorough knowledge of one of the EU official languages and an adequate knowledge of another of these languages. Candidates should note that the selection procedures will be carried out in English, French or German only.

The Director will be selected and appointed by the Commission according to its selection and recruitment procedures. Salaries and conditions of employment are those laid down in the Staff Regulations for AD 14 grade officials of the European Communities. The Commission applies an equal opportunities policy. The link to the on-line application at which you can find full job description and the selection criteria is: http://ec.europa.eu/dgs/personnel_administration/seniormanagementvacancies/CV_Encadext/index.cfm. If you encounter technical problems, please send an e-mail to: ADMIN-MANAGEMENT-ONLINE@ec.europa.eu.



<http://ec.europa.eu>

ScienceCareers.org

The closing date
for application is
5 July 2007.

On-line application
will not be possible
after 12.00 noon
Brussels time.

Office of Naval Research HEAD, WARFIGHTER PERFORMANCE S&T DEPARTMENT

The Office of Naval Research (ONR) is seeking an outstanding individual to serve in this Civil Service position in the Senior Executive Service (SES). Salary range is \$111,676 to \$168,000 per year, depending on qualifications. In addition to salary, career SES appointees are eligible to compete for performance awards and bonuses.

As a Department Head, the incumbent participates with other top management officials in advising on matters concerning the policies and personnel of the science and technology program and in recommending to the Chief of Naval Research the scientific and technical contents of an integrated science and technology program. In support of the approved program and overall Office of Naval Research mission requirements, the incumbent manages an extensive Departmental research and development program focused on the integration of basic research, applied research, and advanced technology development in the fields of science and technology such as computational neuroscience, cognitive science, manpower, personnel, training, human factors, occupational and environmental health, medicine of naval operations (undersea, Marine Corps, surface, aerospace) and combat/contingency medicine. The incumbent is responsible and accountable for planning and executing the Department's program. The incumbent: provides leadership to and establishes the broad direction of the program; establishes the objectives, policies, and priorities pertinent to the program; oversees and ensures the effective accomplishment of the extensive activities of the Department's Divisions; and coordinates and cooperates with other Departments in working to achieve a fully integrated science and technology program in the Office of Naval Research.

For detailed information on qualifications and how to apply, applicants may download a copy of Announcement # NE7-XXXX-4H673666-SES from the ONR web site <http://www.onr.navy.mil/hr>. Applications must be received in the ONR Human Resources Office by the close of business Friday 15 June 2007. Applications will not be accepted that are emailed, faxed, or postmarked after the closing date.

U.S. CITIZENSHIP REQUIRED • AN EQUAL OPPORTUNITY EMPLOYER AND PROMOTES DIVERSITY IN THE WORKPLACE. • WOMEN AND MINORITIES ARE ENCOURAGED TO APPLY.

CELL & DEVELOPMENTAL BIOLOGIST

The Samuel Lunenfeld Research Institute invites applications for a Research Investigator position (assistant to full professor equivalent, according to experience). We are seeking a biologist investigating fundamental questions of cell and developmental biology (areas of interest include neurobiology, stem cell biology, and classic developmental biology).

Research programs utilizing cutting-edge imaging technology or addressing cellular function in the context of development are also sought. The successful candidate will have a PhD and/or MD degree with postdoctoral experience and a strong publication record. You will be expected to develop innovative and highly competitive independent research programs.

The institute is affiliated with the Mount Sinai Hospital and University of Toronto and has diverse strengths in cell biology, developmental biology, biochemistry, and integrative biology. For more information about the institute, please refer to <http://www.mshri.on.ca>. This position will include cross-appointment with the University of Toronto.

We offer competitive salary and startup packages commensurate with experience and qualifications. Applications should include a current CV, summary of research interest and goals, most relevant publications, and three references. Applications and references should be submitted, preferably by e-mail, by September 15, 2007, to:

Chair of the Cell and Developmental Search
Samuel Lunenfeld Research Institute
e-mail: CellDevSearch@mshri.on.ca



Samuel Lunenfeld
Research Institute

MRC

Laboratory
of Molecular
Biology

Post-Doctoral Scientist

Applications are invited for a Post-Doctoral position in the group of Dr Phil Holliger. Our research focuses on the synthetic biology of nucleic acid replication (see PNAS (2001), 99, 8530; Nature Biotechnol. (2004), 22, 755). The aim of the project is to apply compartmentalization and selection strategies developed in the laboratory to the evolution of an efficient, general RNA polymerase ribozyme, ultimately capable of true self-replication.

Applicants must have a PhD degree, and experience in recombinant DNA technology. Experience in working with RNA, and in particular with aptamers, ribozymes and SELEX, will be considered a bonus. For further information about the post, please contact Dr Phil Holliger, email: ph1@mrc-lmb.cam.ac.uk

This is a three-year appointment with a salary range of £24,993 - £28,214 per annum, depending upon qualifications and experience. This is supported by a flexible pay and reward policy, 30 days annual leave entitlement, an optional MRC final salary pension scheme and excellent on site sports and social facilities.

For further information and an application pack, please contact the Recruitment Team by email: cambridge.recruitment@ssc.mrc.ac.uk or telephone 01793 301154 quoting reference CAM 2007-329. Please include with your application a copy of your CV and names and addresses of two referees who can be contacted prior to interview.

Closing date: 1 July 2007.

For further information about MRC visit www.mrc.ac.uk

The Medical Research Council is an Equal Opportunities Employer.
'Leading Science for Better Health'



Director of Microscopy Neuroscience Institute Stanford University

The Neuroscience Institute at Stanford University (NIS) is seeking a director for their new Imaging Center at the Arastradero facility. The ideal candidate would have a PhD in Cell biology or electrical Engineering with an emphasis on Optical analysis.

Candidates must have extensive experience in 3 of the 4 following areas: 2 photon and confocal microscopy including time-lapse live imaging, TEM and SEM microscopy on biological tissues, Computational Image acquisition, processing and deconvolution, Storage and Acquisition of large datasets. The candidate would be responsible for the day to day operations of the center, the center's operating budget, selecting and purchasing equipment for the center and interfacing with an optical project engineer responsible for assembling microscope equipment. The candidate must be able to work both independently and in collaboration with diverse users, ranging from those seeking microscopy services to those needing training: students, post-docs, and technicians. Practical experience and knowledge in sample preparations, TEM and confocal microscopy and applications are important. Excellent verbal, written and interpersonal communication skills in English are essential. Some grant writing and preparation is required.

Applicants should ask three references to send letters directly to the search committee: email: jsv1@stanford.edu

Dr. Mark Schnitzer, Dr. Stephen Smith and Dr. William Mobley
1201 Welch Road
P.O. Box 5489
Stanford, Ca 94305-5489

FACULTY POSITION ANNOUNCEMENT Pollination Biologist University of California, Davis

The Entomology Department seeks applicants for a Pollination Biologist at the Assistant Professor level (20% AES research and outreach, 80% instruction and research). We seek an outstanding applicant with a Ph.D. degree in entomology or related disciplines with experience and interest related to basic and applied entomology. The appointee will develop an extramurally funded research program on insect pollinators with emphasis on California agricultural systems pertinent to the AES mission. The appointee is required to teach core curriculum courses, supervise graduate students, participate in outreach programs, and perform University service. This position is part of an eight-position recruitment under the new Agriculture Sustainability Institute Initiative, and the appointee will be expected to contribute to the development of and teach in the planned undergraduate major in sustainable agriculture. This appointment is available on or about January 1, 2008.

Applicants must submit online at http://secure.entomology.ucdavis.edu/fac_recruit/login.cfm: curriculum vitae; statement of research and teaching interests; official transcripts, publication list, and reprints of key publications (up to three), and the names and addresses of at least three references. Inquiries should be addressed to:

James Carey, Professor
Entomology Search Committee Chair
Entomology Department
367 Briggs Hall
One Shields Avenue, Davis, CA 95616
(530) 752-6217
jrcarey@ucdavis.edu

Open until filled but to ensure consideration, applications must be received by **August 15, 2007**. A more detailed job description can be obtained from the above address.

UC Davis is an Affirmative Action/Equal Employment Opportunity Employer and is dedicated to recruiting a diverse faculty community. We welcome all qualified applicants to apply, including women, minorities, veterans, and individuals with disabilities.

COURSES & TRAINING



2nd CMP-Summerschool on "Analysing Membrane Proteins: Methods and Approaches"

24th - 29th of September 2007

The European Membrane Biology Network (EMBN) presents its broad know-how in analysing membrane proteins to young scientists from abroad organized by the Center for Membrane Proteomics (CMP) of the Johann Wolfgang Goethe-University. The summer school takes place from 24th - 29th of September 2007 at the Biocenter of the Johann Wolfgang Goethe-University Frankfurt, Germany.

The event focuses on methods to analyse the biological, biophysical, biochemical and structural properties of membrane proteins. Highly qualified MSc. students and PhD students are invited to register for participation. A limited number of fellowships covering travel and lodging expenses will be available.

Further informations and online registration at www.cmp.uni-frankfurt.de

Contact:

Dr. Bernd Maertens
Center for Membrane Proteomics
Max-von-der-Laue-Str. 11
Tel. +49-(0)69-798-29418
B.Maertens@em.uni-frankfurt.de

Coordinator CMP
University of Frankfurt
D-60439 Frankfurt
Fax +49-(0)69-798-29419
www.cmp.uni-frankfurt.de

Fundación BBVA

2007 BBVA FOUNDATION AWARD FOR SCIENTIFIC RESEARCH IN ECOLOGY AND CONSERVATION BIOLOGY

Recognizing particularly significant scientific advances of a theoretical, methodological and/or empirical nature achieved by researchers of any country in the fields of Ecology and/or Conservation Biology.

One award will be given, consisting of a €500,000 cash prize, a diploma and a commemorative artwork.

The BBVA Foundation Awards include two other categories, for innovative projects and knowledge dissemination in biodiversity conservation.

Fundación BBVA

Gran Vía, 12
48001 Bilbao
Spain
Fax: (34) 94 424 46 21

Paseo de Recoletos, 10
28001 Madrid
Spain
Fax: (34) 91 374 34 44
convocatorias@bbva.es

Deadline for entry submission: July 12, 2007

Call conditions, application forms and additional information are available on the Foundation website: www.fbbva.es

WORKSHOPS



EMBL



EMBO Workshop on Common Regulatory Mechanisms in Haemopoiesis and Neurogenesis

EMBL Heidelberg, Oct 3 - 5, 2007

- Ligands and Receptors during Organogenesis
- Signalling Mechanisms in Development and Function
- Chromosomes and Gene Expression
- Communication between Haemopoietic and Nervous System

Confirmed Speakers:

Ralf Adams	George Kollias
Facundo Batista	Reina Mebius
Patrick Charnay	Ira Mellman
Mark Coles	Jeff Milbrandt
Anne Eichmann	Freddy Radtke
Laura Feltri	Mart Saarma
Richard Flavell	Kirsi Sainio
Rudi Grosschedl	Victor Tybulewicz
Frank Grosveld	David Wilkinson
Carlos Ibanez	George Yancopoulos
Rüdiger Klein	

Registration and further info:
<http://cwp.embo.org/w07-13/>

AWARDS



Sheikh Hamdan Bin Rashid Al Maktoum
Award for Medical Sciences

Hamdan Award for Medical Research Excellence

In the field of:

THERAPY IN MALIGNANCY
**MOLECULAR THERAPY IN
DRUG TARGETING (PHARMACOGENOMICS)**
ORGAN & TISSUE TRANSPLANTATION

The prize amount is AED three hundred thousand (AED 300,000) (Approx. US\$ 82,000) to be awarded equally to 3 winners.

The general secretariat is pleased to invite doctors, researchers, universities, research centres and medical scientific societies throughout the world to submit their research work for the awards 2007-2008

Closing Date: November 30, 2007

For further information:

The General Secretariat
Sheikh Hamdan Bin Rashid Al Maktoum
Award for Medical Sciences
P O Box 22252, Dubai, United Arab Emirates
Tel: +971 4 3986777
Fax: +971 4 3984579 / 3980999
E mail: shaward@emirates.net.ae
Website: <http://www.hmaward.org.ae>



**BASIC SCIENCE FACULTY
POSITIONS AVAILABLE**

**Institute of Human Virology
University of Maryland
School of Medicine
Baltimore, Maryland**

The Institute of Human Virology at the University of Maryland, Baltimore School of Medicine (<http://www.ihv.org>) is recruiting highly qualified individuals with established research programs at ranks of tenure-track **Assistant, Associate** and **Full Professor**. Candidates with NIH (R01 and/or P01) funded research programs with expertise in one or more of the following are encouraged to apply: cell biology, structural biology, basic immunology, or systems biology with interest in chronic human viral diseases such as HIV-1. These programs will complement the existing institute programs in molecular pathogenesis, innate immunity, vaccine development, and translational clinical research that focus on chronic viral diseases. The Institute of Human Virology offers excellent laboratory facilities, competitive salary and startup packages, and access to numerous core facilities including state-of-the-art BSL3 and ABSL3 facilities in a rapidly growing academic environment. The level of appointment will be commensurate with the candidate's experience.

Interested applicants are requested to forward a CV in .pdf format to: **Chairperson, IHV Faculty Search Committee, Institute of Human Virology, 725 W. Lombard Street, Baltimore, Maryland, 21201.**

The University of Maryland, Baltimore is an Equal Opportunity, Affirmative Action Employer.

**INSTITUTE OF
HUMAN VIROLOGY**

**University of Maryland
School of Medicine
Baltimore, Maryland**

The Institute of Human Virology at the University of Maryland, Baltimore School of Medicine (<http://www.ihv.org>) is seeking to fill a **tenure-track faculty position** with an investigator with the ability to establish an independent research program centering on the molecular biology/virology of human papilloma virus and its interactions with host cell factors, especially those relevant to cancer. The successful candidate will have a demonstrable track record of relevant publications in peer-reviewed journals and of attracting peer-reviewed funding, preferably related to cancer. The level of appointment will be commensurate with the candidate's experience.

Interested applicants are requested to forward a CV in .pdf format to:

**Chairperson
IHV Faculty Search Committee
Institute of Human Virology
725 W. Lombard Street
Baltimore, Maryland, 21201**

The University of Maryland, Baltimore is an Equal Opportunity, Affirmative Action Employer.

POSITIONS OPEN

The new School of Pharmacy at Loma Linda University (LLU) joins a proud heritage of nearly a century of health professions education. The University motto: To Make Man Whole, combined with the mission of continuing the teaching and healing ministry of Jesus Christ, is the foundation of all programs.

The Department of Pharmaceutical Sciences is committed to educating competent pharmacists who are critical thinkers and understand and employ foundational biomedical knowledge in rational, therapeutic decision making informed by Christian values of caring service.

**CHAIR, DEPARTMENT OF
PHARMACEUTICAL SCIENCES**

The successful applicant will be responsible for starting a graduate program; recruiting, developing, and mentoring faculty; providing oversight of departmental activities; and managing Department resources. The Chair will provide vision and leadership in the facilitation of scholarship, integration within the pharmaceutical sciences curriculum, and faculty service. The Chair will also work closely with other School and University leaders' implementation and assessment of the Pharm.D. curriculum. Qualifications include a Ph.D. in the pharmaceutical sciences or a related chemistry/biology field and current appointment at the **PROFESSOR or ASSOCIATE PROFESSOR** level. Candidates should have a track record of excellence in teaching, leadership, research, and academic service.

FACULTY, MEDICINAL CHEMISTRY

Full-time (12-month) faculty position in medicinal chemistry is available at the **ASSISTANT or ASSOCIATE PROFESSOR** level. A Ph.D. in the respective discipline is required. Preference will be given to candidates having a pharmacy background and two or more years of experience in academics and pharmaceutical research. Successful candidates will develop appropriate pharmaceutical science lectures, guide and mentor both Pharm.D. and graduate students, initiate research programs, and develop collaboration where possible within and outside LLU.

Loma Linda University is located in a quiet suburban neighborhood in the Inland Empire east of Los Angeles. The vast resources of the area provide a wide variety of cultural, education, shopping, and recreational opportunities.

E-mail your curriculum vitae in PDF or M.S. Word format to e-mail: dyaeger@llu.edu.

**URBAN INSECT ECOLOGIST
Illinois Natural History Survey**

Urban Insect Ecologist, at the level of **ASSISTANT PROFESSIONAL SCIENTIST**. Develop and conduct research program that focuses on insects in terrestrial urban ecosystems. Requires Ph.D. in entomology or related discipline. Responsibilities: develop vigorous, externally funded research program; publish research findings in scientific journals; work with cities, state and federal agencies, and University of Illinois. Illinois Natural History Survey is part of the Illinois Department of Natural Resources and an affiliated agency of the University of Illinois at Urbana-Champaign. To apply send cover letter, curriculum vitae, statement of research interests, and contact information for three references to our **Human Resources Office, e-mail: hroffice@inhs.uiuc.edu** (electronic applications required). Position reference #1495, telephone: 217-244-4592, fax: 217-333-4949. Deadline: July 31, 2007. For application requirements and complete position description visit our website: <http://www.inhs.uiuc.edu/opportunities/index.php?action=fulltime&id=131>.

The Beckman Institute Biological Imaging Center at California Institute of Technology has a **SENIOR SCIENTIST** position available to investigate applications of advanced imaging methodologies in developmental biology and neurodegenerative disease studies. Individuals with at least four years of experience in small animal model systems are encouraged to apply. Send curriculum vitae to **Ms. K. Hilands** at: M/C 139-74, 1200 E. California Boulevard, Pasadena, CA 91125.

POSITIONS OPEN
**ASSISTANT/ASSOCIATE PROFESSOR
Neurophysiology**

The College of Veterinary Medicine at North Carolina State University in Raleigh, North Carolina, announces a tenure-track faculty position in neurophysiology with an initial appointment at 70 percent research, 20 to 30 percent teaching, and zero to ten percent service depending upon entering rank. A Ph.D. in neurophysiology or a relevant neuroscience field is required. Candidates also having a D.V.M. or teaching experience in a veterinary professional curriculum are encouraged to apply. To view the full vacancy announcement, with position responsibilities and additional requirements, and to apply, please visit our website: <http://jobs.ncsu.edu> and search by position #B-96-0708. Applications are currently being accepted and the position will be open until August 15, 2007, or until a suitable candidate is identified. Questions about the position can be directed to: **Dr. Lola Hudson, Search Committee Chair, College of Veterinary Medicine, North Carolina State University, 4700 Hillsborough Street, Raleigh, NC 27606, e-mail: lola_hudson@ncsu.edu.**

Affirmative Action/Equal Opportunity Employer. In addition, NC State University welcomes all persons without regard to sexual orientation. For those individuals with disabilities requiring accommodation please contact telephone: 919-515-3148.

RESEARCH ASSISTANT PROFESSOR

Position available August 16, 2007, in the Department of Surgical Oncology at the University of Illinois at Chicago to work on anticancer activity of bacterial redox proteins. Experience required in gene cloning, protein purification, animal handling, mammalian cell genetics, preclinical pharmacology and pharmacokinetics, and cancer cell biology, evidenced by publication in international journals. Required Ph.D. degree in microbiology, molecular biology, or biochemistry. Salary commensurate with qualifications and experience. Only selected applicants will be contacted for further correspondence. If interested, send curriculum vitae with names of three references by July 2, 2007, to **Tanya Eitzenhoefer, University of Illinois at Chicago-Department of Surgical Oncology at e-mail: tanya@uic.edu.** *Affirmative Action/Equal Opportunity Employer.*

**RESEARCH ASSISTANT PROFESSOR
Lung and Vascular Biology**

Research Assistant Professor position to study mechanisms of endothelial repair, vascular inflammation, and pulmonary diseases. Candidates must have Ph.D./M.D. with extensive experience in studying the pathophysiology of lung and/or vascular diseases with genetically modified mouse models or in endothelial progenitor cells/stem cell research. Successful candidate with an excellent publication record *must be a U.S. citizen or permanent resident*. Send curriculum vitae to: **Dr. Youyang Zhao, Department of Pharmacology, University of Illinois at Chicago, 835 S. Wolcott, Chicago, IL 60612. E-mail: yzhao@uic.edu.** *UIC is an Affirmative Action/Equal Opportunity Employer.*

POSTDOCTORAL POSITION is available to study malaria parasite cytoadherence and host cell signaling. Skills required include protein expression and purification, RNA interference (RNAi) studies with retroviral short hairpin RNAi, electrophoretic mobility shift assays, Chromatin Immunoprecipitation assays, et cetera. Send curriculum vitae to: **Dr. D.C. Gowda, Biochemistry and Molecular Biology, Pennsylvania State University College of Medicine, Hershey, Pennsylvania, at e-mail: gowda@psu.edu.** *Pennsylvania State University is committed to Affirmative Action, Equal Opportunity, and to the diversity of its work force.*

POSITIONS OPEN

VICE PRESIDENT/CHIEF, RESEARCH Centre for Addiction and Mental Health (CAMH)

As a world-leading research facility, community-based organization, and education/training institute, Centre for Addiction and Mental Health (CAMH) provides a unique combination of programs in clinical care, research, policy, education, and health promotion. Fully affiliated with the University of Toronto, Canada's largest and most prestigious research-intensive university, CAMH is one of the few institutions worldwide with deep expertise in all four major areas of mental health and addictions research: biomedical, clinical, health systems and services, and population/public health.

In addition to assuming responsibility for the executive oversight of the Program and its team of 700 (including principal investigators, research support staff, students, and volunteers), the Vice President/Chief, Research will lead in developing a strategy to address the positioning of CAMH Research within the changing landscape of the provincial health system.

As an international leader, CAMH seeks, for this position, an outstanding scientist of considerable stature. A unique combination of qualifications is required: scientific leadership ability, an exceptional track record of scientific achievement and international recognition, a research philosophy that is rooted in clinical/community practice, and the ability to work in a complex environment. The successful candidate will demonstrate disciplinary breadth, a record of accomplishments in translational/multidisciplinary research, and experience in leading change. S/he will possess an M.D. or equivalent, substantial clinical experience, and/or a Ph.D. in a relevant area. S/he will be qualified for appointment at the **ASSOCIATE or FULL PROFESSOR** level.

Applications will be accepted immediately and will be reviewed on a continuing basis, with the Search Committee's consideration of candidates beginning in mid July. Information requests and applications, which must include a letter of interest, curriculum vitae, and the names of and contact information for three referees, should be e-mailed to e-mail: helen.xuc@rayberndtson.ca.

CAMH and the University of Toronto are strongly committed to diversity within their communities and especially welcome applications from visible minority group members, women, Aboriginal persons, persons with disabilities, members of sexual minority groups, and others who may contribute to the further diversification of ideas. All qualified persons are encouraged to apply; however, Canadians and permanent residents of Canada will be given priority.

POSTDOCTORAL RESEARCH POSITION

BioProtection Systems Corporation has an immediate opening for a Postdoctoral scientist to develop new vaccines, and implement cell-based and mouse model efficacy assays. Applicants are required to hold a Ph.D. degree and one to two years of related experience in virology/immunology or a related field. Experience with vaccine development (pseudovirus/virus-like particles) would be a plus. *Competitive candidates will be U.S. citizens or citizens of one of the 26 permanent NATO member countries.* BioProtection Systems Corporation is located in the Iowa State University Research Park in Ames, Iowa. We are focused on the development of prophylactic and therapeutic vaccines for high-priority agents and emerging infectious pathogens. Please send curriculum vitae to e-mail: credentials@bpsys.net.

CAREER OPPORTUNITY

This unique program offers the candidate with an earned Doctorate in the life sciences the opportunity to obtain the Doctor of Optometry (O.D.) degree in 27 months (beginning in March of each year). Employment opportunities exist in research, education, industry, and private practice. Contact the Admissions Office, telephone: 800-824-5526 at the New England College of Optometry, 424 Beacon Street, Boston, MA 02115. Additional information at website: <http://www.neco.edu>, e-mail: admissions@neco.edu.

POSITIONS OPEN

CLINICAL PATHOLOGIST/ MICROBIOLOGIST or CLINICAL LABORATORY SCIENTIST

The Clinical Laboratory Sciences (CLS) Program (website: <http://www.isu.edu/cls/>) of the Department of Biological Sciences (website: <http://www.isu.edu/bios/>) at Idaho State University (ISU) has an opening for a full-time tenure-track faculty position at the level of **ASSISTANT PROFESSOR**, with research and teaching interests in the area of clinical microbiology-bacterial pathogenesis and CLS and will begin with the fall 2007 semester. The position will join an established bacterial pathogenesis research group at the Boise Veterans Administration Medical Center in Boise. The ISU CLS Program faculty offer coursework and research-related courses both on campus and online at the undergraduate and graduate levels, interact with faculty at affiliated clinical sites, and have a strong commitment to student mentoring. The successful candidate will contribute to research/scholarly activity resulting in grants and publications in the area of bacterial host-pathogen interactions; teach CLS-related courses; and provide professional and University service. The position requires a Ph.D. or M.D. in clinical pathology, microbiology, or related field. In addition, s/he must have Medical Technology (American Society for Clinical Pathology) or CLS (National Credentialing Agency for Laboratory Personnel) or equivalent certification, or acquire such certification prior to tenure. The Department of Biological Sciences is committed to aggressive expansion of the CLS Program. Salary, rank, and tenure status are commensurate with qualifications and experience.

Candidates should submit curriculum vitae, no more than three reprints, a statement of research interests and goals, a teaching philosophy statement, and contact information for three references forwarded to: **CLS Search Committee, Department of Biological Sciences, Idaho State University, 921 South 8th Avenue, Mail Stop 8007, Pocatello, ID 83209-8007.**

Screening of applicants will begin June 1, 2007, and continue until the position is filled. *ISU is an Equal Opportunity Employer and welcomes applications from women and minorities.*

HIV TRANSMISSION and PROPHYLAXIS

POSTDOCTORAL POSITION (D.V.M., Ph.D., and/or M.D.) in the Laboratory of **Dr. J. Victor Garcia** to study natural routes of HIV transmission, microbicides and pre-exposure prophylaxis using state-of-the-art humanized mouse models (*Nat. Med.* 12:136-22, 2006, *Journal of Experimental Medicine* 204(4):705-14, 2007). Experience with human stem cells, immunodeficient mouse models of human hematopoiesis and/or molecular biology of HIV is essential for this position. Flow cytometry experience and experience with bone marrow transplantation is highly desirable. Strong written and verbal communication skills in English are required.

Send letter of interest, curriculum vitae, and names of three references to: **Ms. Deborah Solomon, e-mail: deborah.solomon@utsouthwestern.edu, University of Texas Southwestern, Division of Infectious Diseases, 5323 Harry Hines Boulevard, Dallas, TX 75390-9113.** *The University of Texas Southwestern Medical Center at Dallas is an Equal Opportunity, Affirmative Action Employer.*

POSTDOCTORAL POSITION is available at the University of Nebraska, Lincoln, in the area of redox biology/biochemistry/bioinformatics with emphasis on mechanisms of redox regulation, functional characterization of selenium-containing proteins, bioinformatics and functional genomics of thiol-dependent redox proteins and processes, and their roles in cancer and aging. Additional information is at website: <http://genomics.unl.edu/gladyshev>. To apply send curriculum vitae, cover letter of interest, and names of three references to **Vadim Gladyshev** at e-mail: vgladyshev1@unl.edu. *The University of Nebraska, Lincoln, is an Equal Opportunity, Affirmative Action Employer.*

POSITIONS OPEN

A POSTDOCTORAL RESEARCHER POSITION is available immediately at the Louisiana State University Health Science Center, School of Medicine, New Orleans, Louisiana. A Ph.D. in the field of biochemistry, molecular or cellular biology, or a related science field is required. The research goal includes dissecting ubiquitin-mediated regulation of cell division. The candidate will utilize multidisciplinary approaches including biophysical and genetical techniques and appropriate biological systems to attack this NIH-funded project. Experience with a classical genetics system, such as *Drosophila*, is desirable, but not required. The successful candidate will join a new laboratory in the Department of Biochemistry and Molecular Biology that offers strong mentoring and competitive salaries commensurate with research experience. Please e-mail your curriculum vitae, along with contact information for three references, to: **Dr. Edward Wojcik (e-mail: ewojci@lsuhsc.edu), Department of Biochemistry and Molecular Biology, Louisiana State University Health Sciences Center, 1901 Perdido Street, New Orleans, LA 70112.** *LSUHSC is an Equal Opportunity/Affirmative Action Employer.*

POSTDOCTORAL POSITION available immediately to join a molecular cardiology laboratory at the Ohio State University in Columbus, Ohio. Research is focused on understanding calcium transport in cardiac muscle using genetically altered mouse models (website: <http://medicine.osu.edu/physiology/3484.cfm>). A Ph.D. with minimum of two years of experience in molecular biology, biochemistry, and cardiac electrophysiology is preferred. Please send curriculum vitae to **Muthu Periasamy, Ph.D., e-mail: periasamy.1@osu.edu.** *The Ohio State University is an Equal Opportunity/Affirmative Action Employer. Qualified women, minorities, Vietnam-era veterans, disabled veterans, and individuals with disabilities are encouraged to apply.*

MARKETPLACE

MEETINGS

MicroRNAs EUROPE 2007 November 1-2, 2007

University of Cambridge, Cambridge, UK
Inaugural:

Nobel Laureate Aaron Klug (MRC)
Keynotes: **David Baulcombe (UCambridge)**
Keith McCullagh (Santaris Pharma)

EPIGENOMICS and SEQUENCING July 9-10, 2007

NRB-Harvard Medical, Boston, USA
Keynotes: **Manuel Esteller (CNIO, Spain)**
Thomas Jarvie (454 Life Sciences/Roche)

Organized by:

GeneExpression Systems, Inc of USA
For details: call: 001-781-891-8181 or
Visit: <http://www.expressgenes.com>

Oligo Synthesis Reagents

↳ Specialty CPG Supports

↳ Linkers, Spacers, & Modifiers

↳ Bulk Reagent Pricing Available

BIOSEARCH TECHNOLOGIES +1.800.GENOME.1
Advancing Nucleic Acid Technology™ www.btisynthesis.com

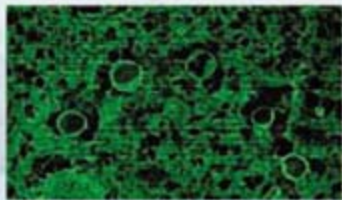
Widely Recognized Original & Guaranteed	KlenTaq1	8¢/u Truncated Taq DNA Polymerase Withstand 99°C



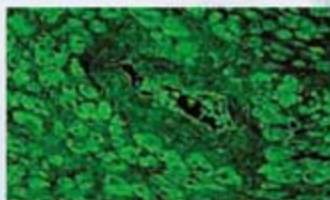
LEADING PROVIDER OF HBV AND HCV
REAGENTS FOR RESEARCH
AND DIAGNOSTIC APPLICATIONS

VIROGEN

IMMUNOHISTOCHEMICAL DETECTION OF GLUTATHIONE

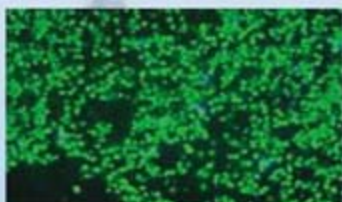


Whole blood cells stained with anti-Glutathione monoclonal antibody, 101-A.

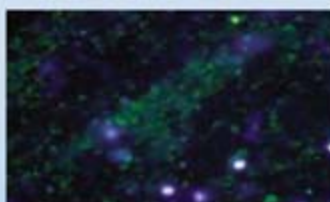


Heart staining with anti-Glutathione monoclonal antibody, 101-A.

DETECT CYSTEINYLATION OF PROTEINS WITH 102-A MONOCLONAL ANTIBODY!



Red Blood Cells stained with anti-Cysteine monoclonal antibody, 102-A.



Red Blood Cells stained with anti-Cysteine monoclonal antibody, 102-A plus DTT.

200 Dexter Avenue, Watertown MA 02472 USA
tel: (617) 926-9167 | fax: (617) 926-9157
order online for fast delivery: www.virogen.com

microRNA Microarray Service

Comprehensive Service

From your sample to fully analyzed microarray data.

The Most Current Sequence Content

All species, Sanger miRBase Version 9.2 (May 2007)

µParaflo™ Microfluidic Chip Technology

Probes optimized, highly reproducible and reliable data.

Customizable Sequence Content

Test your microRNA predictions at no extra cost.

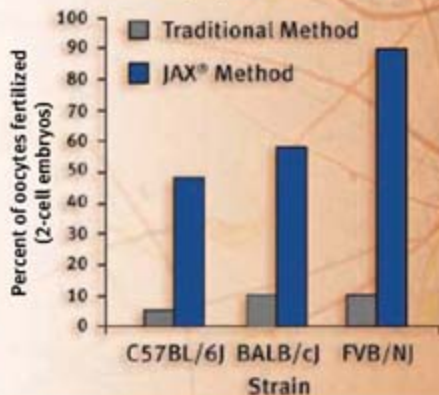


LC Sciences

www.lcsciences.com

Anyone can freeze mouse sperm. We can actually recover it.

JAX® Sperm Cryopreservation Dramatically Improved Fertilization Rates



Are you looking for a better way to manage and protect your mouse colonies? Our scientists have developed innovative methods which make the cryopreservation and recovery of mouse sperm a practical, reliable and cost-effective colony management tool.



To learn more:
1-800-422-MICE, 1-207-288-5845 or jaxservices@jax.org

JAX® Sperm Cryopreservation & Recovery Services
www.jax.org/jaxservices



sbs 赛百盛
SBS Genetech Co., Ltd.

会当凌绝顶 一览众山小

SBS GENETECH

- Custom Services
Custom Oligonucleotides
Custom Peptide synthesis
- Nucleic Acids Isolation & Purification
- Restriction Endonucleases
- DNA Molecular Weight Markers
- PCR-Related Products
- RNA-Related Products
- Protein-Related Products
- SBS PreMix Series-Easy-Do™ PCR PreMix,
Easy-Go™ RT PreMix, Easy-Go™ RT-PCR PreMix
- GoldView™ Nucleic Acid Stain
-An alternative to EB
- Biochemicals, Microtubes & Tips

Tel:+86-10-62969345,+86-10-62969346 Fax:+86-10-82784290
Email: service@sbsbio.com info@sbsbio.com
Website: www.sbsbio.com



What if staying up to date with the latest technology published in journals and patents were as easy as pushing a button?



It is.

With the “Keep Me Posted” alerting feature, SciFinder sends you automatic updates on areas you—and your competitors—are interested in.

You can monitor specific research topics, companies, authors, substances, or sequences, and choose how frequently you receive notifications: daily, monthly, or weekly.

The service isn't just convenient, it's incredibly current. Journal article records often appear in SciFinder before they're even in print. New references, substances, and sequences are added daily. Patents from all the major offices are added within two days of issuance.

As with all SciFinder features, Keep Me Posted is integrated with your workflow. At any point in a search (including the beginning), simply click on the Keep Me Posted button. SciFinder tracks your steps and will generate the appropriate alert—even for complex topics. When you receive a notification, you can follow each reference as you would in a search: find citing or cited articles (with links to the electronic full text), and follow referenced substances and reactions for further information.

Comprehensive, intuitive, seamless—SciFinder doesn't just alert you, it's part of the process. To find out more, call us at 800-753-4227 (North America) or 614-447-3700 (worldwide) or visit www.cas.org/SCIFINDER.



SciFinder®
Part of the process.™



A division of the American Chemical Society. SciFinder is a registered trademark of the American Chemical Society. “Part of the process” is a trademark of the American Chemical Society.

Go the Distance



ULTRAmers™

Ultra High-Fidelity synthesis of oligos up to 200 bases with Mass Spec QC!

IDT continues to push the boundaries of DNA synthesis quality and performance. By leveraging our industry-leading synthesis platform and chemistry, we now offer the custom synthesis of **Ultramers™**; 60-200 base DNA oligos suitable for demanding applications such as cloning and gene construction for use as synthetic template. Save time and trouble with direct synthesis of the entire target fragment!

To maintain our commitment to high quality, a proprietary LC-MS method has also been developed to provide accurate mass assessment for **Ultramers™**. As always, this service is offered free of charge for each oligo with all data accessible online.

Ultramers specifications:

- 60 to 200 DNA bases
- Delivered normalized (3 nanomoles) and lyophilized in tubes
- Ideal for gene construction, cloning and ddRNAI
- PAGE purification and plate synthesis options also available

Go to www.idtdna.com/ultramers for more information.



Innovation and Precision in Nucleic Acid Synthesis

www.idtdna.com

800.328.2661



ISO 9001:2000
FM88954